

DEPARTMENT OF THE INTERIOR
U. S. GEOLOGICAL SURVEY

**Geotechnical description of
Yellow Sea sediments
with some preliminary geological interpretations**

by

James S. Booth¹ and William J. Winters¹

Open-File Report 89-149

This report is preliminary and has not been reviewed
for conformity with U.S. Geological Survey editorial
standards and stratigraphic nomenclature. Any use of
trade names is for descriptive purposes only and does
not imply endorsement by the USGS.

¹Woods Hole, Massachusetts 02543

February 1989

**GEOTECHNICAL DESCRIPTION OF
YELLOW SEA SEDIMENTS**
with some preliminary geological interpretations

James S. Booth and William J. Winters

INTRODUCTION

In August 1985, core samples and high-resolution seismic reflection data were collected in the Yellow Sea near and south of the Shandong Peninsula (Figure 1). As one part of this study, a geotechnical investigation was conducted to establish the basic engineering properties of the sediment, to help identify and analyze potential geohazards, and to supply additional data pertinent to the investigation of geologic processes in the study area. The following is a preliminary report on that work; it provides a general summary of the results of the geotechnical laboratory tests, a brief engineering description of the Yellow Sea sediments, and initial interpretations of the geologic environment as inferred from the geotechnical data.

This investigation received its primary support from the National Science Foundation and the Academia Sinica of the Peoples Republic of China through the Woods Hole Oceanographic Institution (John D. Milliman, Principal Investigator) and the Institute of Oceanology at Qingdao (Professor Yun-shan Qin, Chief Scientist).

We most gratefully acknowledge the invitation, support and cooperation of John Milliman. We also acknowledge the assistance and cooperation of Charles A. Nittrouer and David J. DeMaster of North Carolina State University, also Principal Investigators in the research program, and of their students, Clark Alexander and Ross Elliott, whose help during the field work was invaluable.

METHODS

Field

The sampling program was carried-out August 12-18, 1985 aboard the R/V Science 1, a research vessel operated by the Institute of Oceanology for Academia Sinica. Eleven Kasten cores and eight box cores were recovered from a total of 9 stations (Figure 1). The Kasten cores were tested for vane shear strength at sea and subsampled for later, onshore laboratory index property testing (i.e., water content, liquid limit, plastic limit, and grain specific gravity); the box cores were subcored with 10-cm I.D. poly-vinyl-chloride (PVC) pipe and stored for later triaxial and consolidation testing. Core and site information are provided in Table 1.

CONTENTS

Introduction	1
Methods	1
field	1
laboratory	3
Results and Interpretations	3
shear strength	3
sensitivity	4
index properties	5
consolidation states and properties	6
strength parameters	8
Summary	8
geological	8
geotechnical	9
References	9
Appendices	17
A: nomenclature and symbols	17
B: results of vane shear and index property tests	20
tabular data	21
vane shear strength profiles	27
liquid limit, plastic limit, and water content profiles	38
water content, bulk density, porosity, and grain specific gravity profiles	58
C: results of constant-rate-of-strain consolidation tests	78
tabular data	79
unedited test plots	81
D: results of consolidated-isotropic-undrained triaxial tests	237
tabular data	238
unedited individual test plots	240
unedited multiple test plots	260

Table I
Core listing and station data

Core	Length (m)	Latitude	Longitude	Water Depth (m)
KC-1A	1.05	34° 27.95' N	122° 29.98' E	59
KC-1B	2.25	"	"	"
BC-4	0.50	35° 05.51' N	123° 33.41' E	72
KC-4	2.53	"	"	"
BC-5	0.67	35° 30.00' N	123° 53.00' E	79
KC-5	1.99	"	"	"
BC-6	0.67	35° 43.00' N	123° 11.37' E	73
KC-6	2.92	"	"	"
BC-7	0.65	36° 56.20' N	123° 00.80' E	28
KC-7A	1.63	"	"	"
KC-7B	3.04	"	"	"
BC-8	0.68	36° 43.32' N	123° 00.00' E	34
KC-8	3.02	"	"	"
BC-9	0.65	36° 25.00' N	123° 00.00' E	66
KC-9	1.93	"	"	"
BC-10	0.65	37° 31.33' N	122° 59.77' E	54
KC-10	2.32	"	"	"
BC-11	0.65	36° 07.61' N	121° 49.08' E	38
KC-11	1.27	"	"	"

BC = box core; KC = Kasten core

Undrained shear strength (S_u) was measured at sea with a motorized vane shear device. The four-bladed, 12.7-mm-square vane was inserted normal to the long direction of the core and rotated at approximately 84°/min. Measurements were made at 25 cm intervals beginning at 50 cm below the top of the core (the upper 50 cm was removed for radiometric dating). Although the North Carolina State University Kasten corer (Kuehl and others, 1985) minimizes mechanical disturbance, some disturbance probably took place during coring due to the general softness of the sediment. Thus, because the sediments are fine-grained, the strength values reported herein are probably less than the in-situ values. The inserted vane was rotated 360° after the initial failure and the remolded strength, S_{ur} , was measured. The third vane shear strength parameter, sensitivity (S_t), which is the "natural" shear strength to remolded shear strength ratio, was also calculated. Subsamples were taken from the location of the vane measurement for later index property testing. The subsamples were placed in plastic bags, sealed, and stored in capped core liner sections.

Laboratory

The geotechnical index property tests were conducted as indicated:

- 1) Water content (w) was measured in accordance with standard test method D2216-80 of the American Society for Testing and Materials (ASTM, 1985), except that the samples were dried at 50° C.
- 2) Liquid limit (w_L) values were determined by the cone penetrometer method (standard test BS 1377 of the British Standards Institution).
- 3) Plastic limit (w_P) was measured in accordance with standard test method D4318-84 (ASTM, 1985).
- 4) Grain specific gravity (G_s) measurements were made with an air-comparison pycnometer. The sample chamber was put under a vacuum, then purged with helium.

From these parameters, Plasticity Index (I_p), Liquidity Index (I_L), bulk density (ρ_t), void ratio (e), and porosity (n) were calculated. All index property data were salt-corrected using a salinity of 35^{0/00}.

Constant-rate-of-strain consolidation tests were performed at the top, middle, and bottom of each subcore. Standard test method D4186-82 (ASTM, 1985) was used. The maximum past stress experienced by the sample (σ'_{vm}), compression index (C_c), coefficient of consolidation (c_v), and coefficient of permeability (k) were derived from the test data.

Consolidated, undrained triaxial tests were conducted on selected subcores. Because these PVC cores were relatively short, it was necessary to use small specimens (35 mm diam. x 70 mm length) in the triaxial testing. The method used was based on the ASTM (1985) standard test for unconsolidated, undrained compressive strength (D2850-82). The consolidation stress levels used were (1) assumed in situ stress, (2) 70 kPa, (3) 140 kPa, and (4) 210 kPa. Shearing was accomplished at a rate of 0.15 mm/min. During the tests, data were collected automatically by an HP-85 computer-scanner system. From the basic data set, the angle of internal friction with respect to effective stress (ϕ'), effective stress cohesion (c'), percent strain at failure, undrained shear strength (q_{max}), and other strength, stress, and strain parameters were determined.

Details of all testing procedures are given in Winters (1988).

RESULTS AND INTERPRETATIONS

Shear Strength

The sediments are extremely weak. The highest undrained vane shear strength (S_u) measured was 6.6 kPa (Table 2, Appendix B)) and about one-fifth of the 68 samples possessed strengths below the threshold of measurement of the vane shear apparatus

(i.e., 0.2 kPa). Similarly, four-fifths of the attempts to measure remolded strength were unsuccessful. The down-core strength profiles (Figure 2) show a tendency for S_u to increase with subbottom depth. The predicted strength profile (prediction based on the assumption that the sediments are normally consolidated, and therefore have an S_u/σ'_v value of approximately 0.24) for each of the selected cores is plotted along with the measured profile. The agreement between the two plots is reasonable in each case, which, again, implies a depositional environment (i.e., net sediment accumulation) or, at least, an environment of nonerosion.

Table 2
Vane shear strength and index property data summary

<u>Property</u>	<u>Measurements</u>	<u>Minimum</u>	<u>Average</u>	<u>Maximum</u>
natural shear strength (S_u)[kPa]	54 *	<0.2 **	<3.0 ***	6.6
sensitivity (S_t)	14 †	1.6	>3.6 ‡‡	>6.3 ‡‡
natural water content (w)[%]	100	32	68	144
grain specific gravity (G_s)	100	2.65	2.68	2.73
bulk density (ρ_b)[g/cm ³]	100	1.35	1.64	1.93
porosity (n)[%]	100	45	62	79
liquid limit (w_L)[%]	100	32	58	102
plastic limit (w_P)[%]	100	18	25	36
plasticity index (I_p)[%]	100	11	33	71
liquidity index (I_L)	100	0.67	1.26	2.03

* In 14 of 68 tests the sediment was too weak for accurate strength determination with the vane shear apparatus

** 0.2 kPa is the assumed limit of accurate measurement

*** Values below threshold were not used in the calculation. Therefore average is actually less than 3.0
† strength below measurement threshold in 54 of 68 tests

‡‡ Values below threshold were not used, so numbers represent minima

From a geotechnical perspective, the strength data indicate that these sediments are "very soft" ($S_u \leq 12.2$ kPa) according to classification of Terzaghi and Peck (1967).

Sensitivity

The ratio of "natural" undrained shear strength to remolded shear strength is termed sensitivity (S_t); it is a measure of the strength lost by a sediment when its basic structure has been destroyed. In the majority of cases, remolded shear strength was too low to be measured accurately: only 14 sensitivity determinations were possible, and most of these came from three cores (Table 2). For this reason, and because not even an approximate value can be assigned to the mean or range, sensitivity will not be discussed.

Index Properties

Natural water content (w), grain specific gravity (G_s), liquid limit (w_L), and plastic limit (w_P), and related properties (bulk density (ρ_f), porosity (n), plasticity index (I_P) and liquidity index (I_L)) constitute the suite of index properties for this study. With the exception of grain specific gravity, all of these properties vary over a considerable range (Table 2, Appendix B). In general, this implies a highly variable texture and (or) mineralogy within this basically fine-grained sediment.

Variation in the natural water content of these sediments (32% to 144%) is particularly conspicuous. Because vane shear strengths are uniformly low throughout the cores, and because all cores represent only the upper few meters of sediment, variable degrees of compaction are apparently not responsible for the wide range in water contents. Thus, an environment characterized by a broad range in sediment texture is indicated. Moreover, the average w of 68% suggests that silt is a prominent size class because clay-dominated fine-grained sediment usually has a much higher water content. Spatially, as shown in Figure 3, the higher water content values are associated with the deeper, more distal core sites (with respect to presumed primary point source: the mouth of the Yellow River (Huanghe)). This implies that the sediment texture becomes finer in the offshore direction. The sediment grain-size distribution map of Milliman and others (1985) and the water content isopleth map of this study (Figure 3) are, in fact, similar in the patterns they show. The higher water contents are associated with the finer grain sizes.

There is a tendency for water content to decrease down core, which is the expected trend in any accumulating sediment column below the level of mobil (current-worked) sediment and (or) zone of bioturbation. This gradual dewatering is a response to the ever-increasing degree of compaction upon burial. The index properties that are related to water content in a fully water-saturated sediment (i.e., no gas), specifically bulk density and porosity, display similar variability and trends (see Appendix A), and at average values of 1.64 and 62%, respectively, also suggest that silt is an important size class.

The same basic implications with regard to sediment grain size are present in the Atterberg limits data. Both liquid and plastic limit vary over a wide range (Table 2) and thus suggest a wide range in texture and, possibly, mineralogy. As shown on the composite plasticity chart (Figure 4), however, all the sediments can be basically classified as clays of medium to high compressibility (engineering classification: CL, CH) where, in the engineering sense, "clays" refers to any fine-grained sediment whose behavior is affected by clay minerals. The exact percentages of silt and clay in the textural sense is not known. As with the water contents and related data, plasticity is highest in the samples from the sites in deeper water and probably reflects the sediment grain size distribution.

Liquid limit, which is a fairly sensitive index of changes in texture and composition, is generally invariant down core. Figure 5 shows this consistency as well as the aforementioned spatial trend. Thus, assuming a consistent composition, texture is probably relatively consistent down core, indicating that the same or similar local depositional environments have been sustained during recent geologic time. However, as shown in

Figure 6, there are exceptions. The bottom of core KC-4 is apparently much coarser than the top. Accordingly, the fine-grained sediment may be only a veneer over parts of the region.

Liquidity indices are characteristically greater than one, which is typical of surface sediments, but also indicates a lack of recent, significant erosion.

Changes in grain specific gravity indicate changes in composition. The relatively narrow range shown in these data (2.65–2.73), however, is characteristic of mineral assemblages dominated by marine terrigenous clastics and does not portend significant compositional changes. We believe that the G_s data are consistent with the notion that the sediment in the study area is basically fine-grained and is fairly uniform in composition (mineralogy, organic content, and other components).

Consolidation states and properties

The results of the consolidation tests, along with the strength and index property tests, indicate that the seafloor off the Shandong Peninsula is fundamentally a depositional surface and is compacting normally. This is shown by the values of maximum past vertical stress, σ'_{vm} (Table 3, Appendix C), which are very low but generally increase gradually down the cores. This indicates a normal increase in overburden stress with subbottom depth. OCR ($\sigma'_{vm}/\sigma'_{vo}$) values are high (10-85) at the surface, which is in agreement with values typically reported for marine sediment. However, they decrease rapidly within the upper 50 centimeters and approach a value of 1 below that level (Figure 7). This implies that the seafloor is not an erosional surface.

Compression indices, C_c 's, range from 0.23 to 1.26 and average 0.74. This indicates that these Yellow Sea sediments are of medium to high compressibility; most fine-grained sediments have C_c values less than 1 and the majority are less than 0.5 (Mitchell, 1976). Values of the coefficient of consolidation, c_v , are generally in the 10^{-3} - 10^{-4} cm²/sec range. These values are, again, consistent with the fine-grained nature of the sediment, as are the permeabilities. The coefficient of permeability, k , has a mean value of about 10^{-7} – 10^{-8} cm/sec. The permeability of these sediments is thus classified as “very low” to “practically impermeable” (Lambe and Whitman, 1969). The same areal trends manifested by the index property data are shown by C_c , c_v , and k : values typical of finer sediment are associated with the deepest part of the study area. Consolidation test results are tabulated and plots of the data are presented in Appendix C.

Table 3
Summary of consolidation test results

core	depth in core (m)	σ'_{vo} (kPa)	σ'_{vm} (kPa)	σ'_{e} (kPa)	OCR	C_c	c_v (cm ² /s)	k (cm/s)
KC-1A	0.08	0.42	4.0	3.6	9.5	0.53	6×10^{-4}	3×10^{-8}
	0.25	1.50	5.4	3.9	3.6	0.44	9×10^{-4}	4×10^{-8}
	0.55	3.42	10.9	7.5	3.2	0.43	8×10^{-4}	4×10^{-8}
BC-4	0.04	0.10	2.3	2.2	23	0.92	6×10^{-4}	3×10^{-8}
	0.21	0.67	4.3	3.6	6.4	1.26	4×10^{-4}	5×10^{-8}
	0.42	1.41	9.3	7.9	6.6	0.94	4×10^{-4}	2×10^{-8}
BC-5	0.02	0.07	3.0	2.9	43	1.07	2×10^{-4}	1×10^{-8}
	0.20	0.74	5.7	5.0	7.7	1.00	3×10^{-4}	2×10^{-8}
	0.49	1.82	8.7	6.9	4.8	0.91	3×10^{-4}	1×10^{-8}
BC-6	0.02	0.06	2.6	2.5	43	1.06	3×10^{-4}	5×10^{-8}
	0.18	0.60	5.7	5.1	9.5	1.19	3×10^{-4}	3×10^{-8}
	0.45	1.53	5.2	3.7	3.4	0.96	3×10^{-4}	3×10^{-8}
BC-7	0.04	0.23	4.2	4.0	18	0.34	9×10^{-3}	4×10^{-7}
	0.20	1.27	8.0	6.7	6.3	0.29	3×10^{-3}	8×10^{-8}
	0.46	3.05	22	19	7.2	0.26	2×10^{-3}	6×10^{-8}
BC-8	0.02	0.11	8.1	8.0	74	0.44	2×10^{-3}	8×10^{-8}
	0.18	1.18	15	14	13	0.30	2×10^{-3}	5×10^{-8}
	0.51	3.45	20	17	5.8	0.23	8×10^{-3}	2×10^{-7}
BC-9	0.02	0.07	4.7	4.6	67	1.04	2×10^{-4}	3×10^{-8}
	0.20	0.74	5.6	4.9	7.6	1.12	3×10^{-4}	4×10^{-8}
	0.49	1.82	4.6	2.8	2.5	0.84	3×10^{-4}	4×10^{-8}
BC-10	0.02	0.11	9.3	9.2	85	0.28	2×10^{-2}	6×10^{-7}
	0.18	1.15	12	11	10	0.37	5×10^{-3}	1×10^{-7}
	0.53	3.52	17	14	4.8	0.31	5×10^{-3}	1×10^{-7}
BC-11	0.02	0.07	2.7	2.6	38	0.54	7×10^{-4}	2×10^{-7}
	0.19	1.02	5.4	4.4	5.3	0.55	7×10^{-4}	4×10^{-8}
	0.51	2.88	10.4	7.5	3.6	0.41	1×10^{-3}	4×10^{-8}

symbols:

σ'_{vo} : in situ effective overburden stress

σ'_{e} : excess vertical effective stress ($\sigma'_{vm} - \sigma'_{vo}$)

C_c : compression index

k : coefficient of permeability

σ'_{vm} : maximum past effective vertical stress

OCR : overconsolidation ratio ($\sigma'_{vm} / \sigma'_{vo}$)

c_v : coefficient of consolidation

Strength parameters

The mode of failure and the percentage strain at failure in the CIU triaxial tests are presented in Table 4 and Appendix D. Plastic deformation occurs, rather than failure along discrete planes, and considerable strain is accumulated before peak strength is reached. The amount of strain shown in Table 4 is relatively high, but not unusual, for fine-grained sediments. Also, these strain percentages imply that cements, which lead to brittle failure, are not present in these sediments.

Table 4
Summary of CIU triaxial test results

Core	Failure type	% strain at failure (avg)	S_u/σ'_c	ϕ' (°)	c' (kPa)
BC-5	plastic	16	0.41	35	3
BC-6	plastic	10	0.34	32	2
BC-7	plastic	16	0.36	36	4
BC-8	plastic	18	0.43	38	0
BC-11	plastic	13	0.38	35	4

symbols: S_u : undrained shear strength σ'_c : consolidation stress on triaxial sample prior to shear
 ϕ' : effective friction angle c' : cohesion intercept in terms of effective stress

The strength-overburden ratio, S_u/σ'_c , which averages about 0.40, is slightly higher than the values of 0.2 to 0.3 that are typically reported for terrestrial soils. We are uncertain, with so few samples, if the difference is significant.

Cohesion, c' , and internal friction angle, ϕ' , are the basic strength parameters with respect to effective stress. The values shown in Table 4 for c' are typical for marine muds; the ϕ' values are, in contrast, generally higher than the norm. For most fine-grained marine sediments composed of common clay minerals, CIU-derived values of ϕ' are less than 34° and frequently less than 30° (e.g., see Booth and others, 1985). The reason for the apparently anomalous values cannot be determined without textural and mineralogical analyses. Triaxial test results are tabulated and plots of the data are presented in Appendix D.

SUMMARY

Geological

The surface sediments near and south of the Shandong Peninsula are composed primarily of silts and clays; silts are apparently an important textural component throughout the study area and may be the dominant size class at many sites. The sediments be-

come finer toward the deeper part of the study area. No vertical trends are present in the sediment texture, as inferred from the index property data; however, the silt-clay sediment may only be a veneer over at least part of the region. The surface is depositional: the extremely low shear strengths and high liquidity indices coupled with a lack of evidence for erosion indicate that there is net sediment accumulation throughout most of the study area.

Geotechnical

The Yellow Sea sediments are very soft and composed of silts and clays of medium to high plasticity (classification: CL and CH). The sediments are of medium to high compressibility and have a permeability that ranges from "very low" to "practically impermeable". They exhibit overconsolidated behavior, although they trend toward a state of normal consolidation down core. The S_u/σ'_v values are slightly higher than those for normally consolidated terrestrial soil. The values of ϕ' , compared to data reported for many other marine sediments, are also slightly higher than the norm.

REFERENCES

- American Society for Testing and Materials, 1985, 1985 Annual book of ASTM standards, v. 4.08: Soil and rock; building stones: Philadelphia, ASTM, 1078 p.
- Booth, J. S., Sangrey, D. A., and Fugate, J. K., 1985, A nomogram for interpreting slope stability of fine-grained deposits in modern and ancient marine environments: Journal of Sedimentary Petrology, v. 55, p. 29–36.
- British Standards Institution, 1975, Standard test for liquid limit— cone penetrometer method: London.
- Keuhl, S. A., Nittrouer, C. A., DeMaster, D. J., and Curtin, T. B., 1985, A long, square-barrel gravity corer for sedimentological and geochemical investigation of fine-grained sediments: Marine Geology, v. 62, p. 365–370.
- Milliman, J. D., Qin, Y. S., and Butenko, J., 1985, Geohazards in the Yellow Sea and East China Sea: Proceedings Offshore Technology Conference, 17th, p. 73–81.
- Mitchell, J. K., 1976, Fundamentals of soil behavior: New York, John Wiley, 422 p.
- Lambe, T. W., and Whitman, R. V., 1969, Soil mechanics: New York, John Wiley, 553 p.
- Terzaghi, K., and Peck, R. B., 1967, Soil mechanics in engineering practice: New York, John Wiley, 729 p.
- Winters, W. J., 1988, Geotechnical testing of marine sediment: U. S. Geological Survey Open-File Report 88-36, 52 p.

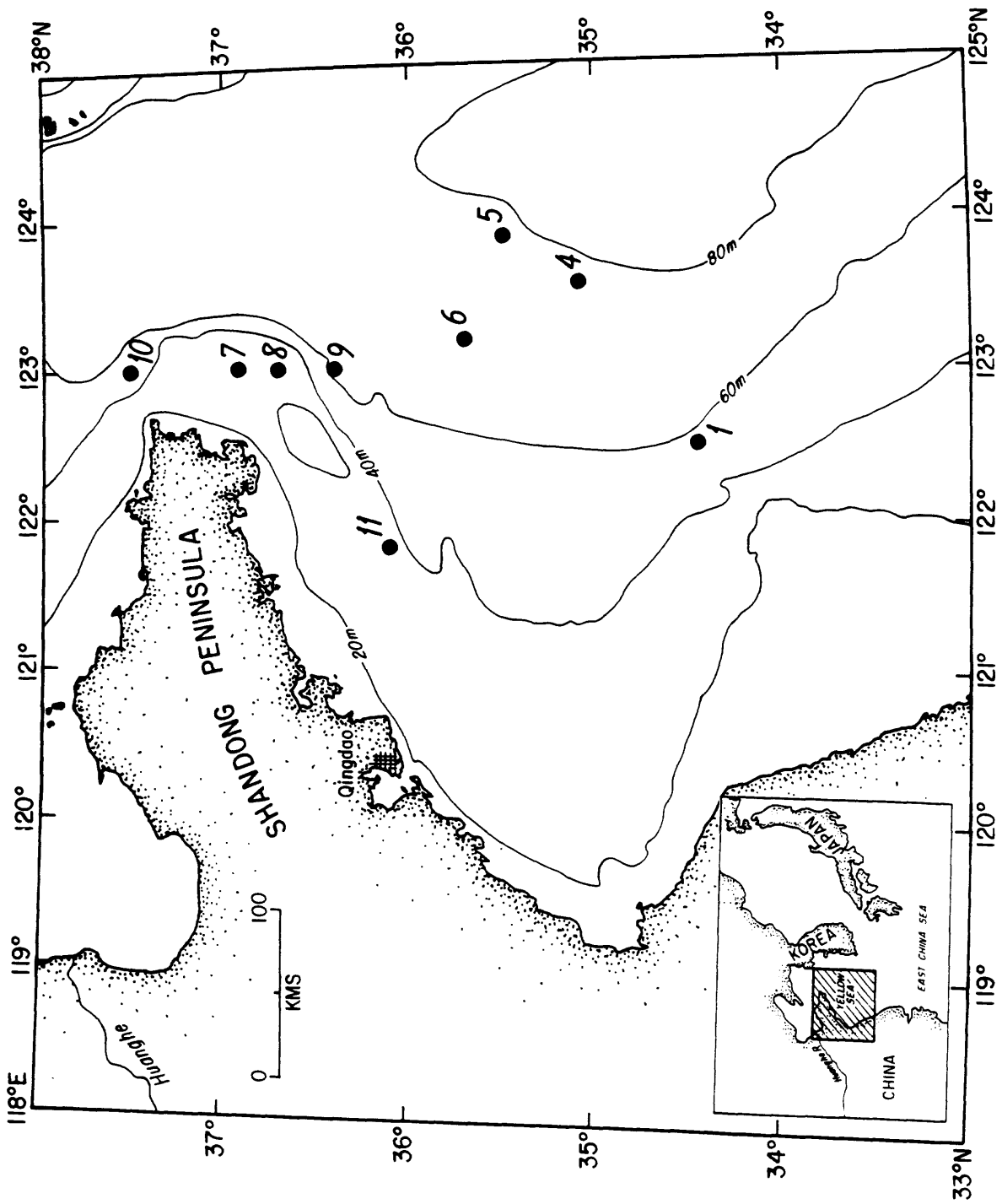


Figure 1: Yellow Sea station locations and bathymetry. Sea floor becomes shallower to the east as it rises to meet the Korean peninsula (see inset).

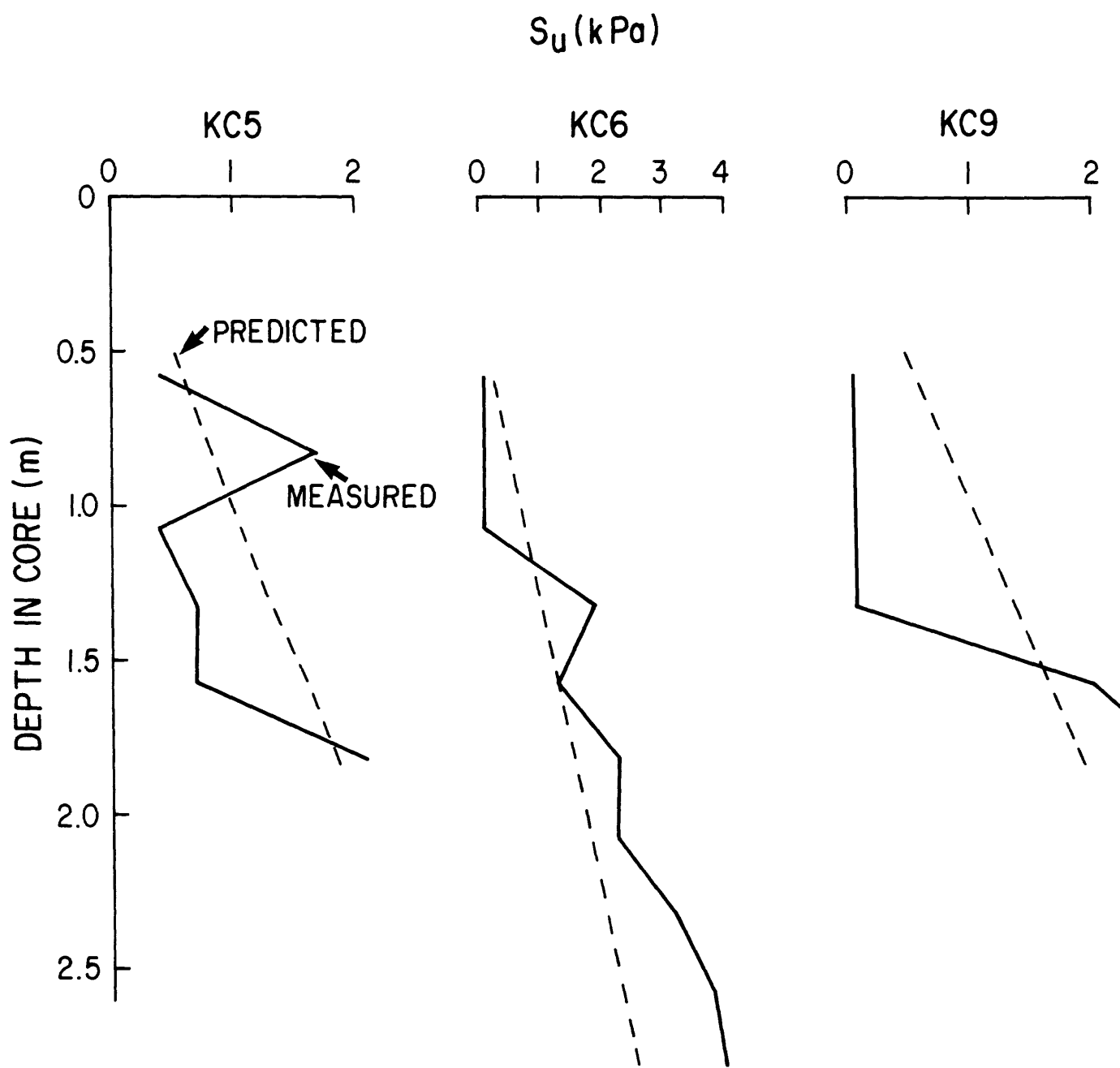


Figure 2: Selected vane shear strength profiles. Dashed lines are strength profiles predicted for each core by assuming that the sediment is normally consolidated (i.e., $S_u/\sigma'_v = 0.24$)

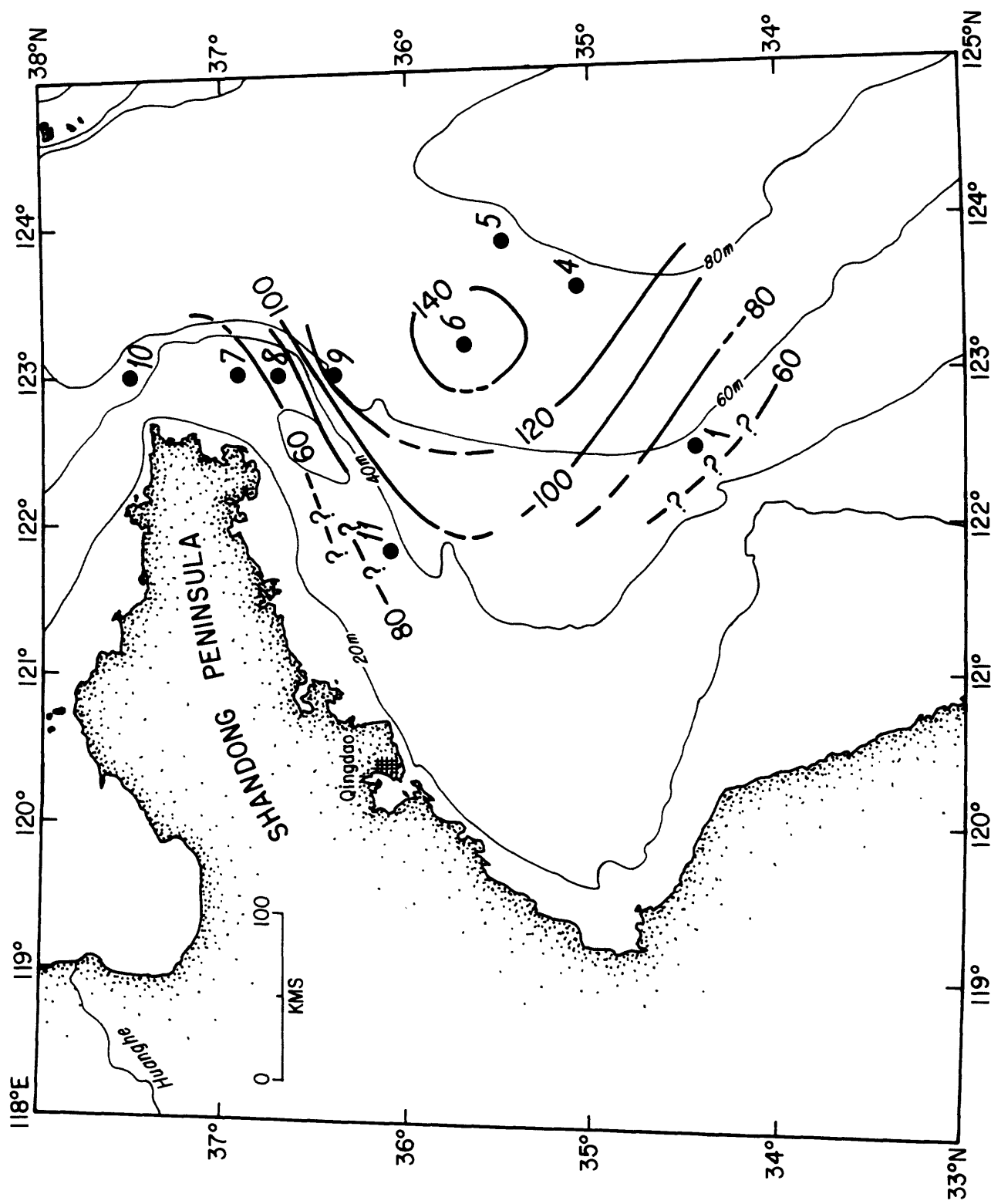


Figure 3: Water content of surface sediment (upper ≈ 5 cm). Values calculated on the basis of percent dry weight.

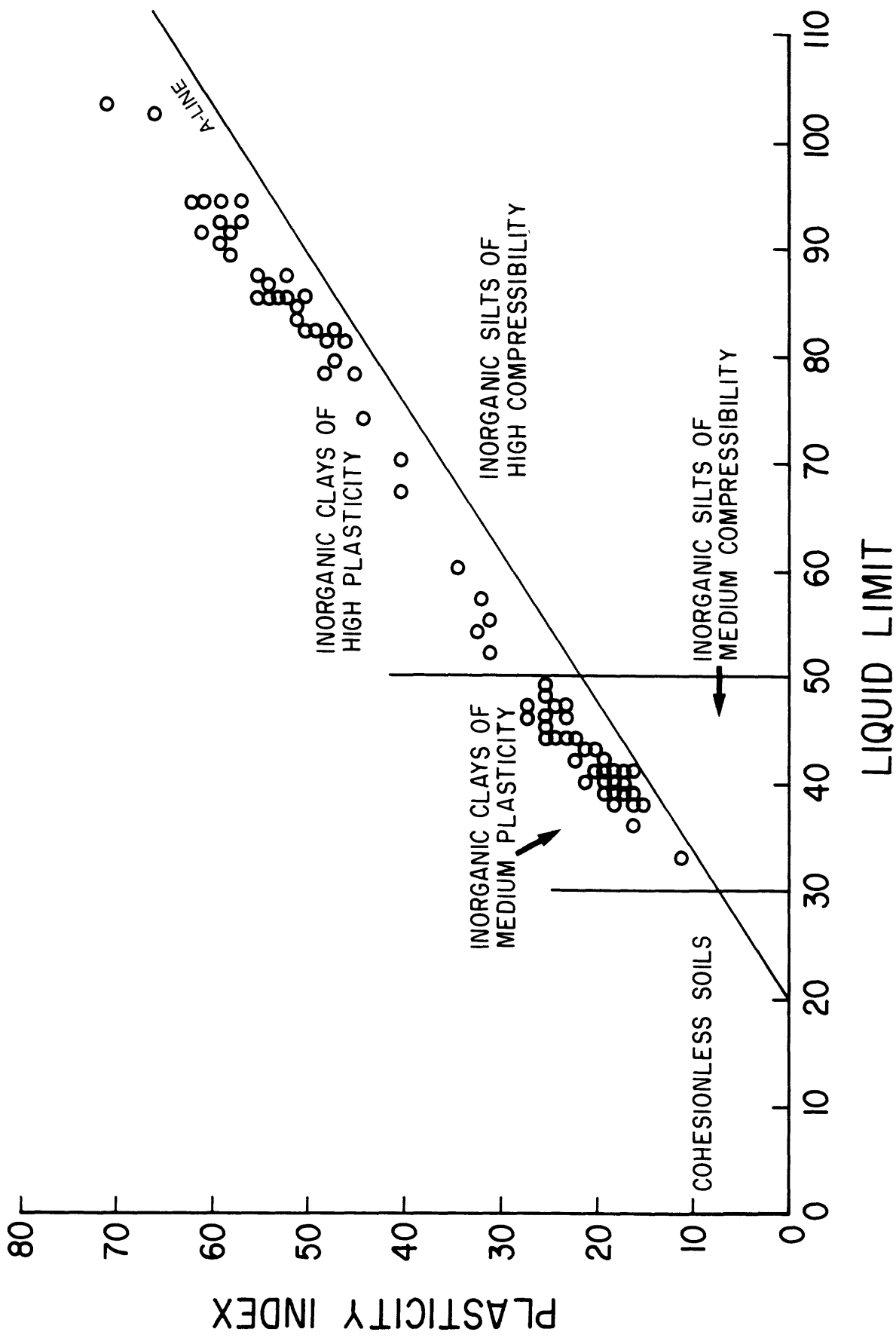


Figure 4: Plasticity chart plot of all samples. Note spread of data points.

LIQUID LIMIT (W_L)

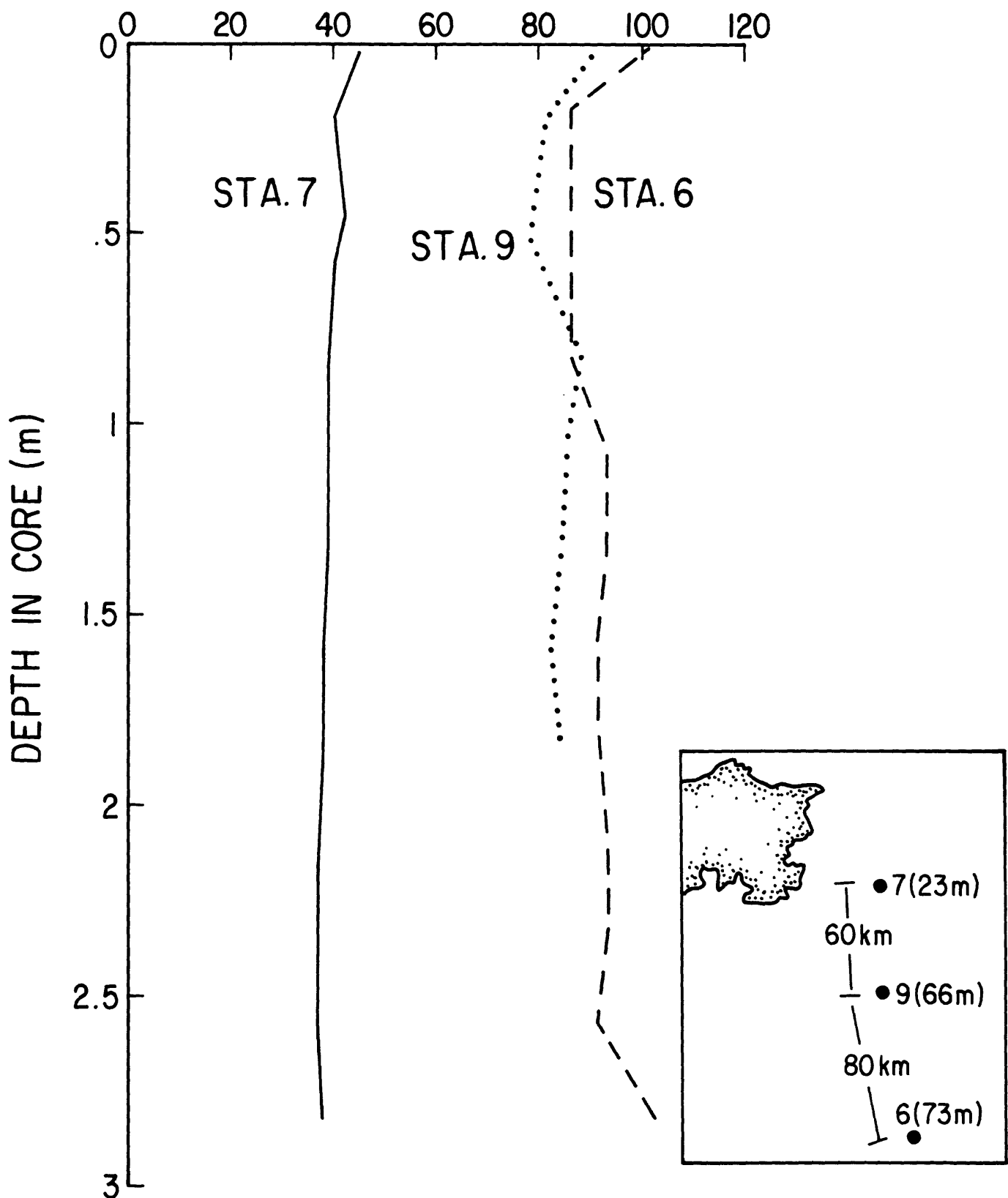


Figure 5: Liquid limit profiles of sites 6, 7, and 9. Inset shows core locations and water depths. The down-core uniformity is evident in the profiles. The offshore trend toward increasing liquid limit values is evident in the inset.

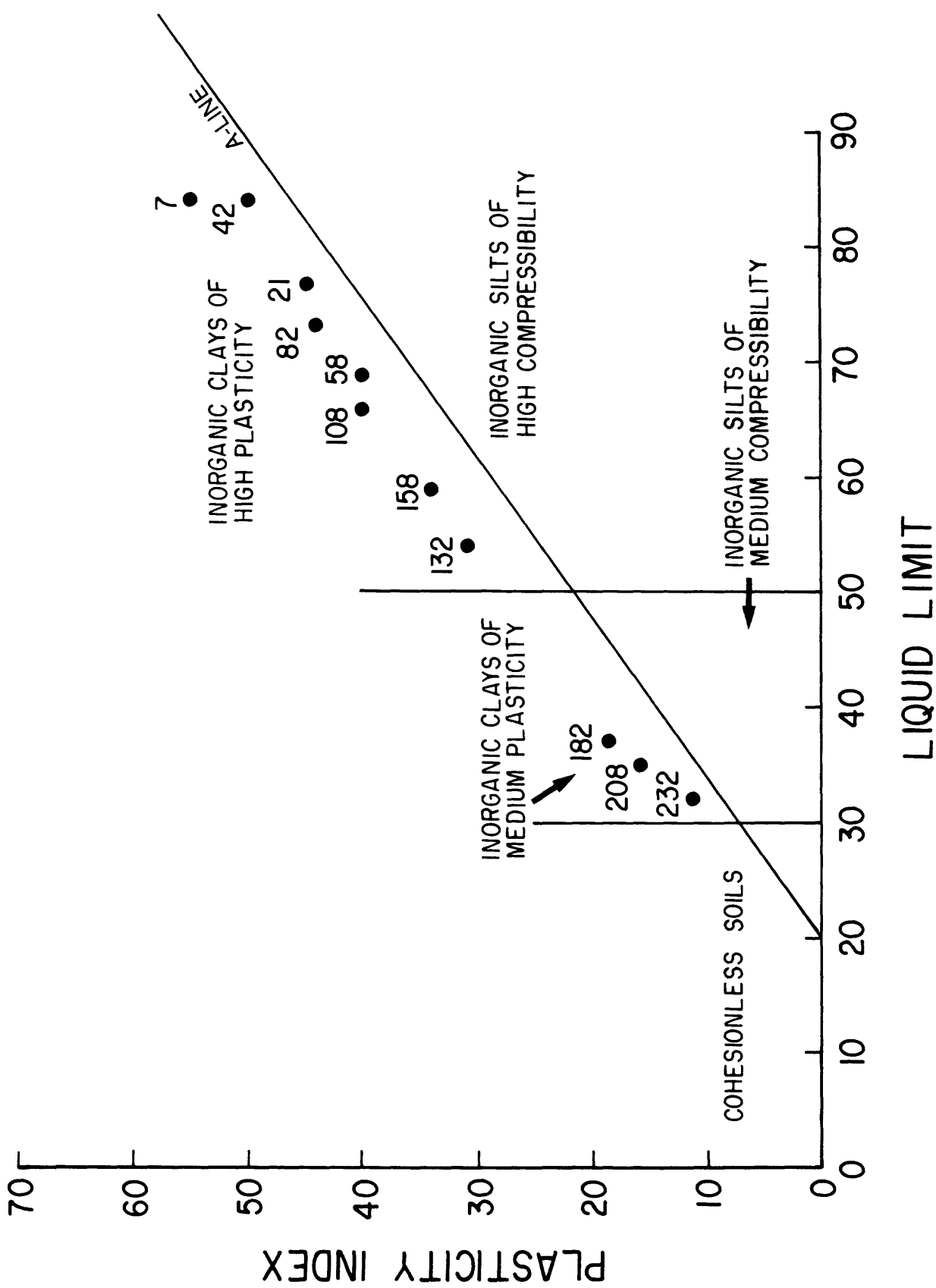


Figure 6: Change in plasticity with depth in core KC-4. Numerals refer to depth (in centimeters) down-core. Top of core (7 cm) has high plasticity; bottom of core (232 cm) is nearly nonplastic.

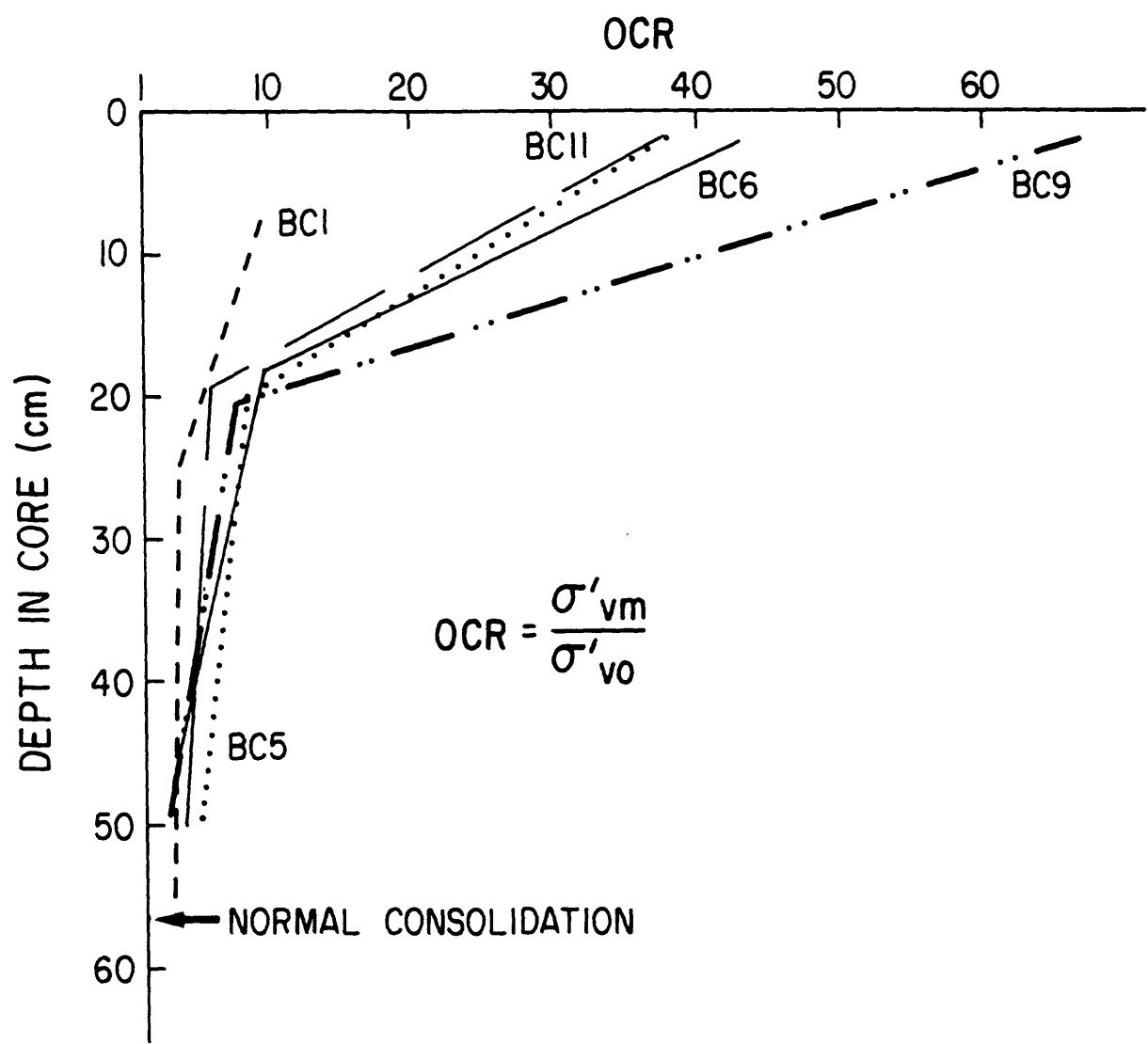


Figure 7: Consolidation state of sediments vs. depth in core. An OCR value of 1 implies that sediment is normally consolidated, values greater than 1 imply a state of overconsolidation.

Appendix A

Nomenclature and Symbols

Nomenclature and Symbols

A_f	coefficient of pore pressure response at failure during a triaxial compression test (change in pore pressure at failure/change in deviator stress)
ASTM	American Society for Testing and Materials
BC	box core
c'	cohesion intercept expressed in terms of effective stress
C_c	compression index (change in e /change in log of vertical effective stress from consolidation test)
C_{cf}	corrected field compression index (Schmertmann method)
C_r	rebound-recompression index
c_v	coefficient of consolidation
$c_v(\sigma'_{vo})$	coefficient of consolidation at the in situ effective overburden stress
$c_v(\sigma'_{vm})$	coefficient of consolidation at the maximum past vertical effective stress
$c_v(\text{avg})$	average coefficient of consolidation for virgin compression
DELTA u	change in pore water pressure (also equals delta PORE)
e	void ratio (volume voids/volume solids)
G_s	grain specific gravity
I_D	disturbance index (Silva method)
I_L	liquidity index
I_P	plasticity index
k	coefficient of permeability
$k(\sigma'_{vo})$	coefficient of permeability at the in situ effective overburden stress
$k(\sigma'_{vm})$	coefficient of permeability at the maximum past vertical effective stress
$k(\text{avg})$	average coefficient of permeability for virgin compression
KC	Kasten core
n	porosity (volume voids/total volume)
OCR	overconsolidation ratio ($\sigma'_{vm}/\sigma'_{vo}$)
p'	normal effective stress acting on a plane inclined at 45° in a triaxial test $(\sigma'_1 + \sigma'_3)/2$
q	shear stress acting on a plane inclined at 45° in a triaxial test $(\sigma_1 - \sigma_3)/2$
S_{rv}	undrained vane shear strength determined on remolded sediment

Nomenclature and symbols (cont.)

S_t	sensitivity (s_{uv}/s_{rv})
S_u	undrained shear strength
S_{ur}	remolded shear strength (vane measurement)
S_{uv}	undrained shear strength (vane measurement)
w	natural water content (weight water/weight solids)
w_L	liquid limit
w_P	plastic limit
w_s	water content of a triaxial sample during undrained shear
ρ_t	bulk density
σ'_c	consolidation stress exerted on a triaxial test sample prior to shear
σ'_e	excess vertical effective stress ($\sigma'_{vm} - \sigma'_{vo}$)
σ'_{vo}	in situ effective overburden stress
σ'_{vm}	maximum past vertical effective stress
σ'_1	vertical effective principal stress
σ'_3	horizontal effective principal stress
ϕ'	friction angle in terms of effective stress
$\phi'(c=0)$	friction angle in terms of effective stress determined from an individual triaxial test assuming no cohesion intercept
$\phi'(c\neq 0)$	friction angle in terms of effective stress determined from a number of triaxial tests performed on similar sediment

Appendix B

Results of Vane Shear and Index Property Tests

**tabular data
profiles**

TABULAR DATA

YS-85-08 Index Properties

Core ID	Depth in core (m)	S_{uv} (kPa)	S_{rv} (kPa)	S_t	w (%)	W_L (%)	W_p (%)	I_p (%)	I_L	G_s	ρ_t (g/cm ³)	e	n	Comments
KC-1a	0.0 -0.11	-	-	-	61	48	23	25	1.51	2.68	1.64	1.63	0.62	CRSC
	0.23-0.27	-	-	-	57	44	19	25	1.52	2.67	1.66	1.52	0.60	CRSC
	0.53-0.58	-	-	-	47	43	19	24	1.17	2.70	1.75	1.27	0.56	CRSC
	0.75-0.80	-	-	-	44	43	19	24	1.04	2.68	1.77	1.18	0.54	
	1.00-1.05	-	-	-	43	43	20	23	1.00	2.65	1.77	1.14	0.53	
	0.55-0.60	2.6	-	-	55	45	18	27	1.37	2.69	1.68	1.48	0.60	
KC-1b	0.80-0.85	6.2	3.9	1.6	54	46	19	27	1.29	2.67	1.68	1.44	0.59	
	1.05-1.10	6.3	2.8	2.3	55	41	19	22	1.64	2.65	1.67	1.46	0.59	
	1.30-1.35	1.9	-	-	52	43	18	25	1.36	2.67	1.70	1.39	0.58	
	1.55-1.60	5.1	1.4	3.6	41	38	19	19	1.16	2.67	1.80	1.09	0.52	
	1.80-1.85	4.9	1.9	2.6	42	39	18	21	1.12	2.68	1.79	1.13	0.53	
	0.0-0.07	-	-	-	129	84	29	55	1.81	2.65	1.37	3.42	0.77	CRSC
BC-4	0.19-0.23	-	-	-	113	77	32	45	1.80	2.70	1.42	3.05	0.75	CRSC
	0.39-0.44	-	-	-	103	84	34	50	1.38	2.69	1.45	2.77	0.73	CRSC
	22													
KC-4	0.55-0.60	1.2	0.4	3.0	102	69	29	40	1.83	2.70	1.45	2.75	0.73	
	0.80-0.85	0.6	-	-	103	73	29	44	1.68	2.68	1.45	2.76	0.73	
	1.05-1.10	2.3	-	-	81	66	26	40	1.38	2.71	1.54	2.20	0.69	
	1.30-1.35	3.3	0.6	5.5	78	54	23	31	1.77	2.69	1.55	2.10	0.68	
	1.55-1.60	3.7	-	-	81	59	25	34	1.65	2.68	1.53	2.17	0.68	
	1.80-1.85	3.7	-	-	35	37	19	18	0.89	2.68	1.87	0.94	0.48	
	2.05-2.10	6.6	3.3	2.0	37	35	19	16	1.13	2.67	1.84	0.99	0.50	
	2.30-2.35	4.3	-	-	30	32	21	11	0.82	2.68	1.93	0.80	0.45	

Symbols are explained in Appendix A.

YS-85-08 Index Properties (continued)

Core ID	Depth in core (m)	S_{uv} (kPa)	S_{rv} (kPa)	S_t (%)	w (%)	w_L (%)	w_p (%)	I_p	I_L	G_s	ρ_t	e	n	Comments
BC-5	0.00-0.05	-	-	-	124	84	32	52	1.77	2.71	1.39	3.36	0.77	CRSC
	0.18-0.22	-	-	-	98	82	31	51	1.31	2.71	1.47	2.66	0.73	CRSC
	0.47-0.54	-	-	-	104	81	31	50	1.46	2.70	1.45	2.81	0.74	CRSC
KC-5	0.55-0.60	0.4	-	-	104	80	34	46	1.52	2.67	1.44	2.78	0.74	
	0.80-0.85	1.7	-	-	99	90	29	61	1.15	2.68	1.46	2.65	0.73	
	1.05-1.10	0.4	-	-	95	81	34	47	1.30	2.70	1.48	2.57	0.72	
	1.30-1.35	0.2	3.5	98	80	32	48	1.38	2.67	1.46	2.62	0.72		
	1.55-1.60	0.7	-	92	84	30	54	1.15	2.69	1.49	2.47	0.71		
	1.80-1.85	2.1	-	-	98	89	30	59	1.15	2.66	1.46	2.61	0.72	
BC-6	0.0-0.04	-	-	-	144	101	35	66	1.66	2.68	1.35	3.86	0.79	CRSC
	0.16-0.20	-	-	-	114	86	31	55	1.51	2.70	1.42	3.08	0.75	CRSC
	0.43-0.51	-	-	-	111	83	32	51	1.55	2.70	1.43	3.00	0.75	CRSC
KC-6	0.55-0.60	-	-	-	111	86	31	55	1.45	2.65	1.42	2.94	0.75	
	0.80-0.85	-	-	-	106	86	34	52	1.38	2.70	1.44	2.86	0.74	
	1.05-1.10	-	-	-	114	93	36	57	1.37	2.71	1.42	3.09	0.76	
	1.30-1.35	1.9	0.7	2.7	110	93	31	62	1.28	2.73	1.43	3.00	0.75	
	1.55-1.60	1.3	-	-	102	91	32	59	1.19	2.66	1.45	2.71	0.73	
	1.80-1.85	2.3	-	-	105	91	34	57	1.25	2.72	1.45	2.86	0.74	
	2.05-2.10	2.2	-	-	99	93	34	59	1.10	2.72	1.47	2.69	0.73	
	2.30-2.35	3.2	-	-	102	93	32	61	1.15	2.70	1.45	2.75	0.73	
	2.55-2.60	3.8	1.0	3.8	96	91	34	57	1.09	2.66	1.47	2.55	0.72	
	2.80-2.85	4.0	1.2	3.3	99	102	31	71	0.95	2.69	1.46	2.66	0.73	

YS-85-08 Index Properties (continued)

Core ID	Depth in core (m)	S_{uv} (kPa)	S_{rv} (kPa)	S_t (%)	w (%)	W_L (%)	W_p (%)	I_p (%)	I_L (%)	C_s	ρ_t (g/cm ³)	e	n	Comments
BC-7	0.0-0.06	-	-	-	57	45	22	23	1.52	2.70	1.67	1.54	0.61	CRSC
	0.18-0.22	-	-	-	46	40	20	20	1.30	2.69	1.76	1.24	0.55	CRSC
	0.44-0.48	-	-	-	40	42	21	21	0.90	2.71	1.82	1.08	0.52	CRSC
KC-7a	0.55-0.60	-	-	-	43	40	21	19	1.16	2.66	1.77	1.14	0.53	
	0.80-0.85	-	-	-	41	40	21	19	1.05	2.69	1.80	1.10	0.52	
	1.05-1.10	0.6	-	-	43	38	21	17	1.29	2.65	1.77	1.14	0.53	
	1.30-1.35	1.6	-	-	41	40	22	18	1.05	2.68	1.80	1.10	0.52	
	1.55-1.60	3.6	-	-	41	38	22	16	1.19	2.68	1.80	1.10	0.52	
	0.55-0.60	3.9	-	-	44	40	21	19	1.21	2.69	1.77	1.18	0.54	
KC-7b	0.80-0.85	4.1	-	-	42	39	20	19	1.16	2.72	1.80	1.14	0.53	
	1.05-1.10	4.0	0.9	4.4	40	39	22	17	1.06	2.70	1.82	1.08	0.52	
	1.30-1.35	2.7	-	-	40	39	21	18	0.93	2.68	1.81	1.07	0.52	
	1.55-1.60	4.3	-	-	36	38	21	17	0.88	2.66	1.85	0.96	0.49	
	1.80-1.85	2.5	-	-	35	38	21	17	0.82	2.69	1.87	0.94	0.48	
	2.05-2.10	4.4	-	-	34	37	22	15	0.80	2.70	1.89	0.92	0.48	
	2.30-2.35	2.1	-	-	32	37	21	16	0.69	2.69	1.91	0.86	0.46	
	2.55-2.60	5.9	-	-	32	37	22	15	0.67	2.68	1.90	0.86	0.46	
	2.80-2.85	5.1	-	-	36	38	22	16	0.88	2.69	1.86	0.97	0.49	

YS-85-08 Index Properties (continued)

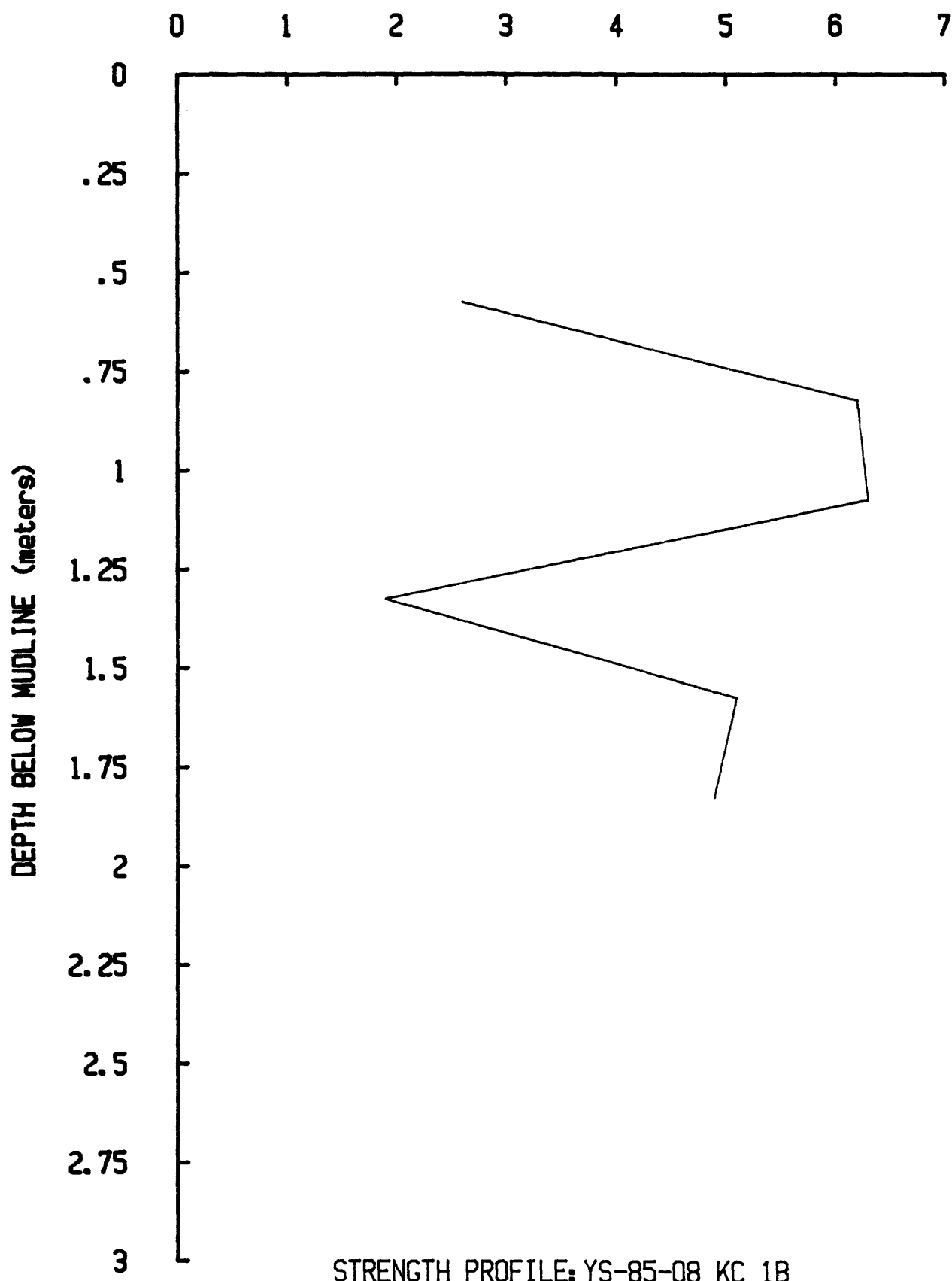
Core ID	Depth in core (m)	S_{uv} (kPa)	S_{rv} (kPa)	S_t	w (%)	W_L (%)	W_p (%)	I_p (%)	I_L (%)	G_s	ρ_t	e	n	Comments
BC-8	0.0-0.04	-	-	-	62	46	23	23	1.68	2.68	1.63	1.66	0.62	CRSC
	0.16-0.20	-	-	-	46	47	22	25	0.96	2.68	1.75	1.23	0.55	CRSC
	0.49-0.54	-	-	-	42	40	23	17	1.12	2.69	1.79	1.13	0.53	CRSC
KC-8	0.55-0.60	-	-	-	45	40	22	18	1.28	2.70	1.77	1.22	0.55	
	0.80-0.85	2.2	-	-	42	39	22	17	1.18	2.69	1.79	1.13	0.53	
	1.05-1.10	2.5	-	-	46	40	22	18	1.33	2.69	1.76	1.24	0.55	
	1.30-1.35	1.4	-	-	47	41	19	22	1.24	2.68	1.74	1.26	0.56	
	1.55-1.60	2.1	-	-	47	42	22	20	1.25	2.69	1.75	1.26	0.56	
	1.80-1.85	0.9	-	-	46	40	22	18	1.33	2.68	1.75	1.23	0.55	
	2.05-2.10	3.3	-	-	45	42	22	20	1.15	2.70	1.77	1.22	0.55	
	2.30-2.35	5.0	0.8	6.3	45	42	22	20	1.15	2.70	1.77	1.22	0.55	
	2.55-2.60	4.0	-	-	43	39	22	17	1.24	2.69	1.78	1.16	0.54	
	2.80-2.85	3.6	-	-	45	43	21	22	1.09	2.66	1.76	1.20	0.54	
BC-9	0.0-0.06	-	-	-	123	90	32	58	1.56	2.65	1.39	3.26	0.77	CRSC
	0.18-0.22	-	-	-	107	81	32	49	1.53	2.68	1.43	2.87	0.74	CRSC
	0.47-0.56	-	-	-	106	78	31	47	1.60	2.67	1.44	2.83	0.74	CRSC
KC-9	0.55-0.60	-	-	-	86	77	29	48	1.19	2.66	1.50	2.29	0.70	
	0.80-0.85	-	-	-	95	88	30	58	1.12	2.70	1.48	2.57	0.72	
	1.05-1.10	-	-	-	108	85	31	54	1.43	2.65	1.43	2.86	0.74	
	1.30-1.35	-	-	-	83	84	30	54	0.98	2.70	1.52	2.24	0.69	
	1.55-1.60	2.0	-	-	98	82	31	51	1.31	2.68	1.46	2.63	0.72	
	1.80-1.85	2.7	-	-	94	84	31	53	1.19	2.66	1.47	2.50	0.71	

YS-85-08 Index Properties (continued)

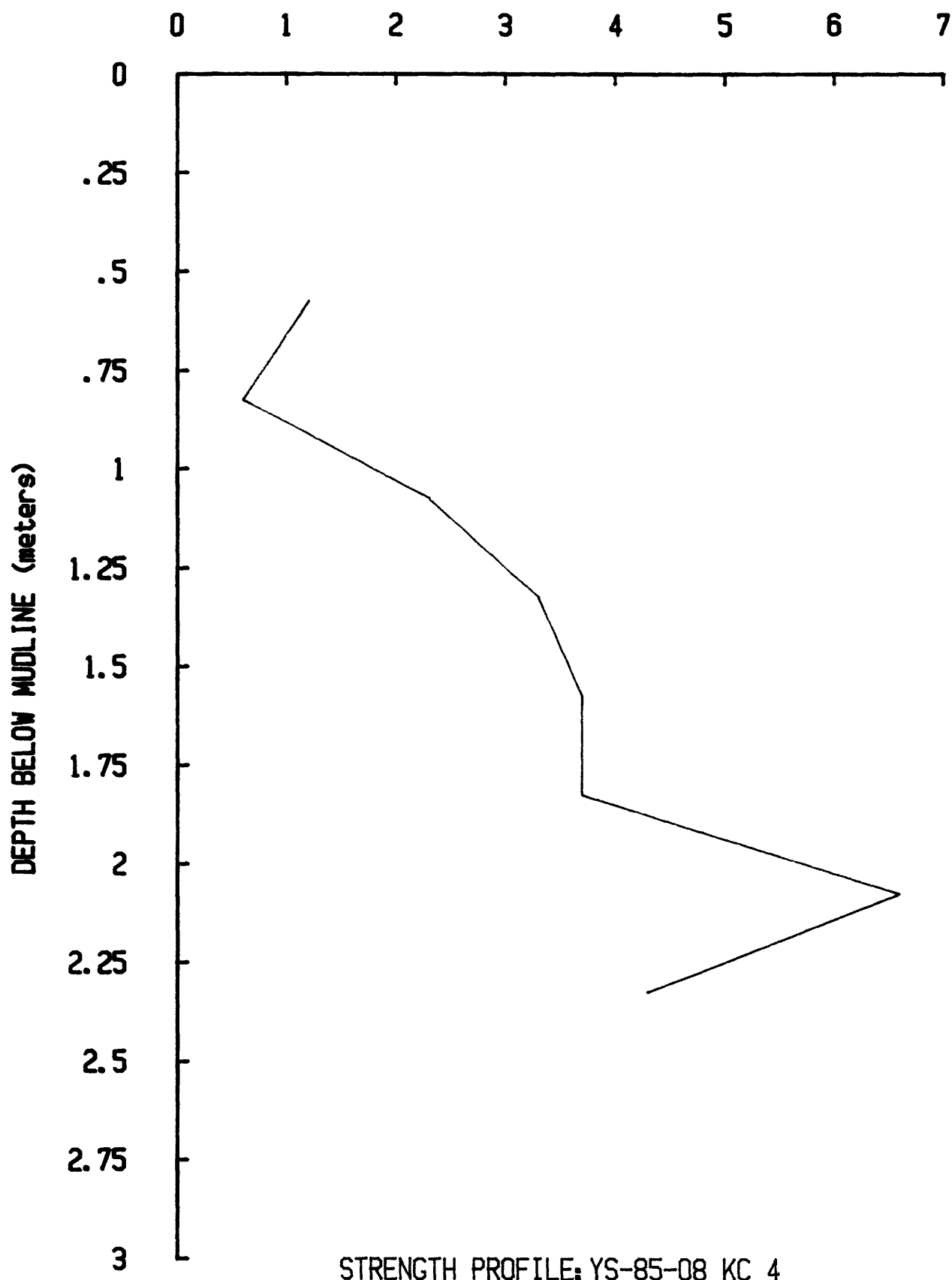
Core ID	Depth in core (m)	S _{uv} (kPa)	S _{rv} (kPa)	S _t (%)	w (%)	W _L (%)	W _P (%)	I _P (%)	I _L (%)	G _s	ρ _t (g/cm ³)	e	n	Comments
BC-10	0.0-0.04	-	-	-	53	40	24	16	1.73	2.69	1.70	1.43	0.59	CRSC
	0.16-0.20	-	-	-	54	41	22	19	1.68	2.68	1.69	1.45	0.59	CRSC
	0.50-0.56	-	-	-	45	42	21	21	1.14	2.70	1.77	1.22	0.55	CRSC
KC-10	0.55-0.60	-	-	-	45	46	22	24	0.96	2.67	1.76	1.20	0.55	
	0.80-0.85	-	-	-	41	43	21	22	0.91	2.67	1.80	1.09	0.52	
	1.05-1.10	-	-	-	57	53	21	32	1.12	2.71	1.67	1.54	0.61	
	1.30-1.35	-	-	-	43	40	21	19	1.16	2.66	1.77	1.14	0.53	
	1.55-1.60	1.9	-	-	38	40	22	18	0.89	2.69	1.84	1.02	0.51	
	1.80-1.85	3.8	-	-	36	39	22	17	0.82	2.66	1.85	0.96	0.49	
	2.05-2.10	3.2	0.6	5.3	42	39	22	17	1.18	2.70	1.80	1.13	0.53	
BC-11	0.0-0.04	-	-	-	89	56	24	32	2.03	2.68	1.50	2.39	0.70	CRSC
	0.17-0.21	-	-	-	57	45	20	25	1.48	2.68	1.66	1.53	0.60	CRSC
	0.48-0.54	-	-	-	46	47	22	25	0.96	2.68	1.69	1.45	0.59	CRSC
KC-11	0.55-0.60	1.7	-	-	62	51	20	31	1.34	2.68	1.63	1.66	0.62	
	0.80-0.85	0.5	-	-	51	43	19	24	1.33	2.68	1.71	1.37	0.58	
	1.05-1.10	5.2	-	-	46	45	18	27	1.05	2.65	1.74	1.22	0.55	

PROFILES
Vane shear strength

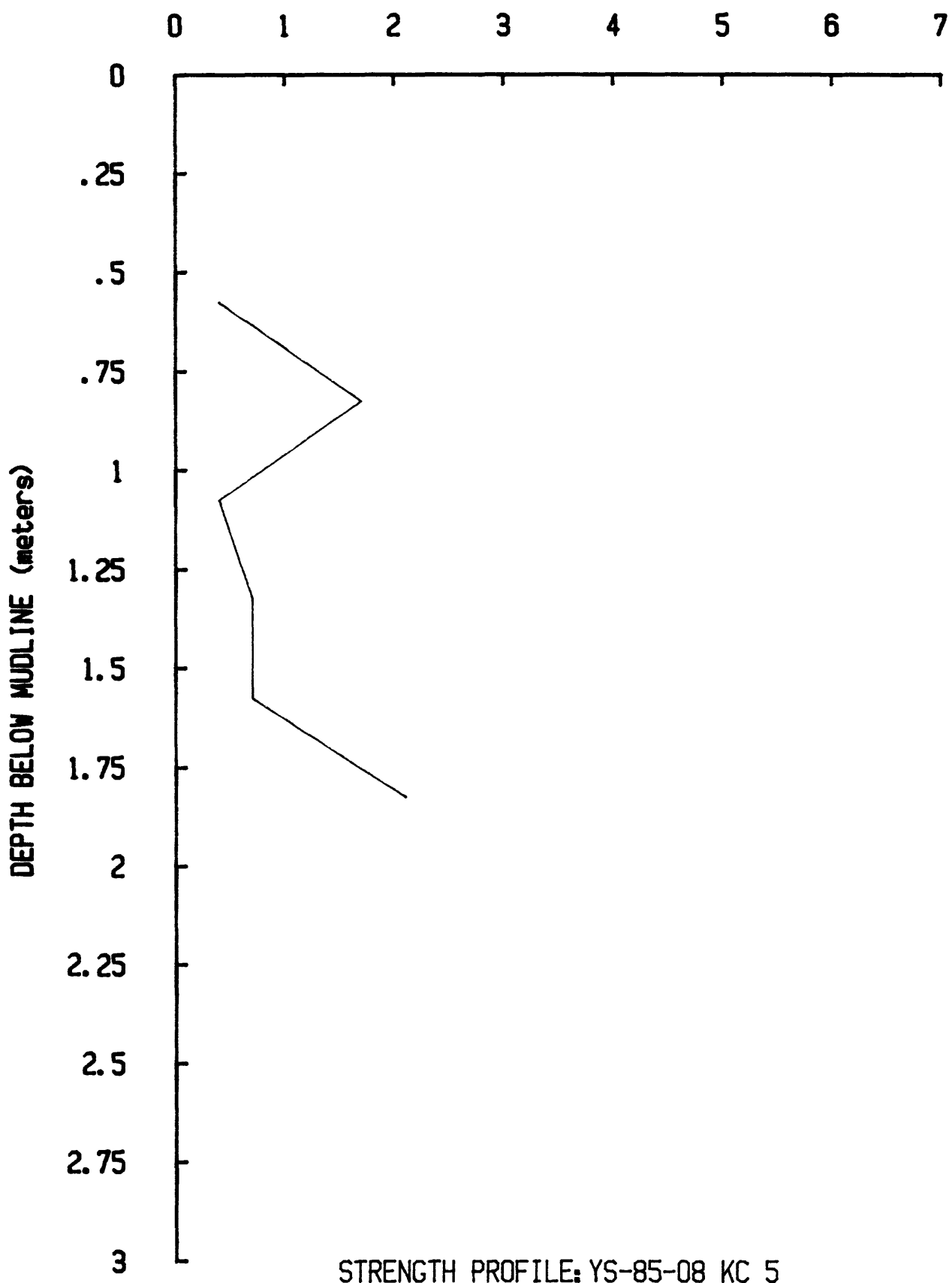
VANE SHEAR STRENGTH (kPa)



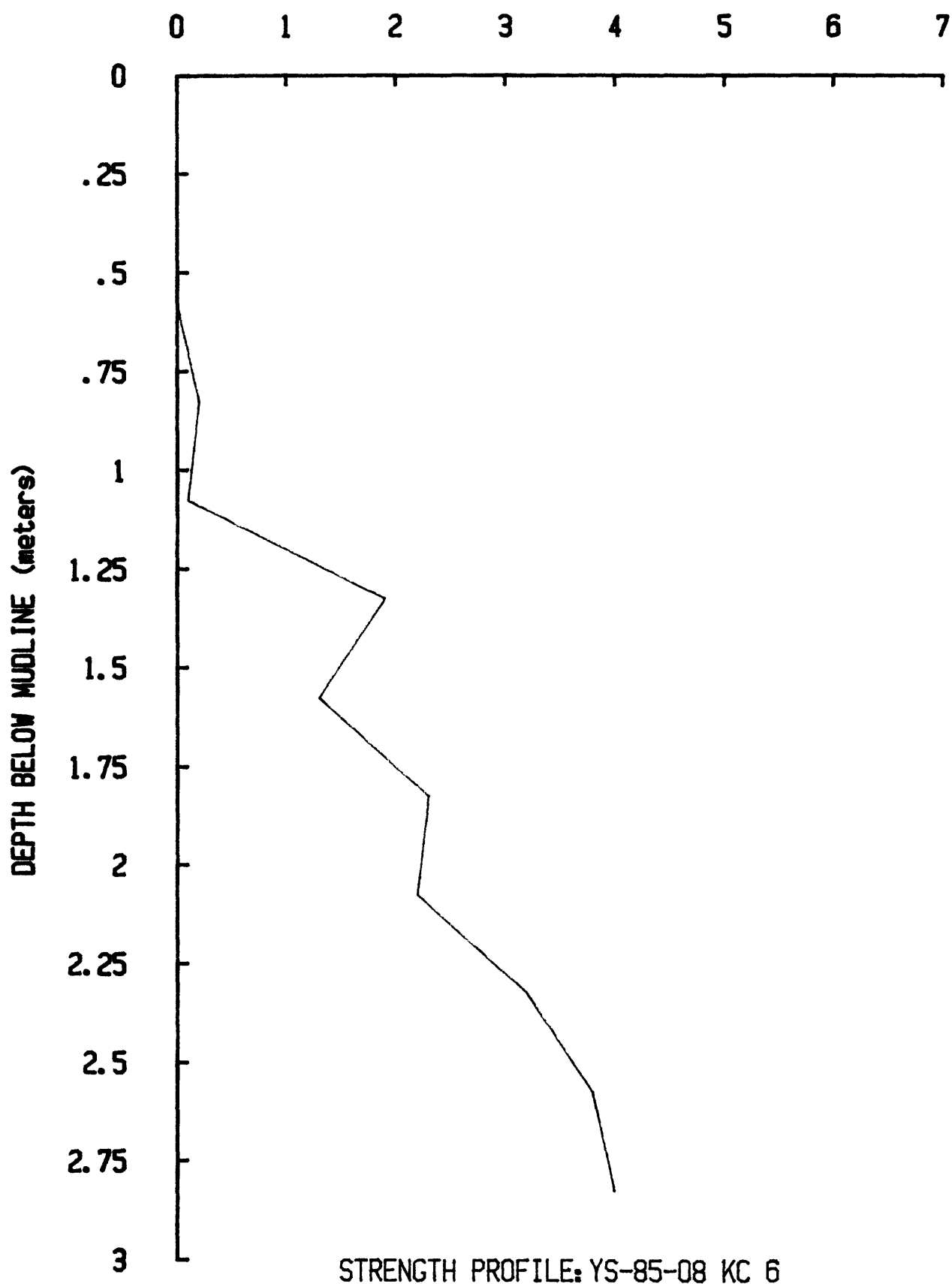
VANE SHEAR STRENGTH (kPa)



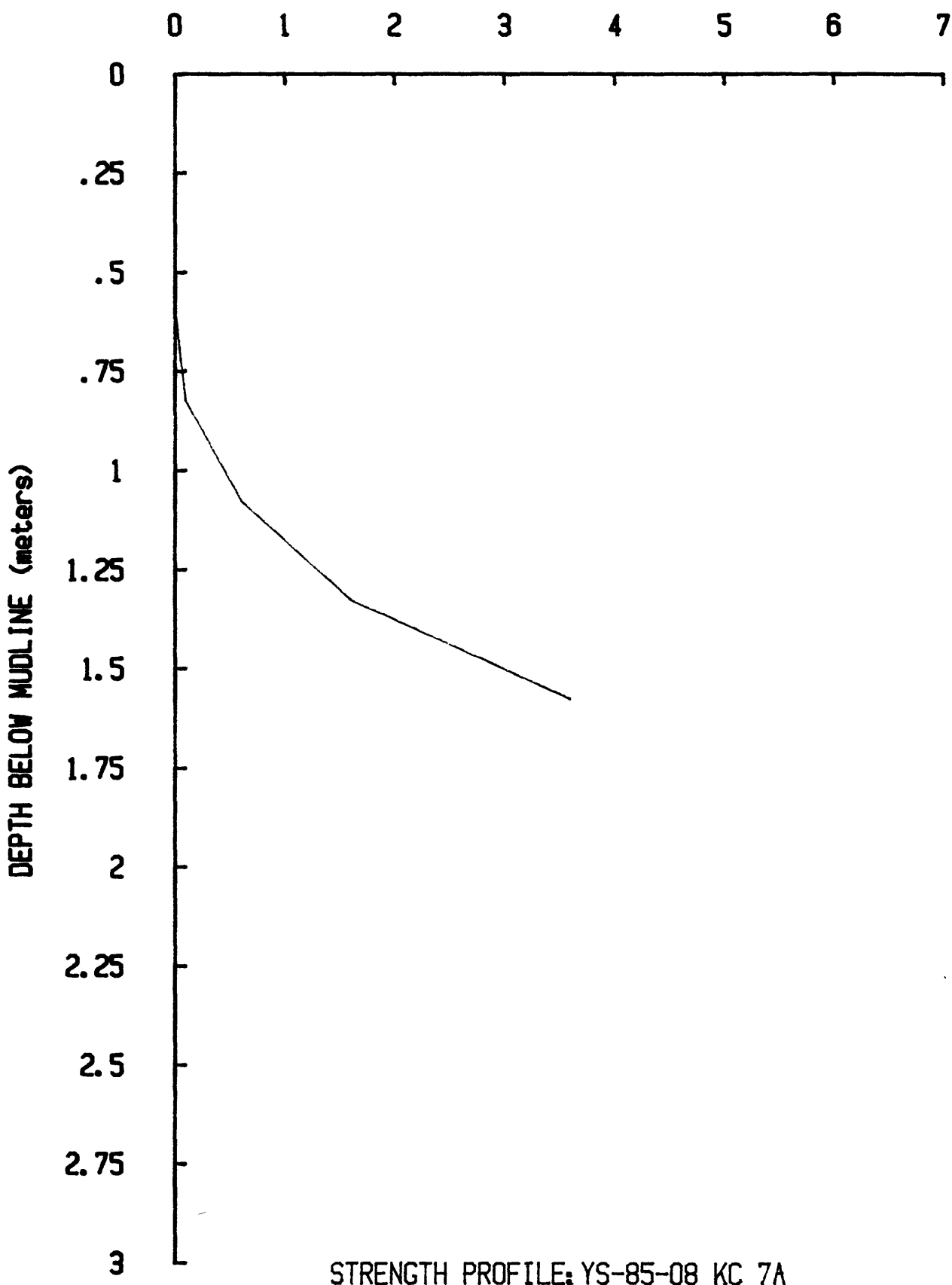
VANE SHEAR STRENGTH (kPa)



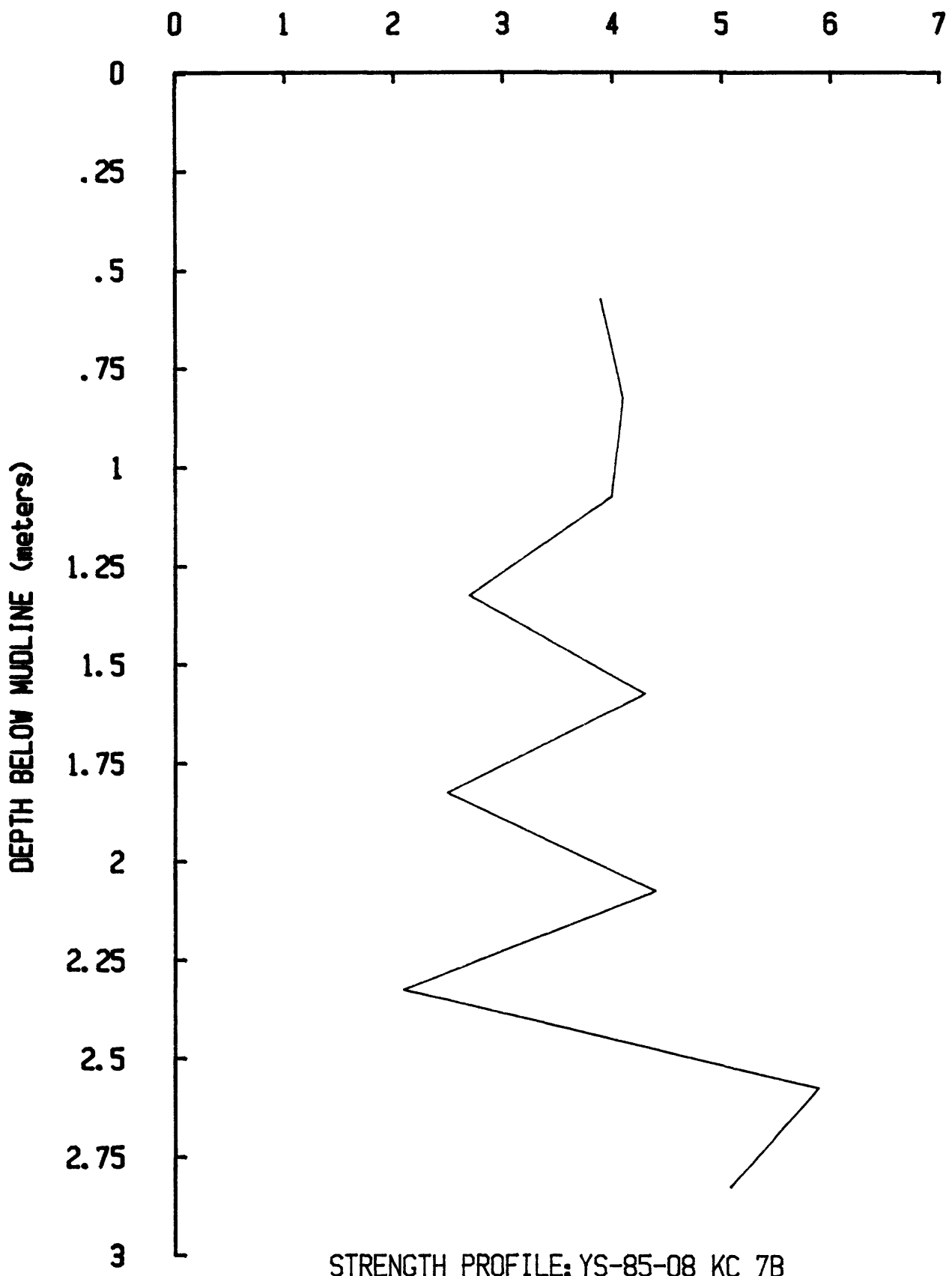
VANE SHEAR STRENGTH (kPa)



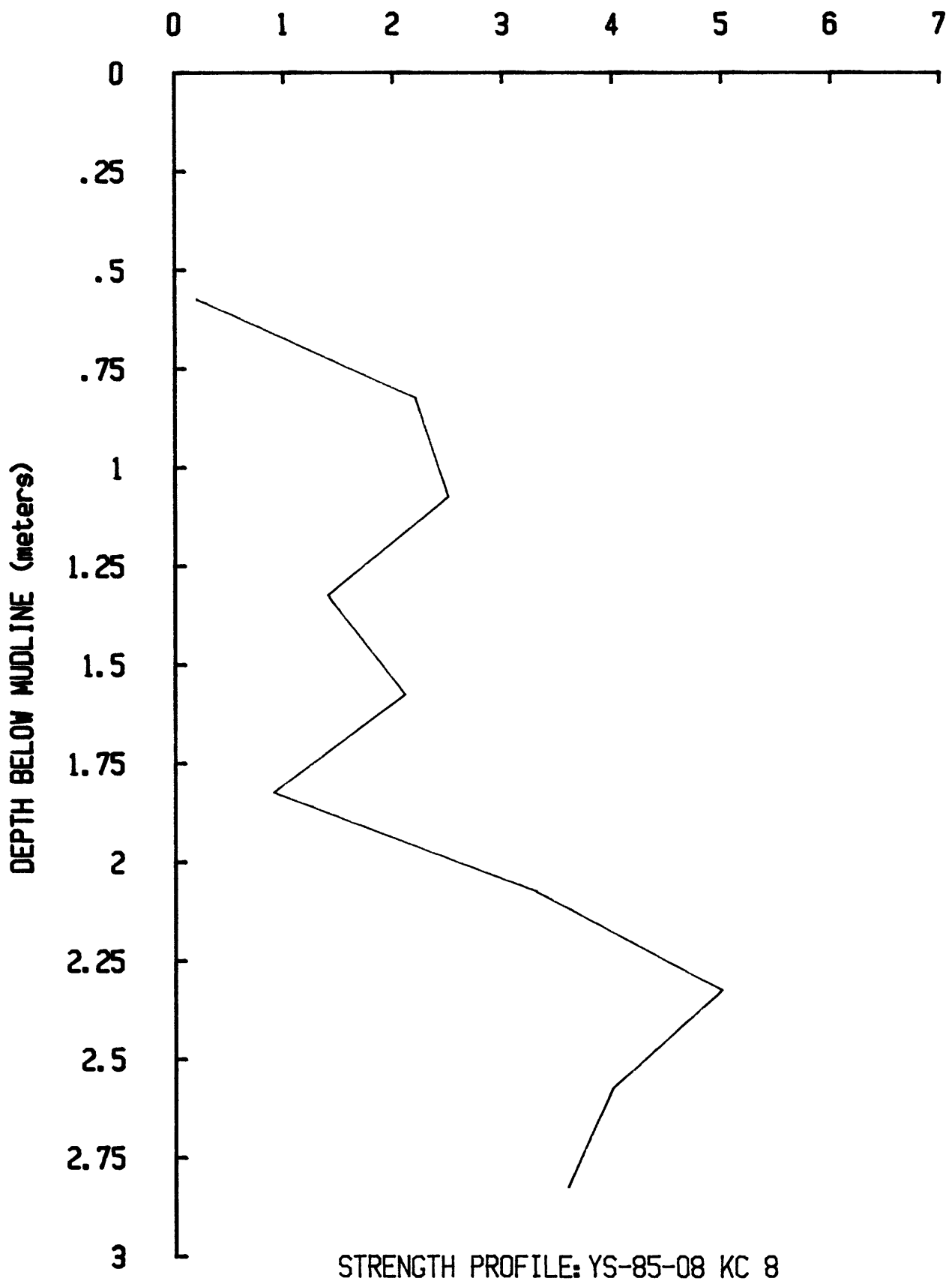
VANE SHEAR STRENGTH (kPa)



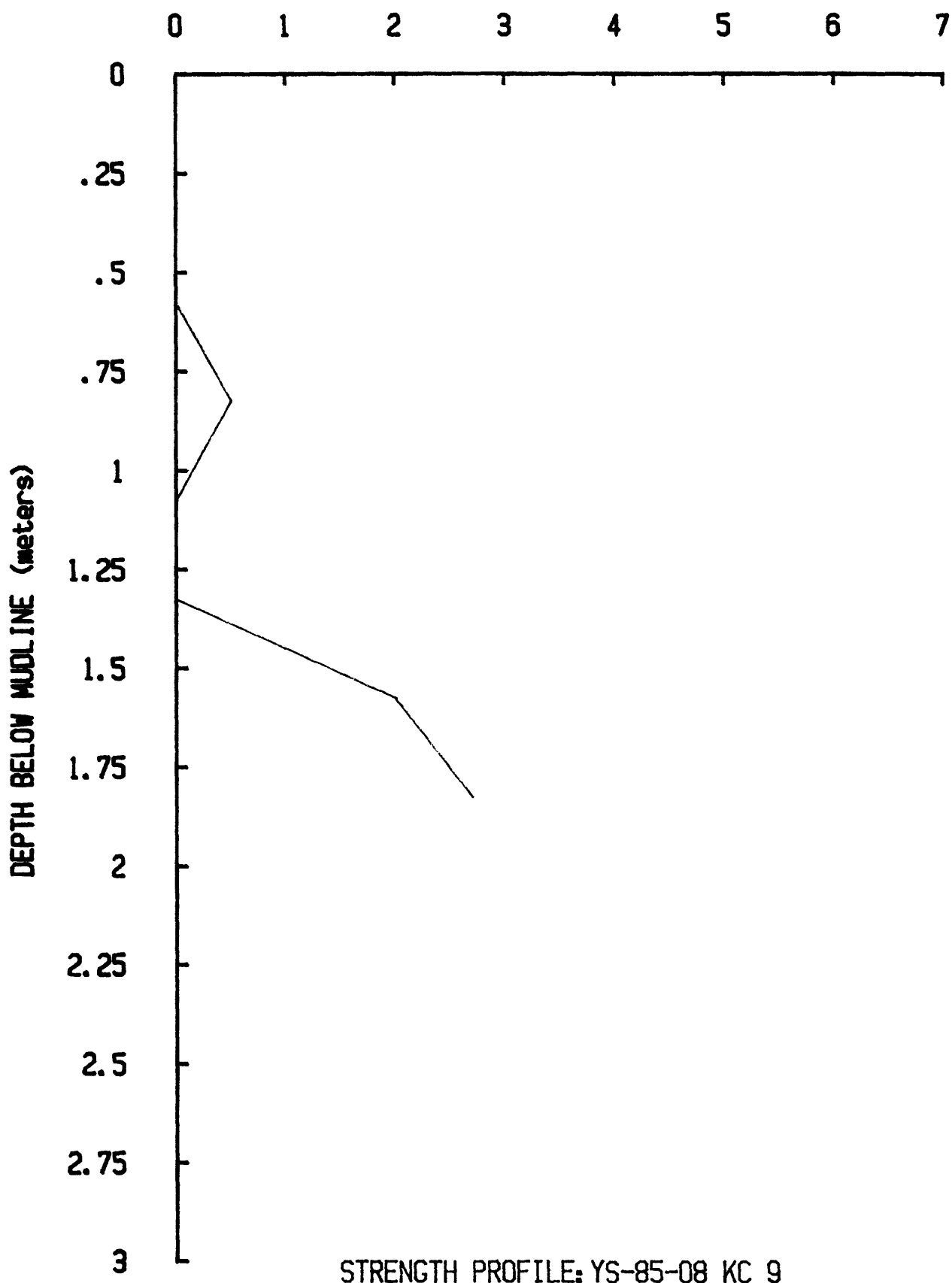
VANE SHEAR STRENGTH (kPa)



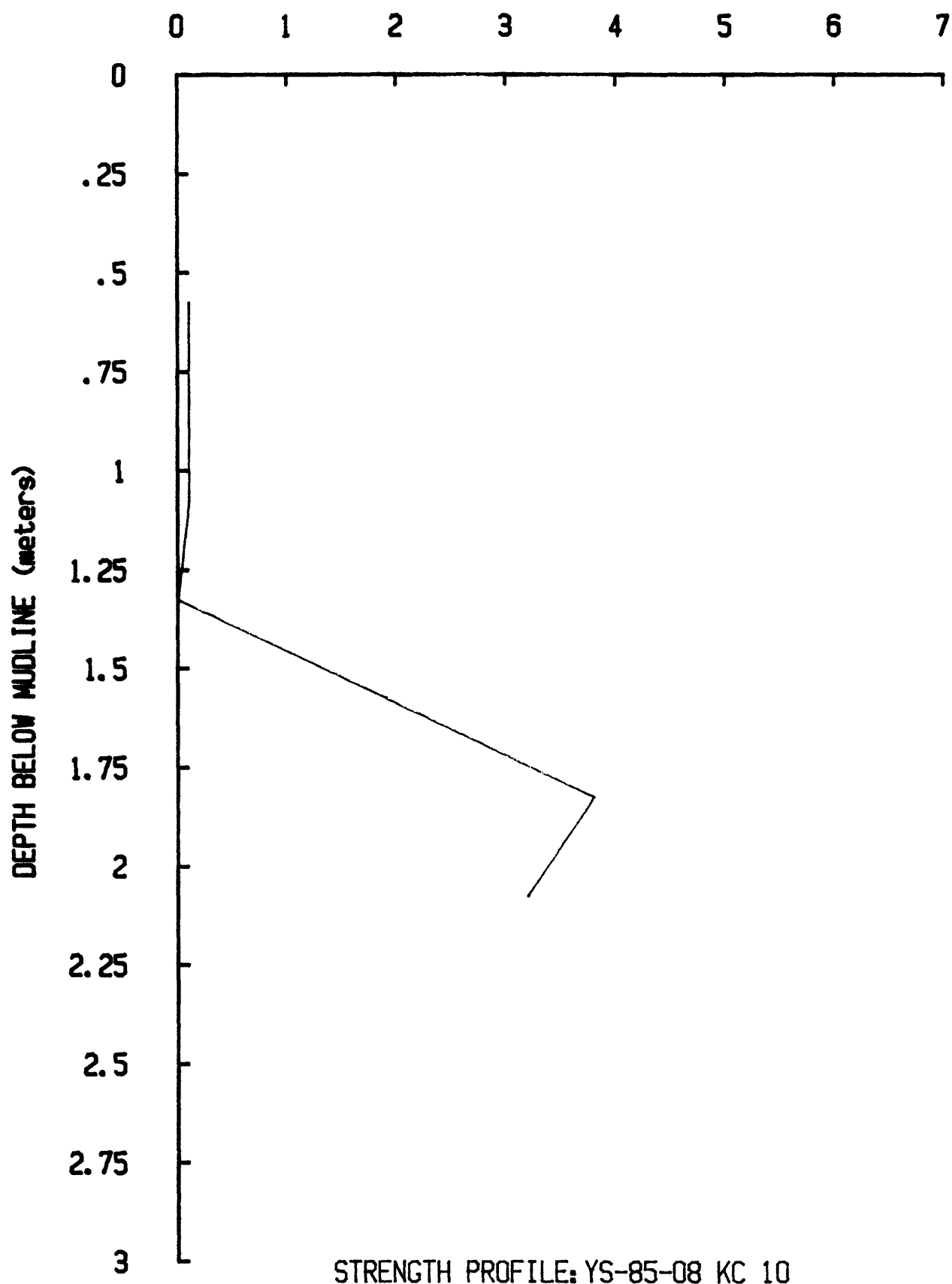
VANE SHEAR STRENGTH (kPa)



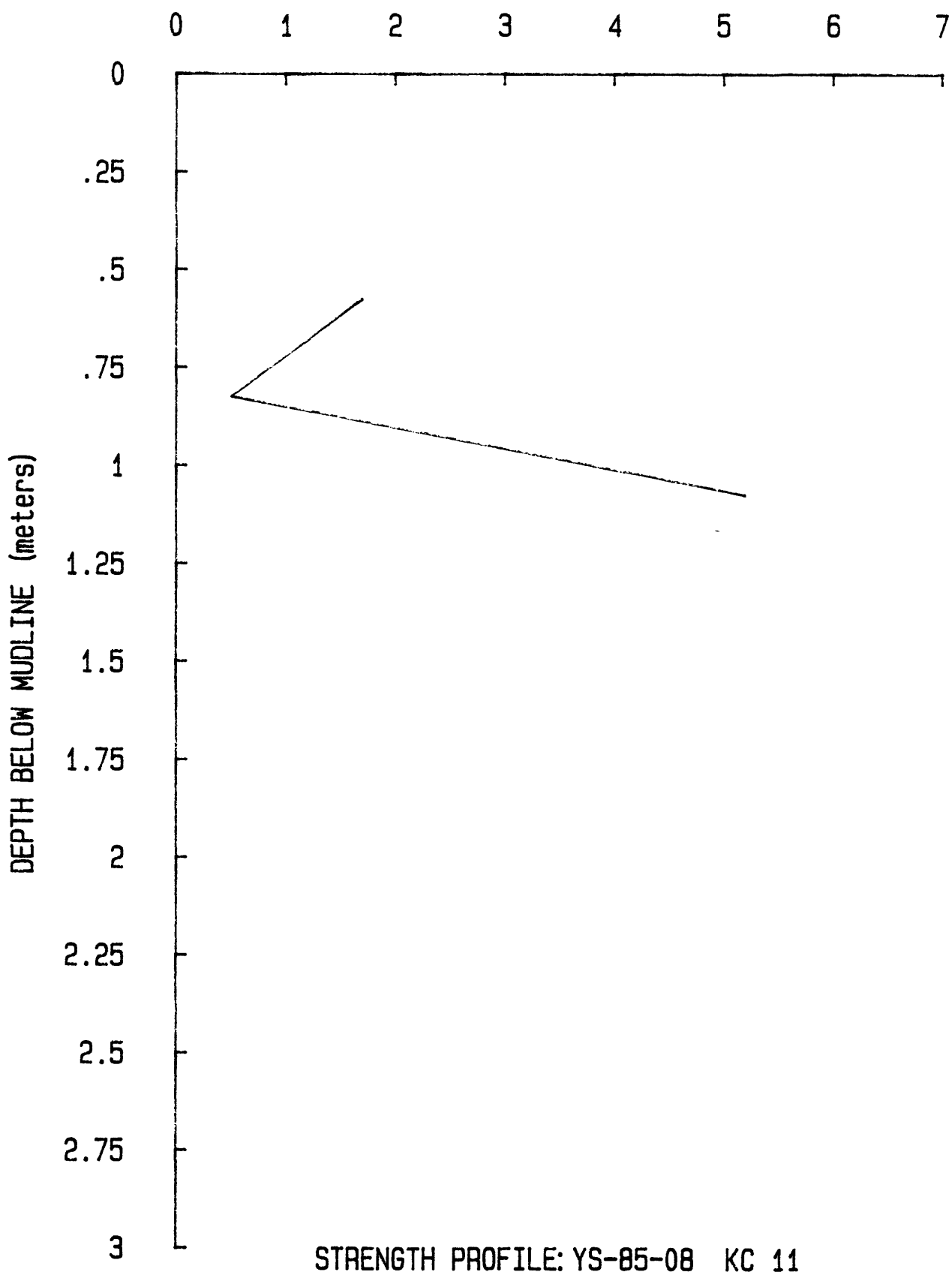
VANE SHEAR STRENGTH (kPa)



VANE SHEAR STRENGTH (kPa)

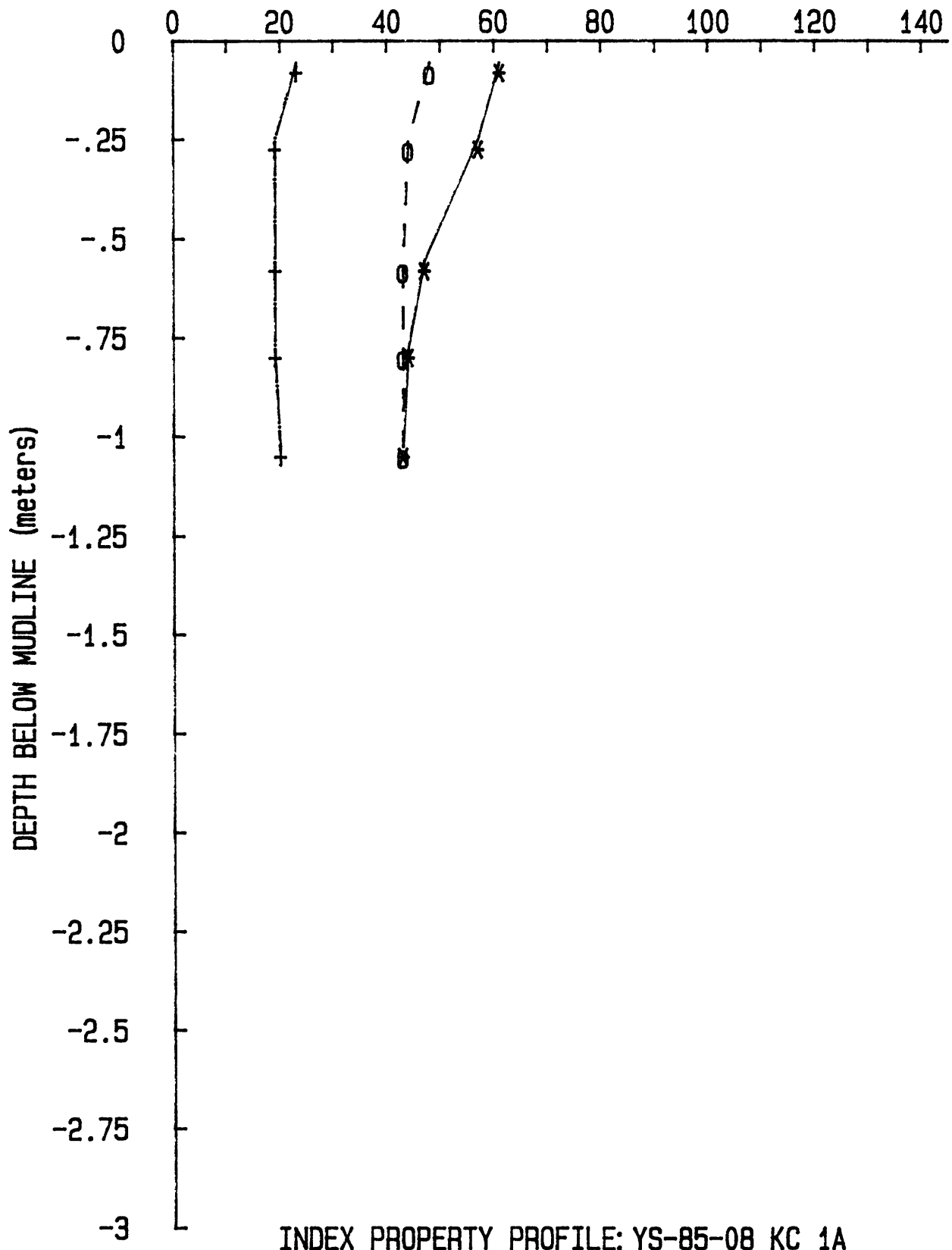


VANE SHEAR STRENGTH (kPa)

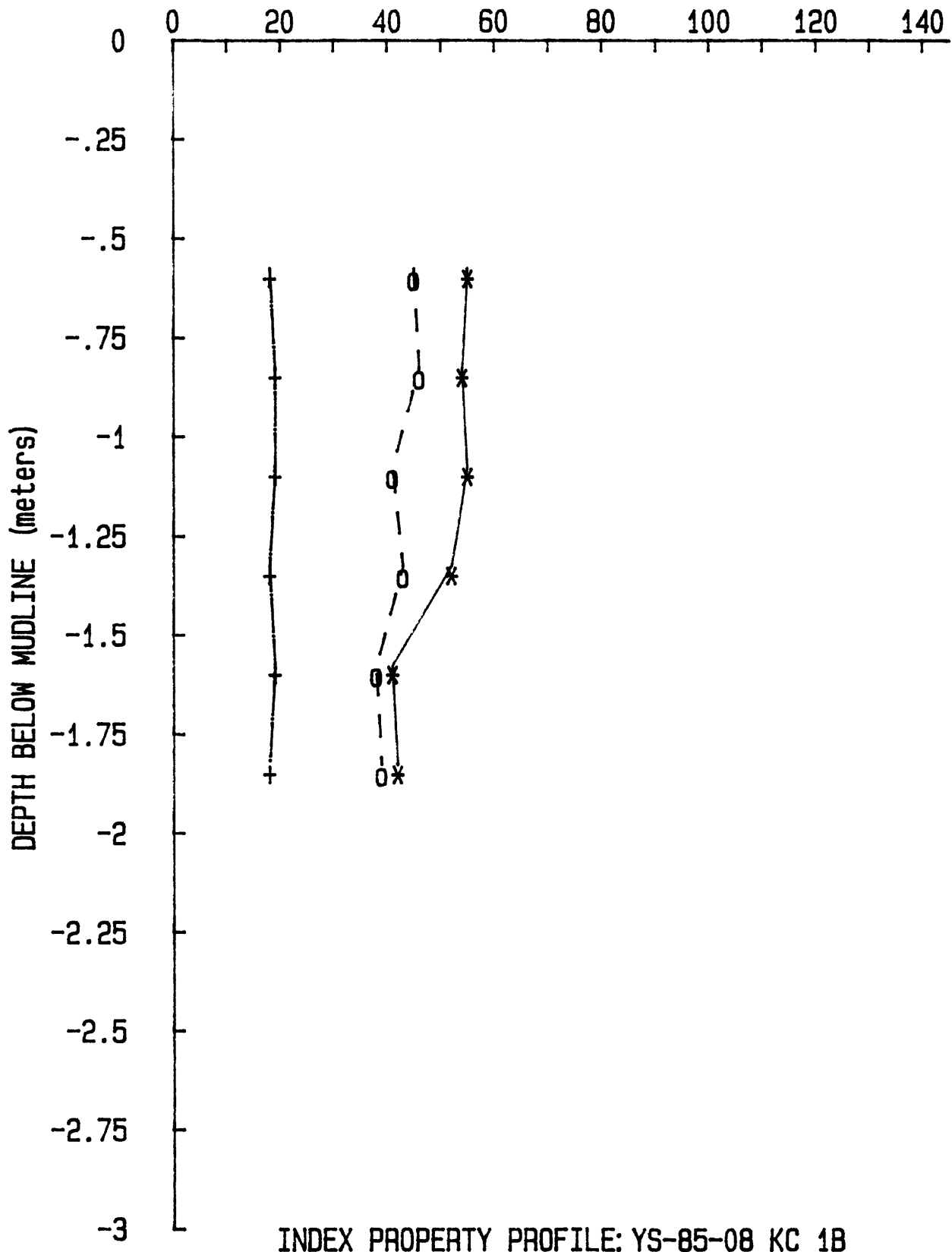


PROFILES
Liquid limit
Plastic limit
Water content

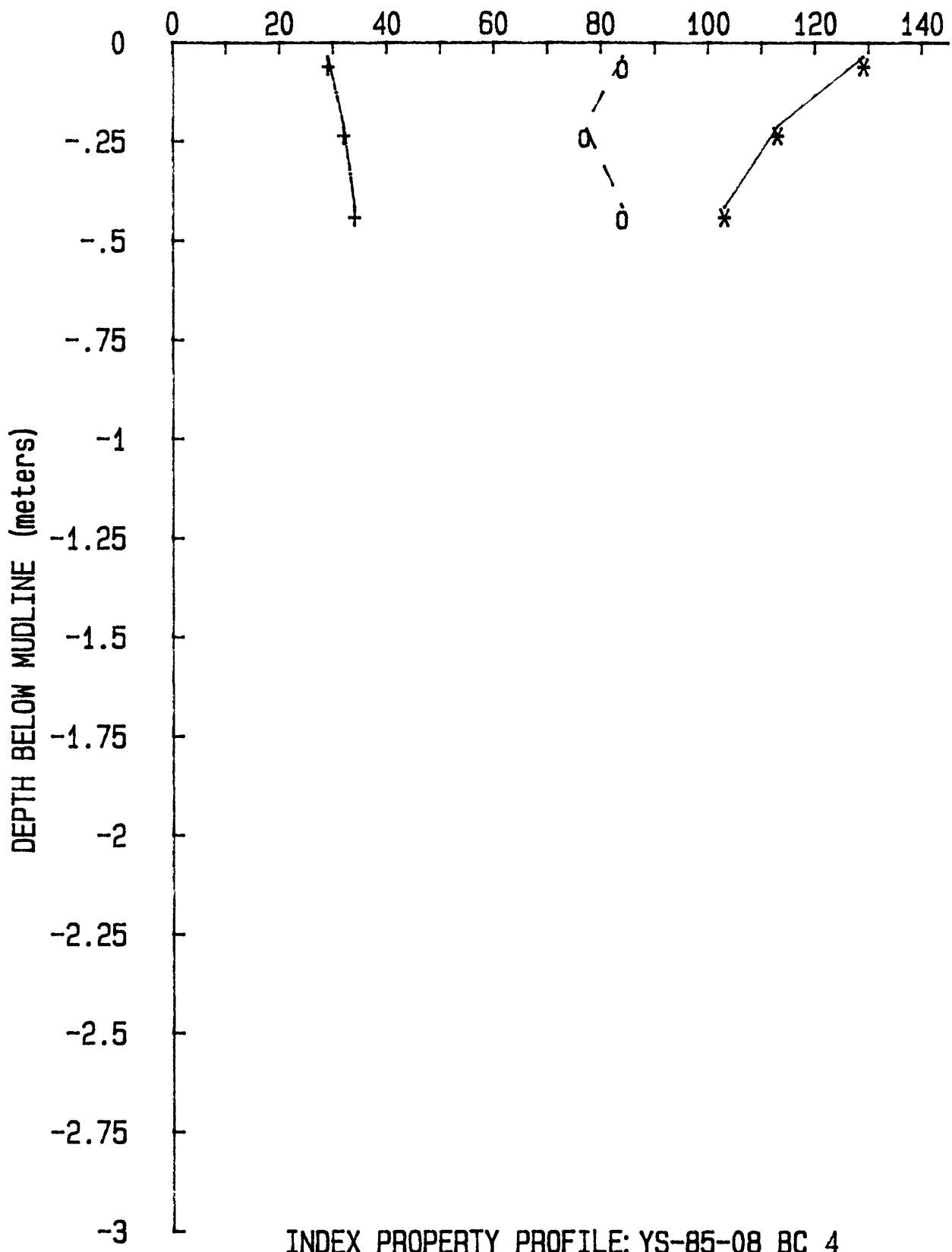
*- WATER CONTENT o--- LIQUID LIMIT +___. PLASTIC LIMIT



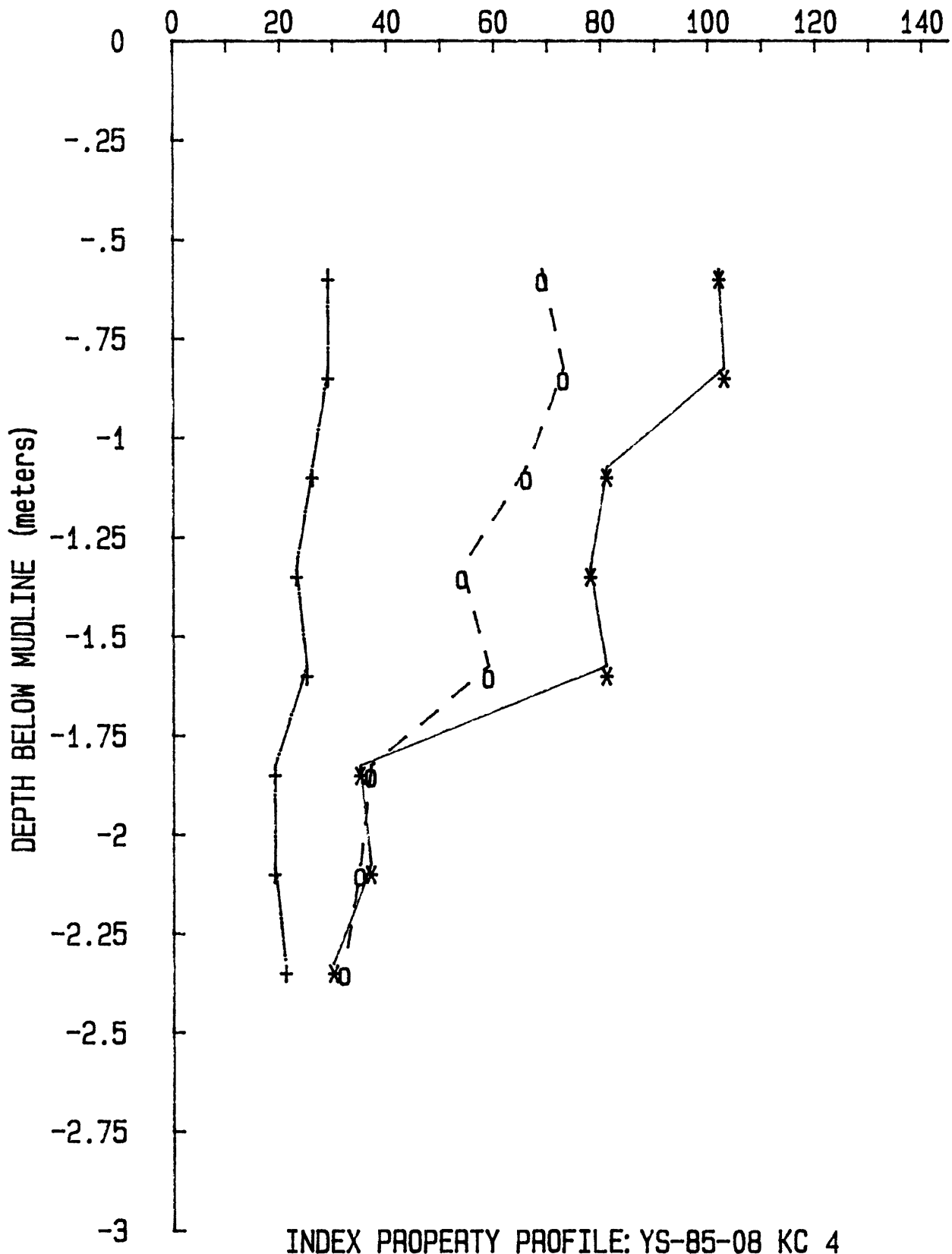
*- WATER CONTENT o--- LIQUID LIMIT +_._ PLASTIC LIMIT

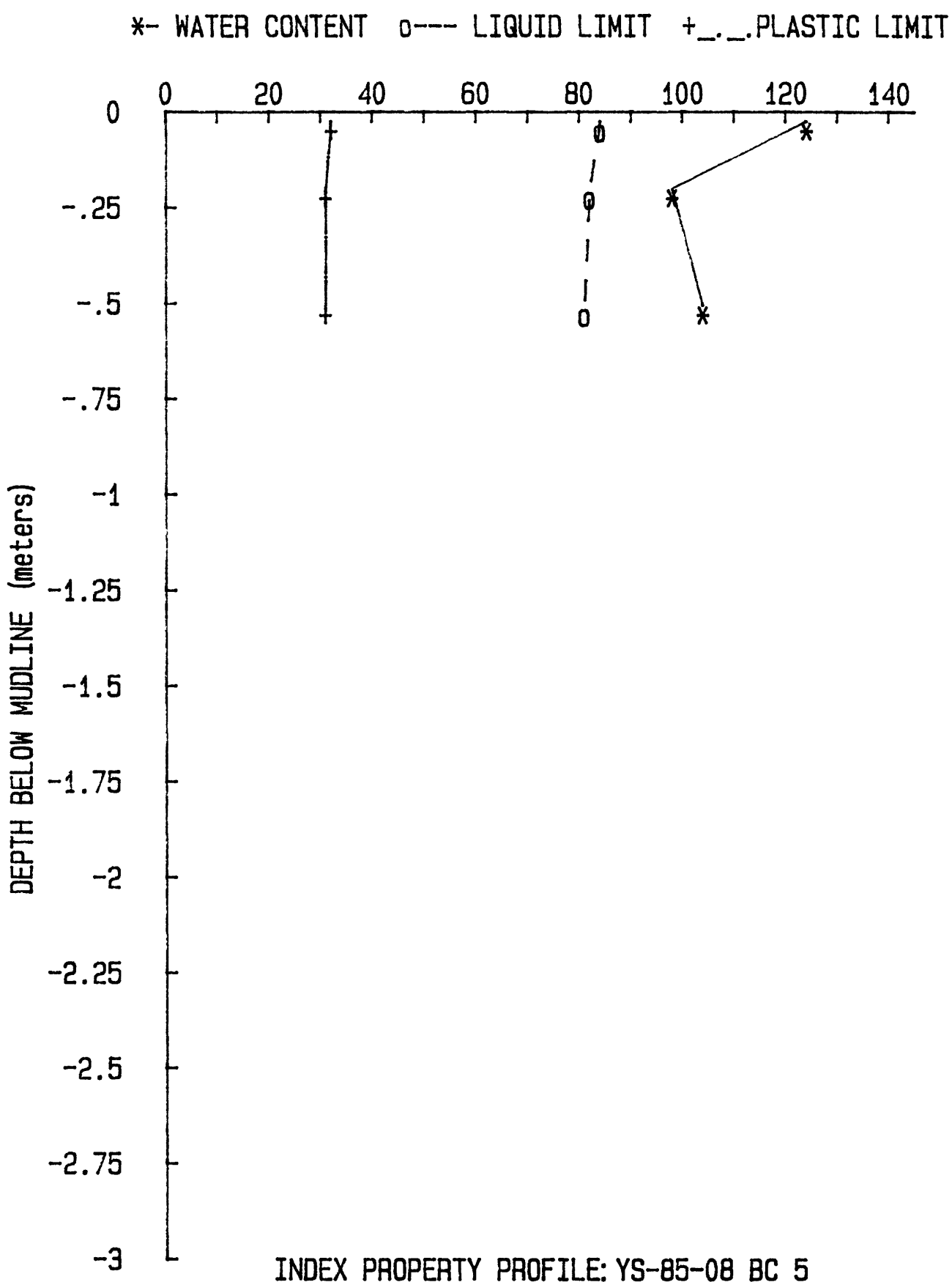


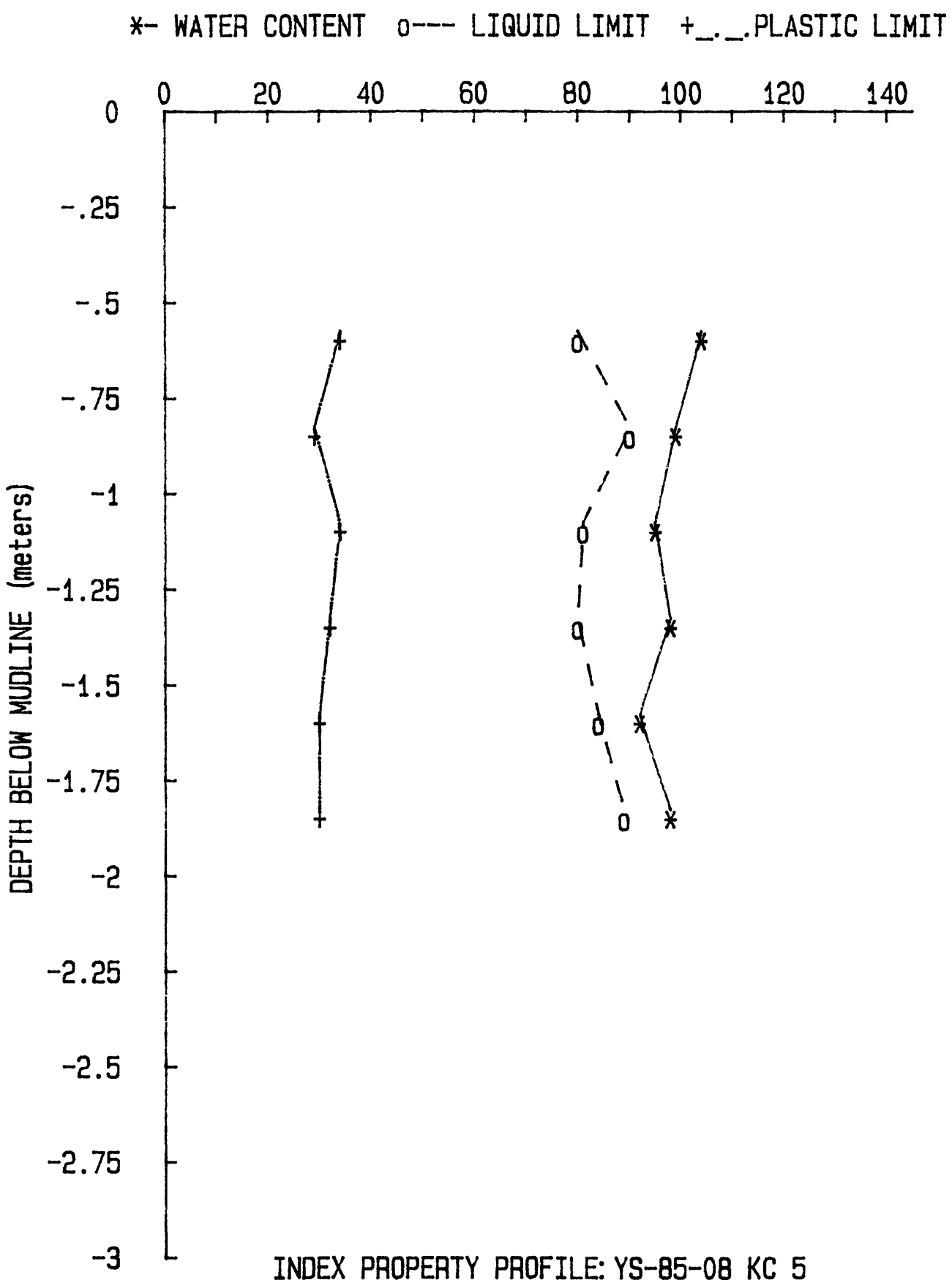
*- WATER CONTENT o--- LIQUID LIMIT +_._ PLASTIC LIMIT



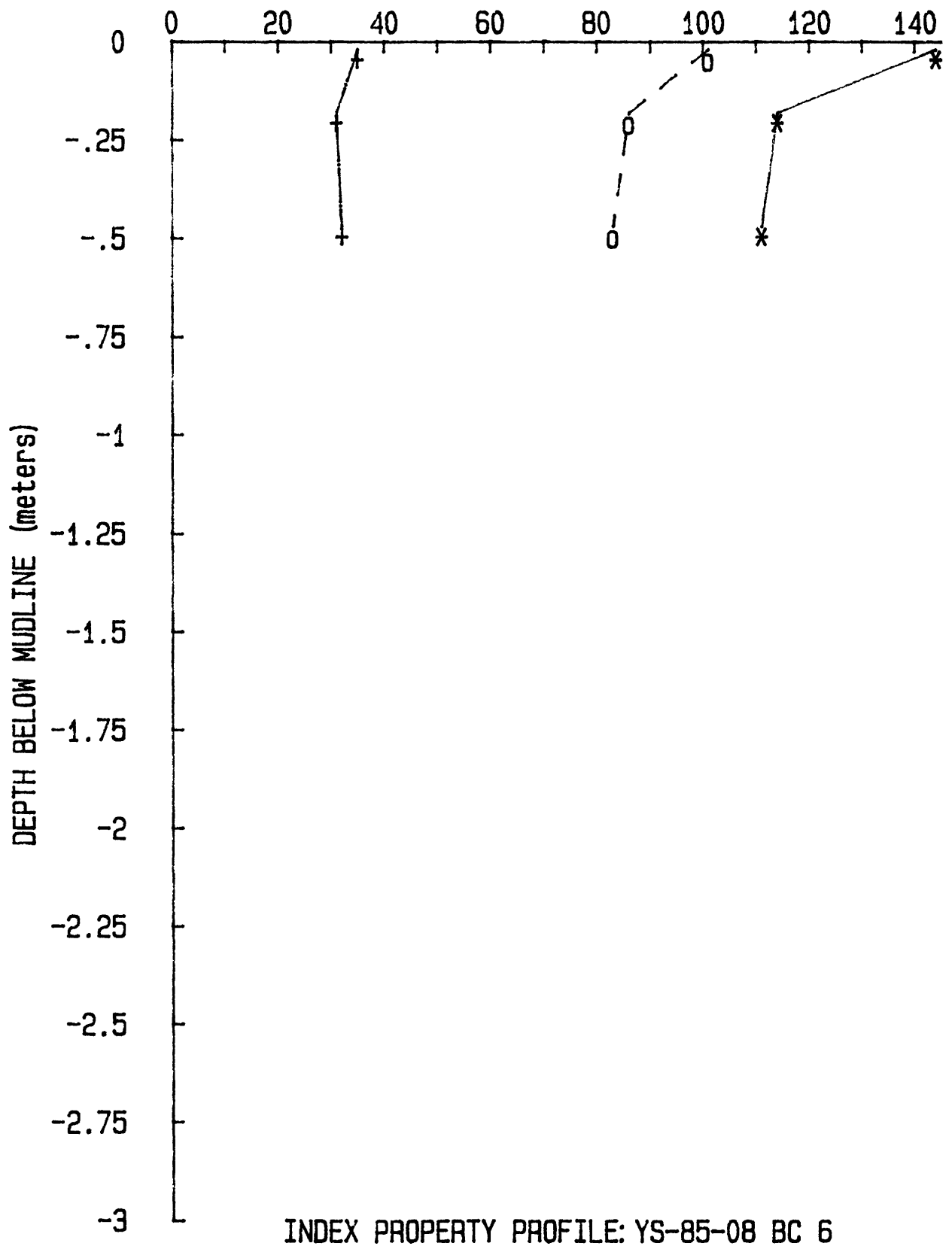
*- WATER CONTENT o--- LIQUID LIMIT +--- PLASTIC LIMIT



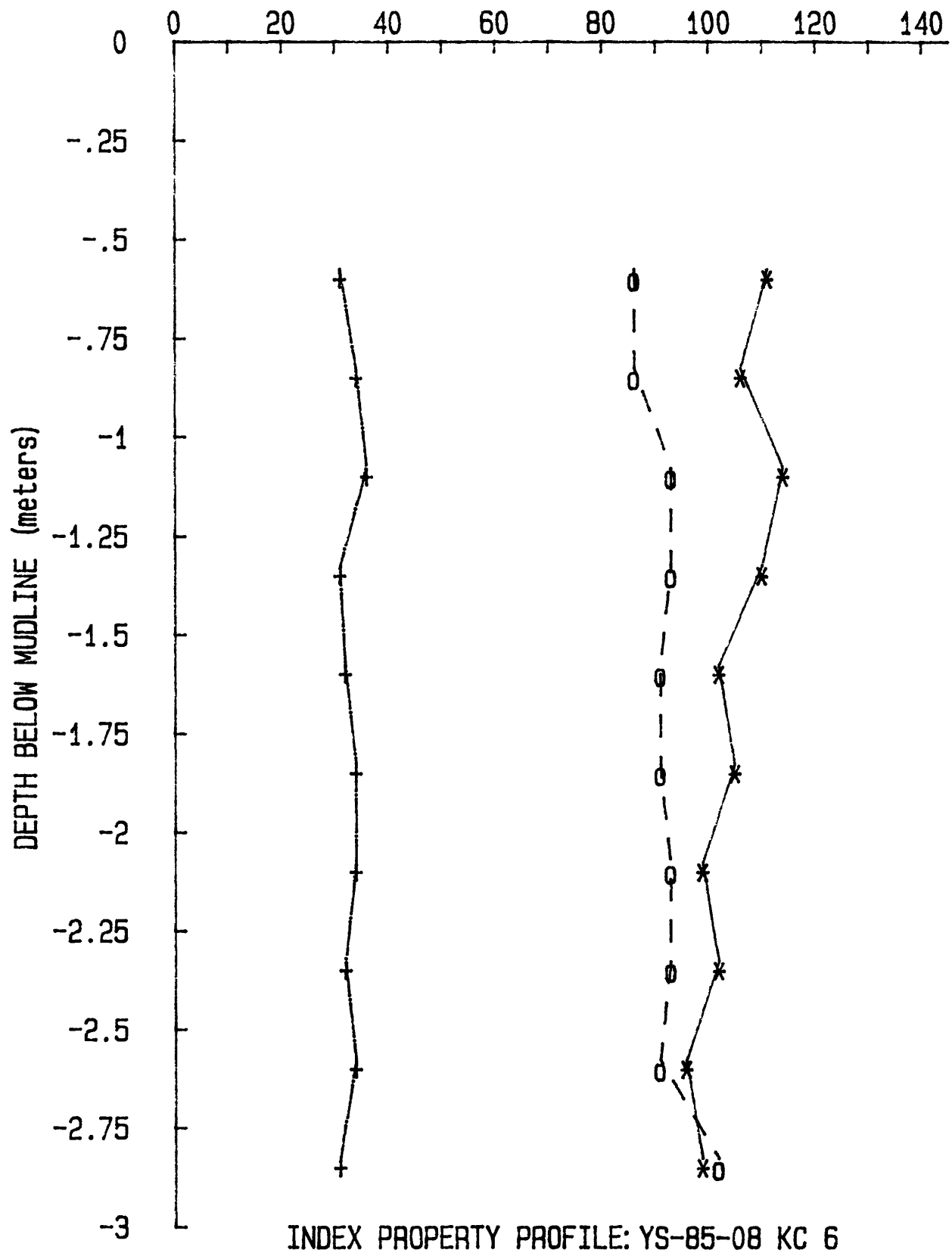




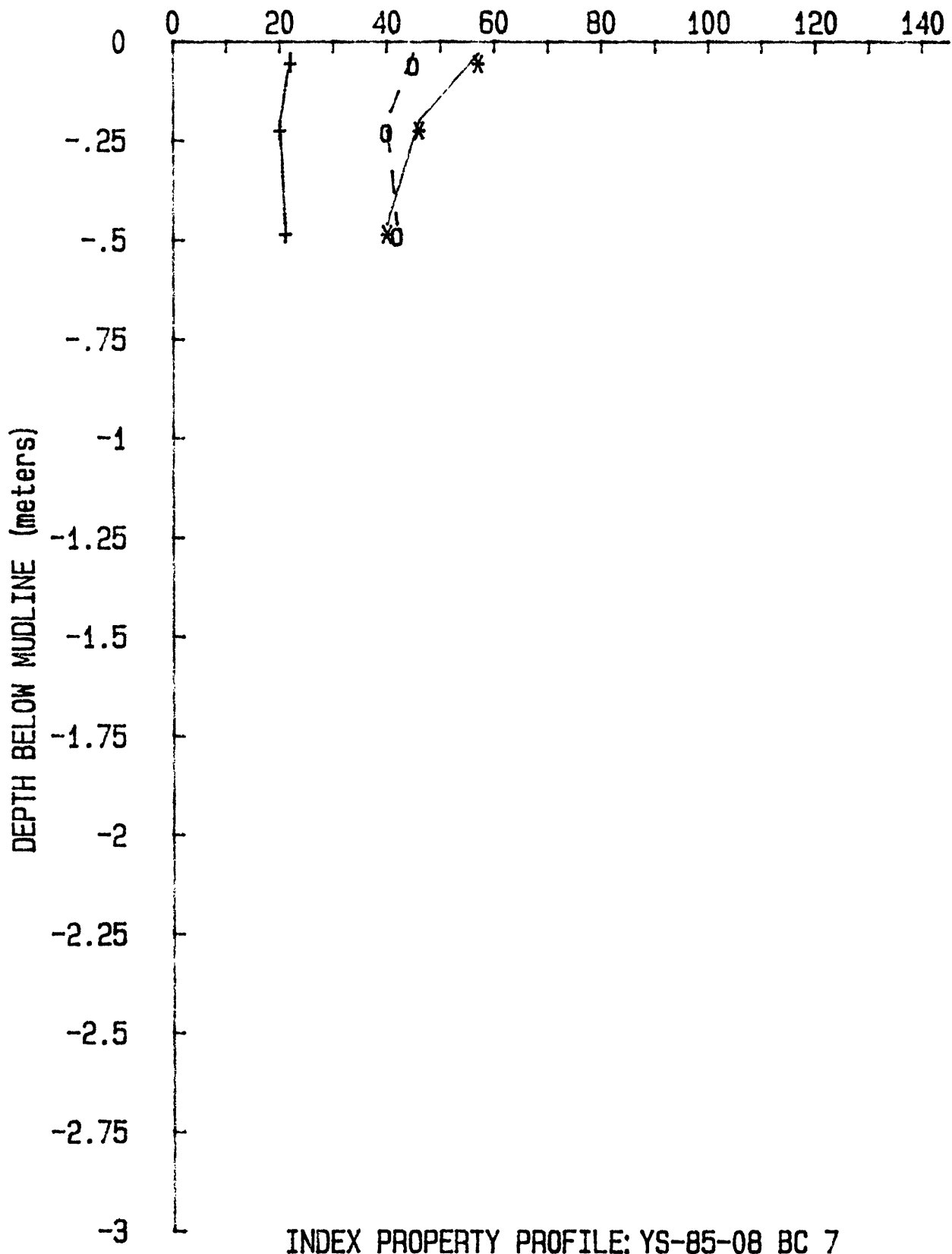
*- WATER CONTENT 0--- LIQUID LIMIT +_._.PLASTIC LIMIT



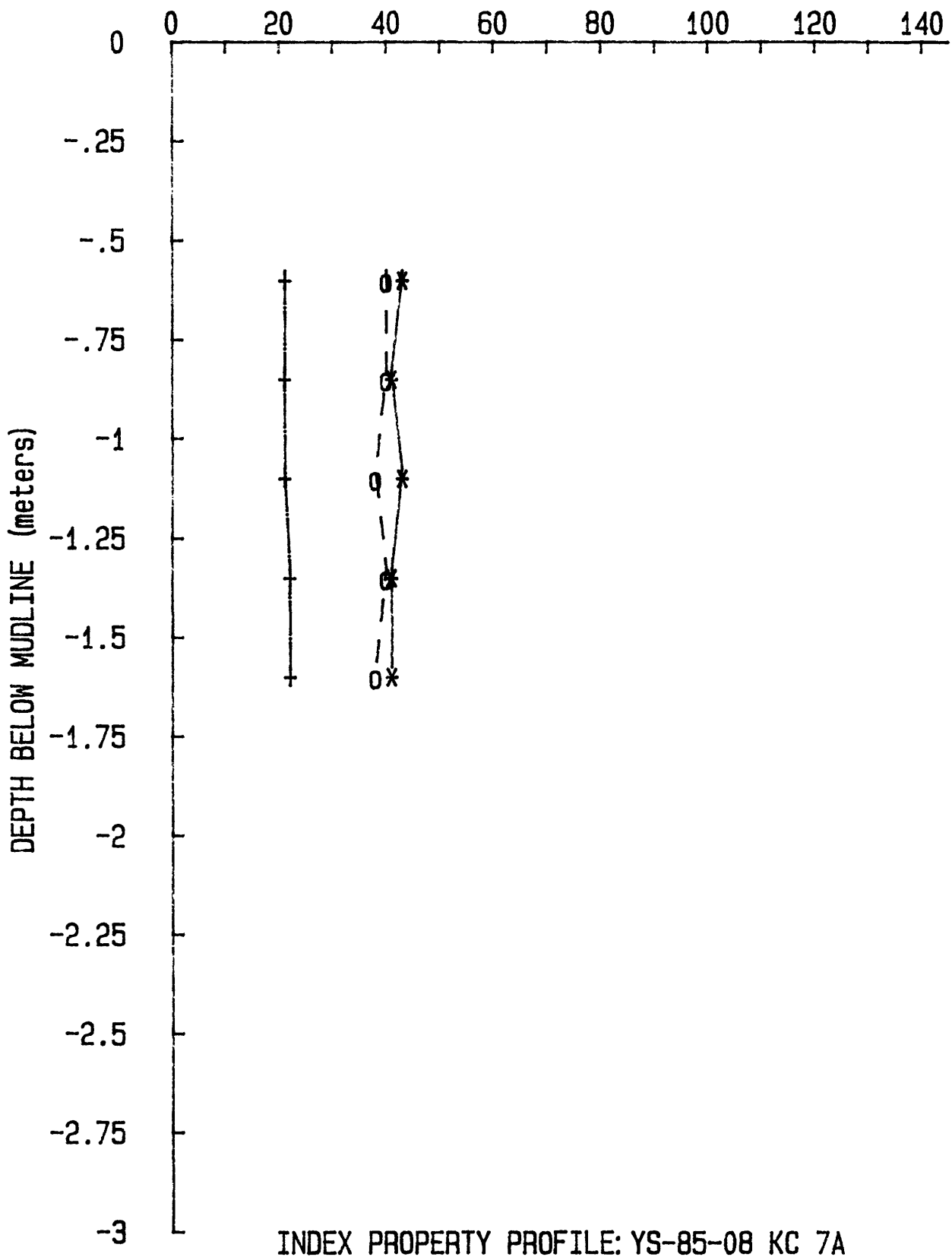
*- WATER CONTENT o--- LIQUID LIMIT +_._.PLASTIC LIMIT



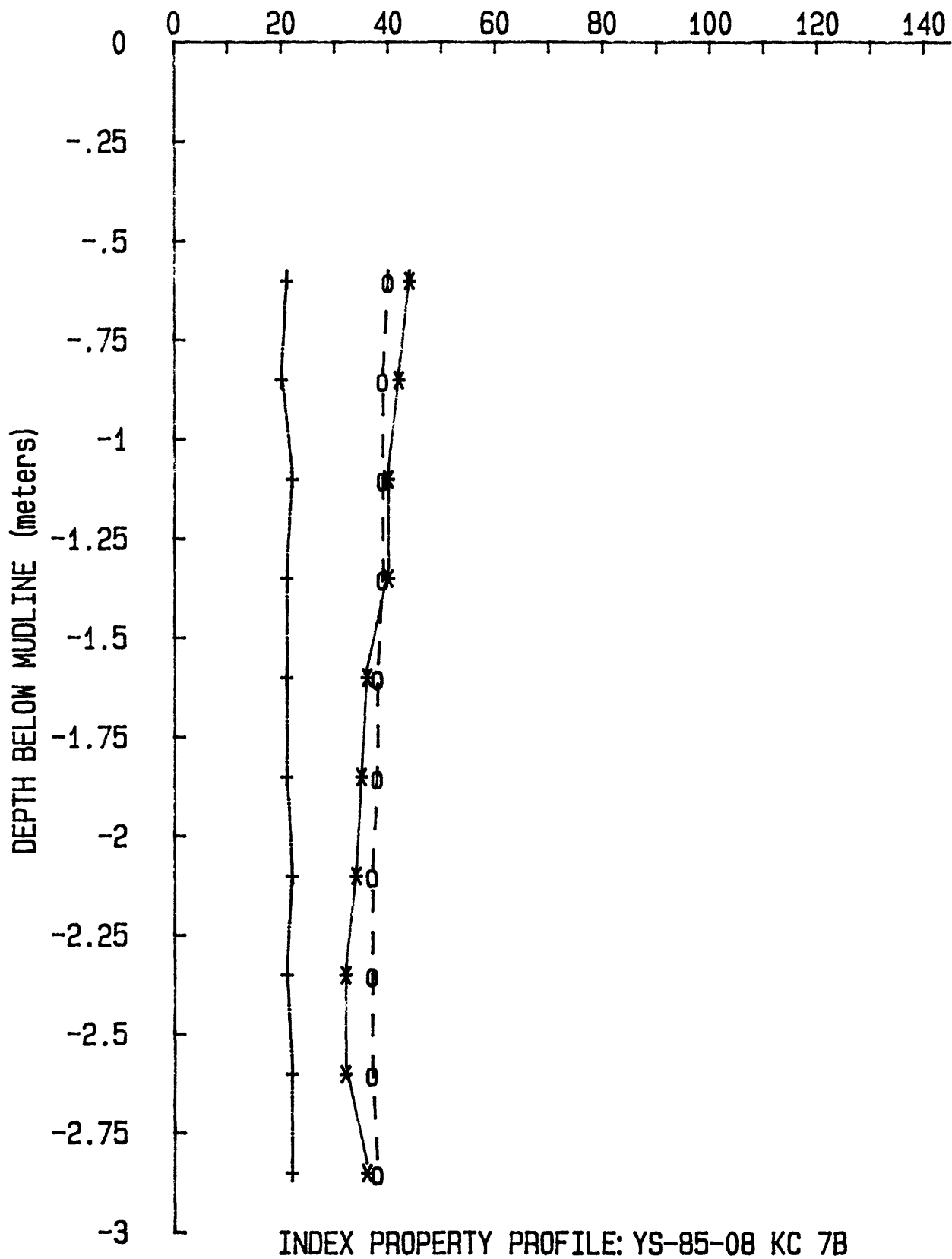
*- WATER CONTENT 0--- LIQUID LIMIT +_._ PLASTIC LIMIT



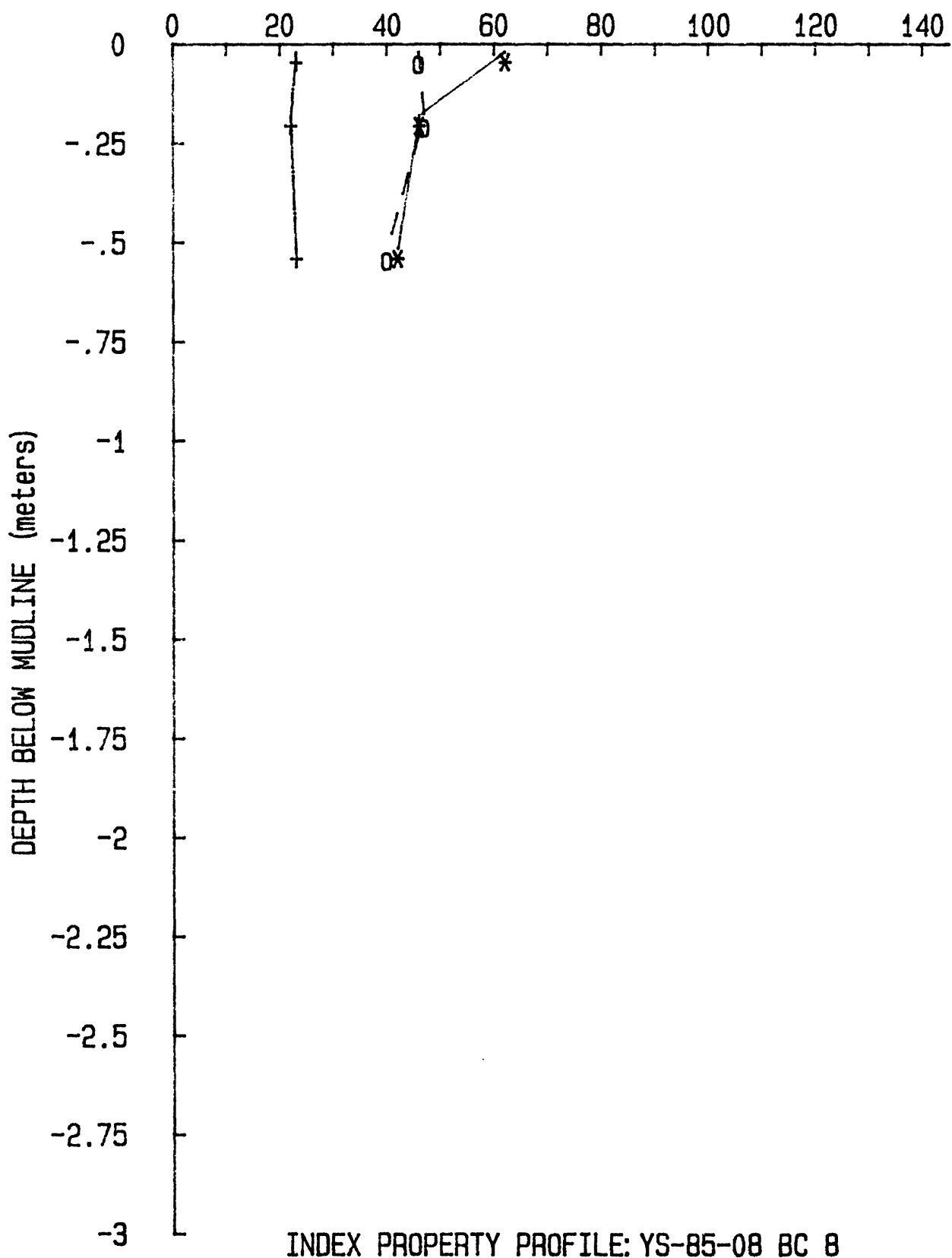
*- WATER CONTENT o--- LIQUID LIMIT +-- PLASTIC LIMIT



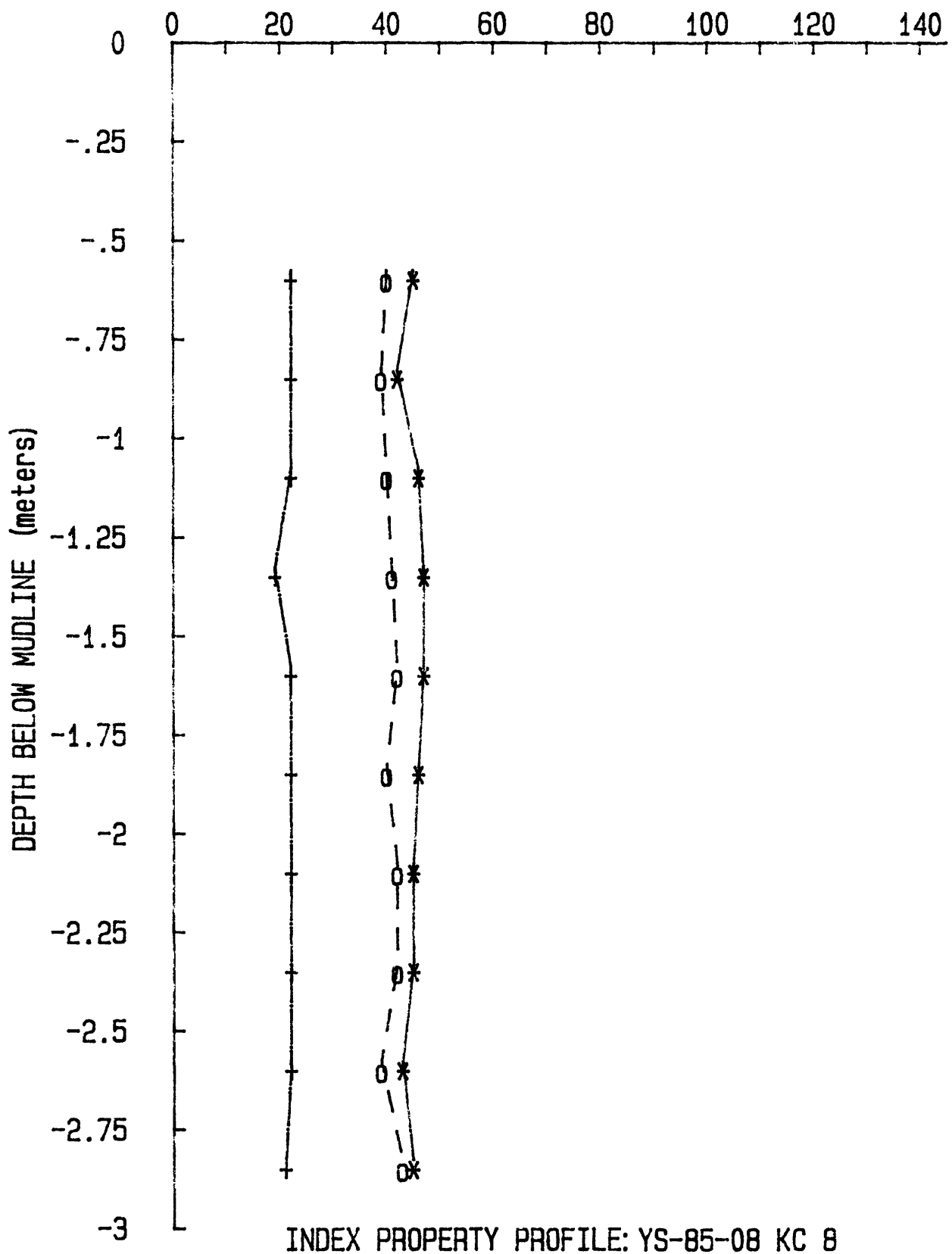
*-- WATER CONTENT 0--- LIQUID LIMIT +_._. PLASTIC LIMIT

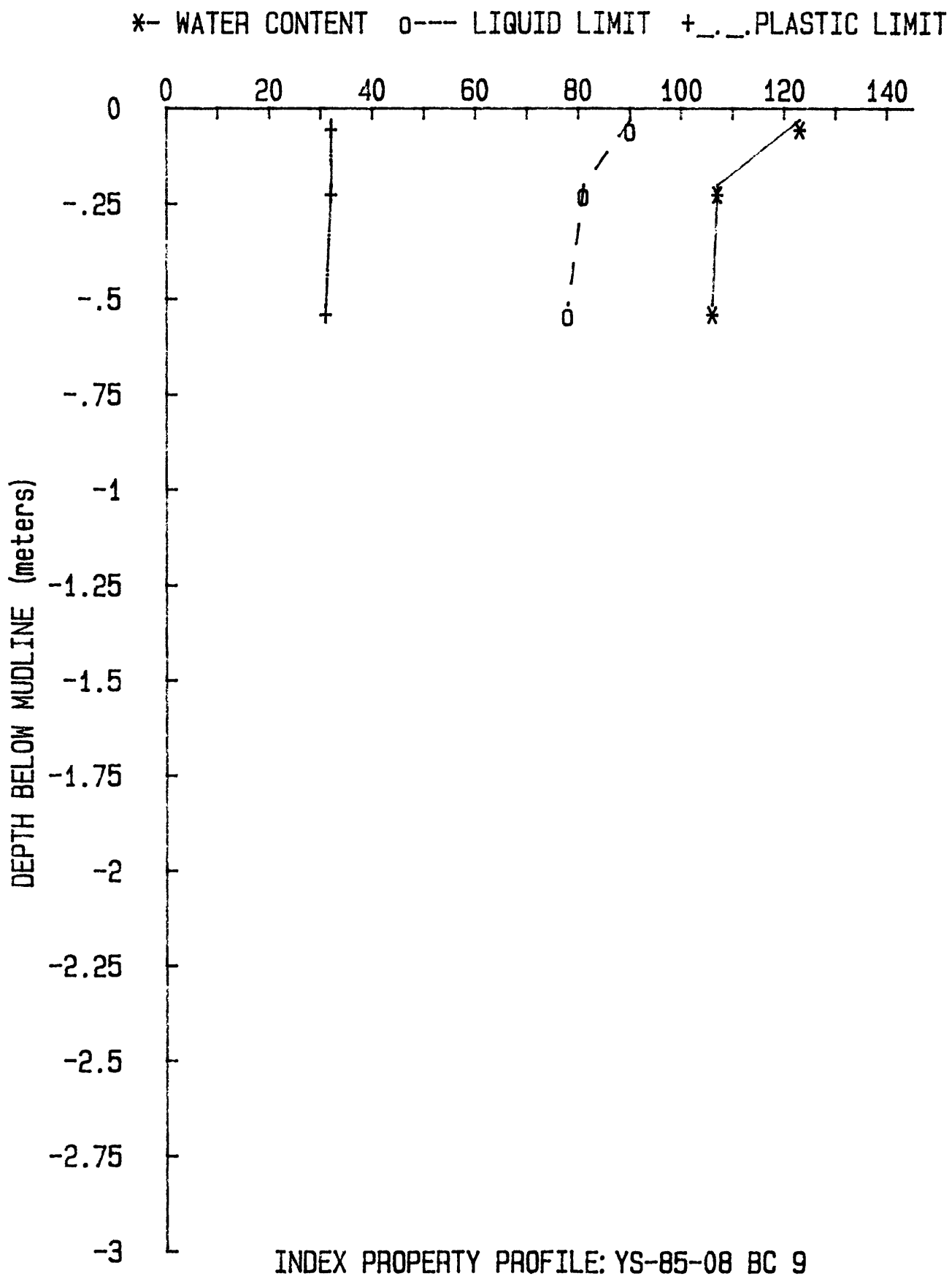


*- WATER CONTENT o--- LIQUID LIMIT +_._. PLASTIC LIMIT

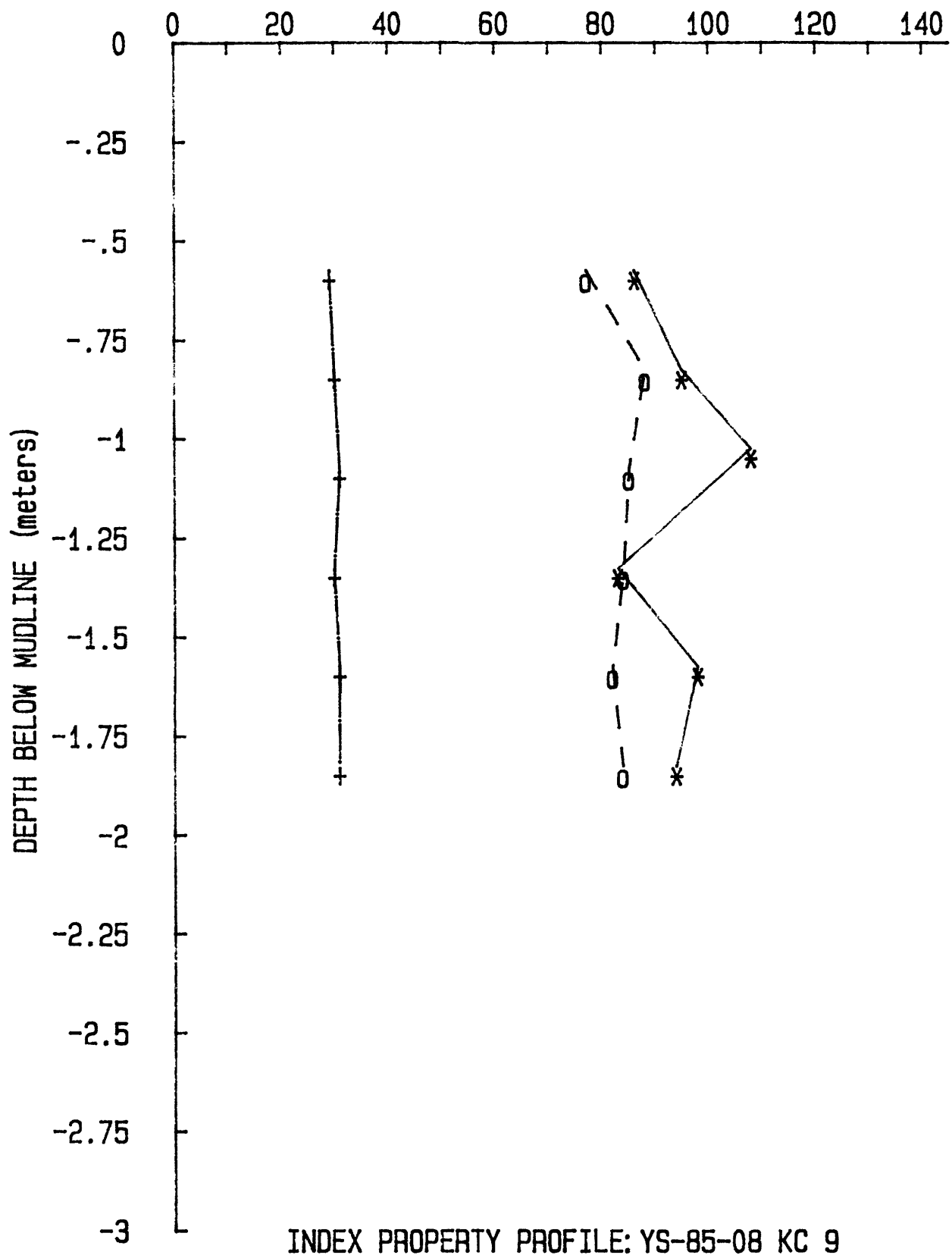


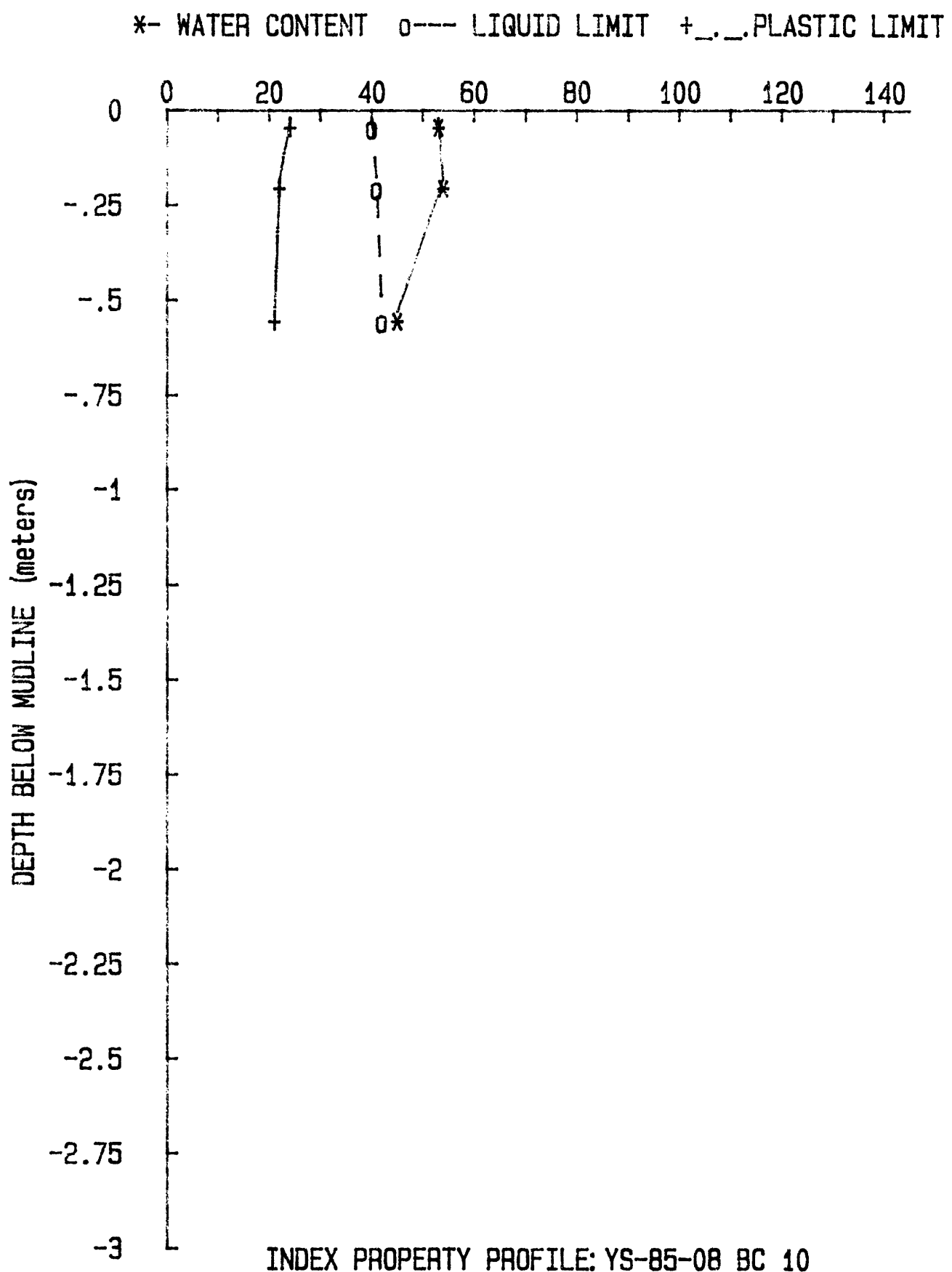
*- WATER CONTENT o--- LIQUID LIMIT +-- PLASTIC LIMIT



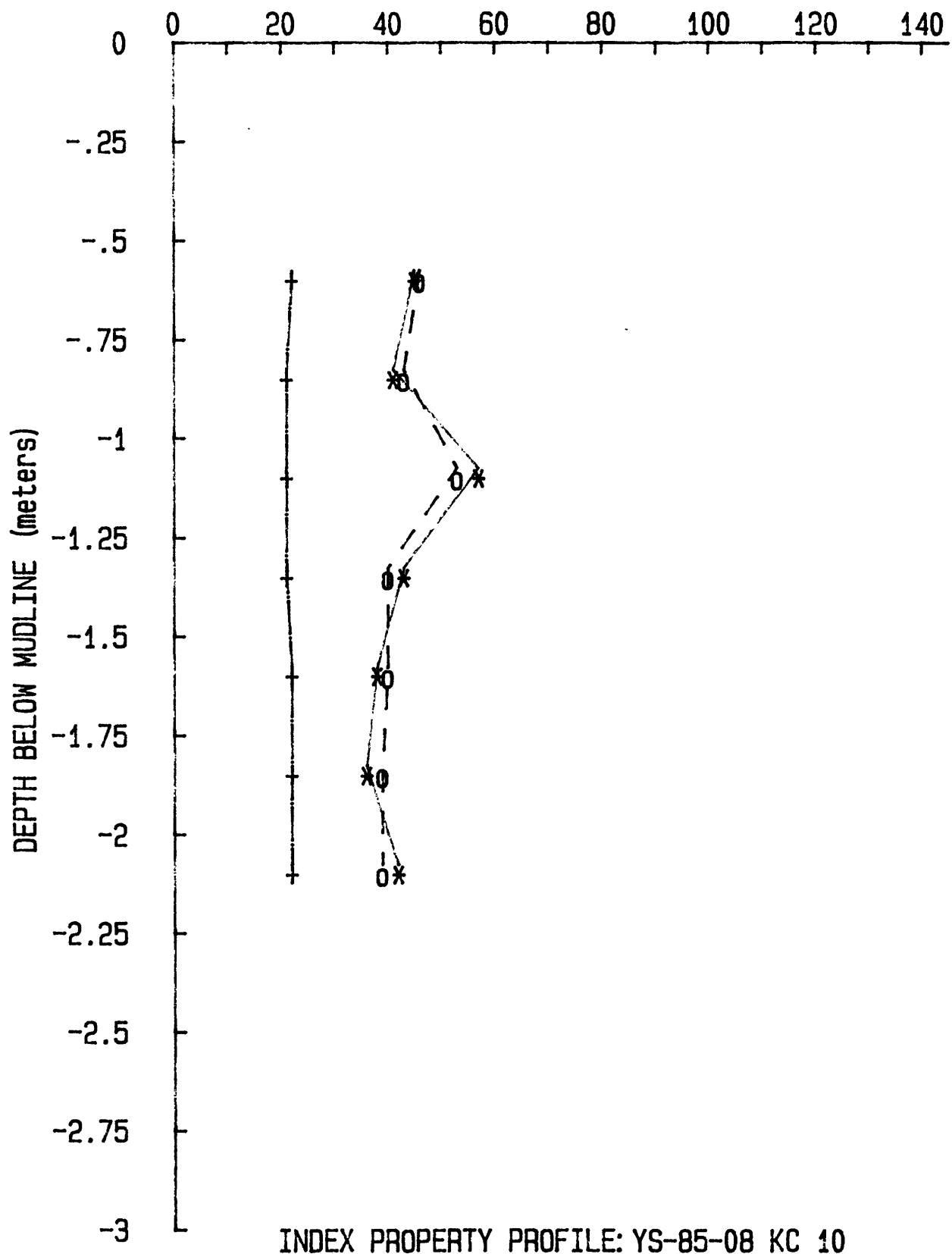


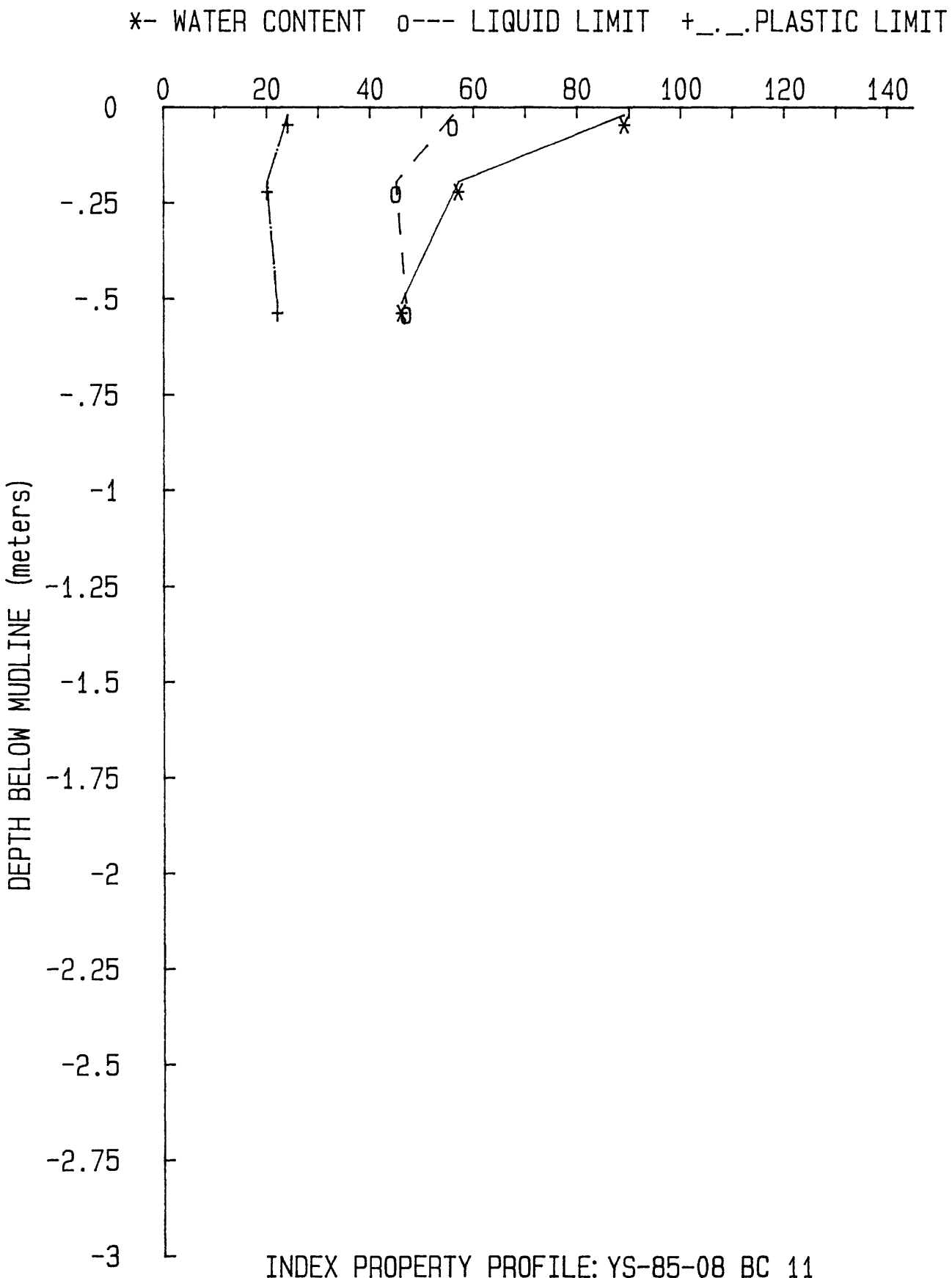
*- WATER CONTENT o--- LIQUID LIMIT +_._.PLASTIC LIMIT



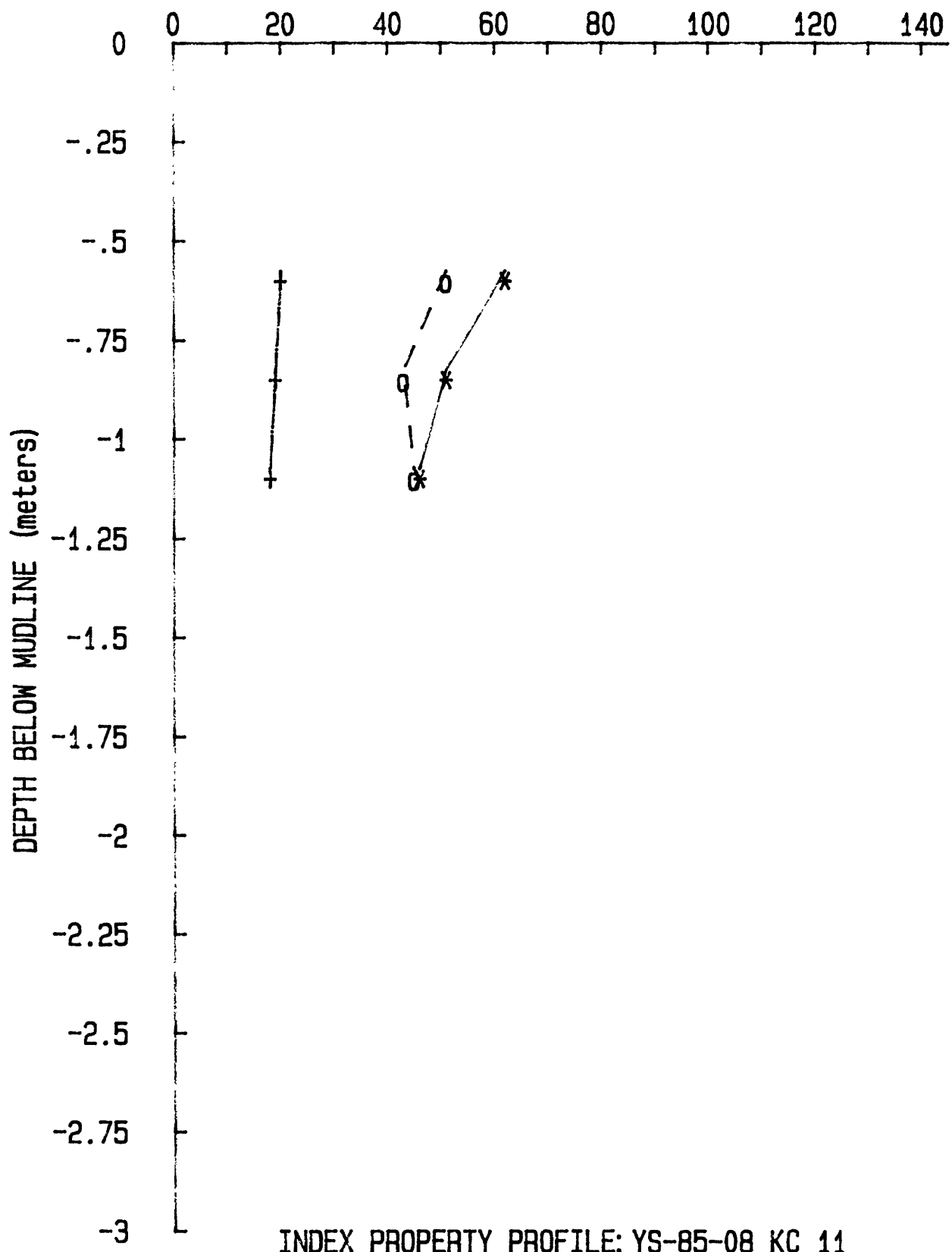


*- WATER CONTENT o--- LIQUID LIMIT +-- PLASTIC LIMIT

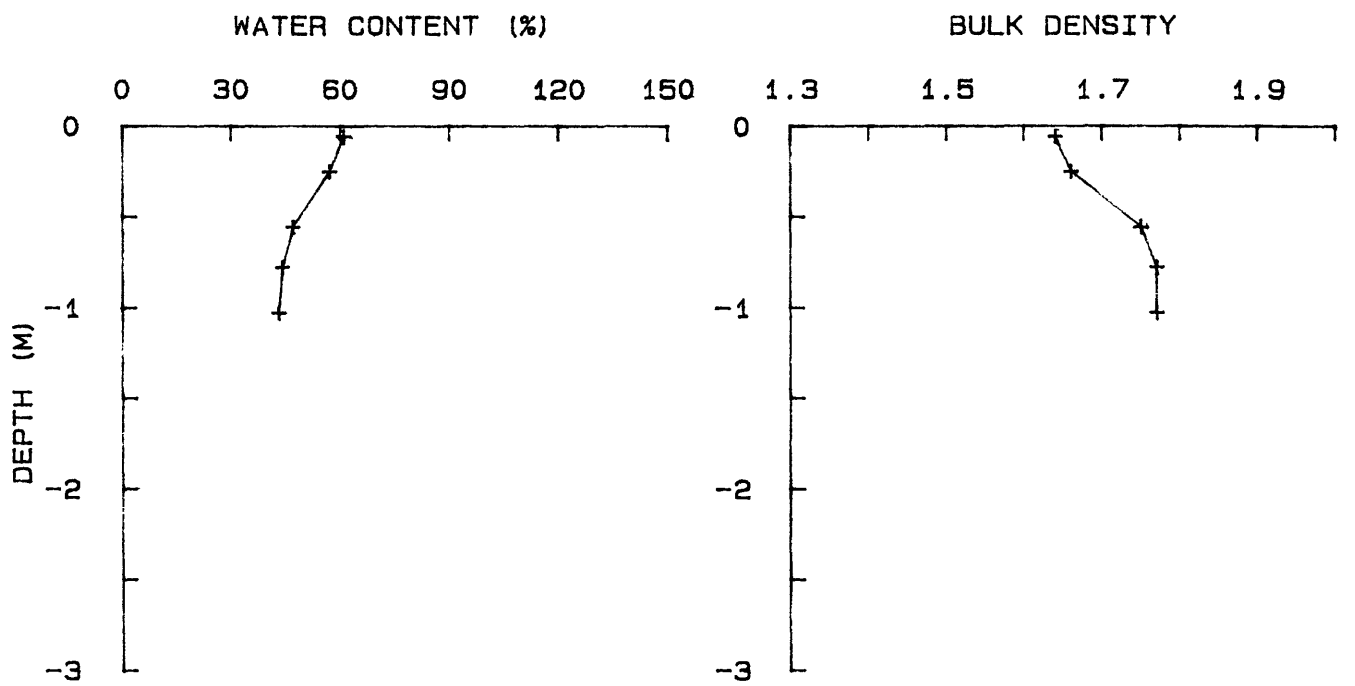




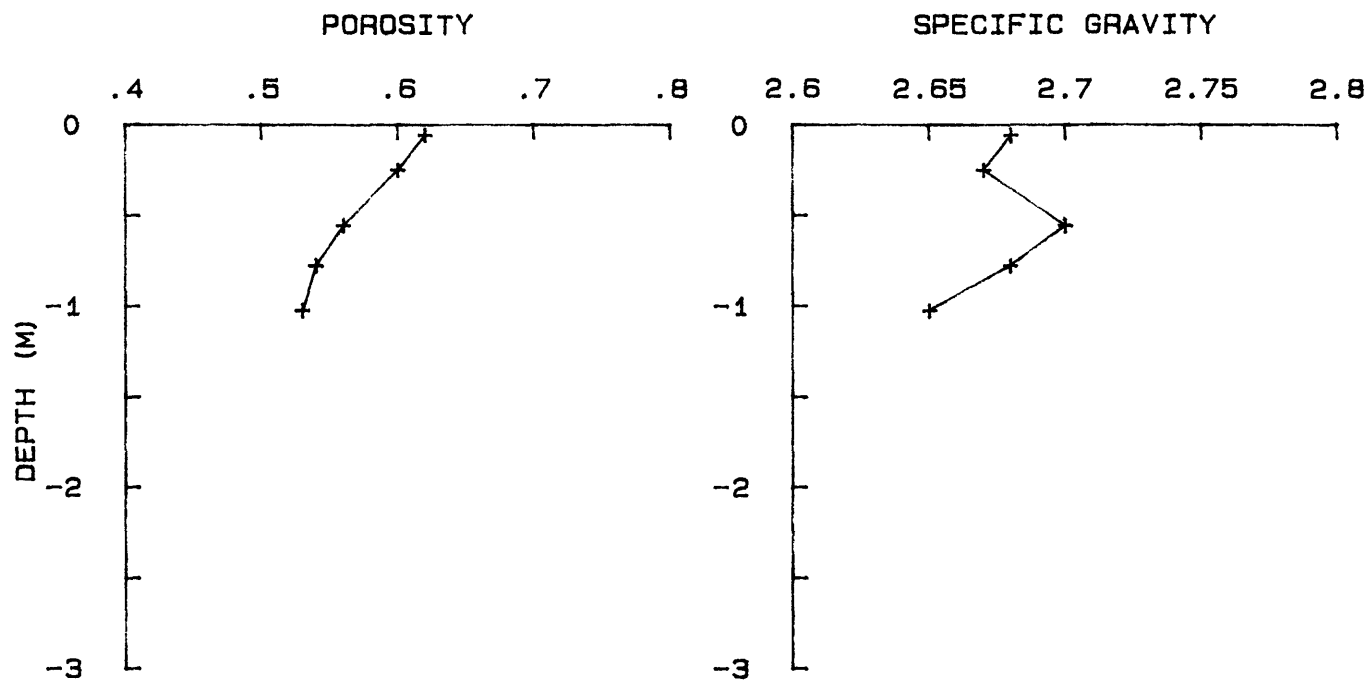
*- WATER CONTENT o--- LIQUID LIMIT +-- PLASTIC LIMIT

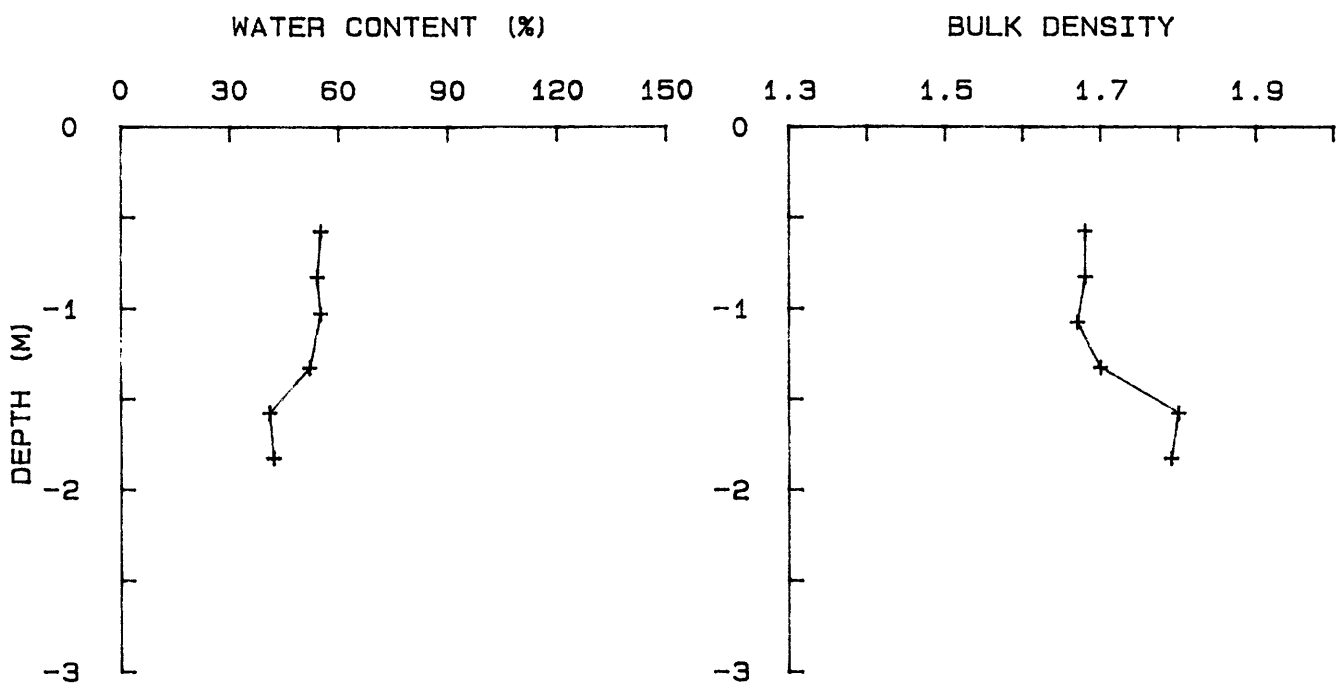


PROFILES
Water content
Bulk density
Porosity
Grain specific gravity

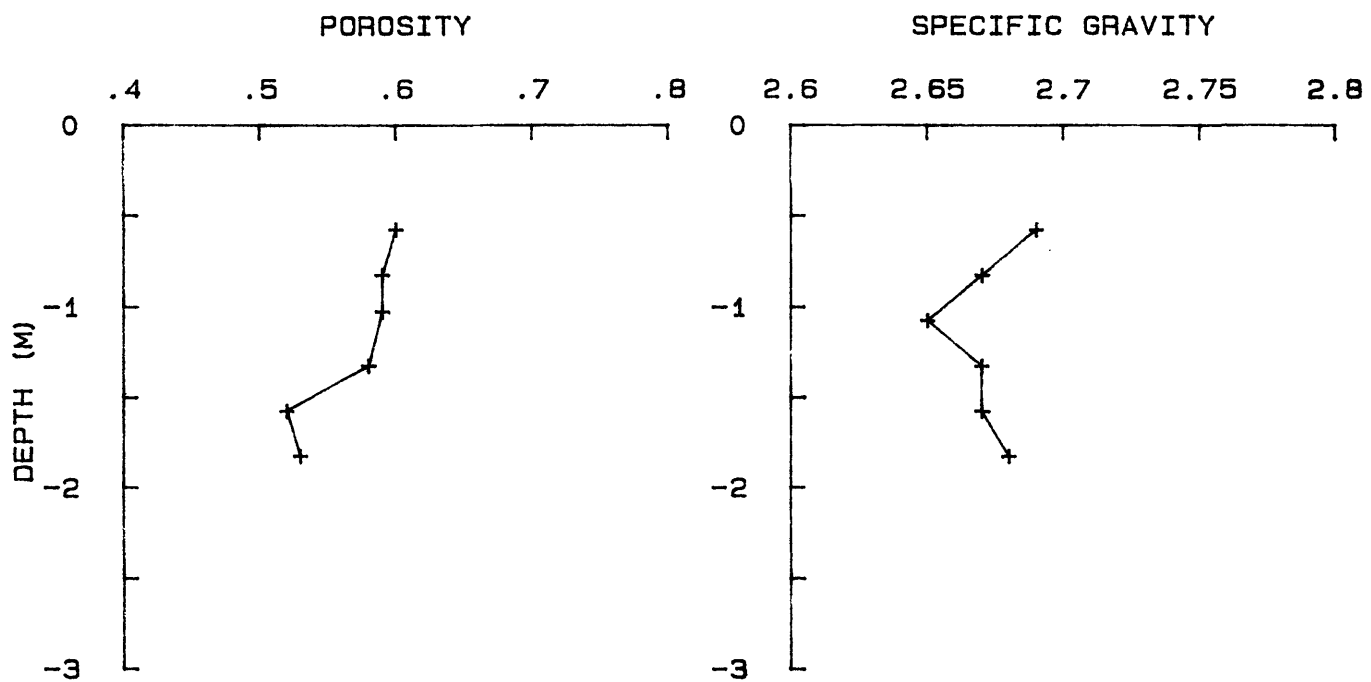


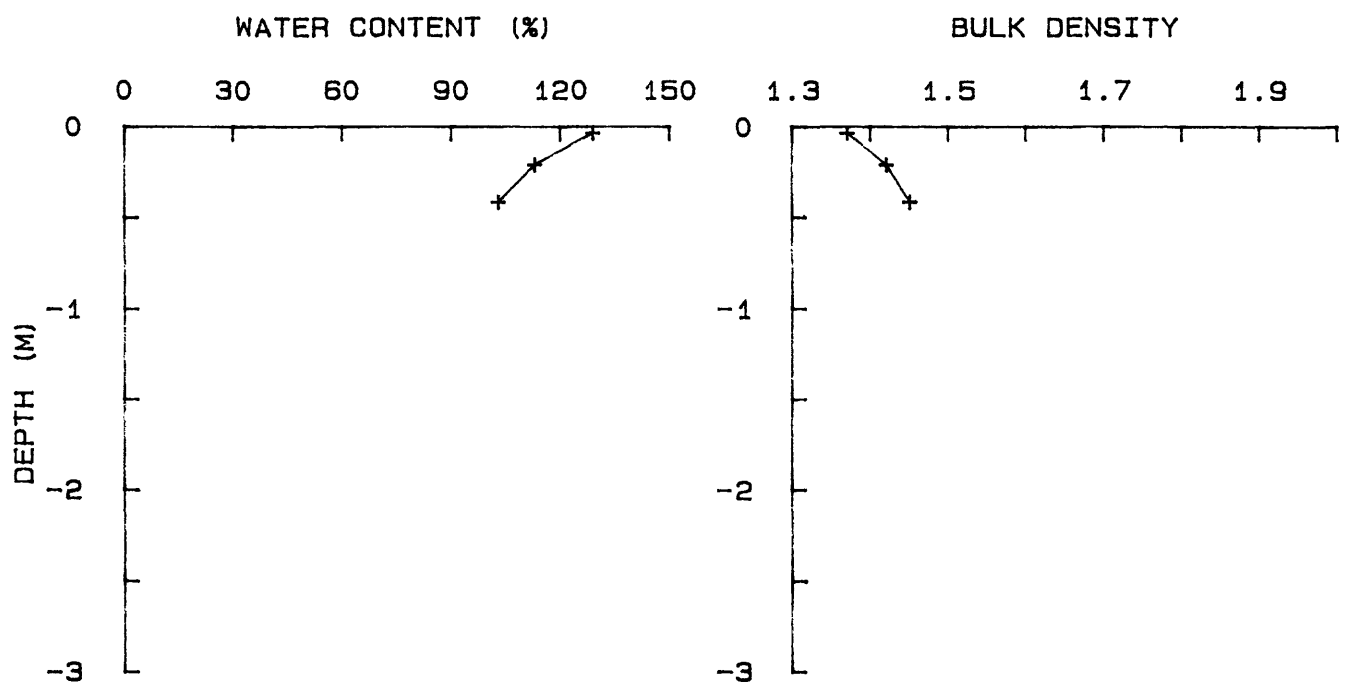
YS-85-08 KC 1A



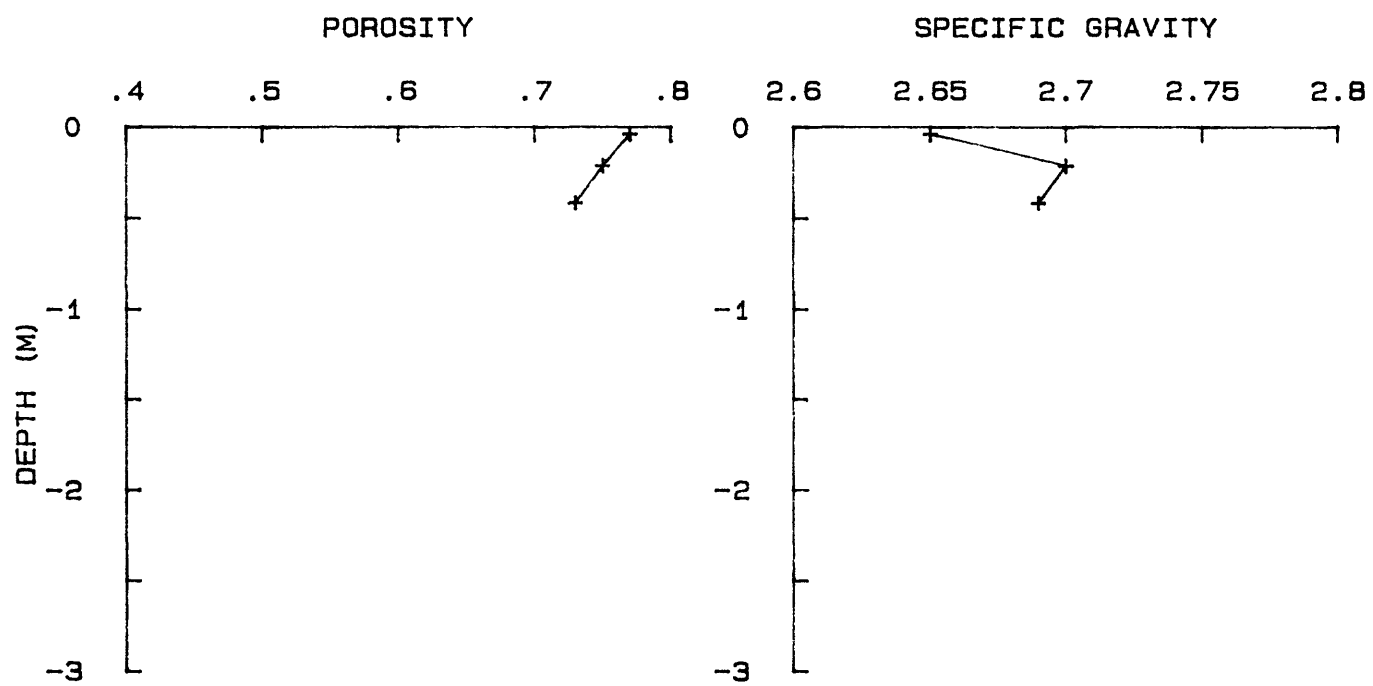


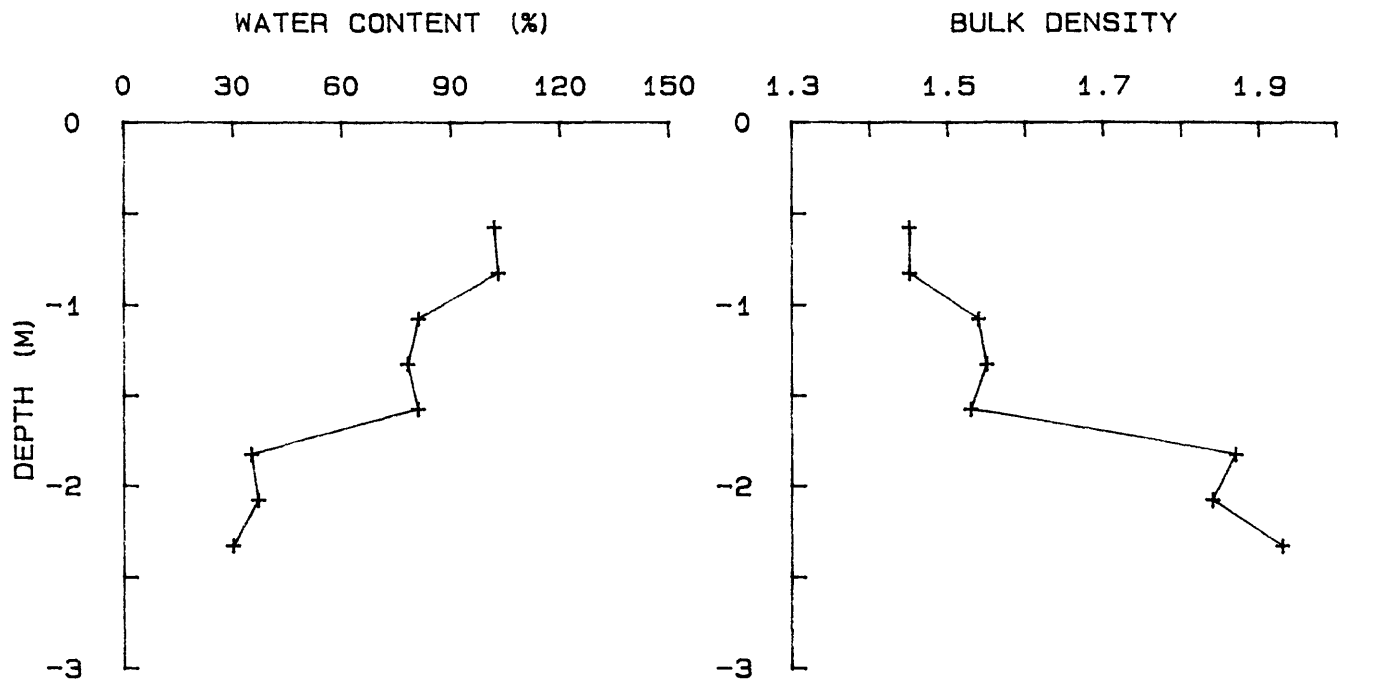
YS-85-08 KC 1B



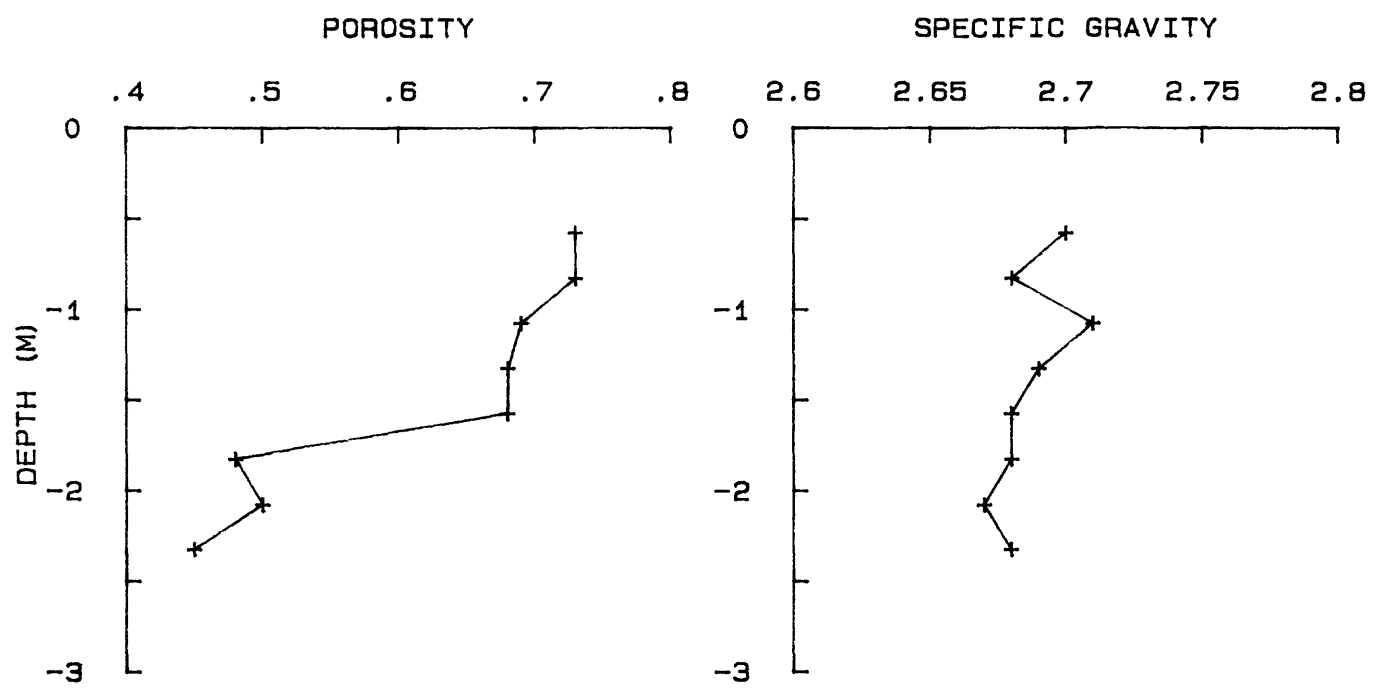


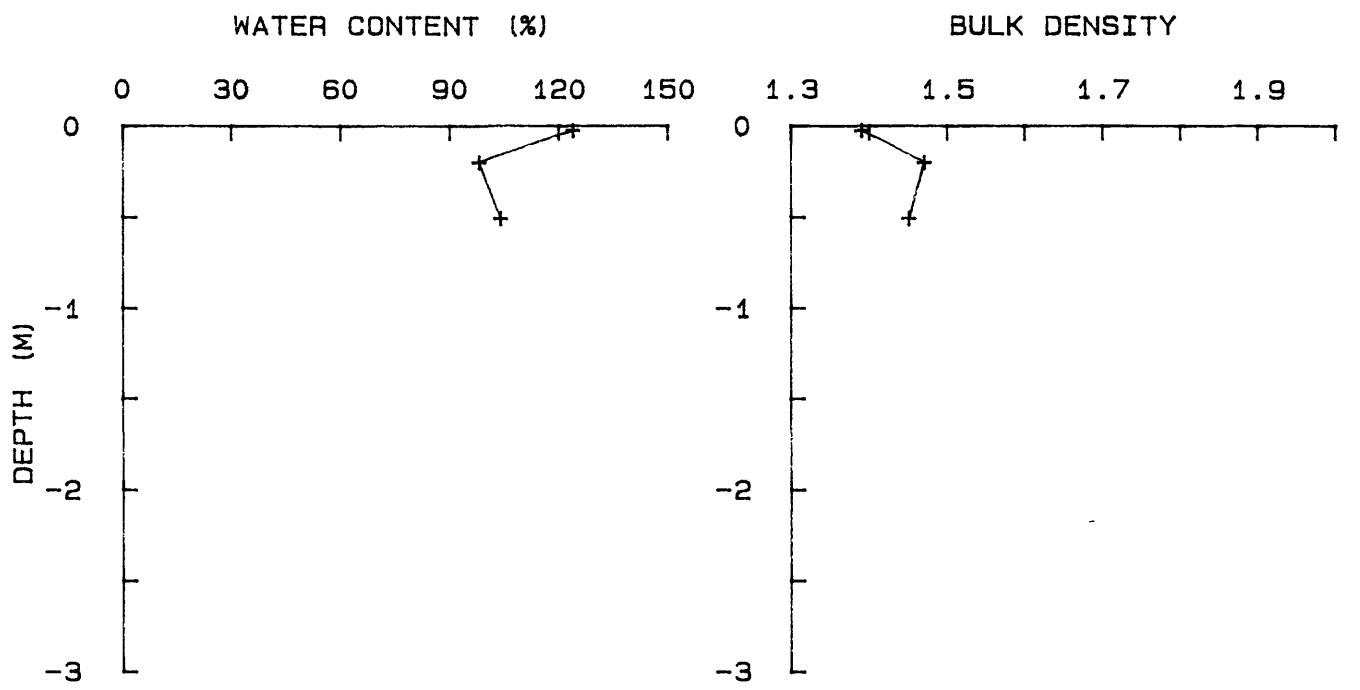
YS-85-08 BC 4



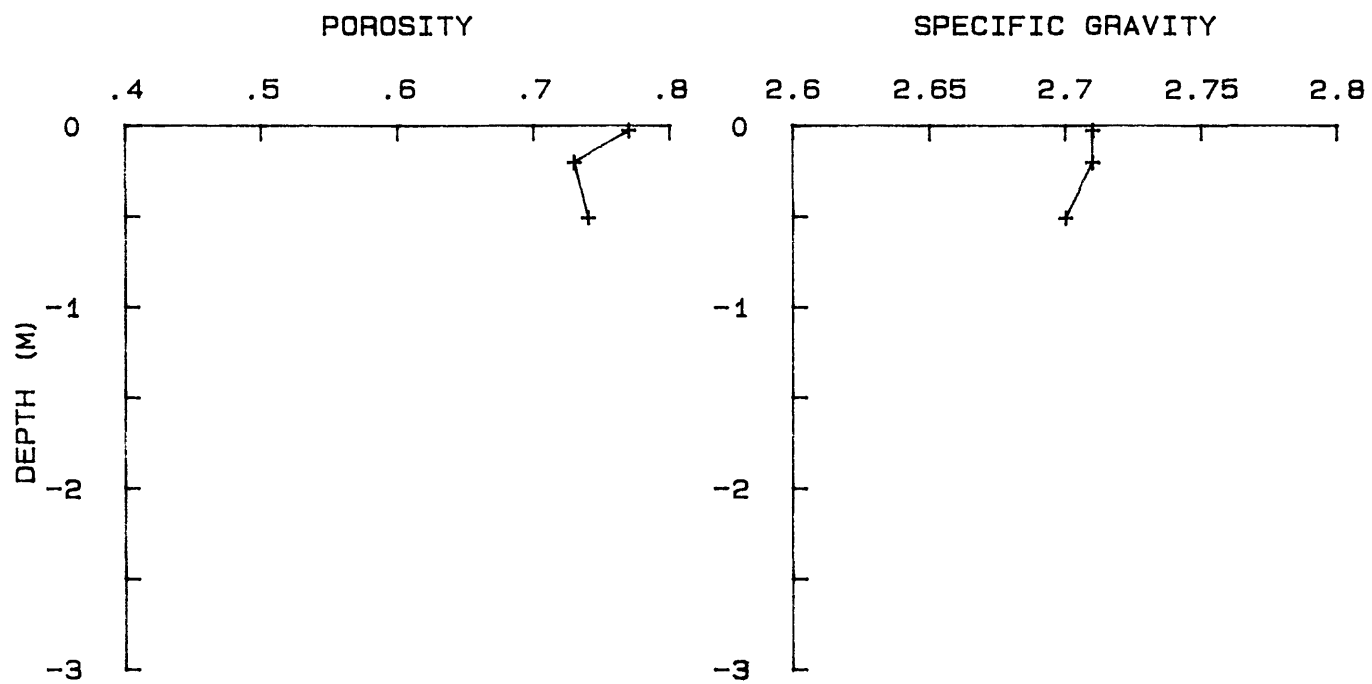


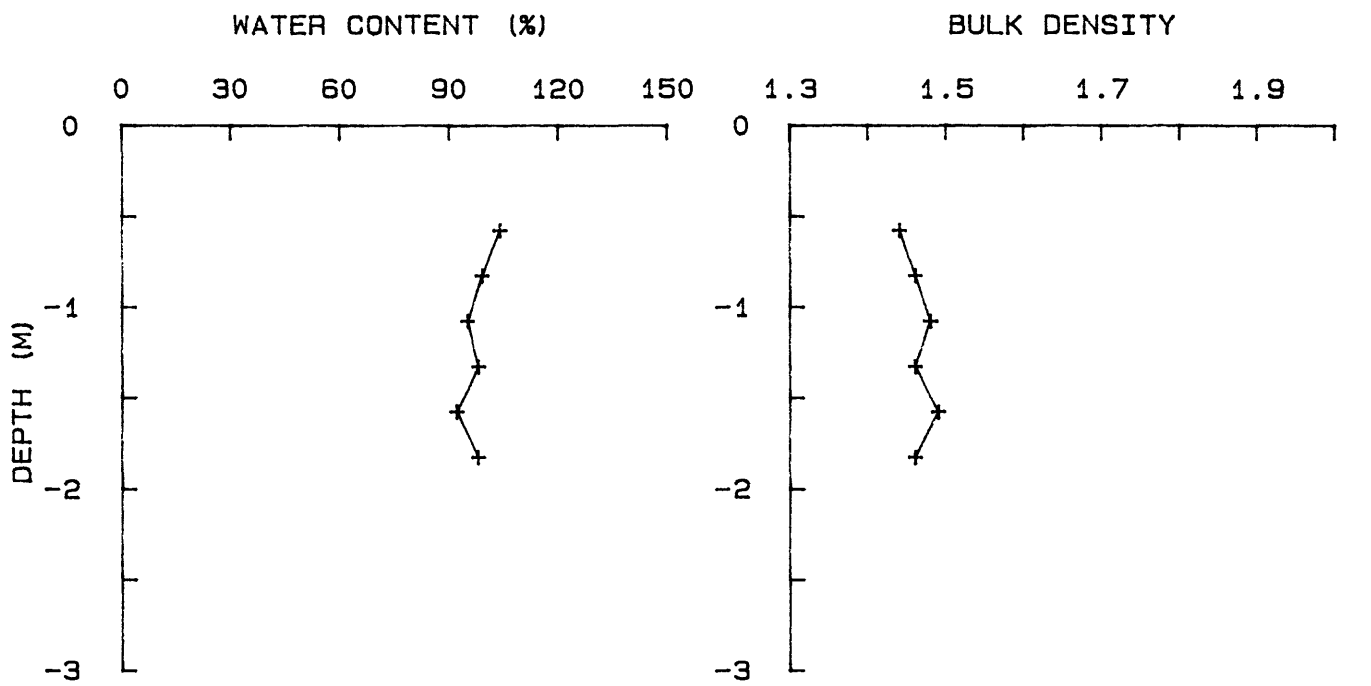
YS-85-08 KC 4



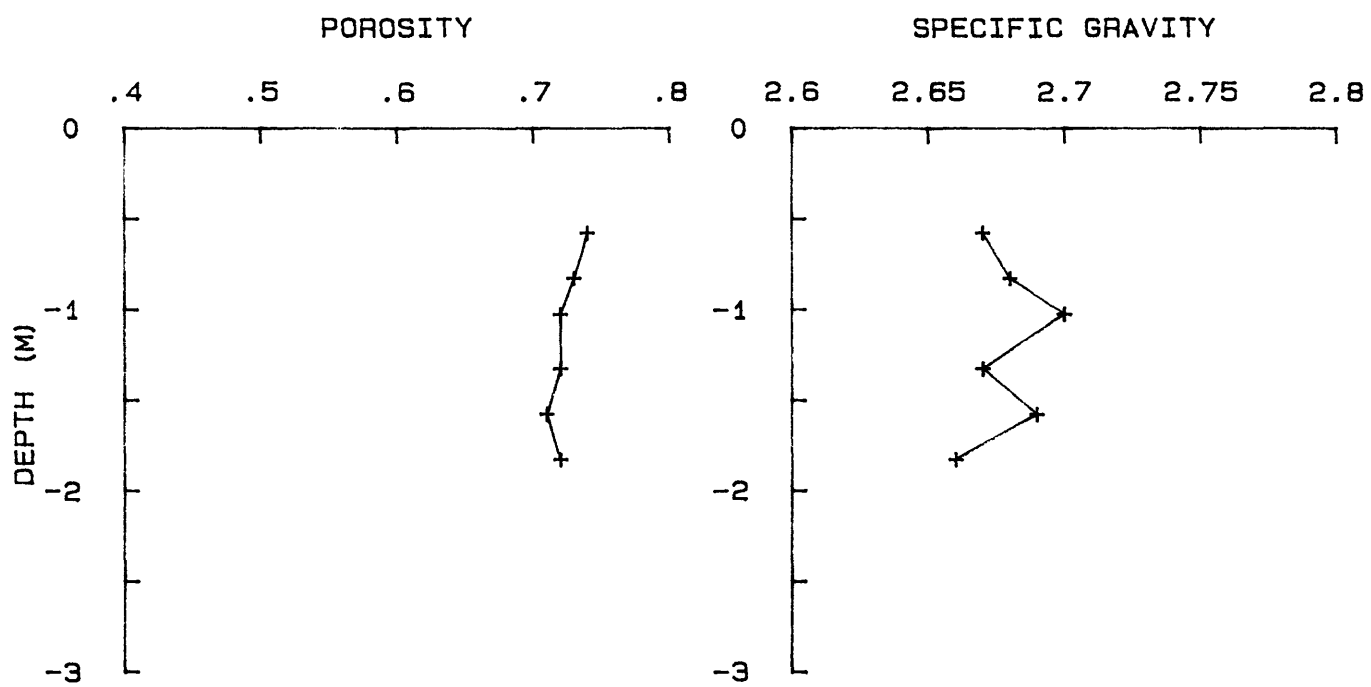


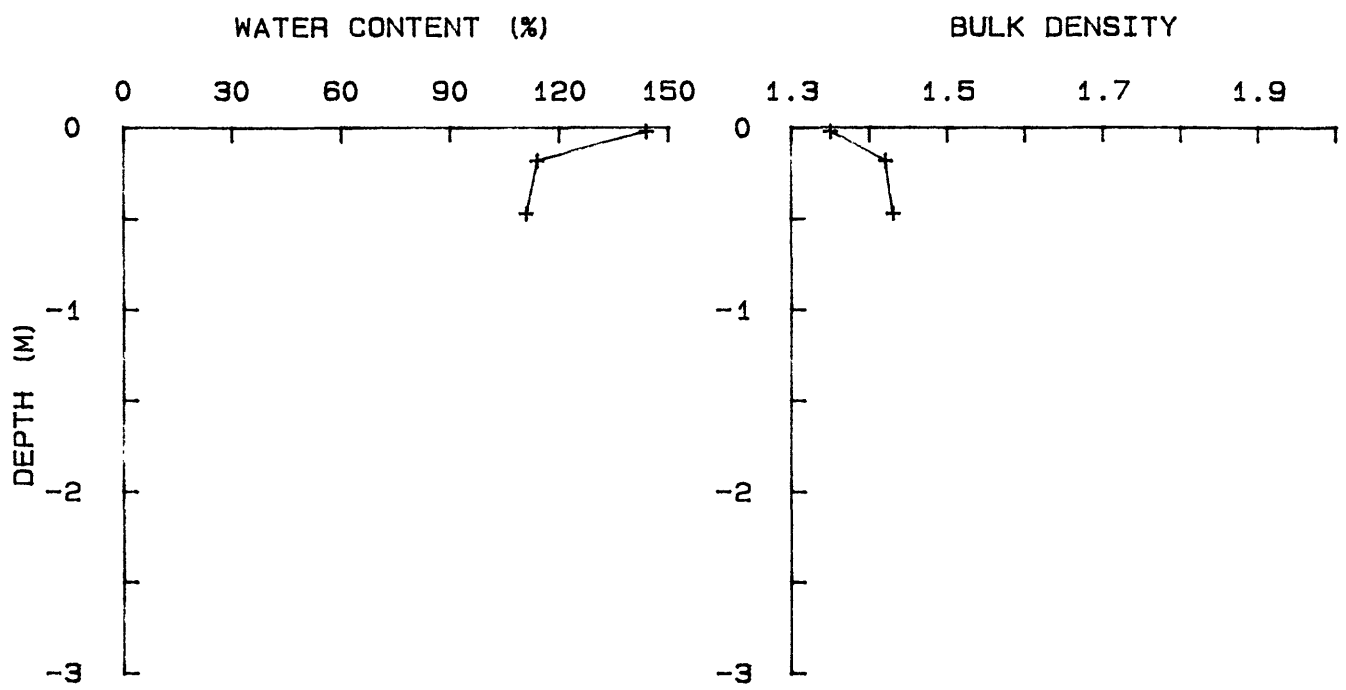
YS-85-08 BC 5



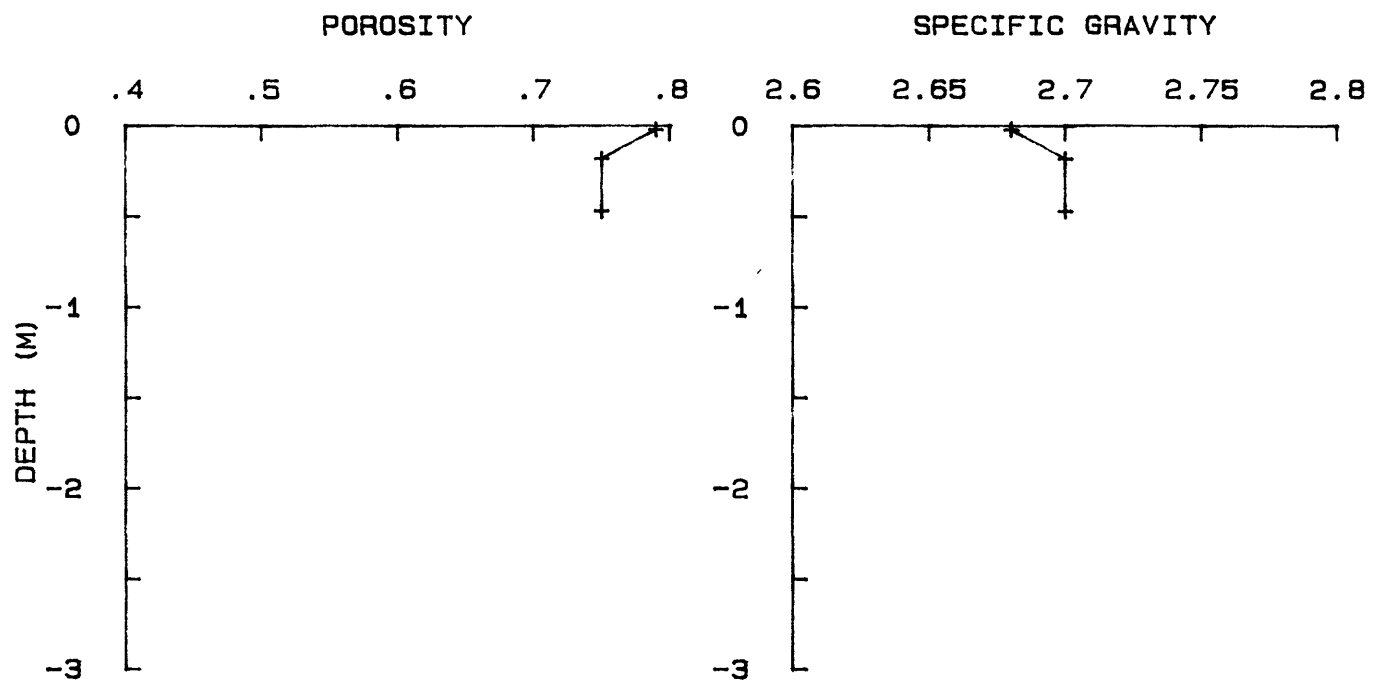


YS-85-08 KC 5

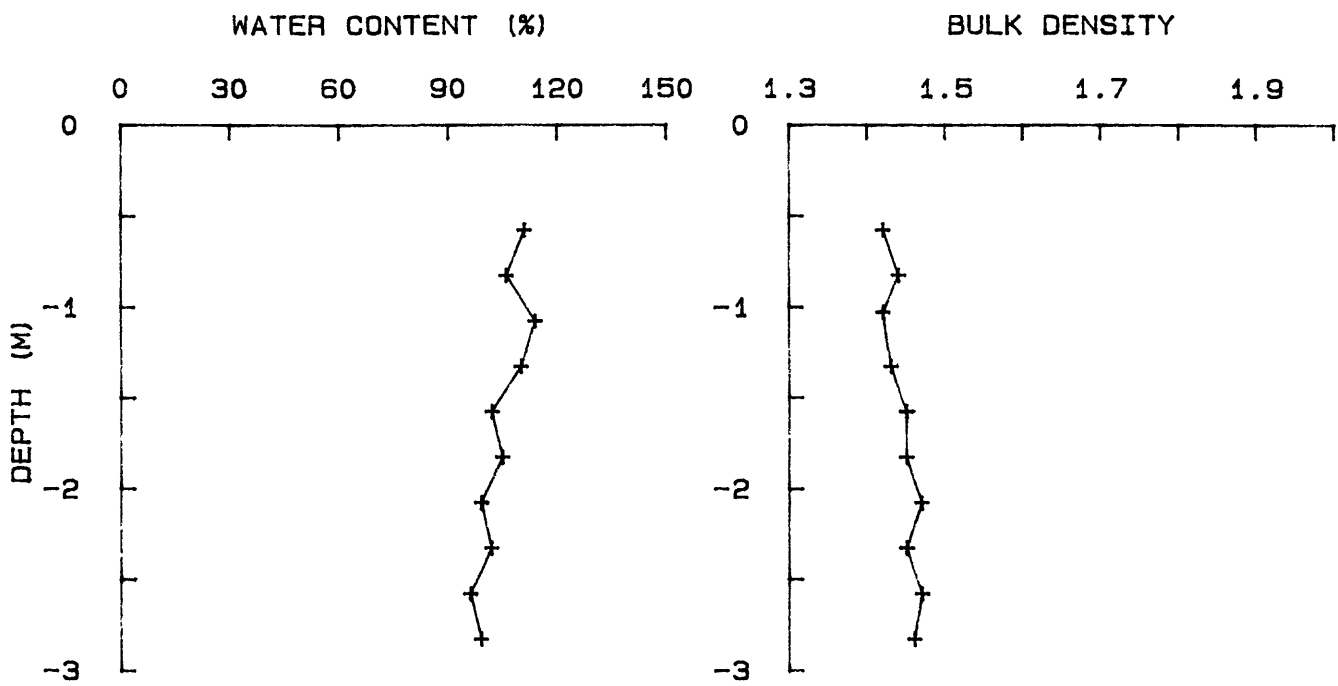




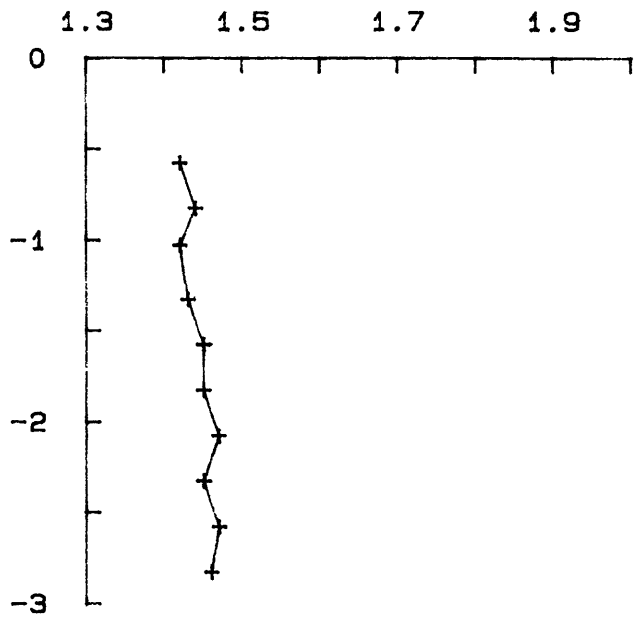
YS-85-08 BC 6



WATER CONTENT (%)

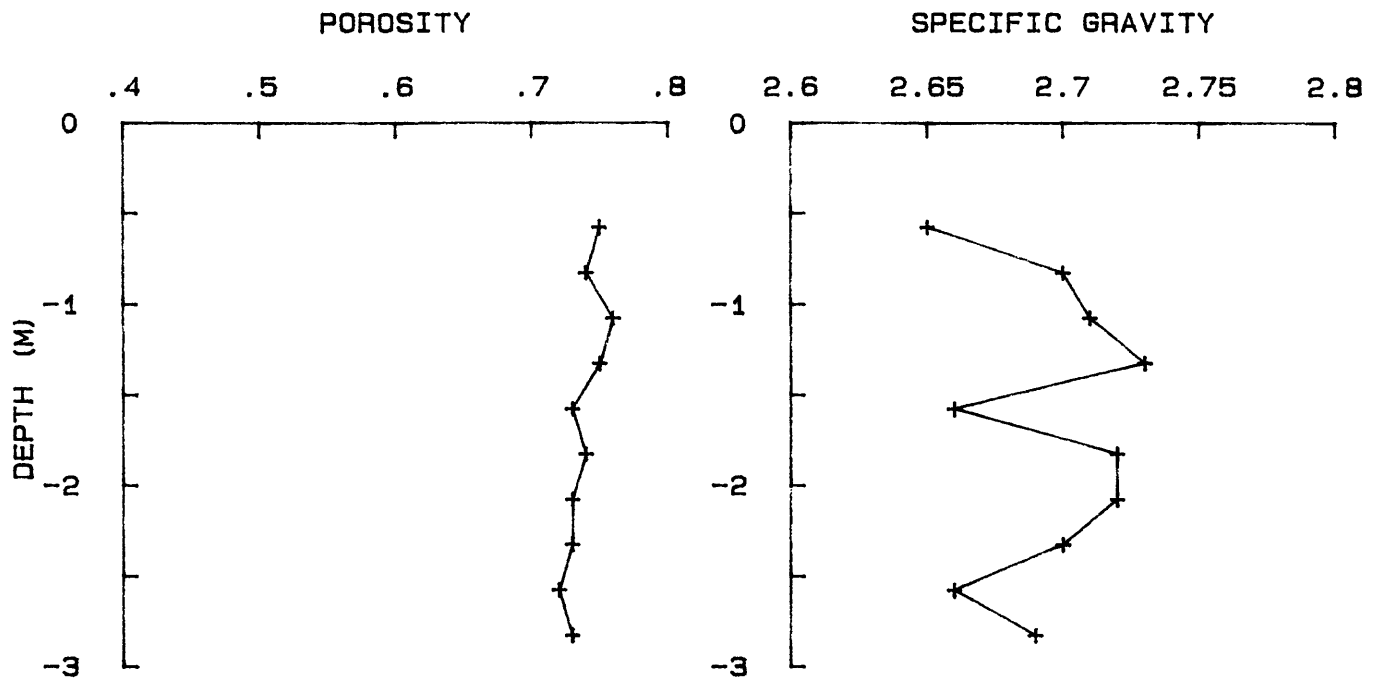


BULK DENSITY

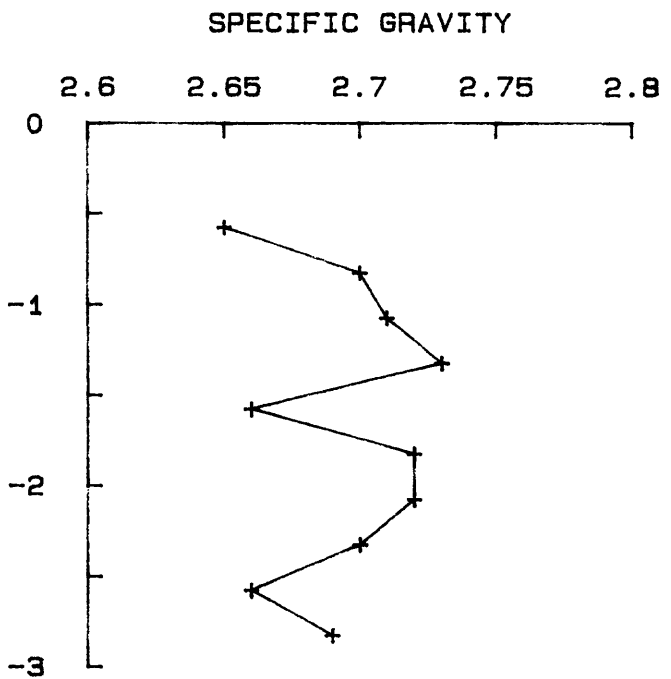


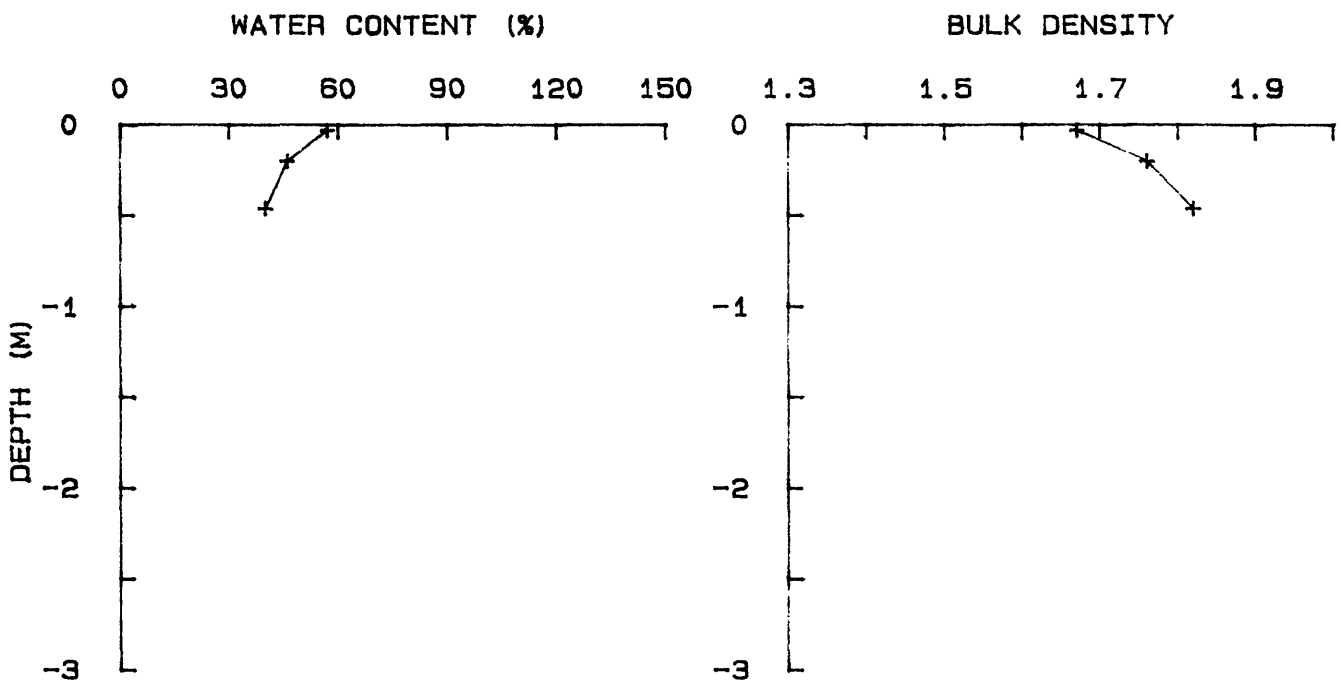
YS-85-08 KC 6

POROSITY

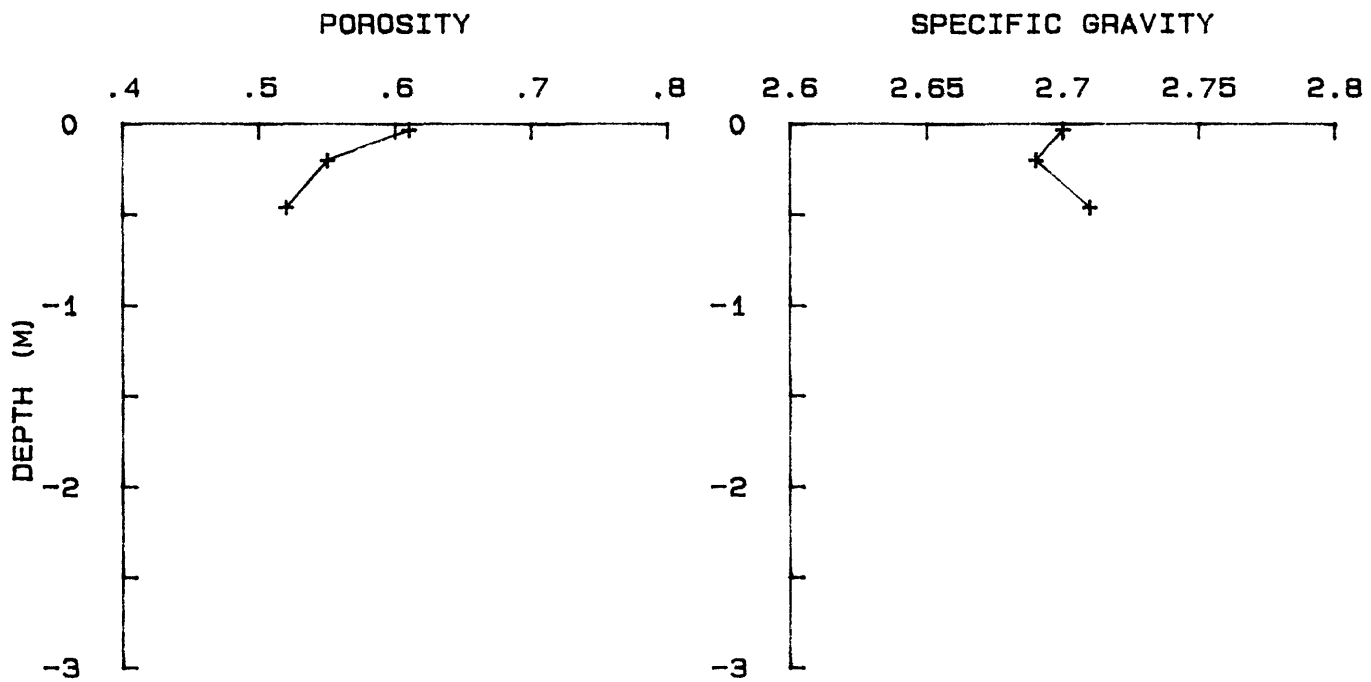


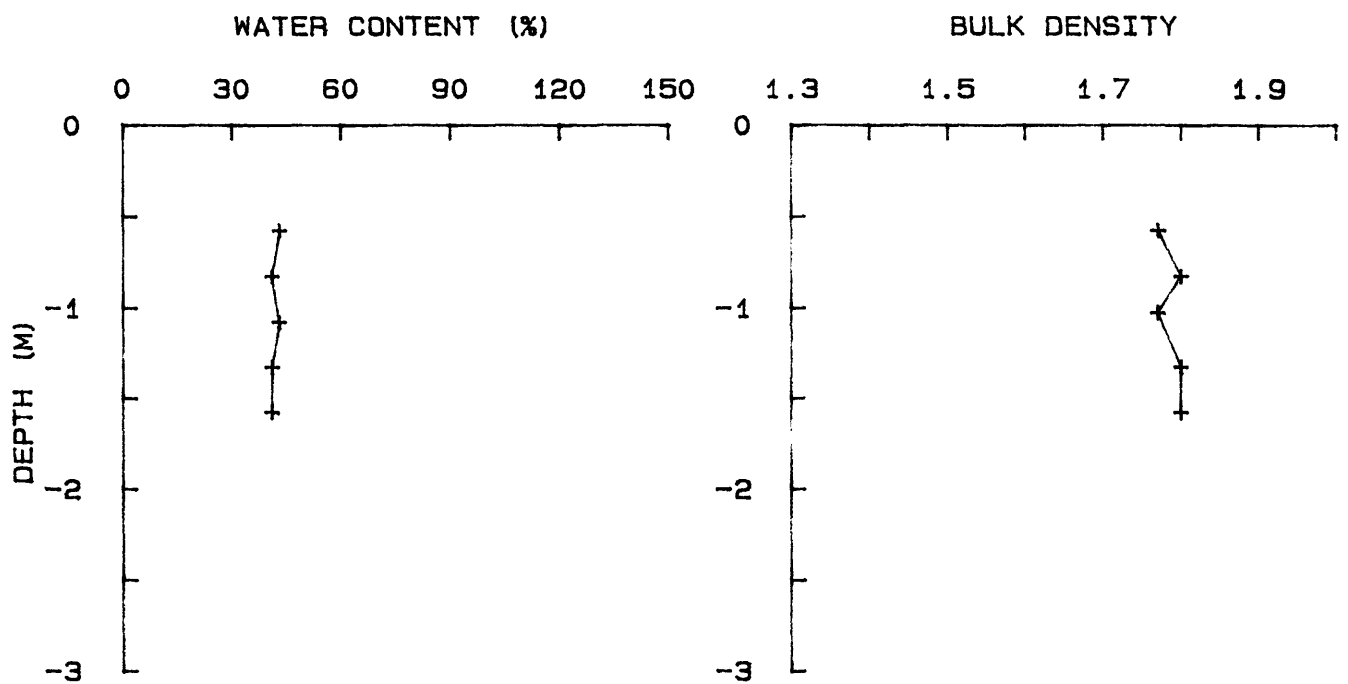
SPECIFIC GRAVITY



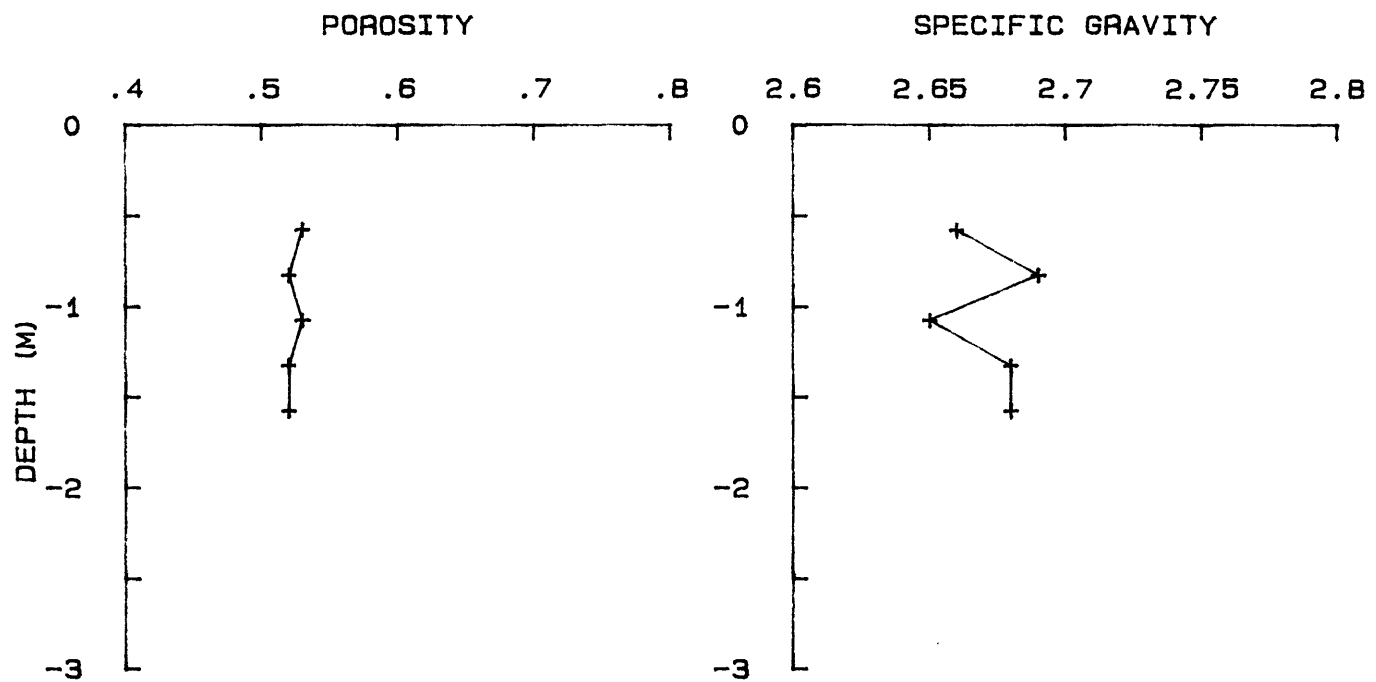


YS-85-08 BC 7

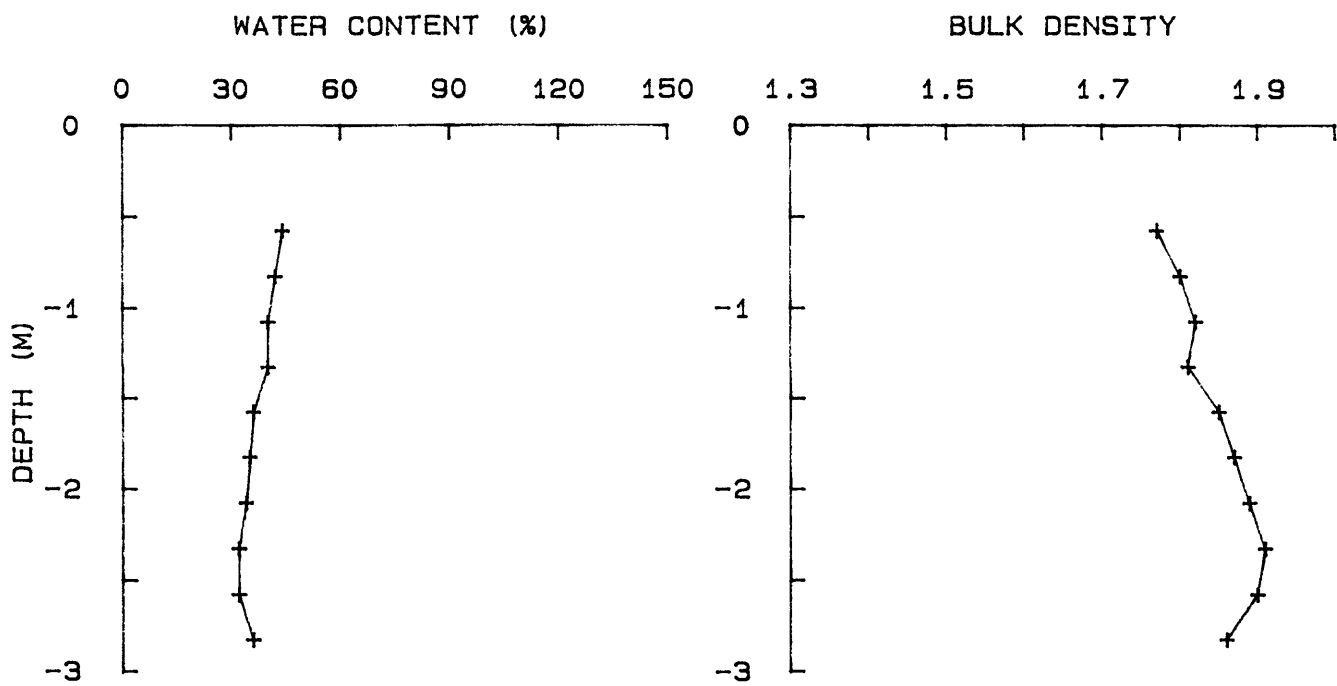




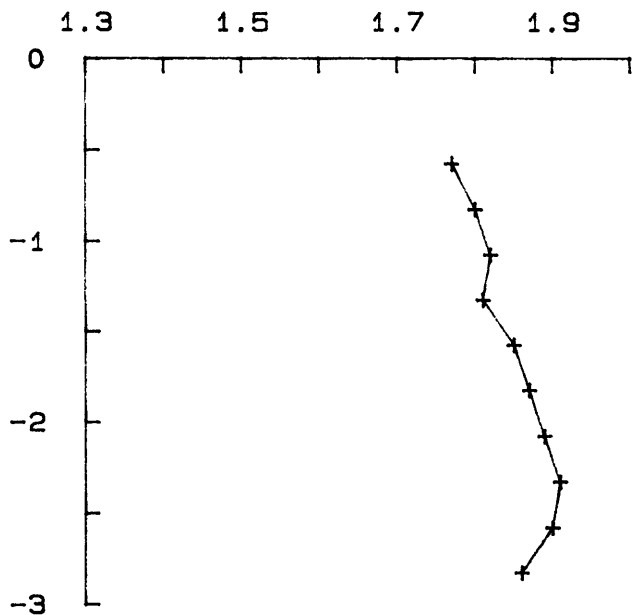
YS-85-08 KC 7A



WATER CONTENT (%)

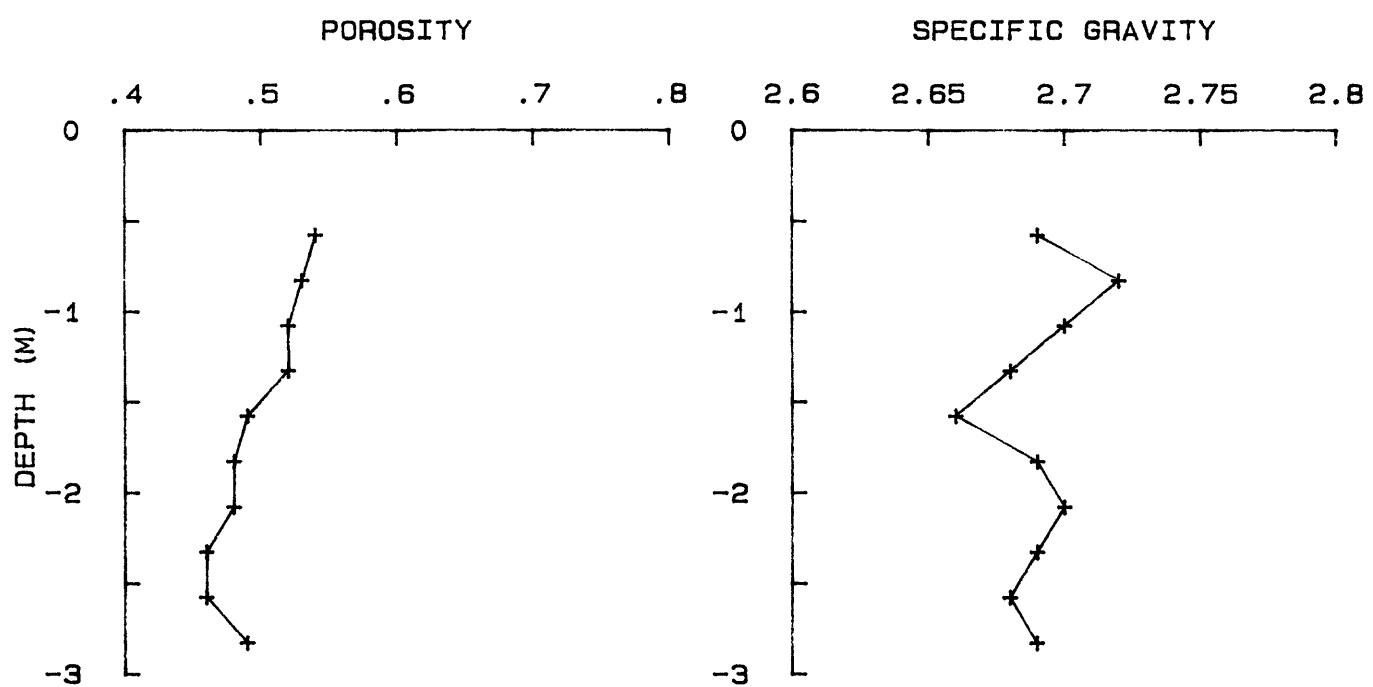


BULK DENSITY

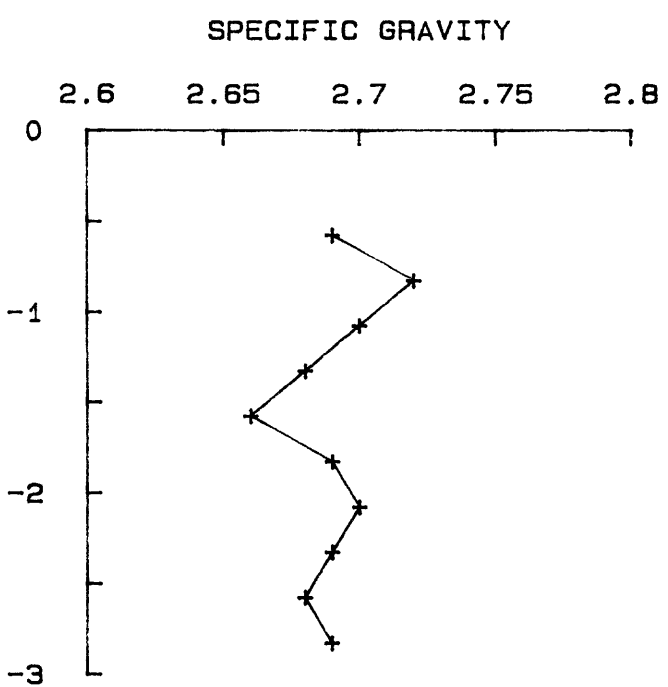


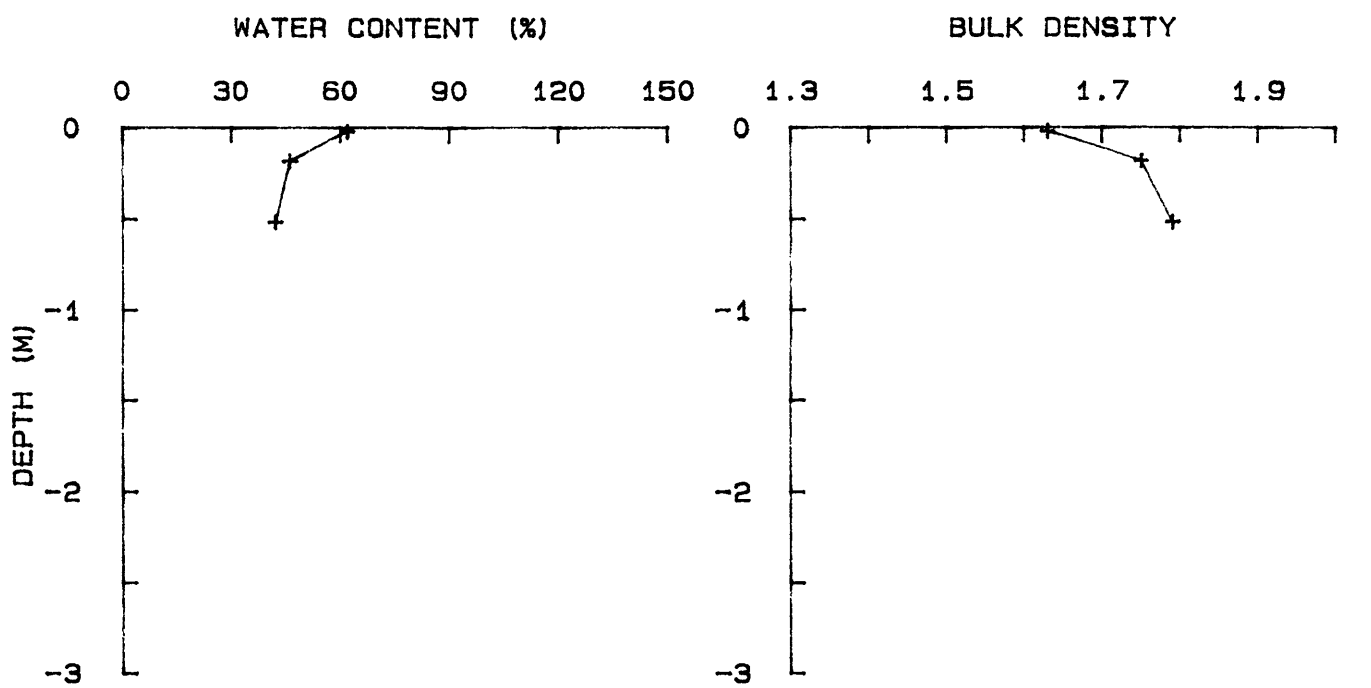
YS-85-08 KC 7B

POROSITY

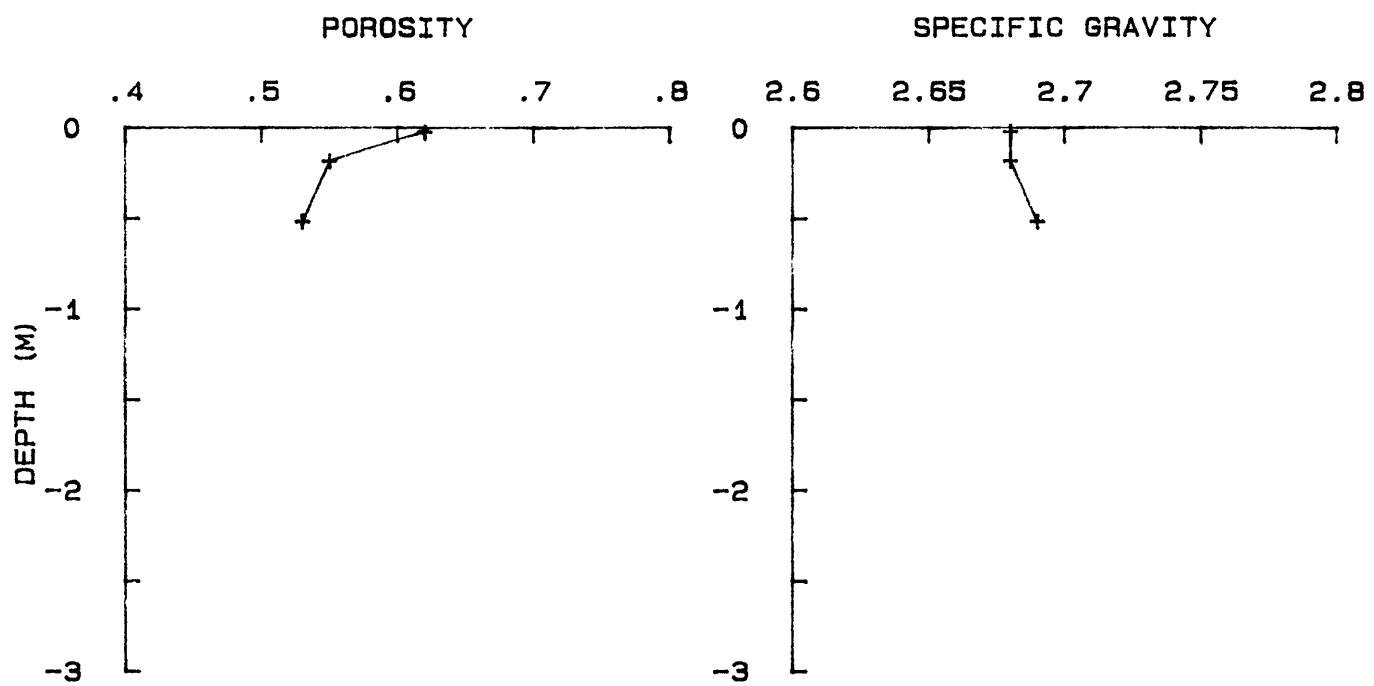


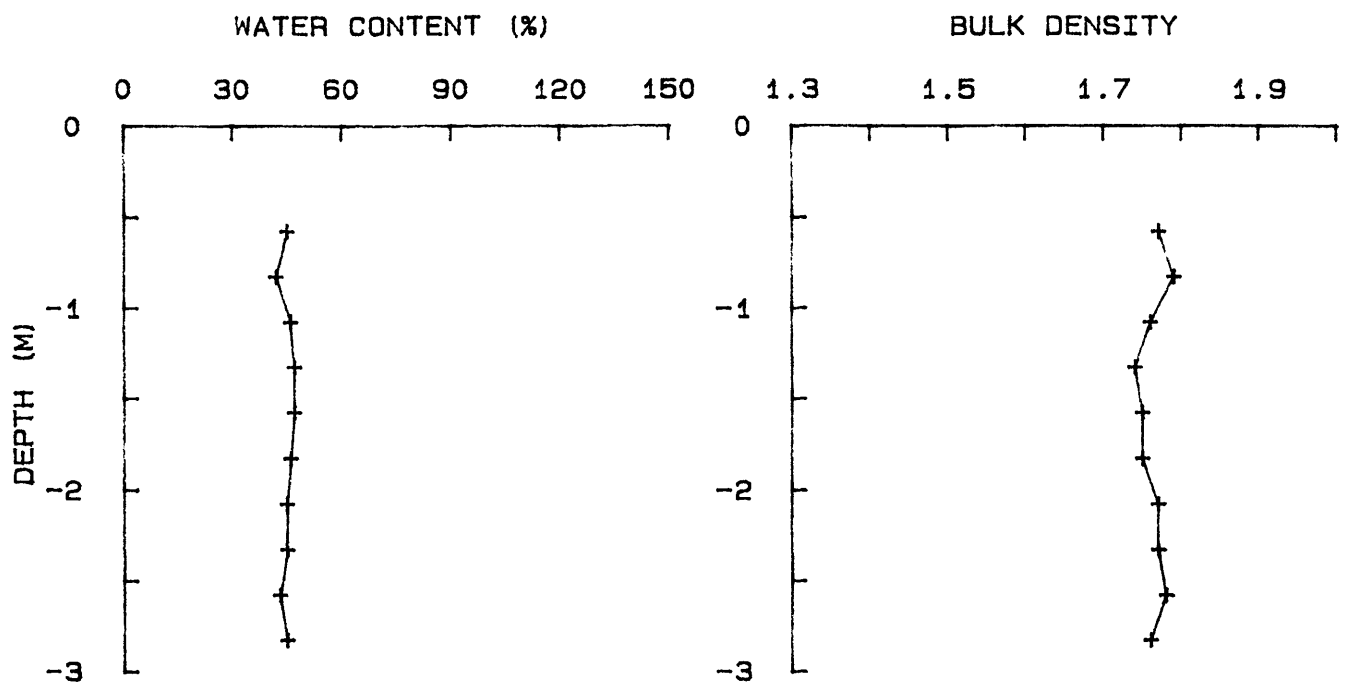
SPECIFIC GRAVITY



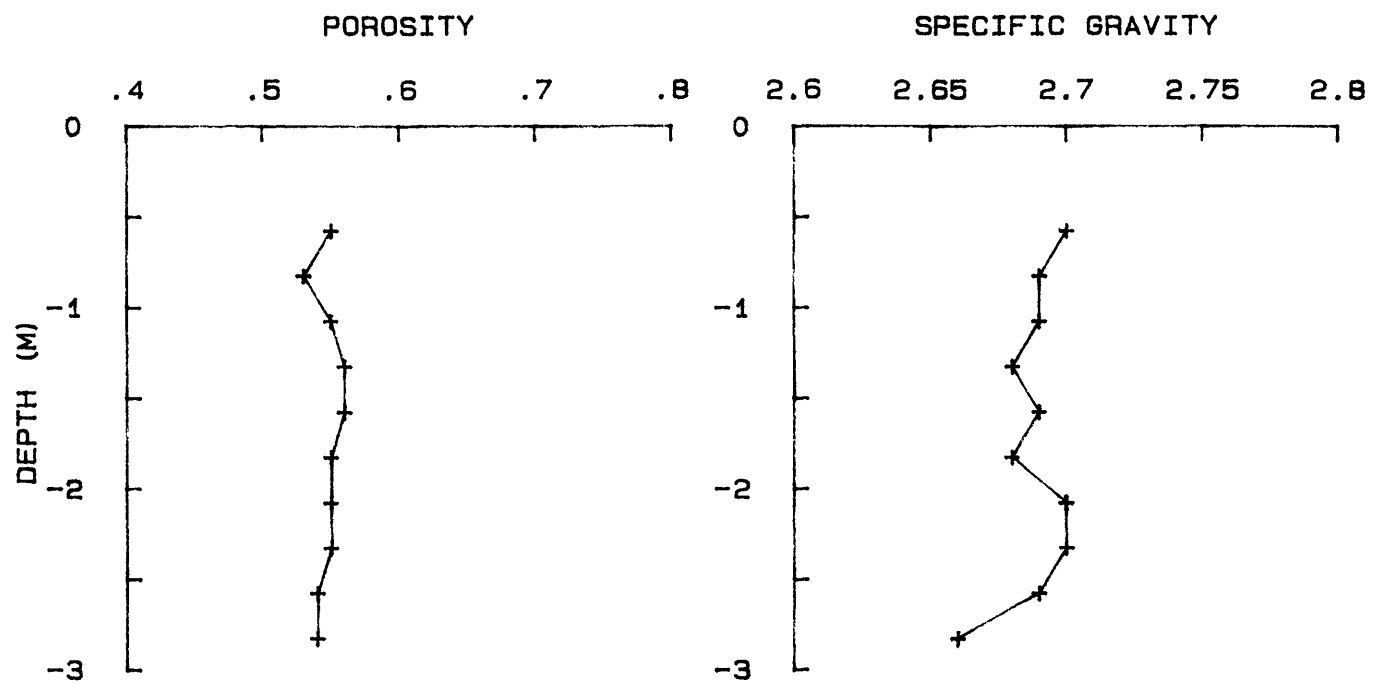


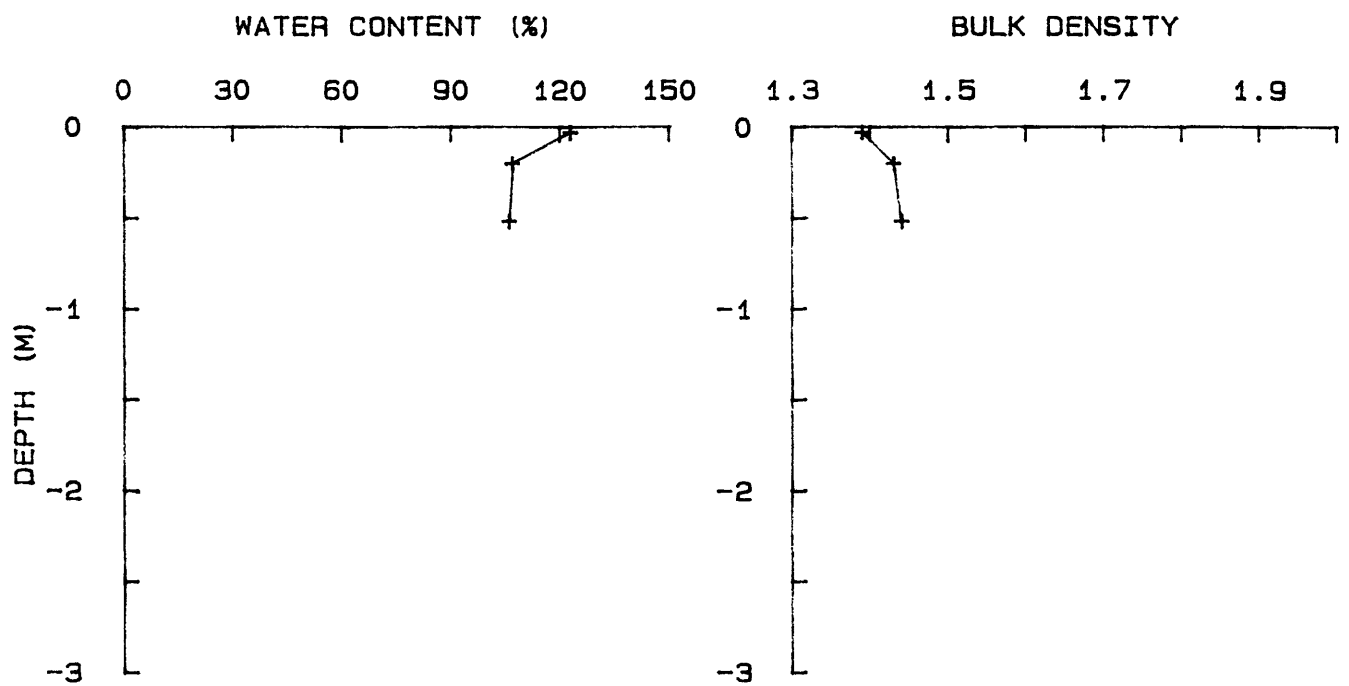
YS-85-08 BC 8



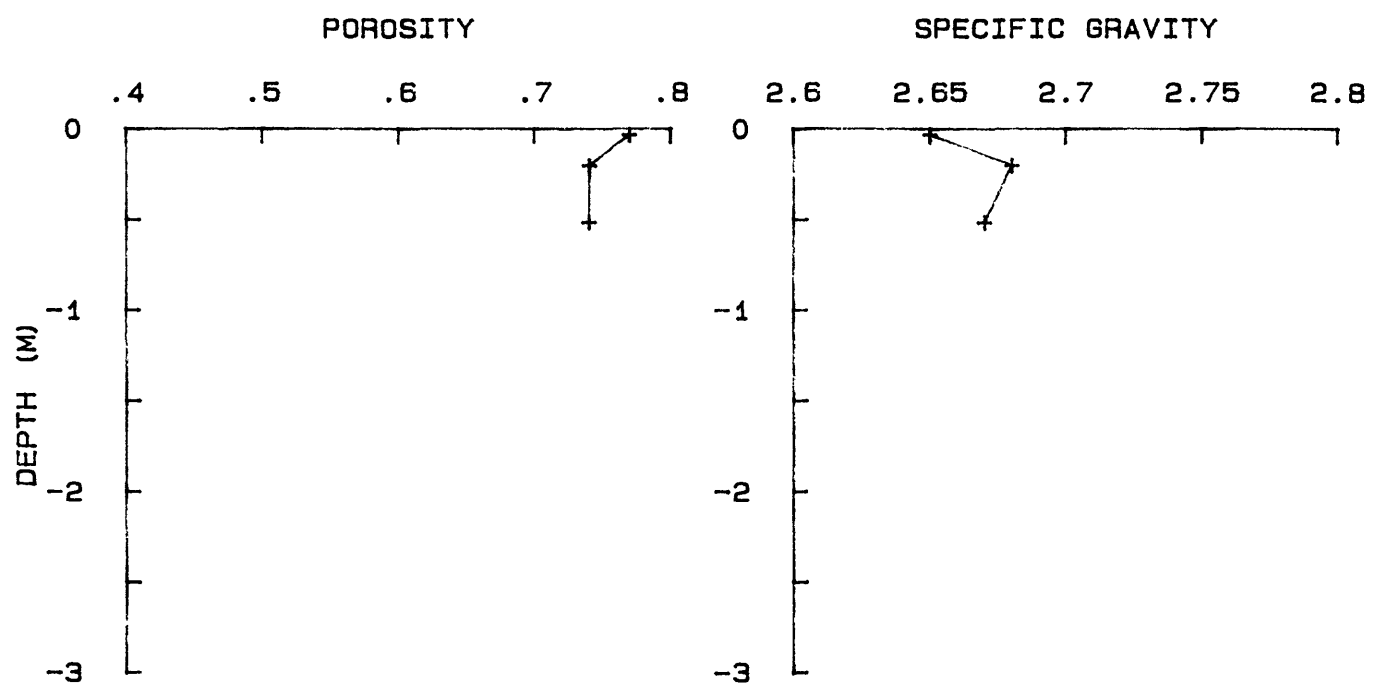


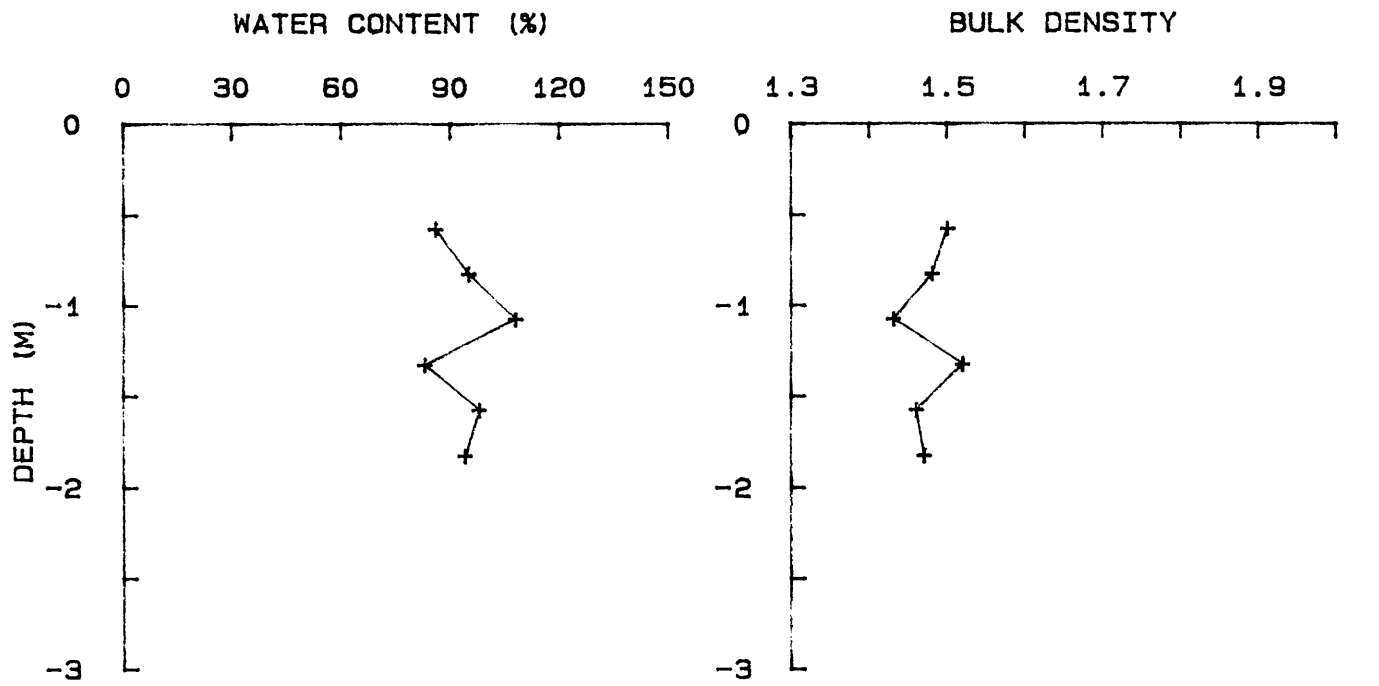
YS-85-08 KC 8



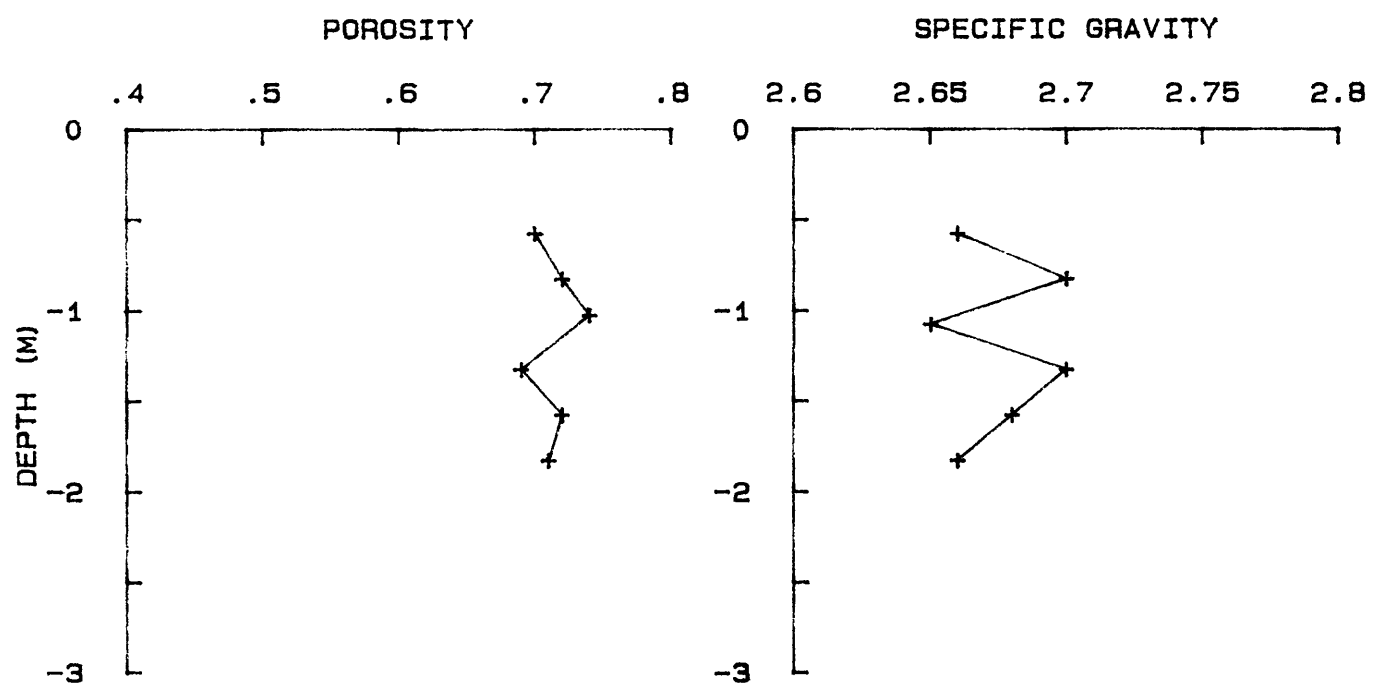


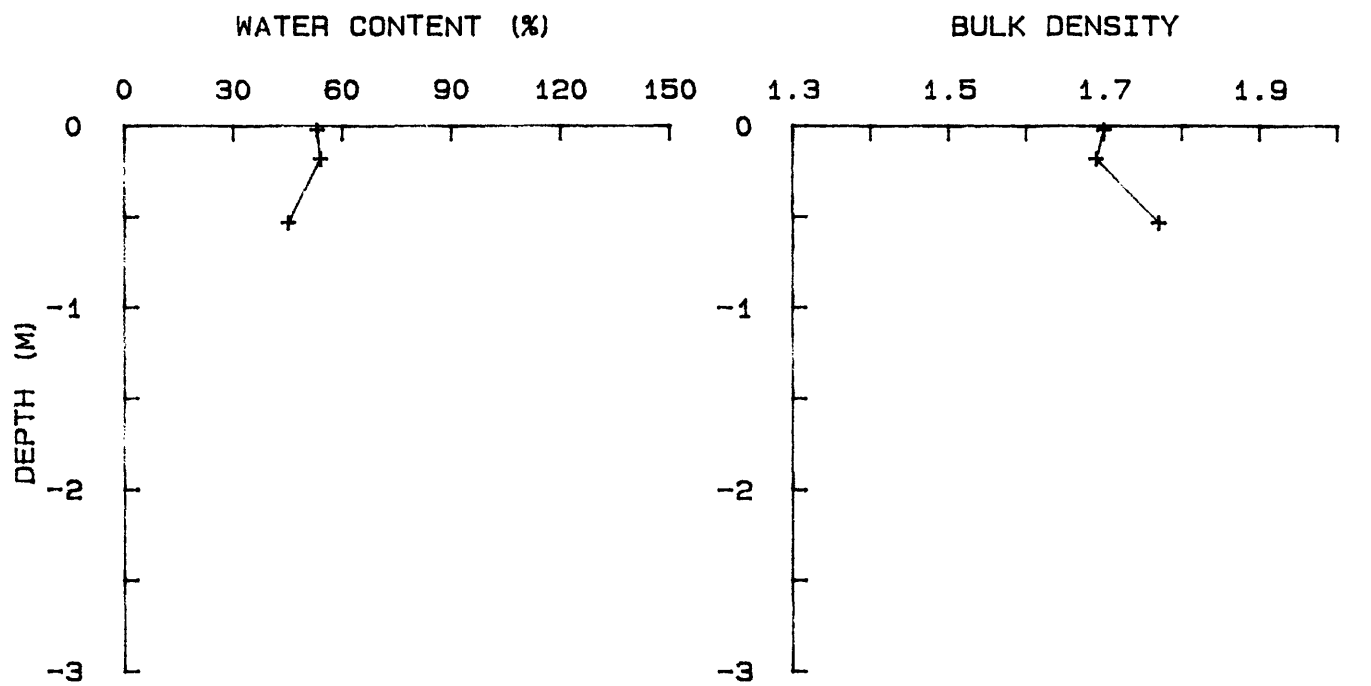
YS-85-08 BC 9



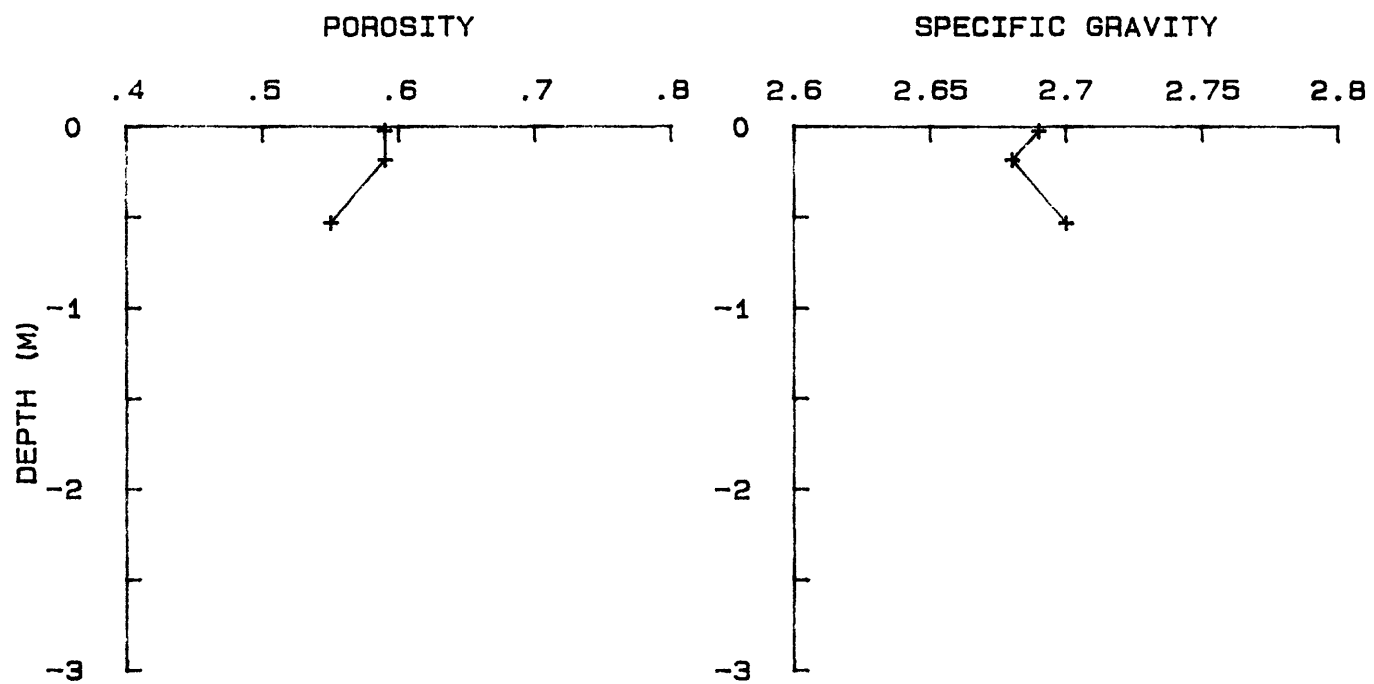


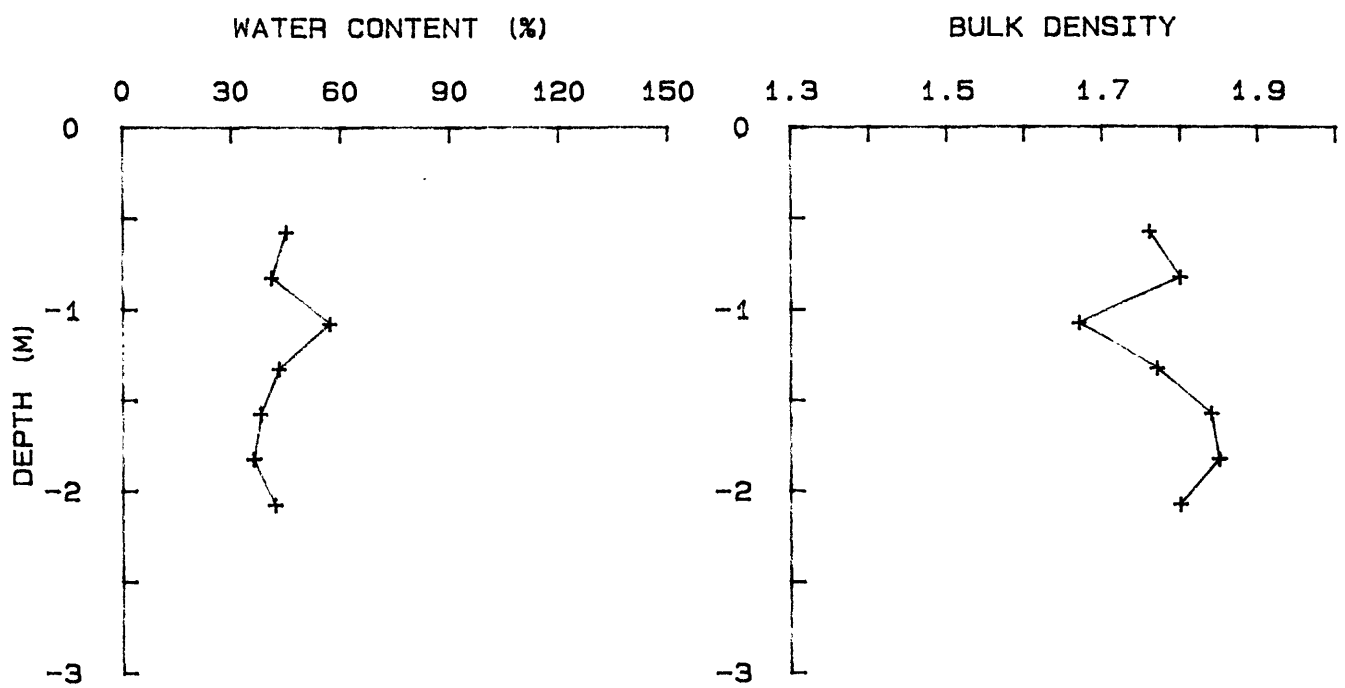
YS-85-08 KC 9



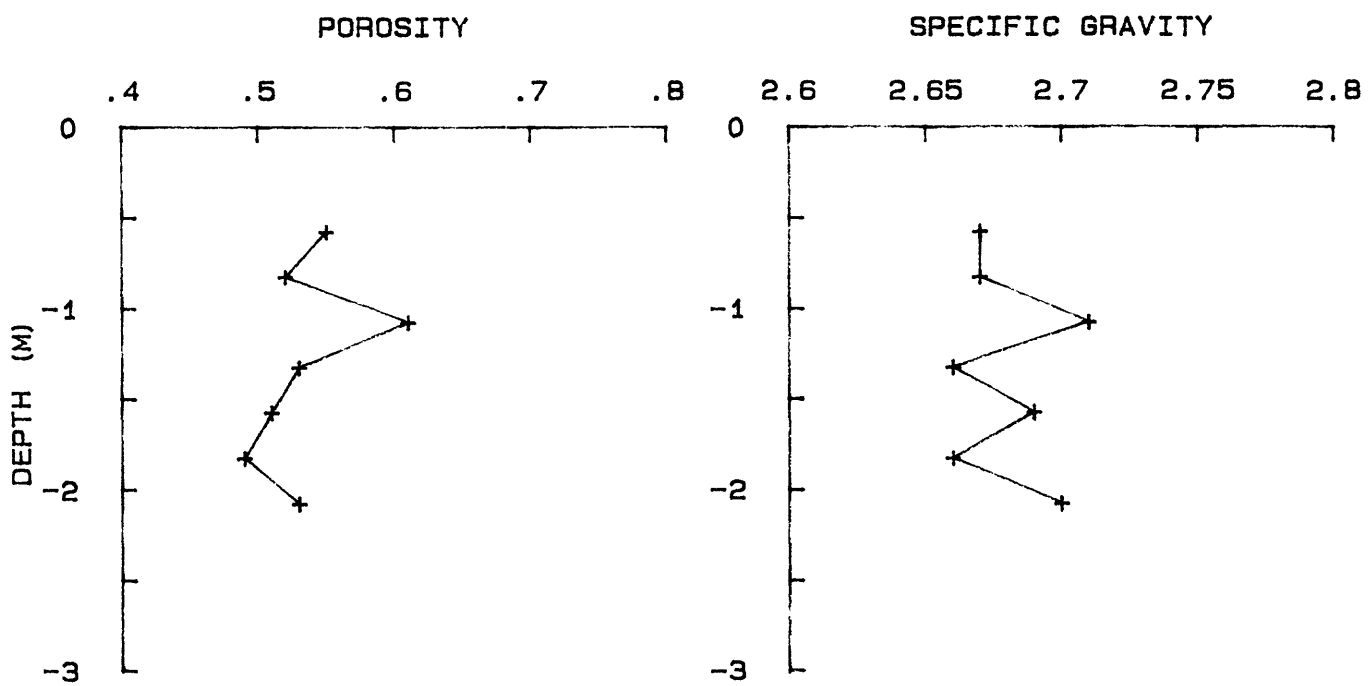


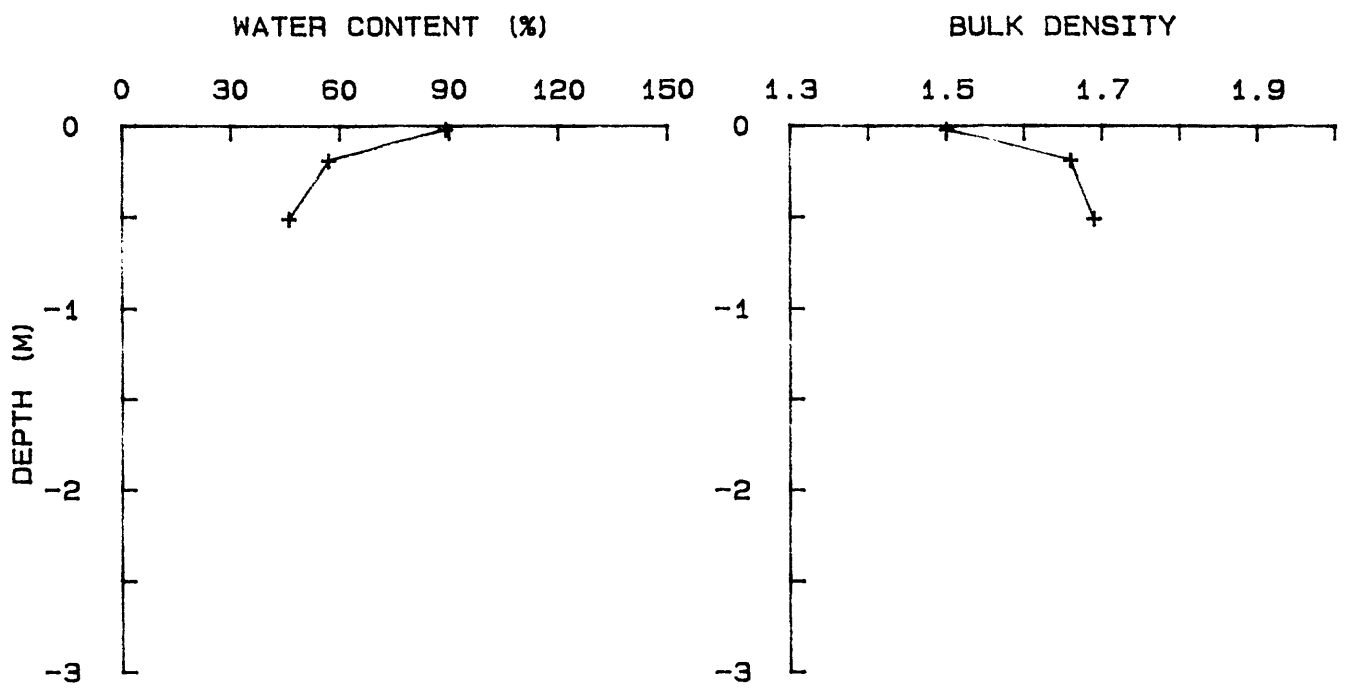
YS-85-08 BC 10



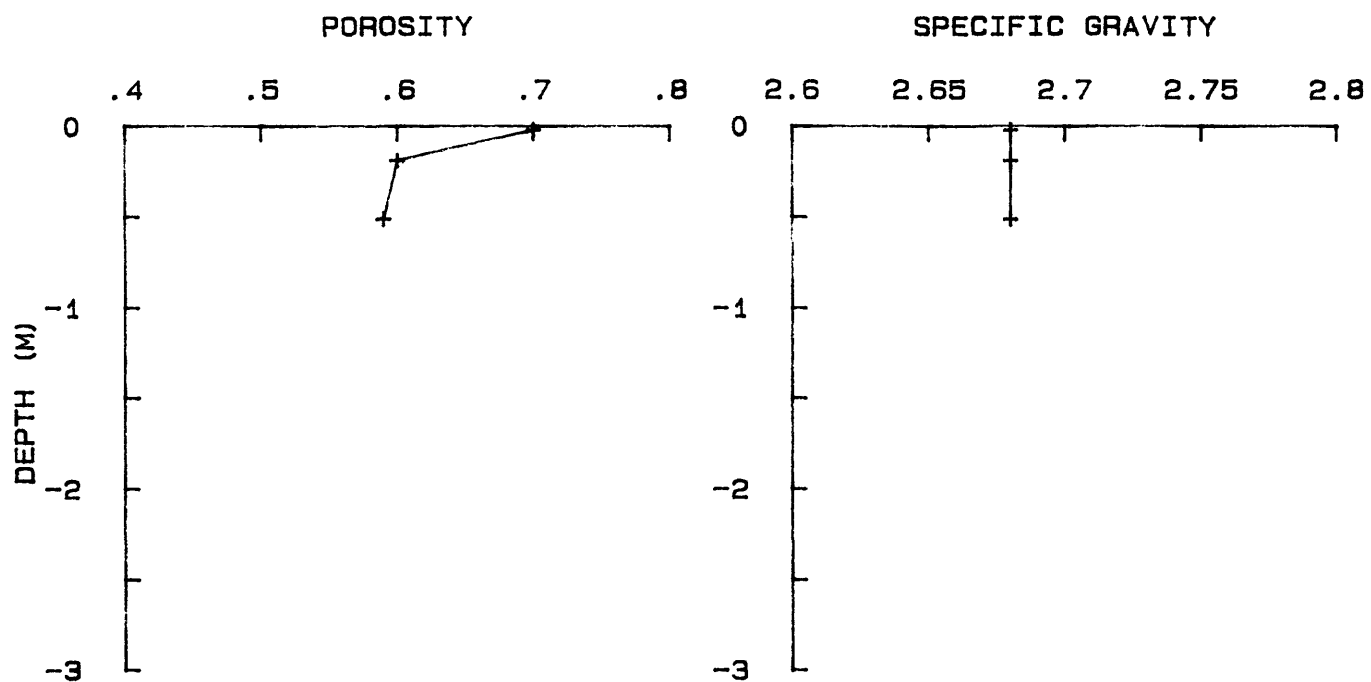


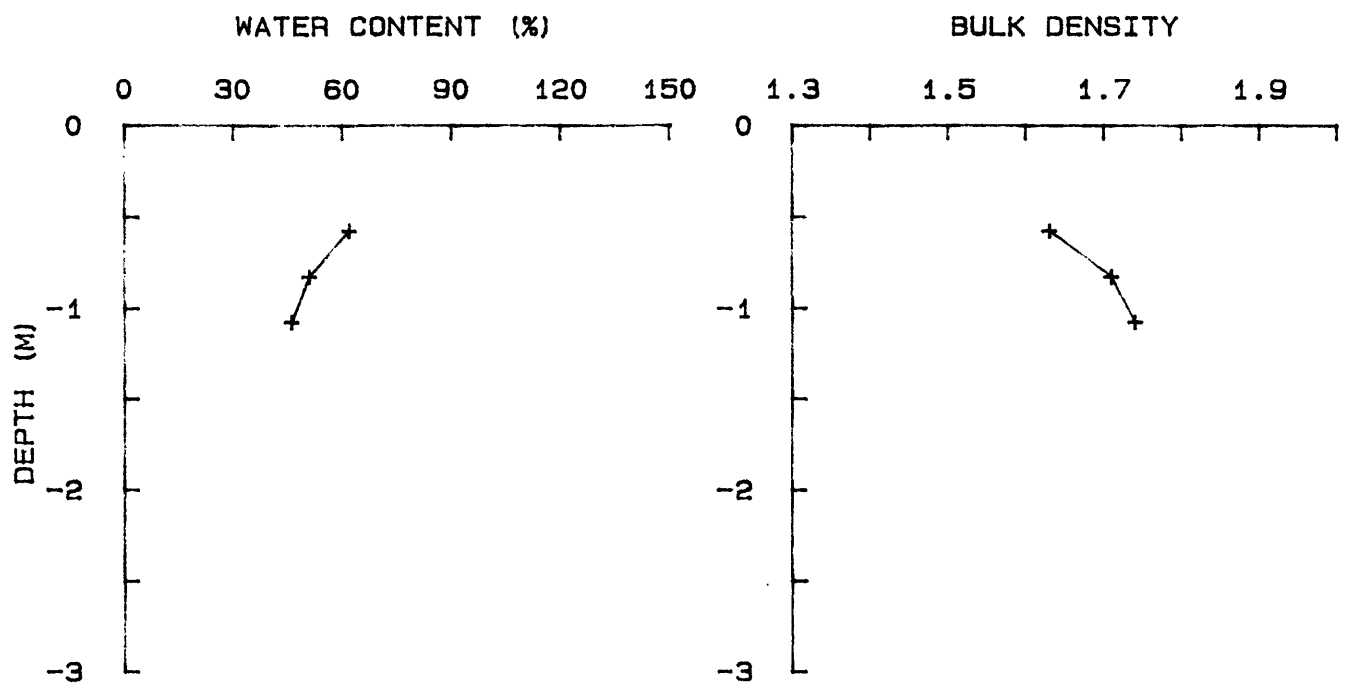
YS-85-08 KC 10



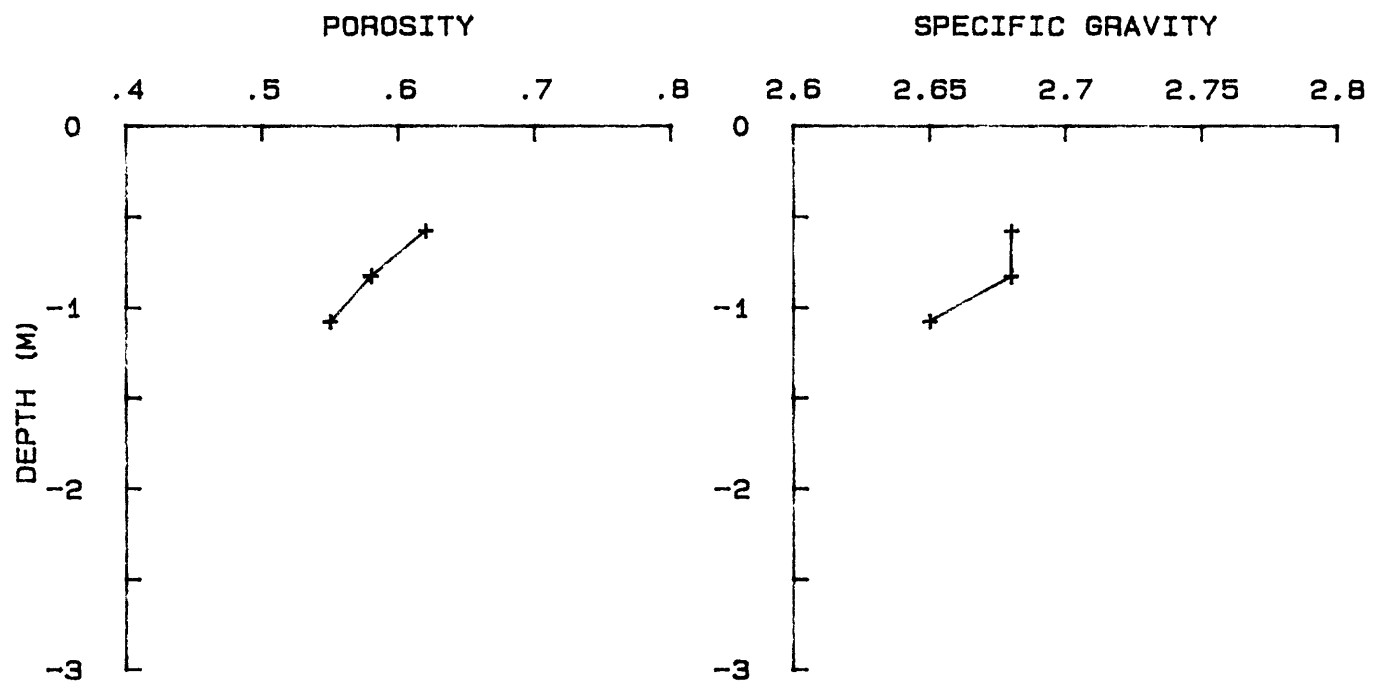


YS-85-08 BC 11





YS-85-08 KC 11



Appendix C

Results of Constant-Rate-of-Strain Consolidation Tests

**tabular data
unedited test plots**

TABULAR DATA

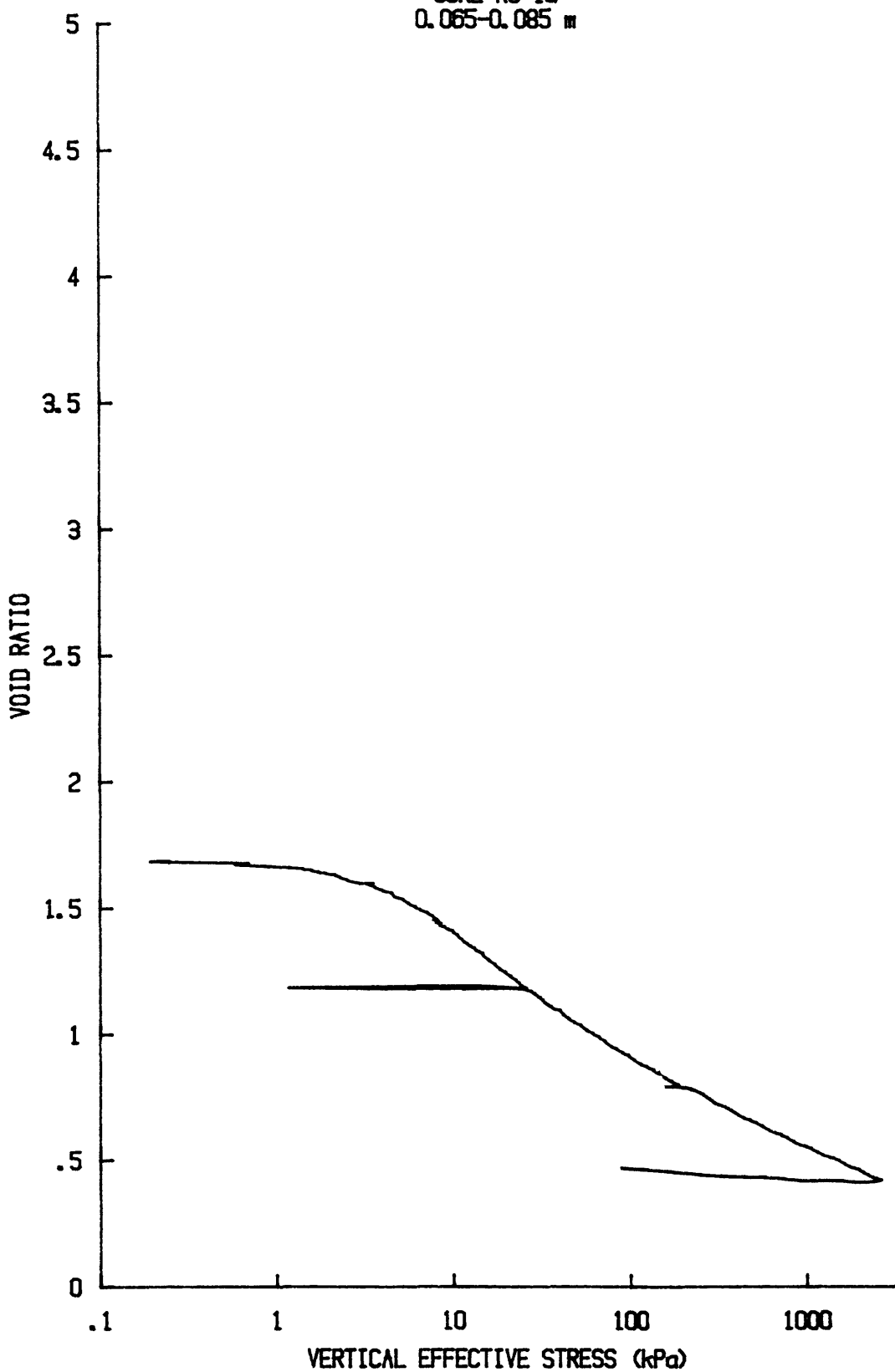
YS-85-08 Consolidation Test Results

Core ID	Test No.	Depth in core (m)	w (%)	σ'_{vo} (kPa)	σ'_{vm} (kPa)	$\sigma'e$ (%)	OCR	Cc	Ccf	Cr	$c_v(\sigma'_{vo})$ (cm^2/s)	$c_v(\sigma'_{vm})$ (cm^2/s)	$c_v(\text{ave})$ (cm^2/s)	$k(\sigma'_{vm})$ (cm/s)	$k(\text{ave})$ (cm/s)	I _D	Comments		
KC-1a	CR037	0.075	64	0.42	4.0	3.6	9.5	0.53	0.57	0.004	1×10^{-3}	6×10^{-4}	7×10^{-7}	3×10^{-8}	0.22				
	CR047	0.25	63	1.50	5.4	3.9	3.6	0.44	0.47	0.006	1×10^{-3}	7×10^{-4}	1×10^{-6}	5×10^{-7}	4×10^{-8}	0.23			
	CR041	0.55	56	3.42	10.9	7.5	3.2	0.43	0.46	0.005	1×10^{-3}	8×10^{-4}	8×10^{-7}	2×10^{-7}	4×10^{-8}	0.28			
BC-4	CR038	0.035	158	0.10	2.3	2.2	23	0.91	0.92	—	2×10^{-3}	6×10^{-4}	1×10^{-6}	3×10^{-8}	0.31				
	CR049	0.21	140	0.67	4.3	3.6	6.4	1.26	1.30	0.08	7×10^{-3}	1×10^{-3}	4×10^{-4}	9×10^{-6}	5×10^{-8}	0.23			
	CR042	0.42	110	1.41	9.3	7.9	6.6	0.94	1.11	—	3×10^{-3}	5×10^{-4}	1×10^{-6}	3×10^{-7}	2×10^{-8}	0.27			
	CR033	0.02	139	0.07	3.0	2.9	43	1.07	1.14	0.04	4×10^{-4}	2×10^{-4}	$—$	5×10^{-7}	1×10^{-8}	0.21			
BC-5	CR053	0.20	111	0.74	5.7	5.0	7.7	1.00	1.08	0.09	4×10^{-3}	7×10^{-4}	3×10^{-4}	3×10^{-6}	7×10^{-7}	2×10^{-8}	0.26		
	CR029	0.49	109	1.82	8.7	6.9	4.8	0.91	1.04	0.03	1×10^{-3}	3×10^{-4}	5×10^{-7}	2×10^{-7}	1×10^{-8}	0.29			
	CR056	0.49	111	1.86	3.5	1.6	1.9	0.78	0.84	0.09	5×10^{-4}	3×10^{-4}	2×10^{-4}	3×10^{-7}	2×10^{-7}	0.22	Remolded		
	CR039	0.02	156	0.06	2.6	2.5	43	1.06	1.08	0.006	—	2×10^{-3}	3×10^{-4}	$—$	7×10^{-6}	5×10^{-8}	0.26		
C2	CR050	0.18	127	0.60	5.7	5.1	9.5	1.19	1.23	0.06	—	3×10^{-3}	3×10^{-4}	4×10^{-6}	6×10^{-6}	3×10^{-8}	0.15		
	CR043	0.45	120	1.53	5.2	3.7	3.4	0.96	1.05	—	7×10^{-3}	1×10^{-2}	3×10^{-4}	4×10^{-6}	5×10^{-8}	0.19			
	CR034	0.04	64	0.23	4.2	4.0	18	0.34	0.35	—	3×10^{-3}	9×10^{-3}	$—$	3×10^{-5}	4×10^{-7}	0.23			
BC-6	CR054	0.20	51	1.27	8.0	6.7	6.3	0.29	0.31	0.01	3×10^{-2}	1×10^{-3}	3×10^{-3}	9×10^{-6}	4×10^{-7}	8×10^{-8}	0.24		
	CR030	0.46	44	3.05	22	19	7.2	0.26	0.29	—	3×10^{-3}	1×10^{-3}	2×10^{-3}	3×10^{-7}	2×10^{-7}	6×10^{-8}	0.28		
	CR057	0.46	44	3.08	7.1	4.0	2.3	0.21	0.23	—	2×10^{-3}	6×10^{-4}	4×10^{-7}	4×10^{-7}	2×10^{-7}	2×10^{-8}	0.30	Remolded	
	CR040	0.02	60	0.11	8.1	8.0	74	0.44	0.65	—	2×10^{-3}	2×10^{-3}	$—$	1×10^{-6}	8×10^{-8}	0.27			
C3	CR048	0.18	49	1.18	15	14	13	0.30	0.35	0.002	9×10^{-3}	2×10^{-3}	2×10^{-3}	4×10^{-6}	5×10^{-8}	0.29			
	CR044	0.51	44	3.45	20	17	5.8	0.23	0.26	—	2×10^{-2}	5×10^{-3}	8×10^{-3}	4×10^{-6}	8×10^{-7}	0.32			
	CR035	0.02	129	0.07	4.7	4.6	67	1.04	1.13	0.005	—	5×10^{-4}	2×10^{-4}	$—$	6×10^{-7}	3×10^{-8}	0.25		
BC-7	CR055	0.205	120	0.74	5.6	4.9	7.6	1.12	1.23	0.06	$—$	9×10^{-3}	3×10^{-4}	$—$	1×10^{-5}	4×10^{-8}	0.28		
	CR031	0.49	110	1.82	4.6	2.8	2.5	0.84	0.97	0.01	4×10^{-3}	2×10^{-3}	3×10^{-4}	4×10^{-6}	5×10^{-6}	4×10^{-8}	0.26		
	CR058	0.51	107	1.90	3.7	1.8	1.9	0.66	0.74	0.02	4×10^{-4}	2×10^{-4}	3×10^{-7}	3×10^{-7}	2×10^{-7}	2×10^{-8}	0.26	Remolded	
	CR040	0.11	59	0.11	9.3	9.2	85	0.28	0.33	—	7×10^{-3}	2×10^{-2}	5×10^{-3}	$—$	2×10^{-6}	6×10^{-8}	0.27		
BC-8	CR035	0.02	129	0.07	4.7	4.6	67	1.04	1.13	0.005	—	5×10^{-4}	2×10^{-4}	$—$	6×10^{-7}	1×10^{-7}	0.27		
	CR048	0.18	49	1.18	15	14	13	0.30	0.35	0.002	9×10^{-3}	2×10^{-3}	5×10^{-3}	4×10^{-6}	5×10^{-7}	1×10^{-7}	0.32		
	CR044	0.51	44	3.45	20	17	5.8	0.23	0.26	—	2×10^{-2}	5×10^{-3}	8×10^{-3}	4×10^{-6}	8×10^{-7}	2×10^{-8}	0.32		
	CR036	0.02	59	0.11	9.3	9.2	85	0.28	0.33	—	7×10^{-3}	2×10^{-2}	5×10^{-3}	$—$	2×10^{-6}	6×10^{-8}	0.27		
C4	CR051	0.18	56	1.15	12	11	1.0	0.37	0.45	0.01	2×10^{-2}	3×10^{-3}	5×10^{-3}	4×10^{-6}	5×10^{-6}	1×10^{-6}	1×10^{-7}	0.27	
	CR032	0.53	50	3.52	17	14	4.8	0.31	0.33	0.004	2×10^{-2}	5×10^{-3}	5×10^{-3}	4×10^{-6}	5×10^{-7}	2×10^{-7}	2×10^{-8}	0.26	
	CR045	0.015	87	0.07	2.7	2.6	38	0.54	0.58	0.02	—	1×10^{-3}	7×10^{-4}	$—$	1×10^{-6}	2×10^{-7}	0.22	S1. Questionable	
BC-9	CR052	0.19	64	1.02	5.4	4.4	5.3	0.55	0.61	0.01	1×10^{-2}	5×10^{-3}	7×10^{-4}	1×10^{-5}	4×10^{-6}	4×10^{-8}	0.30		
	CR046	0.51	58	2.88	10.4	7.5	3.6	0.41	0.45	0.01	1×10^{-3}	4×10^{-4}	1×10^{-3}	4×10^{-7}	2×10^{-7}	4×10^{-8}	0.25		
	CR059	0.51	57	2.91	4.3	1.4	1.5	0.35	0.38	0.02	3×10^{-4}	6×10^{-4}	3×10^{-4}	7×10^{-7}	2×10^{-7}	1×10^{-8}	0.25	Remolded	
	CR044	0.51	44	3.45	20	17	5.8	0.23	0.26	—	2×10^{-2}	5×10^{-3}	8×10^{-3}	4×10^{-6}	8×10^{-7}	2×10^{-8}	0.26	Remolded	

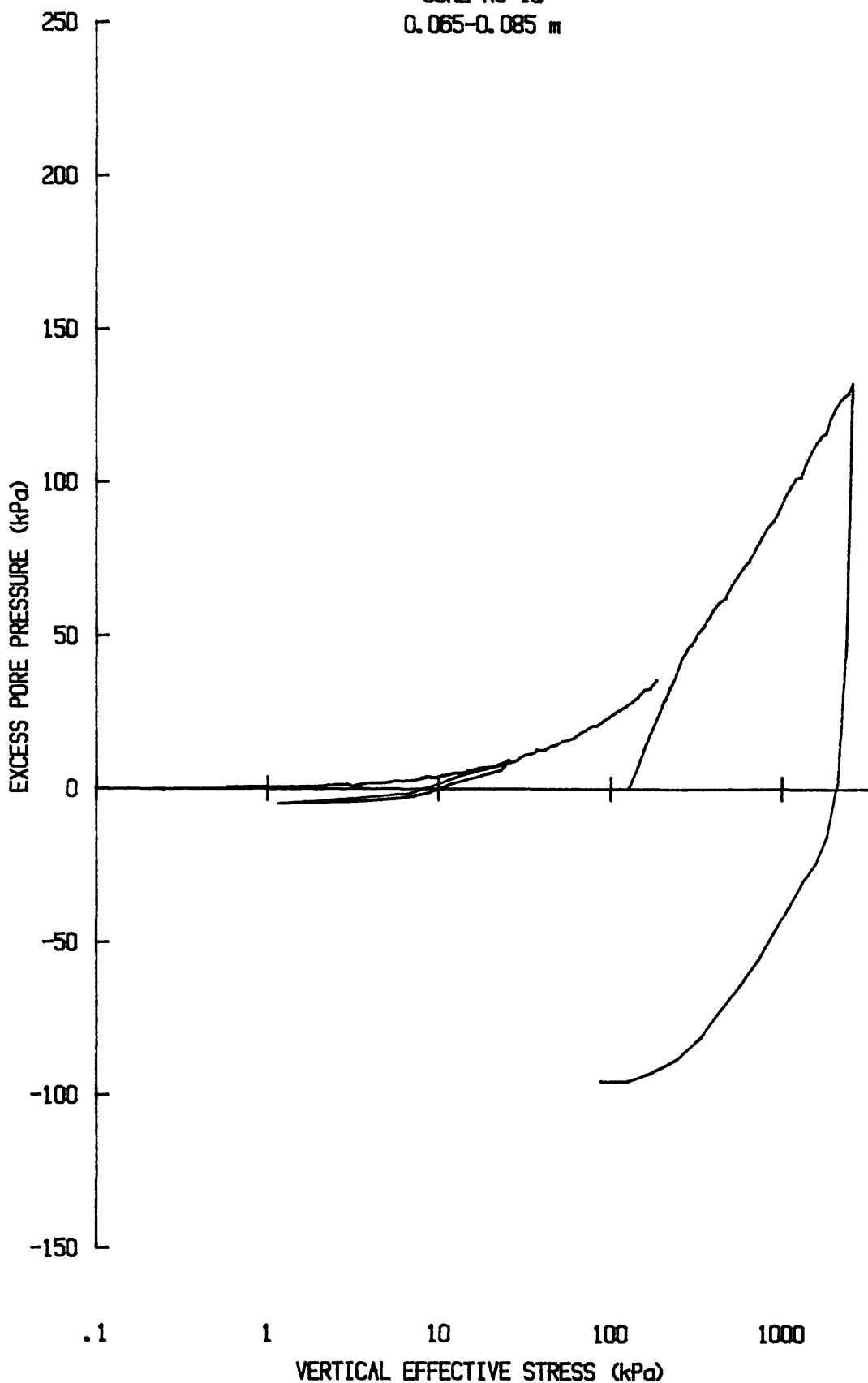
Symbols are explained in Appendix A.

TEST PLOTS

e vs log p' for: CR037S8501
YS-85-08
CORE KC-1a
0.065-0.085 in



u vs $\log p'$ for CR037S8501
YS-85-08
CORE KC-1a
0.065-0.085 m

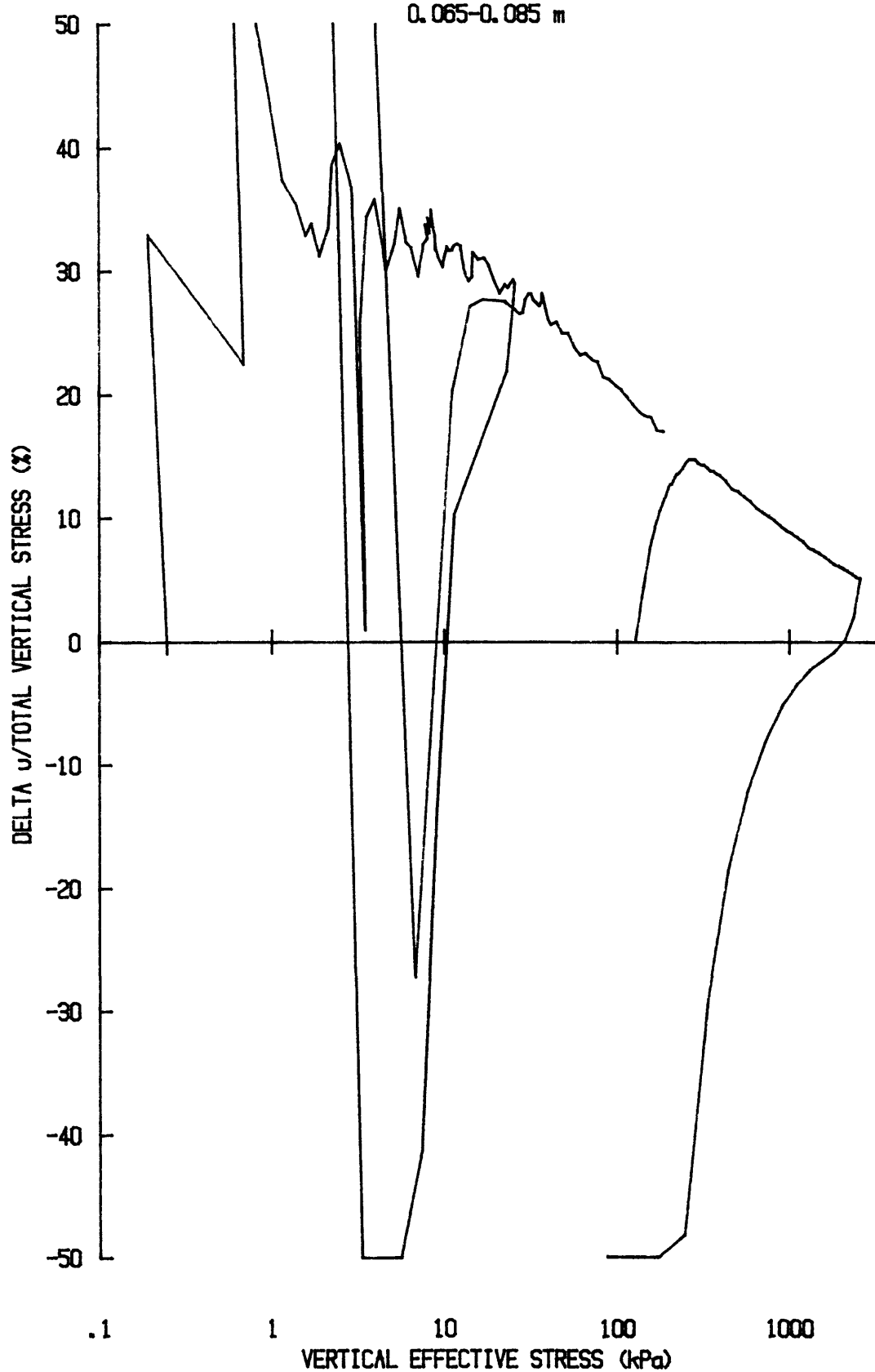


du/Sv for: CR037S8501

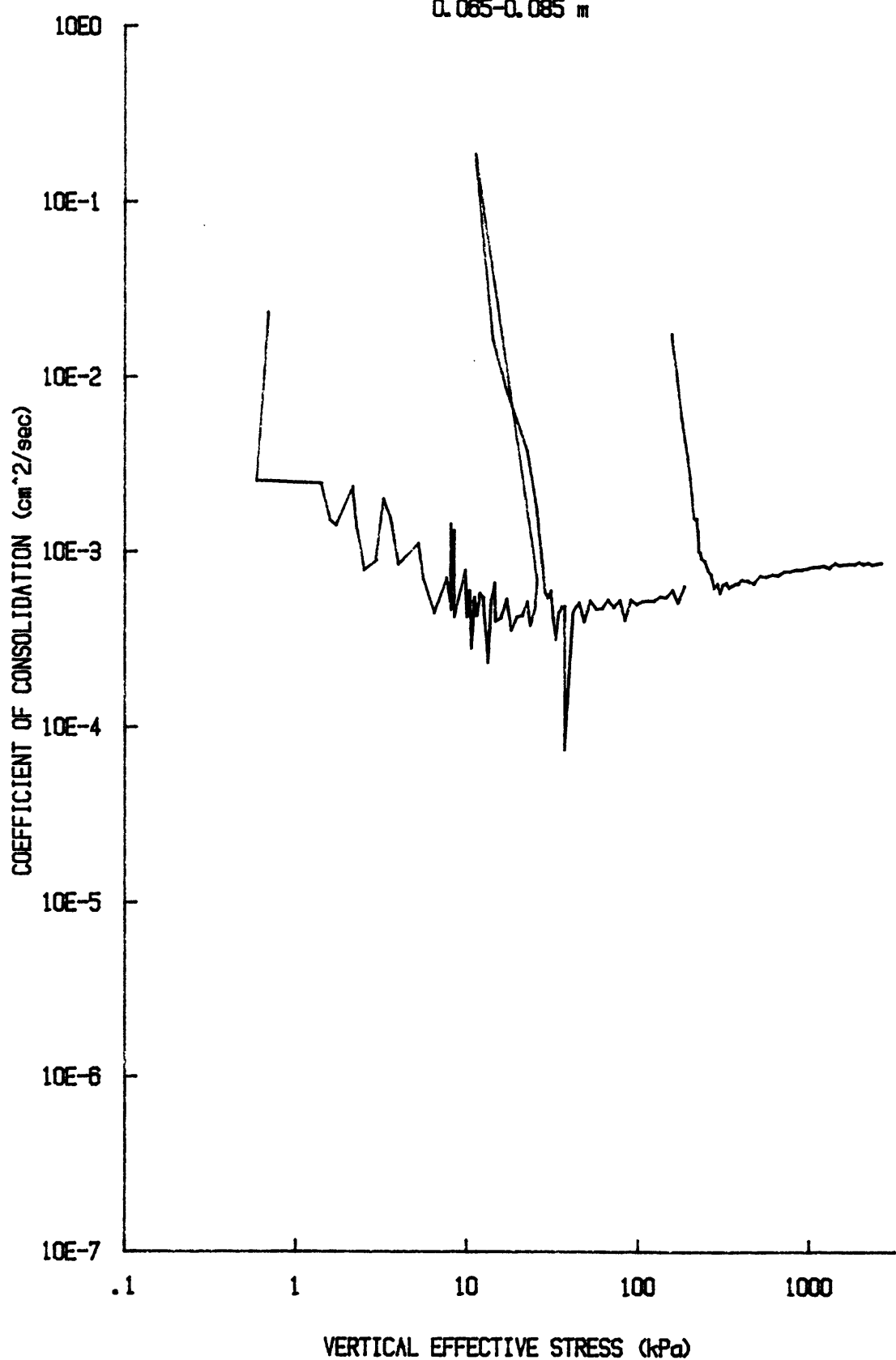
YS-85-08

CORE KC-1a

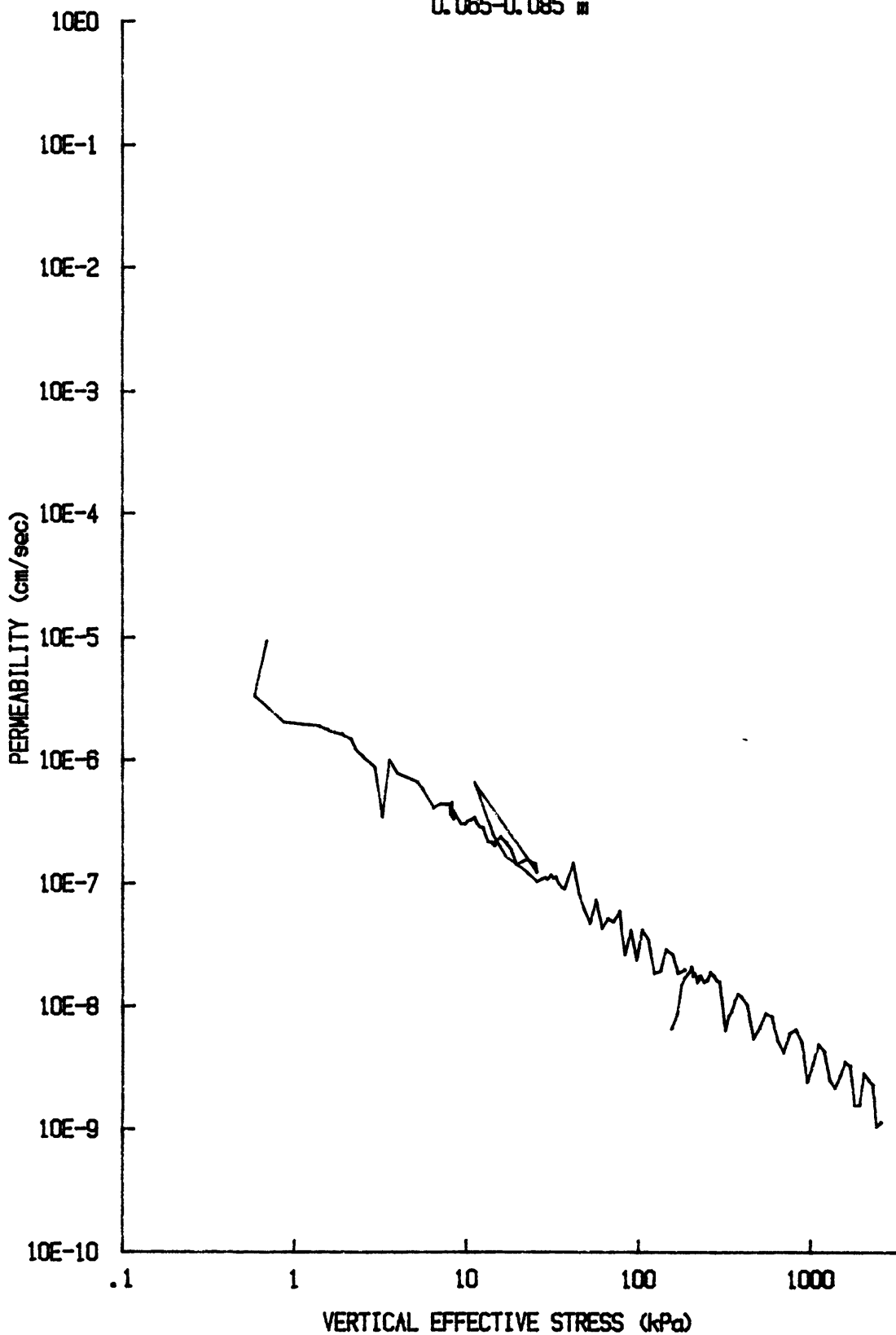
0.065-0.085 m



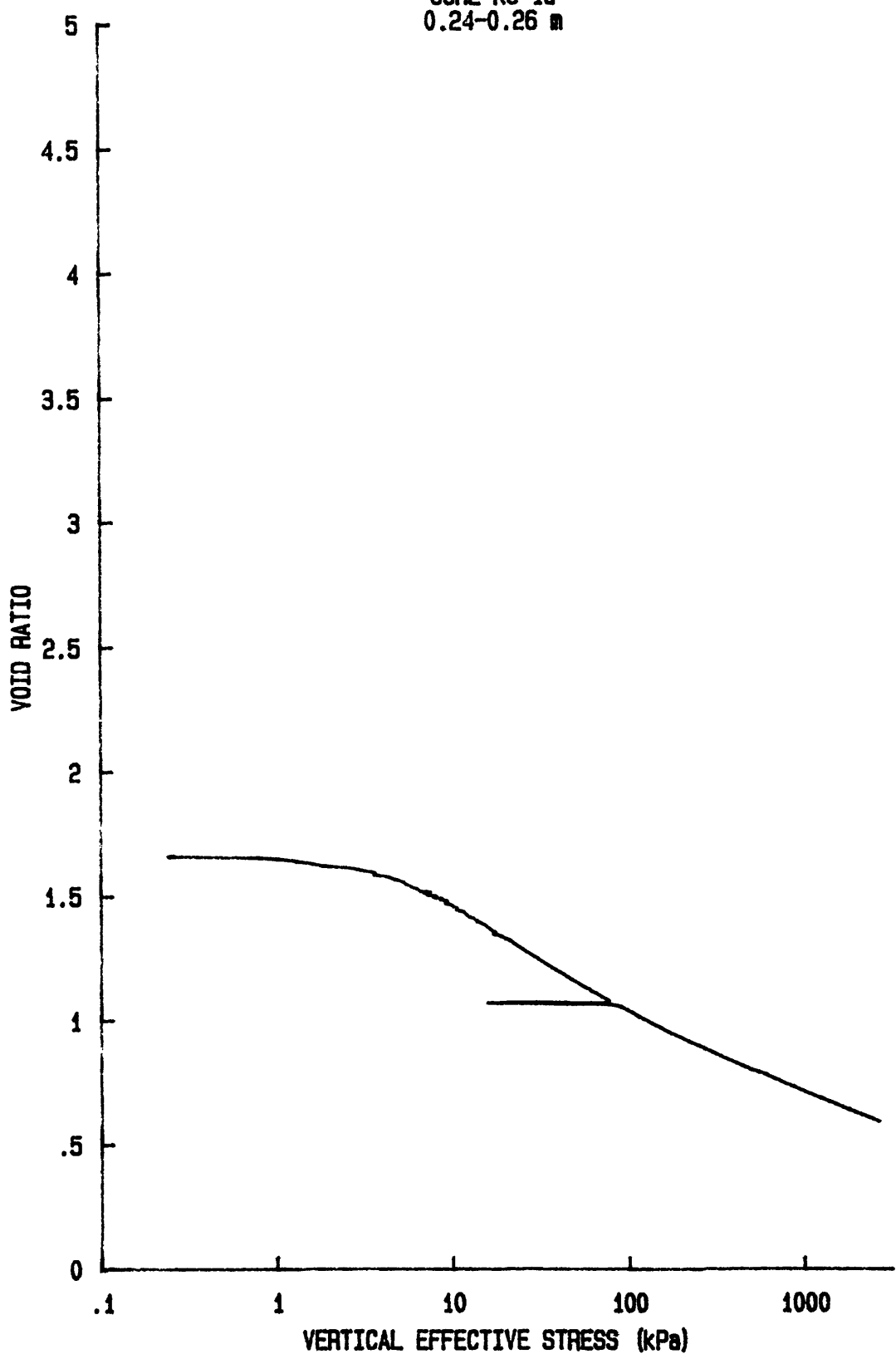
C_v vs $\log p'$ for CR037S8501
YS-85-08
CORE KC-1a
0.065-0.085 m



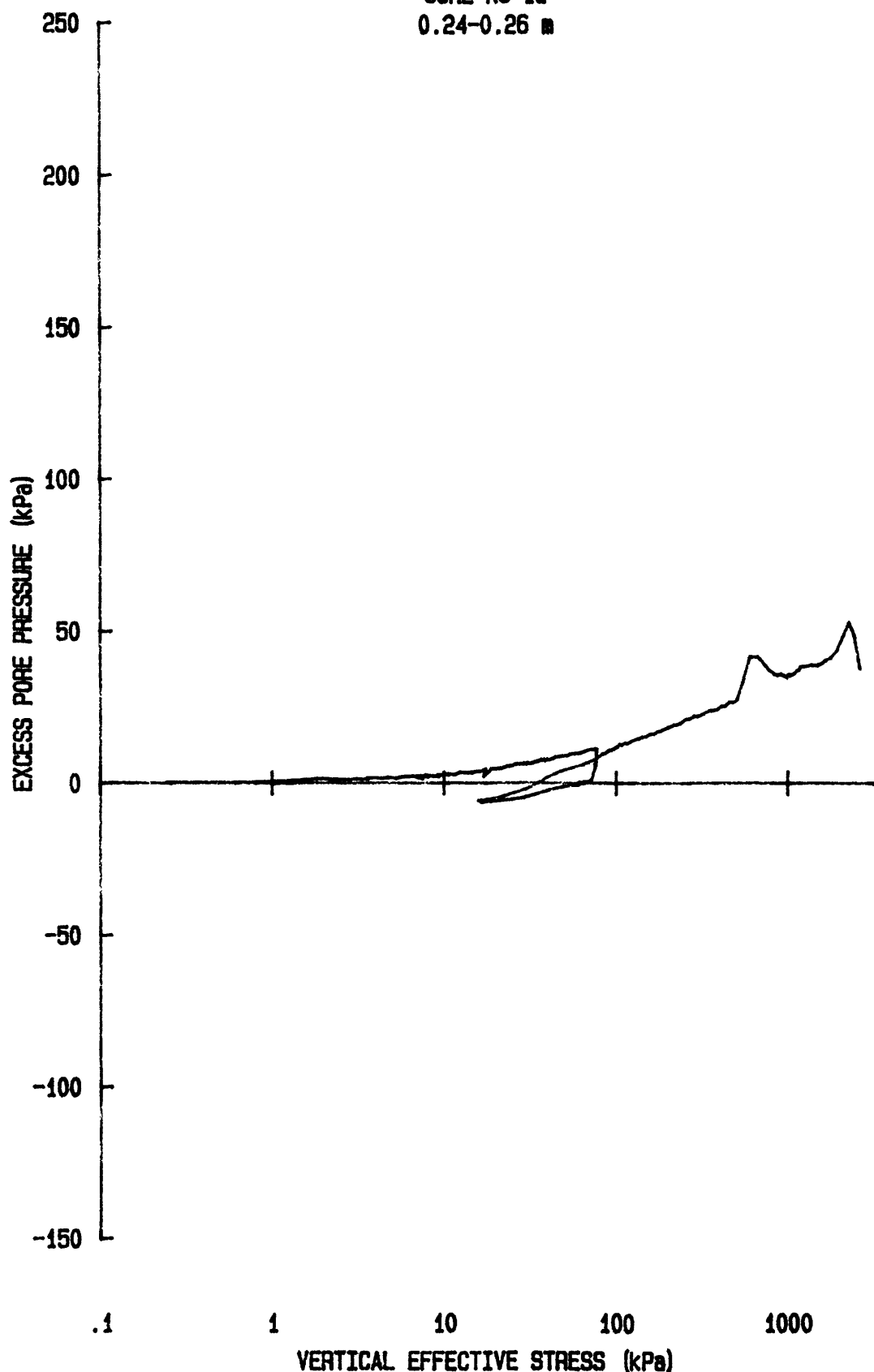
k vs $\log p'$ for CR037S8501
YS-85-08
CORE KC-1a
0.065-0.085 "



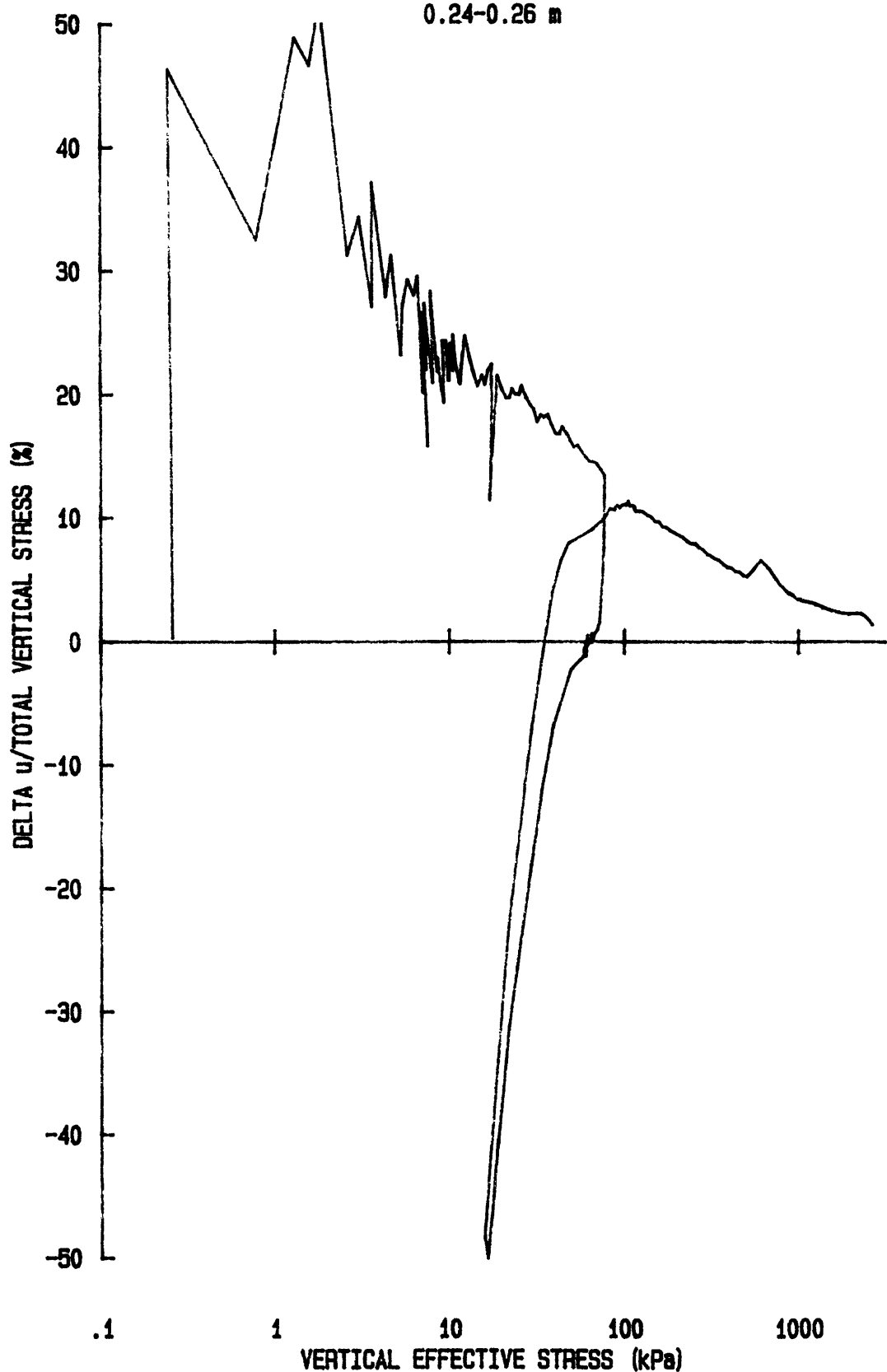
e vs log p' for: CR047S8501
YS-85-08
CORE KC-1a
0.24-0.26 m



u vs $\log p'$ for: CR047S8501
YS-85-08
CORE KC-1a
0.24-0.26 m



du/Sv for: CR047S8501
YS-85-08
CORE KC-1a
0.24-0.26 m

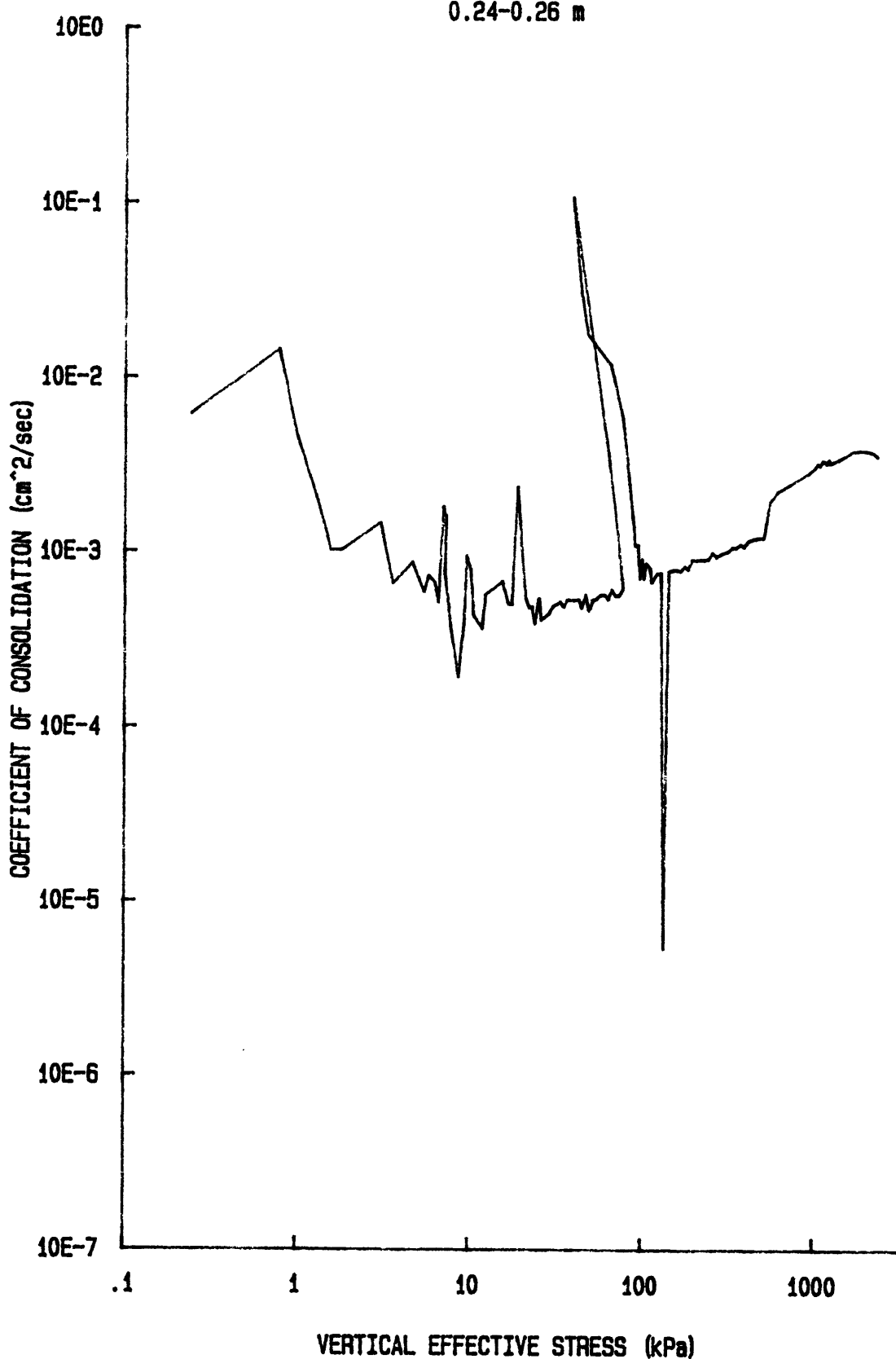


C_v vs $\log p'$ for: CR047S8501

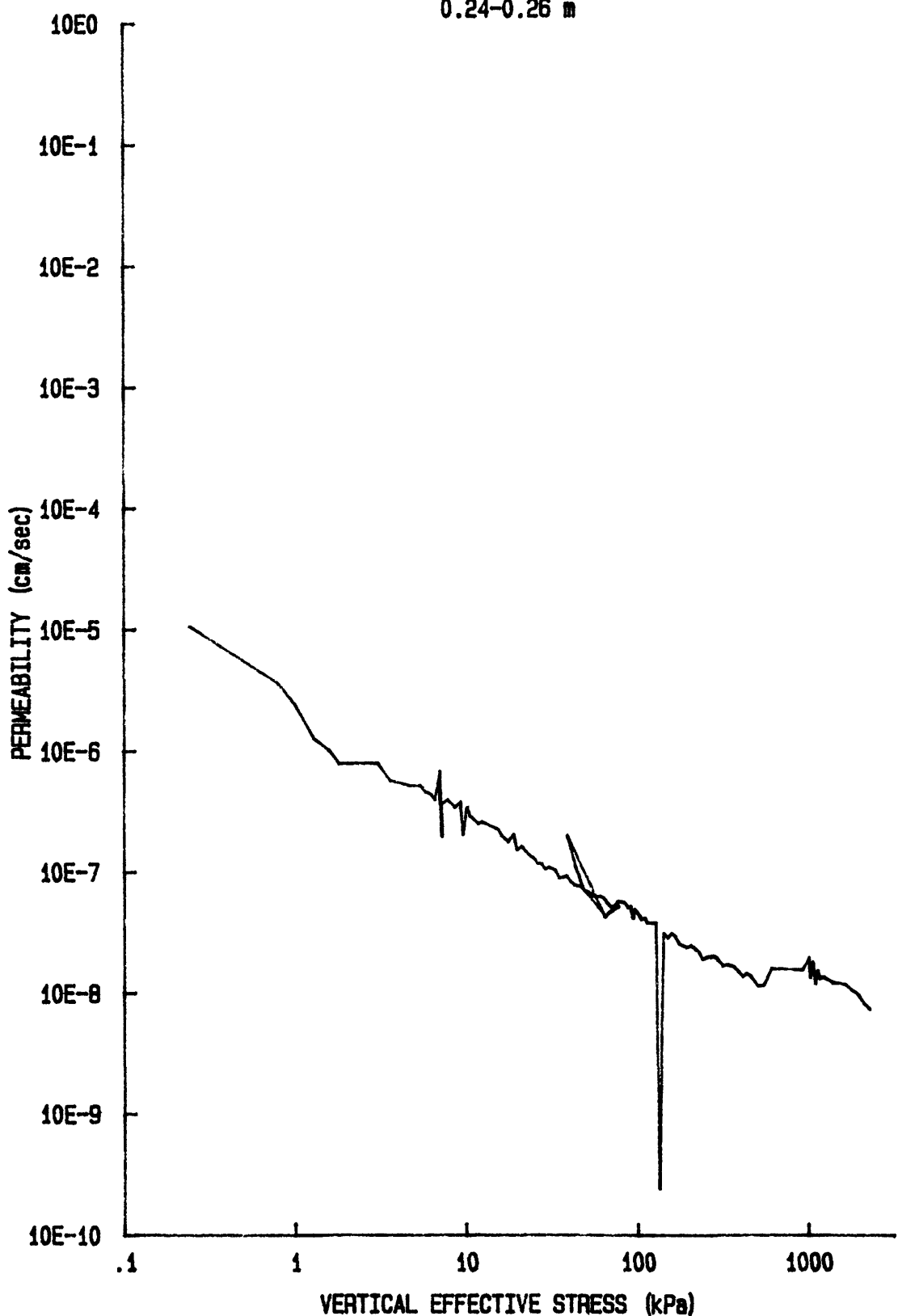
YS-85-08

CORE KC-1a

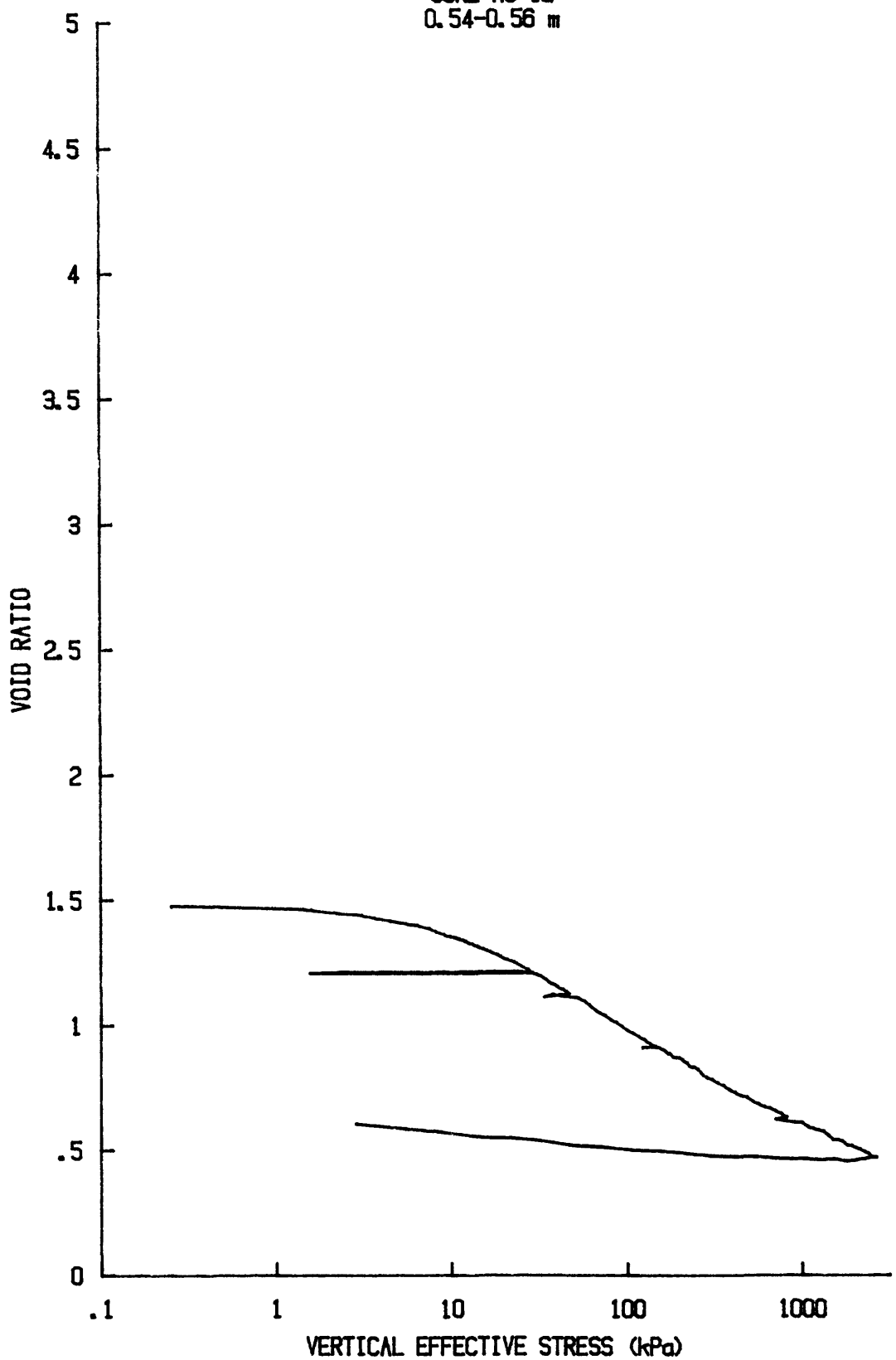
0.24-0.26 m



k vs $\log p'$ for: CR047S8501
YS-85-08
CORE KC-1a
0.24-0.26 m



e vs log p' for CR041S8501
YS-85-08
CORE KC-1a
0.54-0.56 m

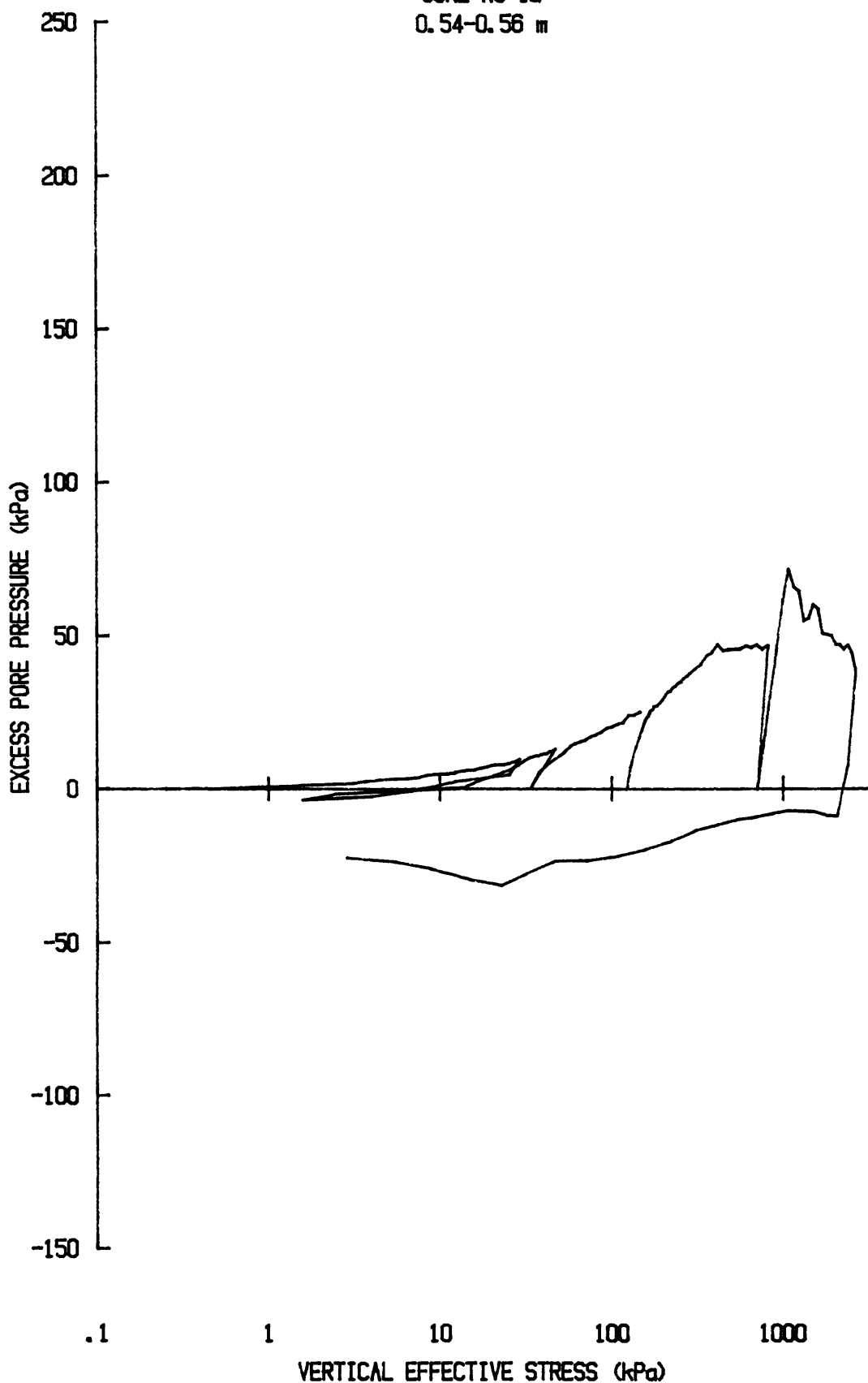


u vs $\log p'$ for: CR041S8501

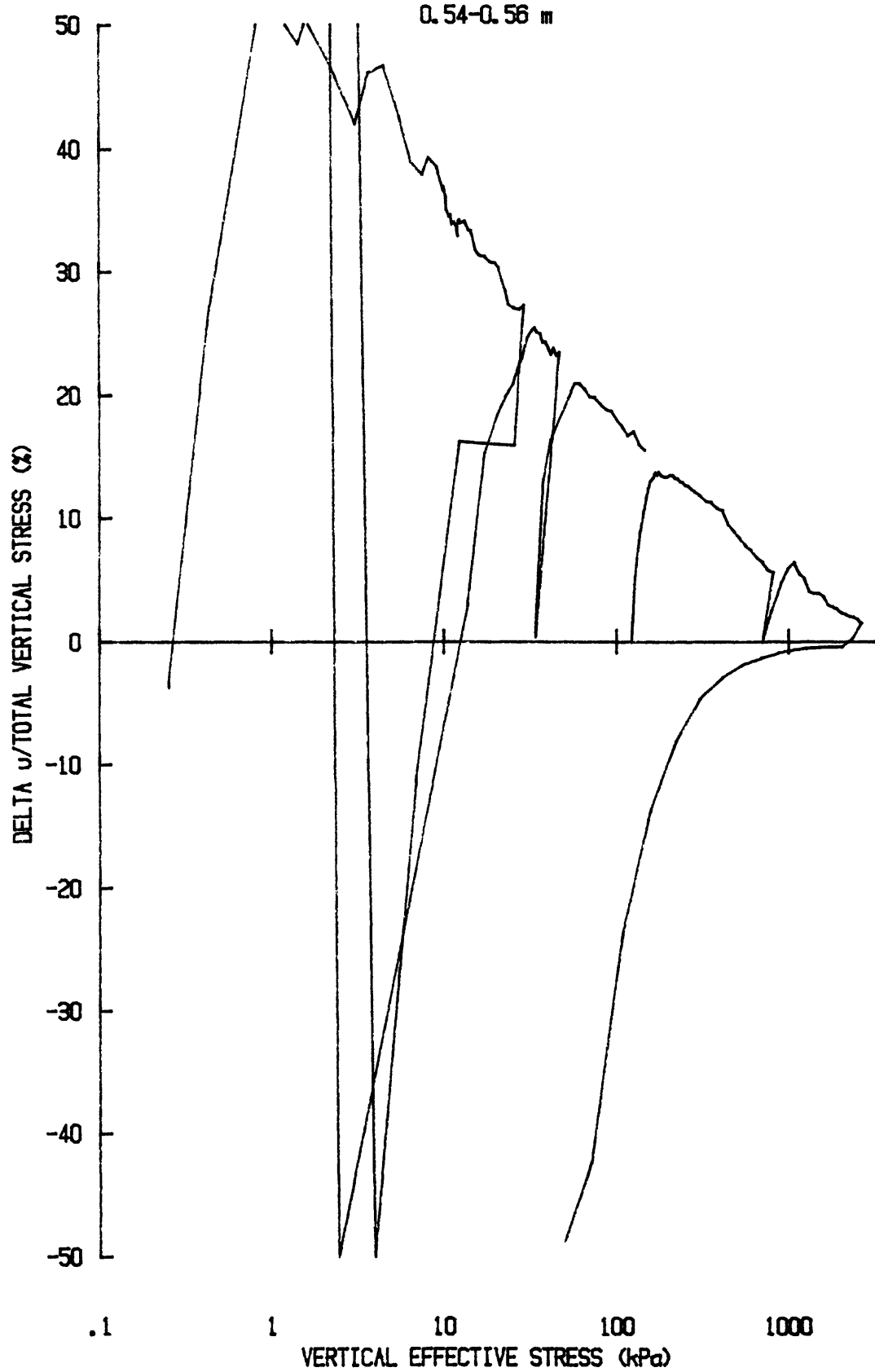
YS-85-08

CORE KC-1a

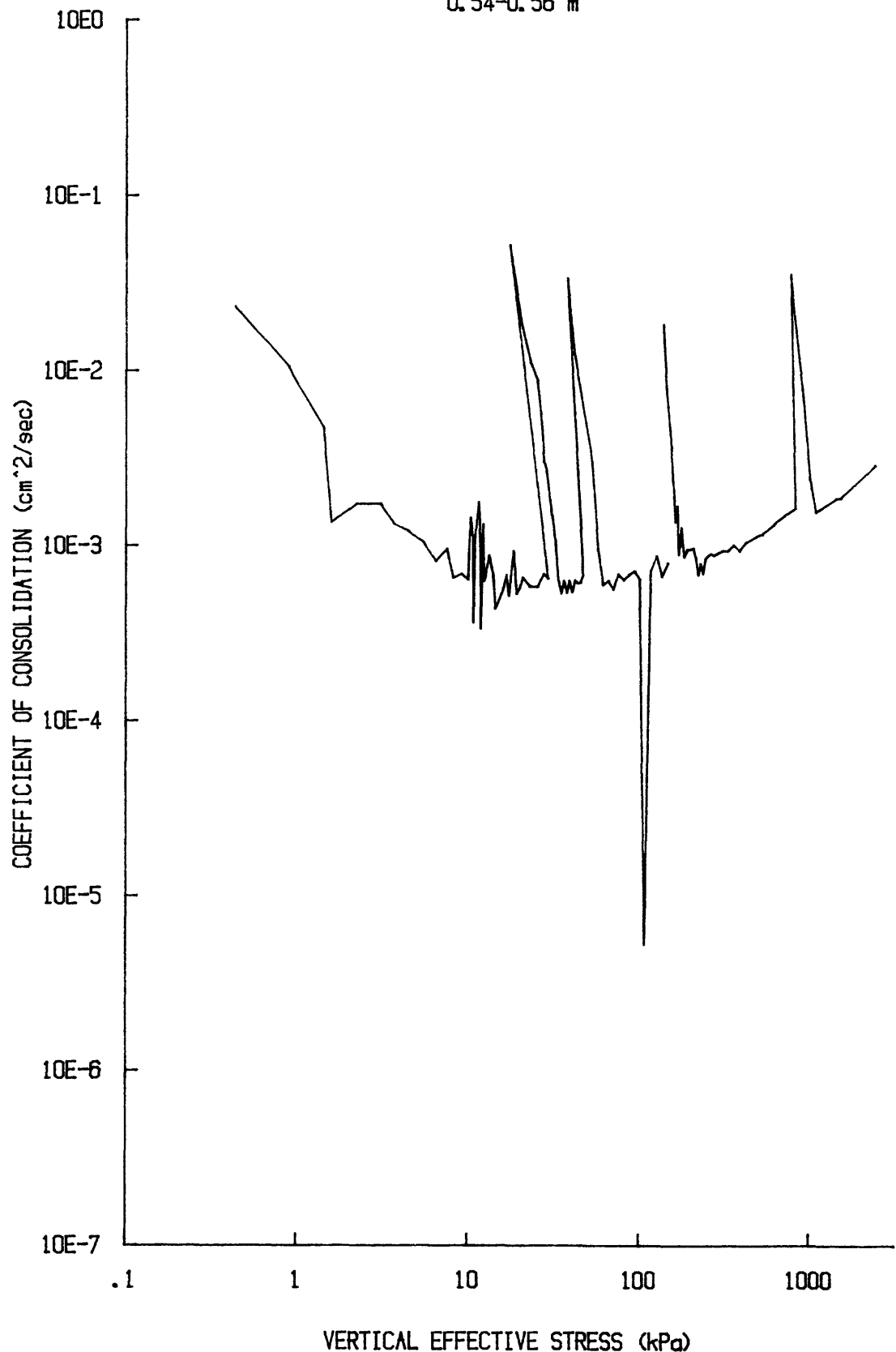
0.54-0.56 m



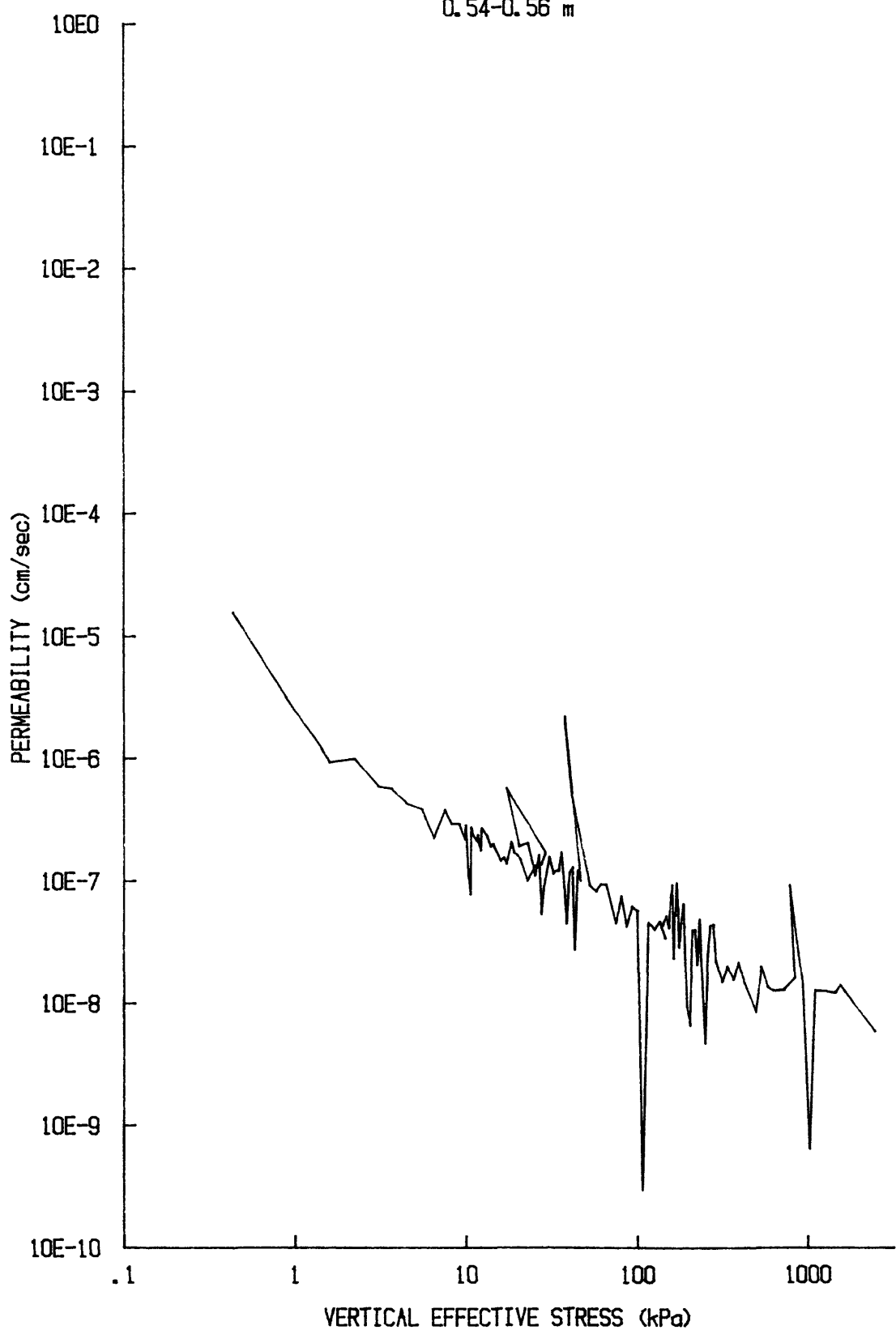
du/Sv for: CR041S8501
YS-85-08
CORE KC-1a
0.54-0.56 m



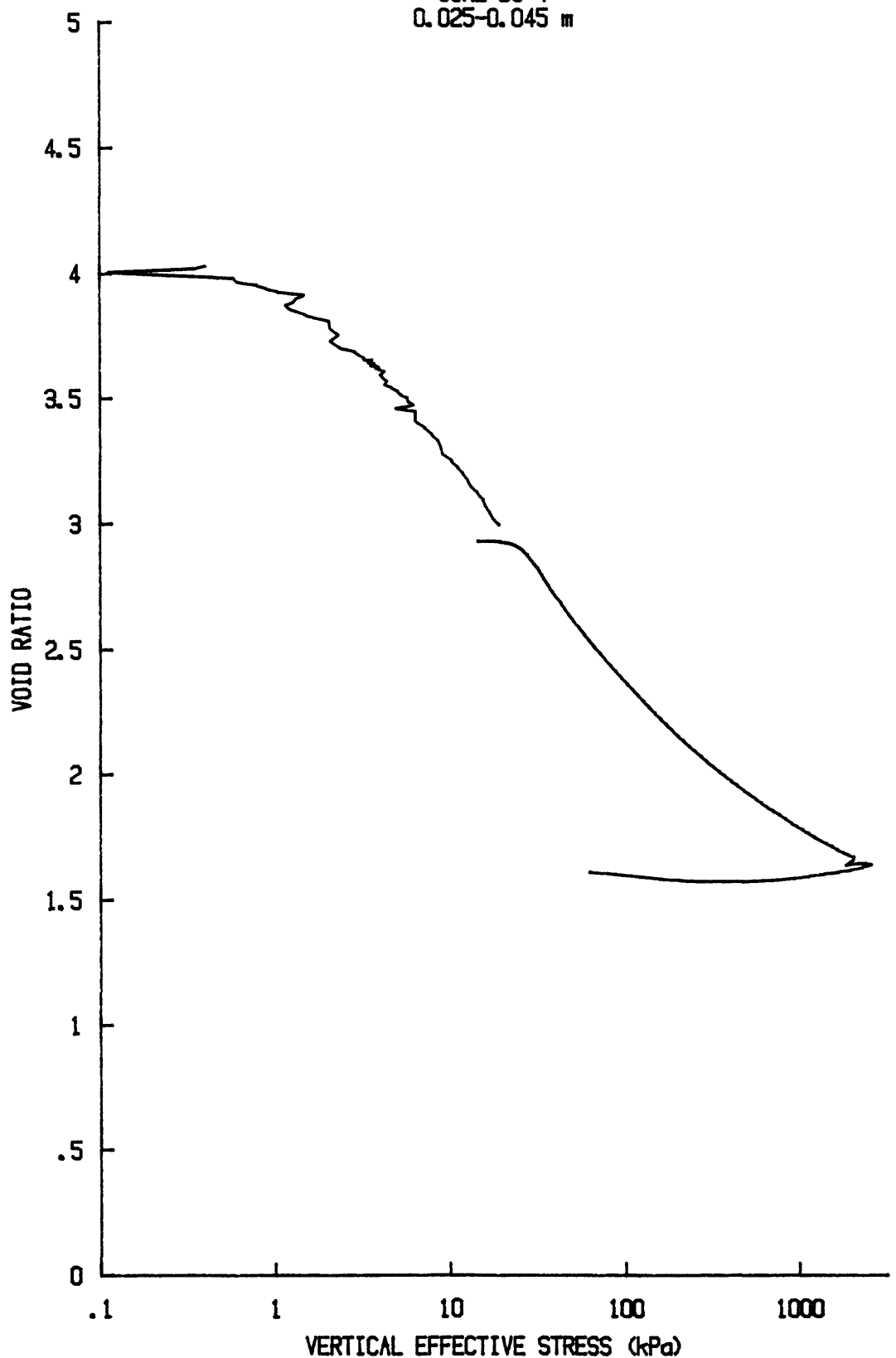
C_v vs $\log p'$ for CR041S8501
YS-85-08
CORE KC-1a
0.54-0.56 m



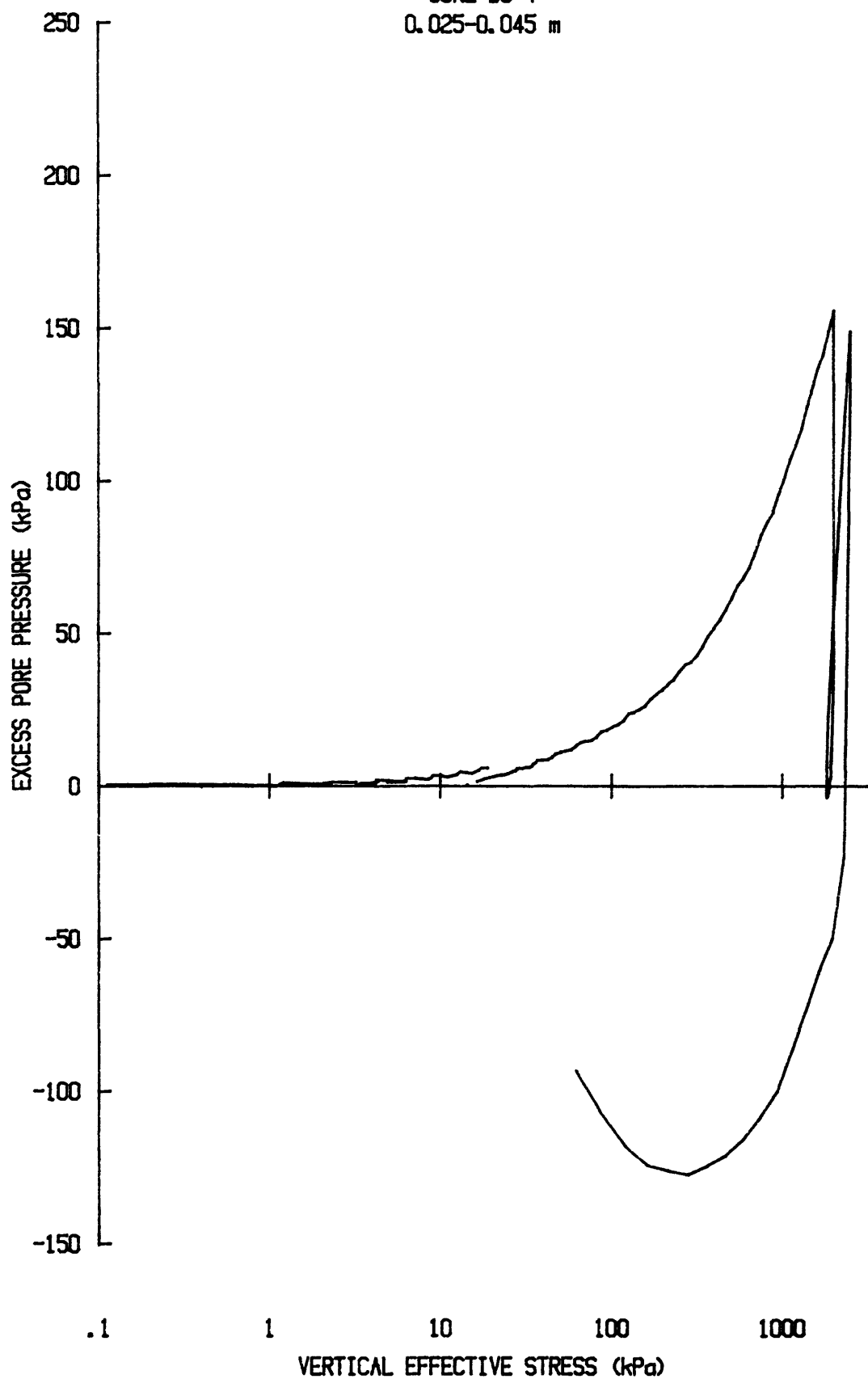
k vs $\log p'$ for: CR041S8501
YS-85-08
CORE KC-1a
0.54-0.56 m



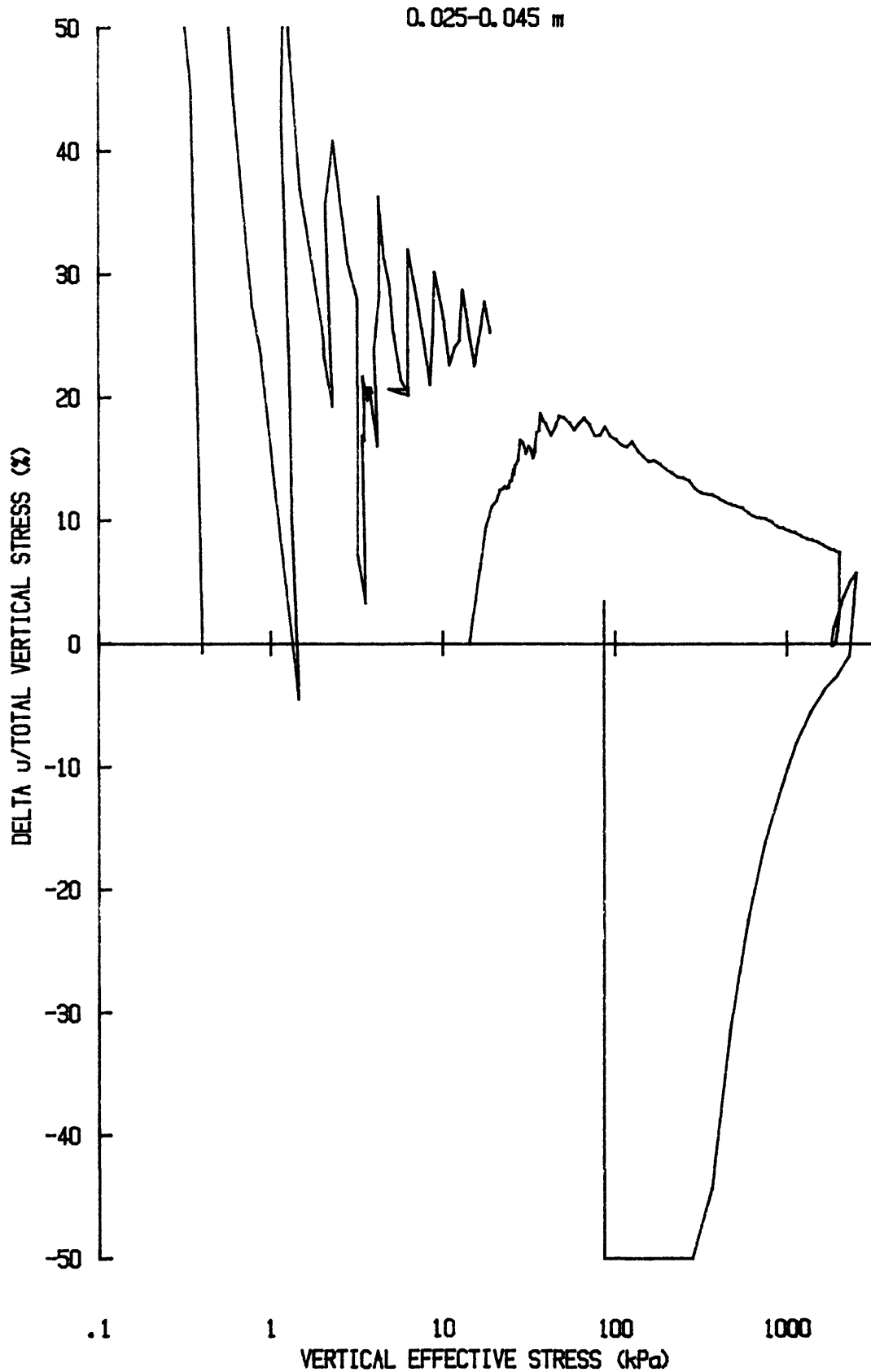
e vs $\log p'$ for: CR038S8504
YS-85-08
CORE BC-4
0.025-0.045 m



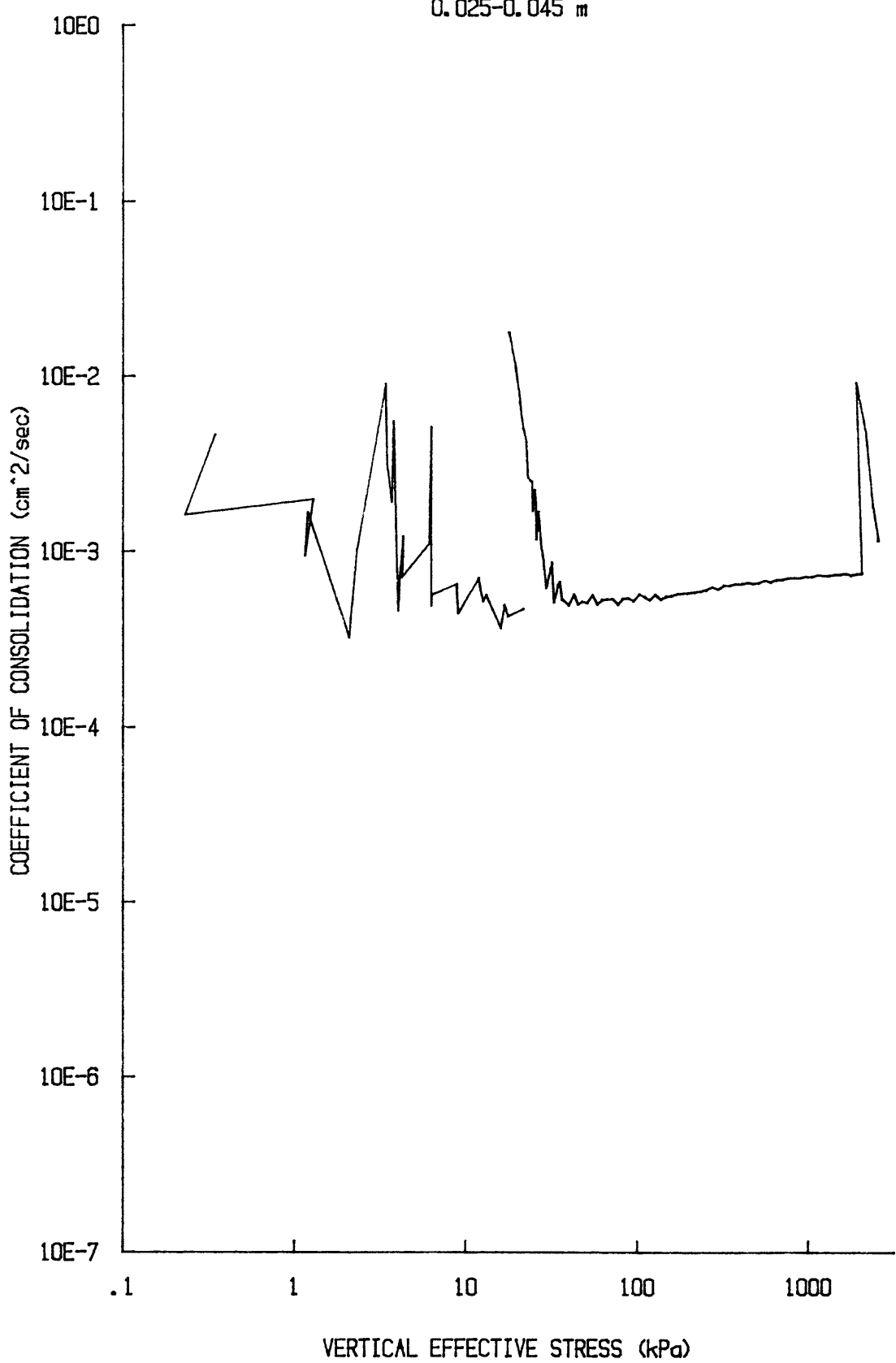
u vs $\log p'$ for CR038S8504
YS-85-08
CORE BC-4
0.025-0.045 m



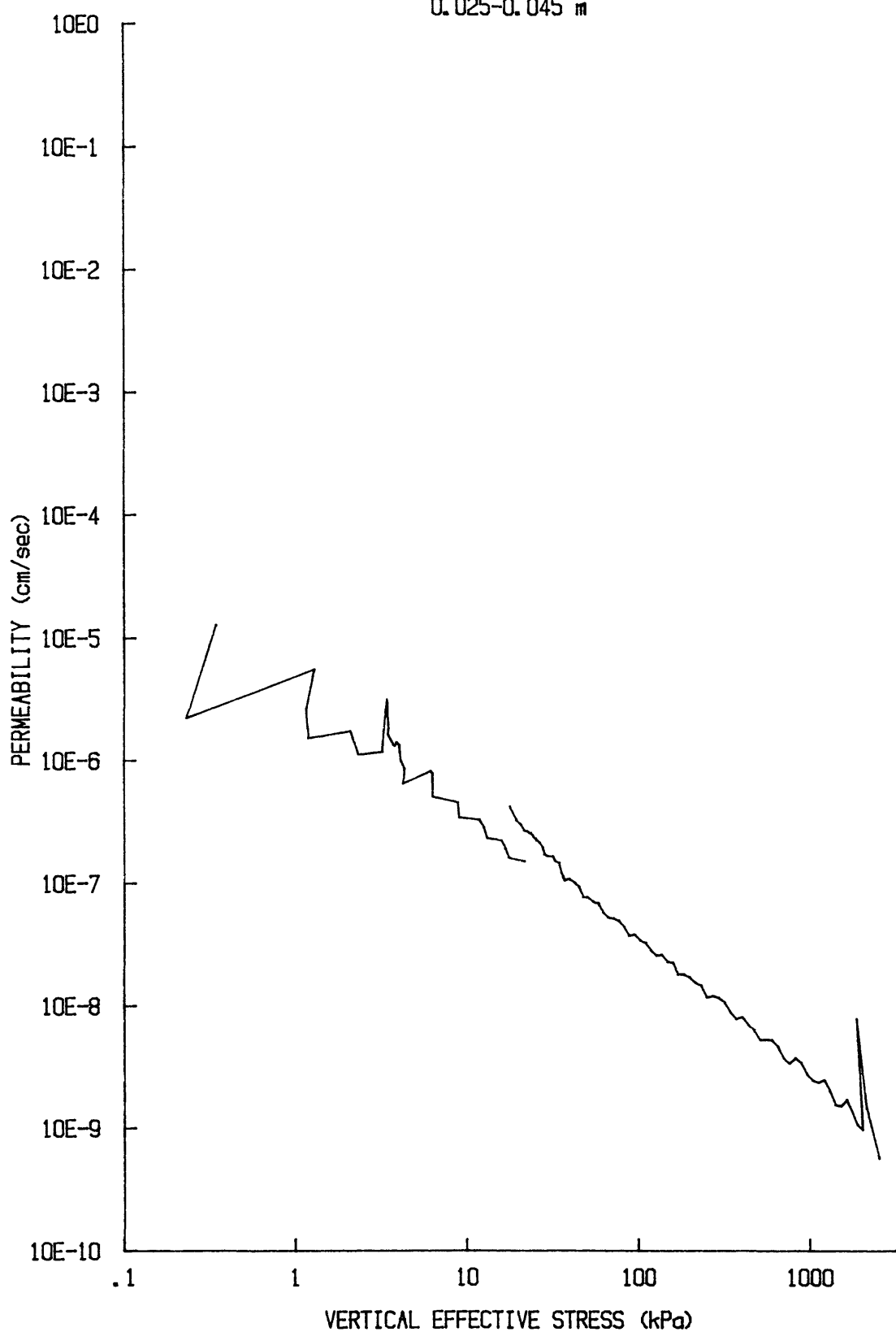
du/Sv for: CR038S8504
YS-85-08
CORE BC-4
0.025-0.045 m



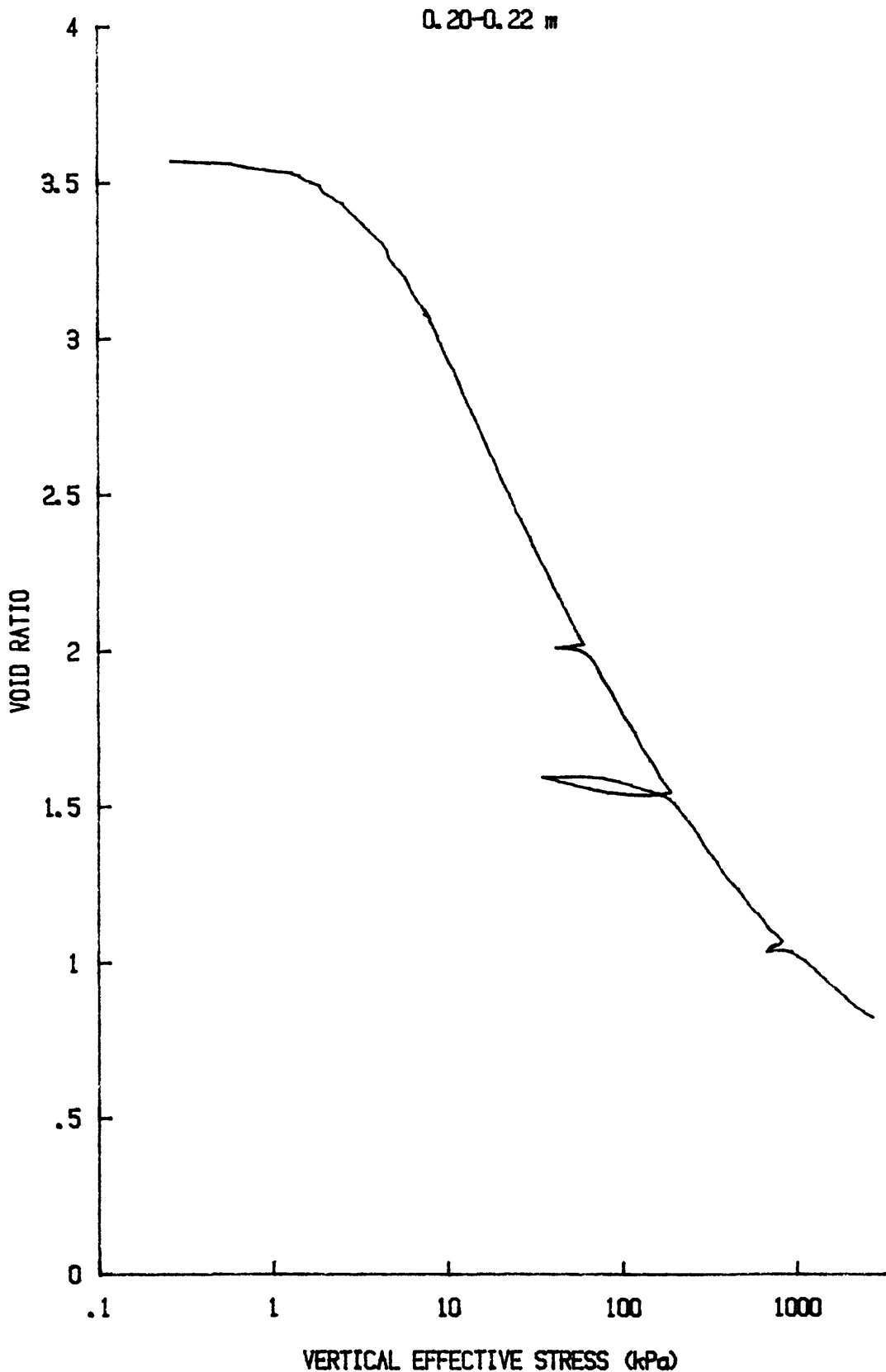
C_v vs $\log p'$ for: CR038S8504
YS-85-08
CORE BC-4
0.025-0.045 m



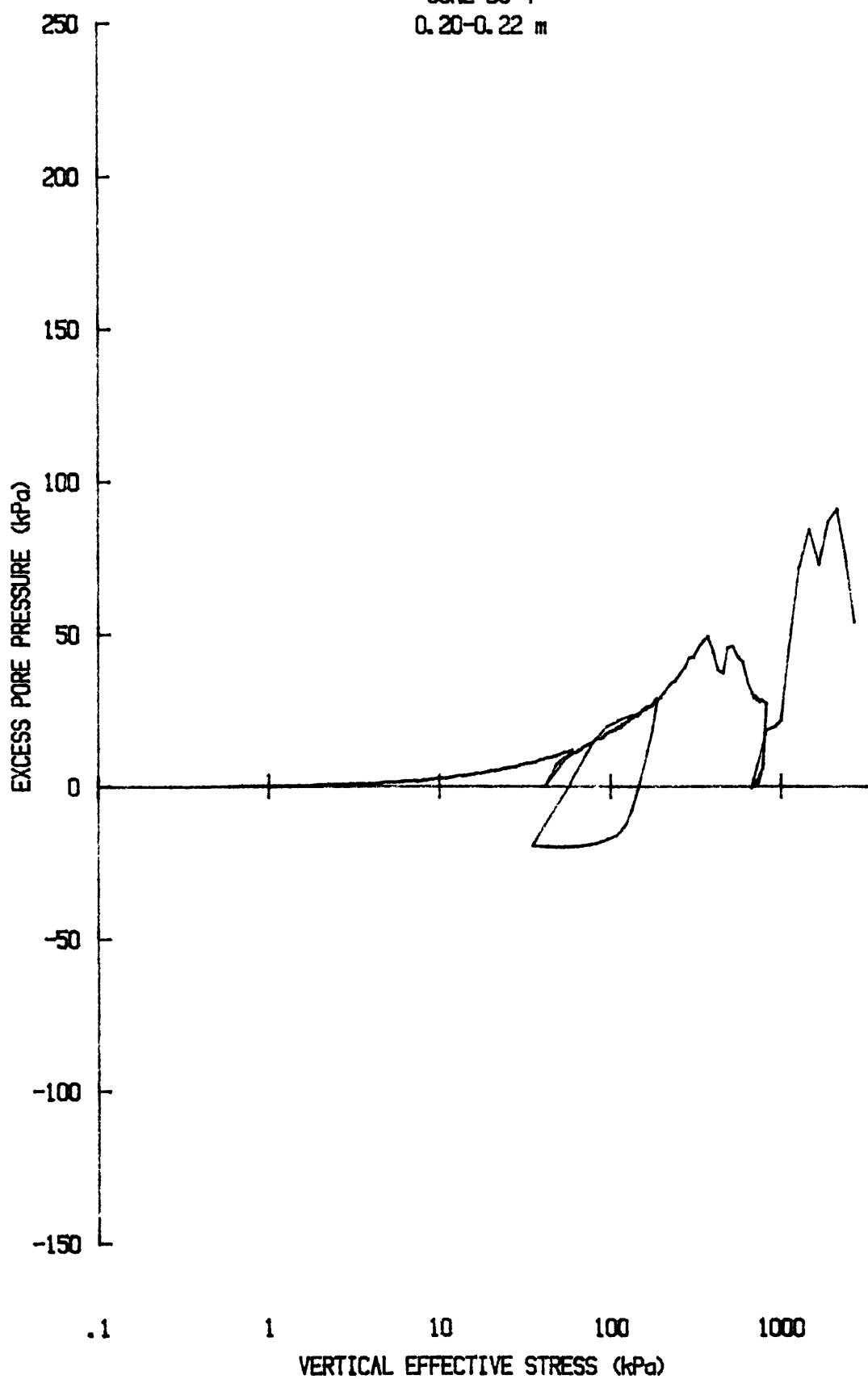
k vs $\log p'$ for: CR038S8504
YS-85-08
CORE BC-4
0.025-0.045 m



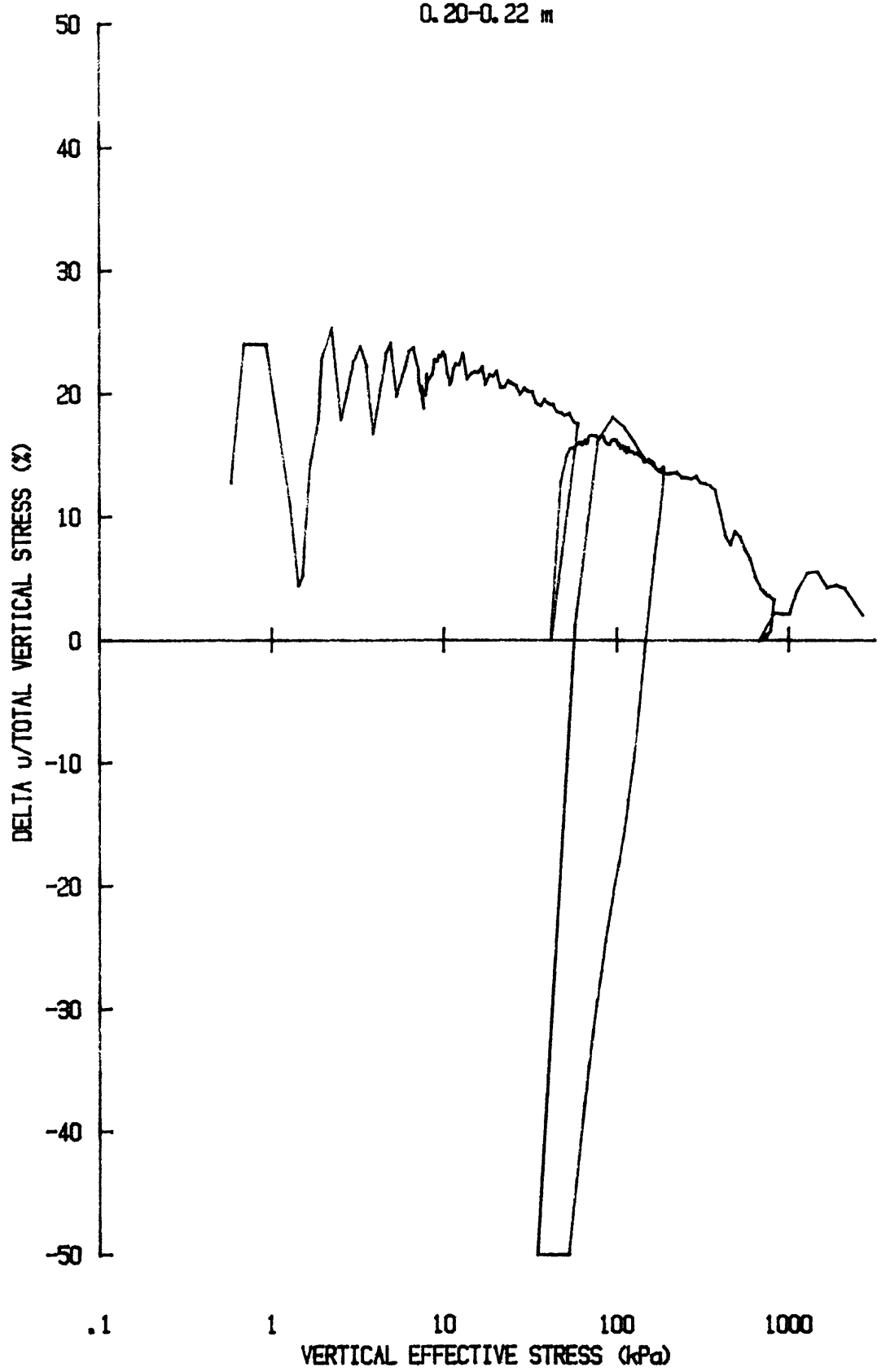
e vs log p' for: CR049S8504
YS-85-08
CORE BC-4
0.20-0.22 m



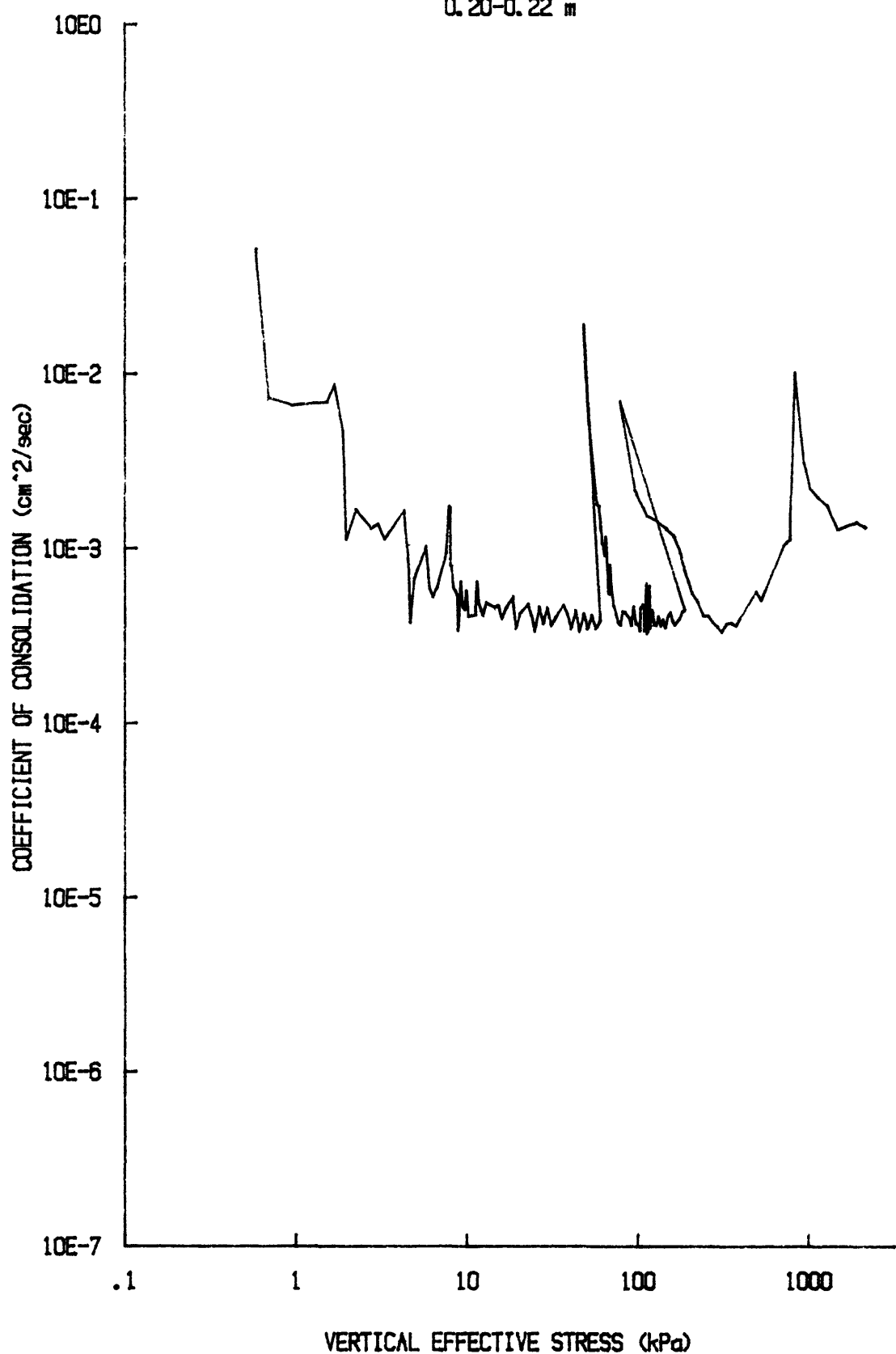
u vs $\log p'$ for CR049S8504
YS-85-08
CORE BC-4
0.20-0.22 m



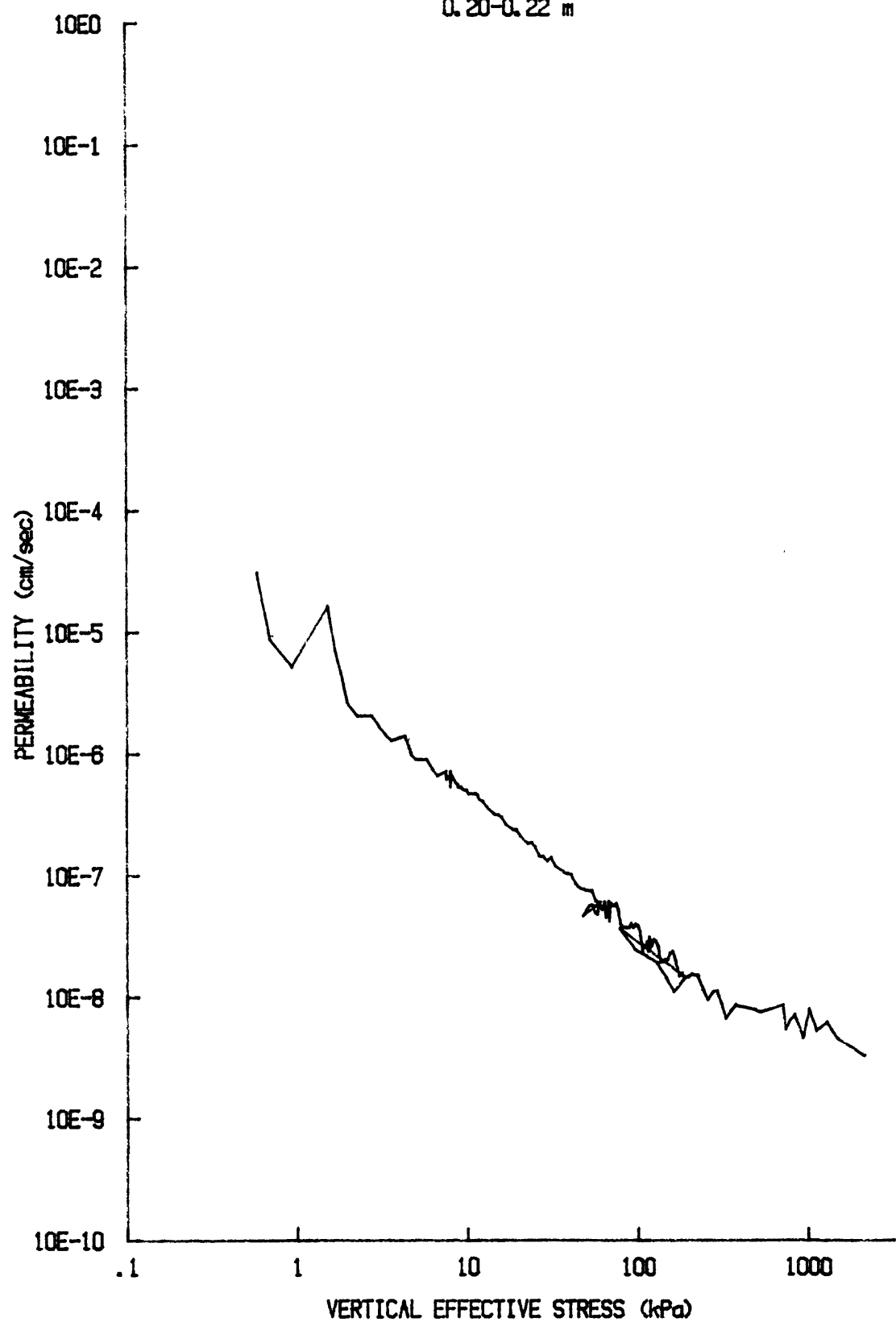
du/Sv for: CR049S8504
YS-85-08
CORE BC-4
0.20-0.22 m



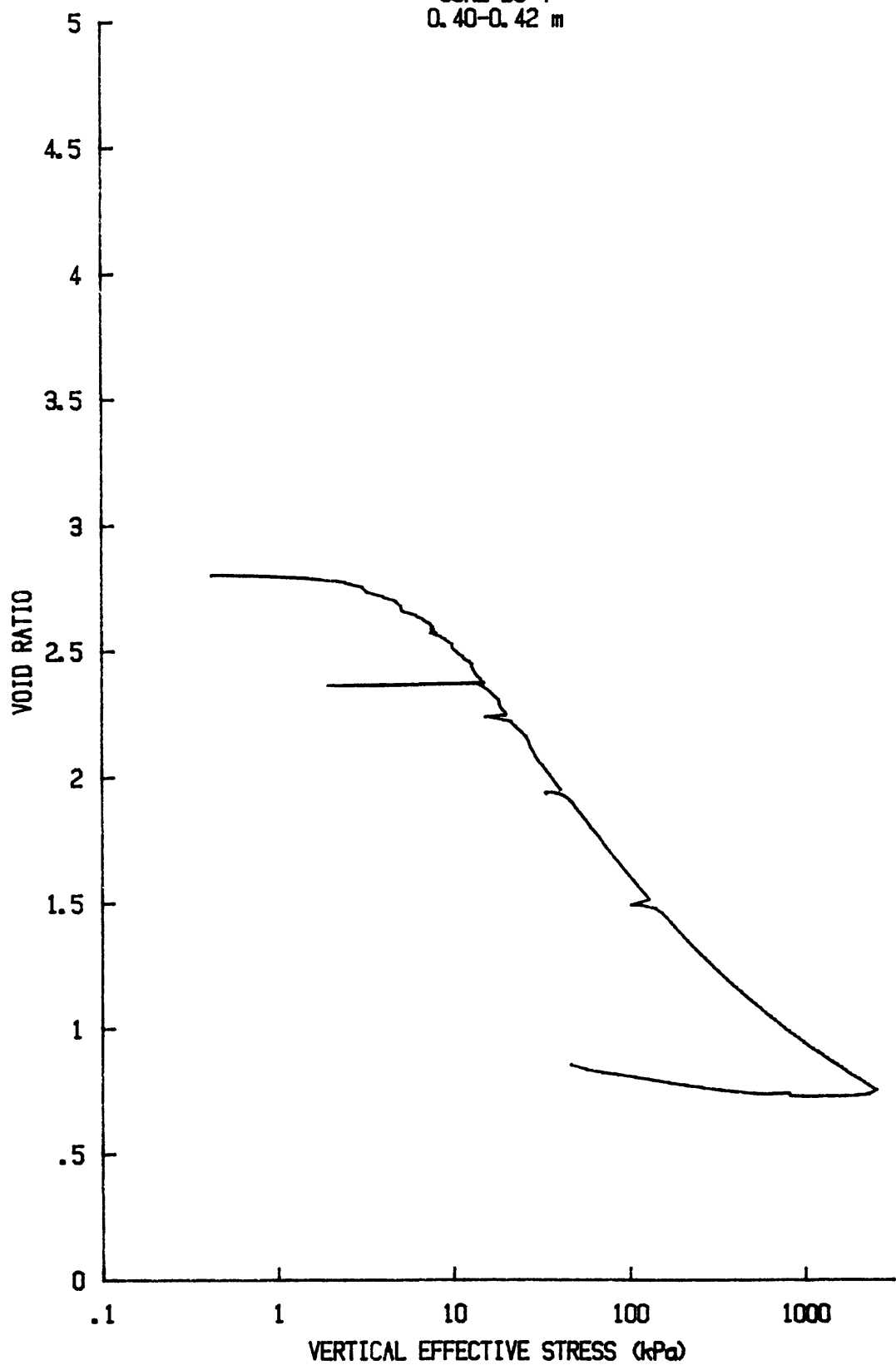
C_v vs $\log p'$ for CR049S8504
YS-85-08
CORE BC-4
0.20-0.22 m



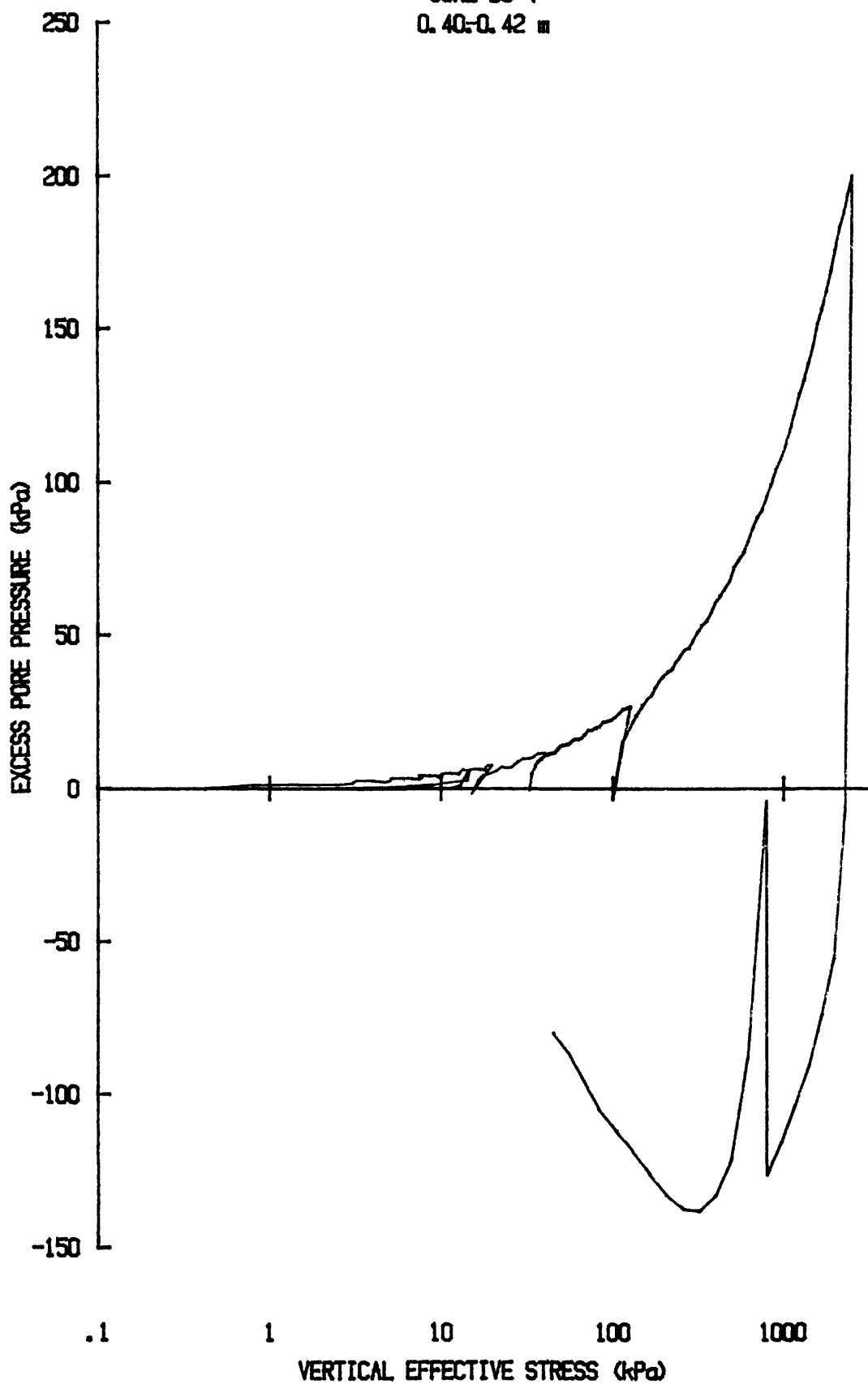
k vs $\log p'$ for CR049S8504
YS-85-08
CORE BC-4
0.20-0.22 m



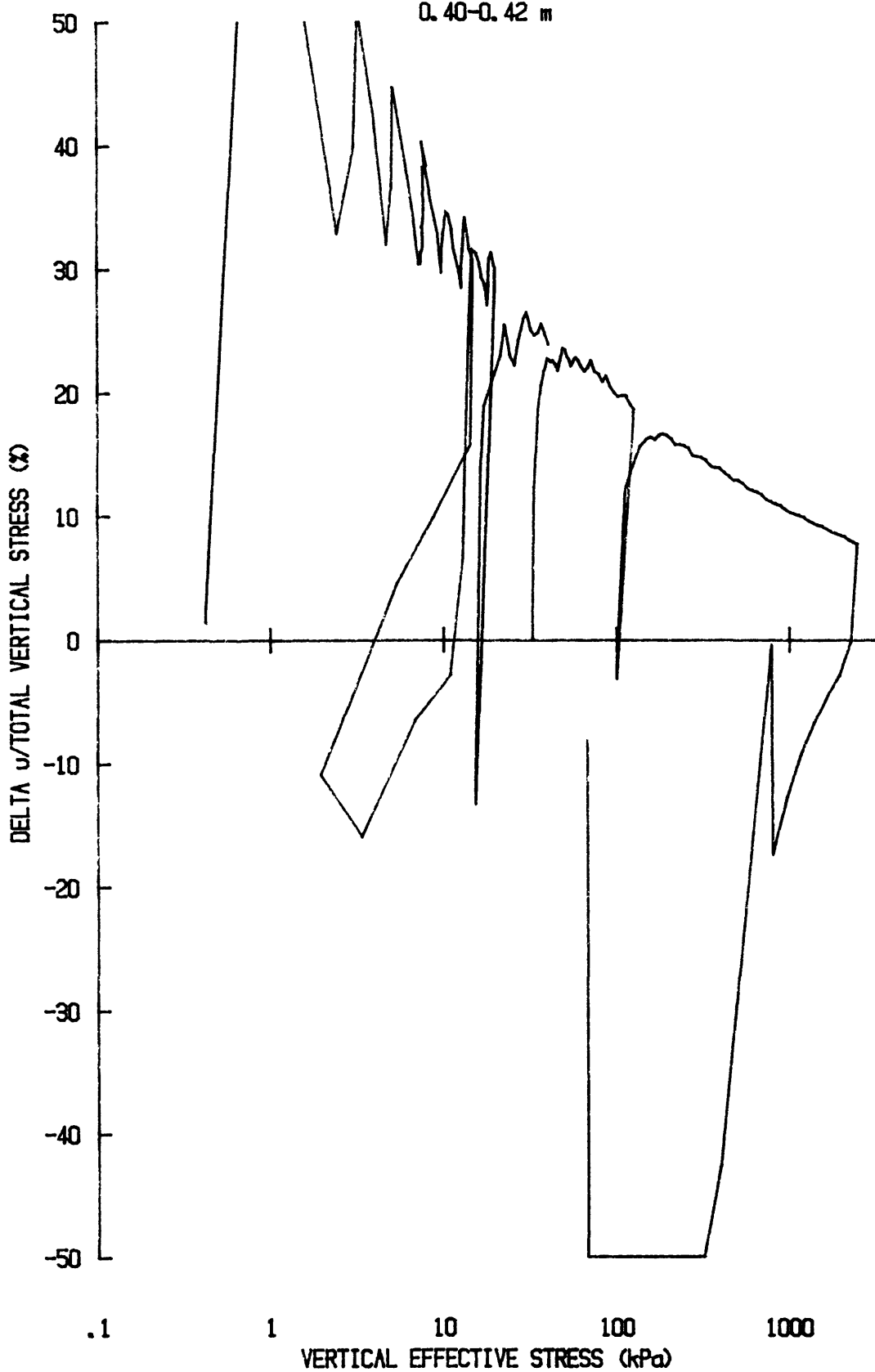
e vs $\log p'$ for: CR042S8504
YS-85-08
CORE BC-4
0.40-0.42 m



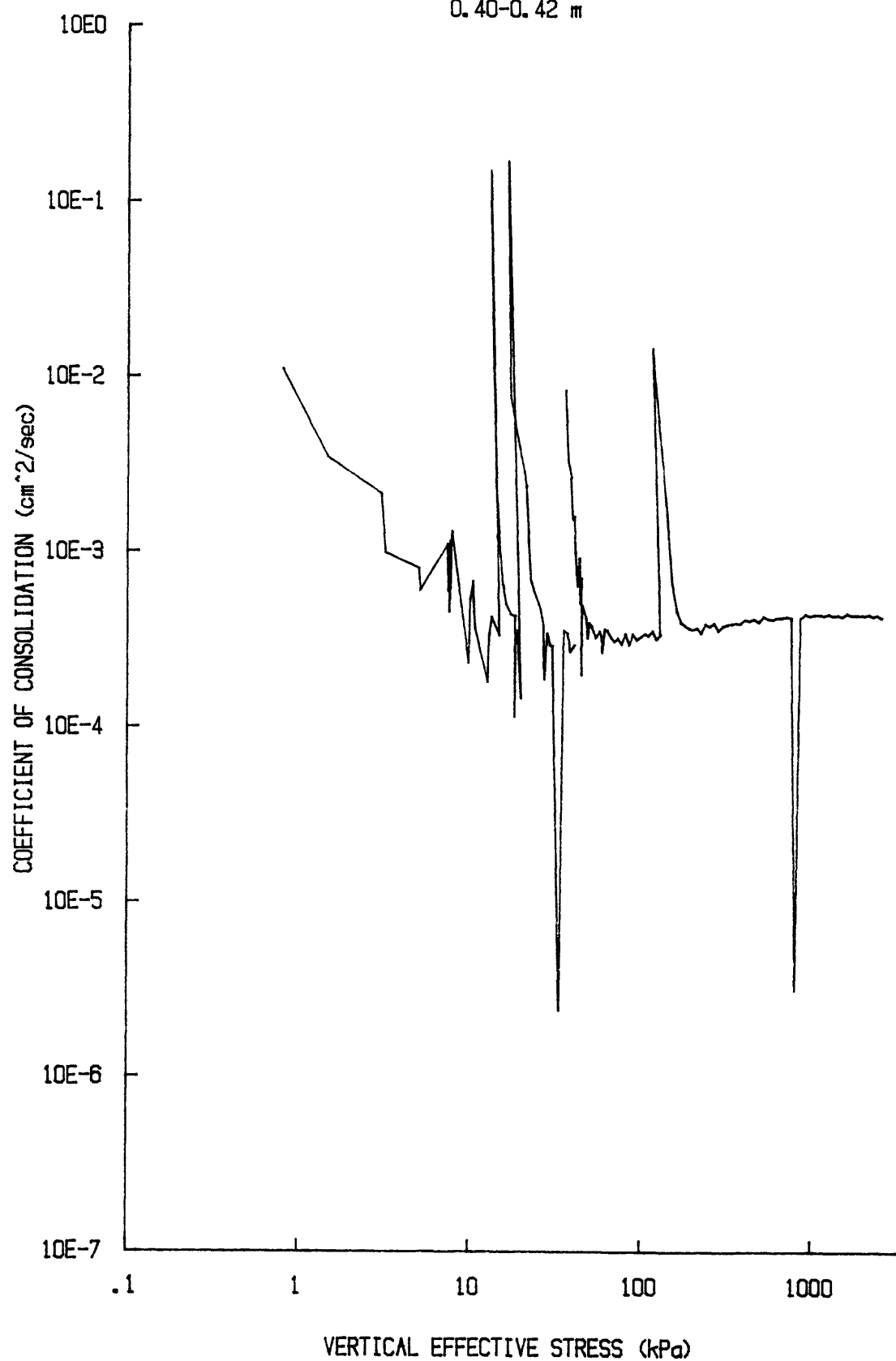
u vs $\log p'$ for CR042S86N4
YS-85-08
CORE BC-4
0.40-0.42 m



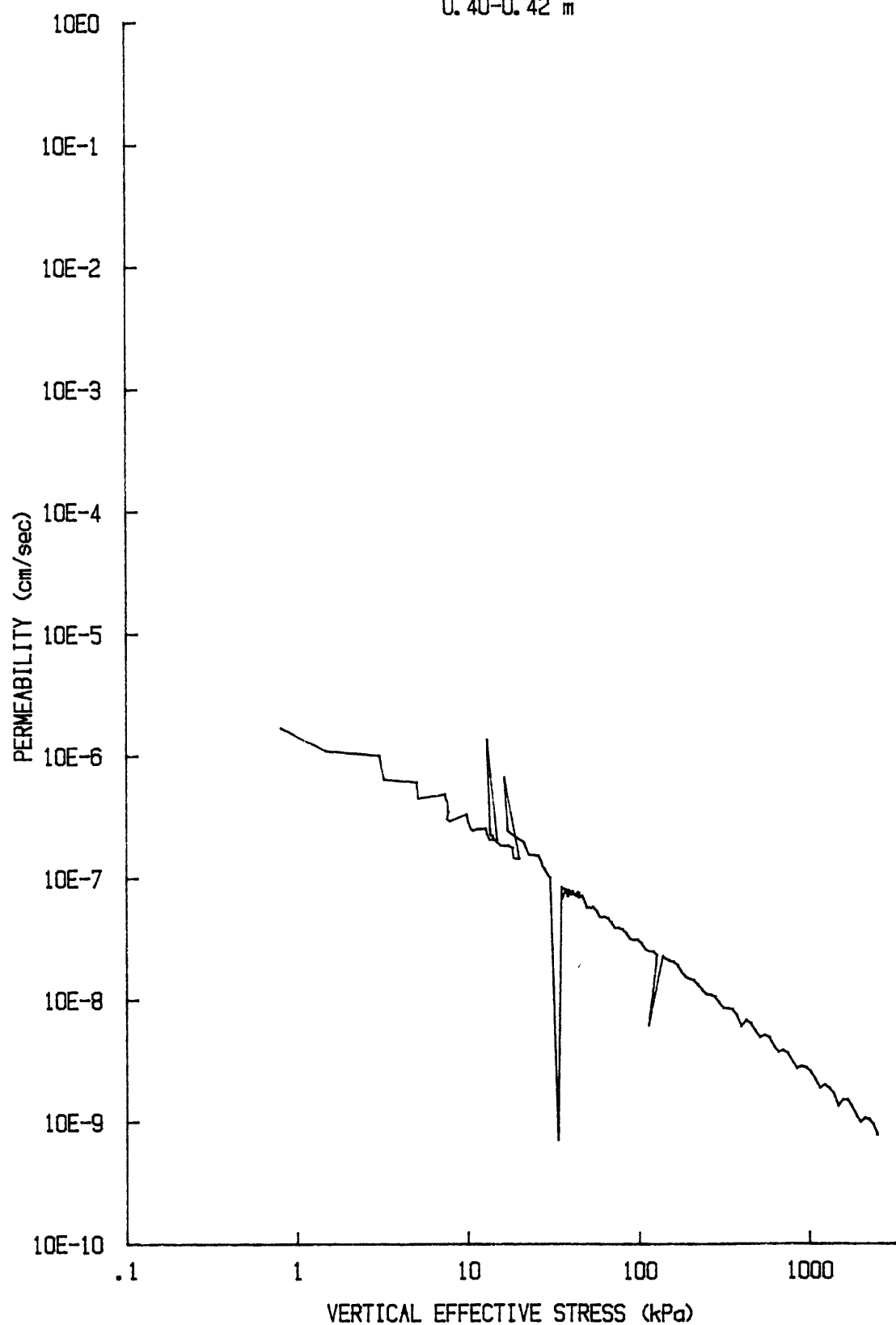
du/Sv for: CR042S8504
YS-85-08
CORE BC-4
0.40-0.42 m



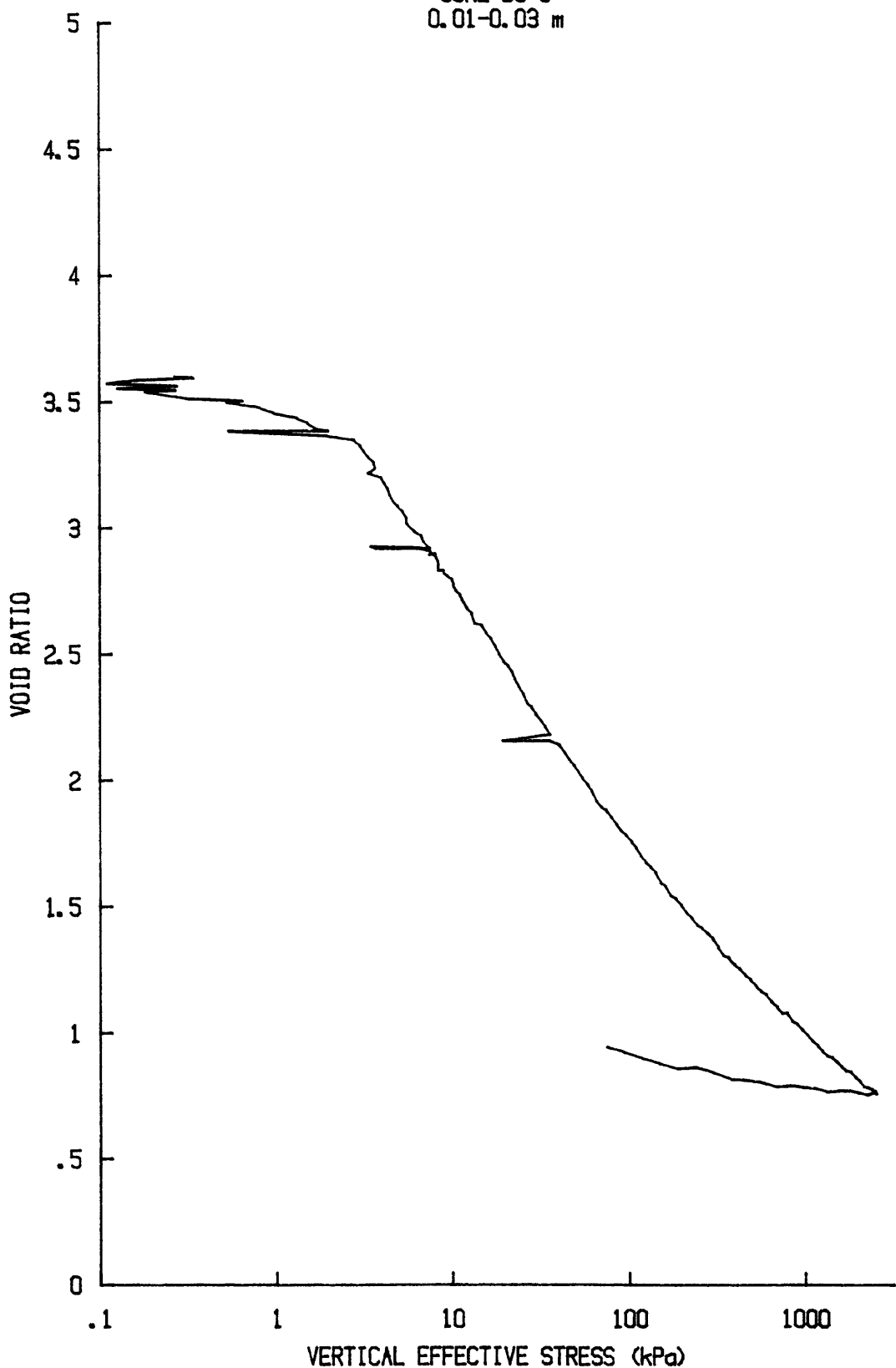
C_v vs $\log p'$ for: CR042S8504
YS-85-08
CORE BC-4
0.40-0.42 m



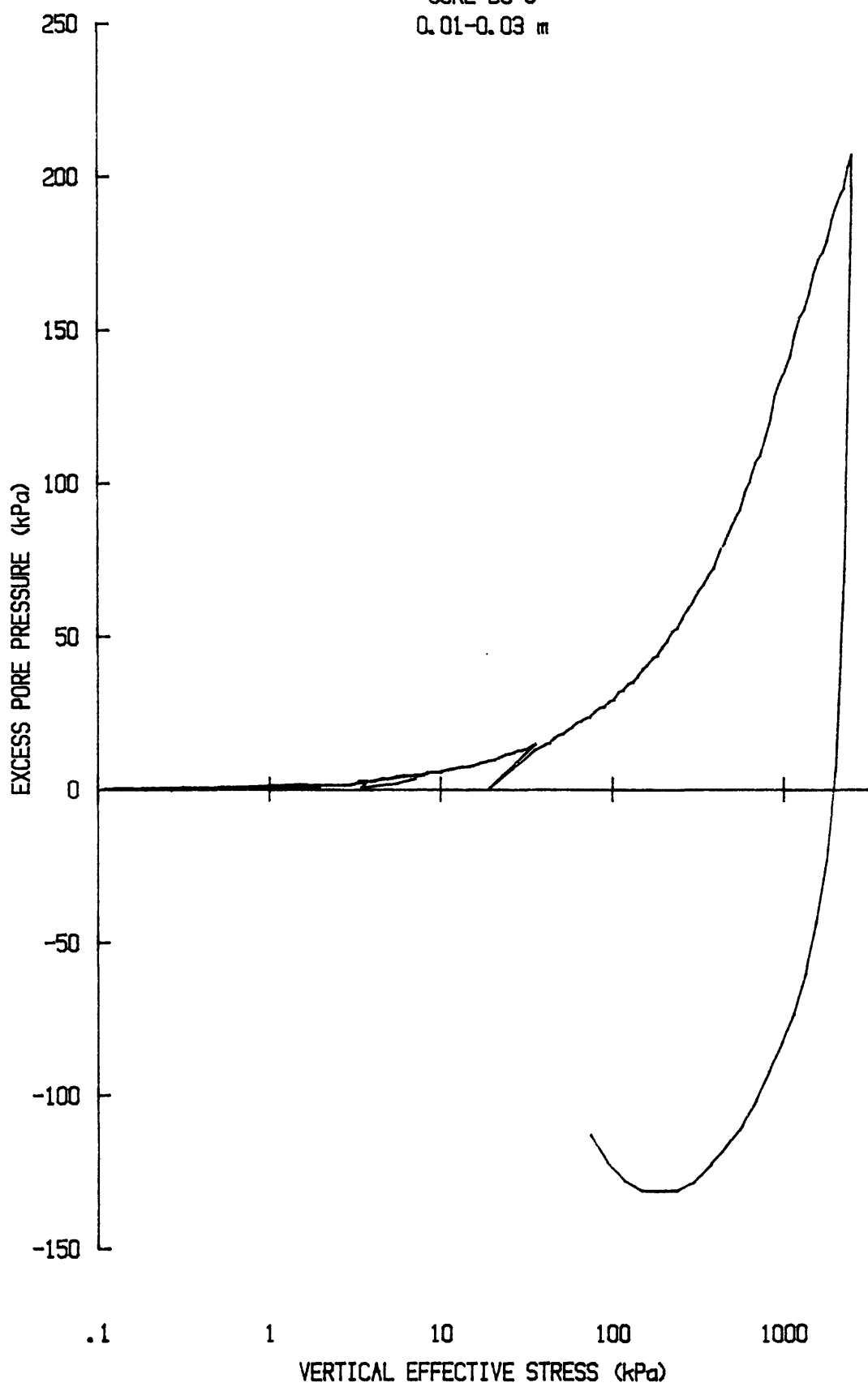
k vs $\log p'$ for: CR042S8504
YS-85-08
CORE BC-4
0.40-0.42 m

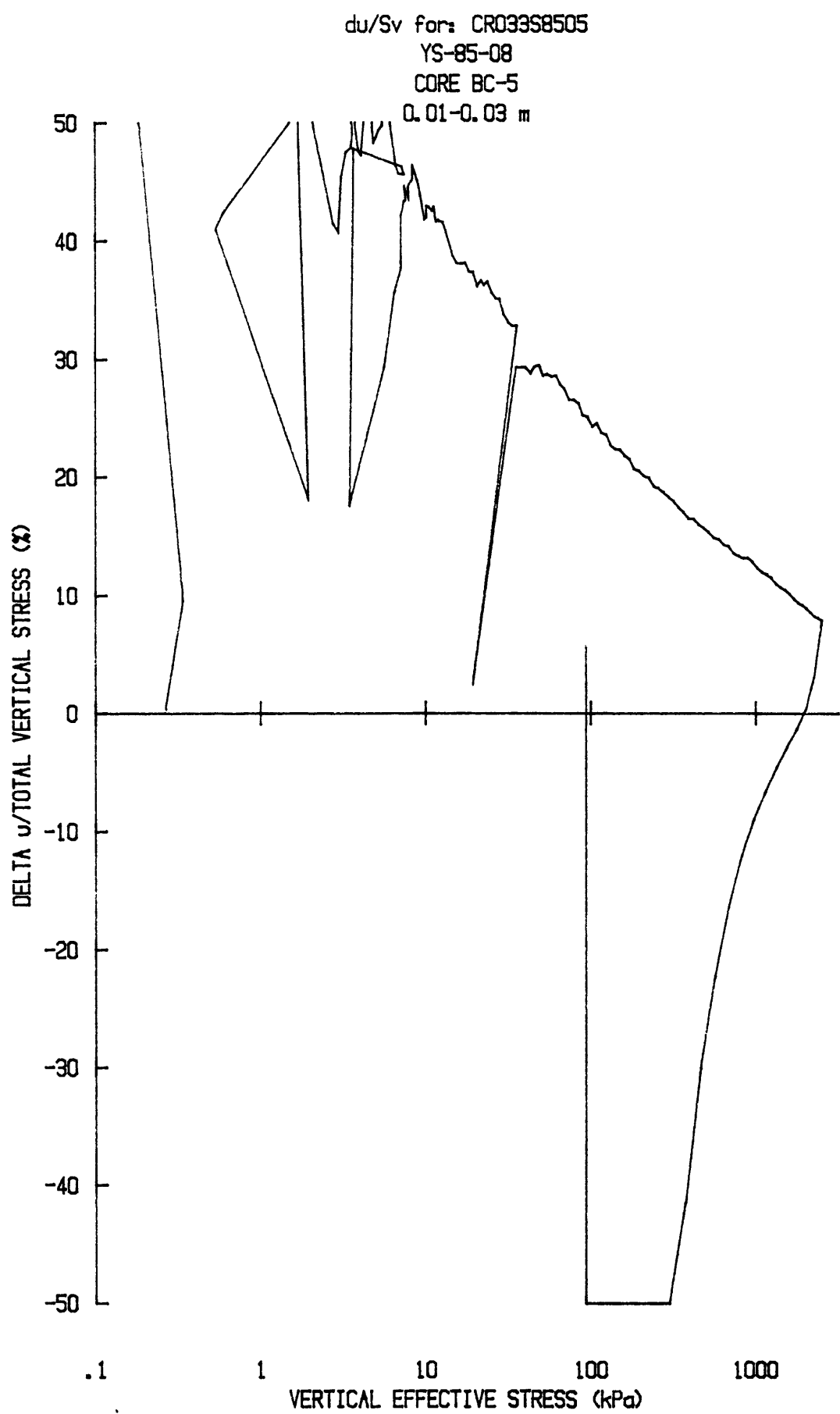


e vs log p' for: CR033S8505
YS-85-08
CORE BC-5
0.01-0.03 m

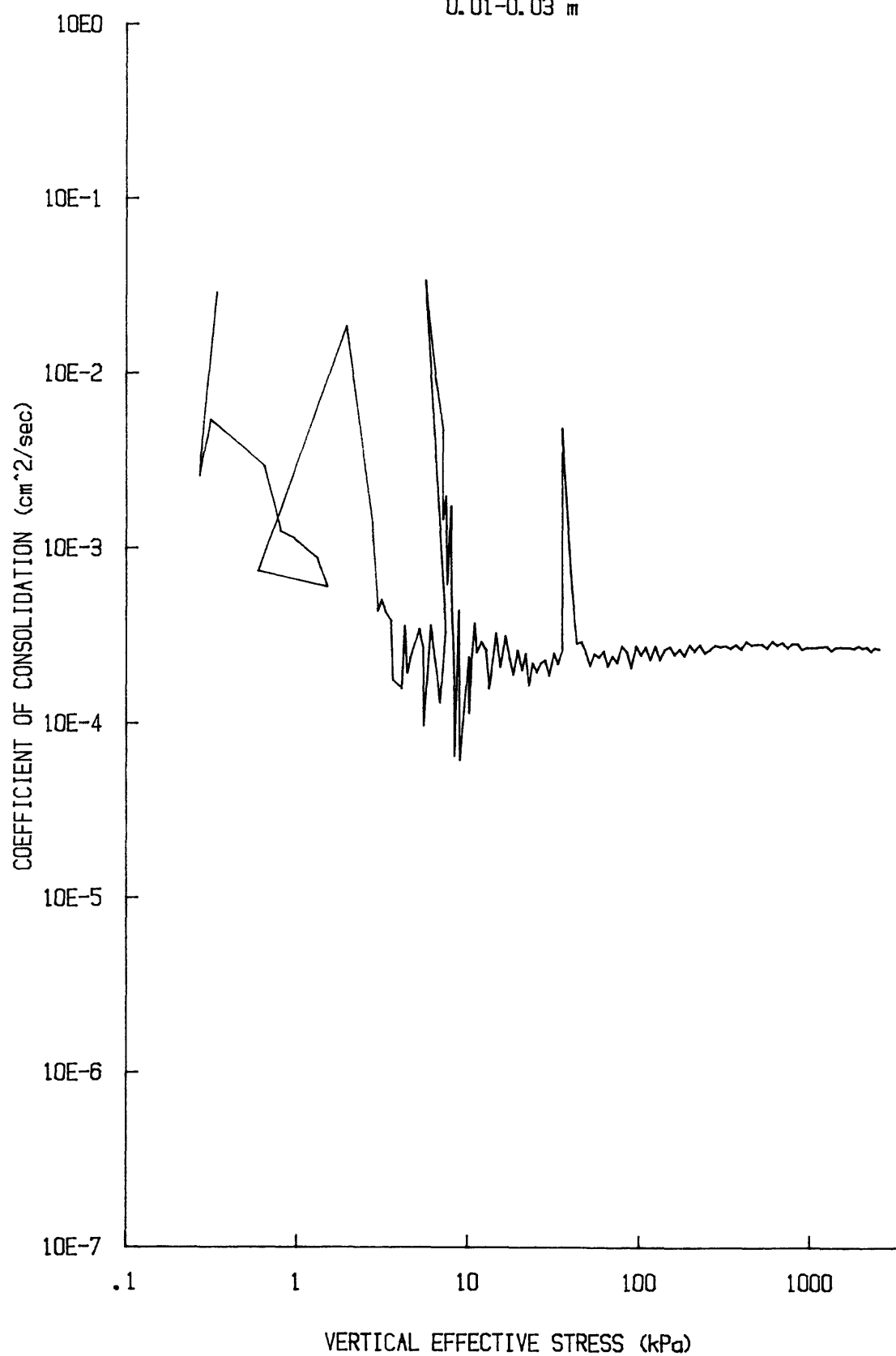


u vs $\log p'$ for: CR033S8505
YS-85-08
CORE BC-5
0.01-0.03 m

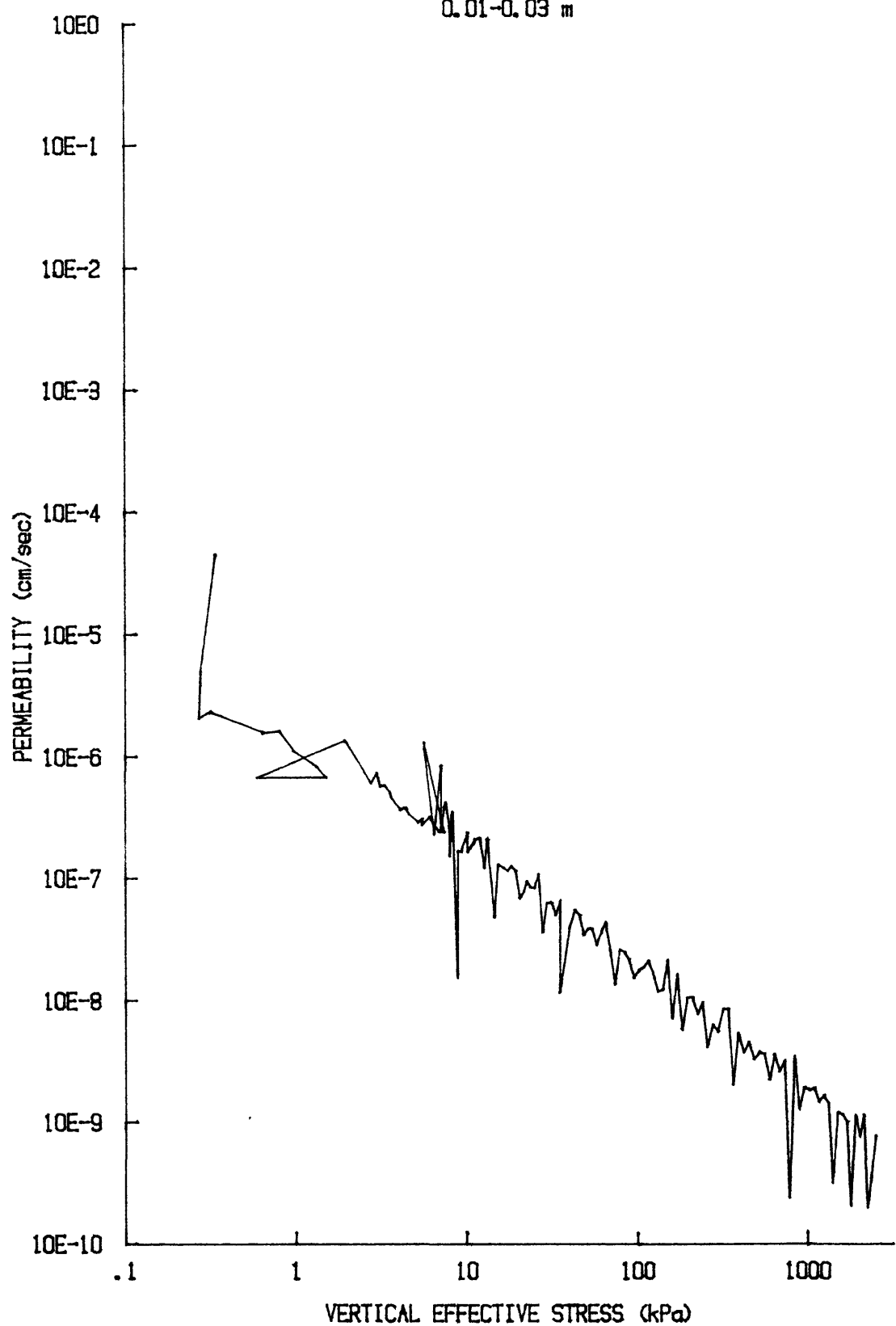




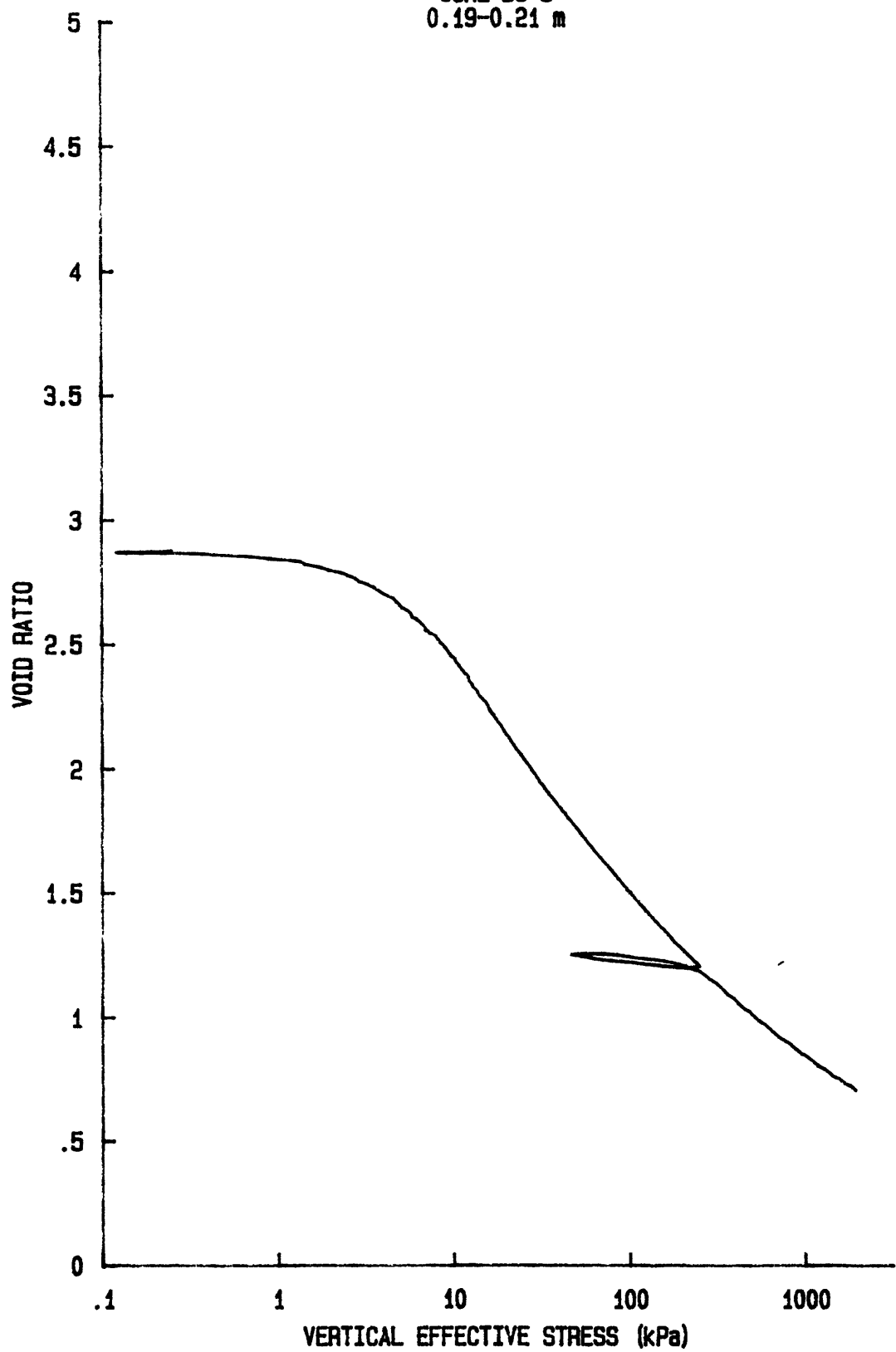
C_v vs $\log p'$ for: CR033S8505
YS-85-08
CORE BC-5
0.01-0.03 m



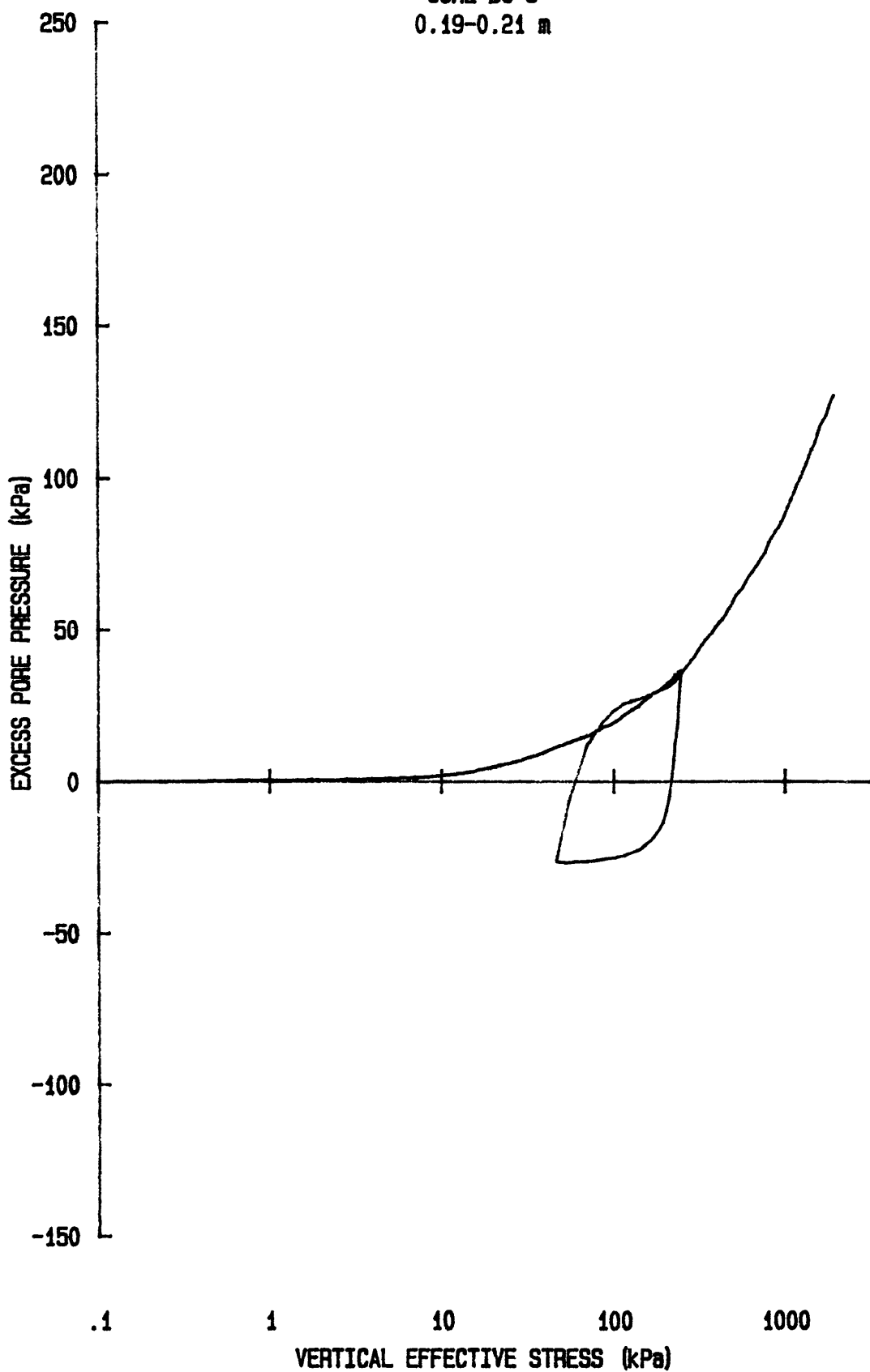
k vs $\log p'$ for CR033S8505
YS-85-08
CORE BC-5
0.01-0.03 m



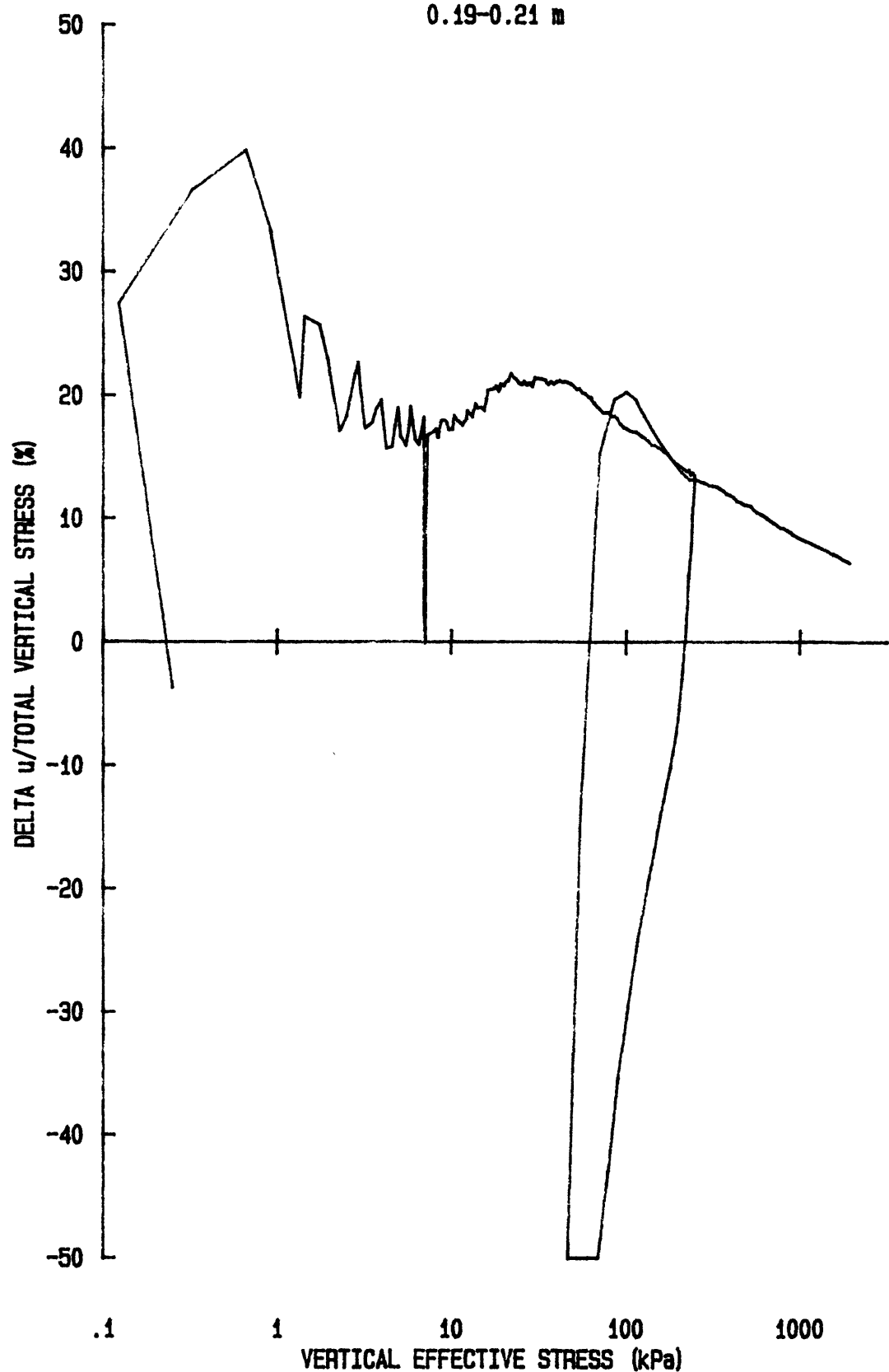
e vs log p' for: CR053S8505
YS-85-08
CORE BC-5
0.19-0.21 m



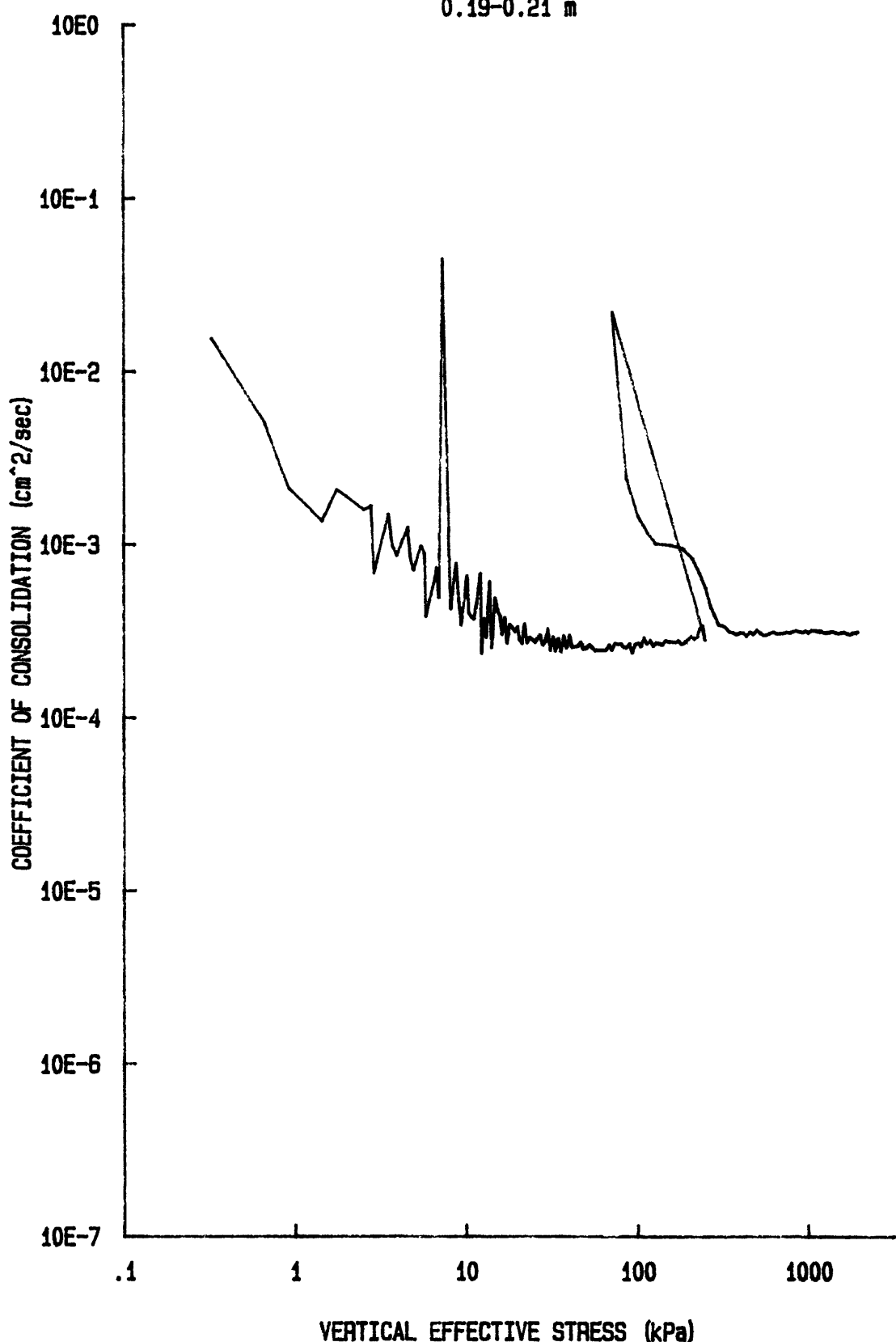
u vs log p' for: CR053S8505
YS-85-08
CORE BC-5
0.19-0.21 m



du/Sv for: CR053S8505
YS-85-08
CORE BC-5
0.19-0.21 m



Cv vs log p' for: CR053S8505
YS-85-08
CORE BC-5
0.19-0.21 m

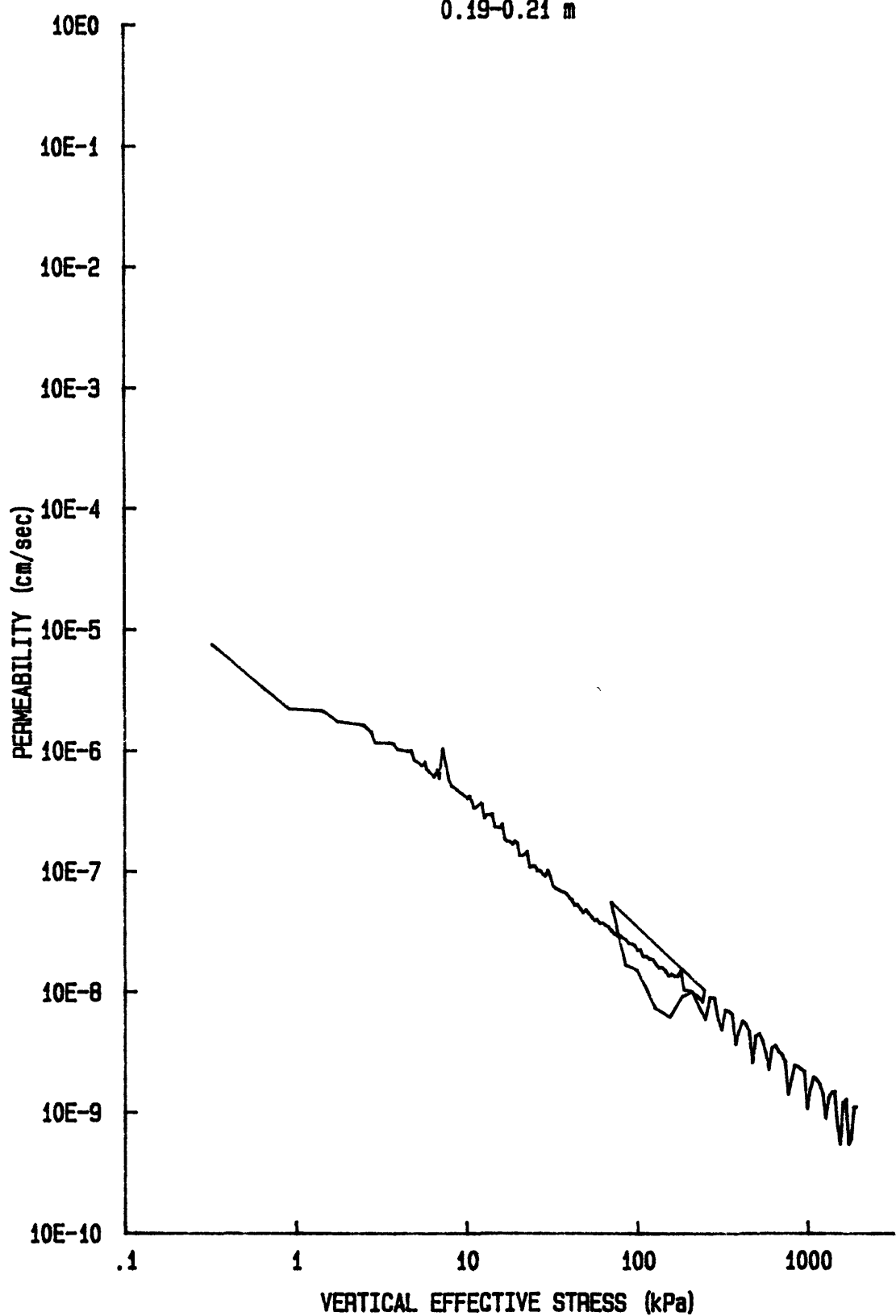


k vs log p' for: CR053S8505

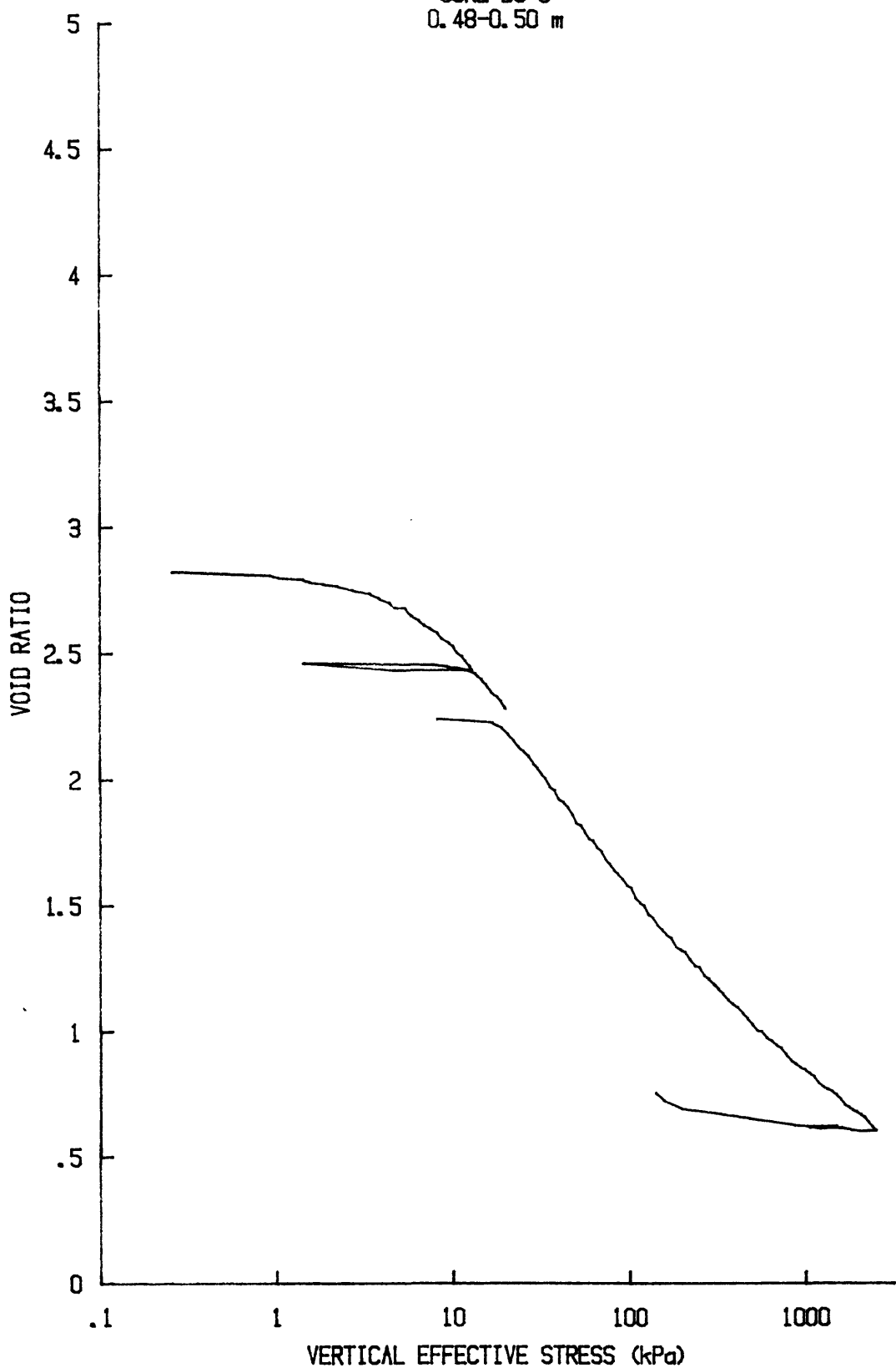
YS-85-08

CORE BC-5

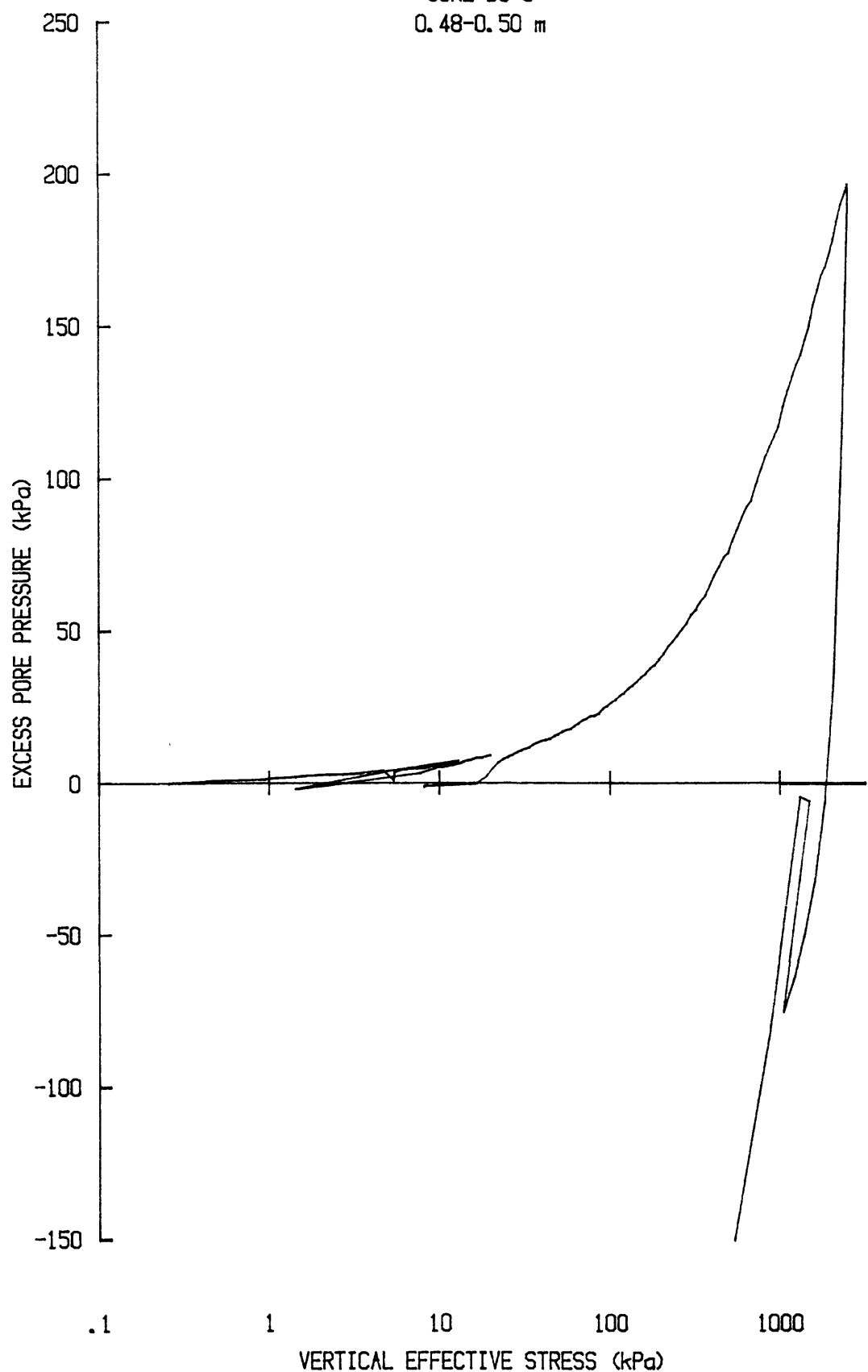
0.19-0.21 m



e vs log p' for: CR029S8505
YS-85-08
CORE BC-5
0.48-0.50 m



u vs $\log p'$ for: CR029S8505
YS-85-08
CORE BC-5
0.48-0.50 m

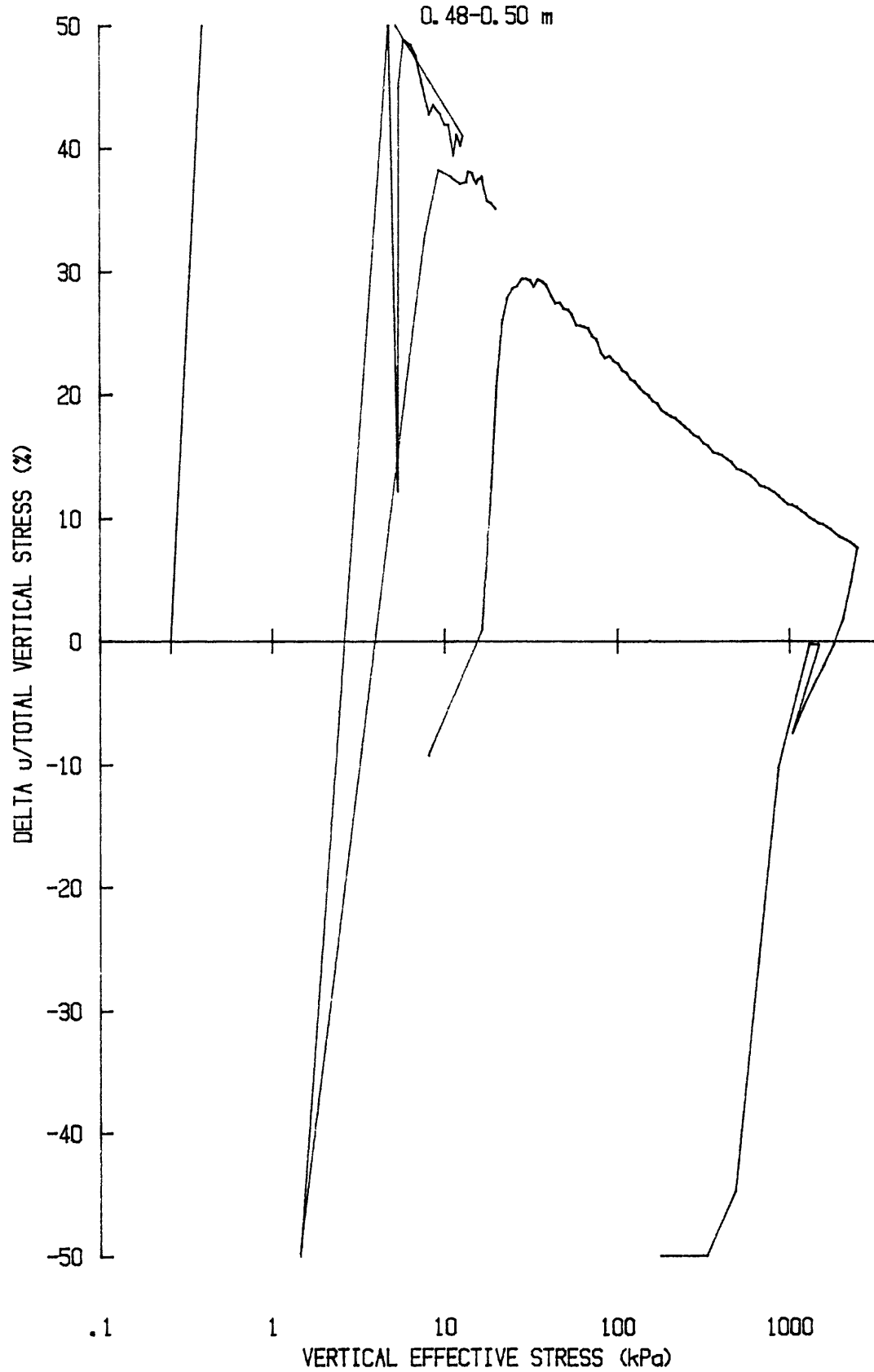


du/Sv for: CR029S8505

YS-85-08

CORE BC-5

0.48-0.50 m

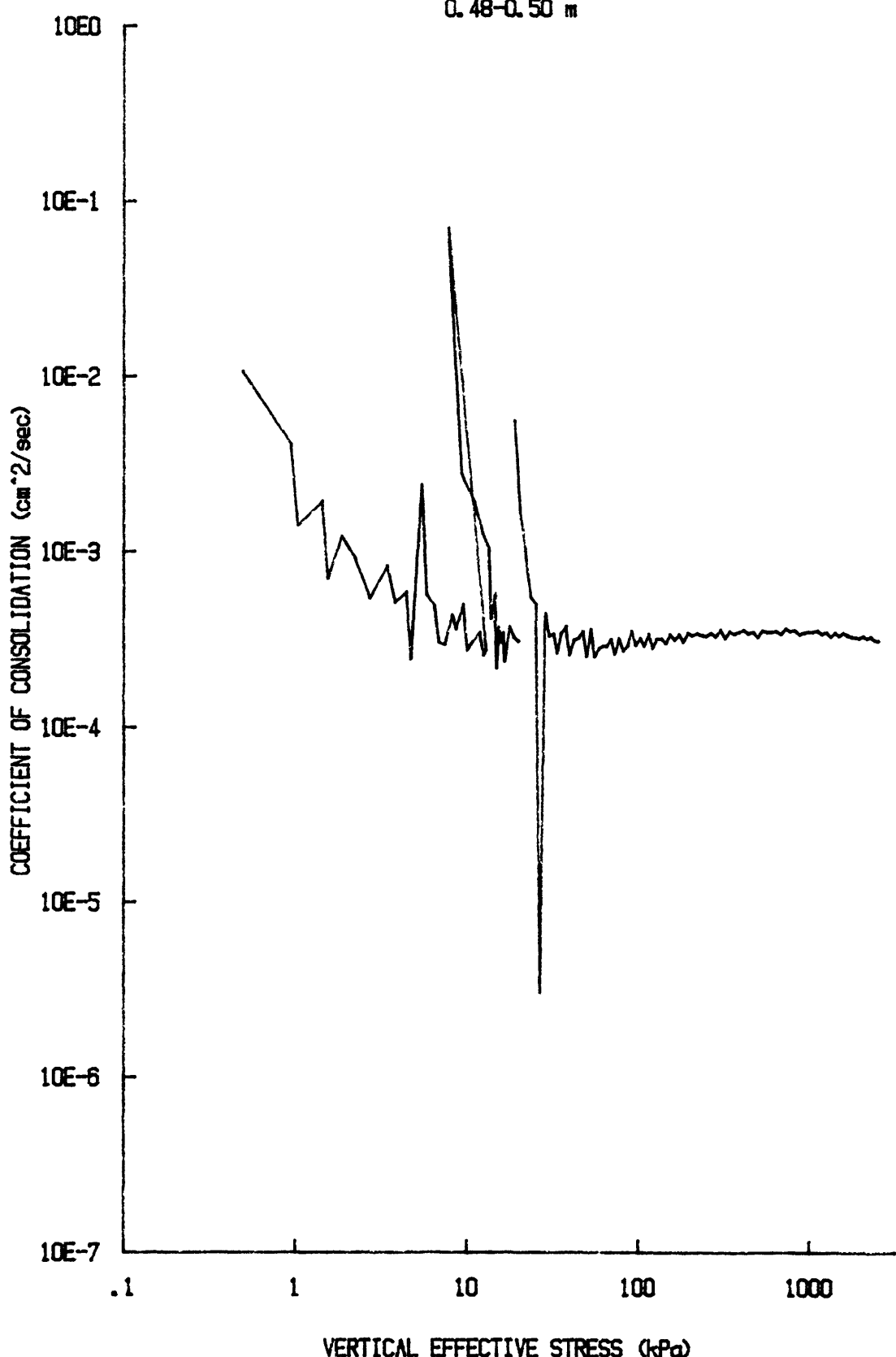


C_v vs $\log p'$ for CR029S8505

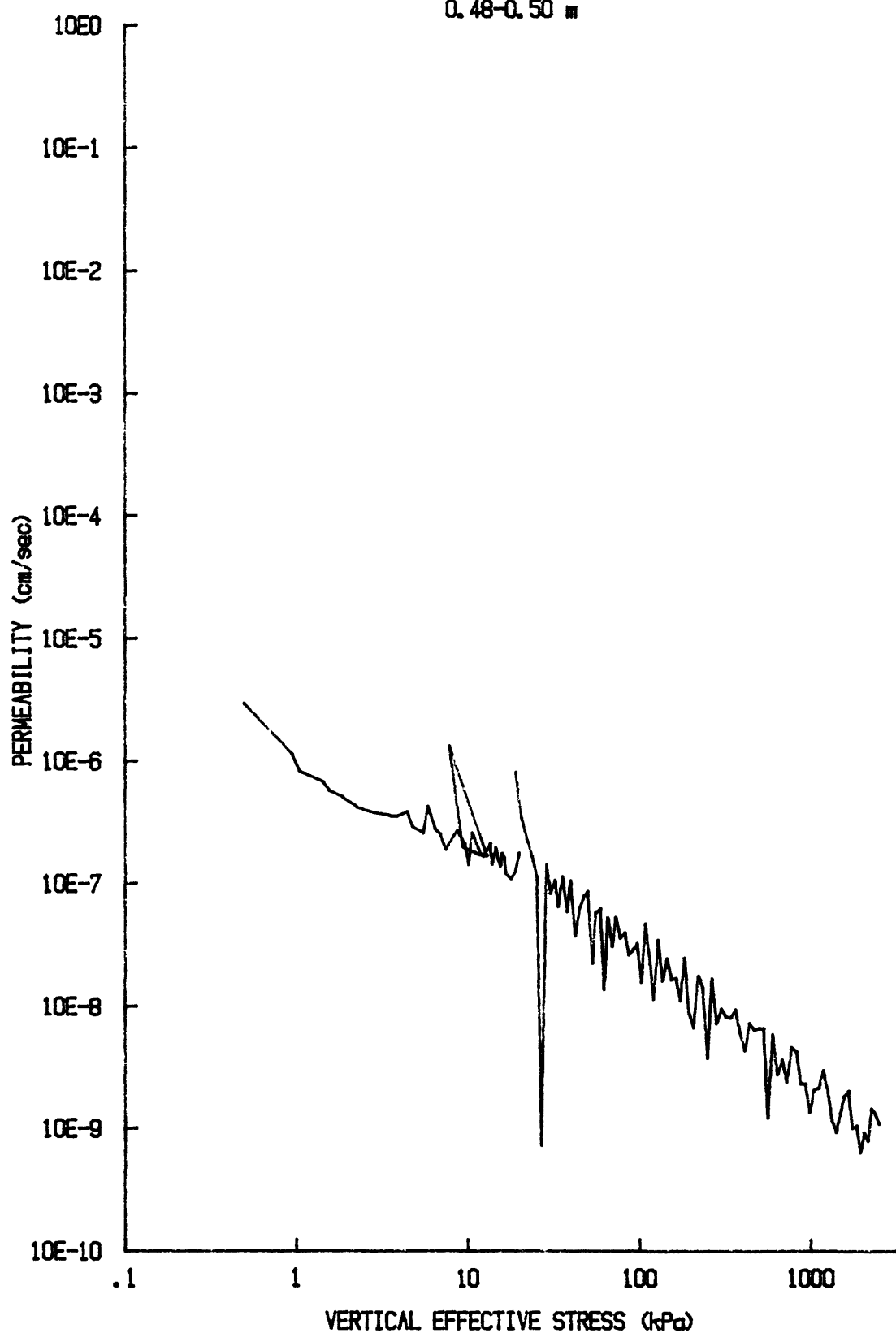
YS-85-08

CORE BC-5

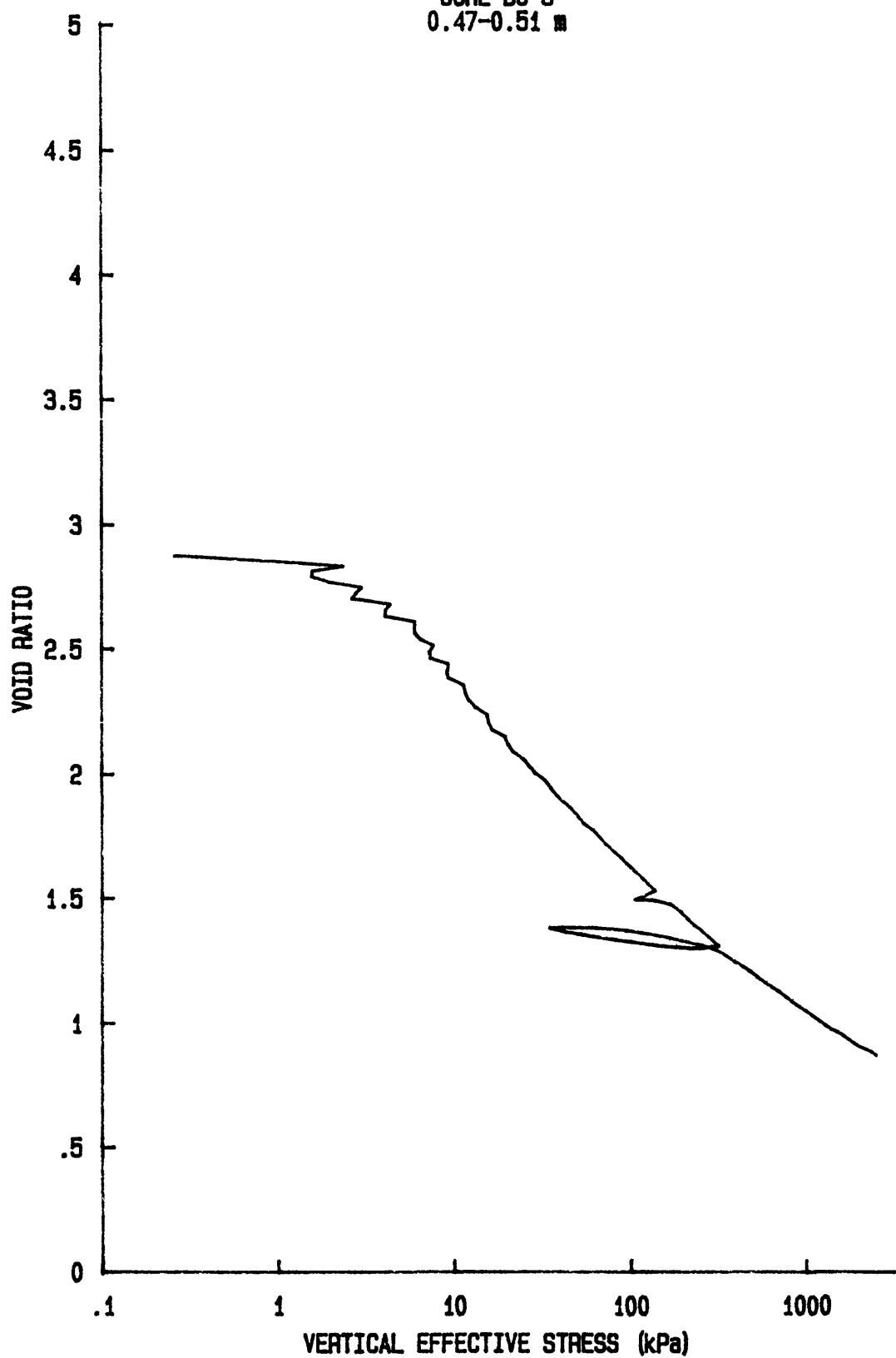
0.48-0.50 m



k vs $\log p'$ for CR029S8505
YS-85-08
CORE BC-5
0.48-0.50 m



e vs log p' for: CR056S8505
YS-85-08
CORE BC-5
0.47-0.51 m

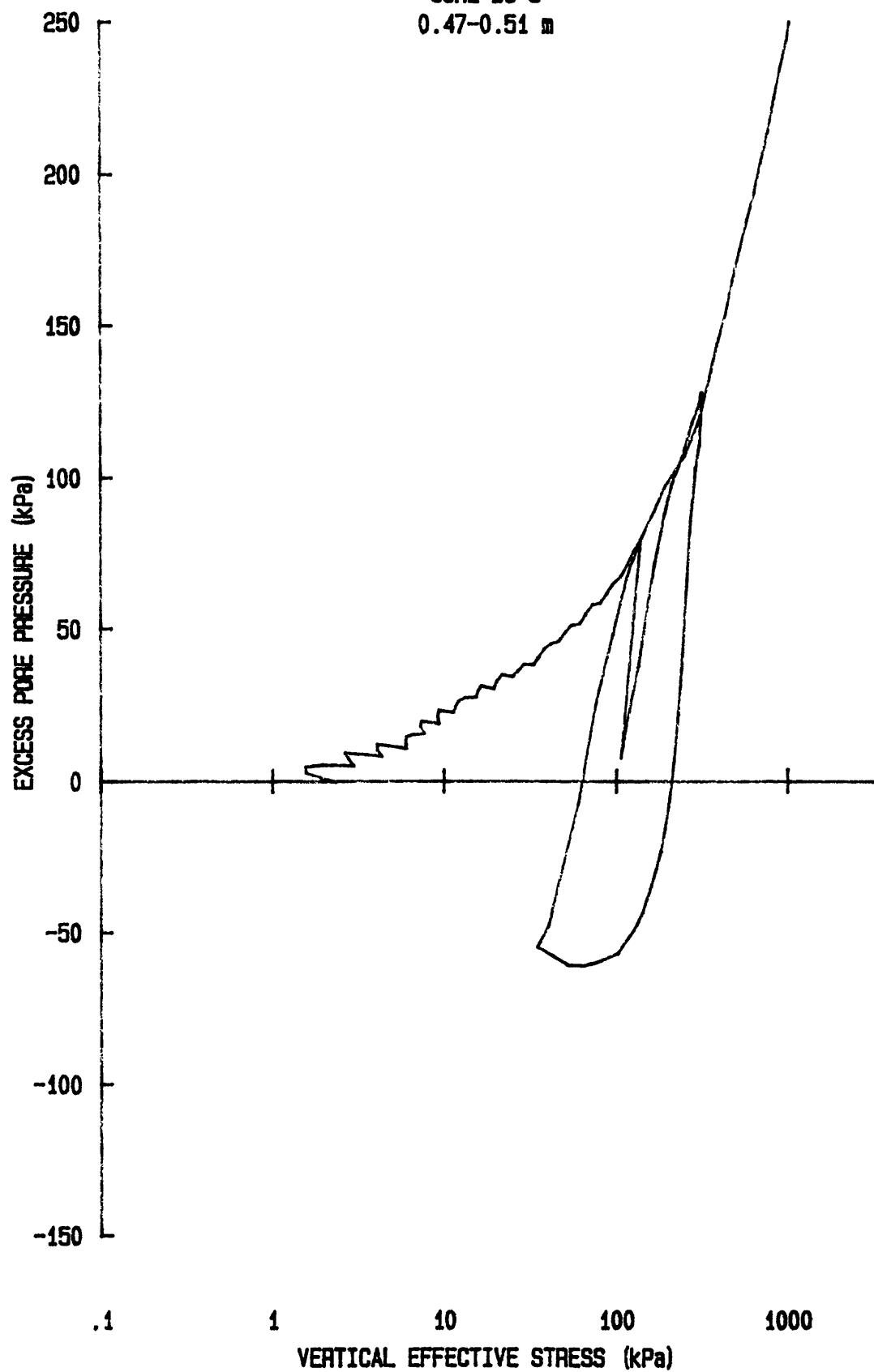


u vs $\log p'$ for: CR056S8505

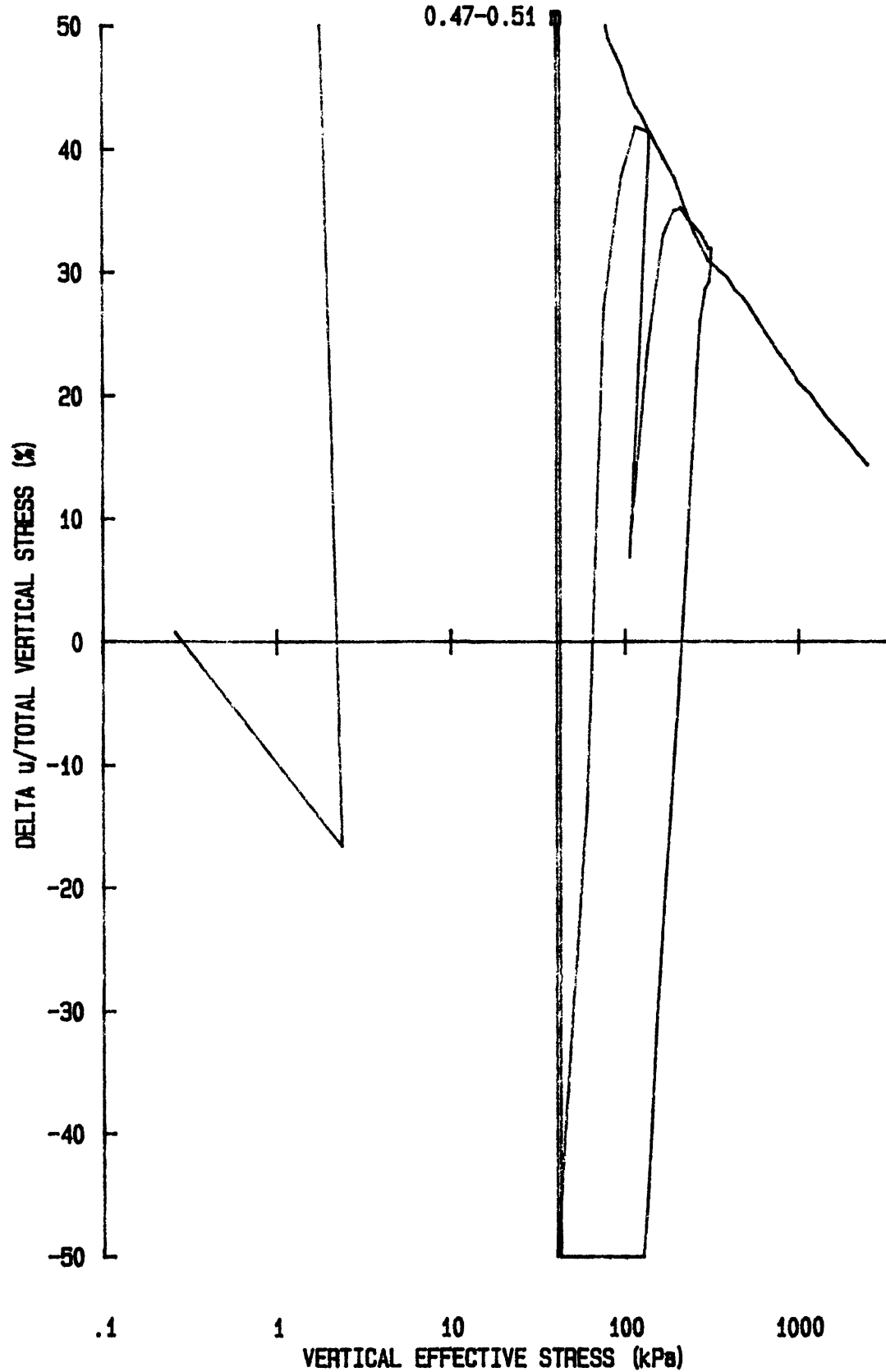
YS-85-08

CORE BC-5

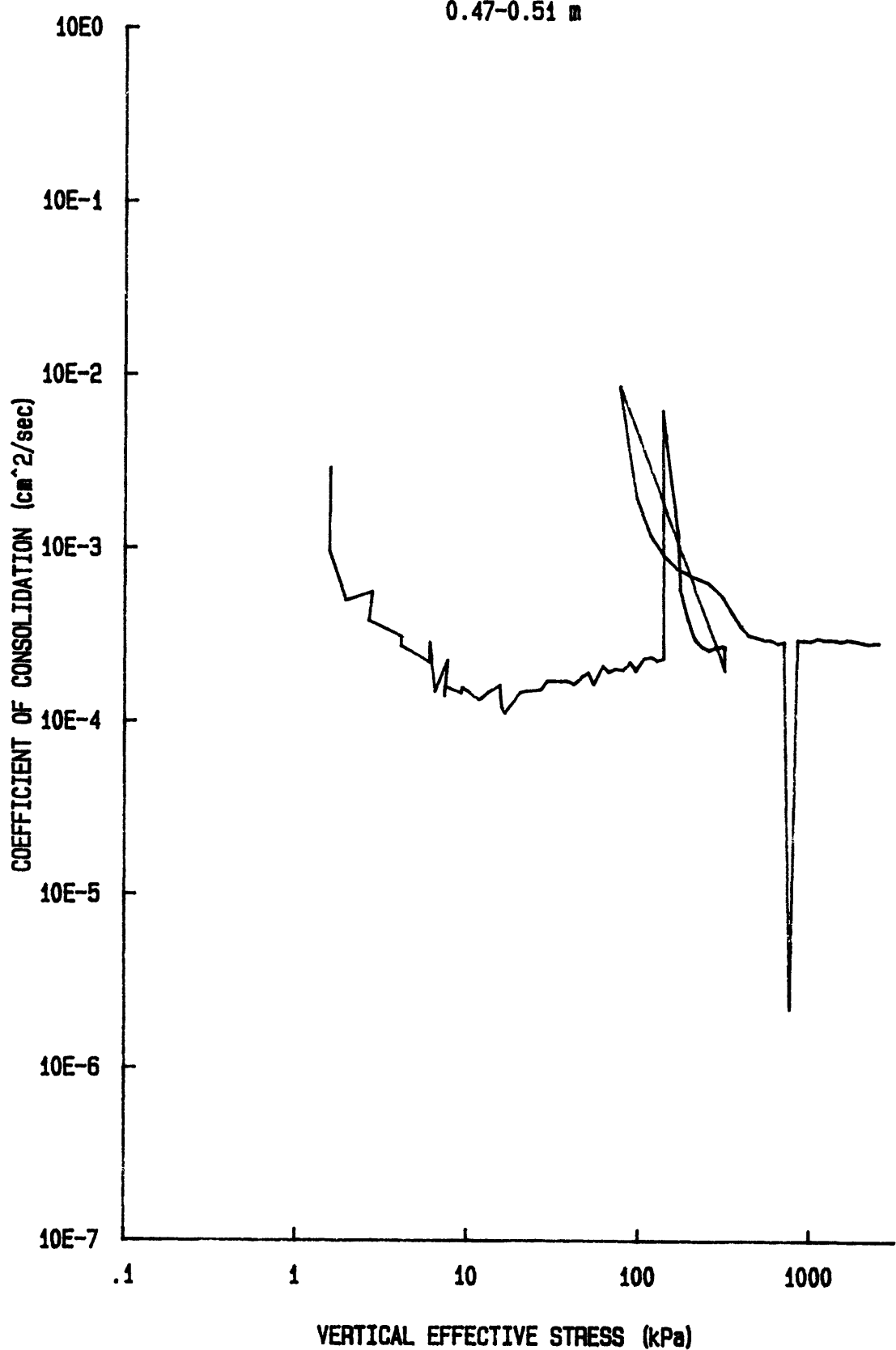
0.47-0.51 m



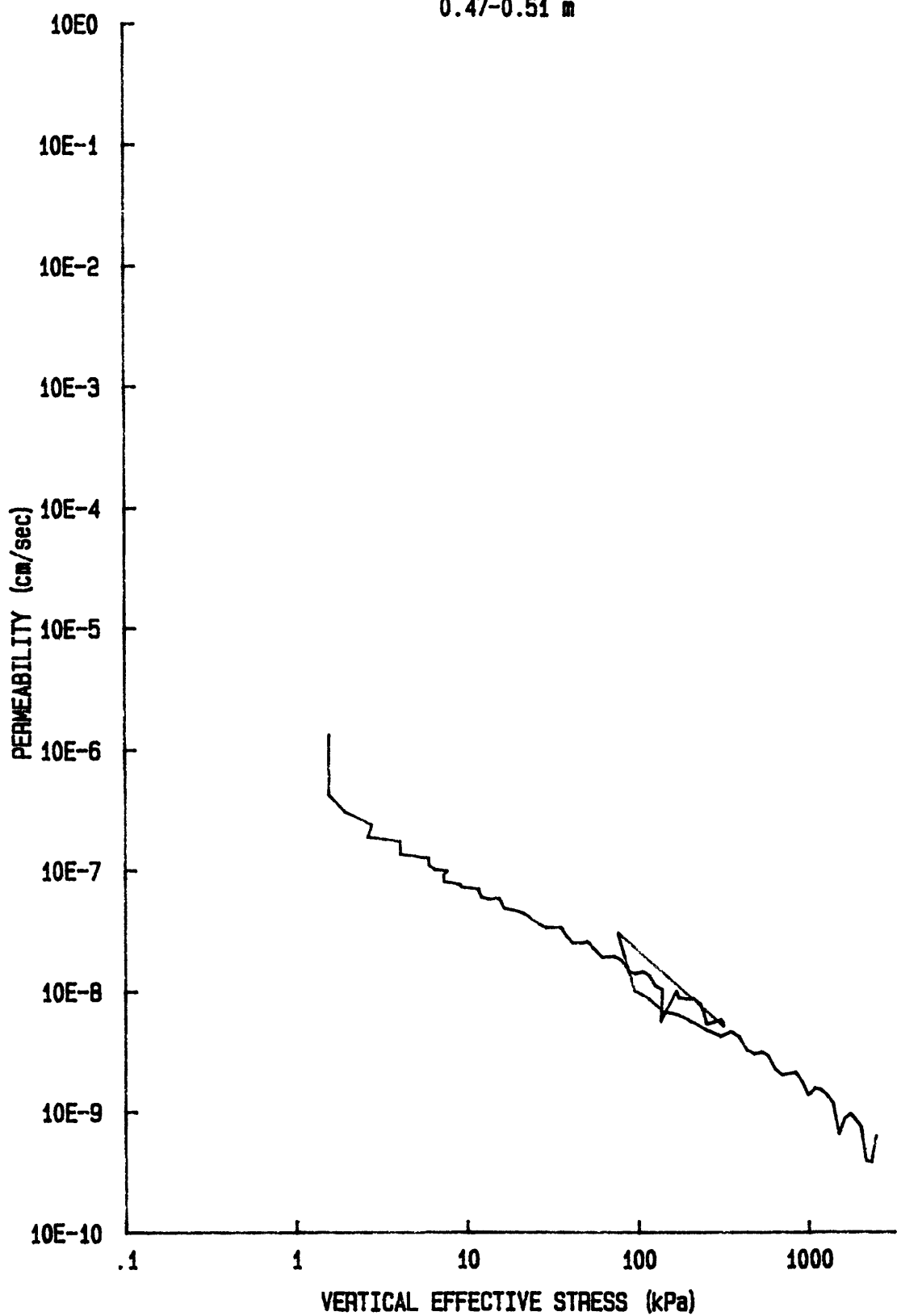
du/Sv for: CR056S8505
YS-85-08
CORE BC-5
0.47-0.51



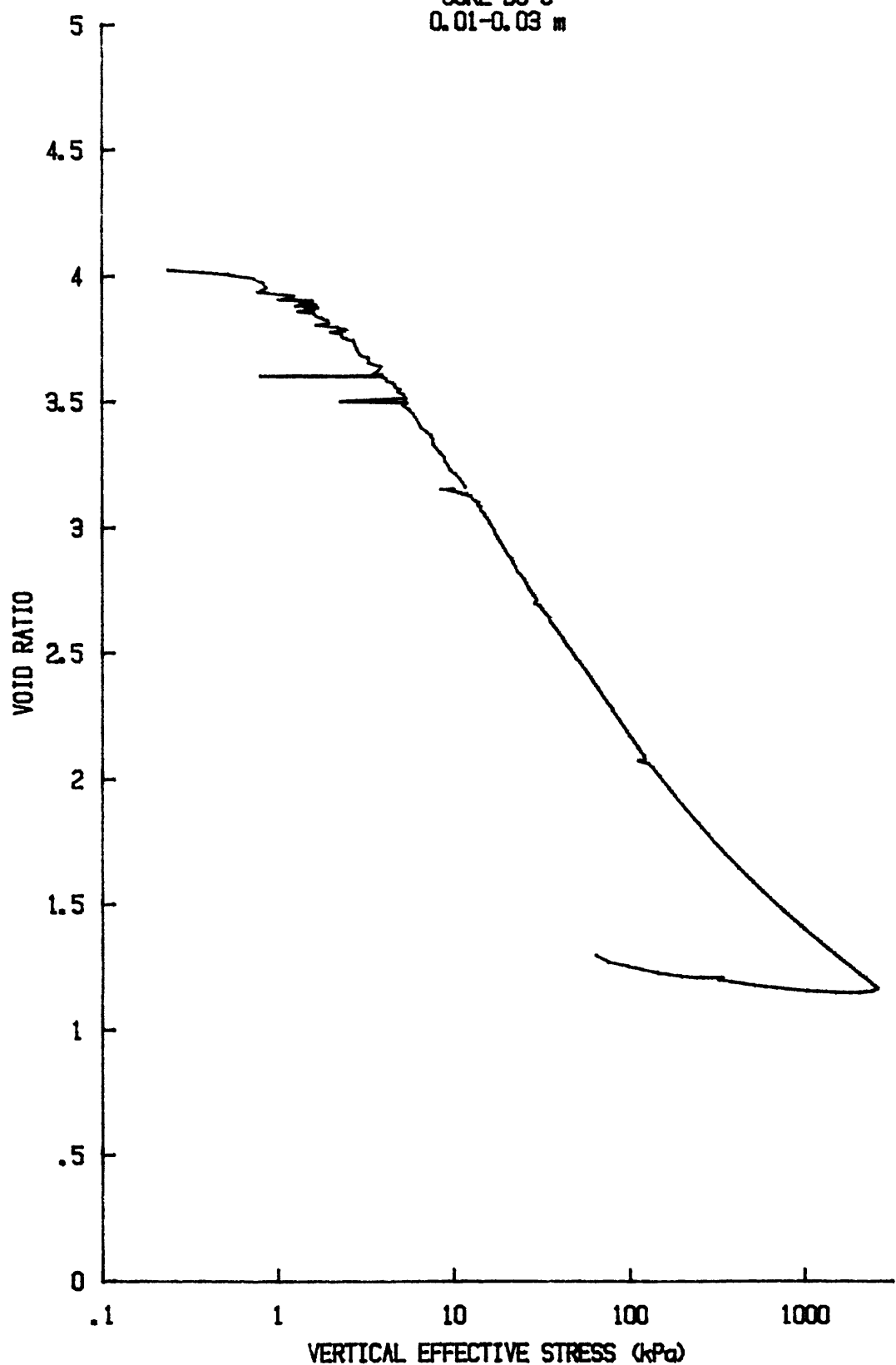
C_v vs log p' for: CR056S8505
YS-85-08
CORE BC-5
0.47-0.51 m



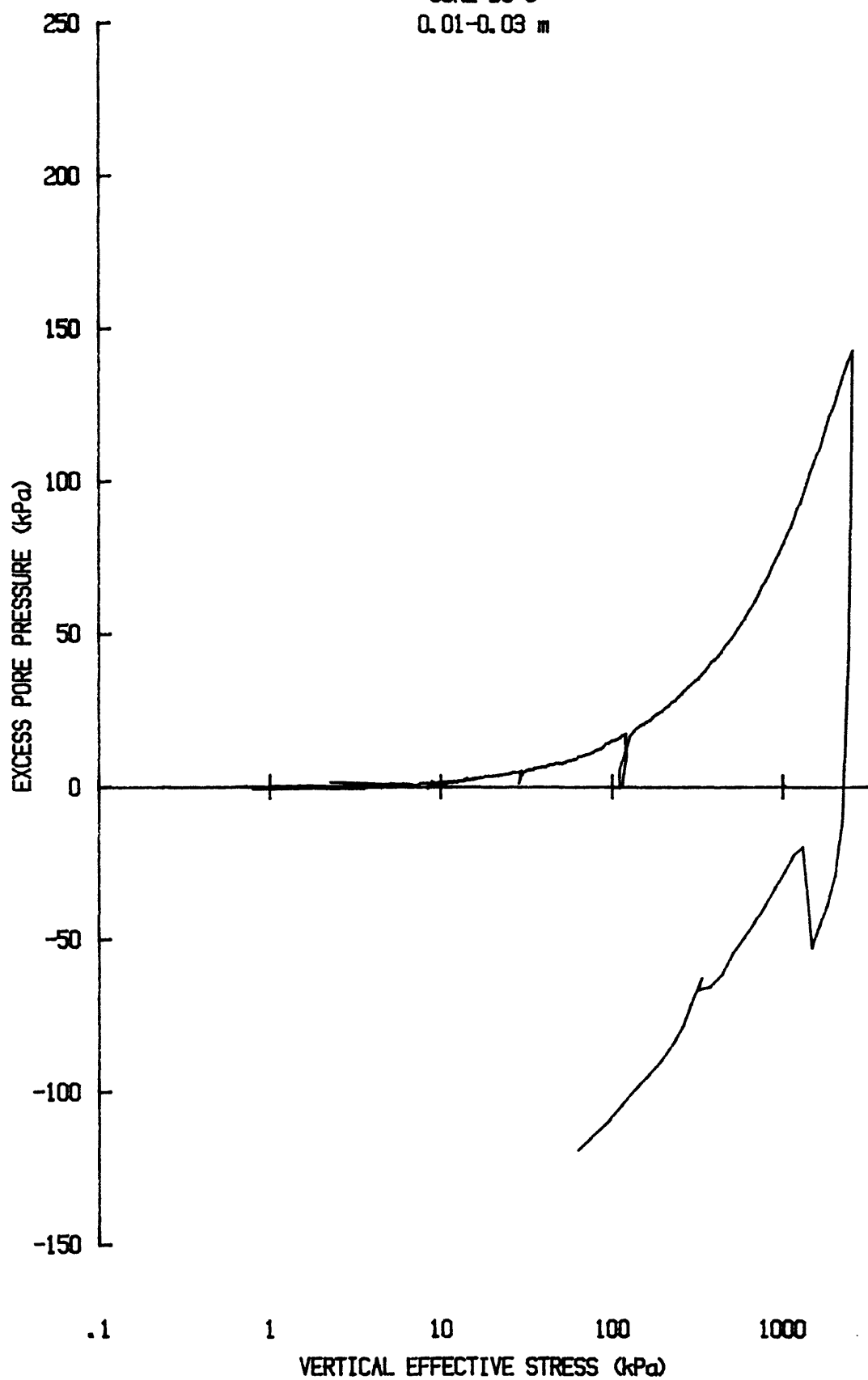
k vs $\log p'$ for: CR056S8505
YS-85-08
CORE BC-5
0.47-0.51 m



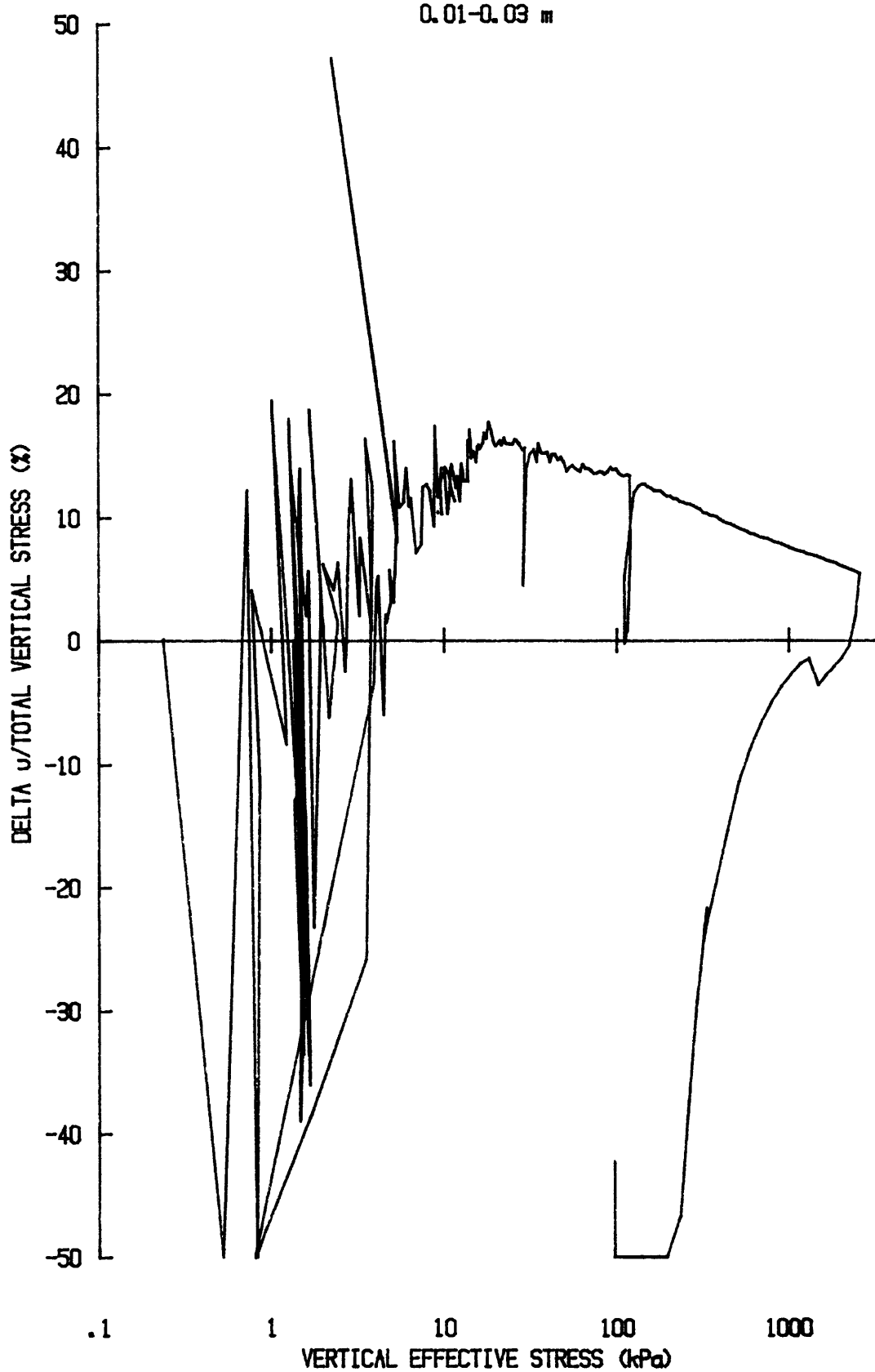
e vs $\log p'$ for CR03958506
YS-85-08
CORE BC-6
0.01-0.03 m



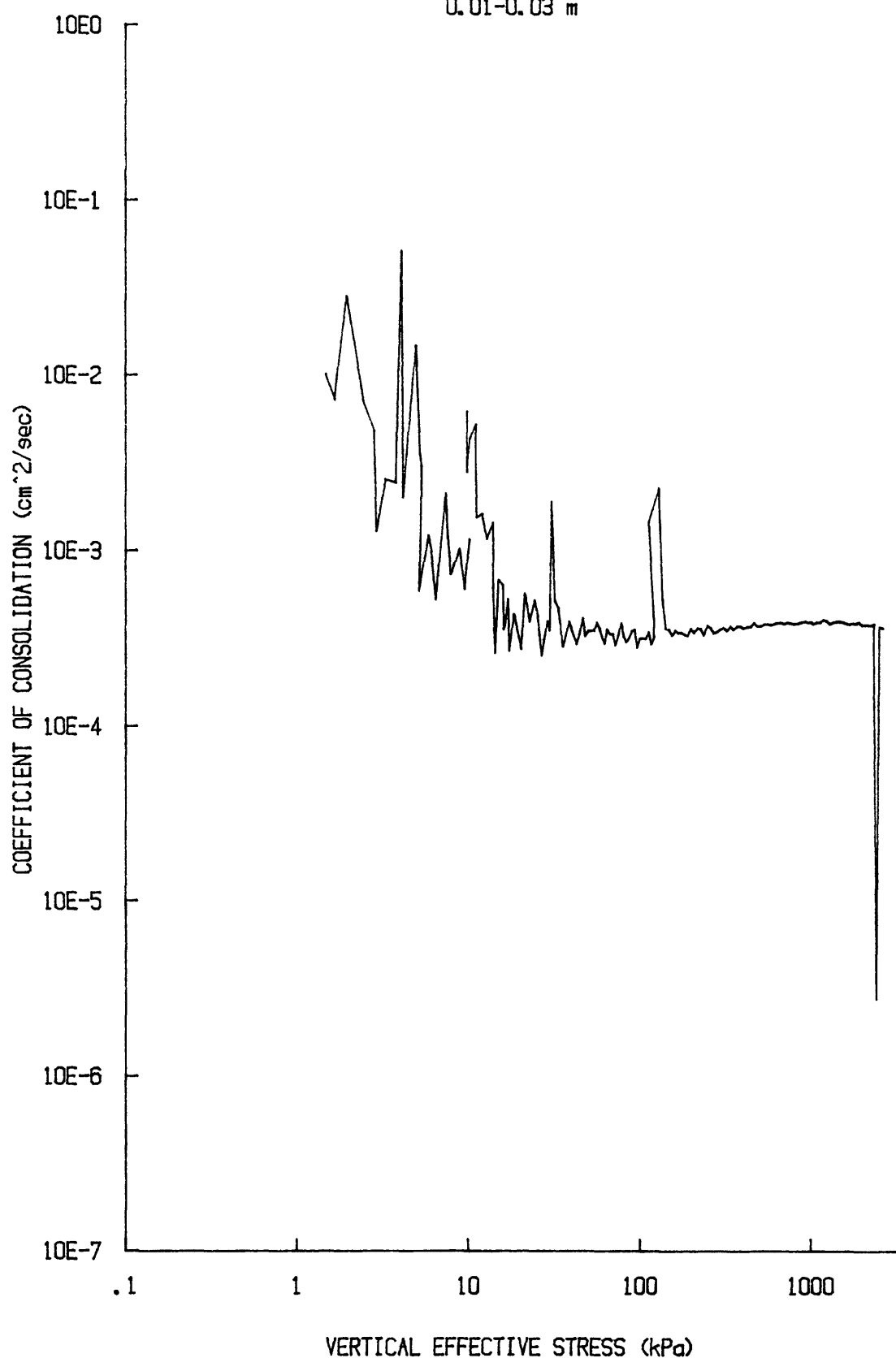
u vs $\log p'$ for CR039S8506
YS-85-08
CORE BC-6
0.01-0.03 m



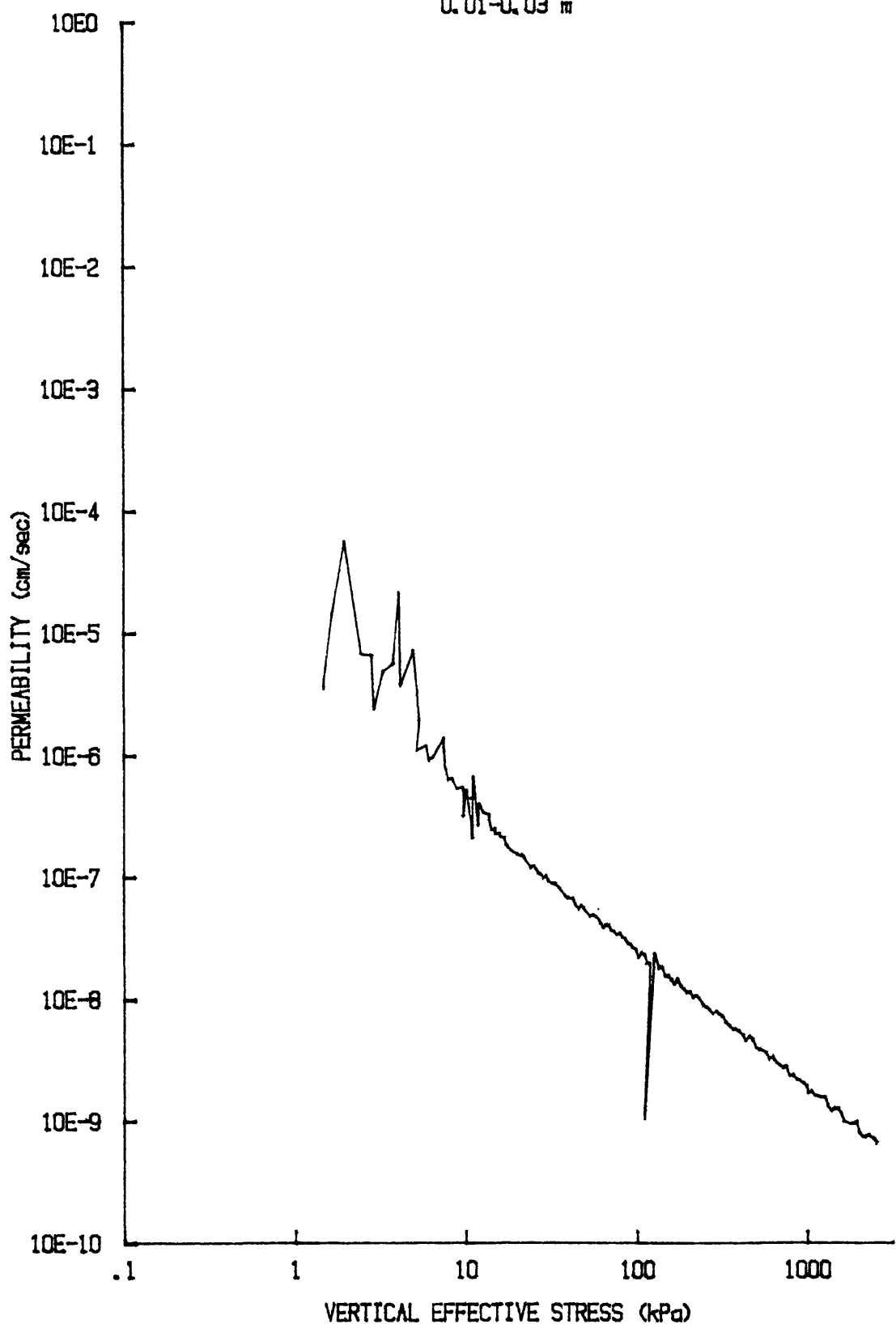
du/Sv for: CR039S8506
YS-85-08
CORE BC-6
0.01-0.03 m



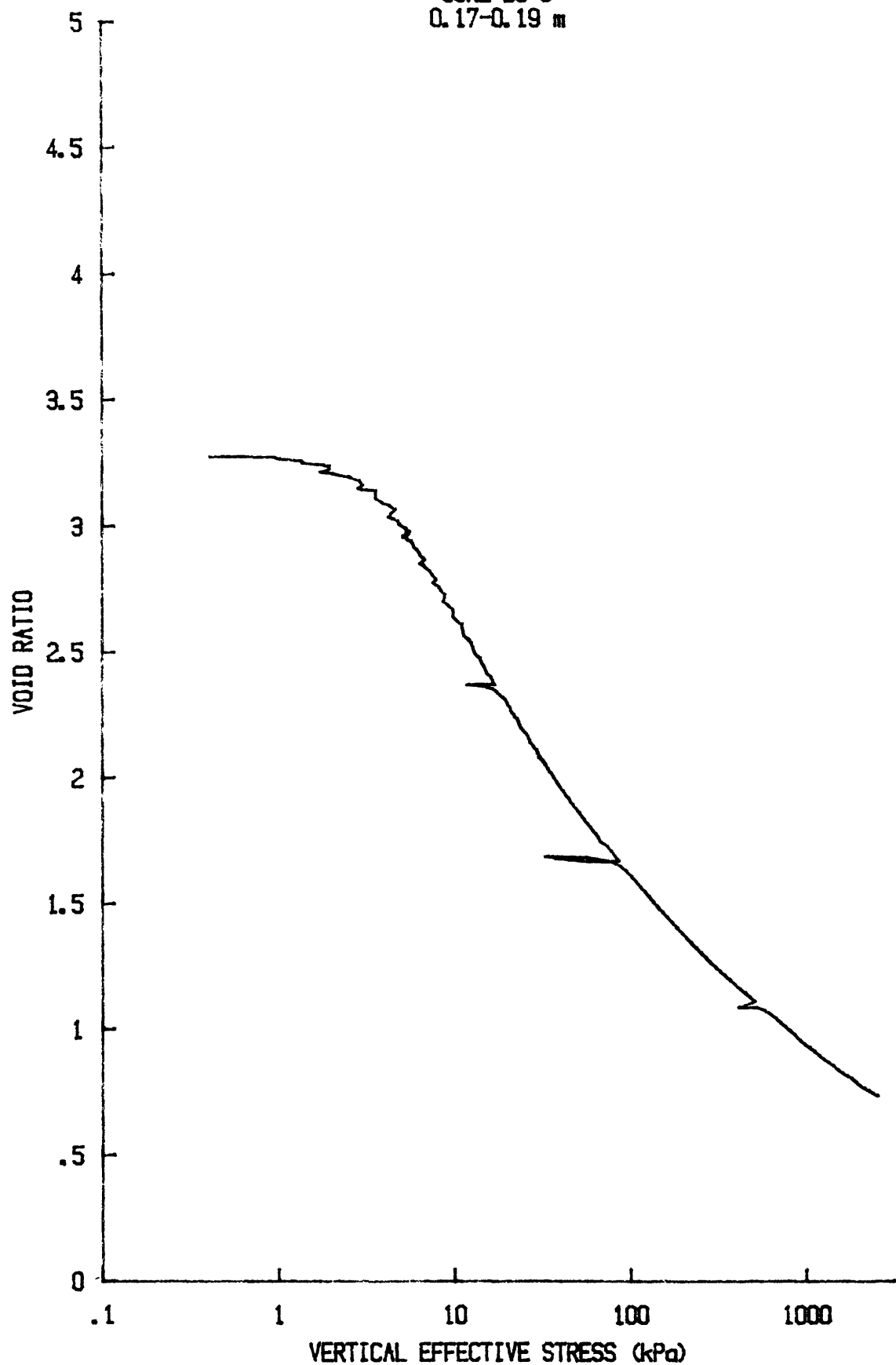
C_v vs $\log p'$ for: CR039S8506
YS-85-08
CORE BC-6
0.01-0.03 m



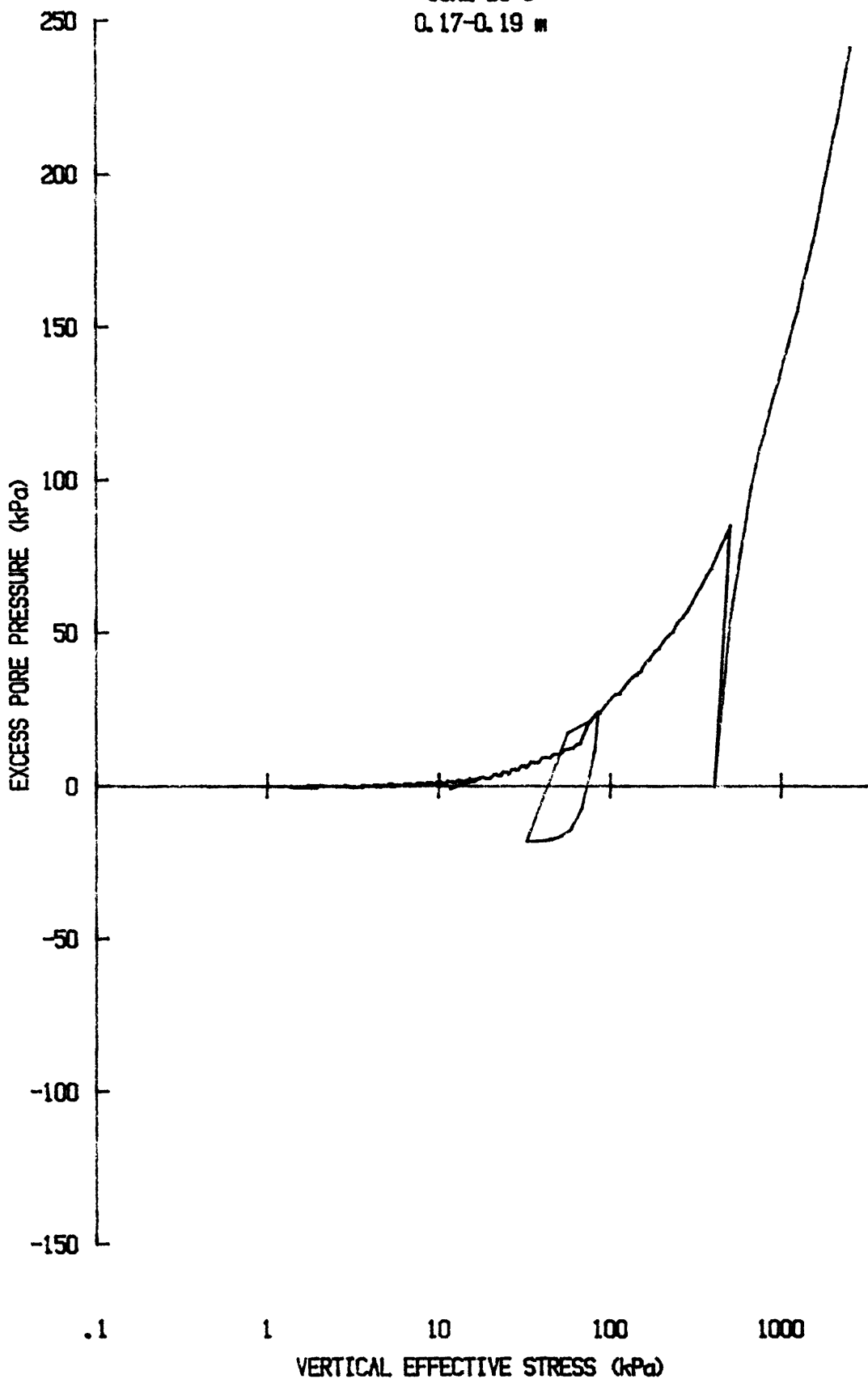
k vs $\log p'$ for CR039S8506
YS-85-08
CORE BC-6
0.01-0.03 m



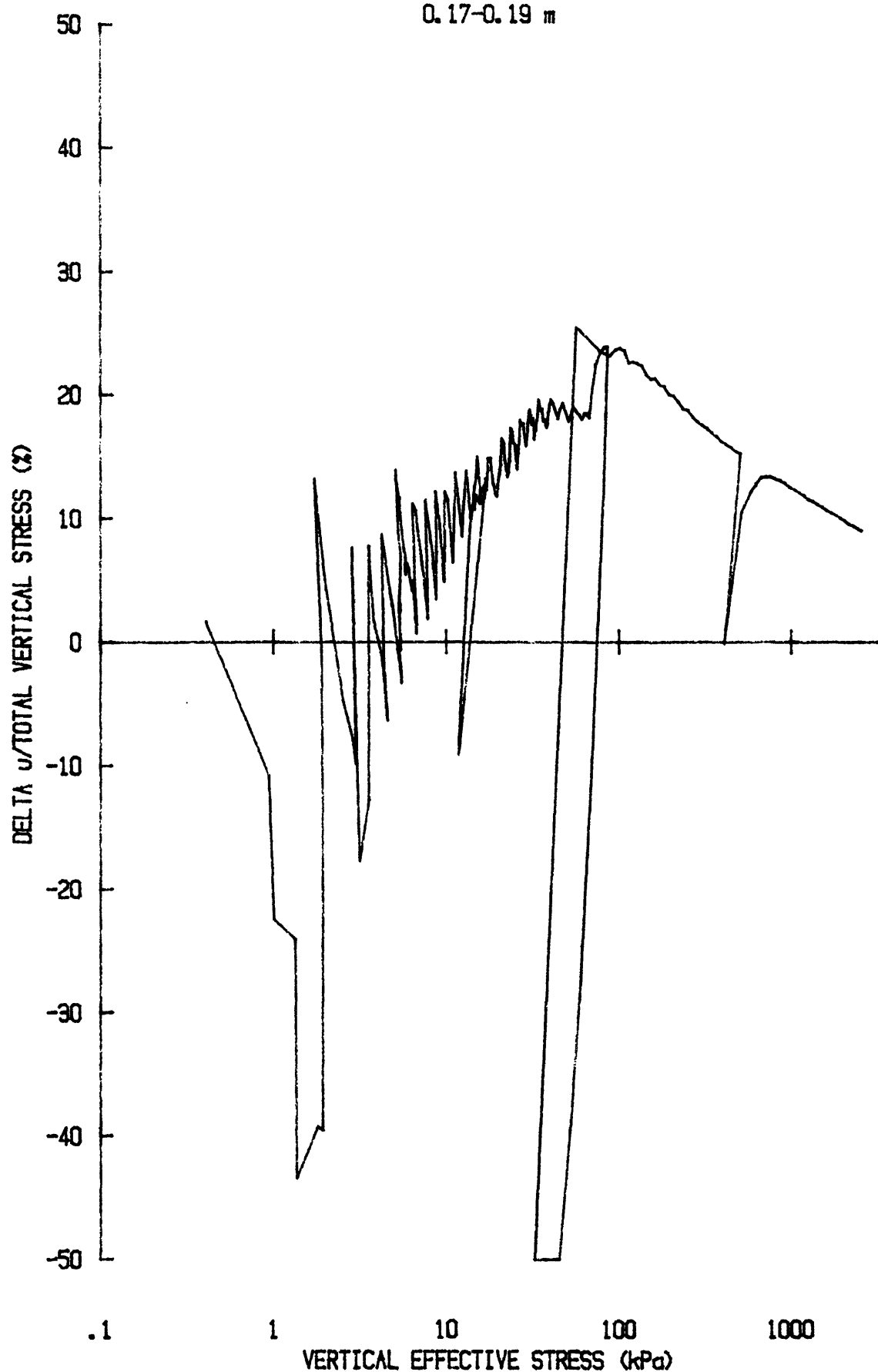
e vs $\log p'$ for: CR050S8506
YS-85-08
CORE BC-6
0.17-0.19 m



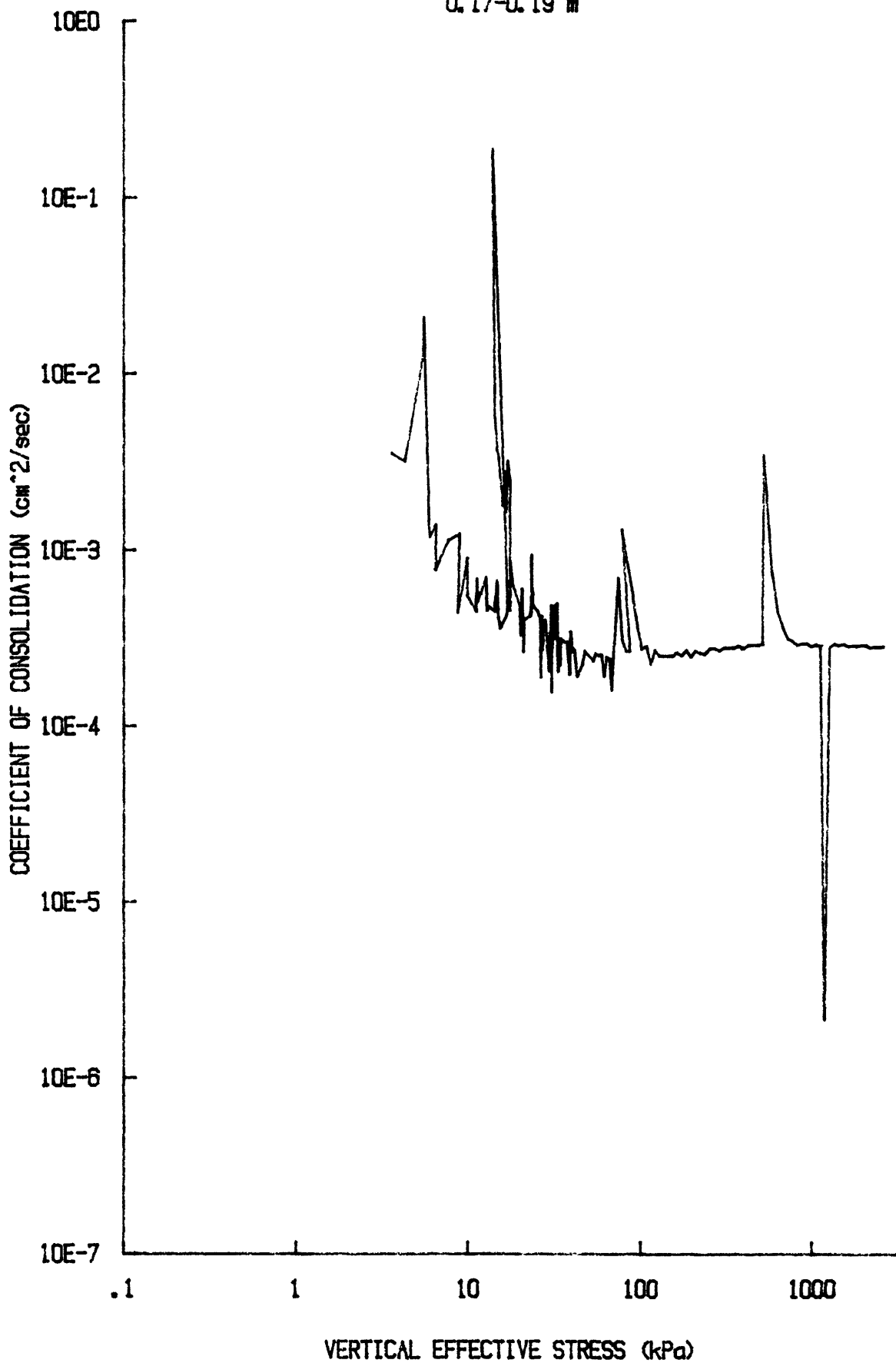
u vs $\log p'$ for CR050S8506
YS-85-08
CORE BC-6
0.17-0.19 m



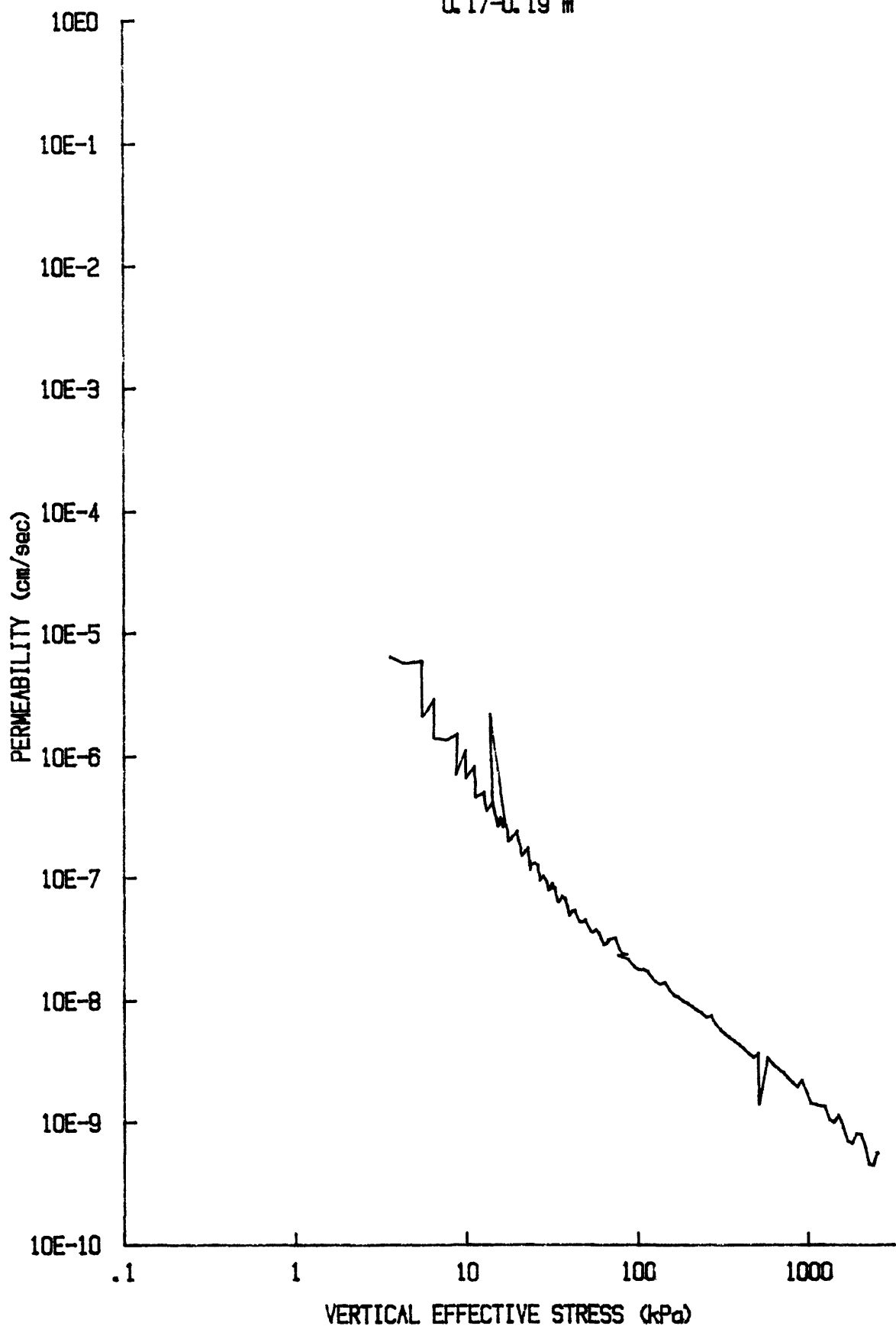
du/Sv for: CR050S8506
YS-85-08
CORE BC-6
0.17-0.19 m



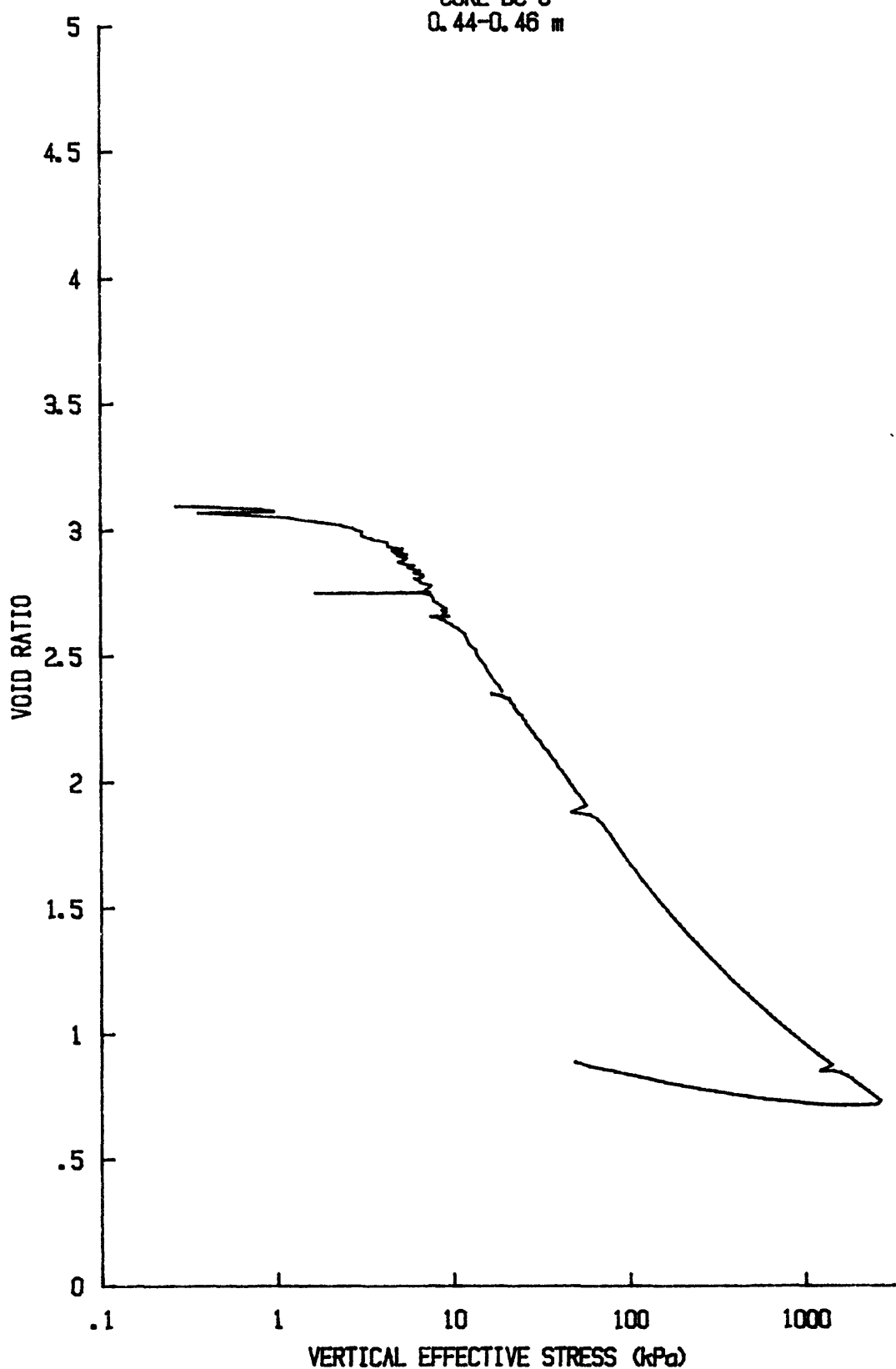
C_v vs $\log p'$ for CR050S8506
YS-85-08
CORE BC-6
 $0.17-0.19 \text{ m}$



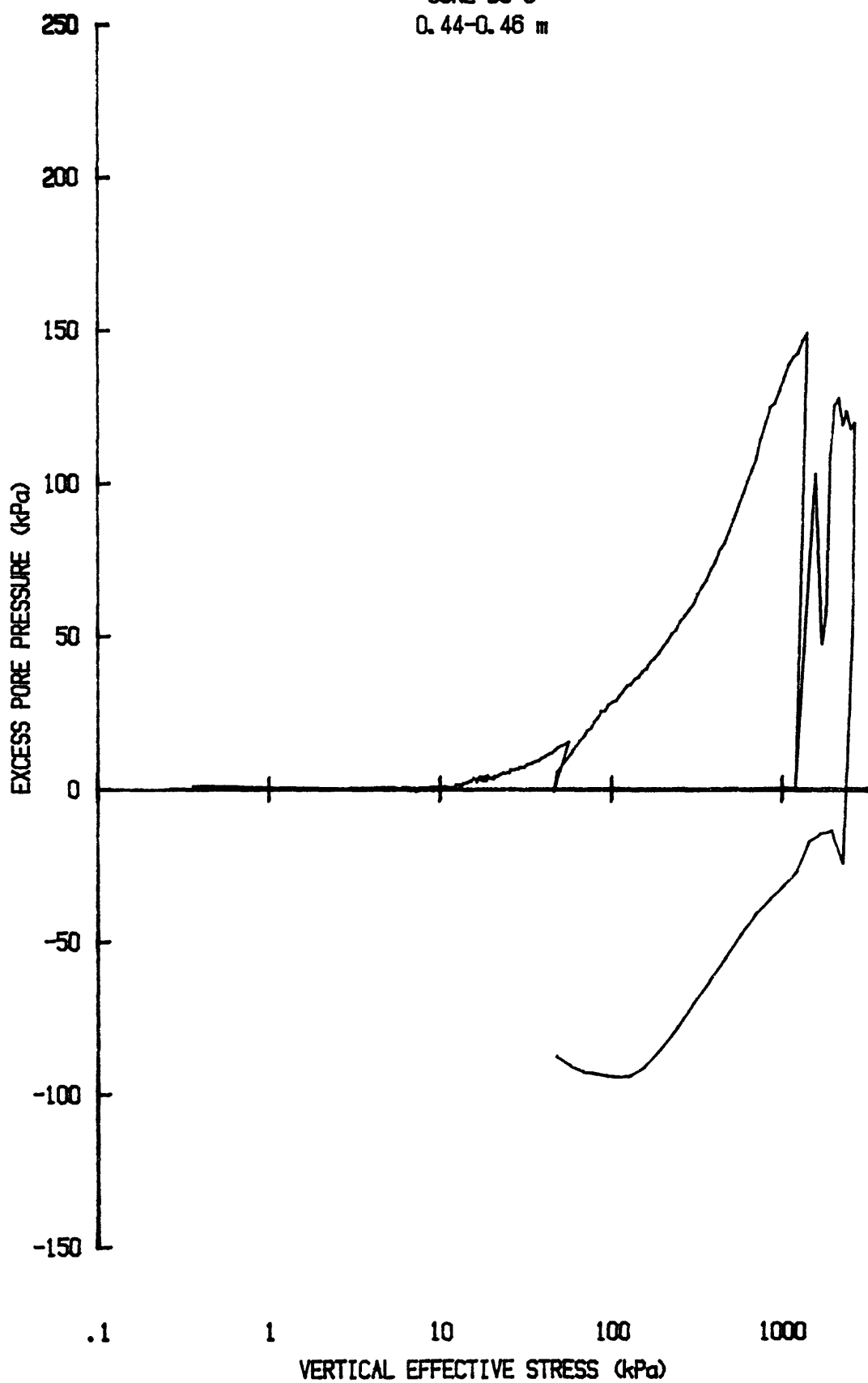
k vs $\log p'$ for CR05058506
YS-85-08
CORE BC-6
0.17-0.19 m



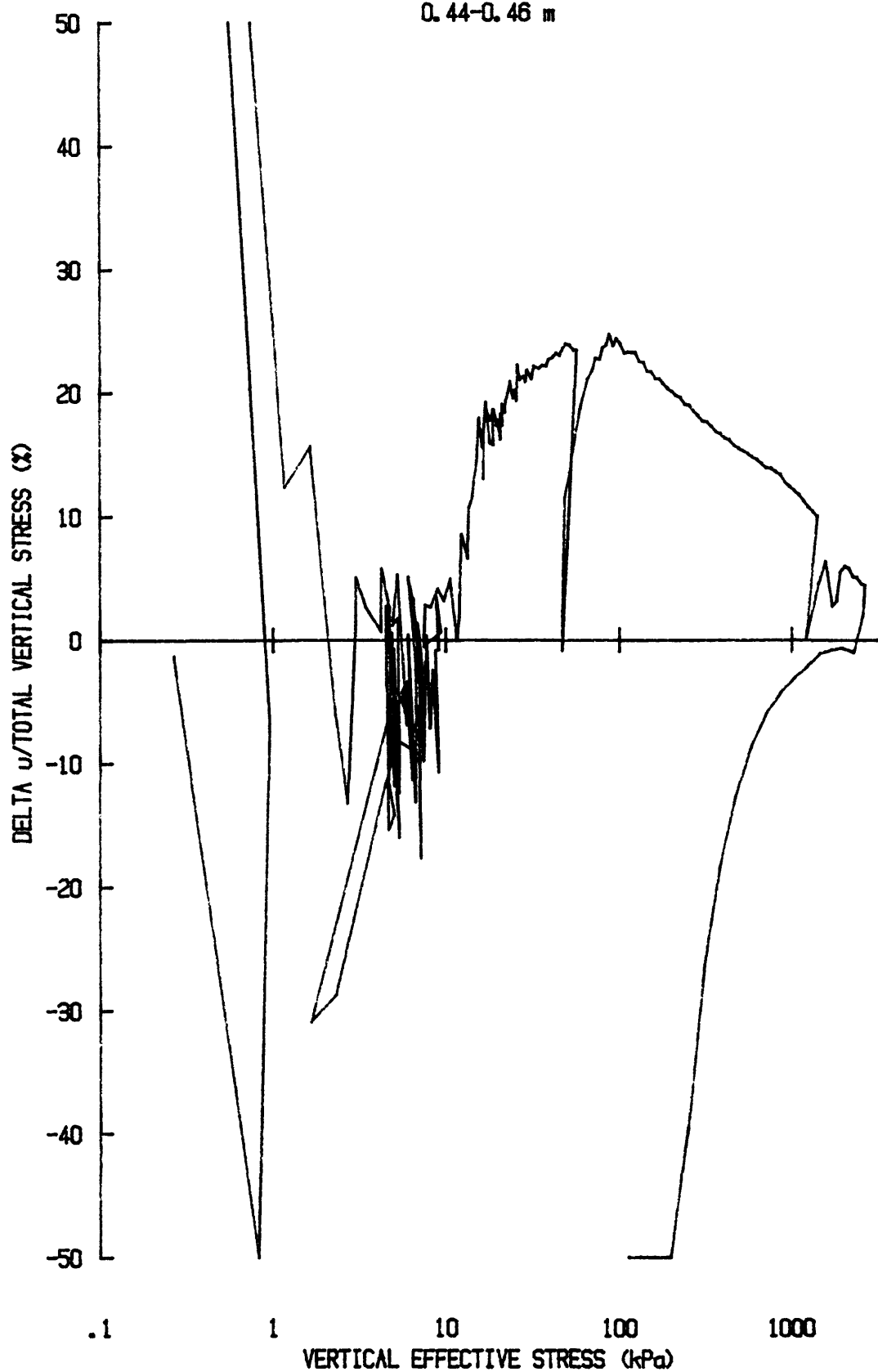
e vs $\log p'$ for CR043S8506
YS-85-08
CORE BC-6
0.44-0.46 m



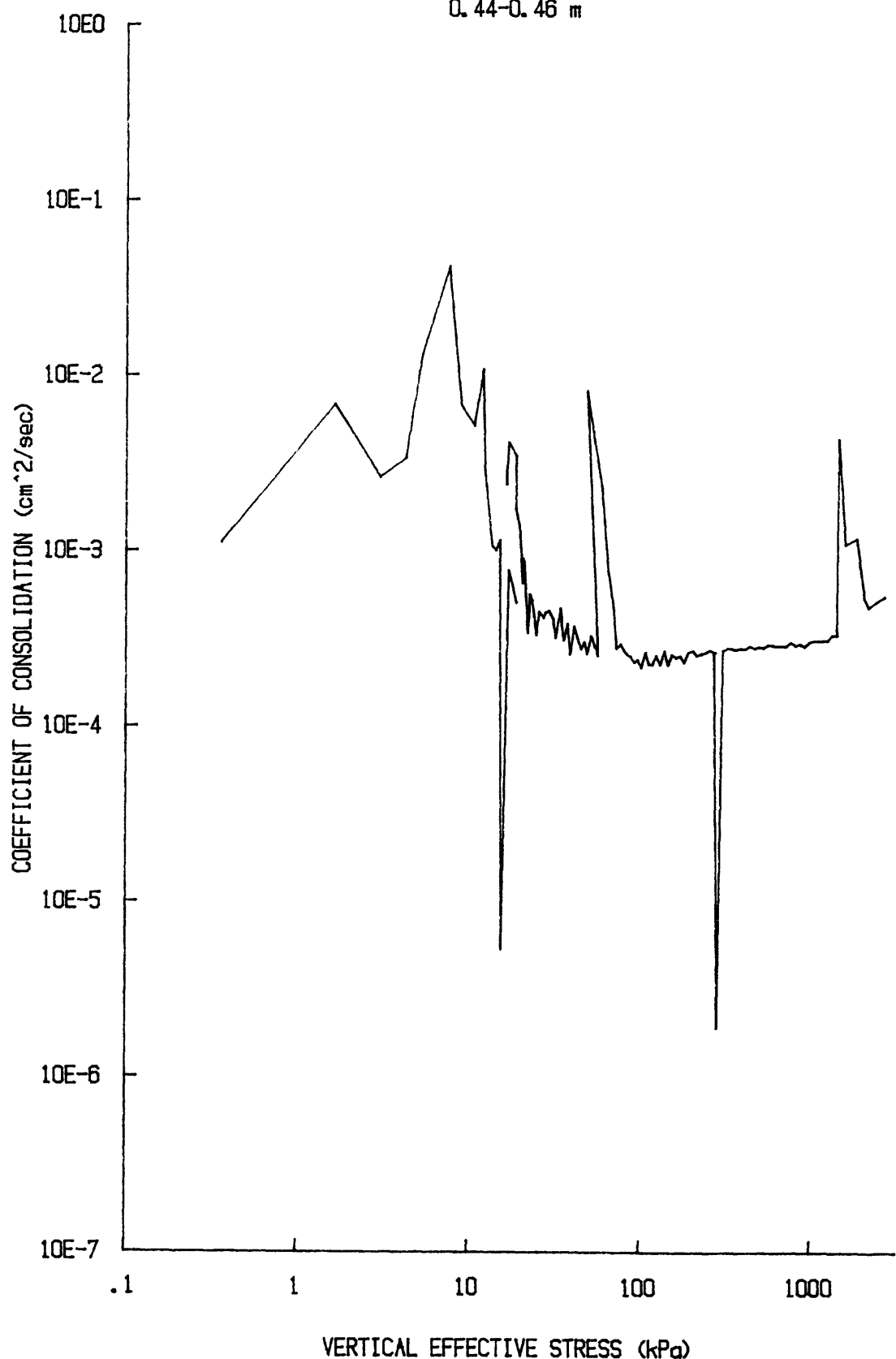
u vs $\log p'$ for CR043S8506
YS-85-08
CORE BC-6
0.44-0.46 m



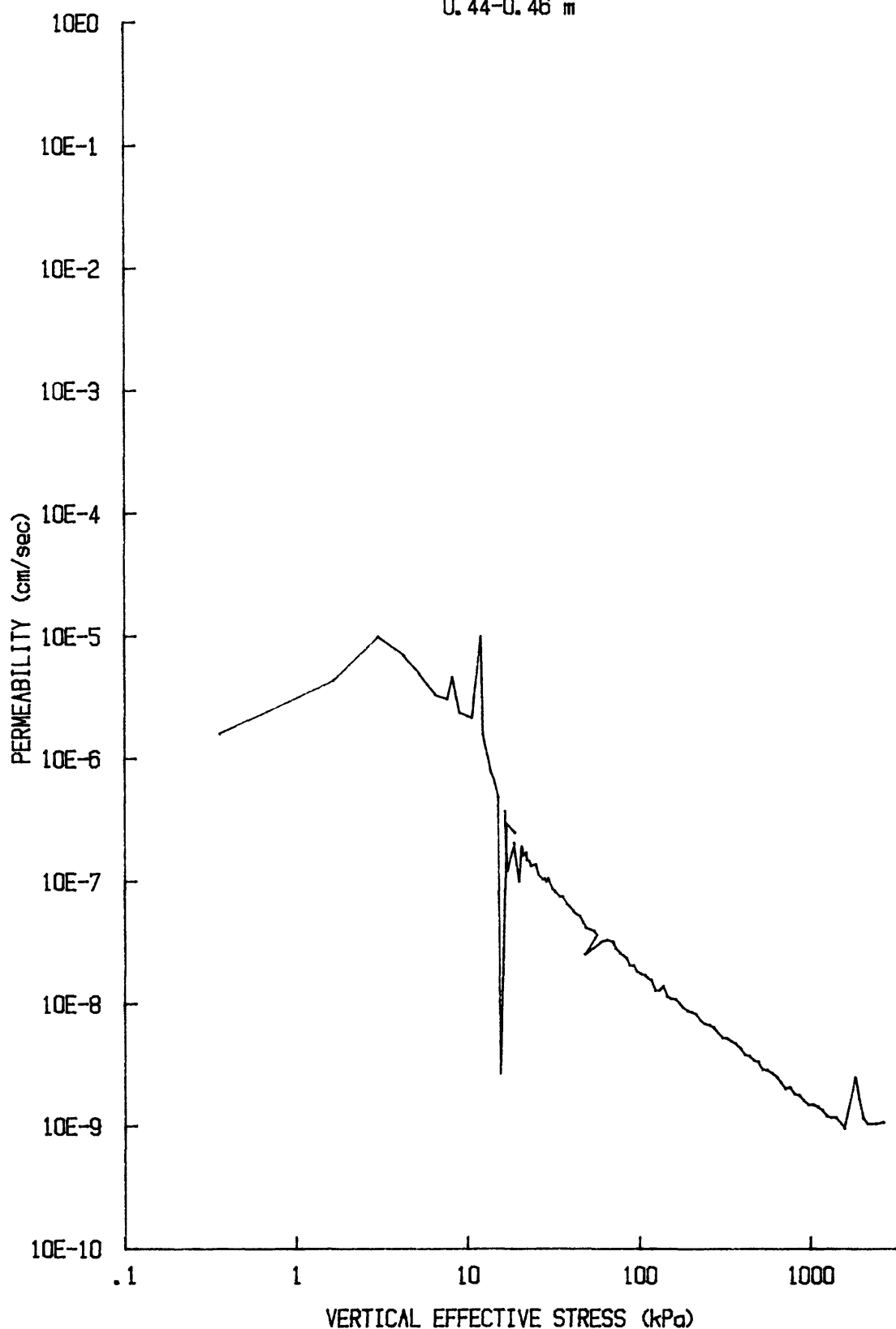
du/Sv for: CR043S8506
YS-85-08
CORE BC-6
0.44-0.46 m



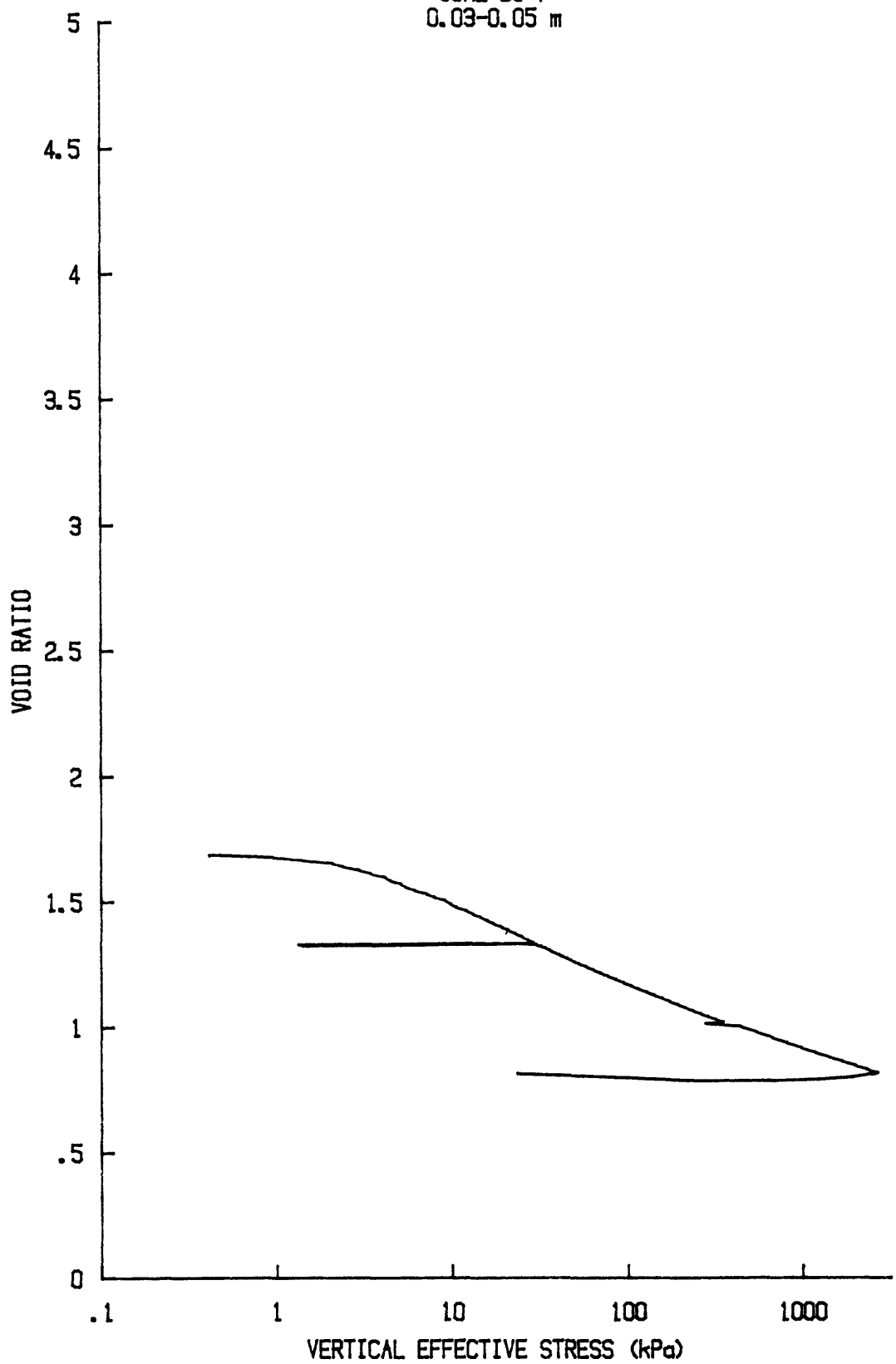
C_v vs $\log p'$ for: CR043S8506
YS-85-08
CORE BC-6
0.44-0.46 m



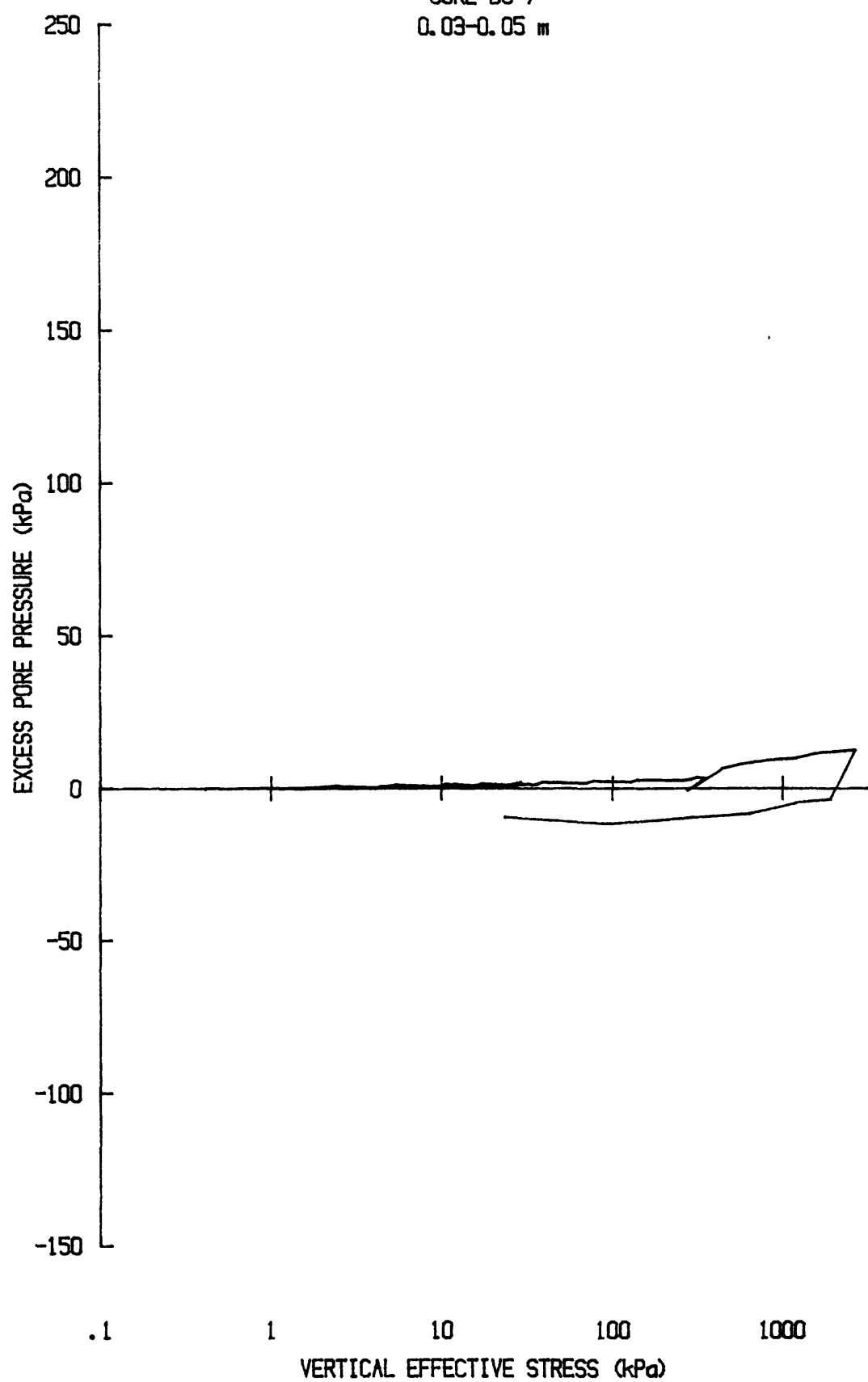
k vs $\log p'$ for: CR043S8506
YS-85-08
CORE BC-6
0.44-0.46 m



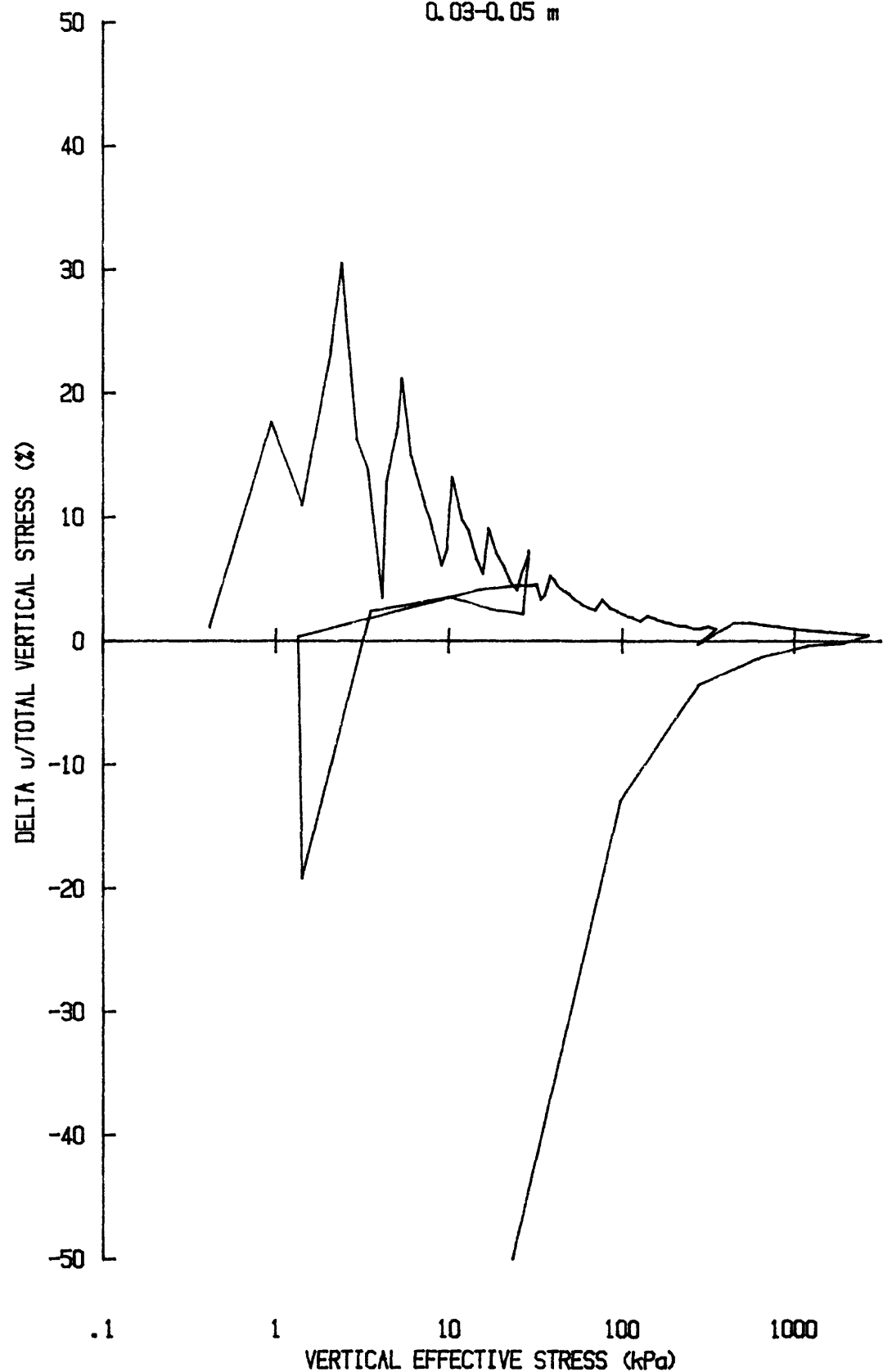
e vs $\log p'$ for: CR034S8507
YS-85-08
CORE BC-7
0.03-0.05 m



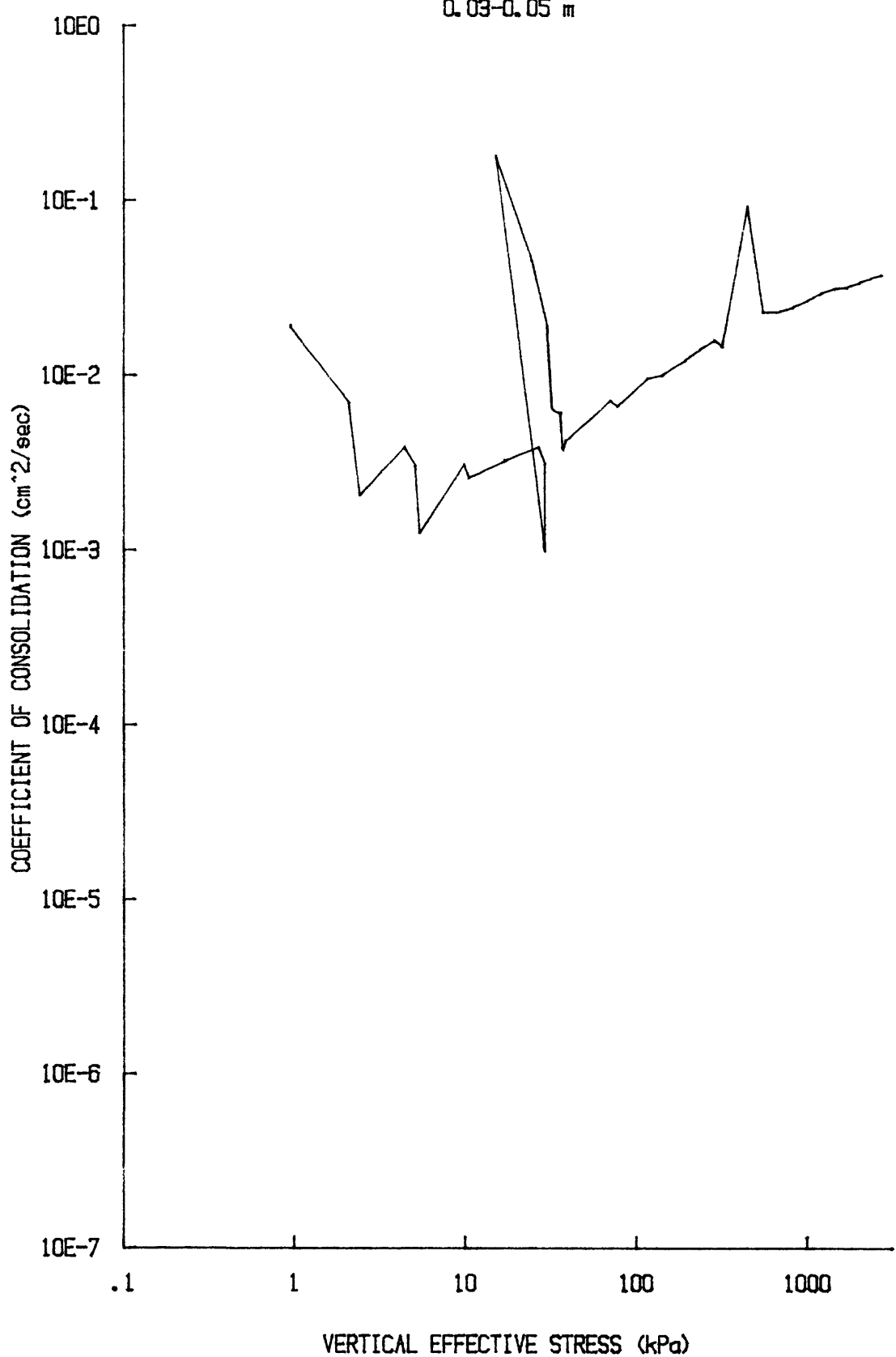
u vs $\log p'$ for: CR034S8507
YS-85-08
CORE BC-7
0.03-0.05 m



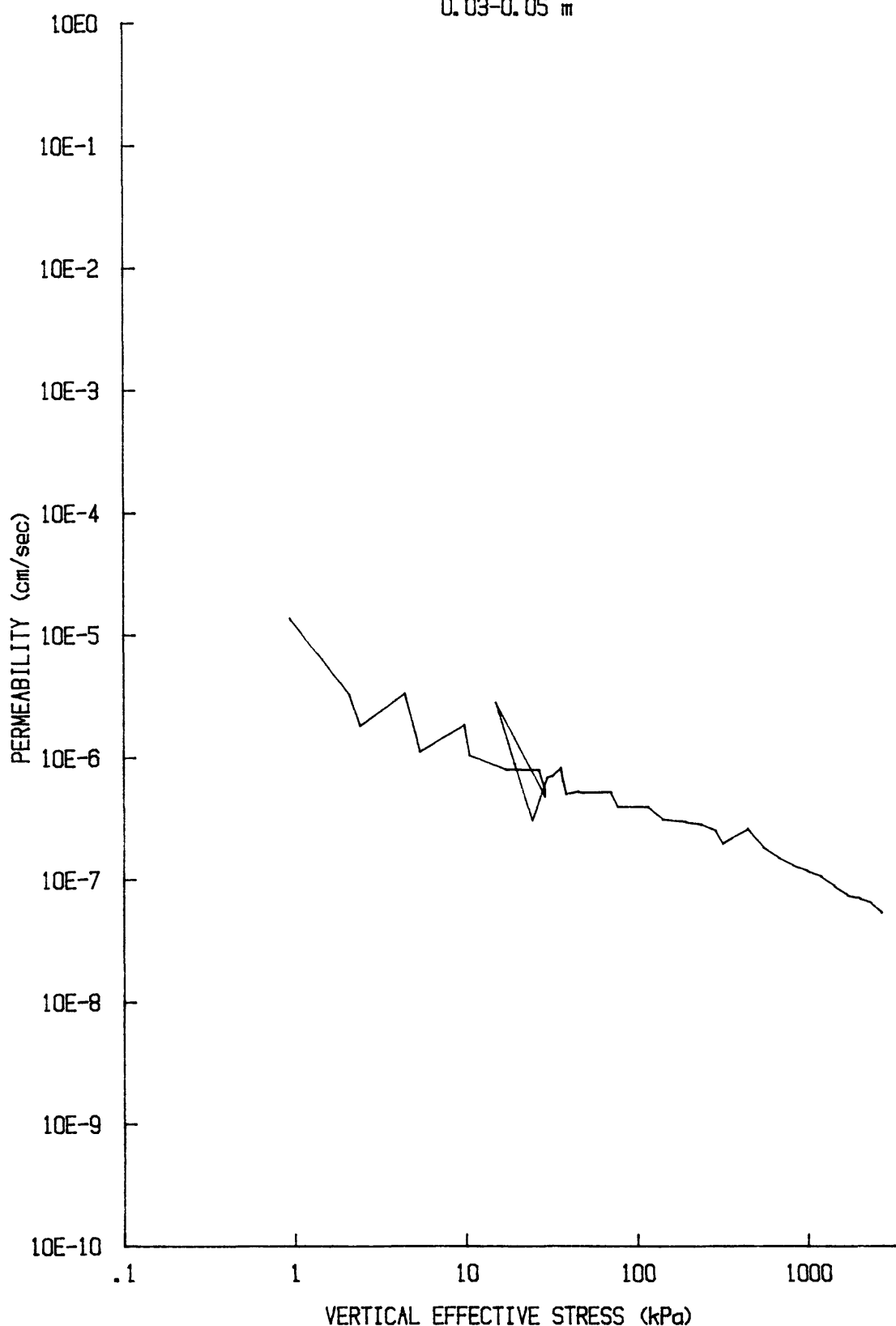
du/Sv for: CR034S8507
YS-85-08
CORE BC-7
0.03-0.05 m



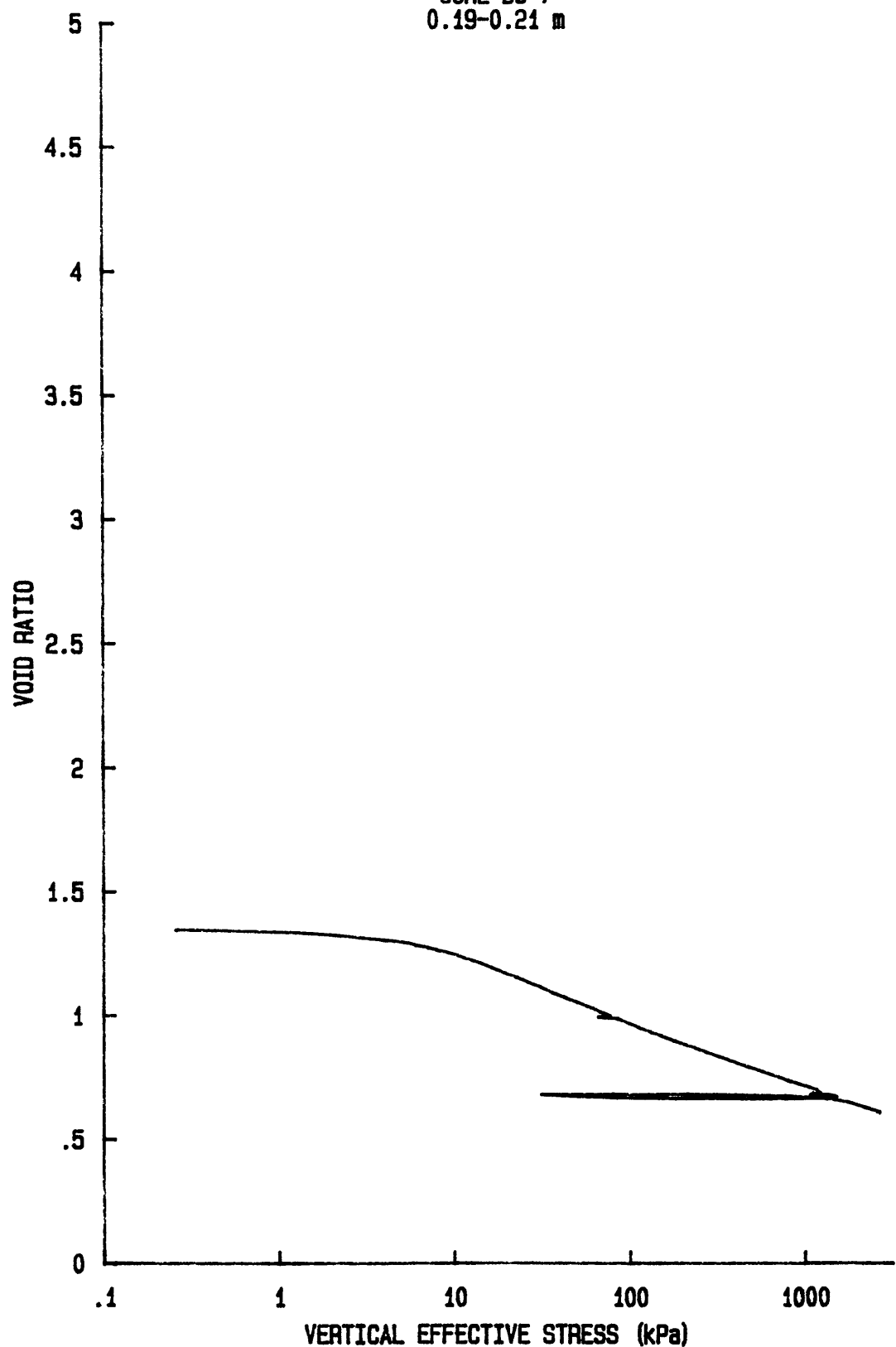
C_v vs $\log p'$ for CR034S8507
YS-85-08
CORE BC-7
0.03-0.05 m



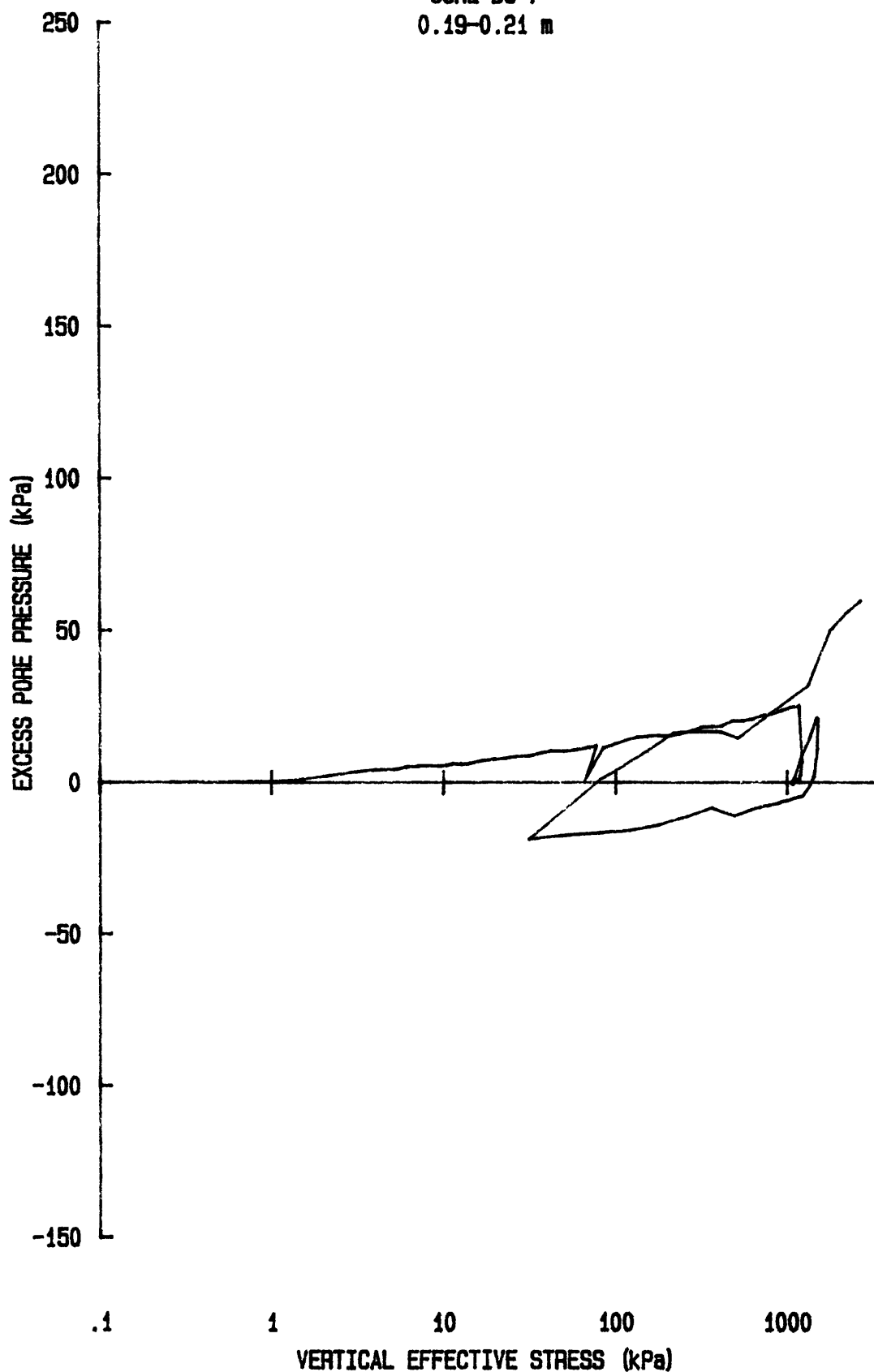
k vs $\log p'$ for: CR034S8507
YS-85-08
CORE BC-7
0.03-0.05 m



e vs log p' for: CR054S8507
YS-85-08
CORE BC-7
0.19-0.21 m



u vs $\log p'$ for: CR054S8507
YS-85-08
CORE BC-7
0.19-0.21 m

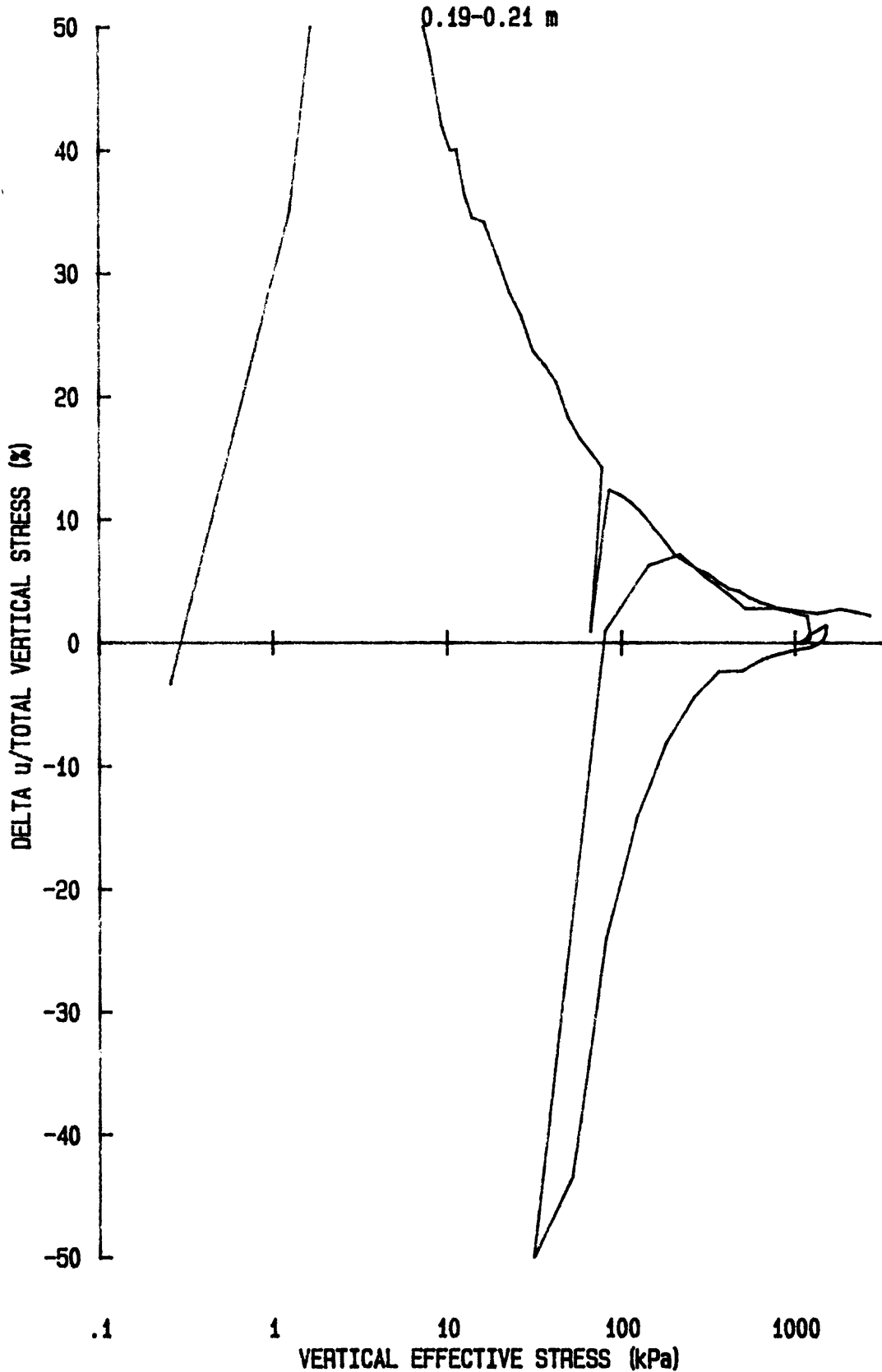


du/Sv for: CR054S8507

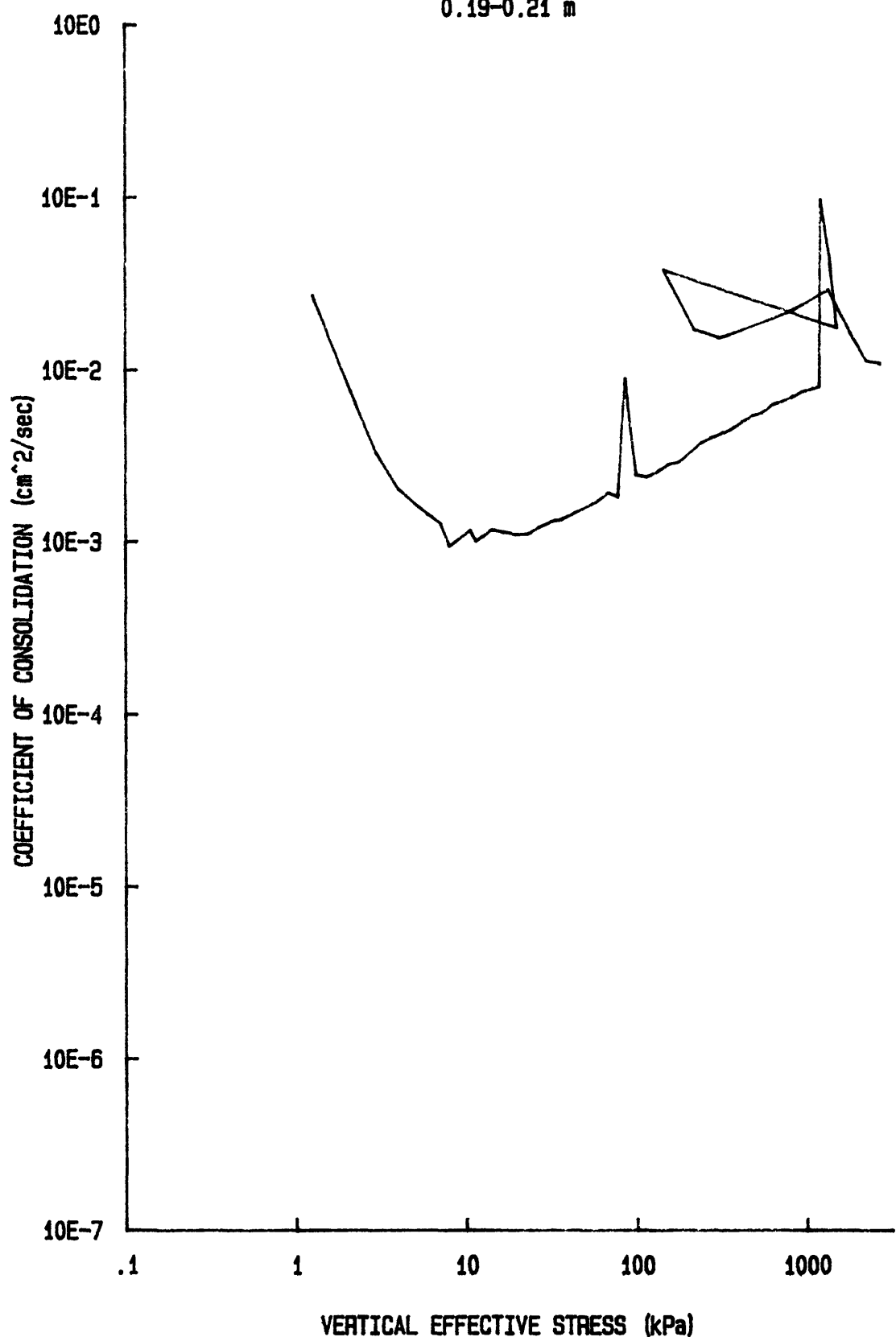
YS-85-08

CORE BC-7

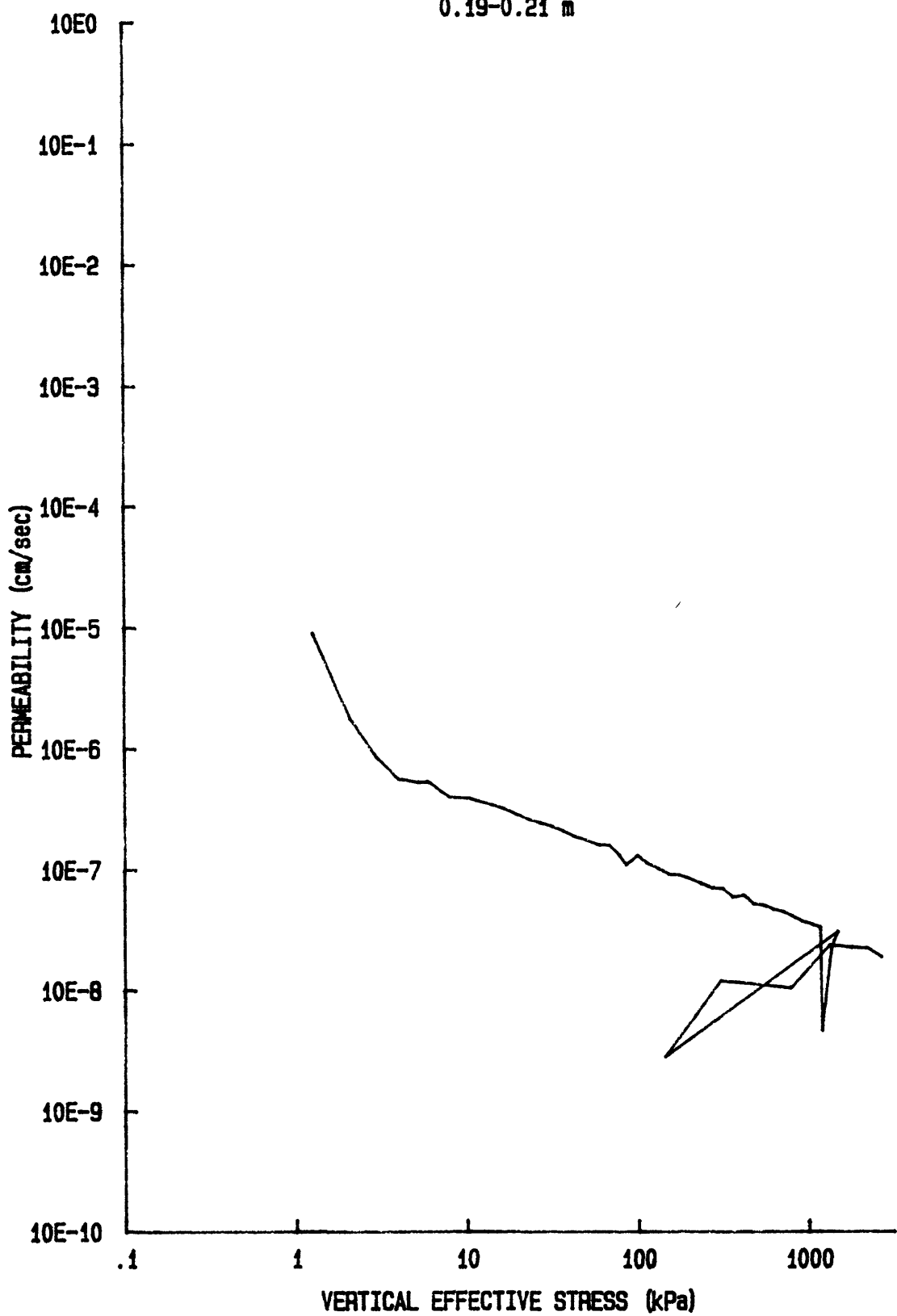
0.19-0.21 m



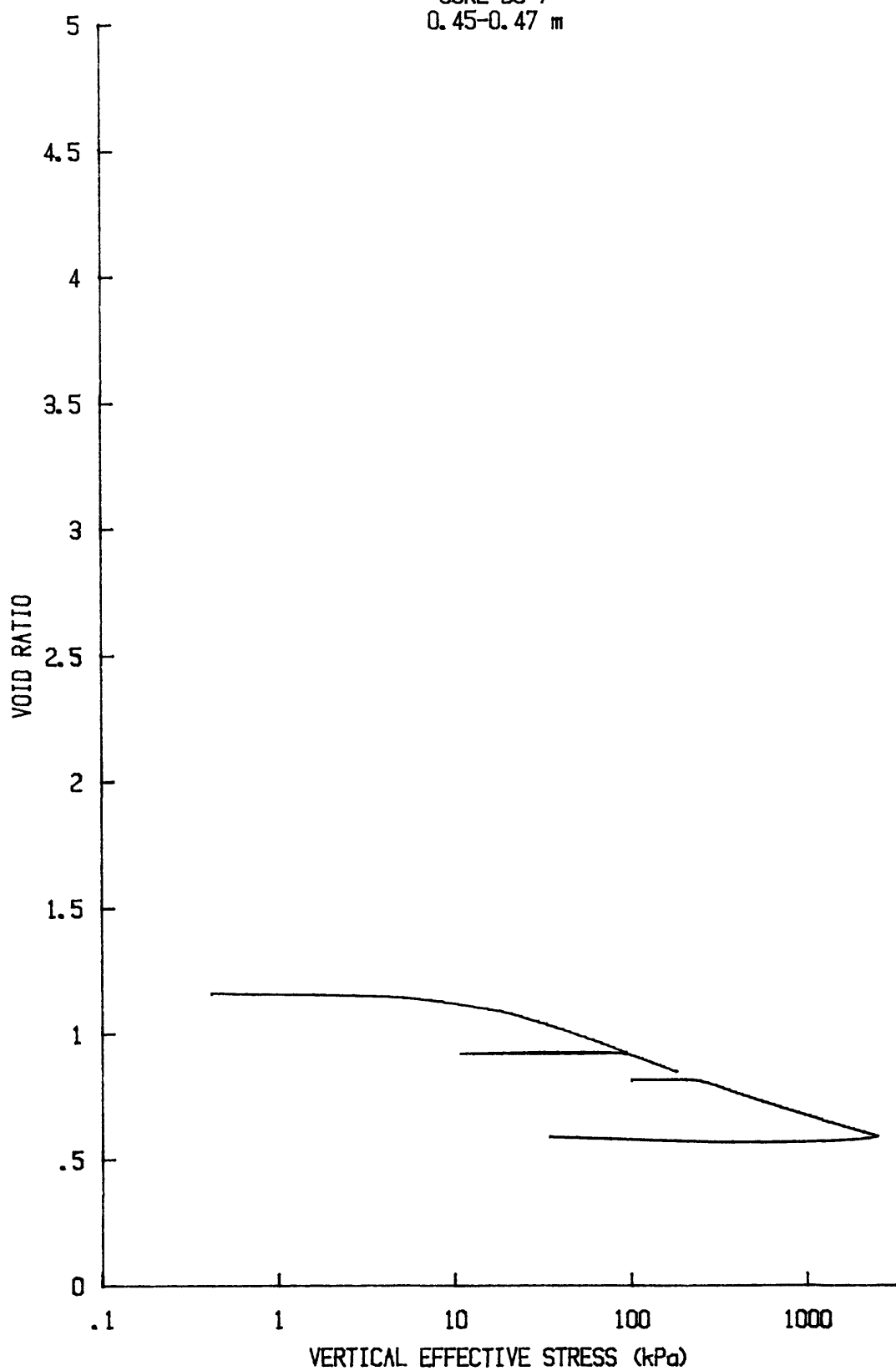
C_v vs log p' for: CR054S8507
YS-85-08
CORE BC-7
0.19-0.21 m



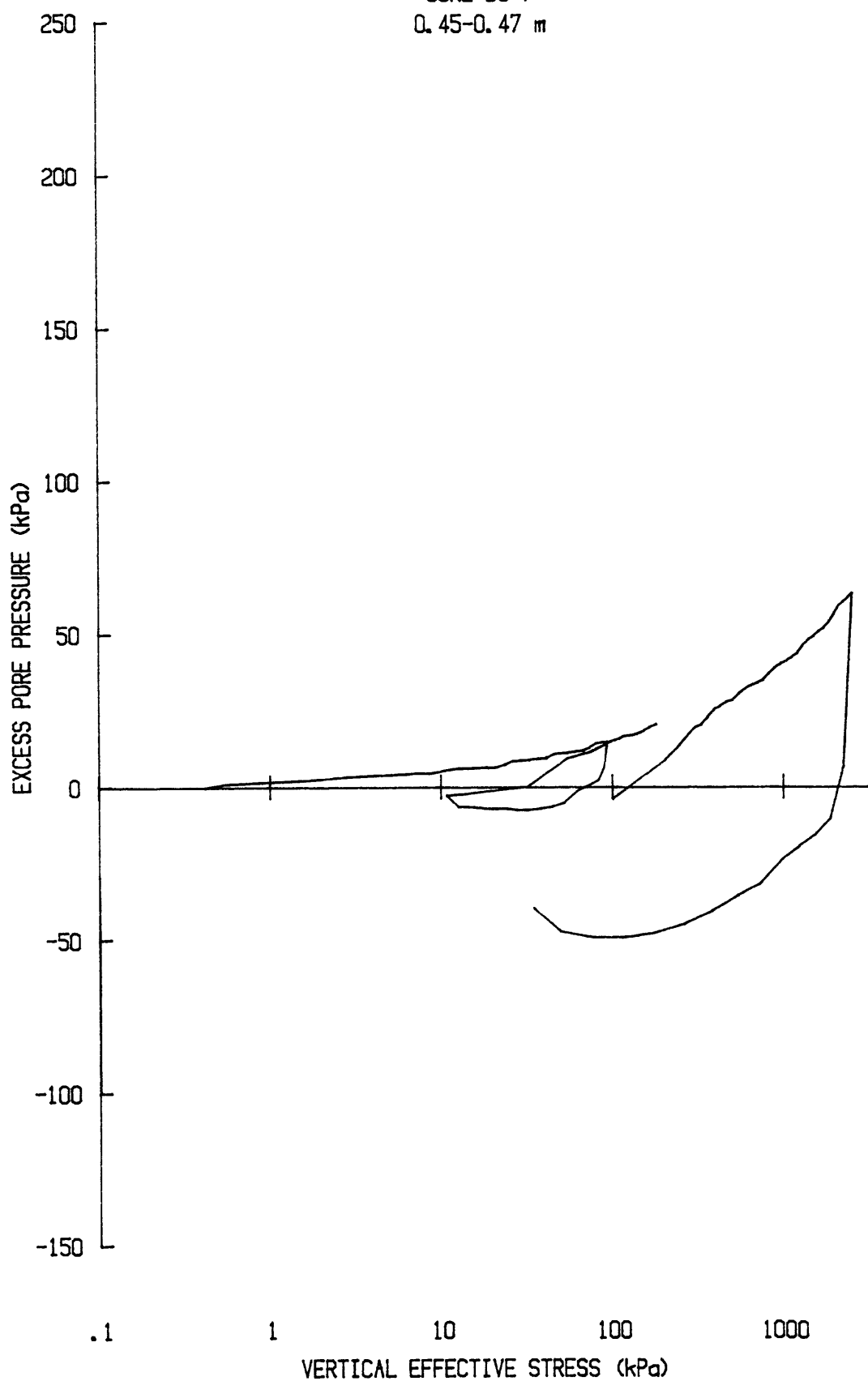
k vs log *p'* for: CR054S8507
YS-85-08
CORE BC-7
0.19-0.21 m



e vs $\log p'$ for: CR030S8507
YS-85-08
CORE BC-7
0.45-0.47 m



u vs $\log p'$ for: CR030S8507
YS-85-08
CORE BC-7
0.45-0.47 m

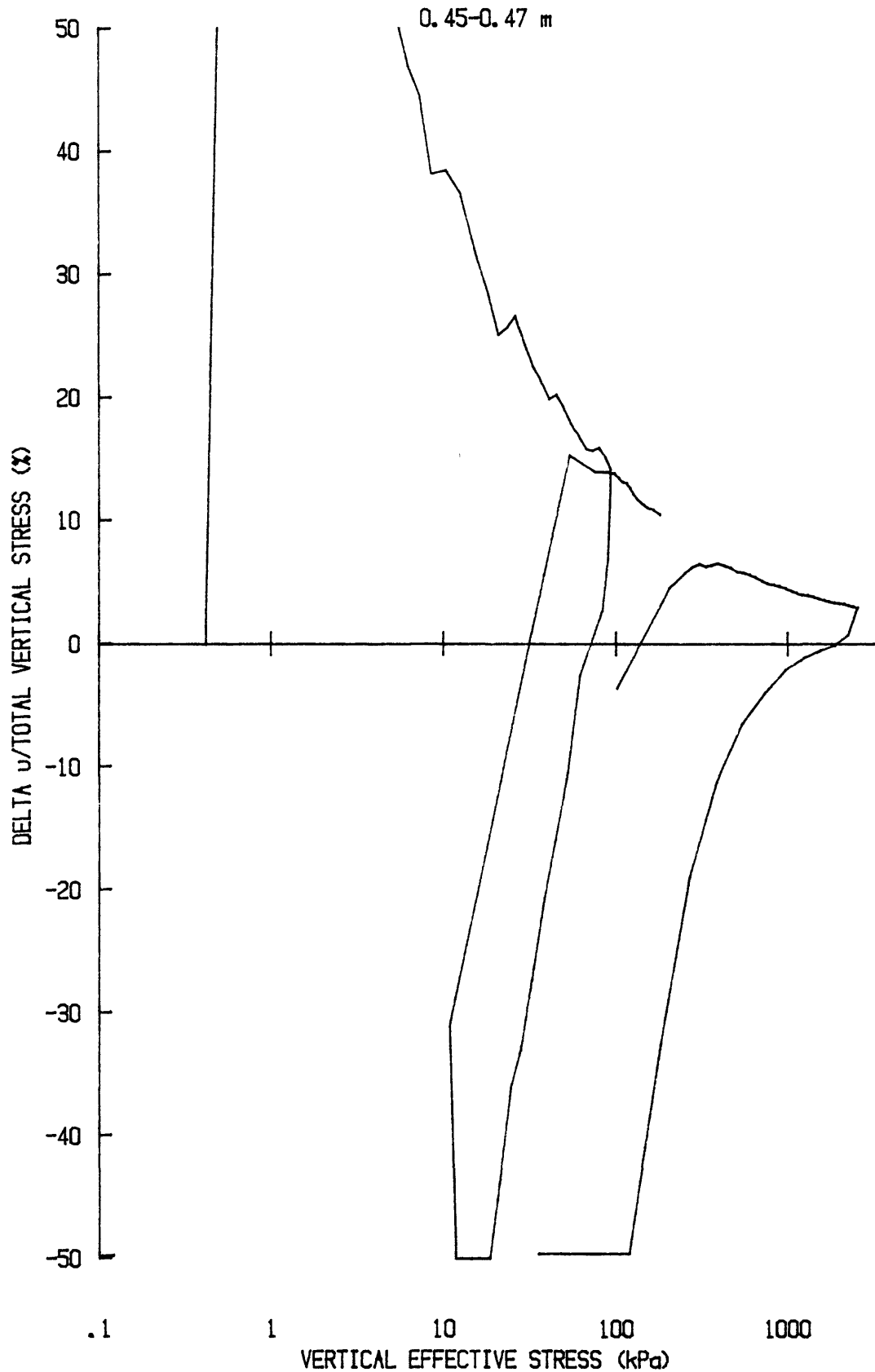


du/Sv for: CR030S8507

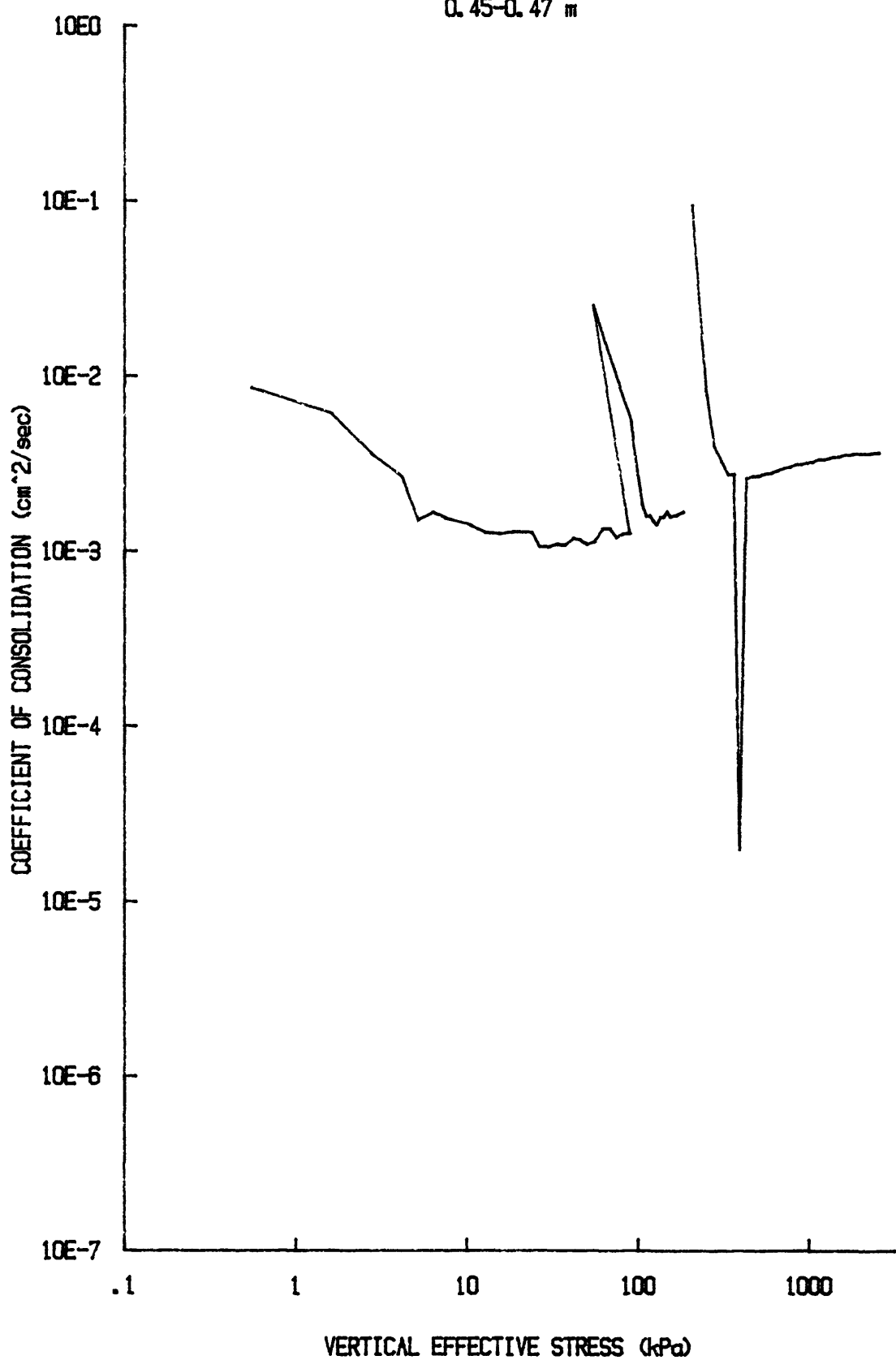
YS-85-08

CORE BC-7

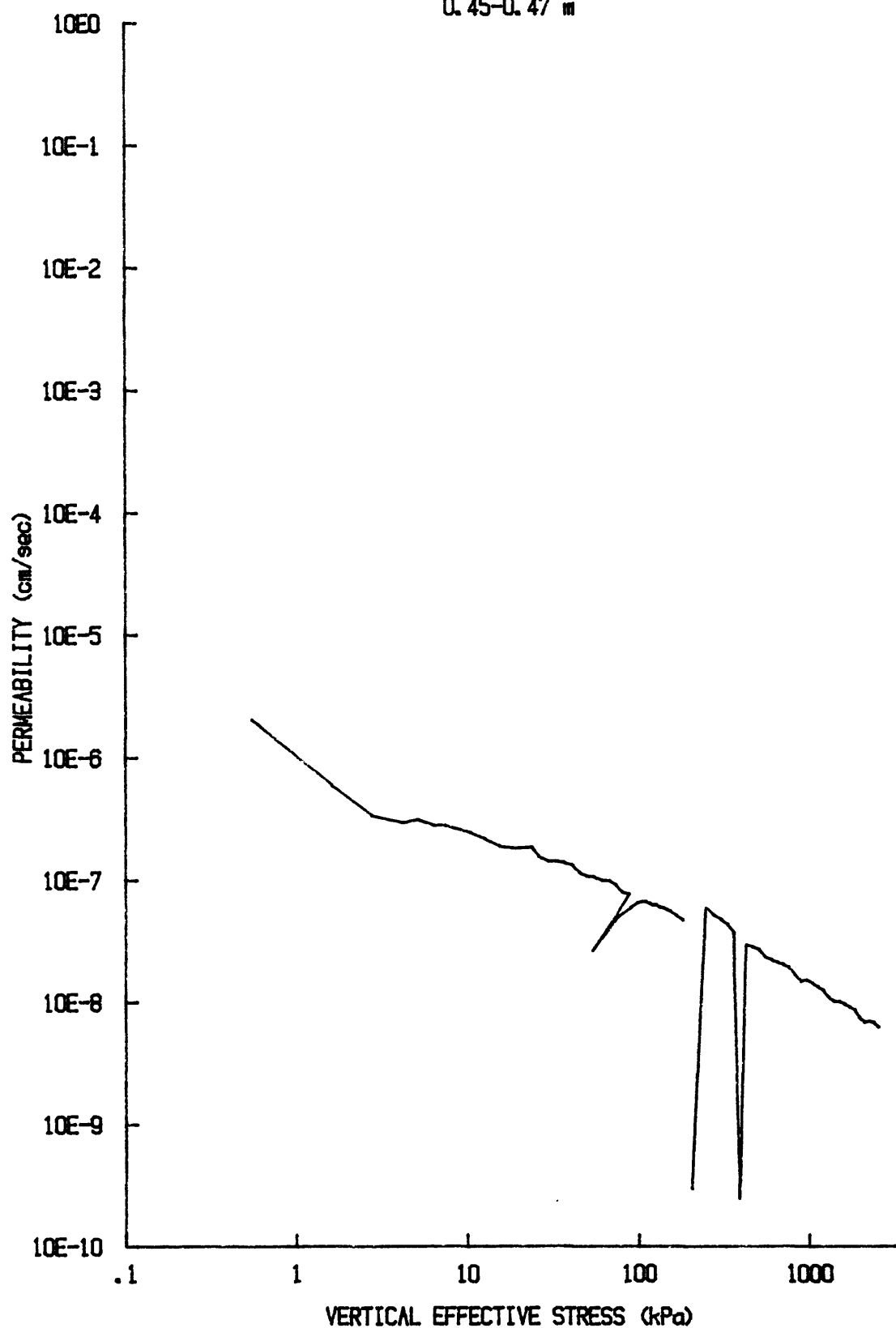
0.45-0.47 m



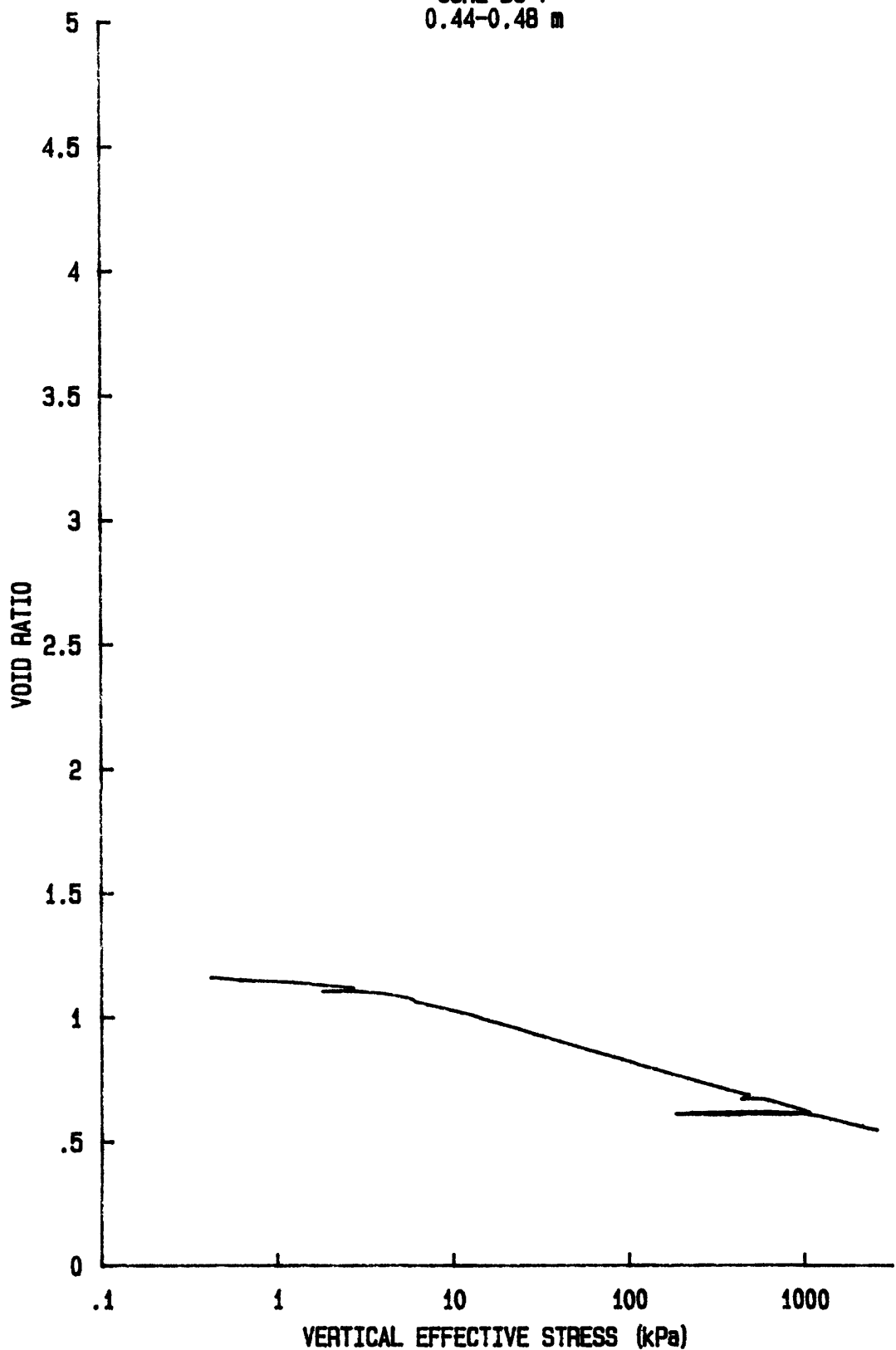
C_v vs $\log p'$ for: CR030S8507
YS-85-08
CORE BC-7
0.45-0.47 m



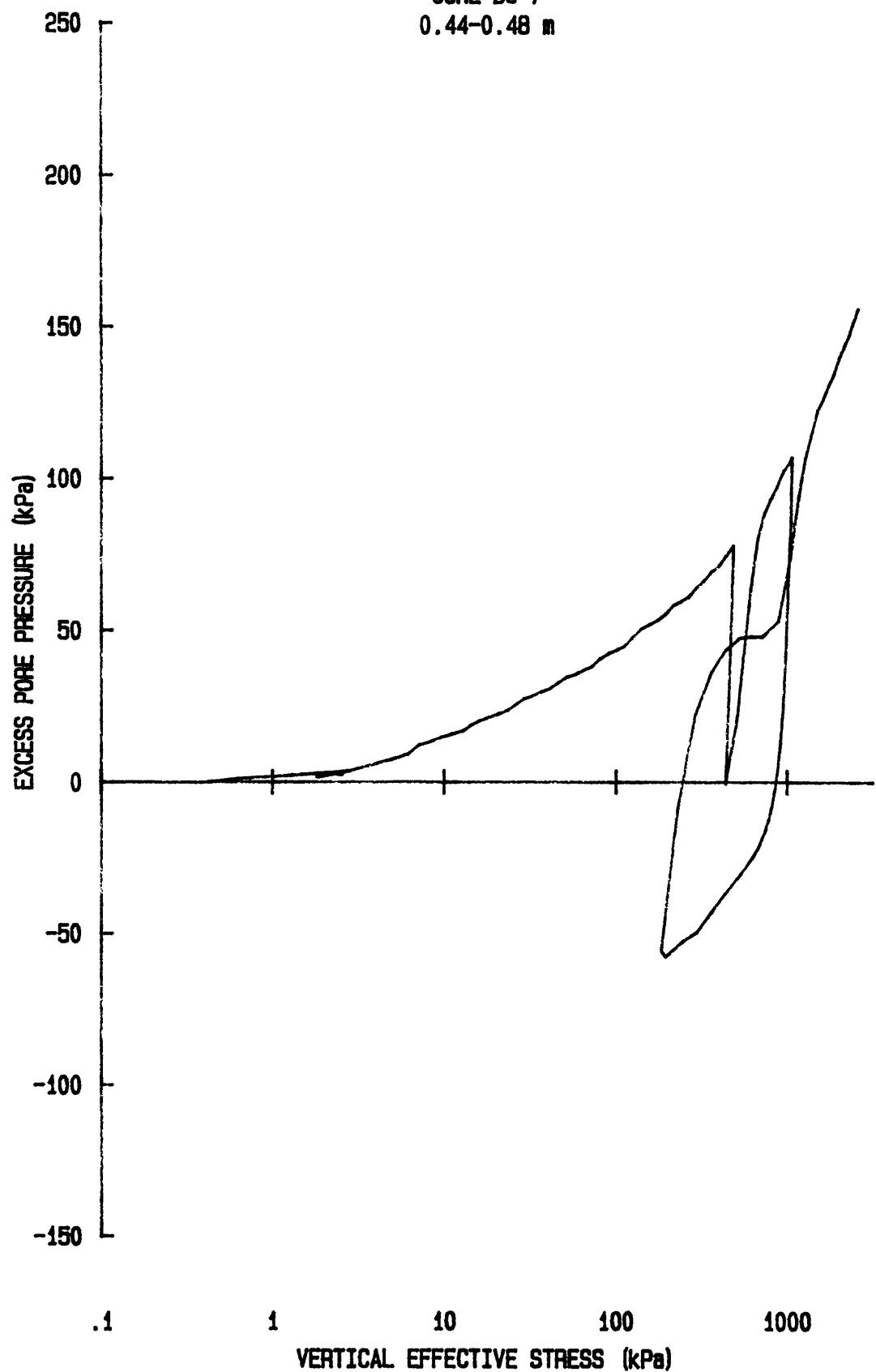
k vs $\log p'$ for CR030S8507
YS-85-08
CORE BC-7
0.45-0.47 m



e vs log p' for: CR057S8507
YS-85-08
CORE BC-7
0.44-0.48 m



u vs log p' for: CR057S8507
YS-85-08
CORE BC-7
0.44-0.48 m

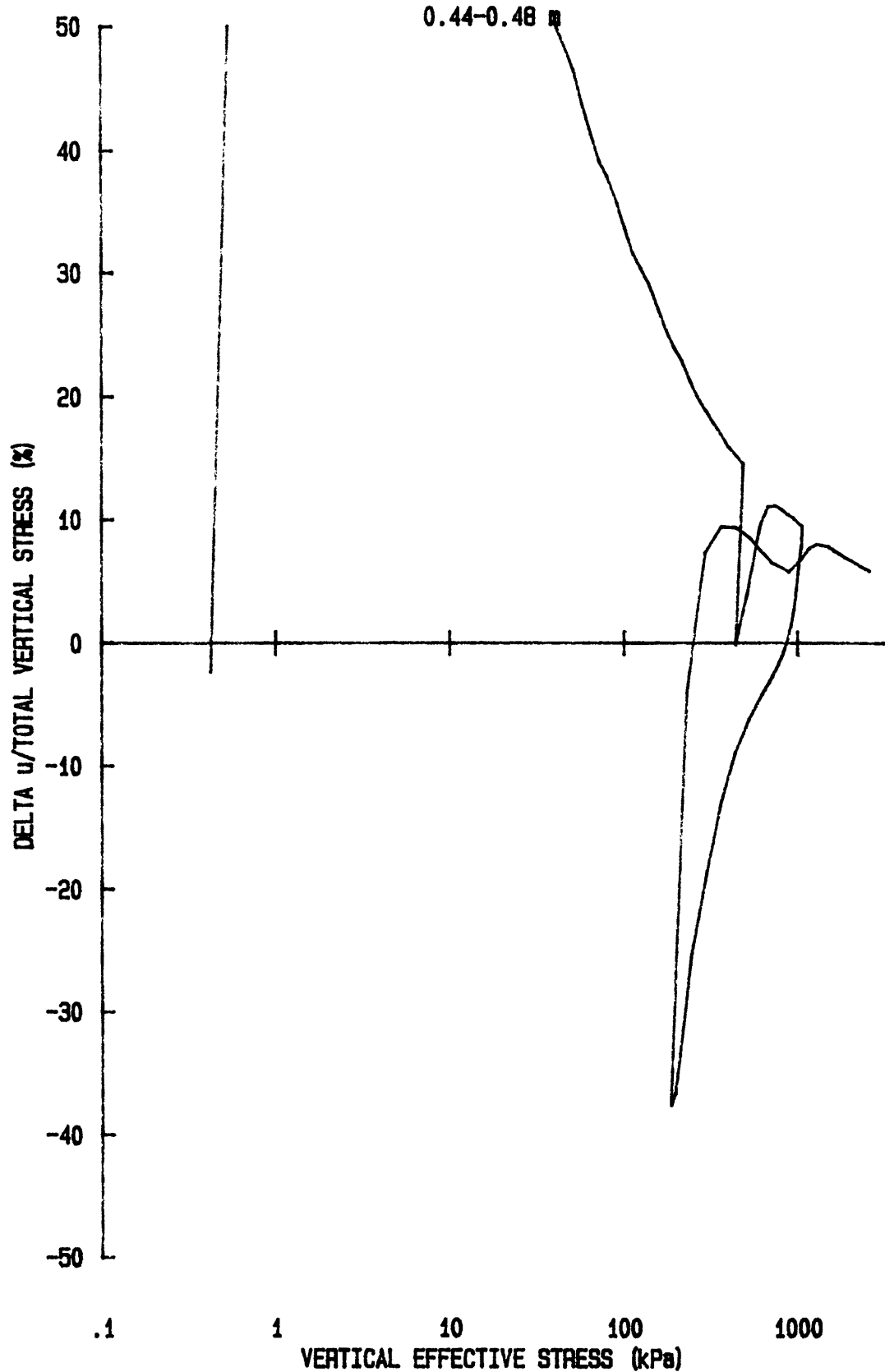


du/Sv for: CR057S8507

YS-85-08

CORE BC-7

0.44-0.48 m

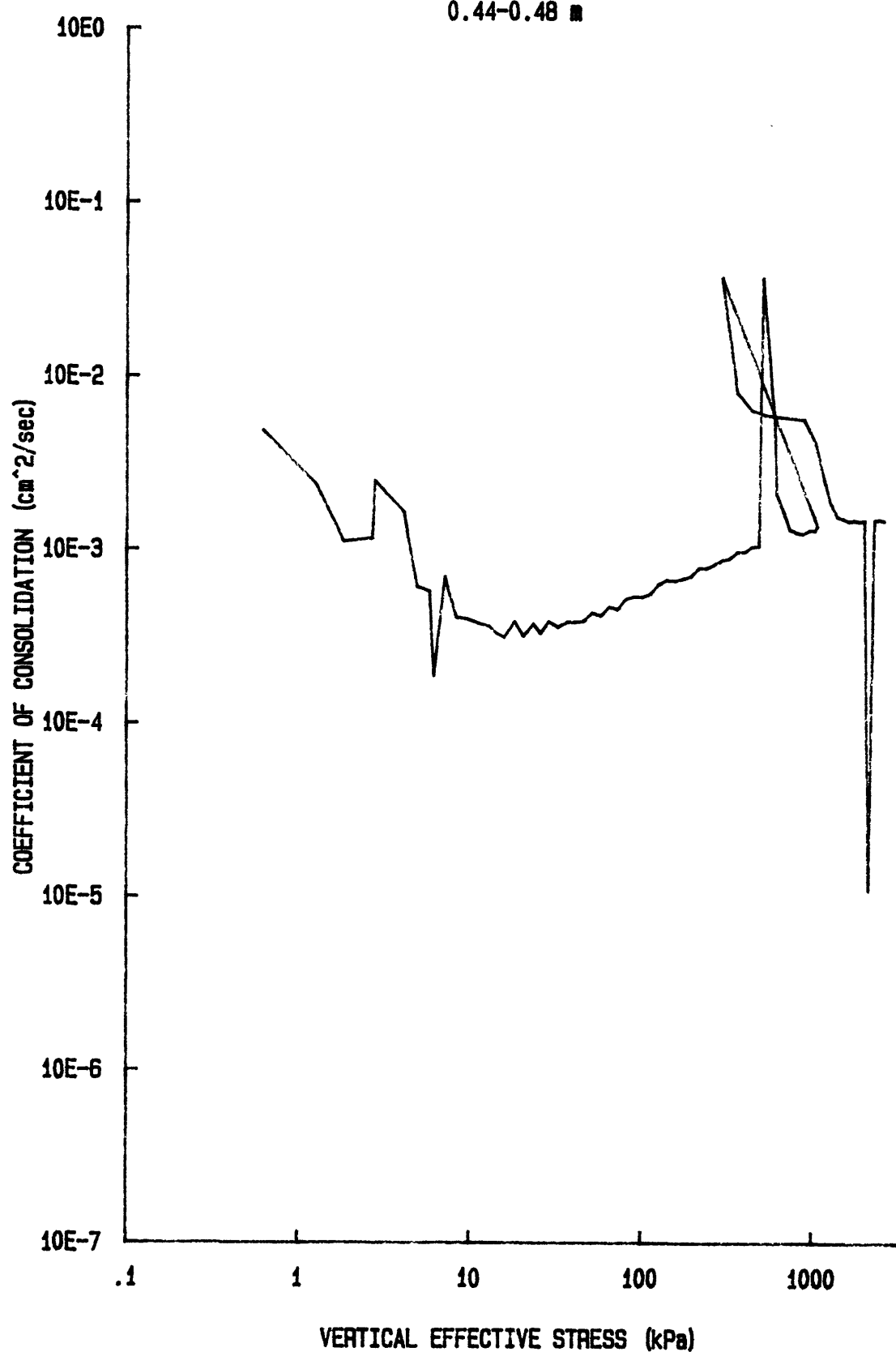


C_v vs $\log p'$ for: CR057S8507

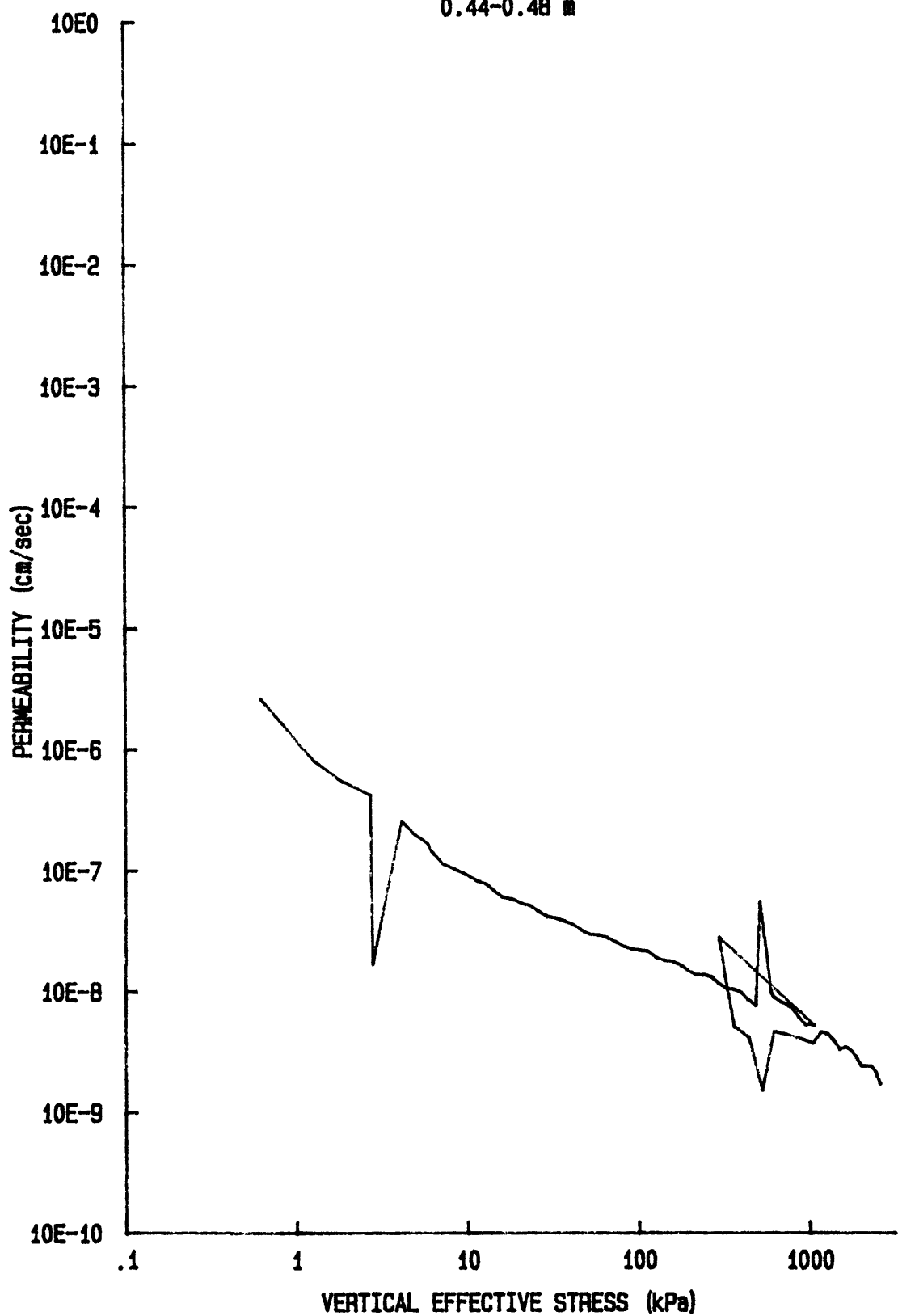
YS-85-08

CORE BC-7

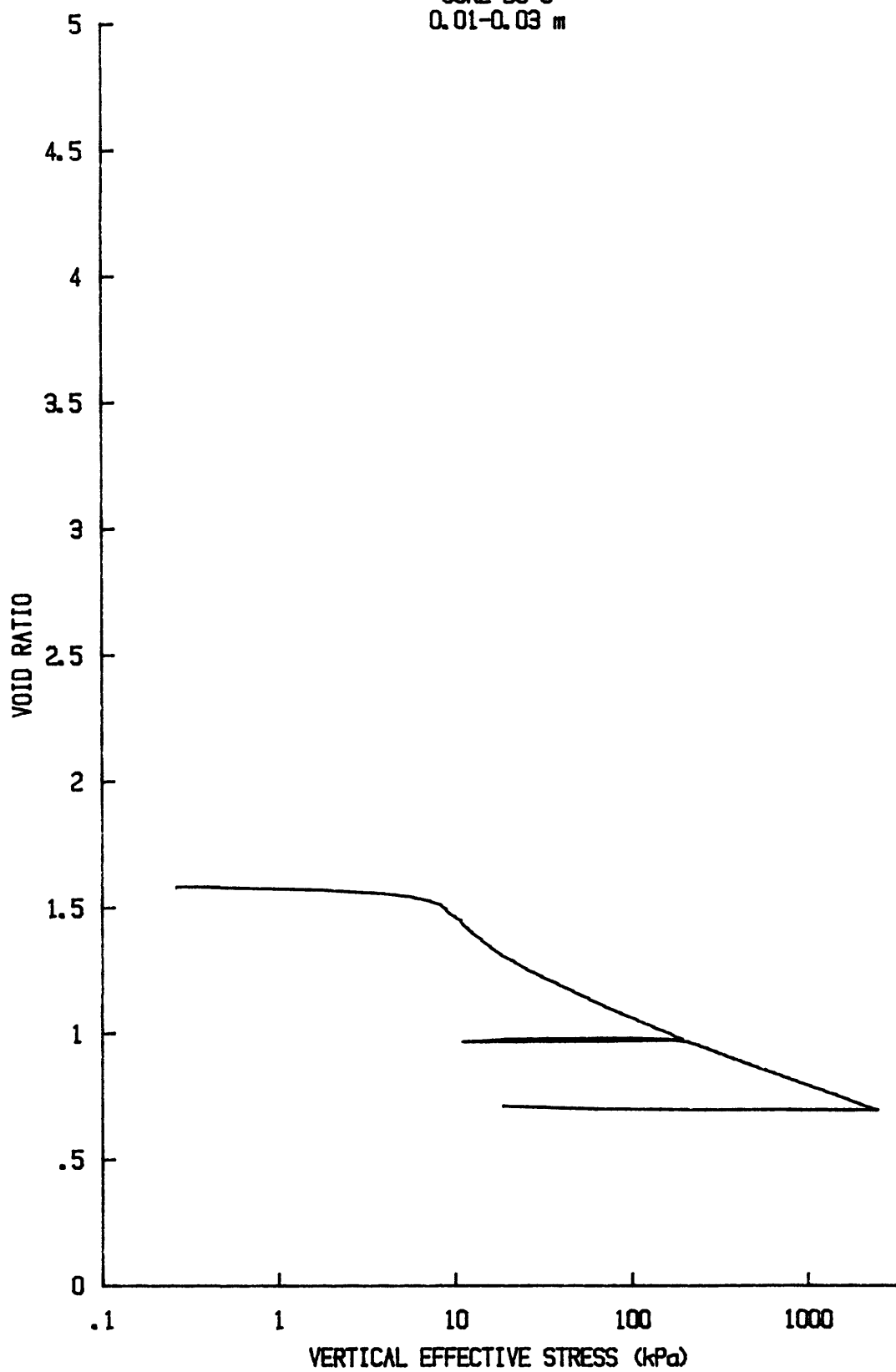
0.44-0.48 m



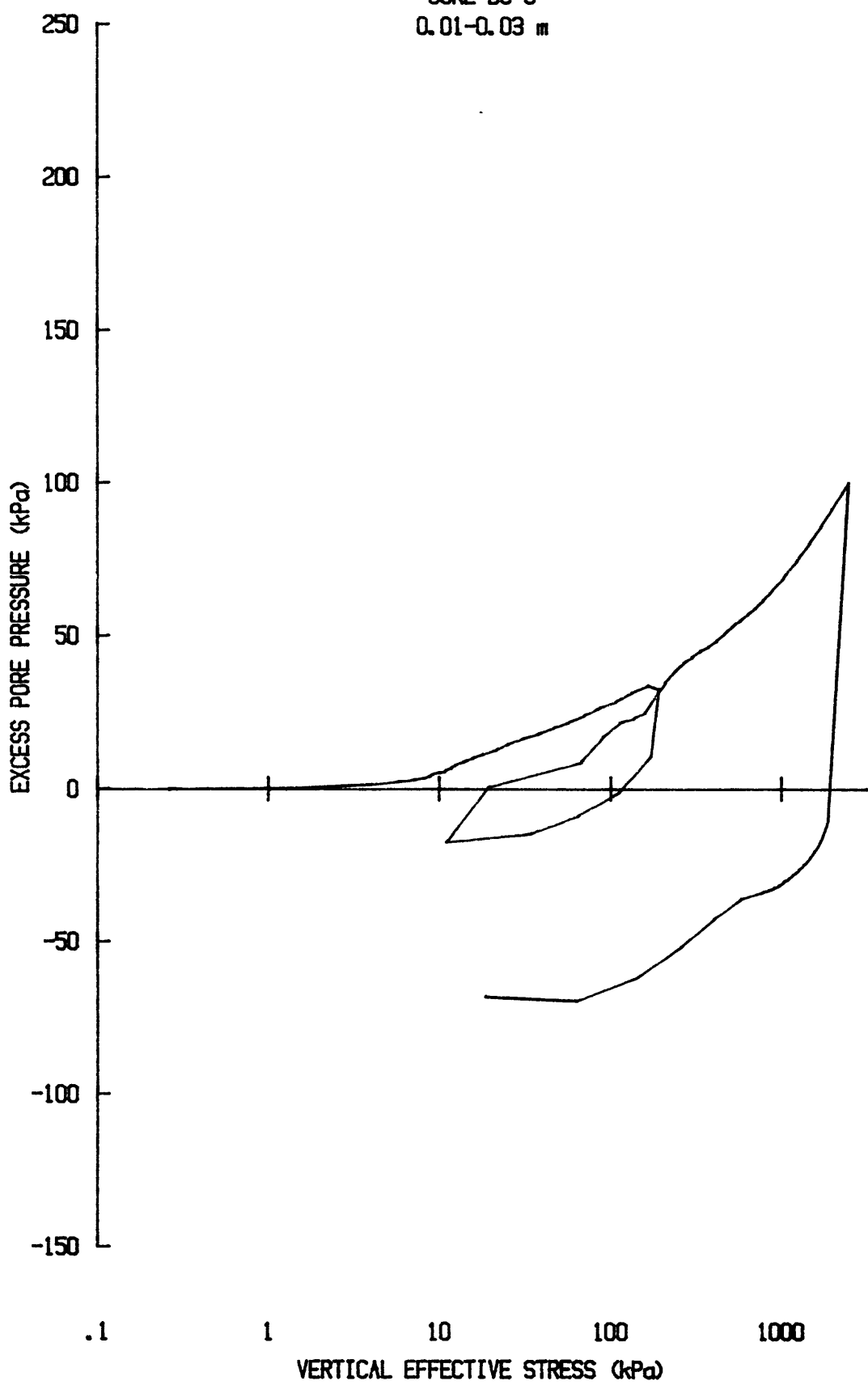
k vs $\log p'$ for: CR057S8507
YS-85-08
CORE BC-7
0.44-0.48 m



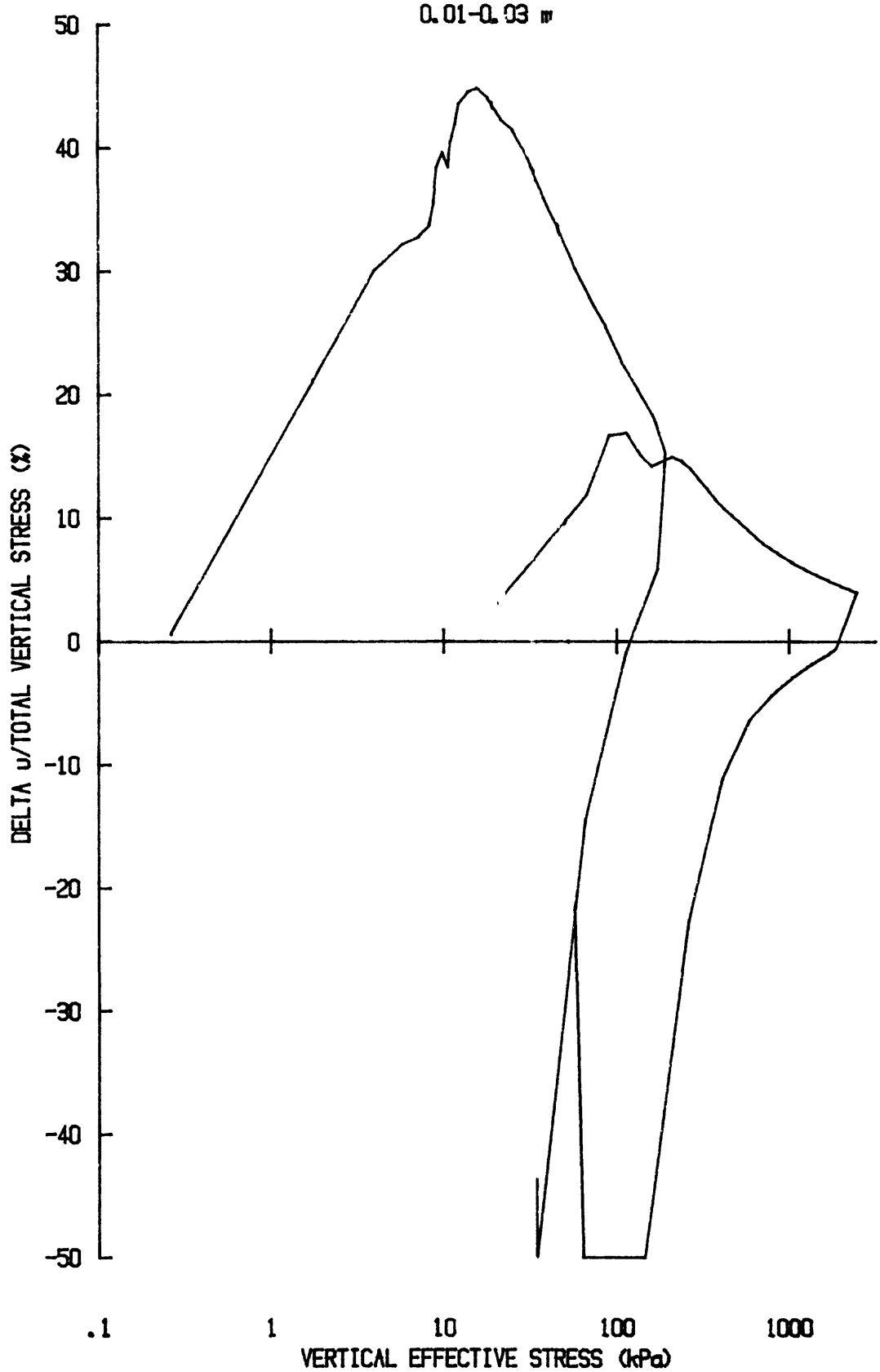
e vs log p' for: CR040S8508
YS-85-08
CORE BC-8
0.01-0.03 m



u vs $\log p'$ for: CR040S8508
YS-85-08
CORE BC-8
0.01-0.03 m



du/Sv for: CR040S8508
YS-85-08
CORE BC-8
0.01-0.03 "

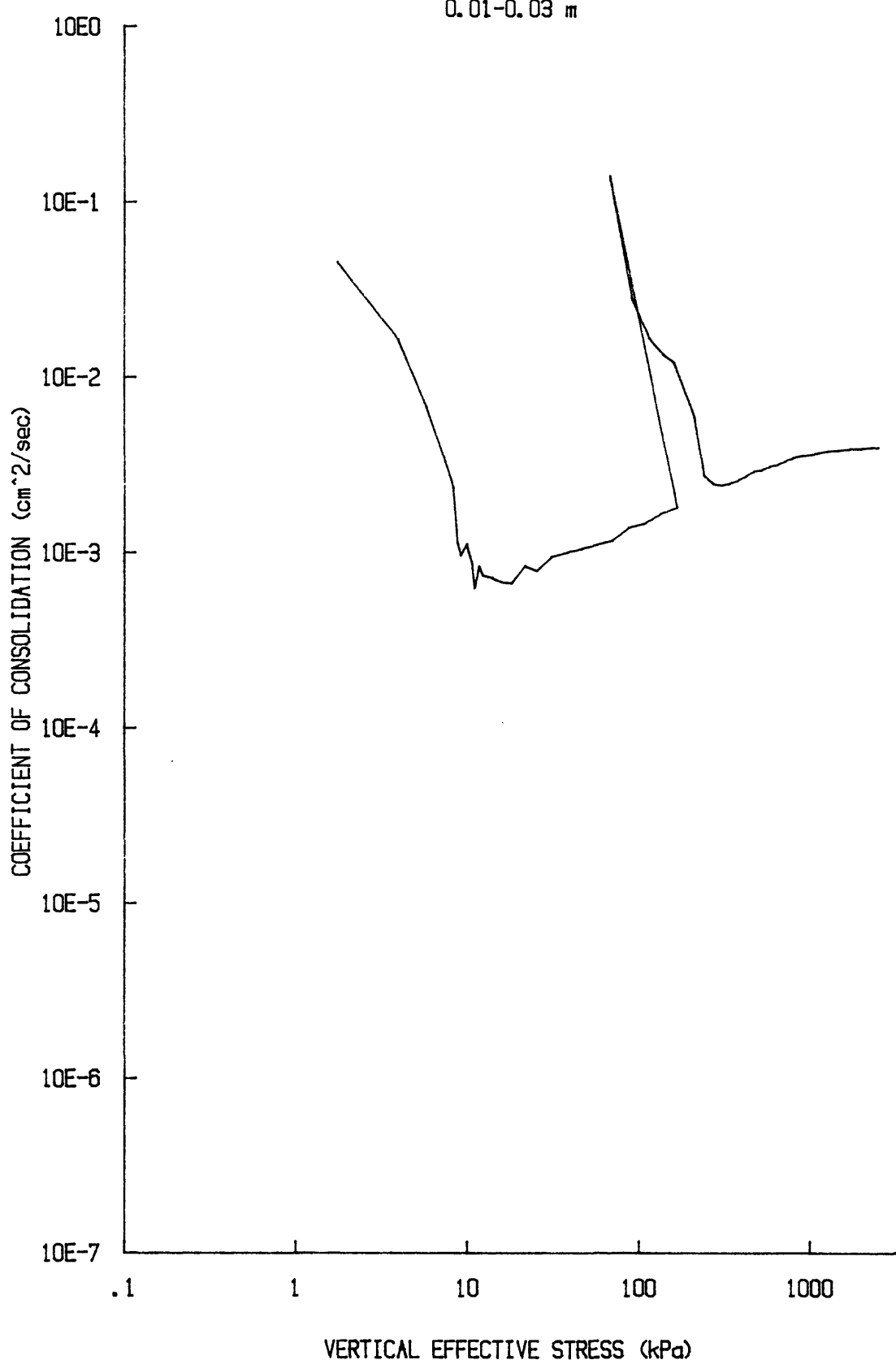


C_v vs $\log p'$ for CR040S8508

YS-85-08

CORE BC-8

0.01-0.03 m

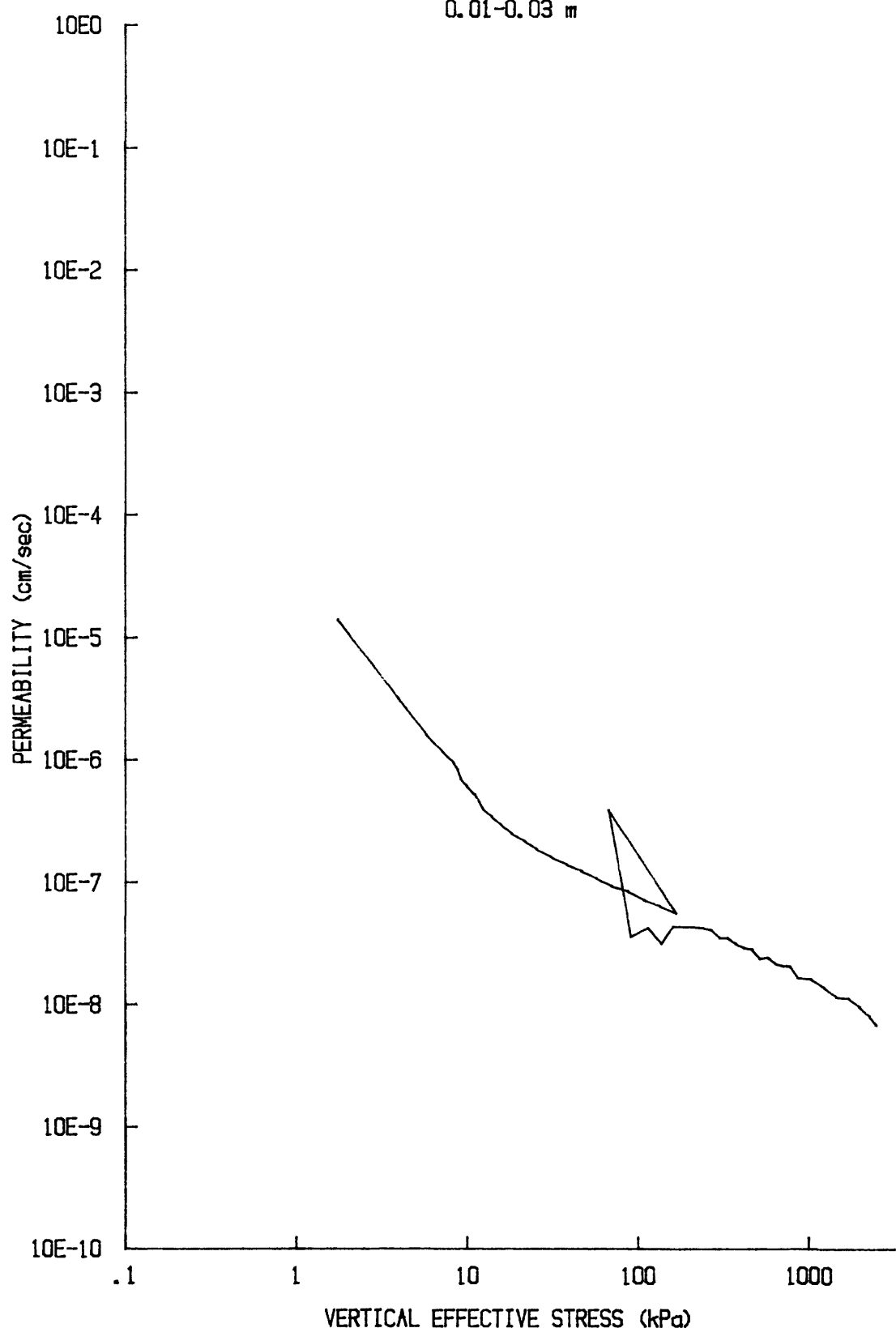


k vs $\log p'$ for: CRO40S8508

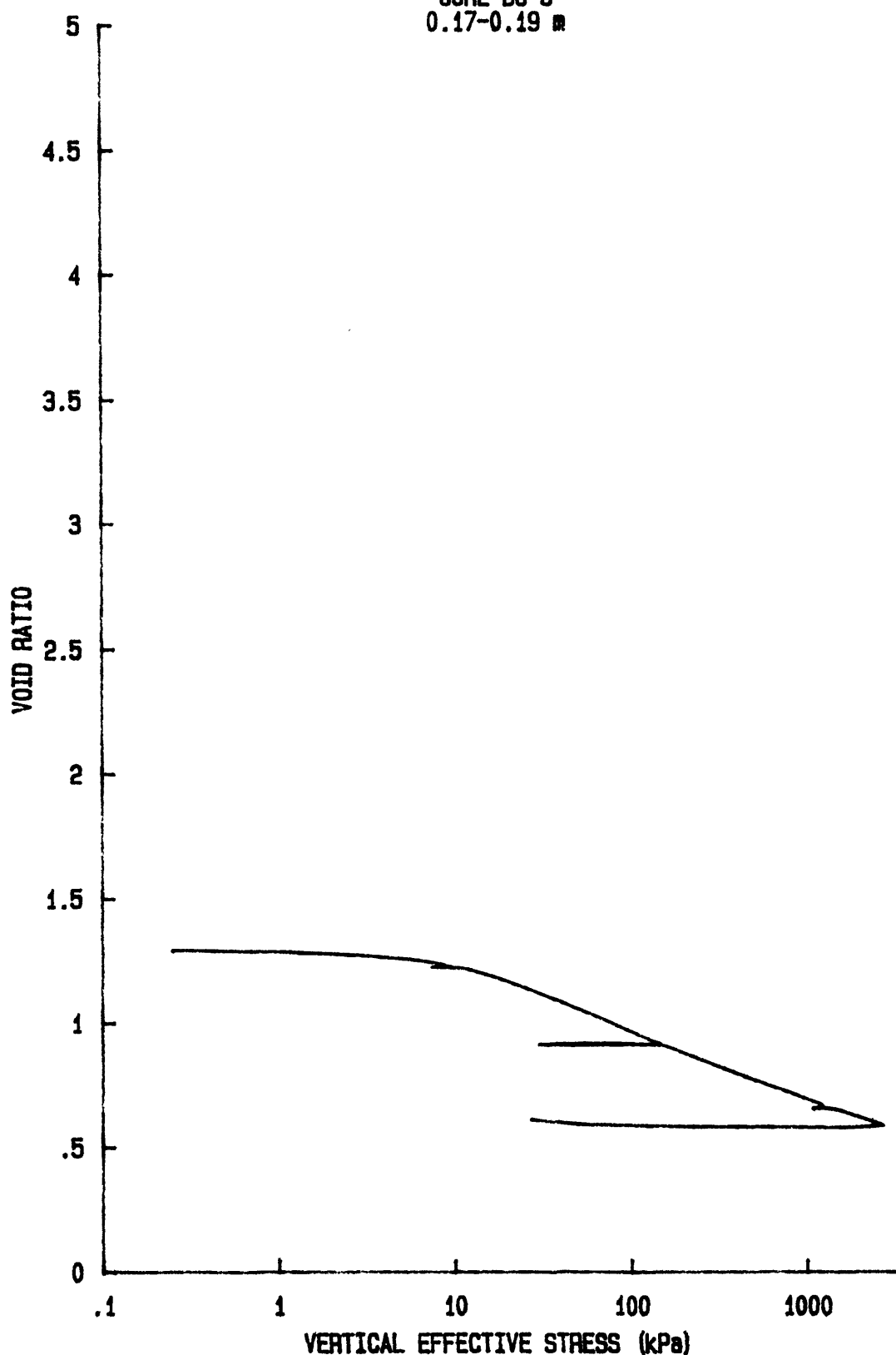
YS-85-08

CORE BC-8

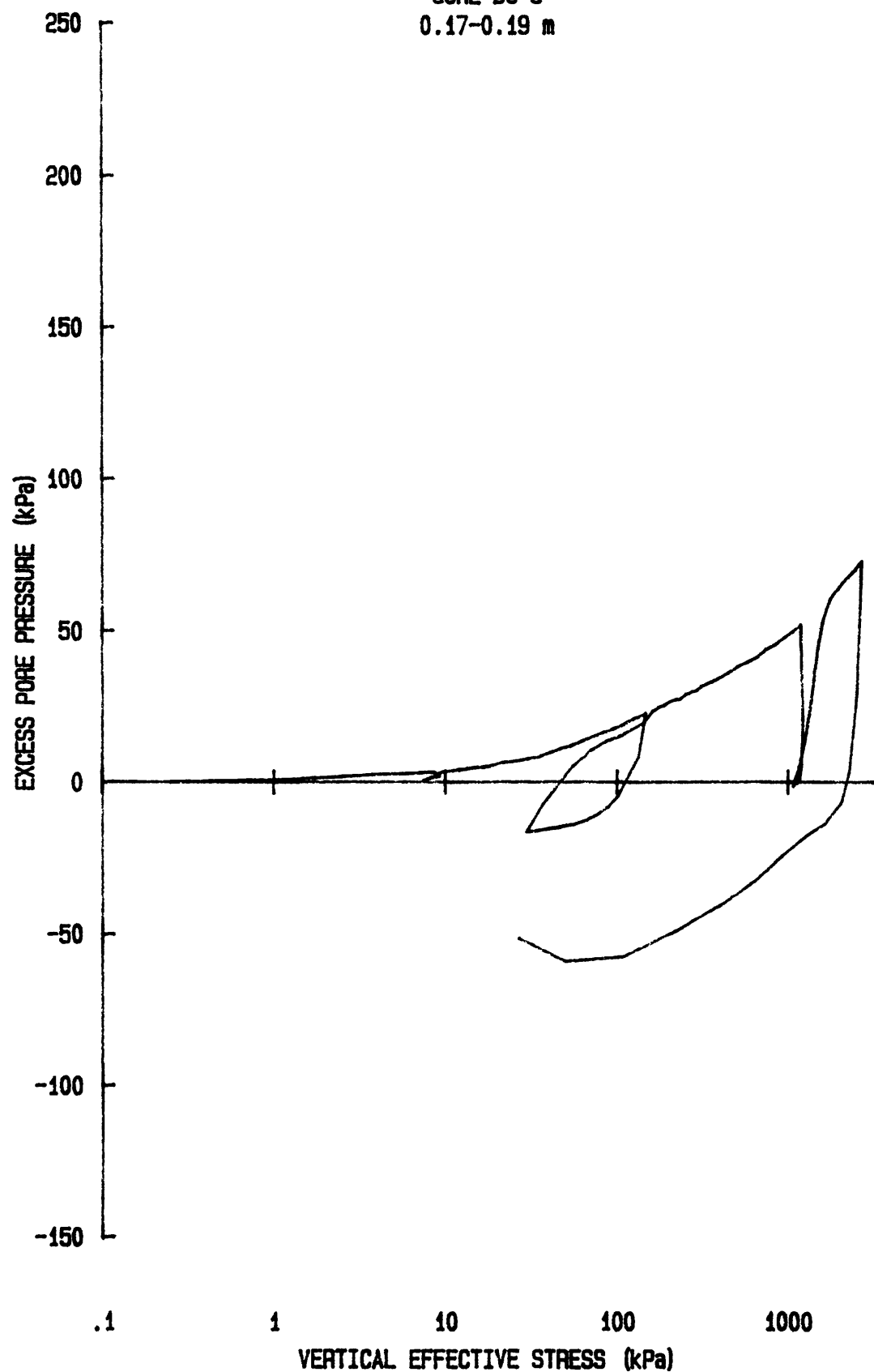
0.01-0.03 m



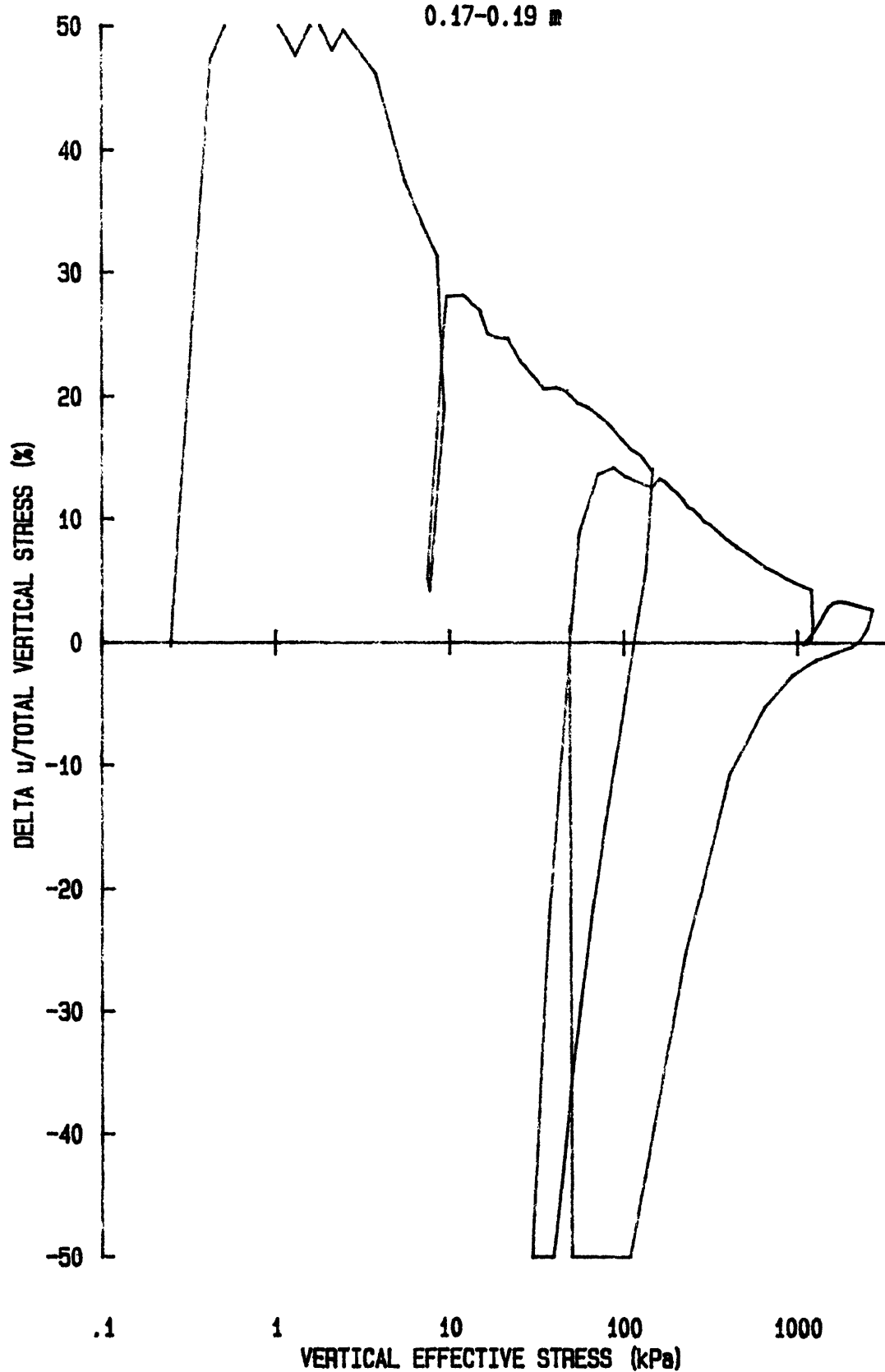
e vs log p' for: CR048S8508
YS-85-08
CORE BC-8
0.17-0.19 m



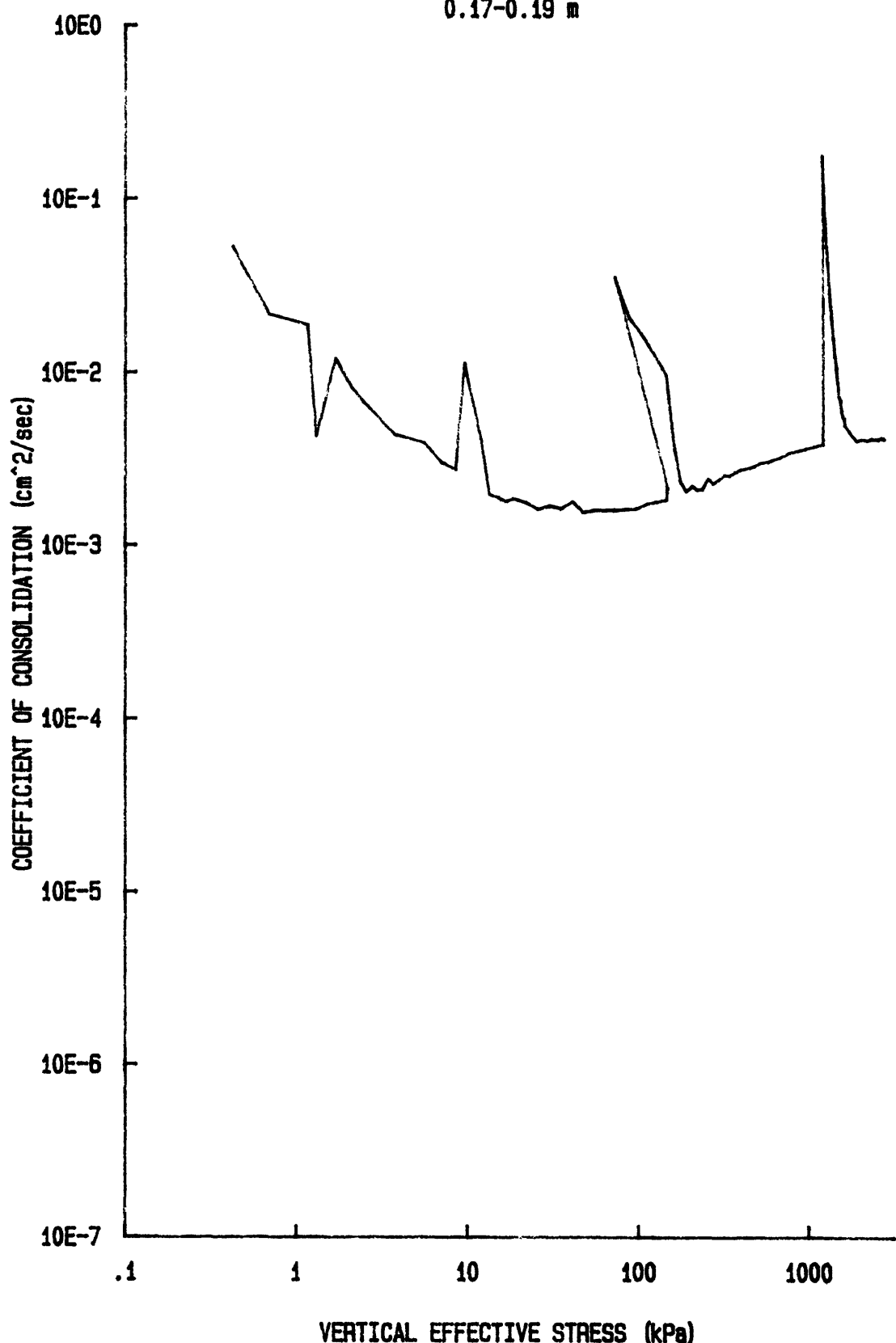
u vs $\log p'$ for: CR048S8508
YS-85-08
CORE BC-8
0.17-0.19 m



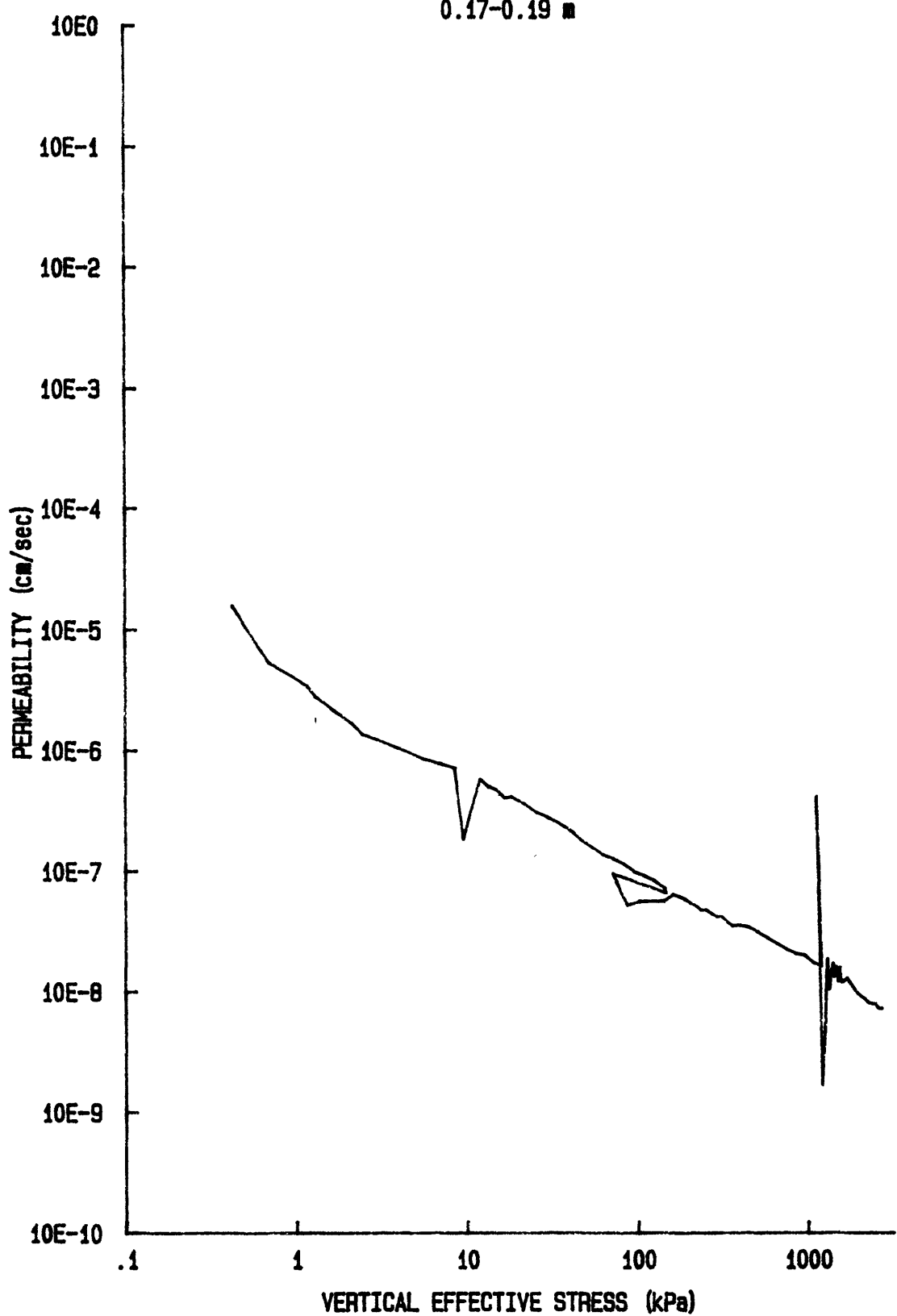
du/Sv for: CR048S8508
YS-85-08
CORE BC-8
0.17-0.19 in



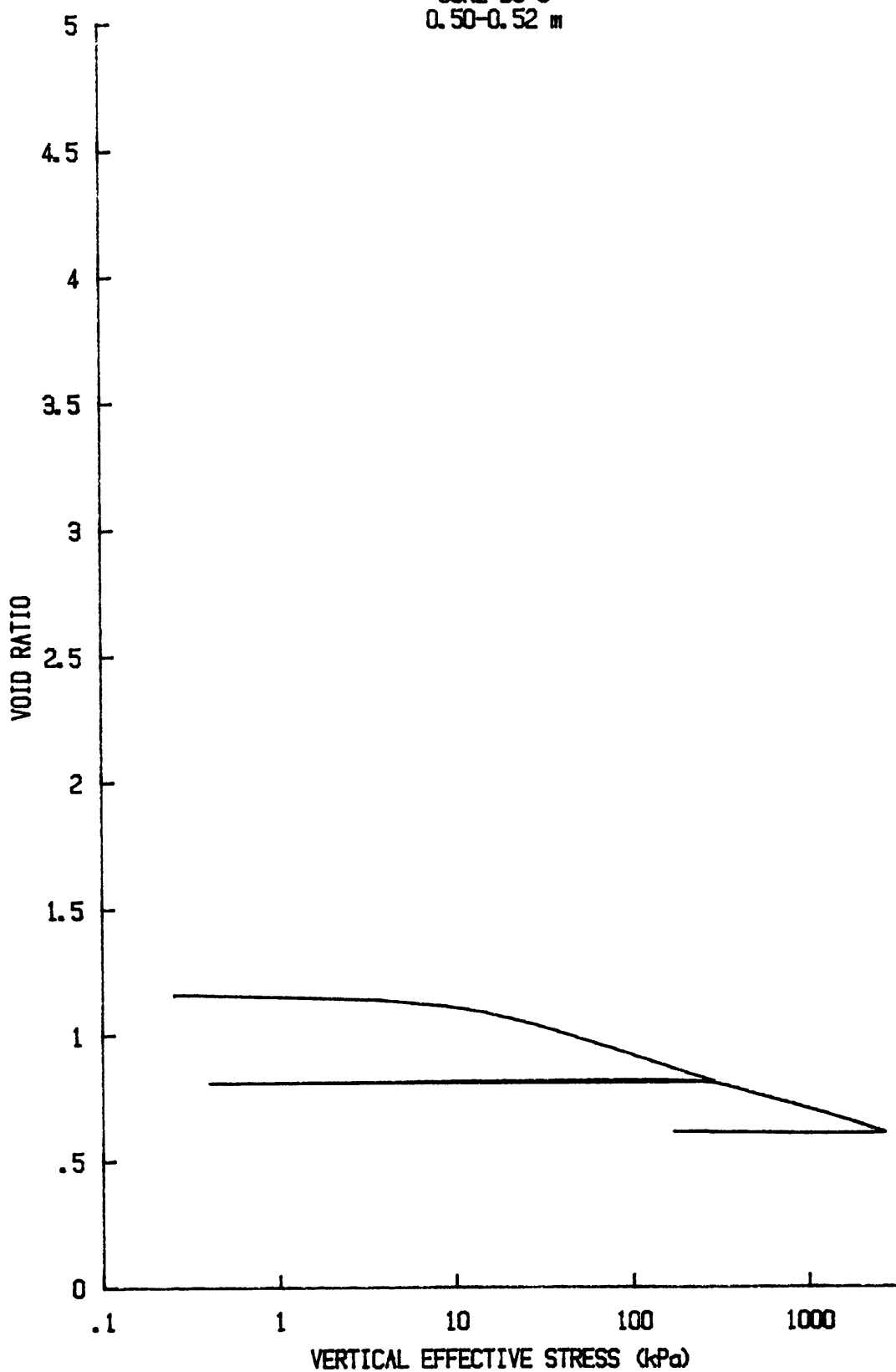
Cv vs log p' for: CR048S8508
YS-85-08
CORE BC-8
0.17-0.19 m



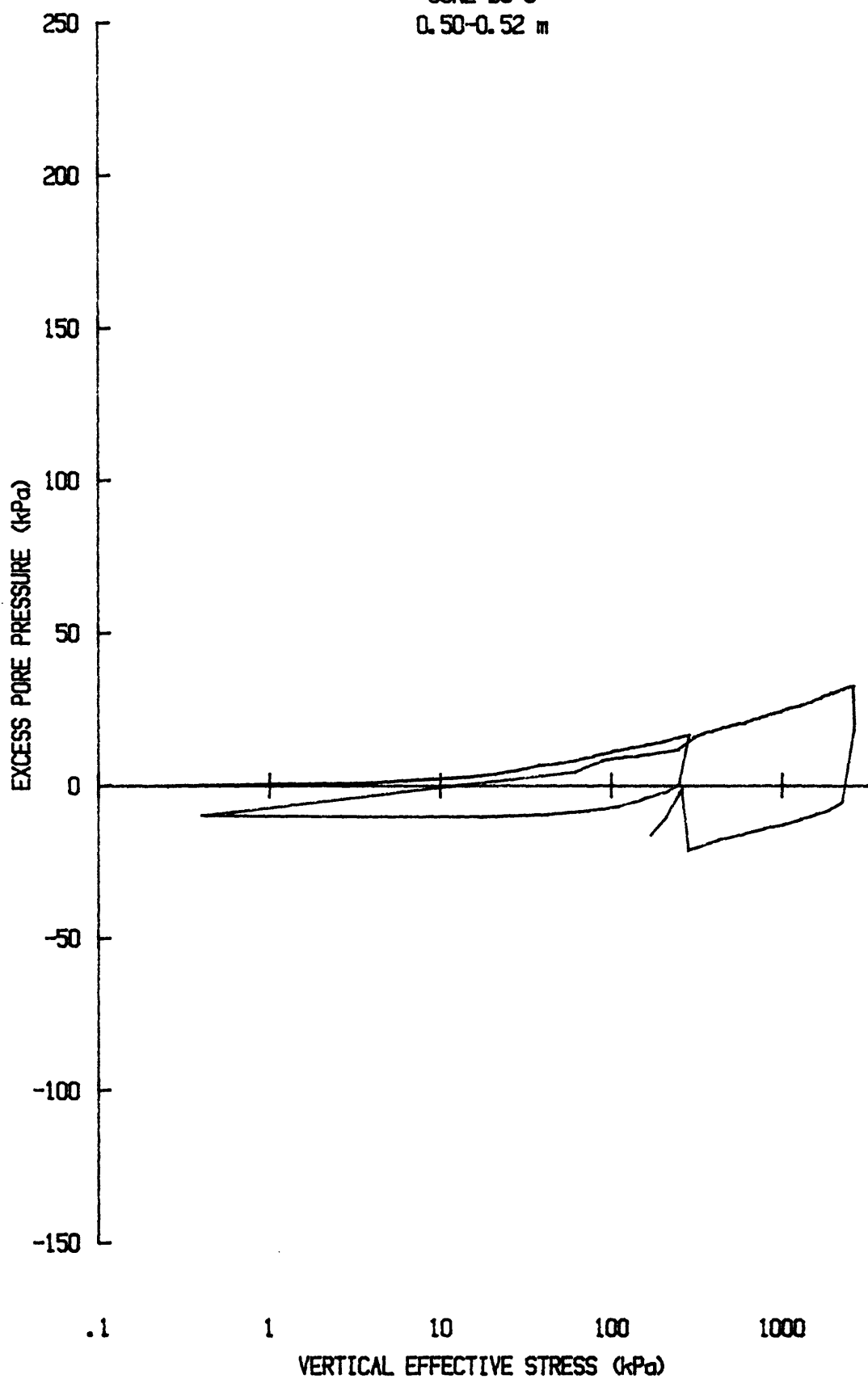
k vs $\log p'$ for: CR048S8508
YS-85-08
CORE BC-8
0.17-0.19 m



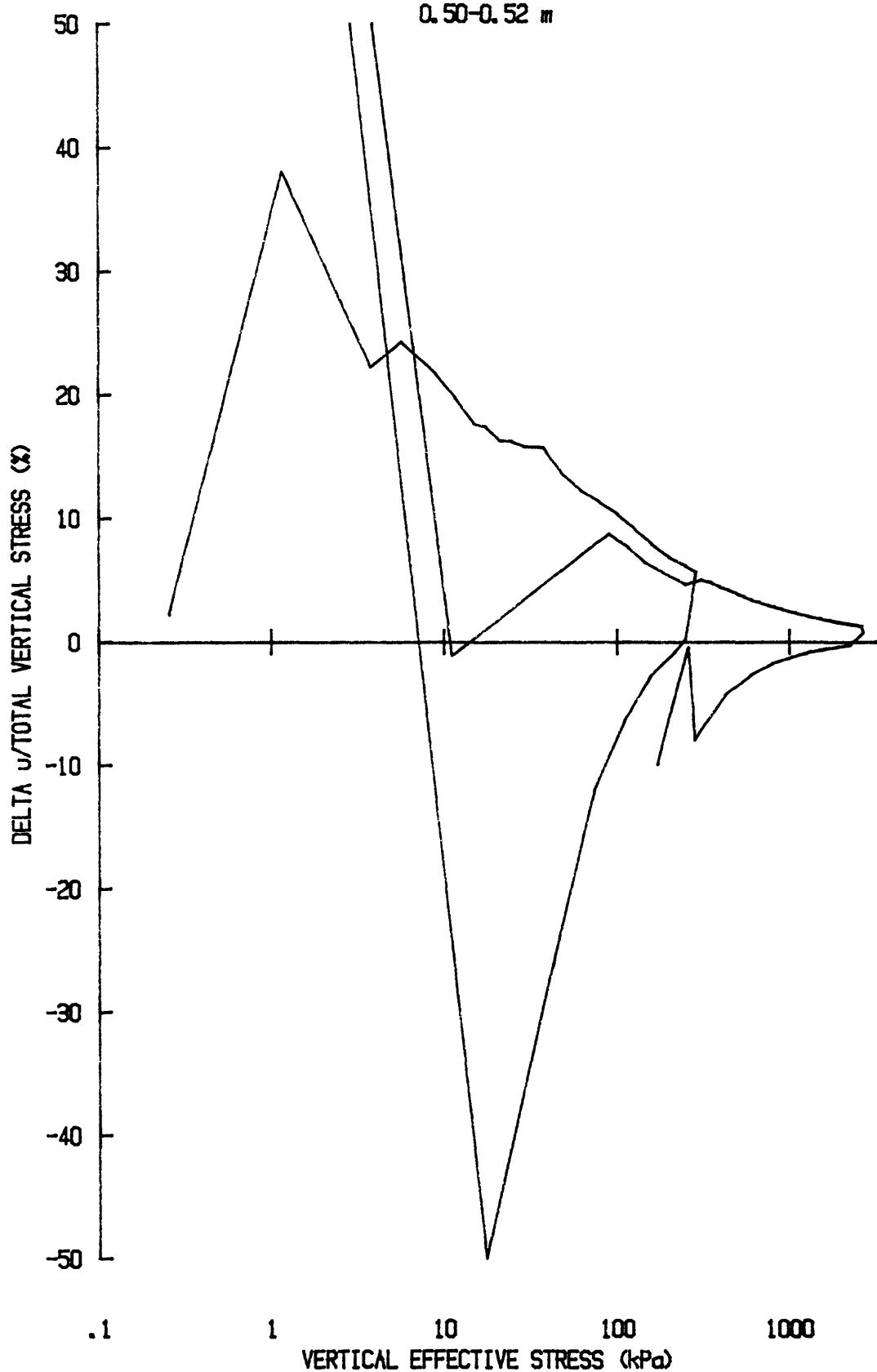
e vs $\log p'$ for CR044S8508
YS-85-08
CORE BC-8
0.50-0.52 m



u vs $\log p'$ for CR044S8508
YS-85-08
CORE BC-8
0.50-0.52 m



du/Sv for: CR044S8508
YS-85-08
CORE BC-8
0.50-0.52 m

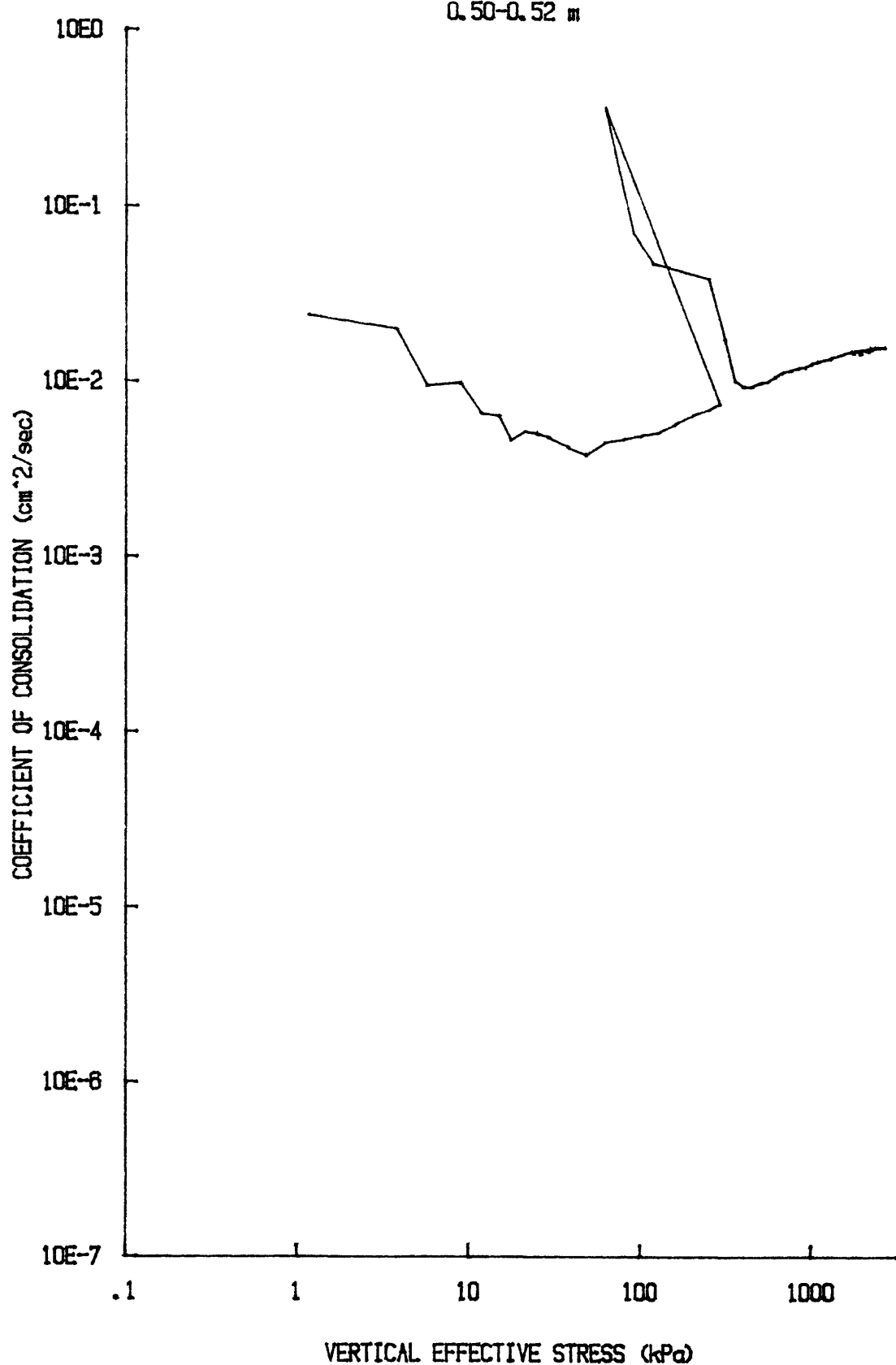


C_v vs $\log p'$ for: CR044S8508

YS-85-08

CORE BC-8

0.50-0.52 m

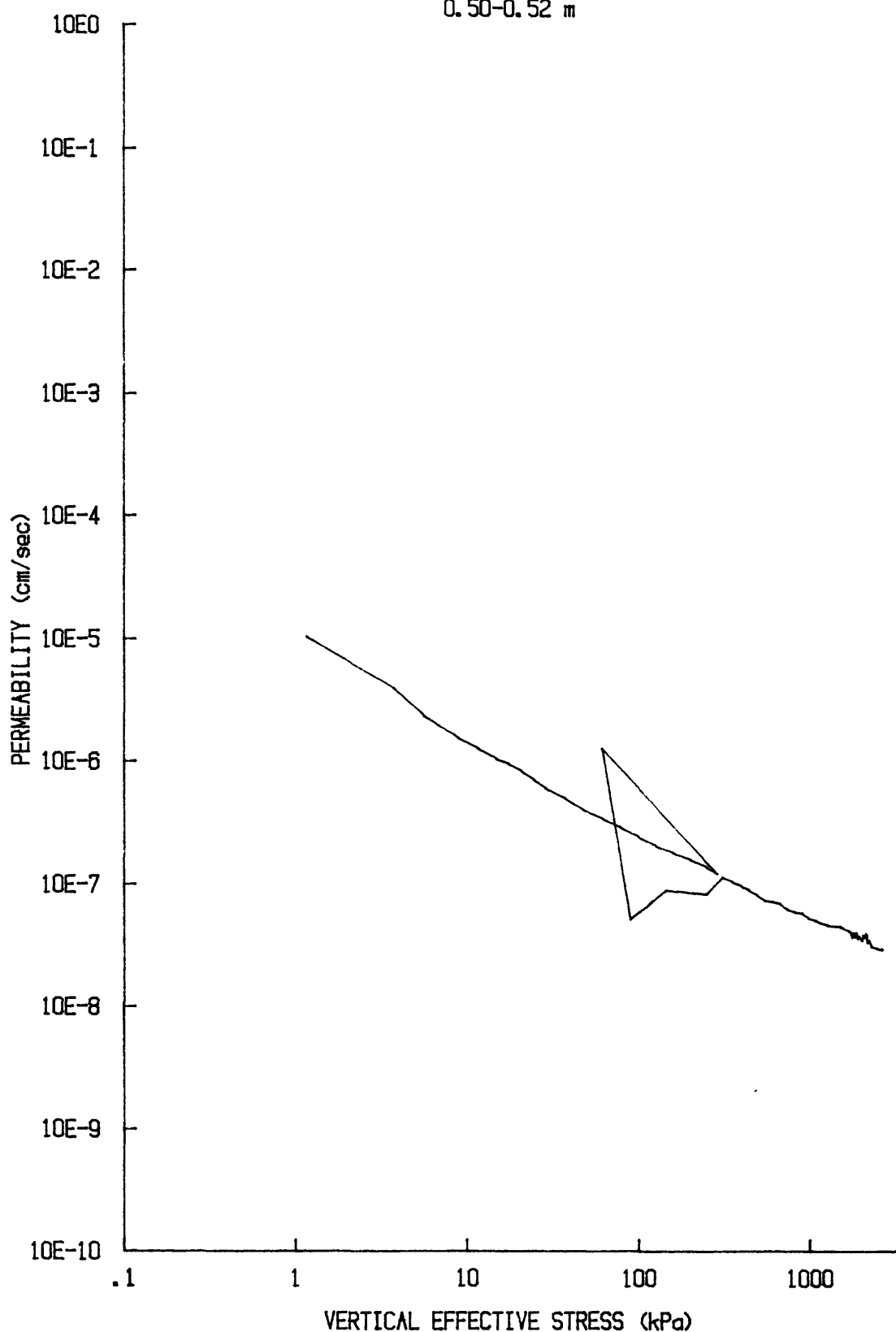


k vs $\log p'$ for CR044S8508

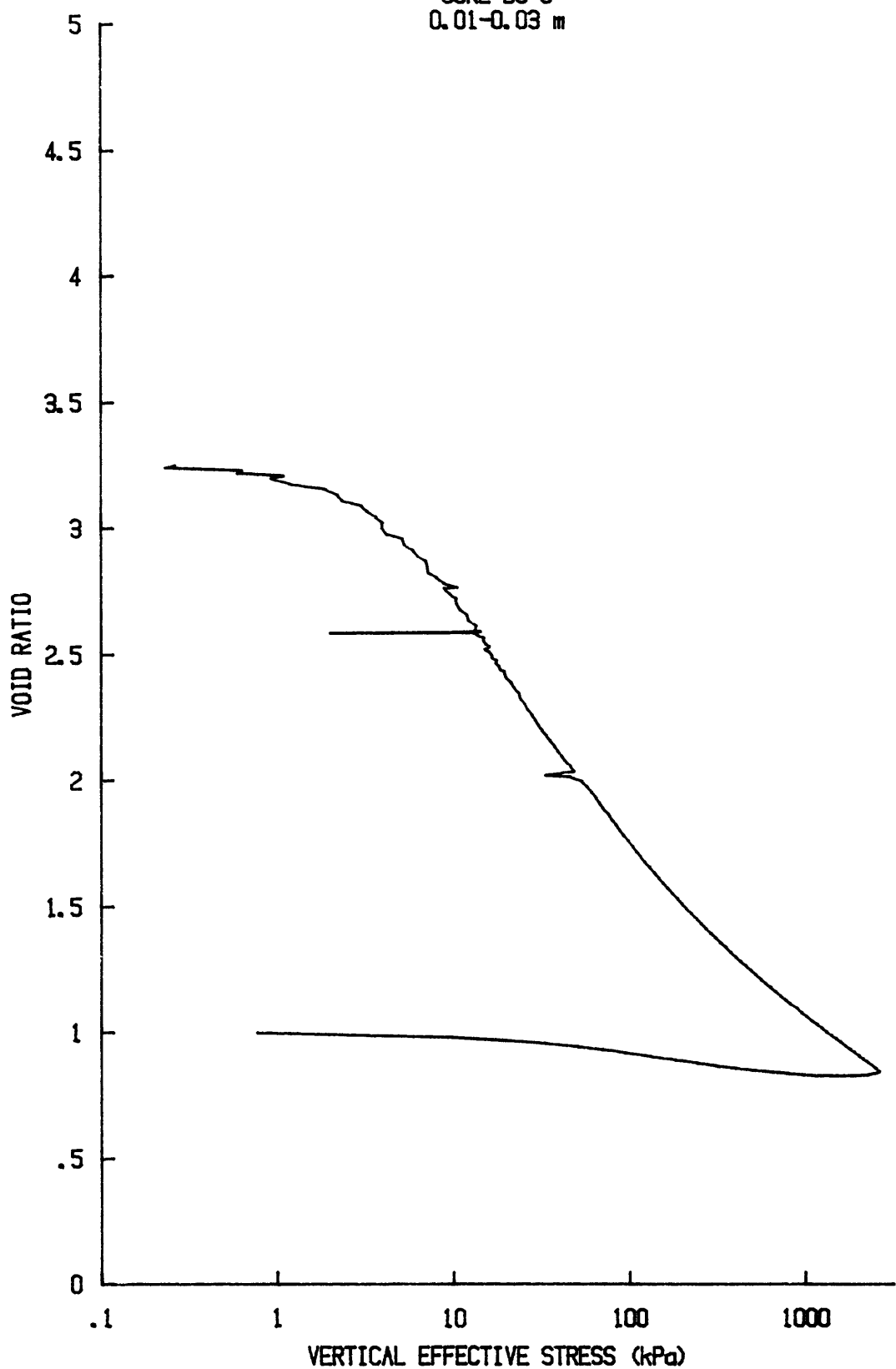
YS-85-08

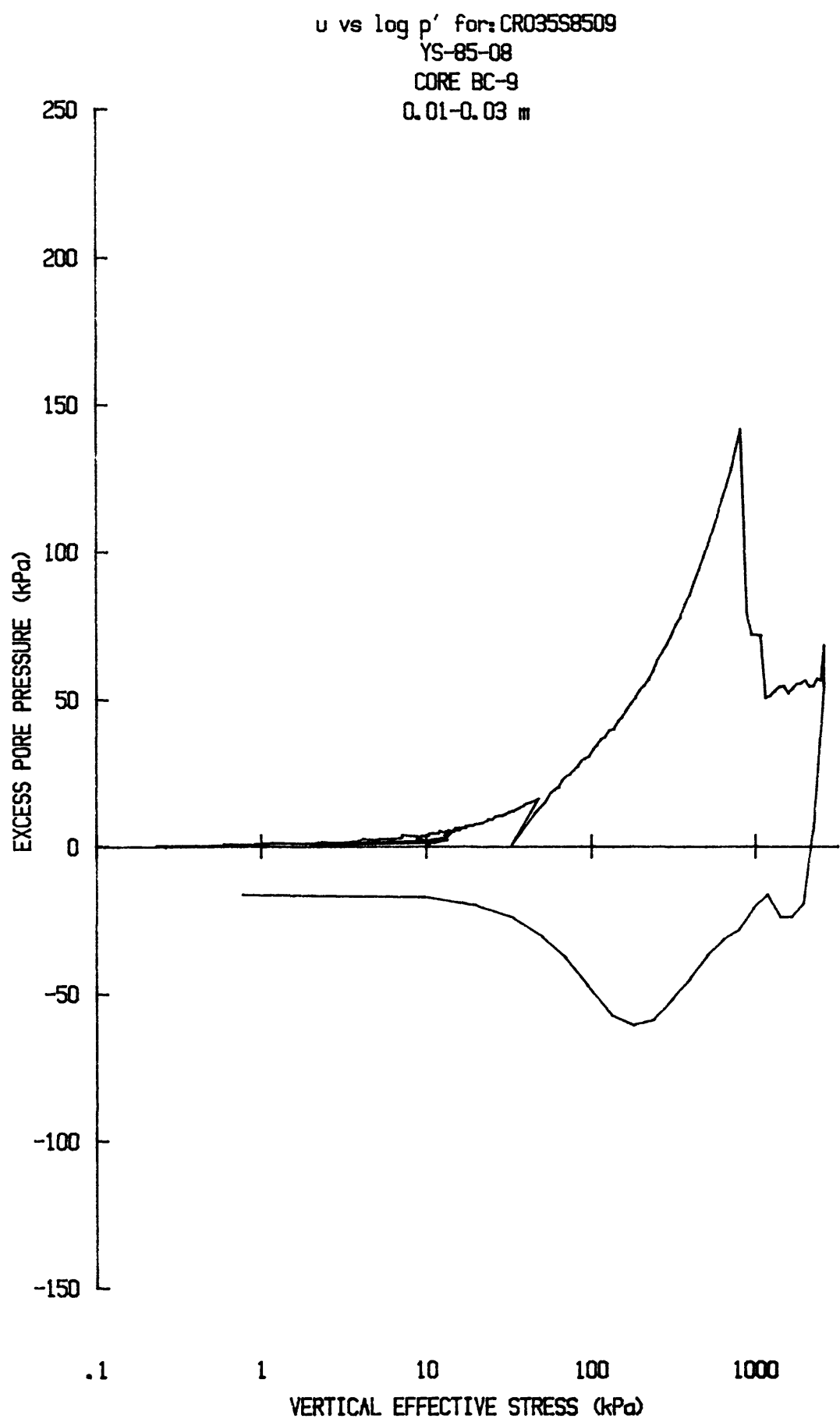
CORE BC-8

0.50-0.52 m

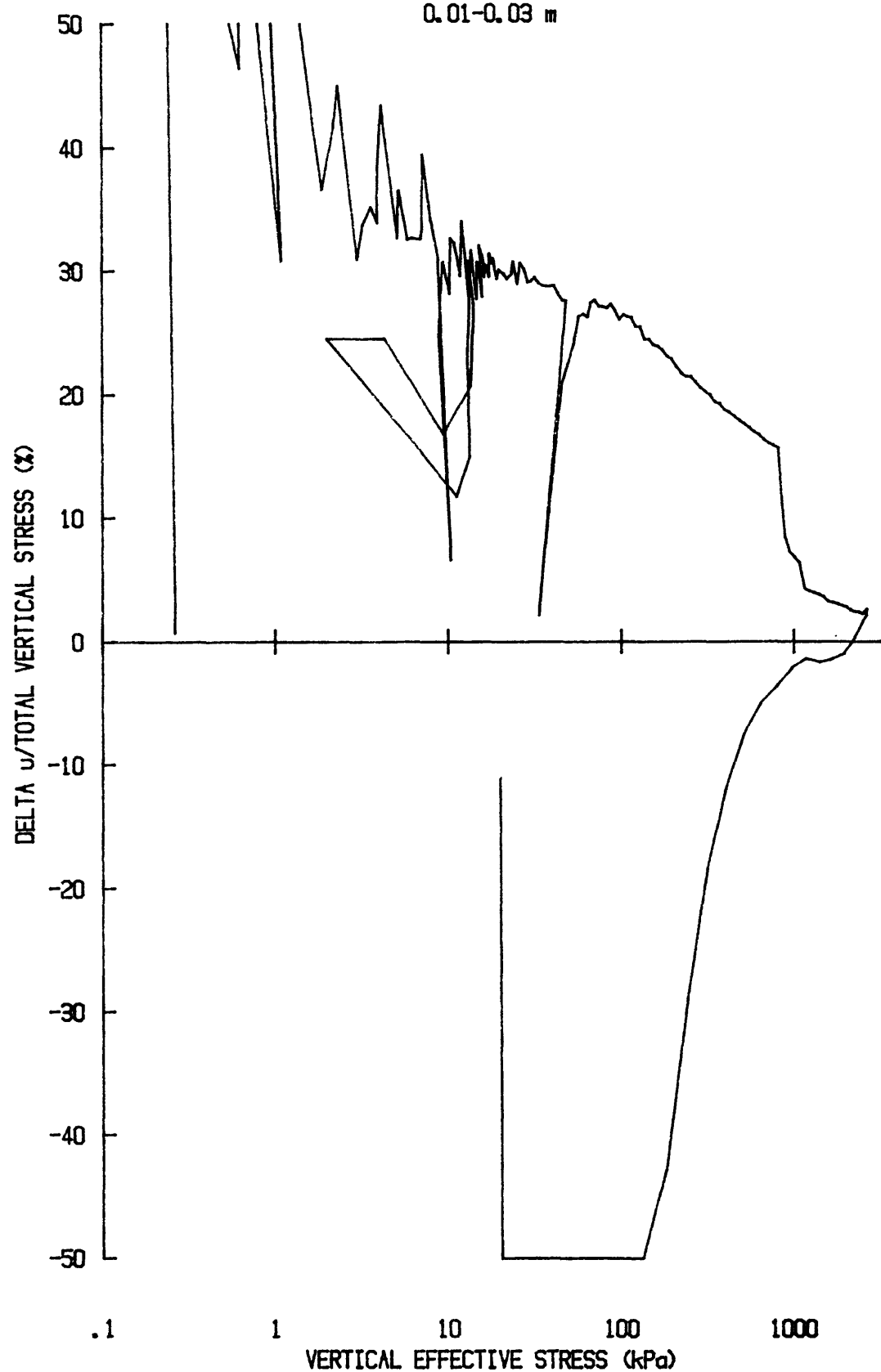


e vs $\log p'$ for: CR035S8509
YS-85-08
CORE BC-9
0.01-0.03 m

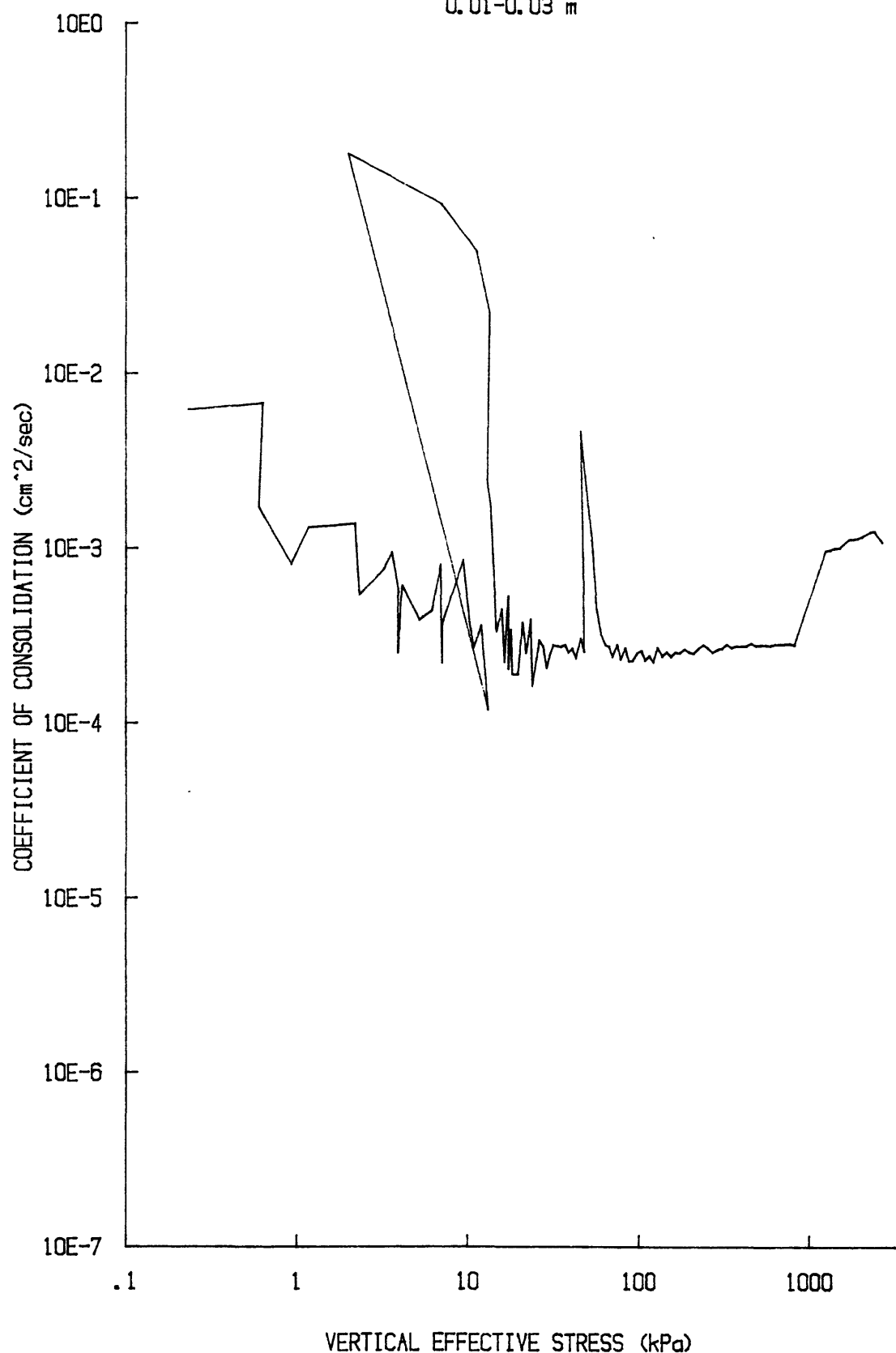




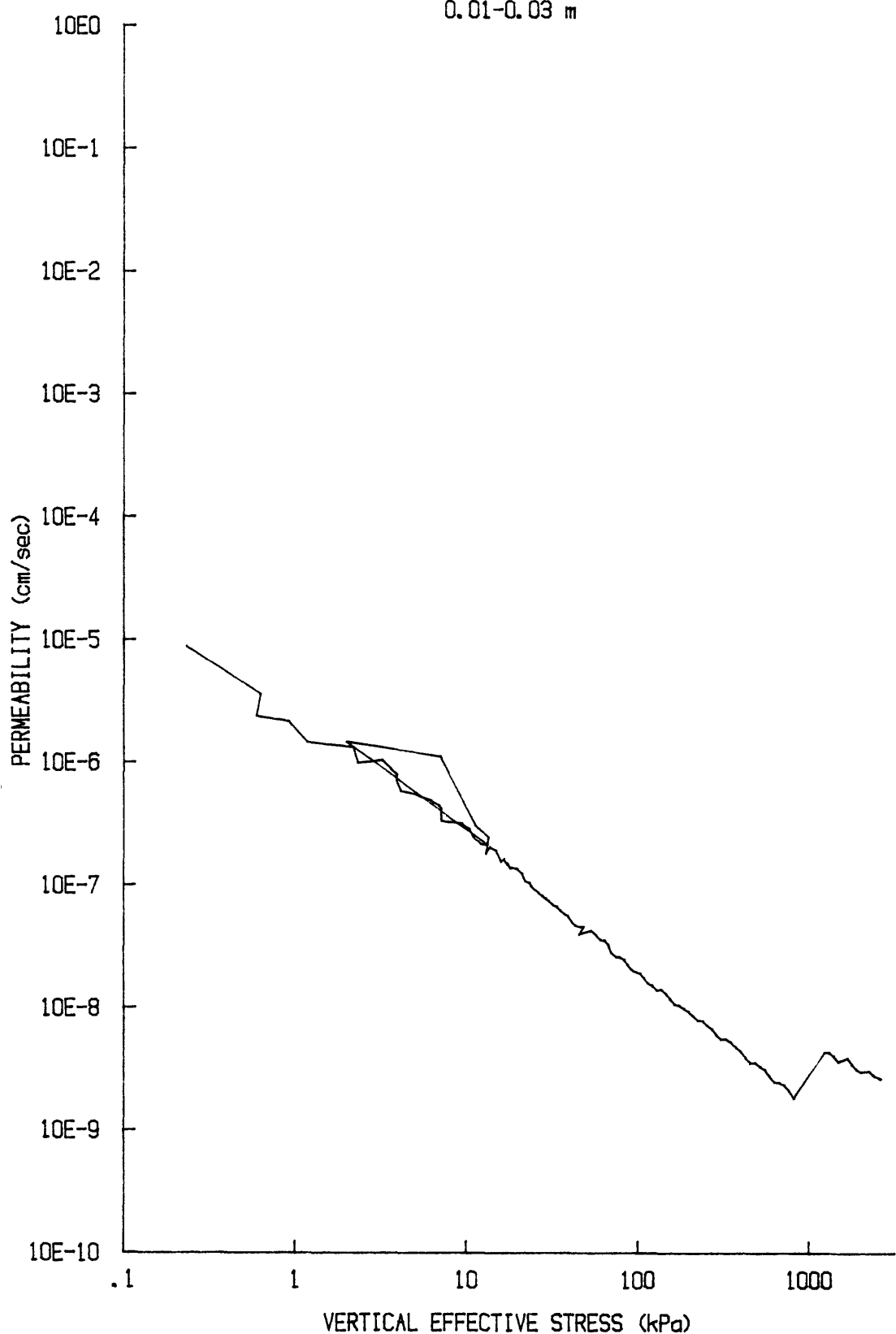
du/Sv for: CR035S8509
YS-85-08
CORE BC-9
0.01-0.03 m



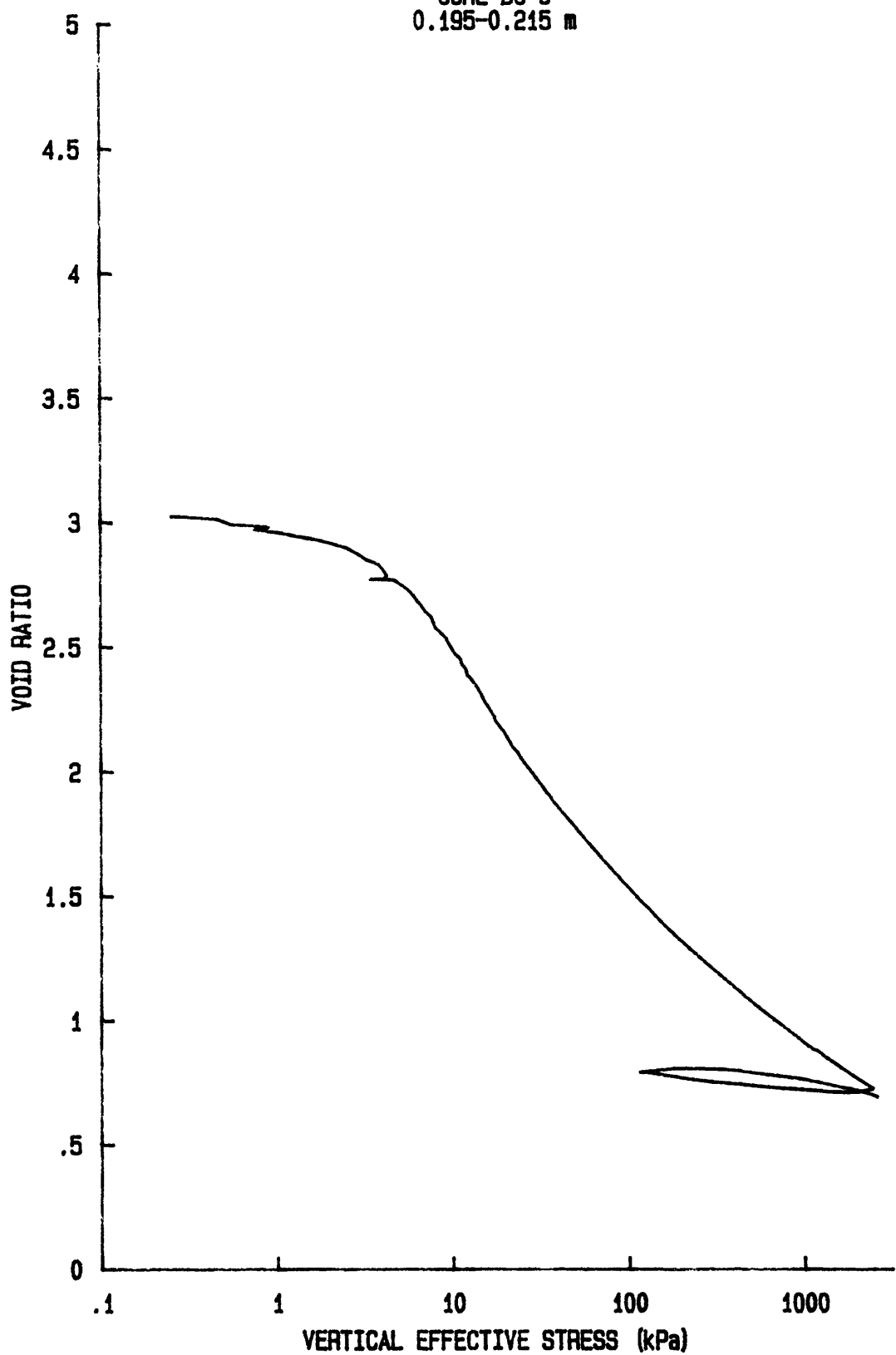
C_v vs $\log p'$ for: CR035S8509
YS-85-08
CORE BC-9
0.01-0.03 m



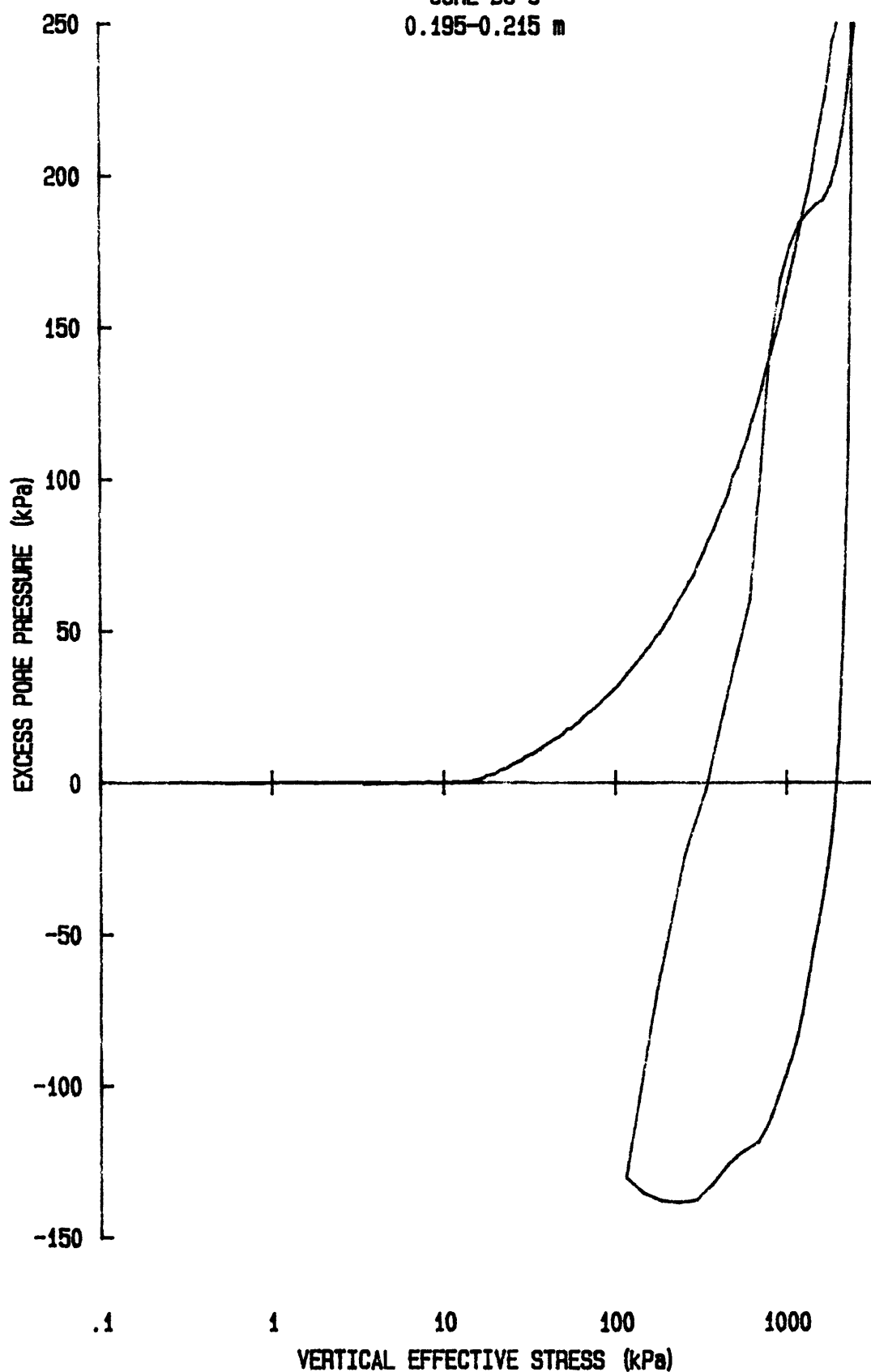
k vs $\log p'$ for CR035S8509
YS-85-08
CORE BC-9
0.01-0.03 m



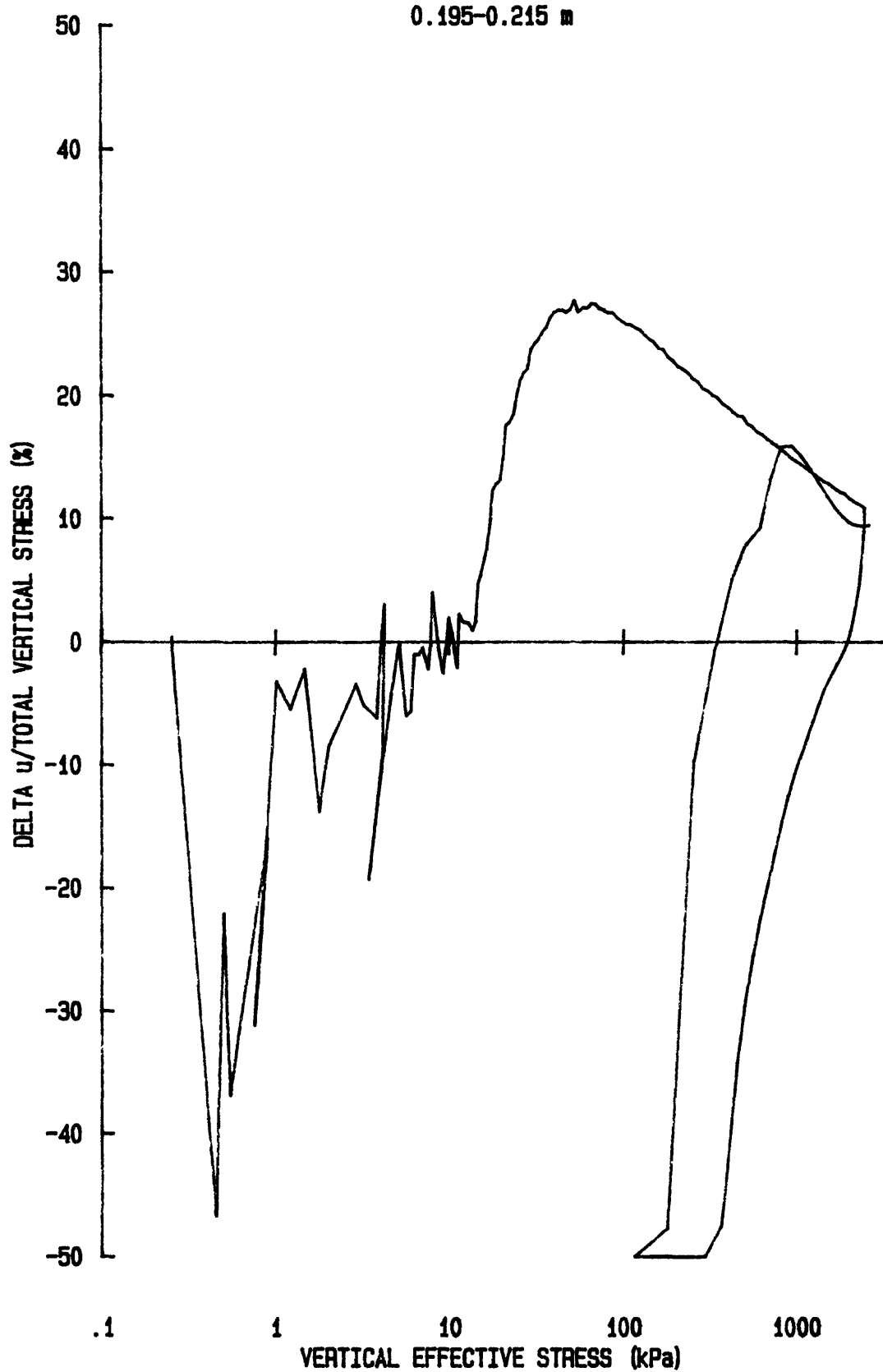
e vs log p' for: CR055S8509
YS-85-08
CORE BC-9
0.195-0.215 m



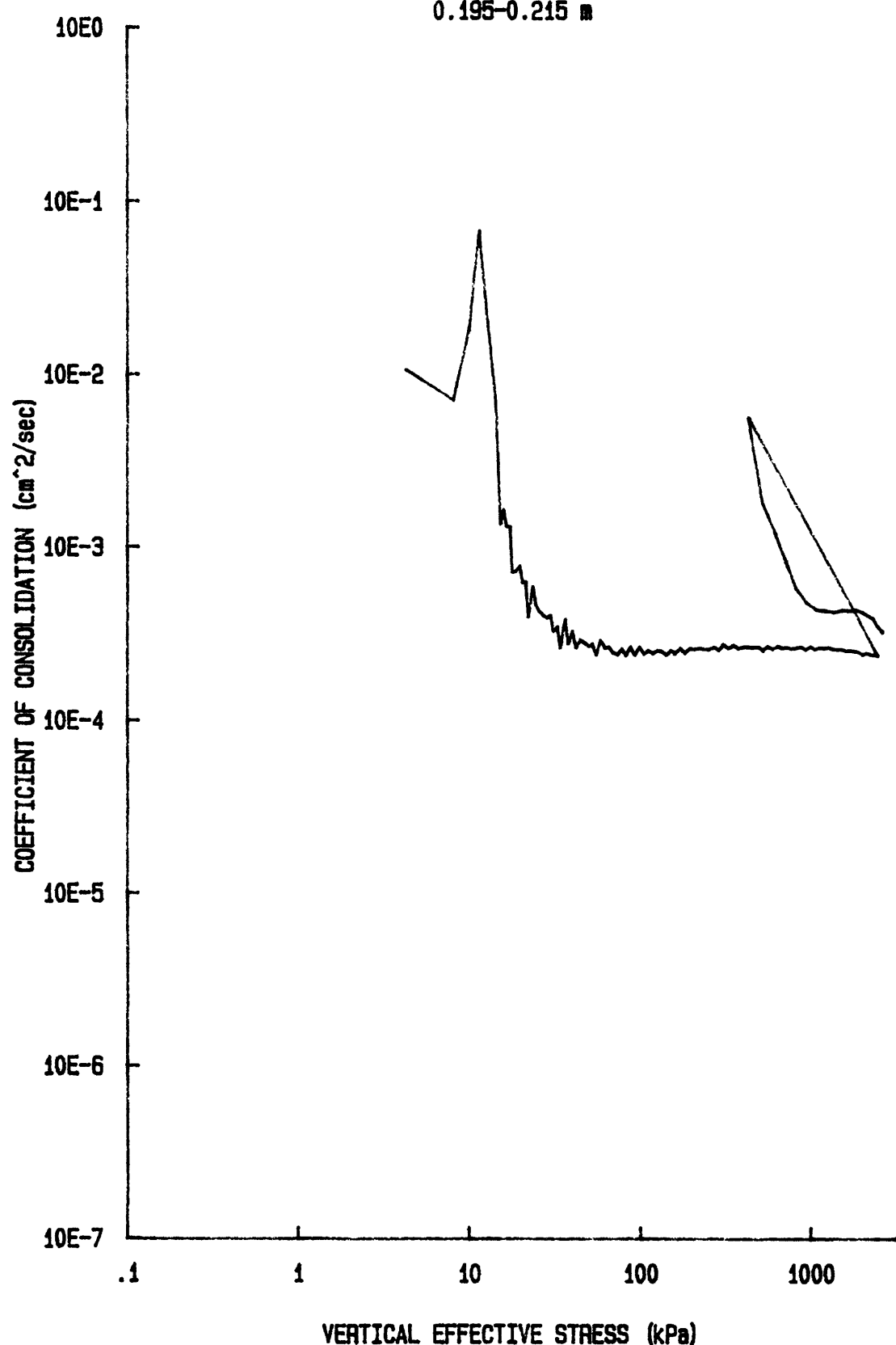
u vs log p' for: CR055S8509
YS-85-08
CORE BC-9
0.195-0.215 m



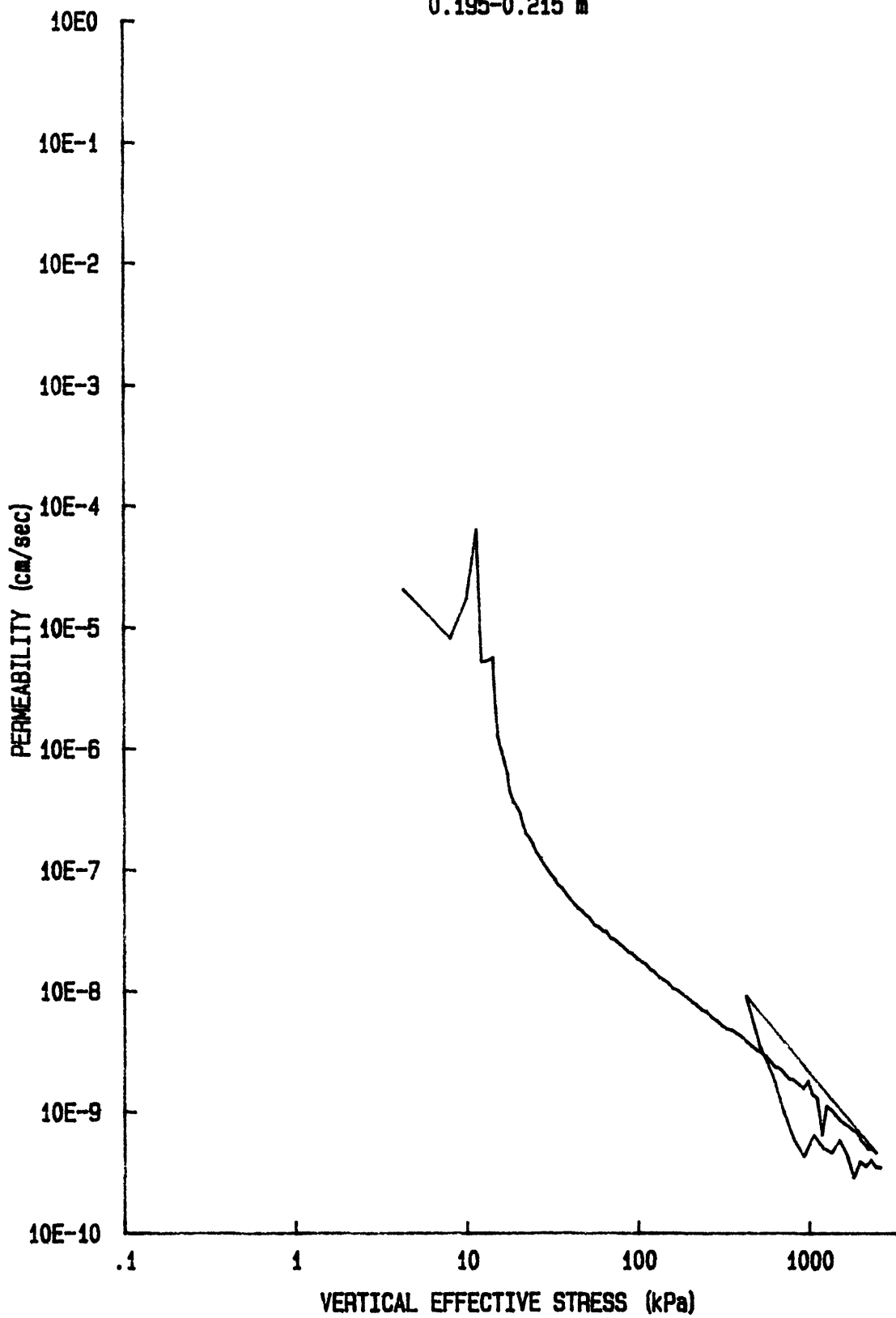
du/Sv for: CR055S8509
YS-85-08
CORE BC-9
0.195-0.215 m



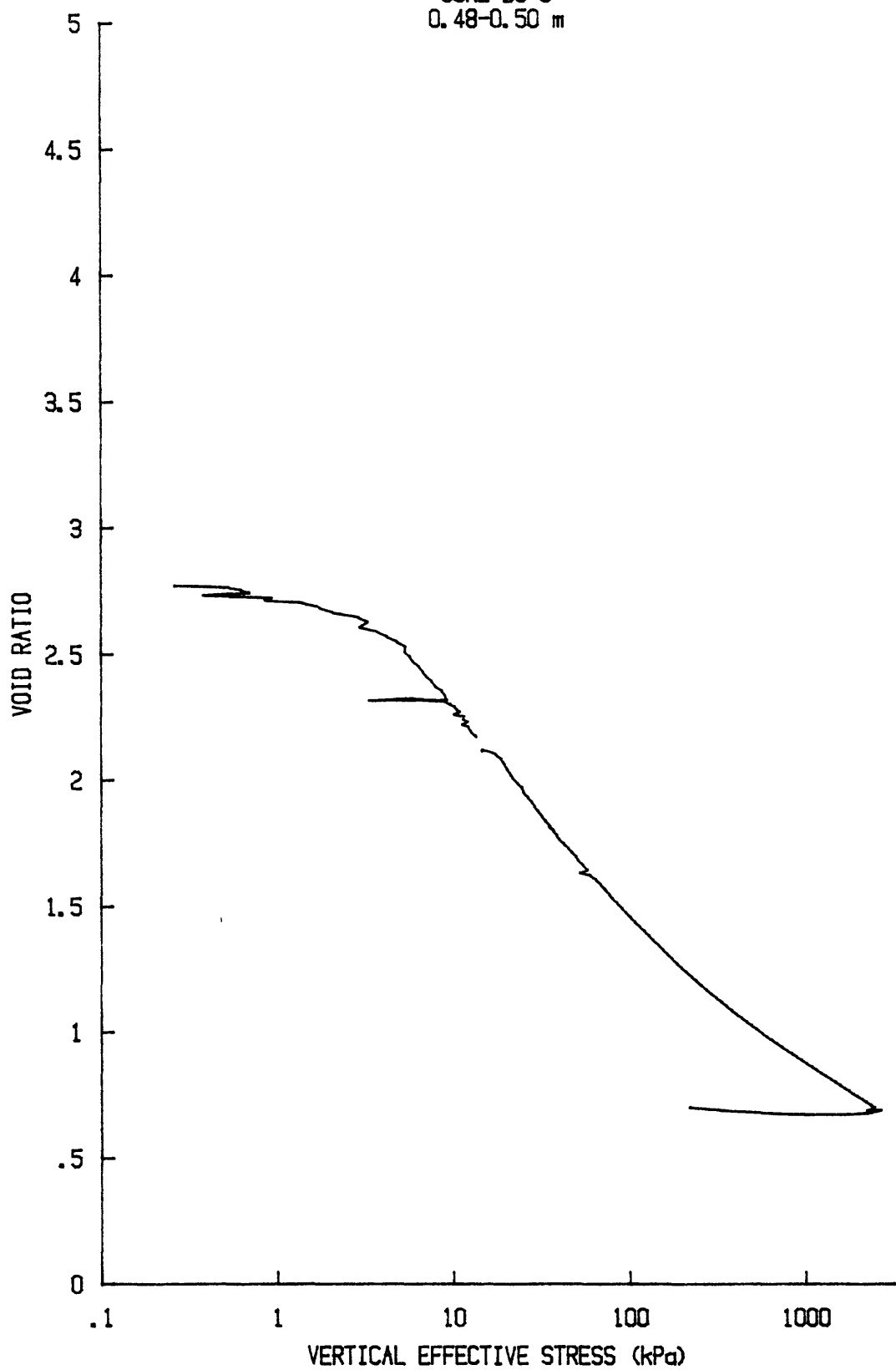
C_v vs $\log p'$ for: CR05598509
YS-85-08
CORE BC-9
0.195-0.215 m



k vs $\log p'$ for: CR055S8509
YS-85-08
CORE BC-9
0.195-0.215 m



e vs log p' for: CR031S8509
YS-85-08
CORE BC-9
0.48-0.50 m

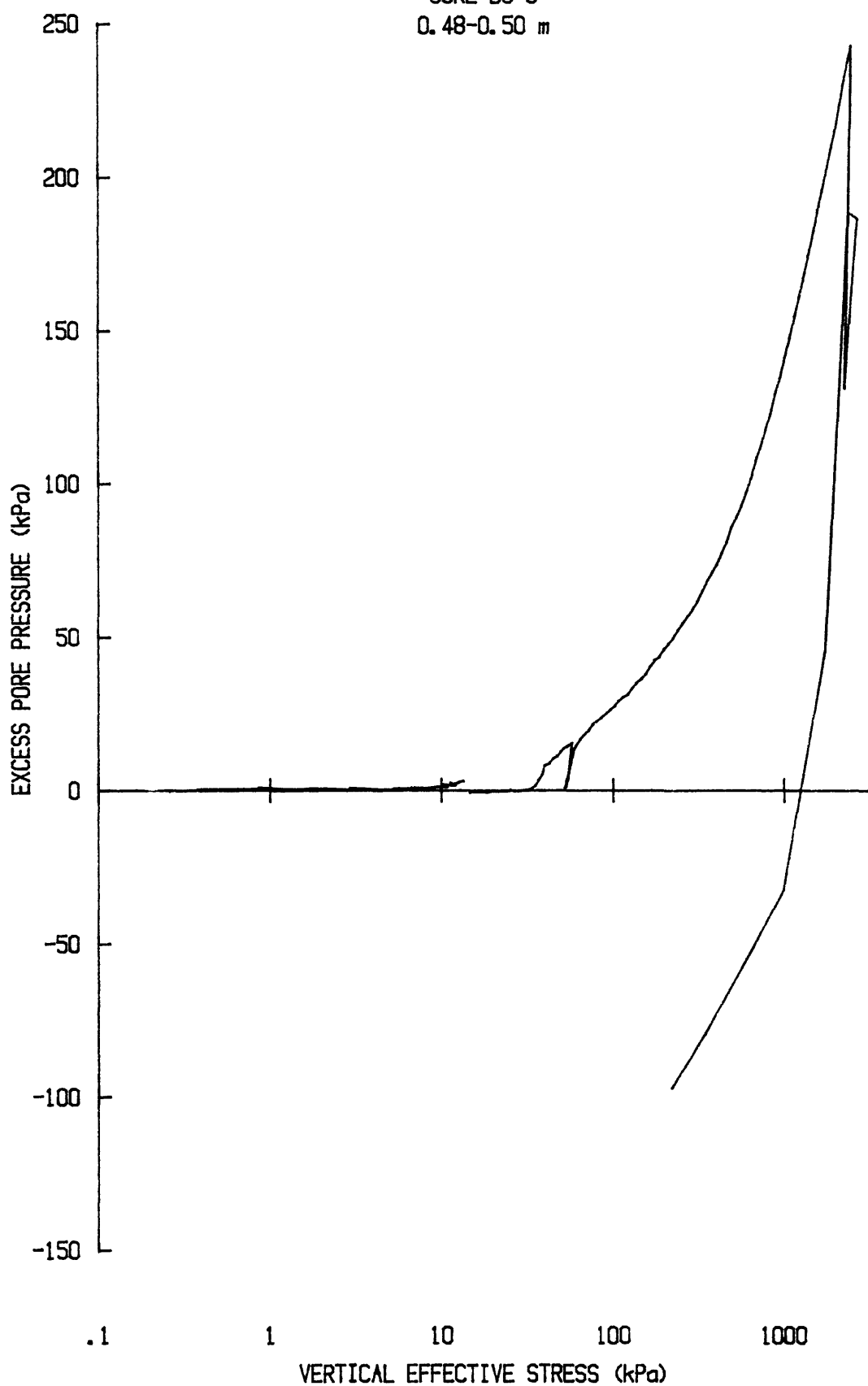


u vs $\log p'$ for: CR031S8509

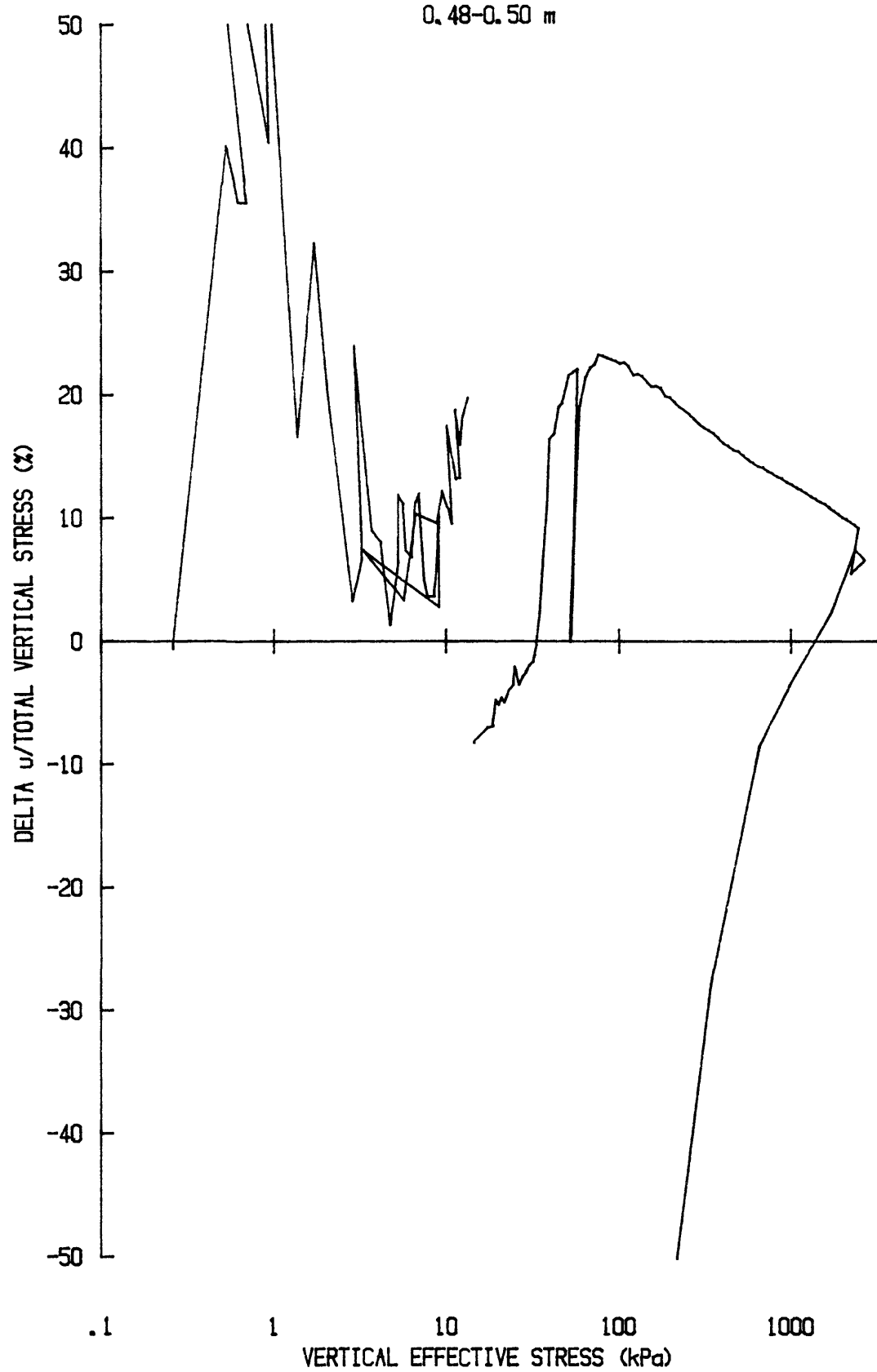
YS-85-08

CORE BC-9

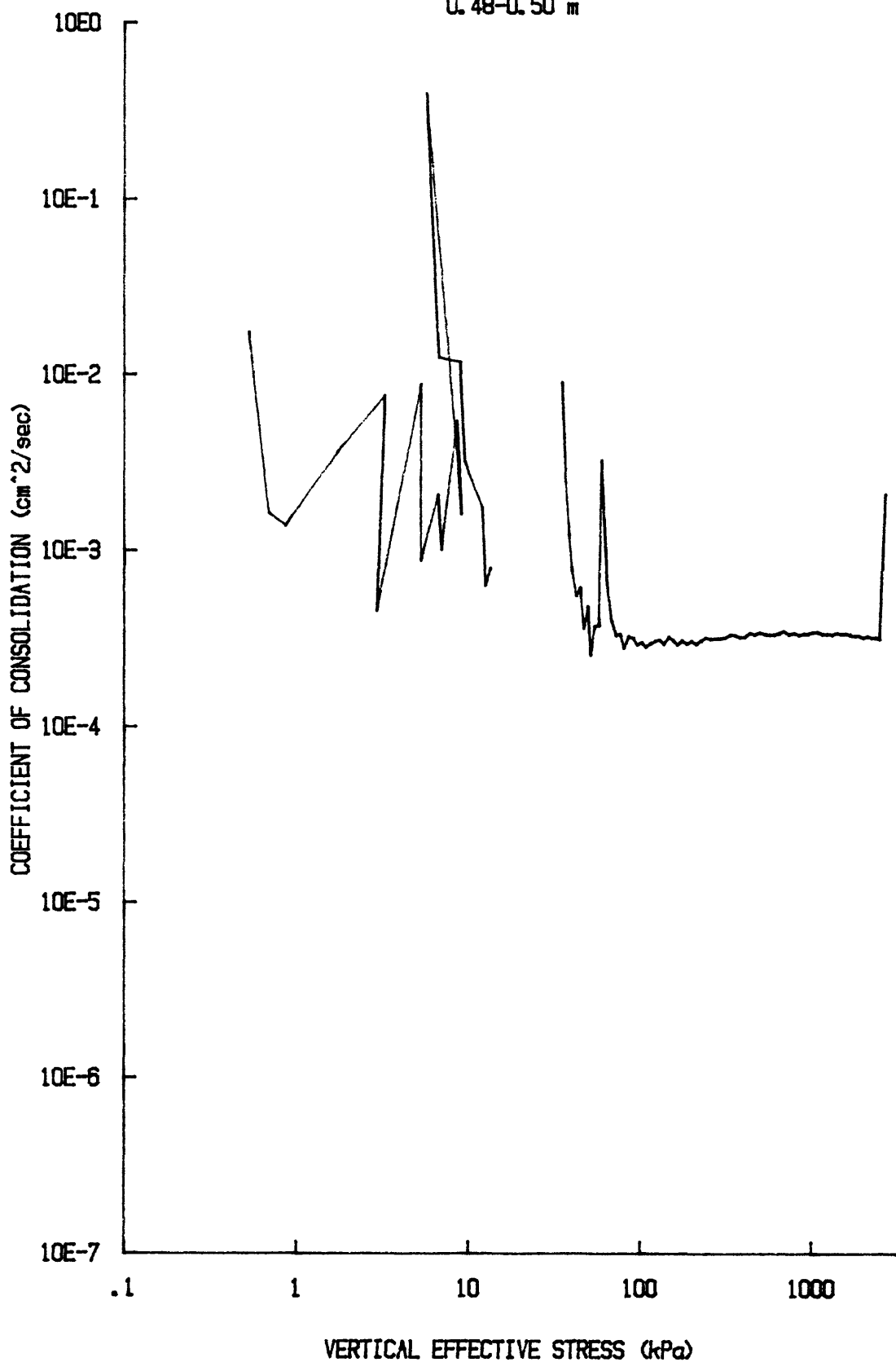
0.48-0.50 m



du/Sv for: CR031S8509
YS-85-08
CORE BC-9
0.48-0.50 m



C_v vs $\log p'$ for: CR031S8509
YS-85-08
CORE BC-9
0.48-0.50 m

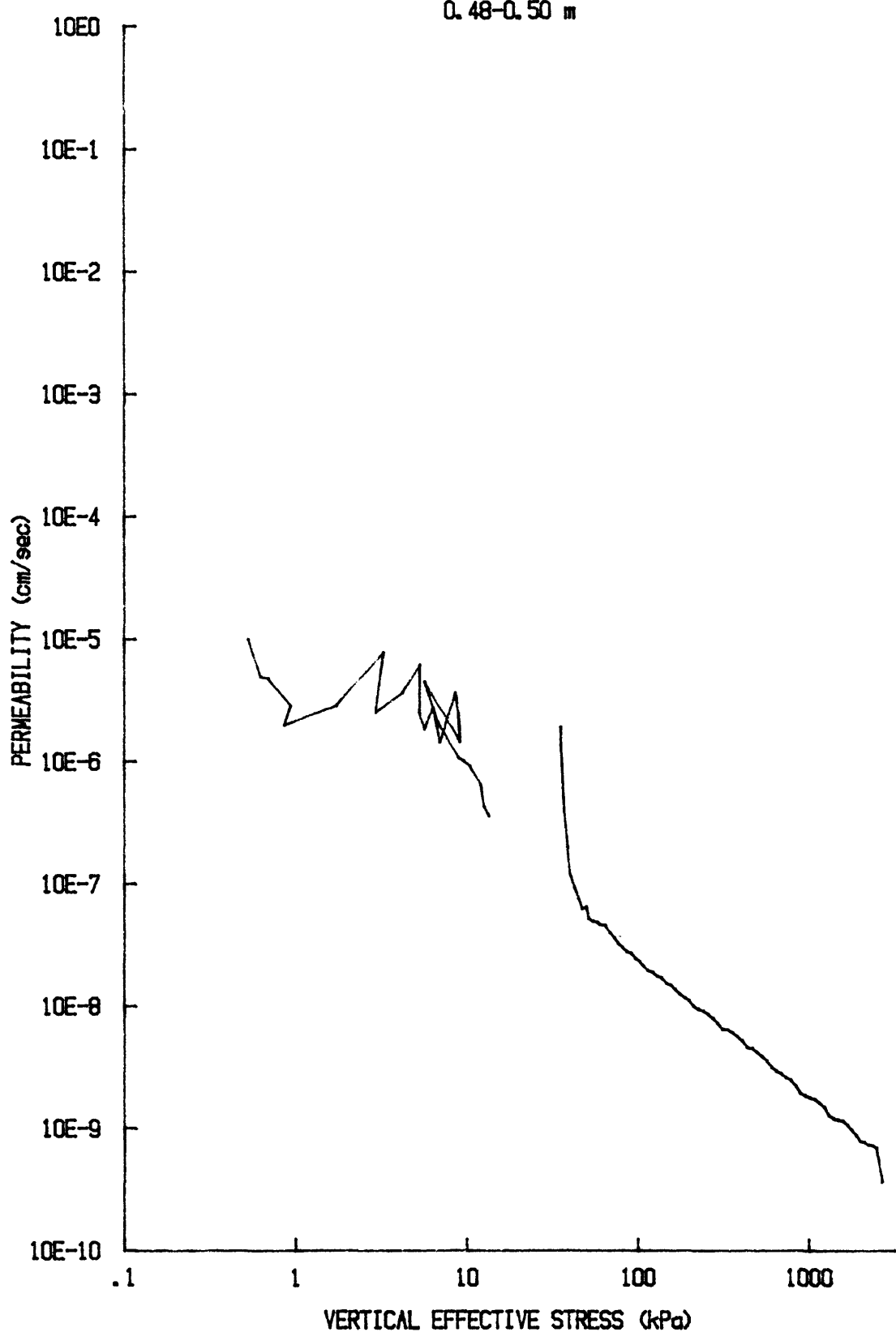


k vs $\log p'$ for CR031S8509

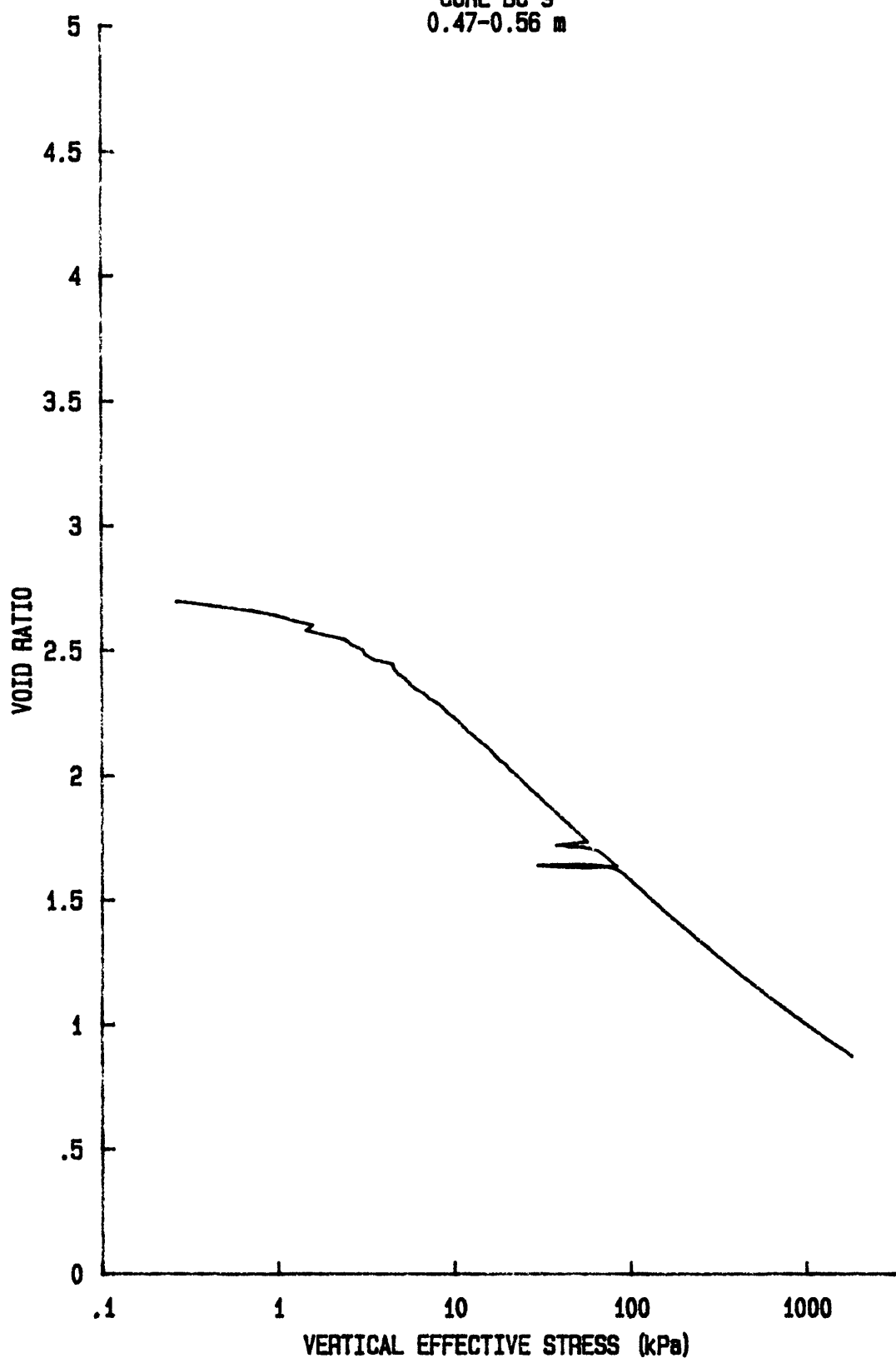
YS-85-08

CORE BC-9

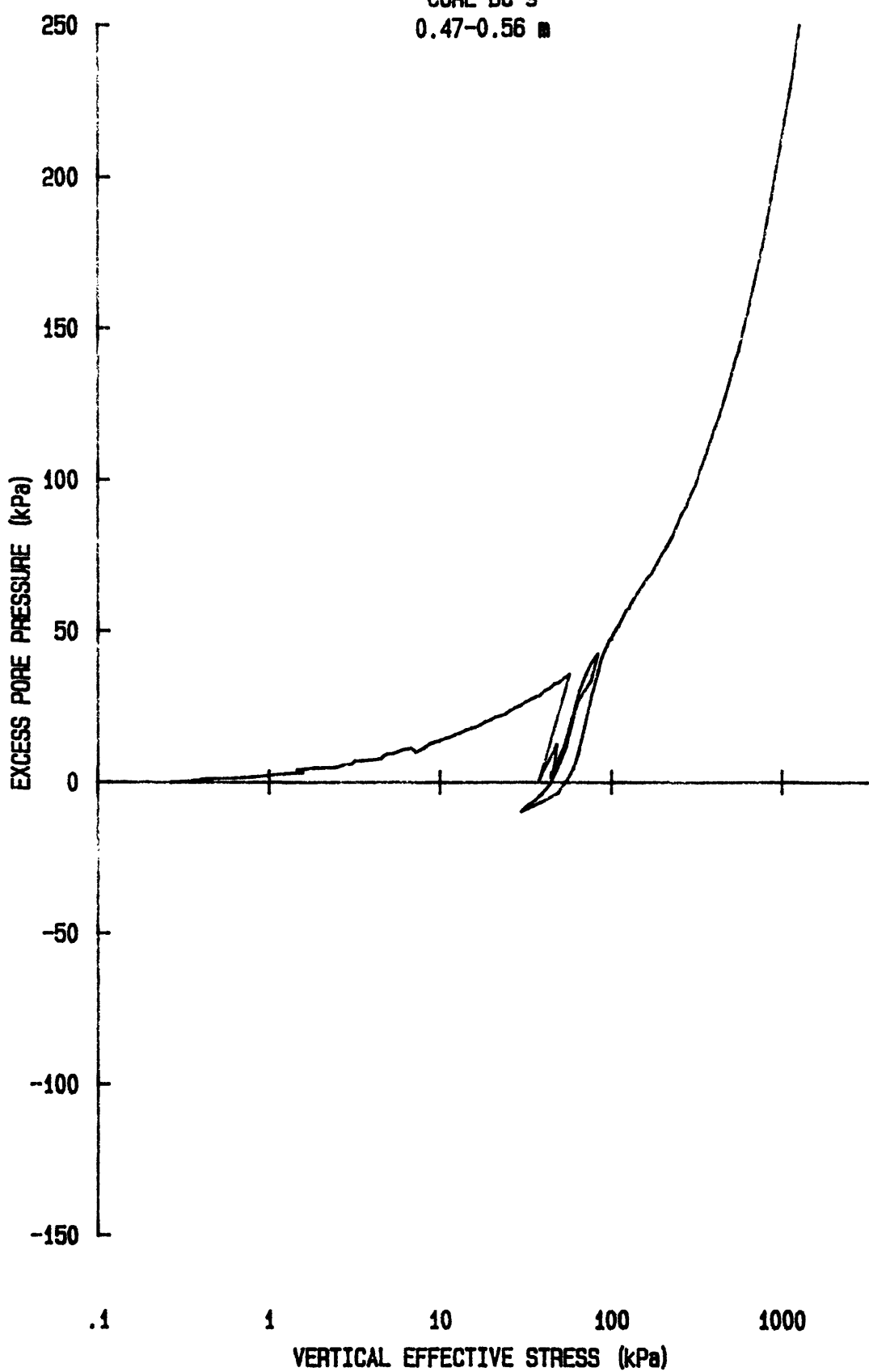
0.48-0.50 m



e vs log p' for: CR058S8509
YS-85-08
CORE BC-9
0.47-0.56 m



u vs $\log p'$ for: CR058S8509
YS-85-08
CORE BC-9
0.47-0.56 in

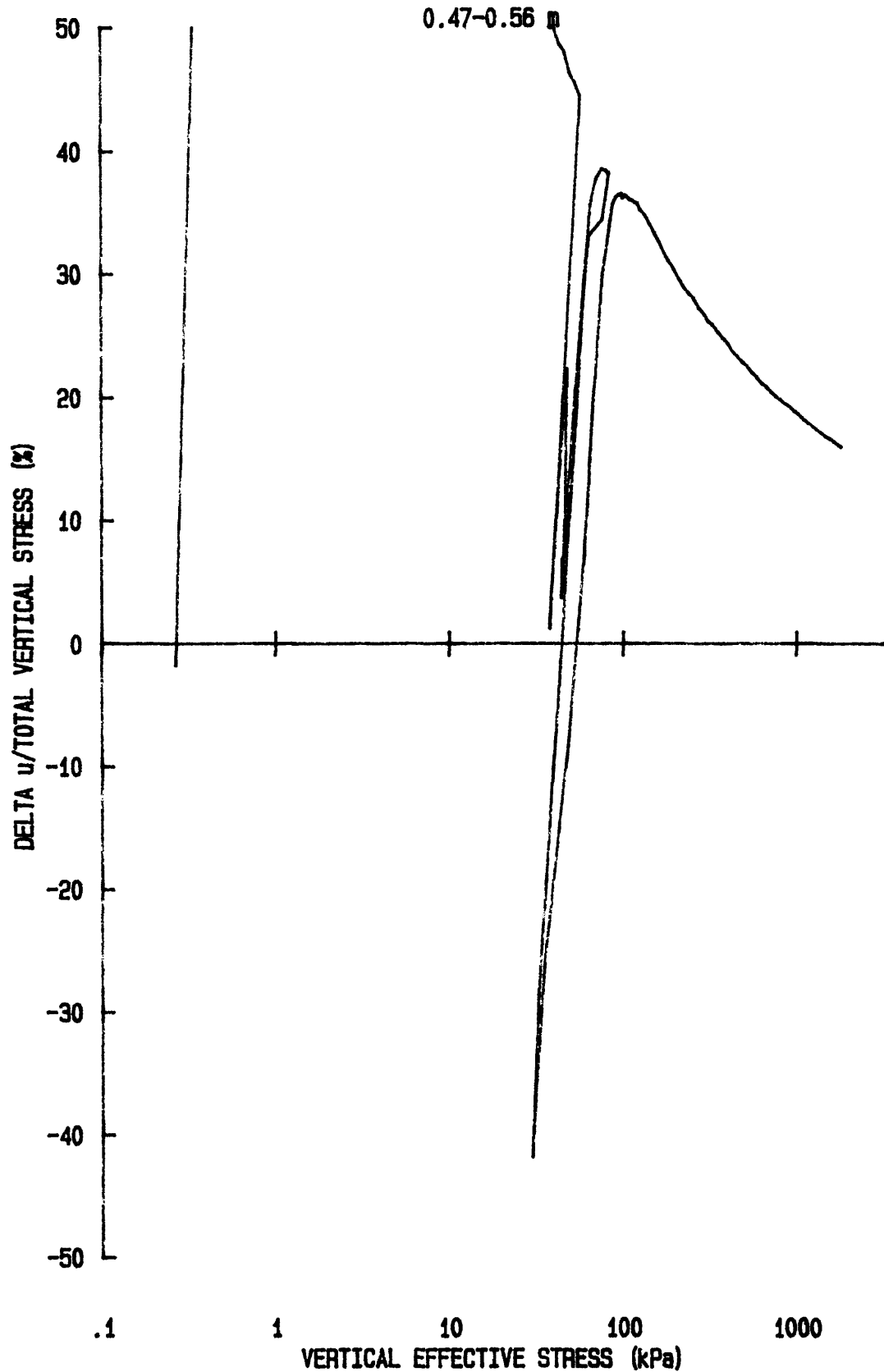


du/Sv for: CR058S8509

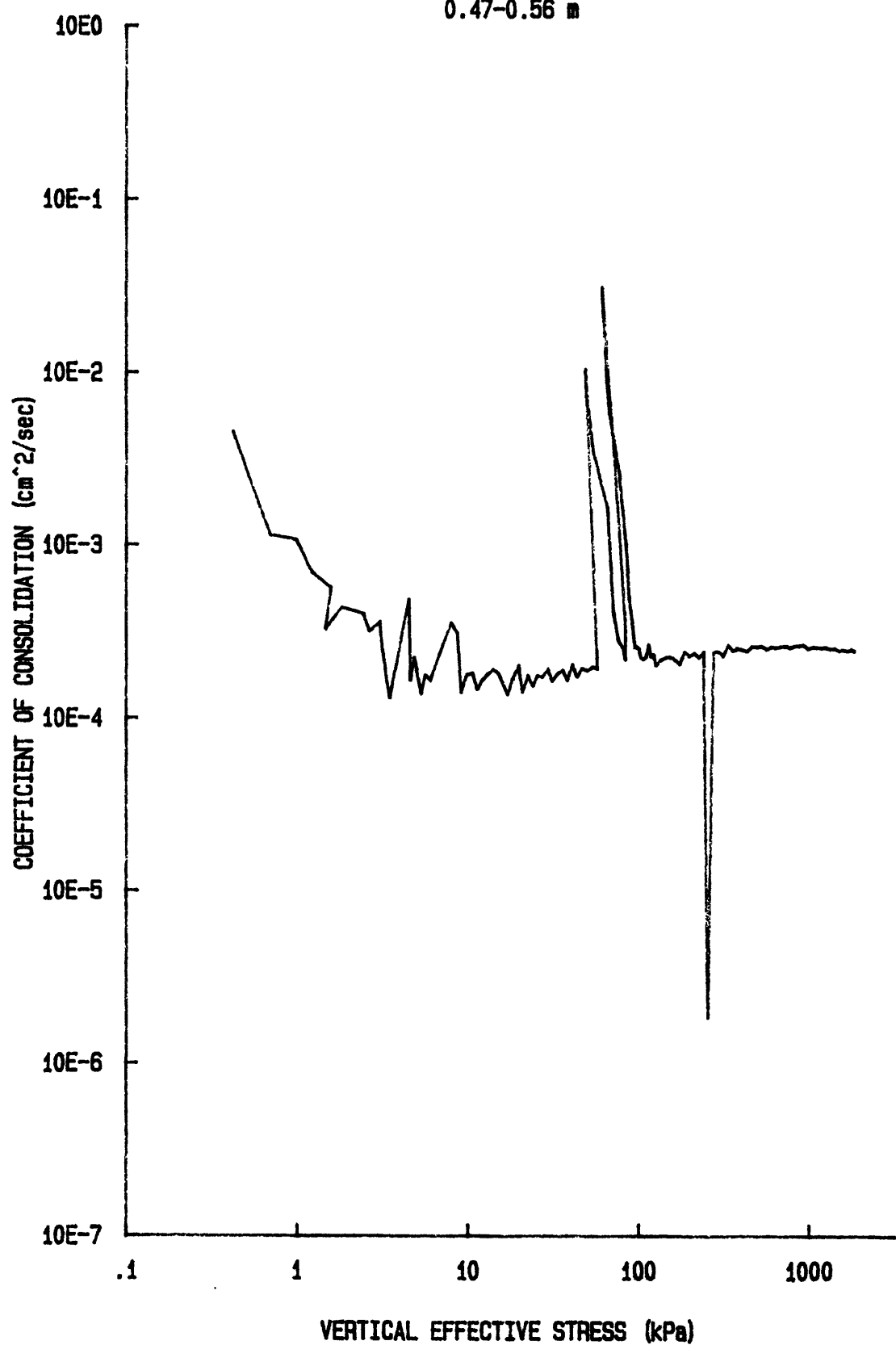
YS-85-08

CORE BC-9

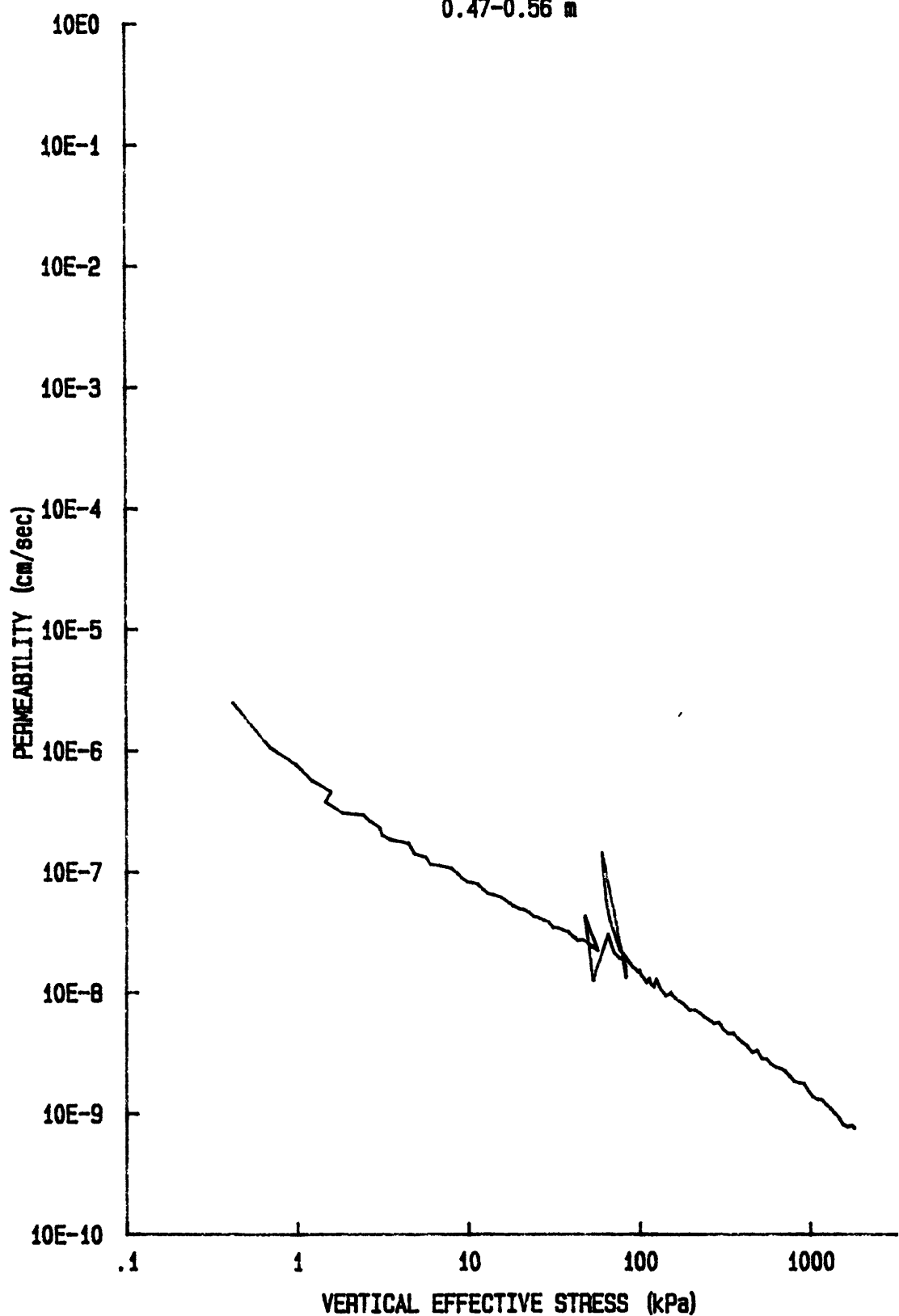
0.47-0.56 m



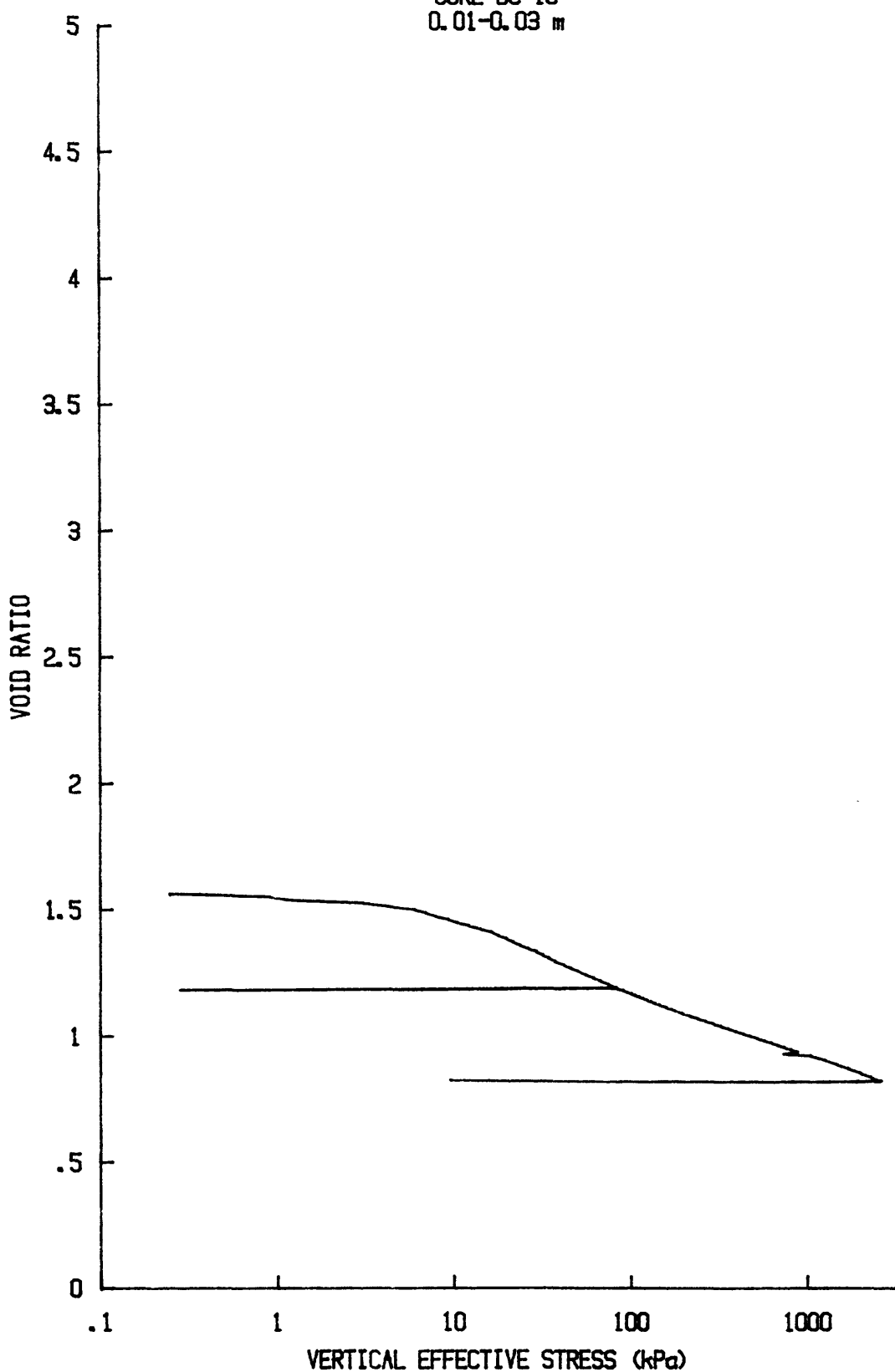
Cv vs log p' for: CR058S8509
YS-85-08
CORE BC-9
0.47-0.56 m



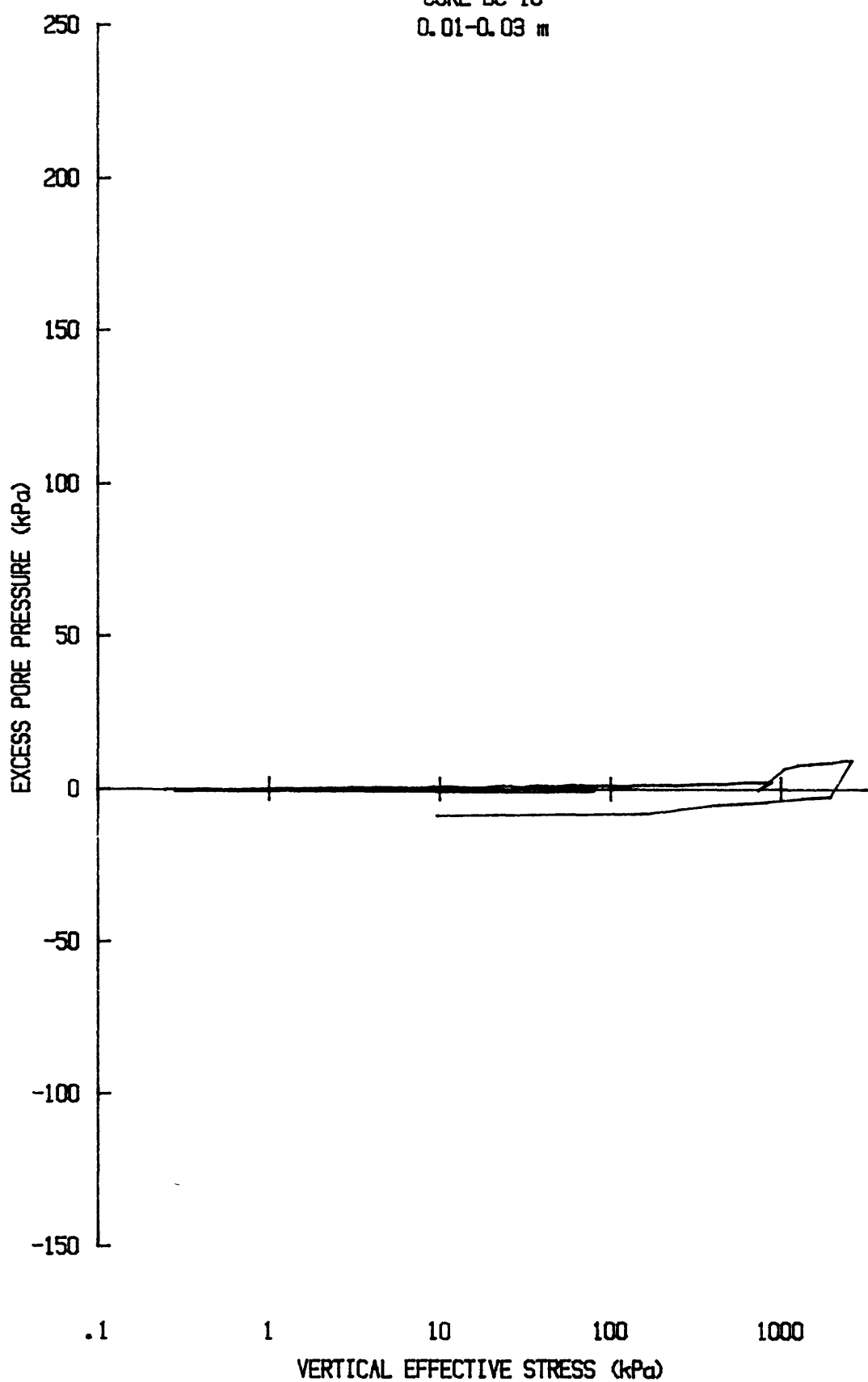
k vs $\log p'$ for: CR058S8509
YS-85-08
CORE BC-9
0.47-0.56 m



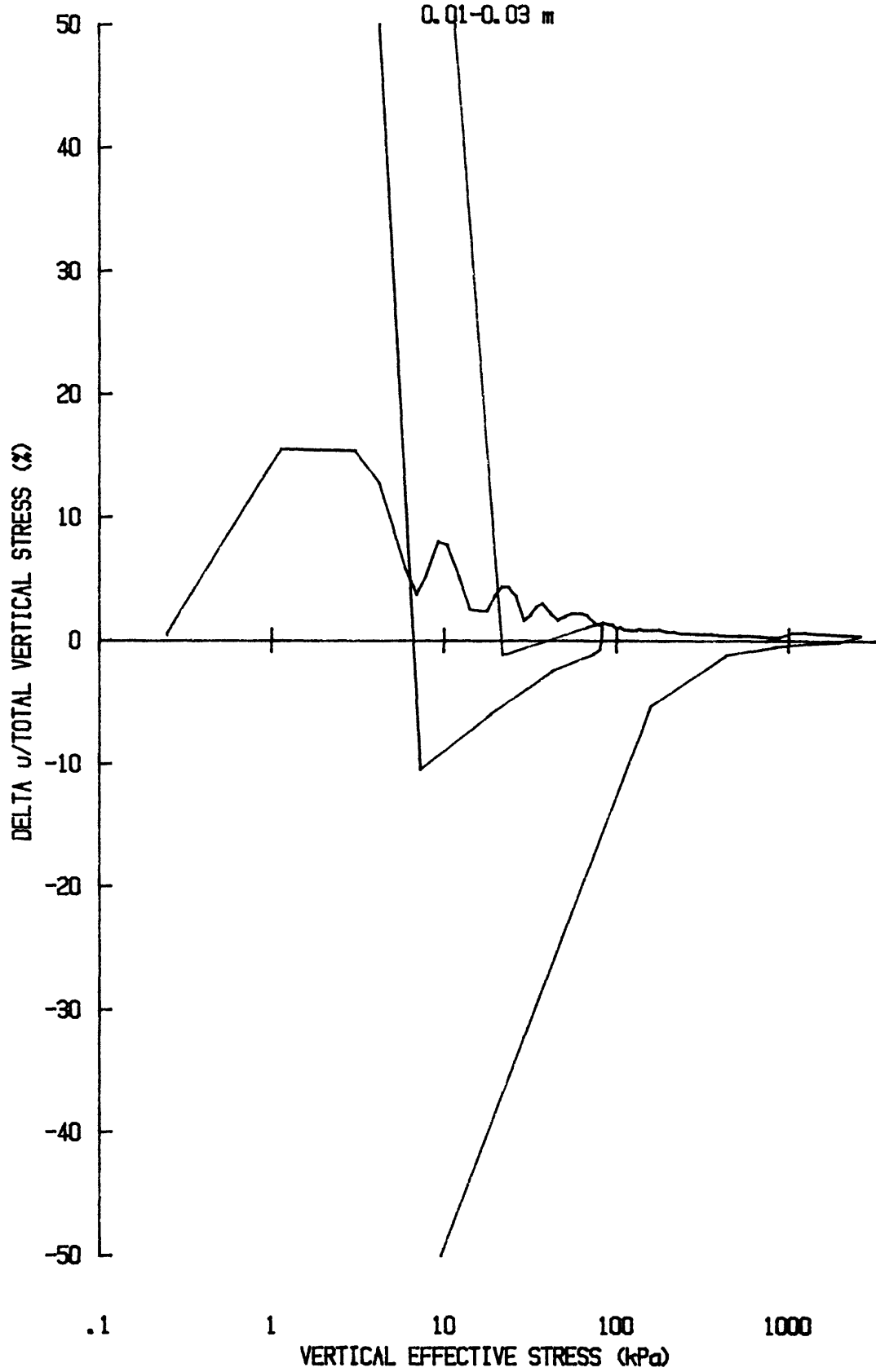
e vs $\log p'$ for CR036S8510
YS-85-08
CORE BC-10
0.01-0.03 m



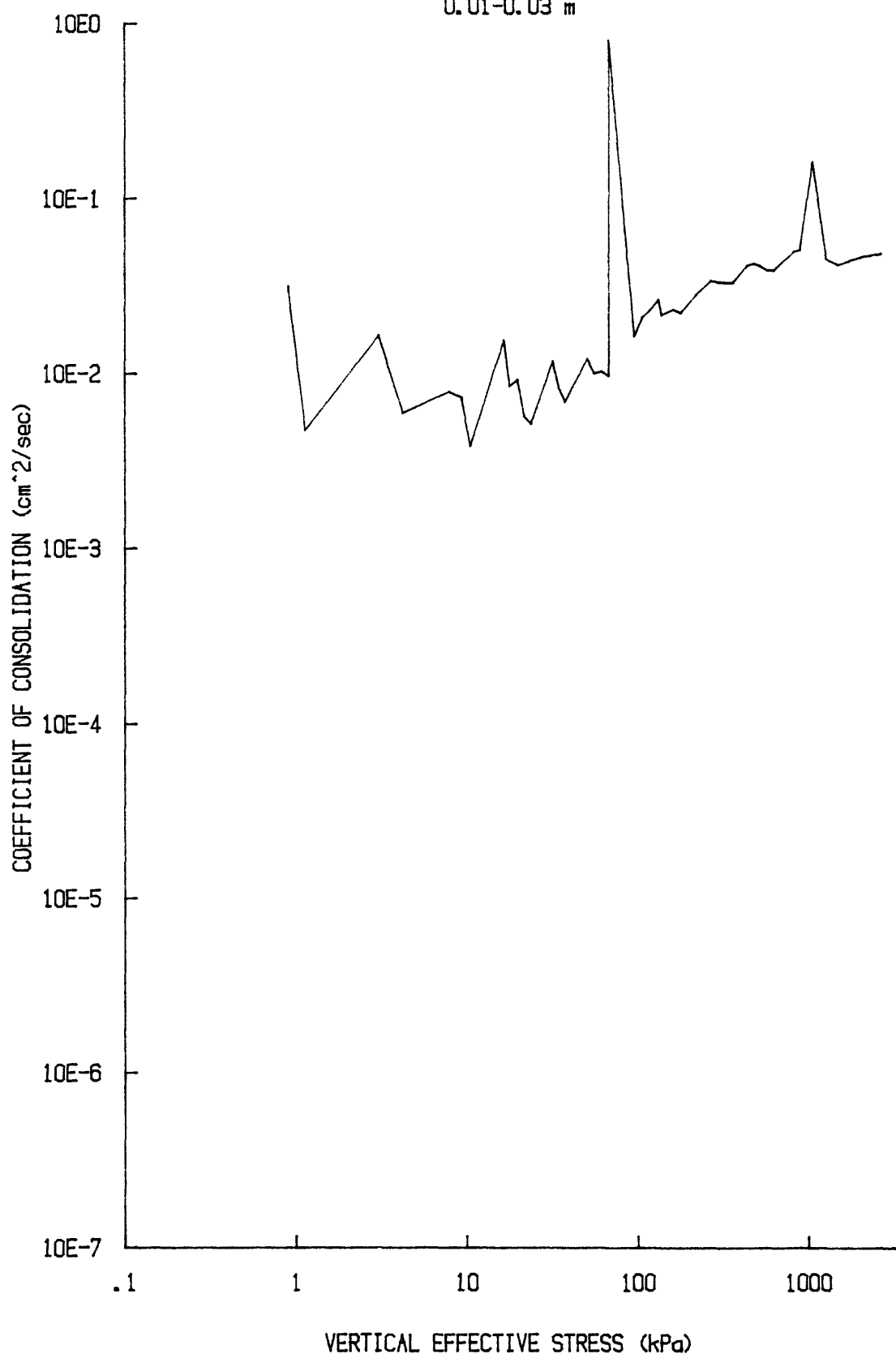
u vs $\log p'$ for: CR036S8510
YS-85-08
CORE BC-10
0.01-0.03 m



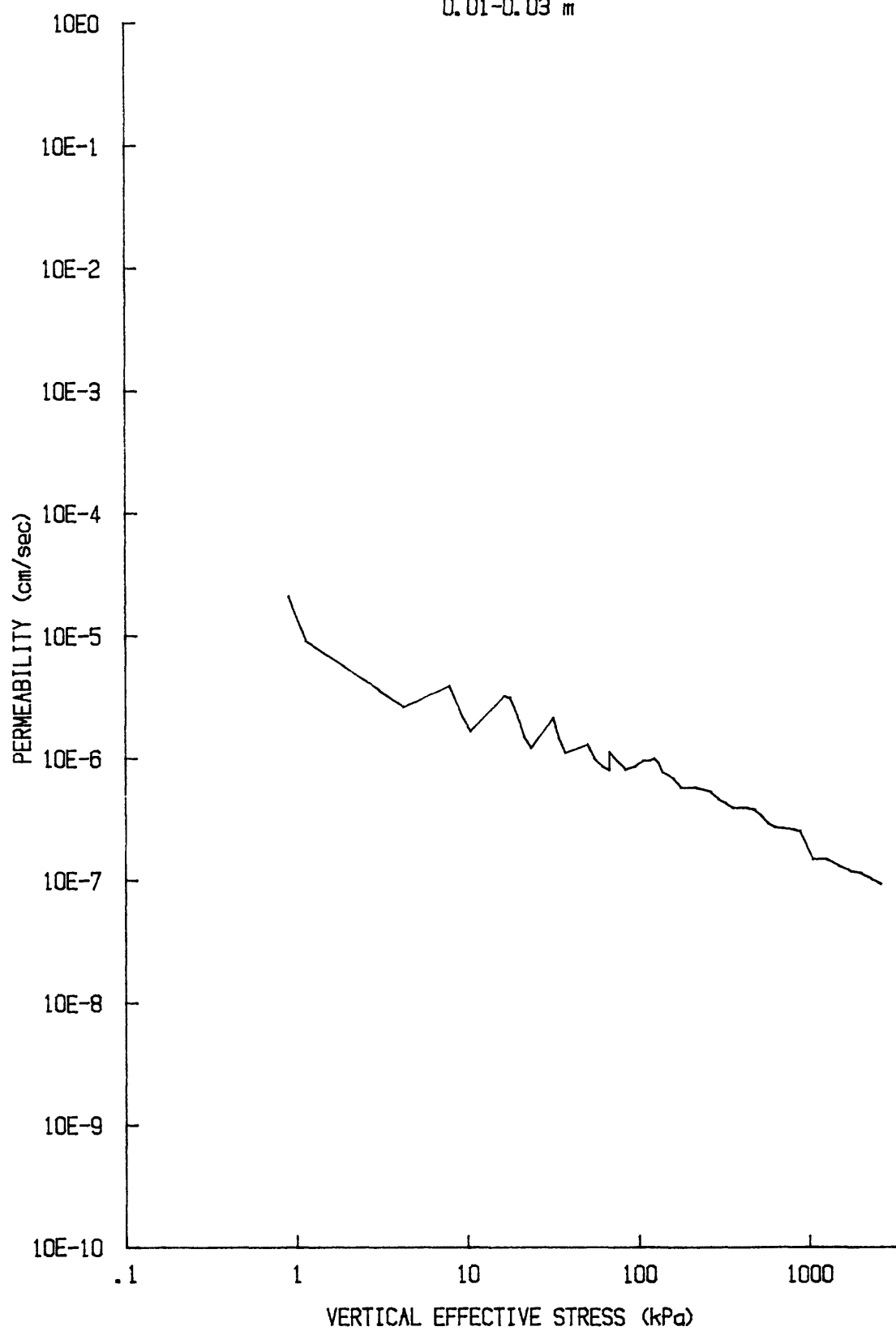
du/Sv for: CR036S8510
YS-85-08
CORE BC-10
0.01-0.03 m



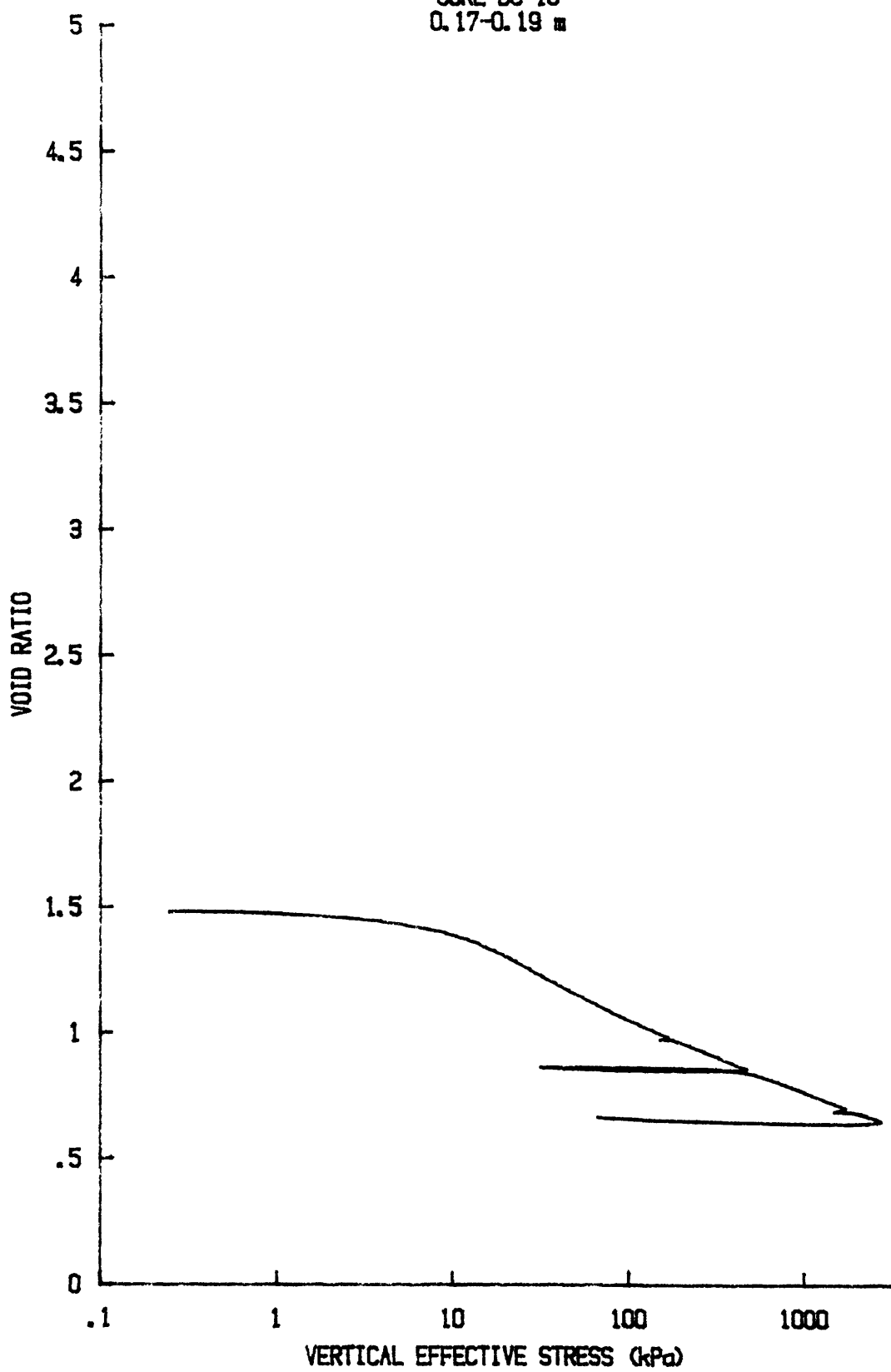
C_v vs $\log p'$ for: CR036S8510
YS-85-08
CORE BC-10
0.01-0.03 m



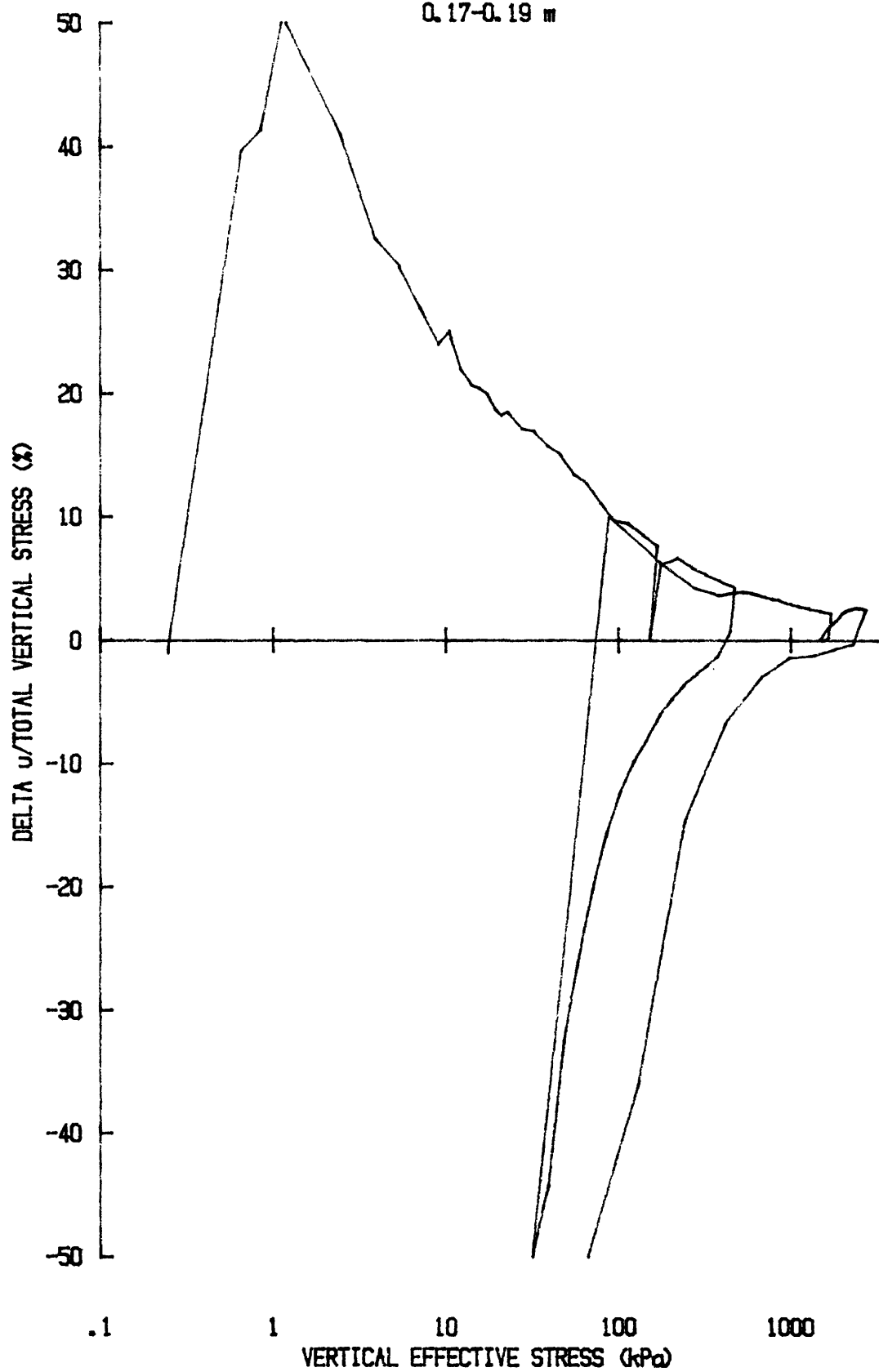
k vs $\log p'$ for: CR036S8510
YS-85-08
CORE BC-10
0.01-0.03 m



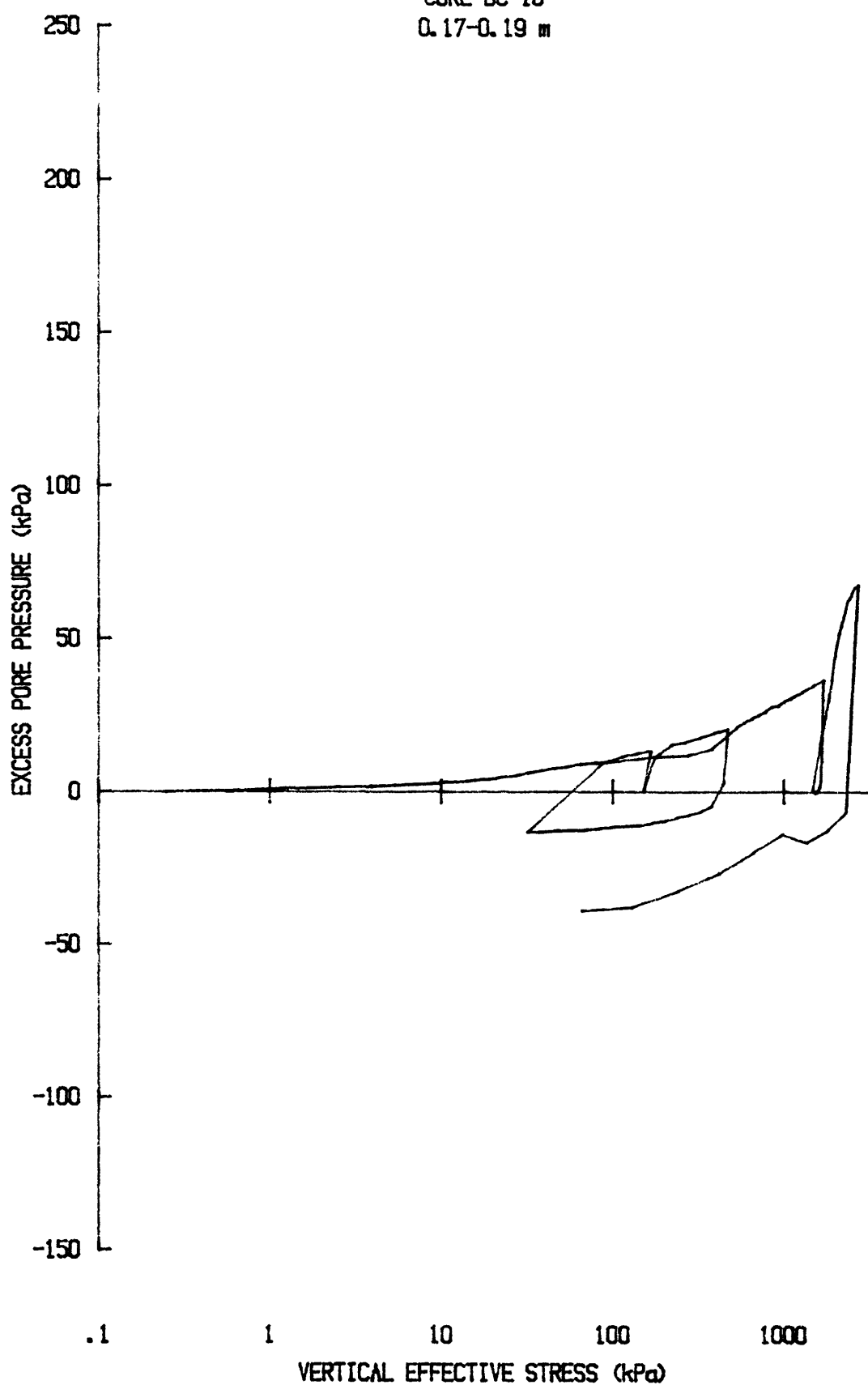
e vs $\log p'$ for CR051S8510
YS-85-08
CORE BC-10
0.17-0.19 m



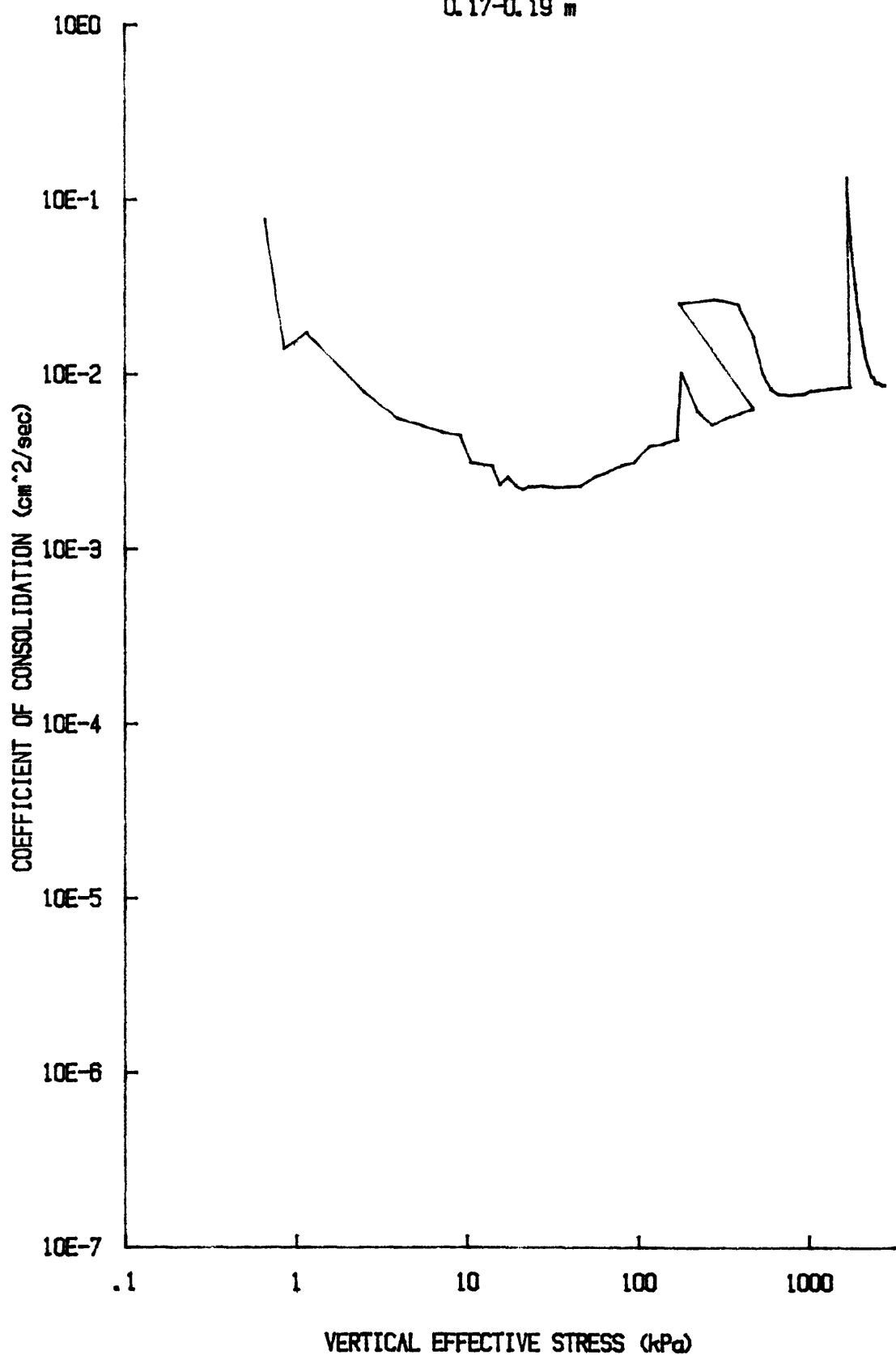
du/Sv for: CR051S8510
YS-85-08
CORE BC-10
0.17-0.19 m



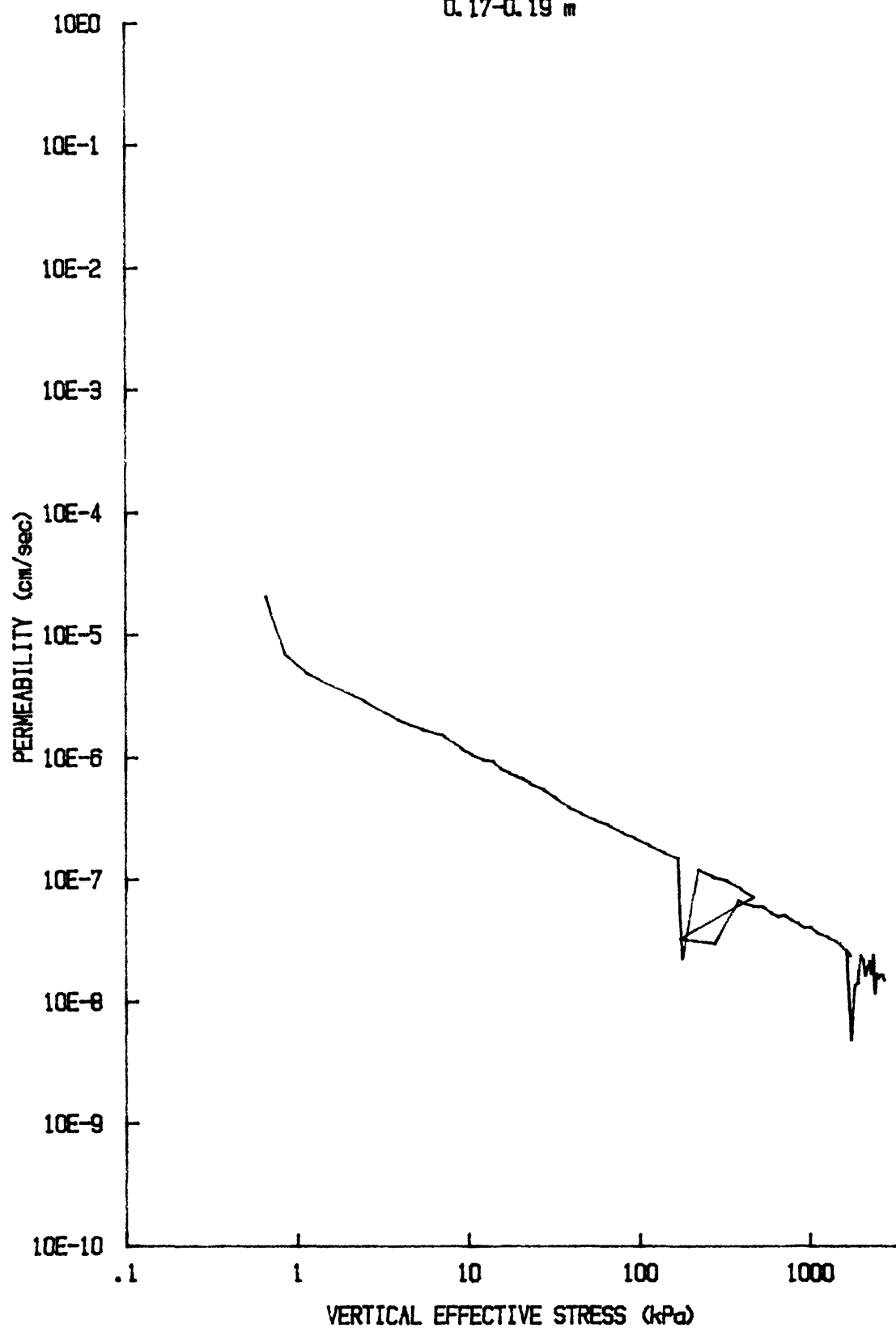
u vs $\log p'$ for CR051S8510
YS-85-08
CORE BC-10
0.17-0.19 m



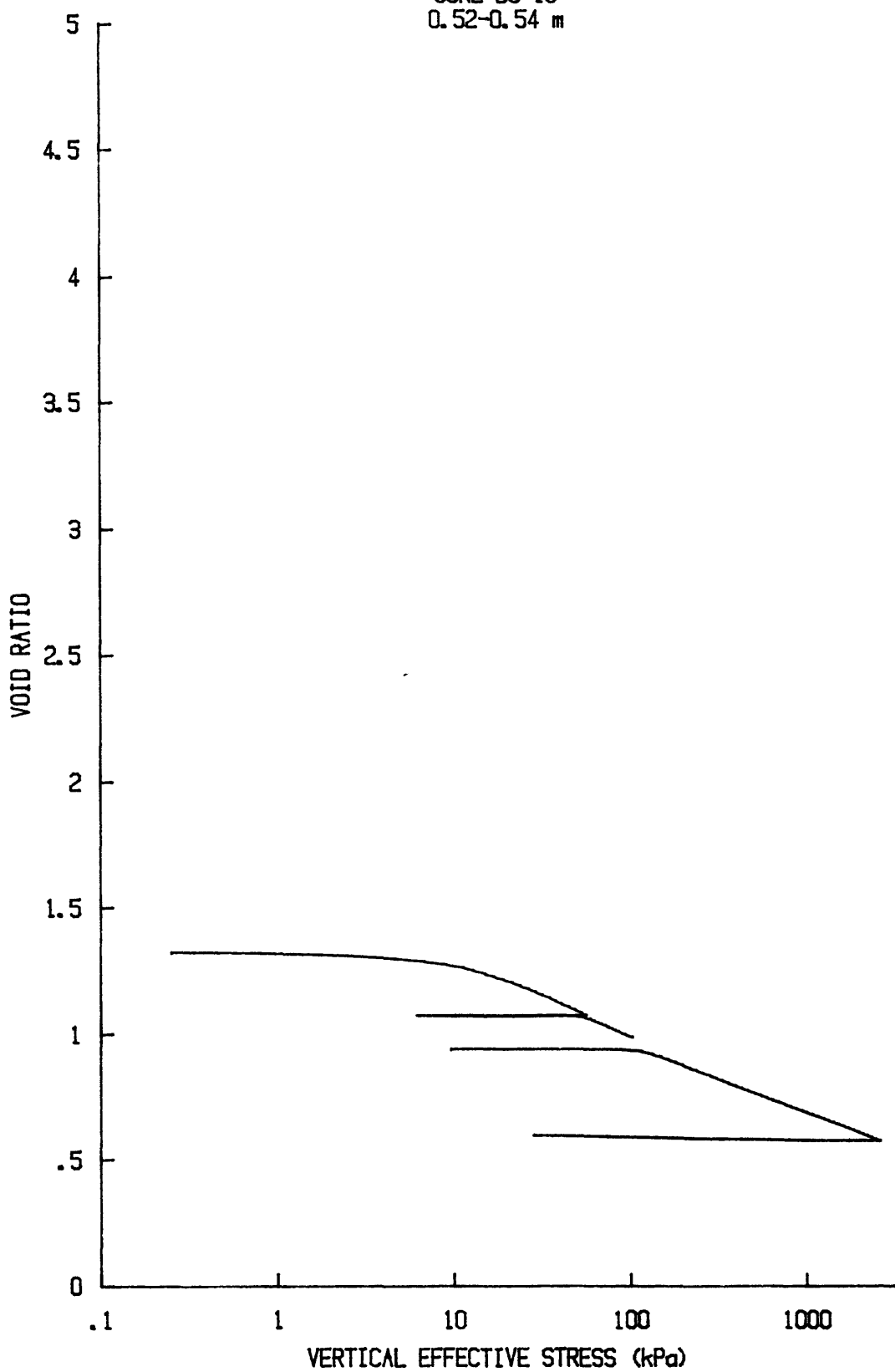
C_v vs $\log p'$ for CR051S8510
YS-85-08
CORE BC-10
0.17-0.19 m



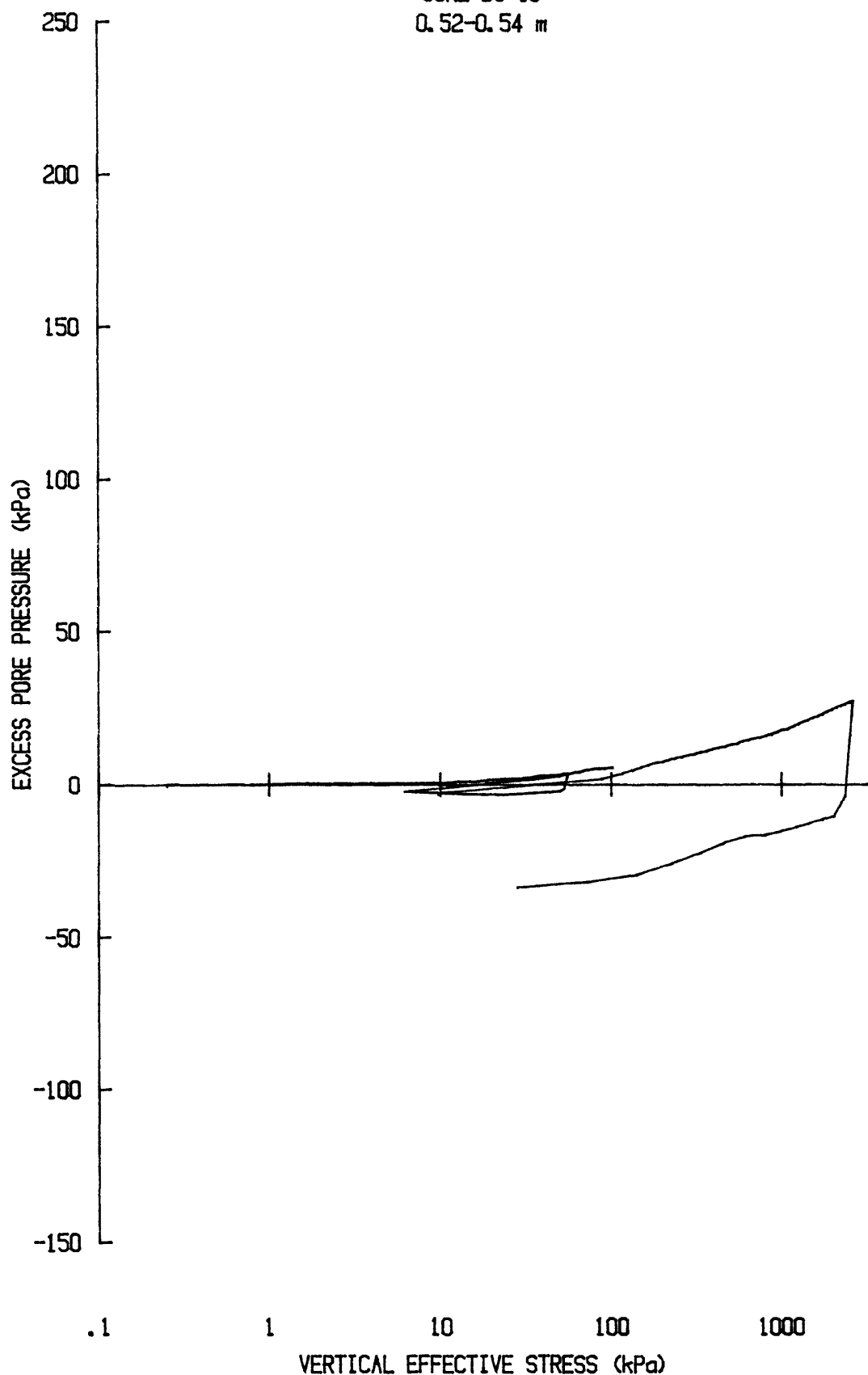
k vs $\log p'$ for CR051S8510
YS-85-08
CORE BC-10
0.17-0.19 m



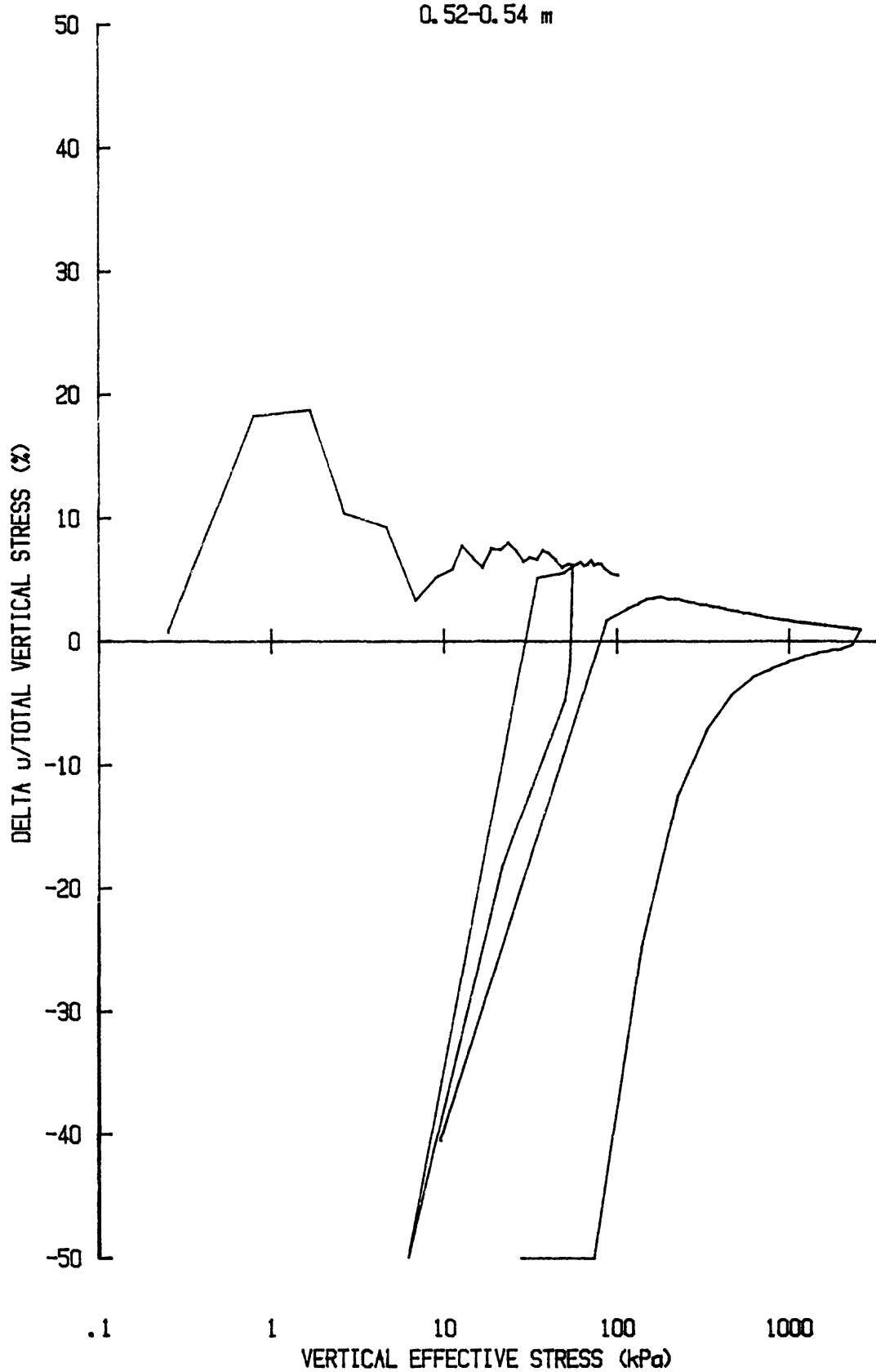
e vs $\log p'$ for: CR032S8510
YS-85-08
CORE BC-10
0.52-0.54 m



u vs $\log p'$ for CR032S8510
YS-85-08
CORE BC-10
0.52-0.54 m



du/Sv for: CR032S8510
YS-85-08
CORE BC-10
0.52-0.54 m

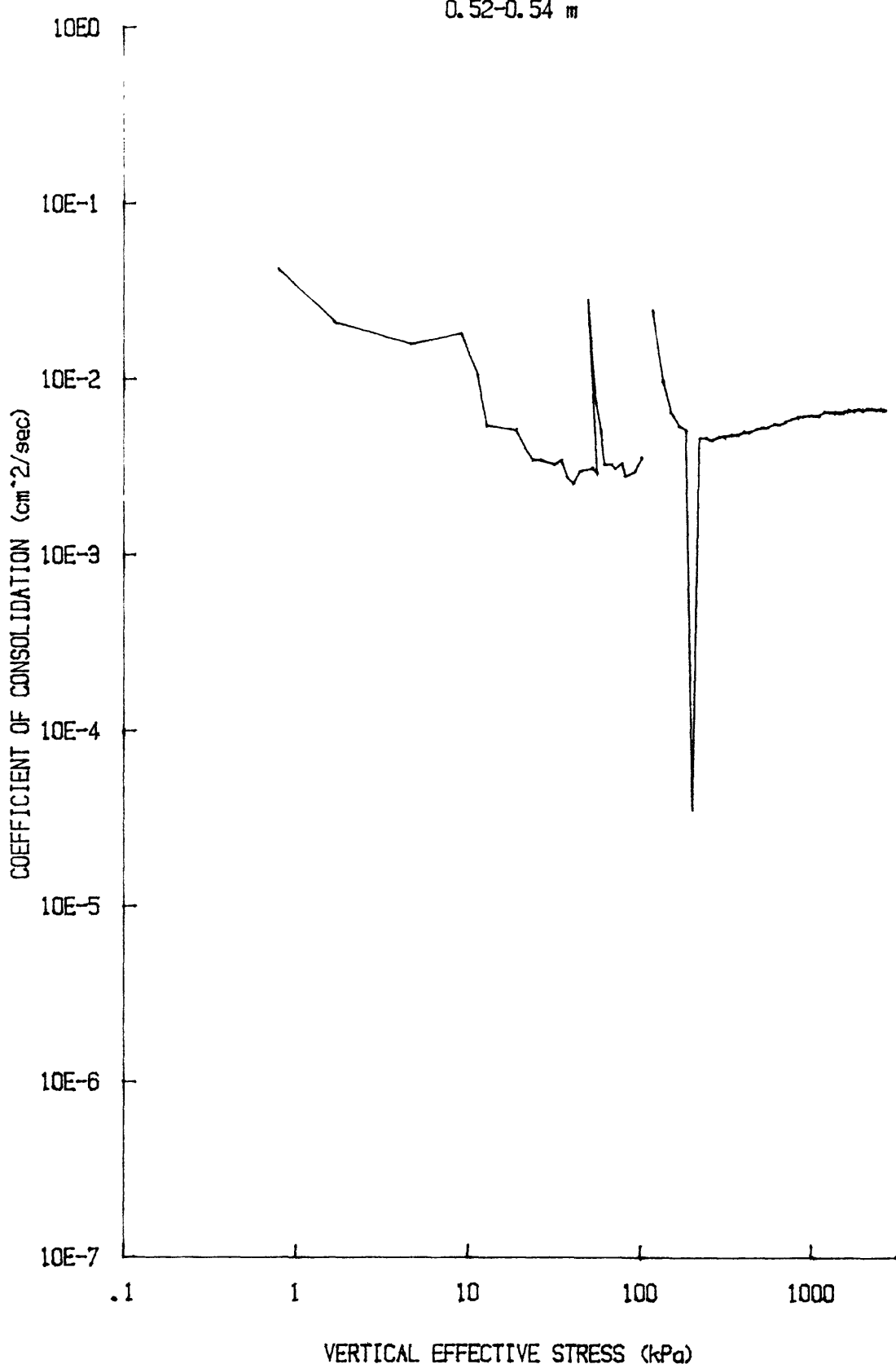


C_v vs $\log p'$ for: CR032S8510

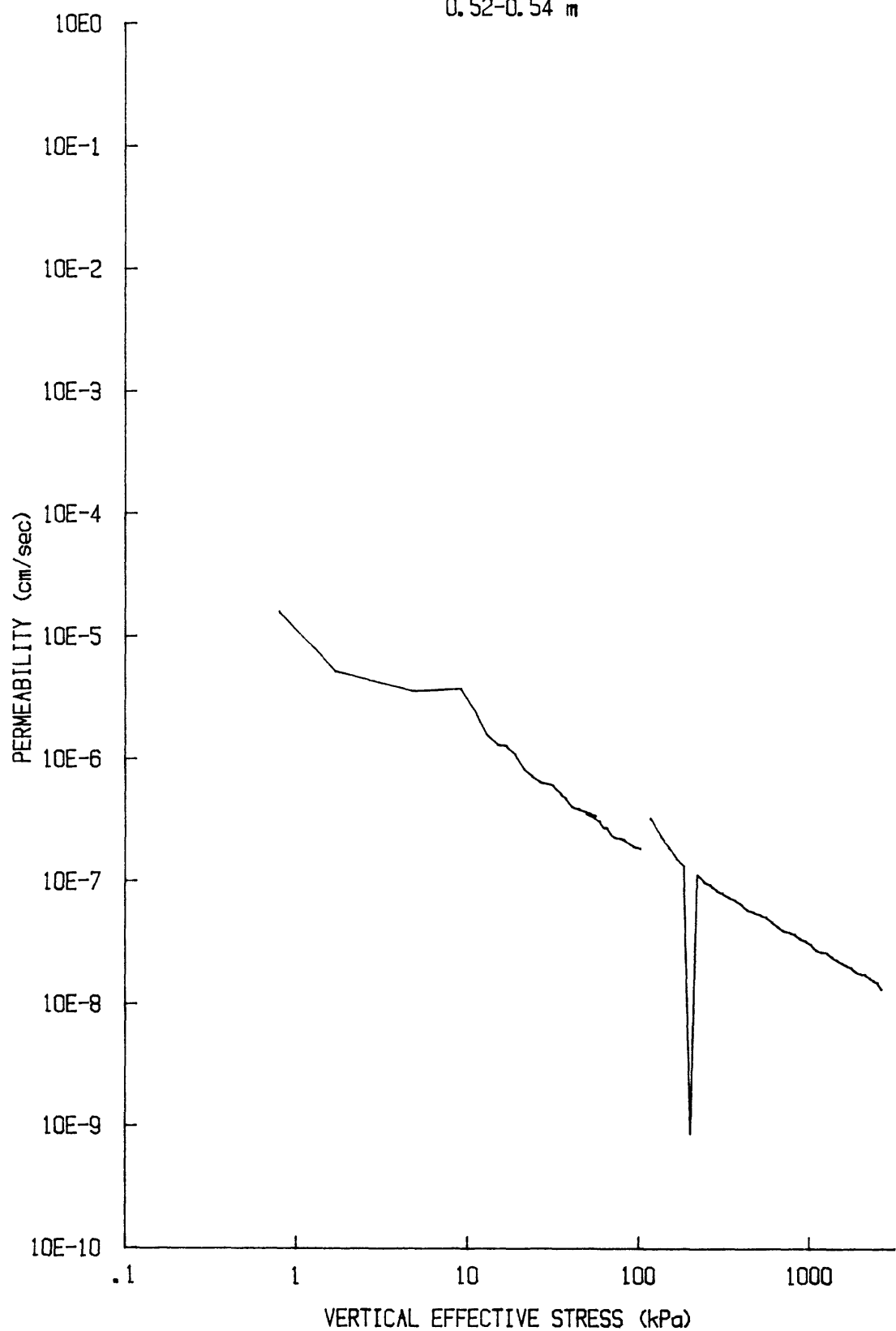
YS-85-08

CORE BC-10

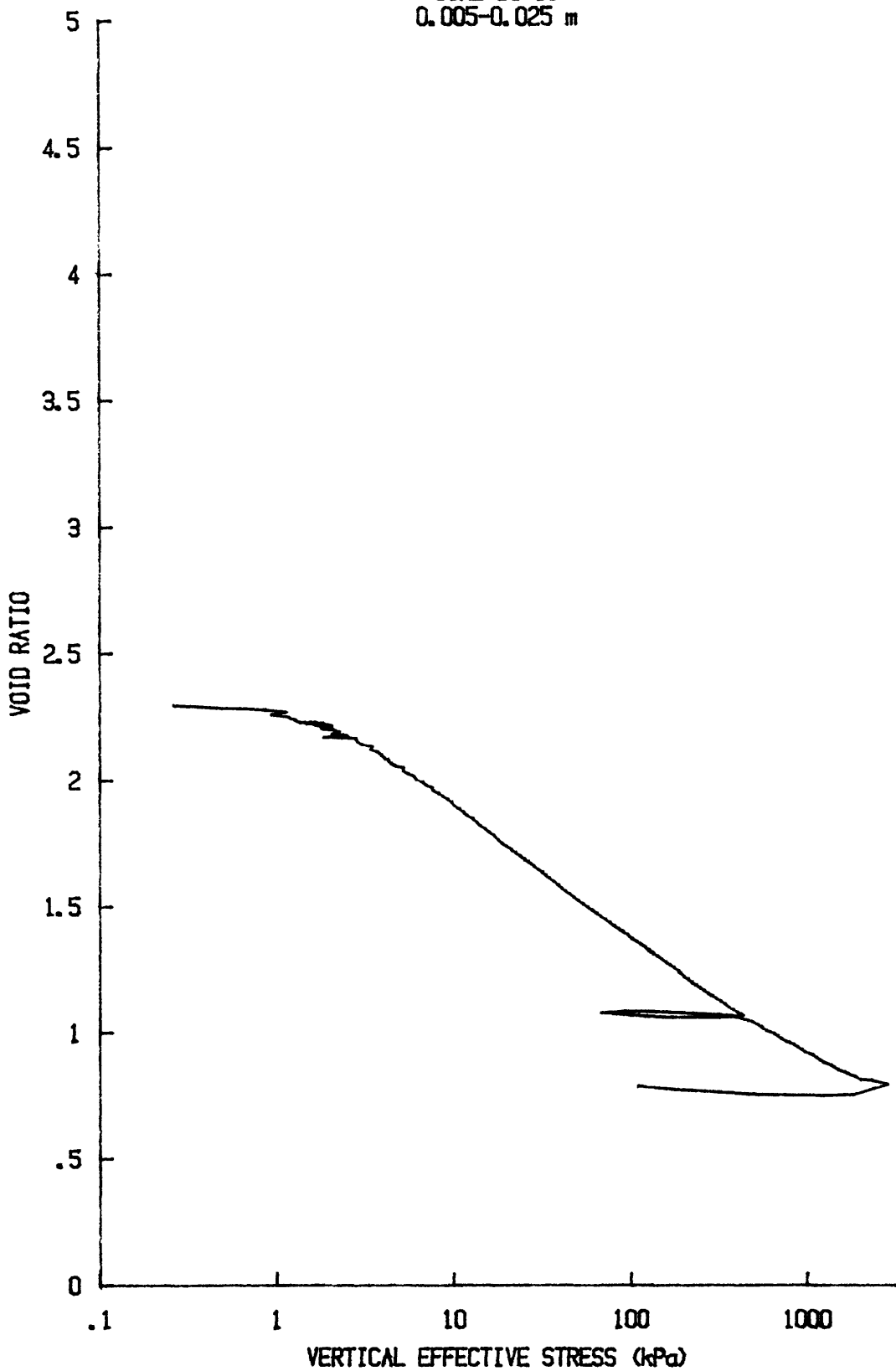
0.52-0.54 m



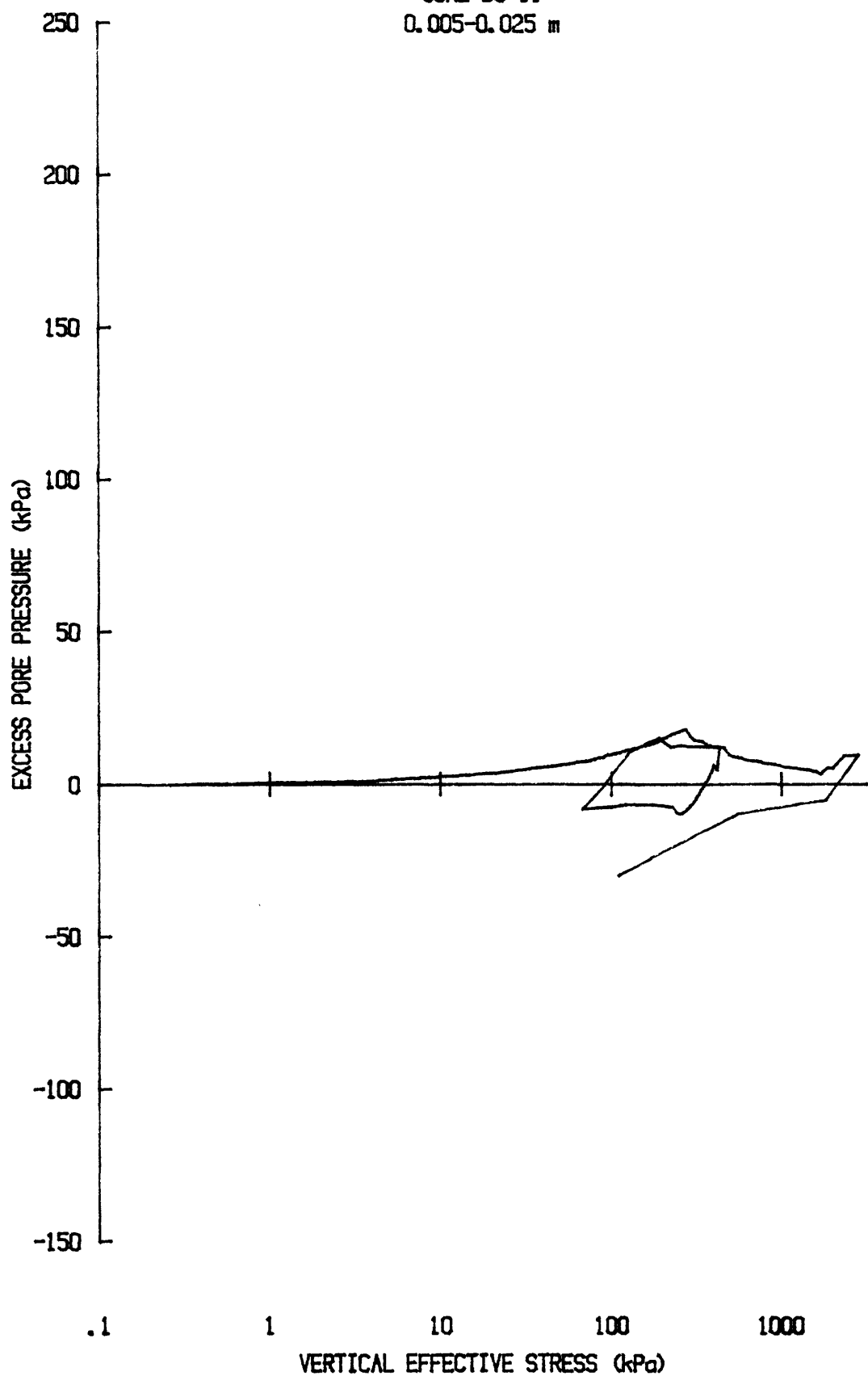
k vs $\log p'$ for: CR032S8510
YS-85-08
CORE BC-10
0.52-0.54 m



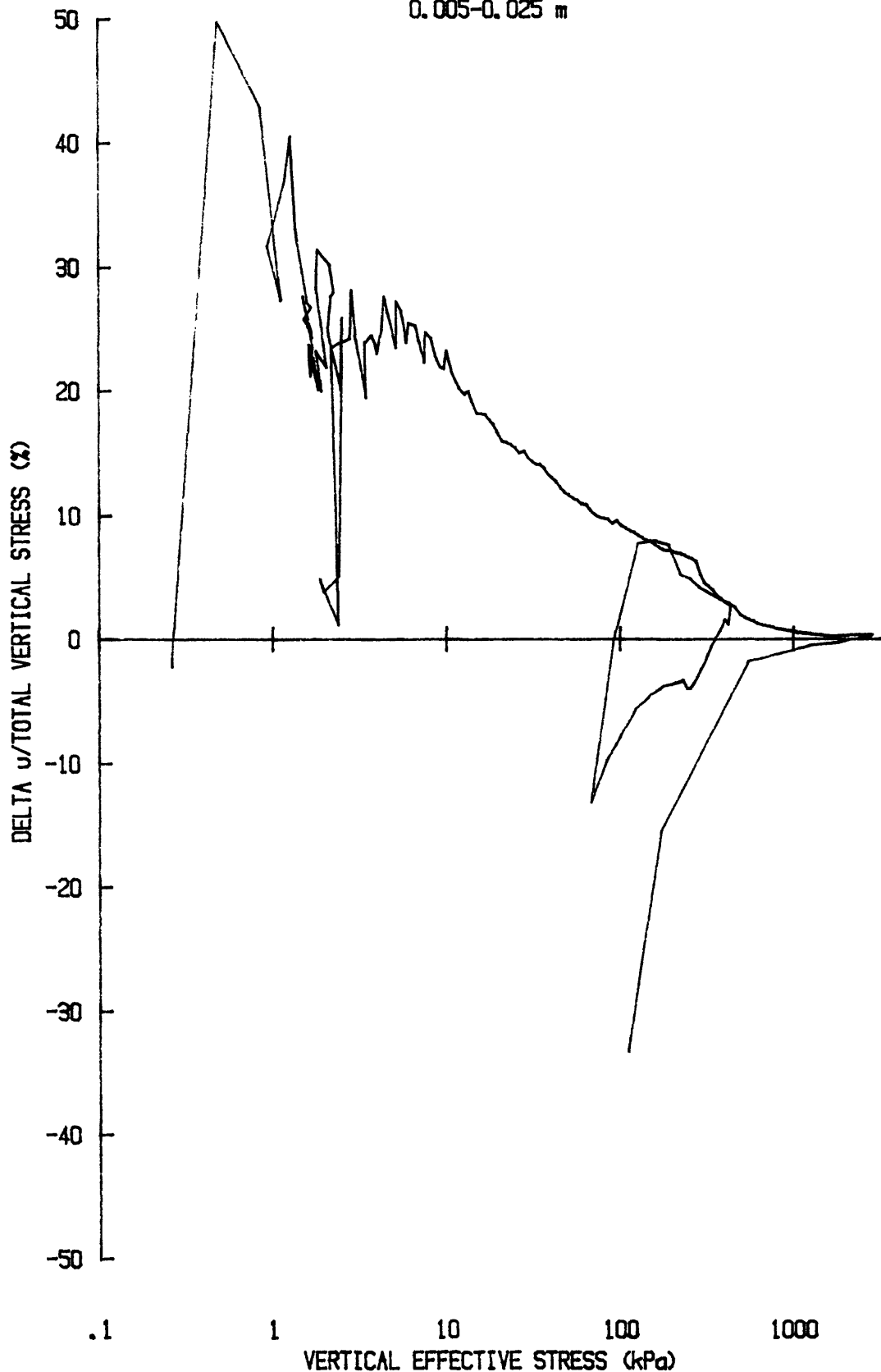
e vs $\log p'$ for CR045S8511
YS-85-08
CORE BC-11
0.005-0.025 m



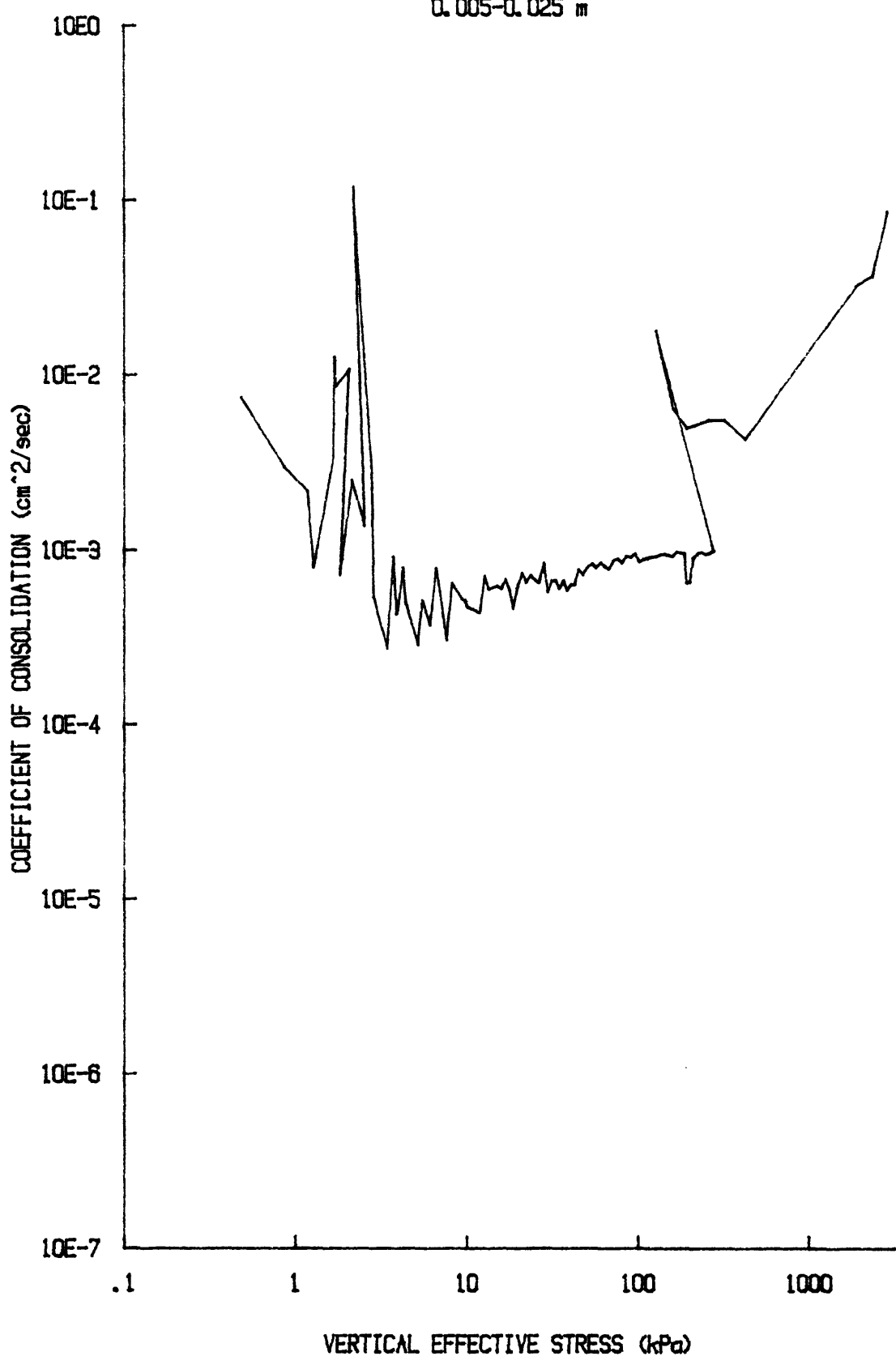
u vs $\log p'$ for CR045S8511
YS-85-08
CORE BC-11
0.005-0.025 m



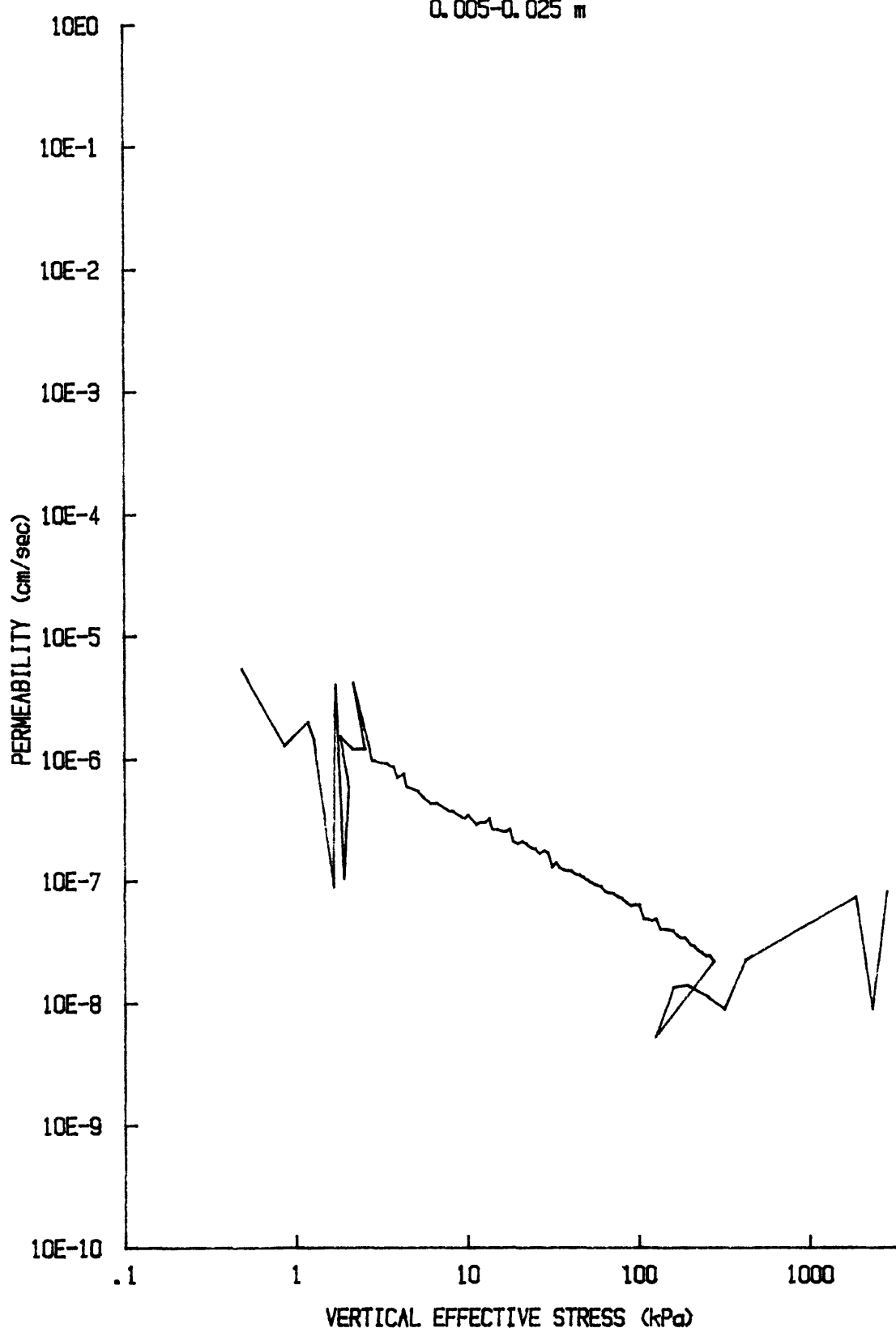
du/Sv for: CR045S8511
YS-85-08
CORE BC-11
0.005-0.025 m



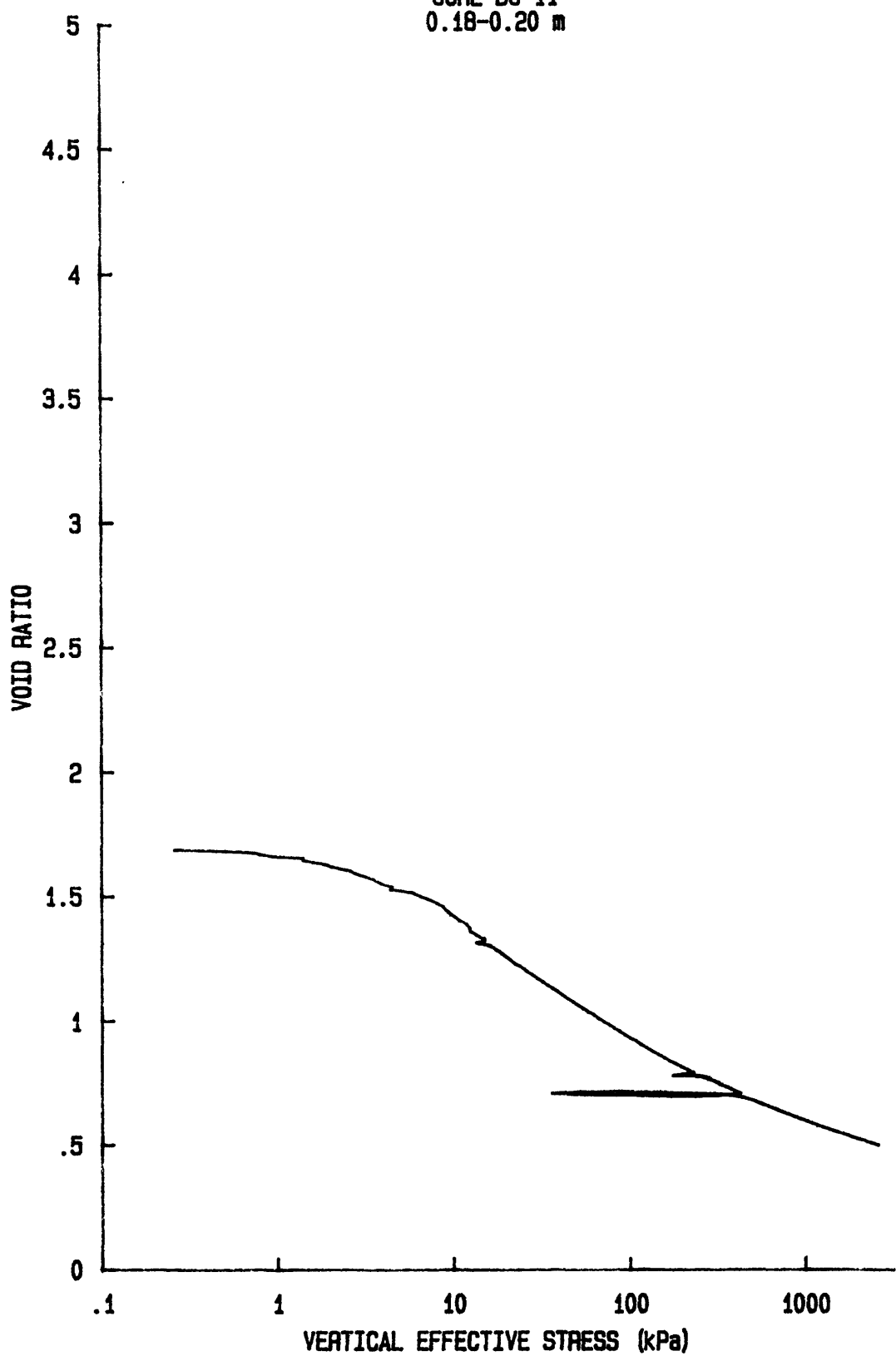
C_v vs $\log p'$ for: CR045S8511
YS-85-08
CORE BC-11
0.005-0.025 m



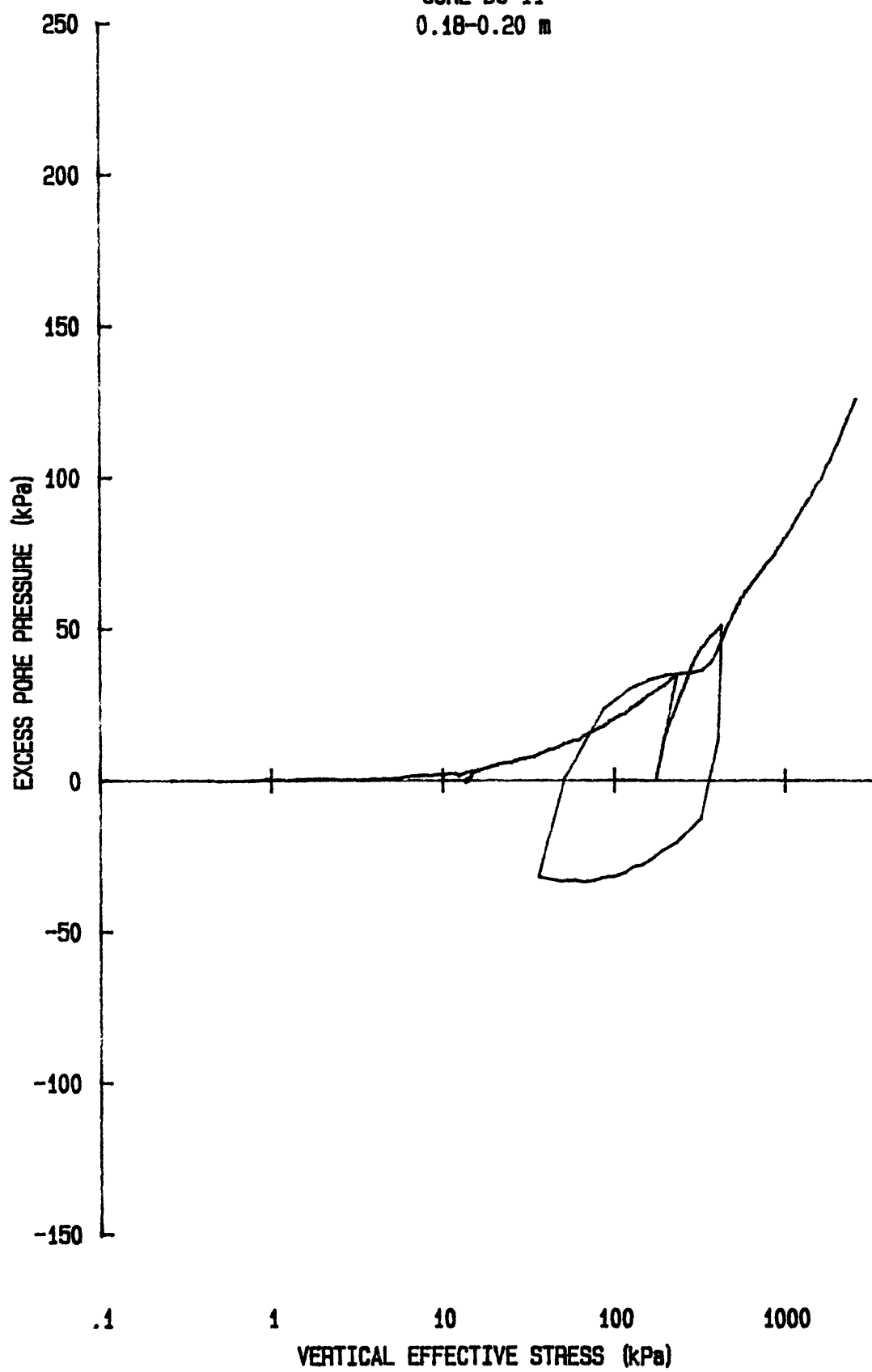
k vs $\log p'$ for CR045S8511
YS-85-08
CORE BC-11
0.005-0.025 m



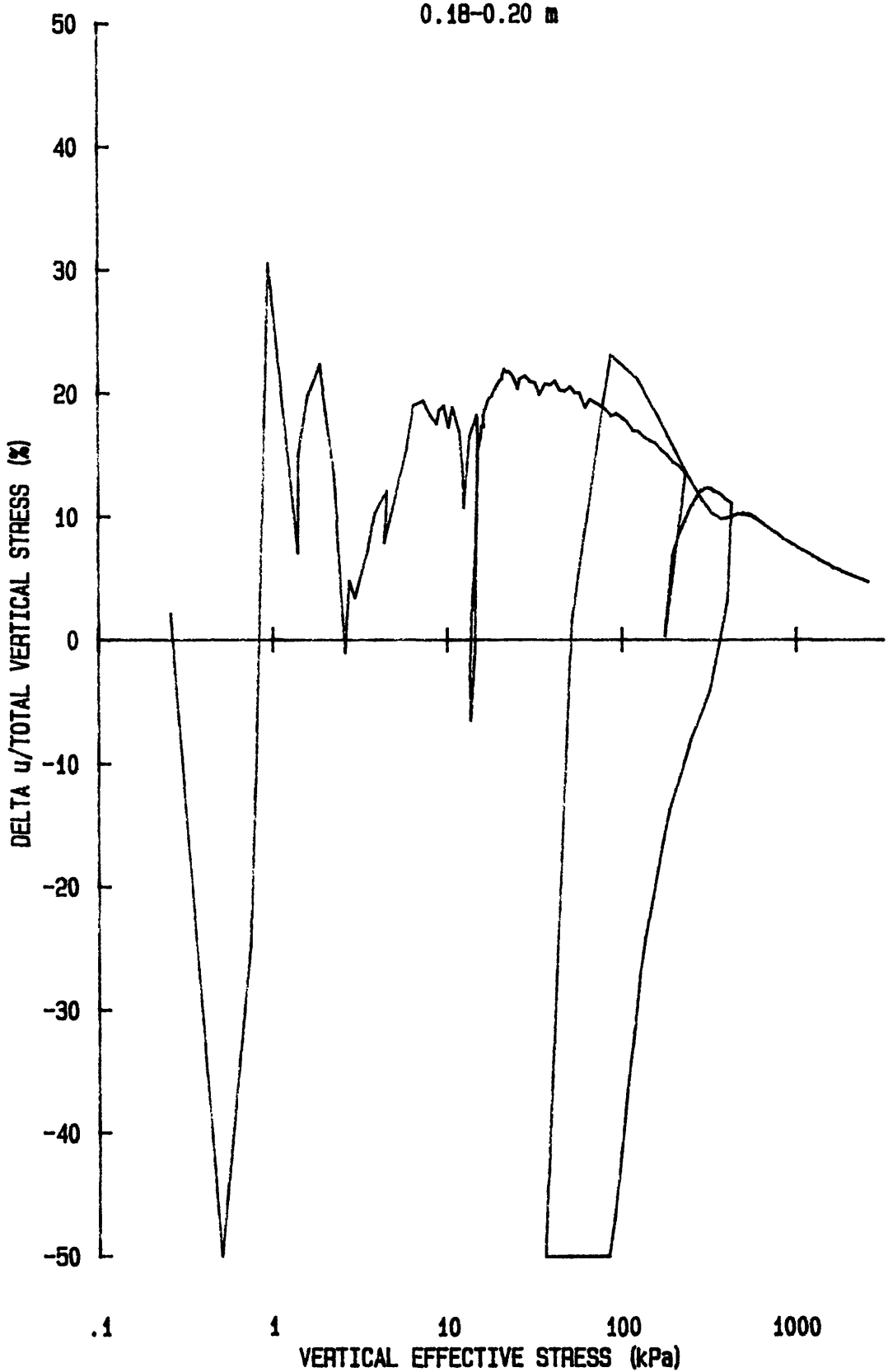
e vs $\log p'$ for: CR052S8511
YS-85-08
CORE BC-11
0.18-0.20 m



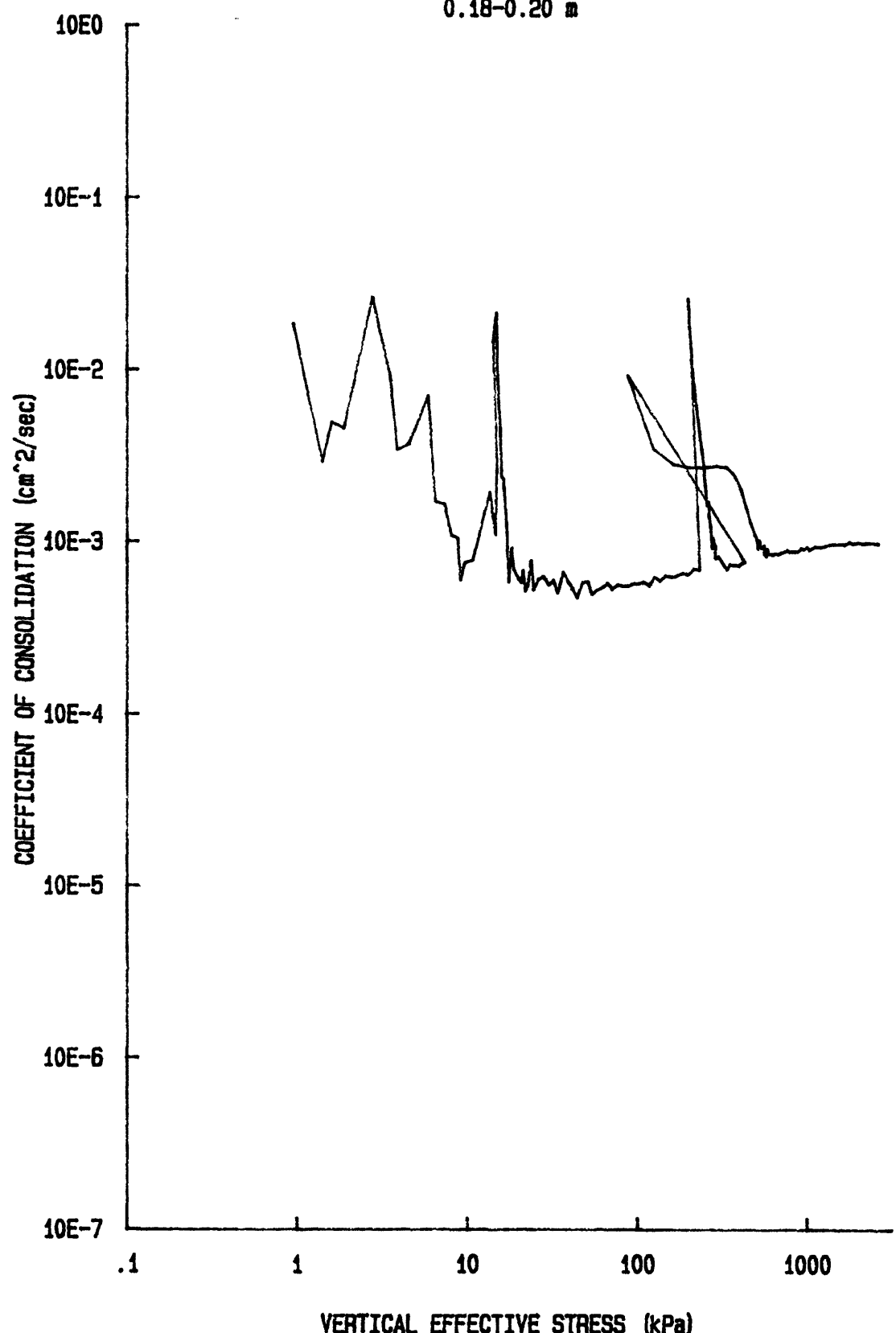
u vs $\log p'$ for: CR052S8511
YS-85-08
CORE BC-11
0.18-0.20 m



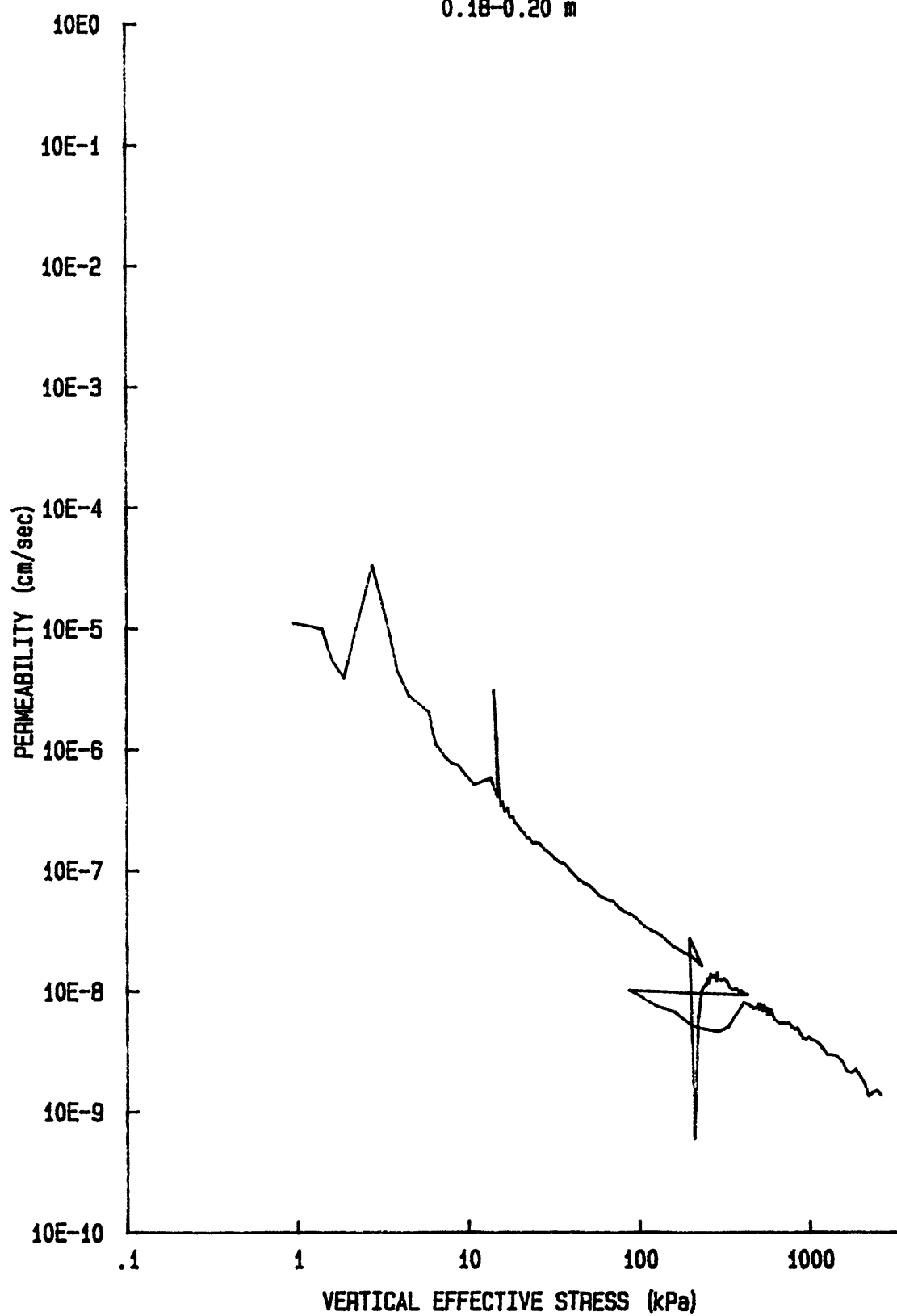
du/Sv for: CR052S8511
YS-85-08
CORE BC-11
0.18-0.20 m



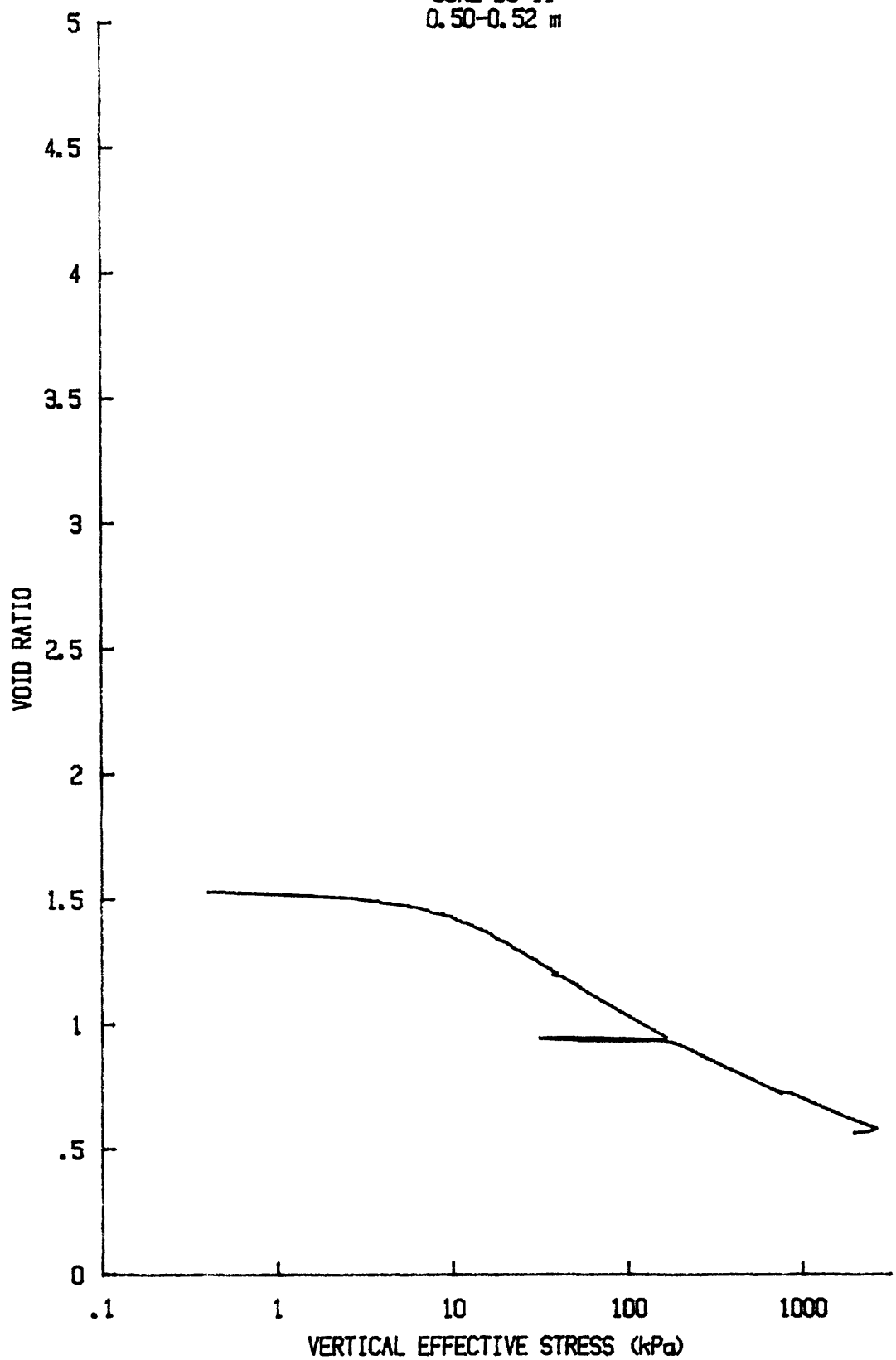
Cv vs log p' for: CR052S8511
YS-85-08
CORE BC-11
0.18-0.20 m



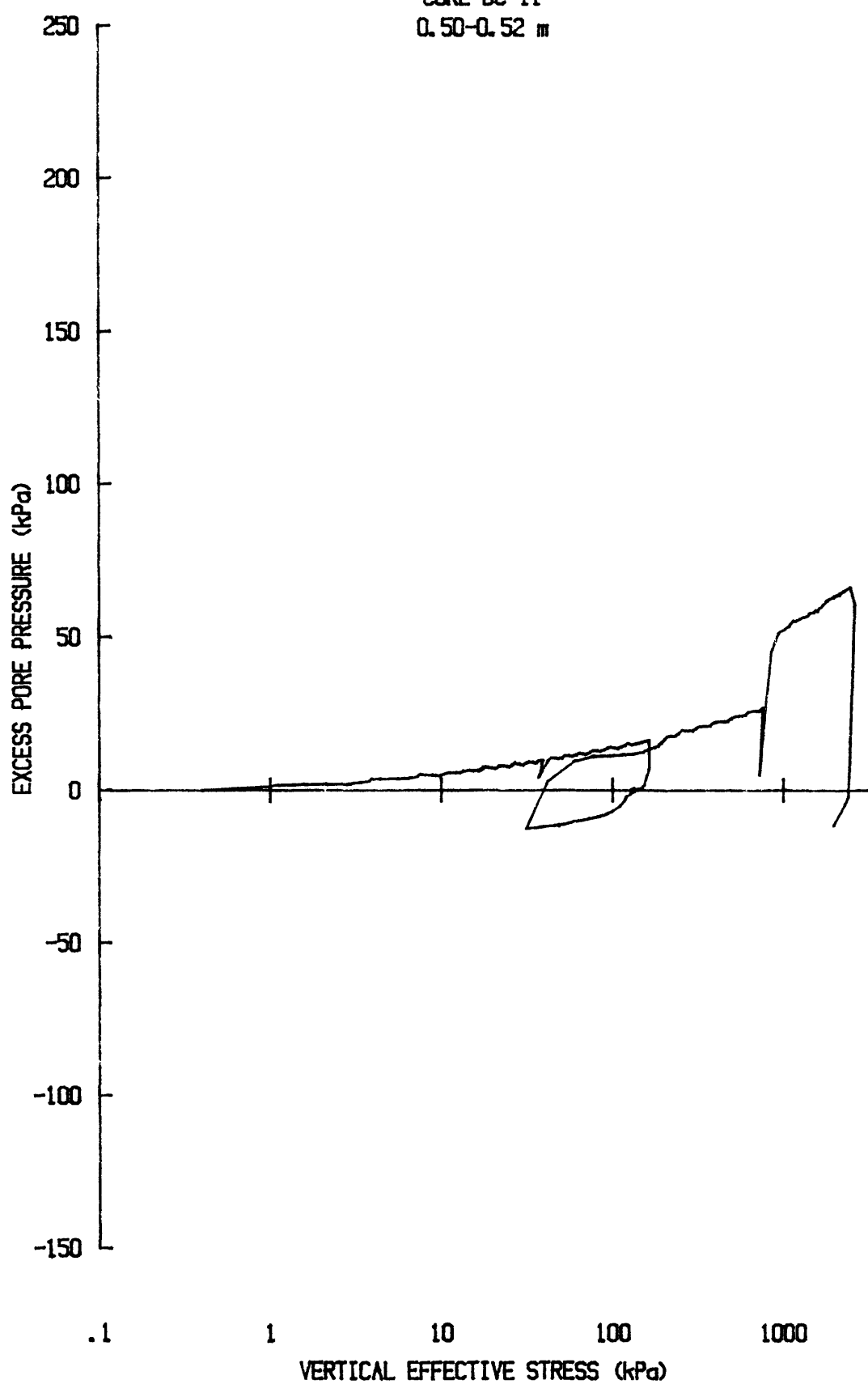
k vs $\log p'$ for: CR052S8511
YS-85-08
CORE BC-11
0.18-0.20 m



e vs $\log p'$ for: CR046S8511
YS-85-08
CORE BC-11
0.50-0.52 m



u vs $\log p'$ for: CRO46S8511
YS-85-08
CORE BC-11
0.50-0.52 m

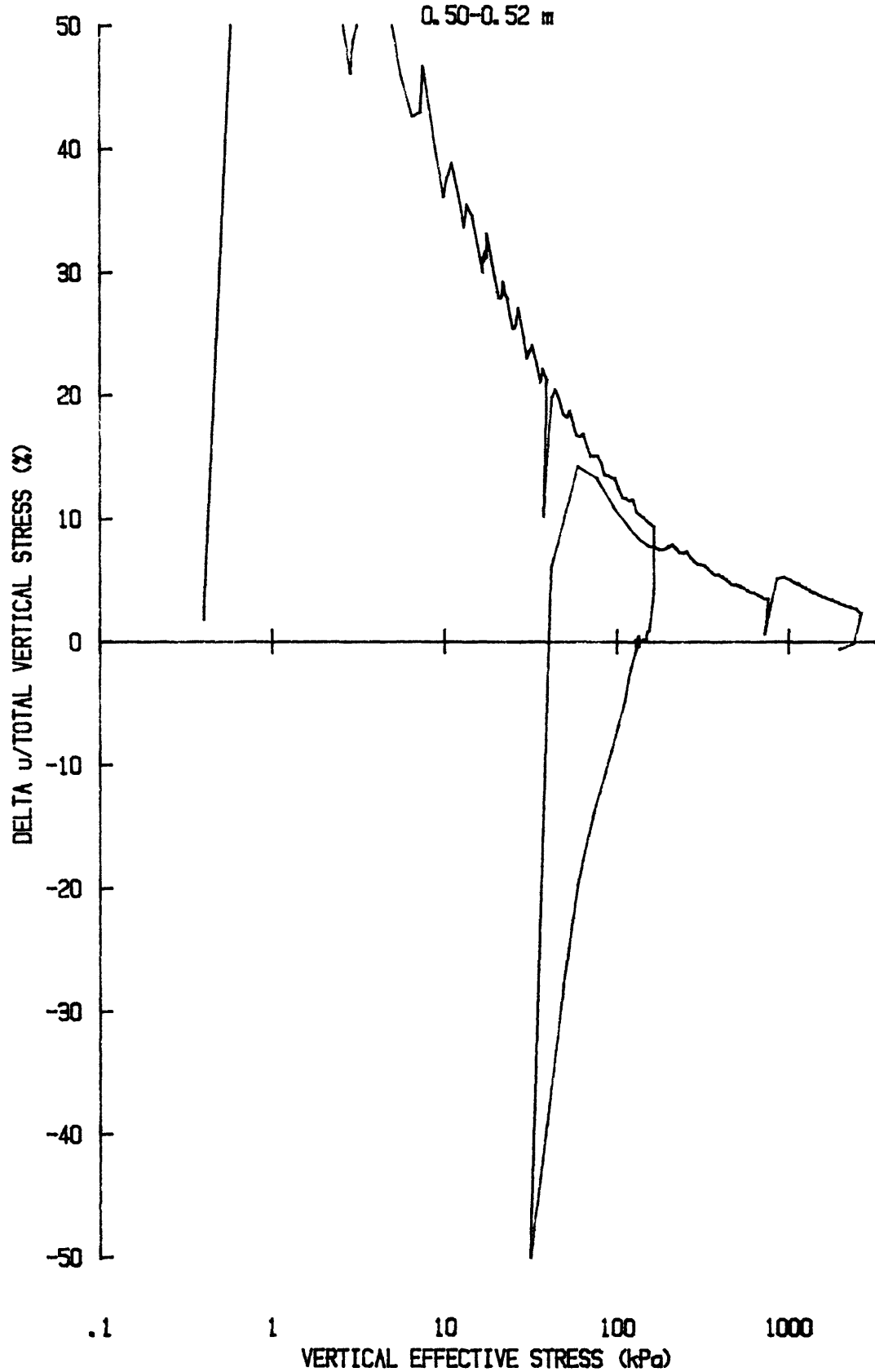


du/Sv for: CR046S8511

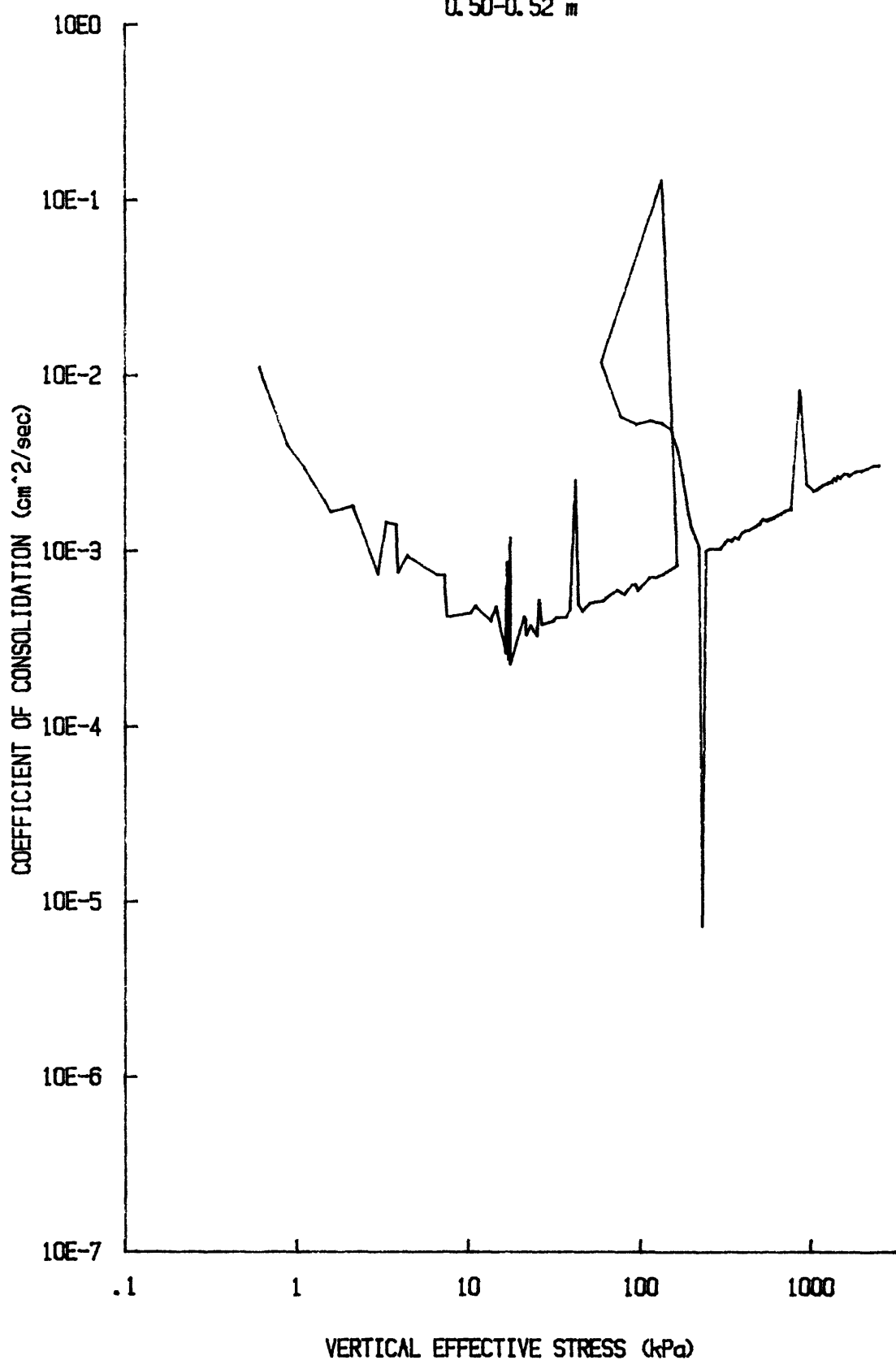
YS-85-08

CORE BC-11

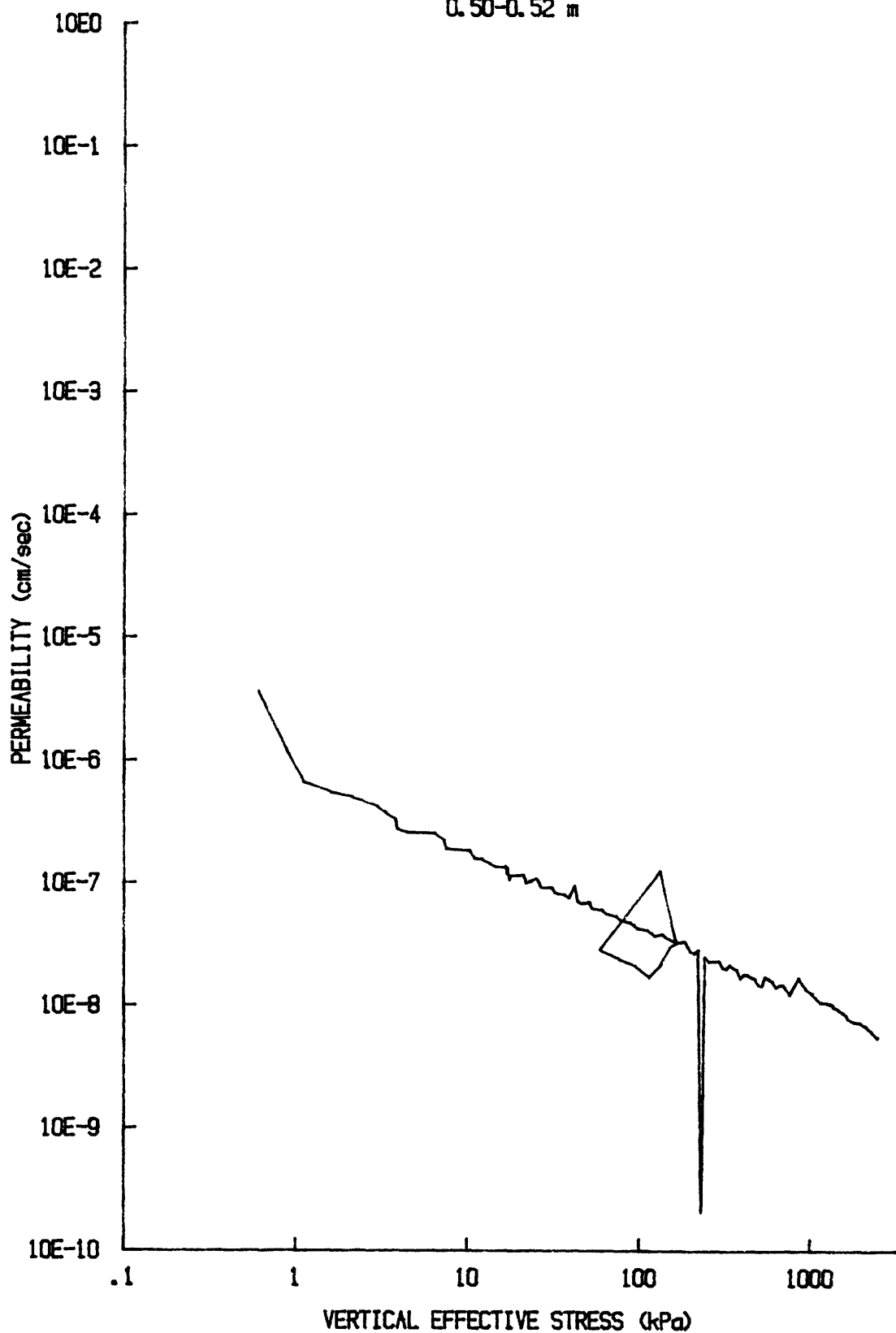
0.50-0.52 in



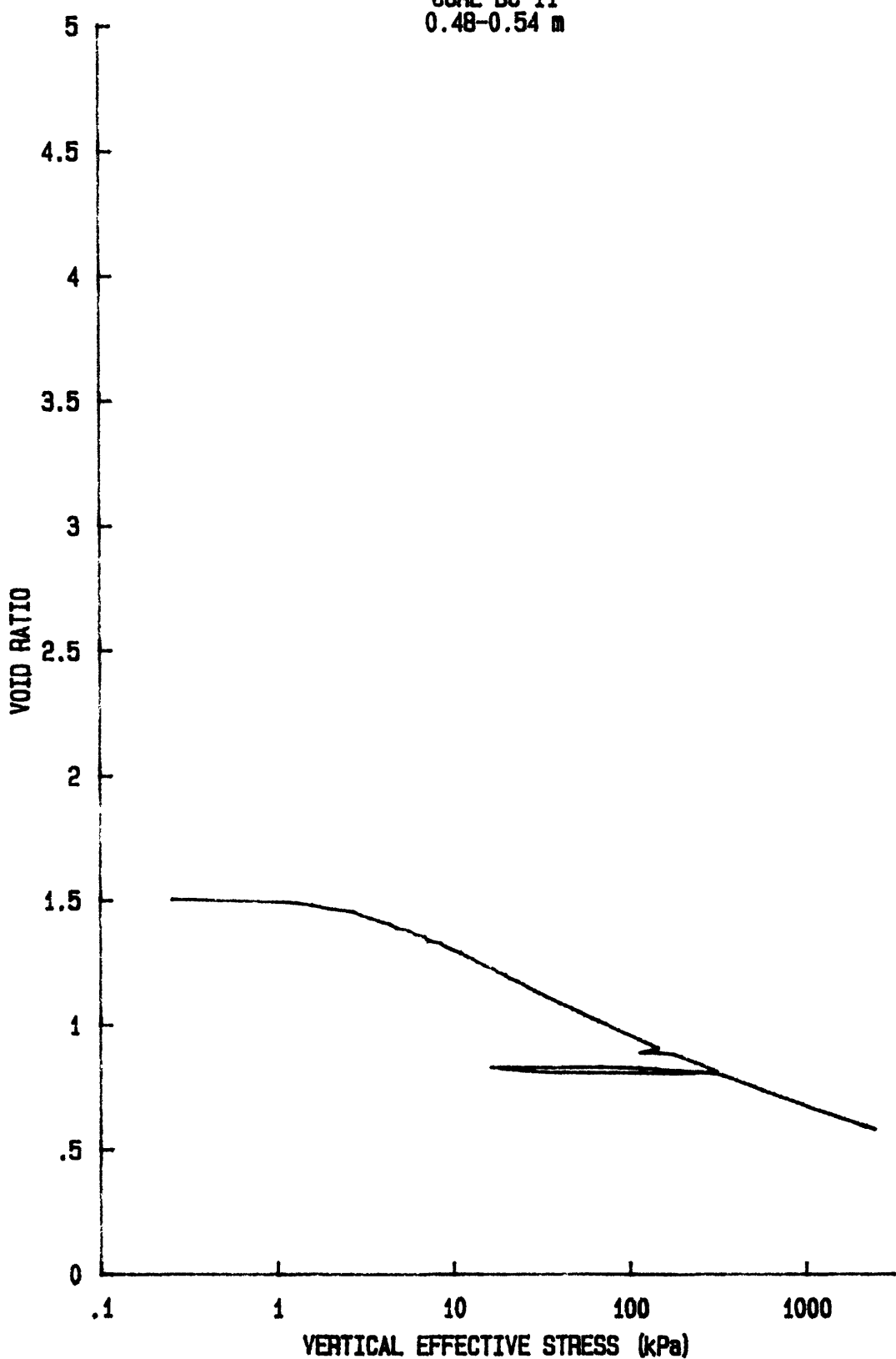
C_v vs $\log p'$ for: CR046S8511
YS-85-08
CORE BC-11
0.50-0.52 m



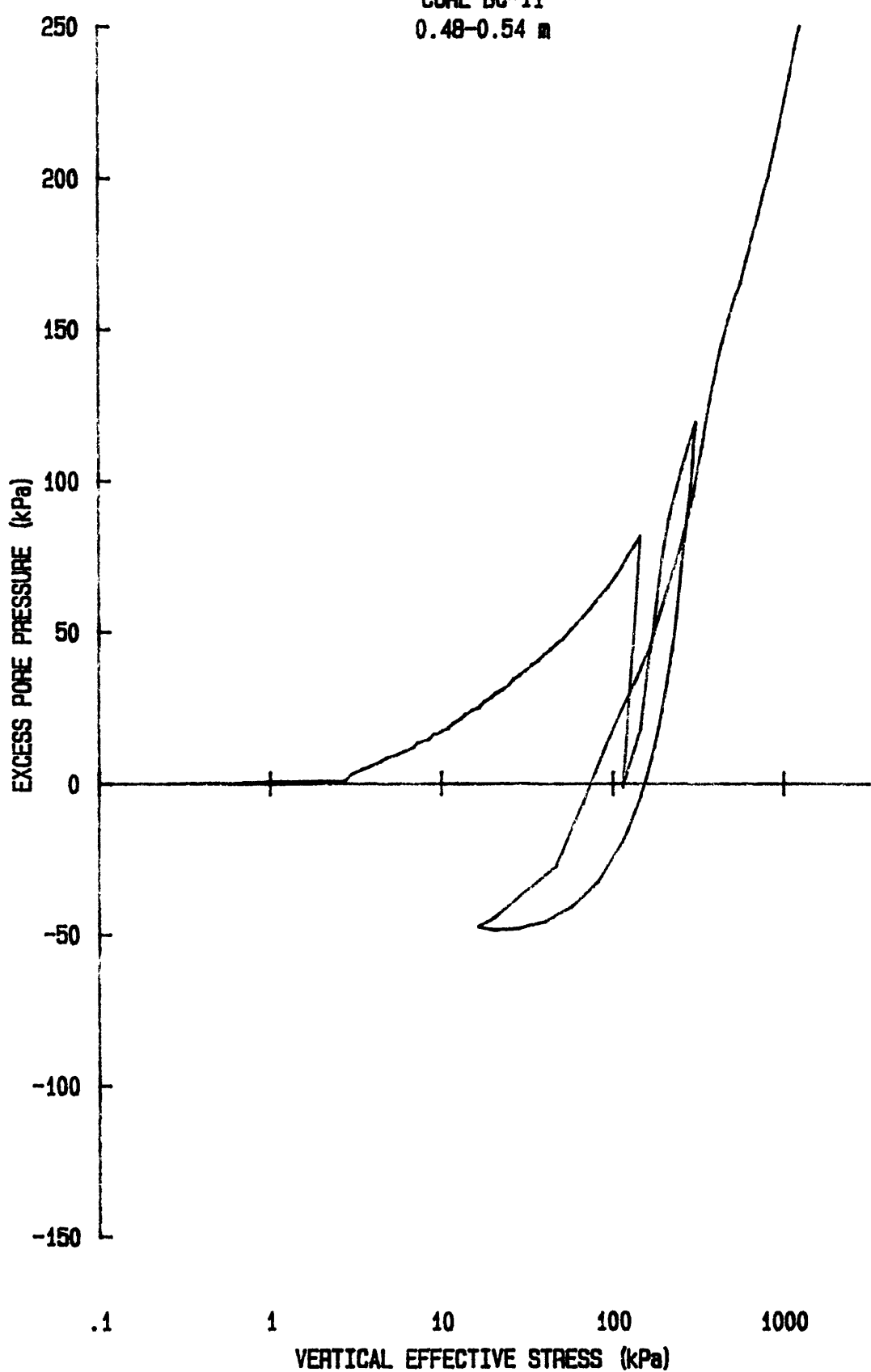
k vs $\log p'$ for CR046S8511
YS-85-08
CORE BC-11
0.50-0.52 m



e vs log p' for: CR059S8511
YS-85-08
CORE BC-11
0.48-0.54 m



u vs $\log p'$ for: CR059S8511
YS-85-08
CORE BC-11
0.48-0.54 m

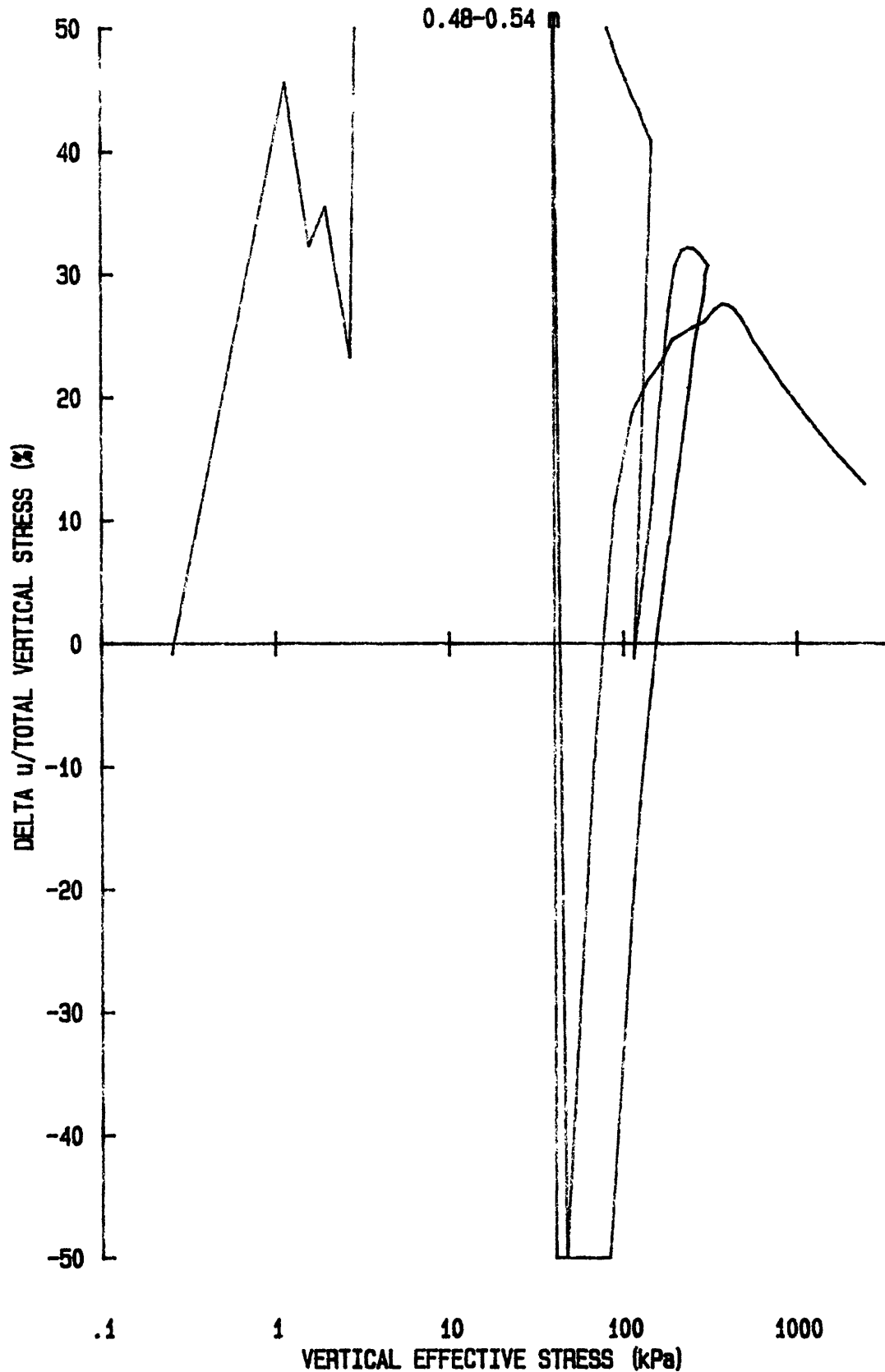


du/Sv for: CR059S8511

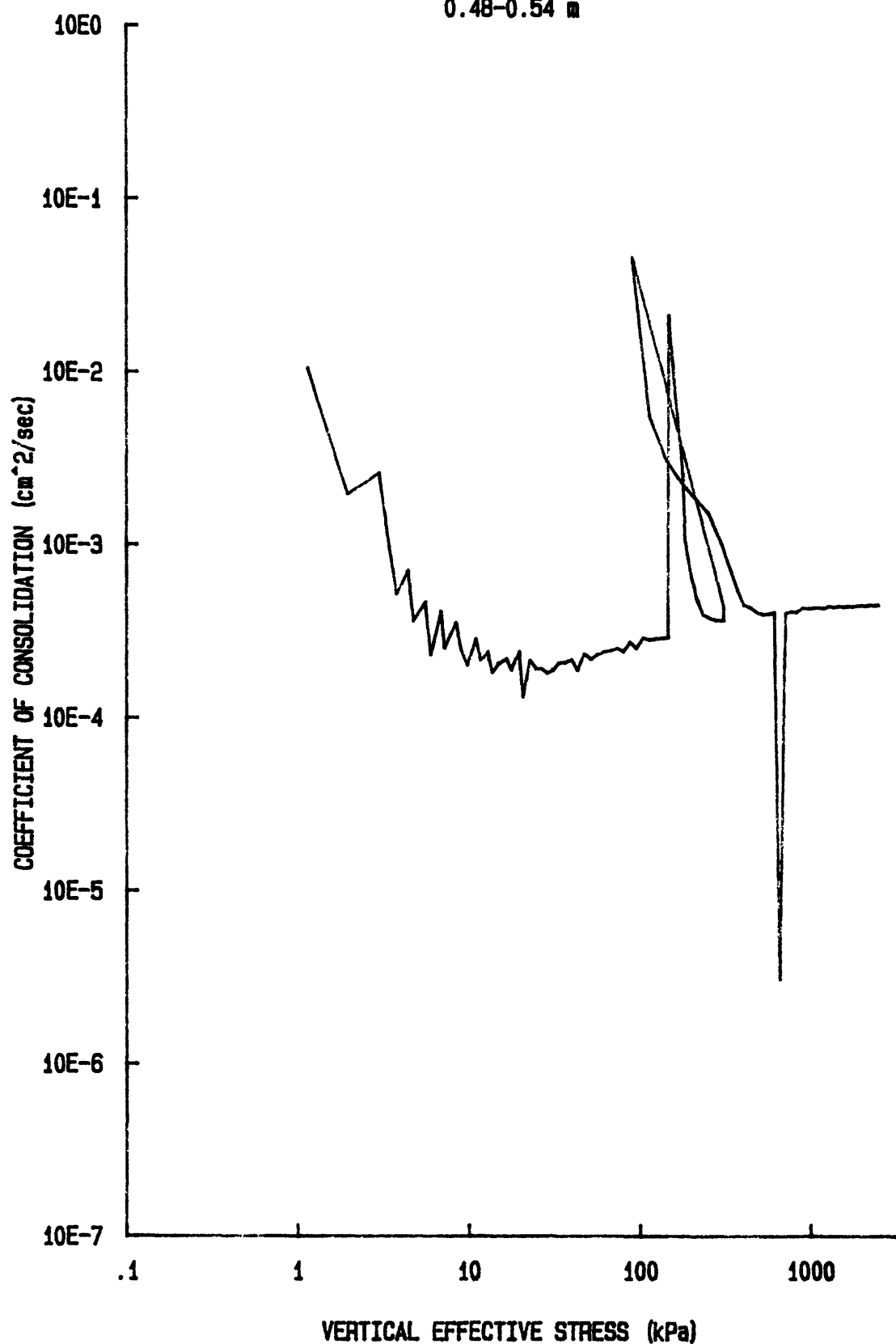
YS-85-08

CORE BC-11

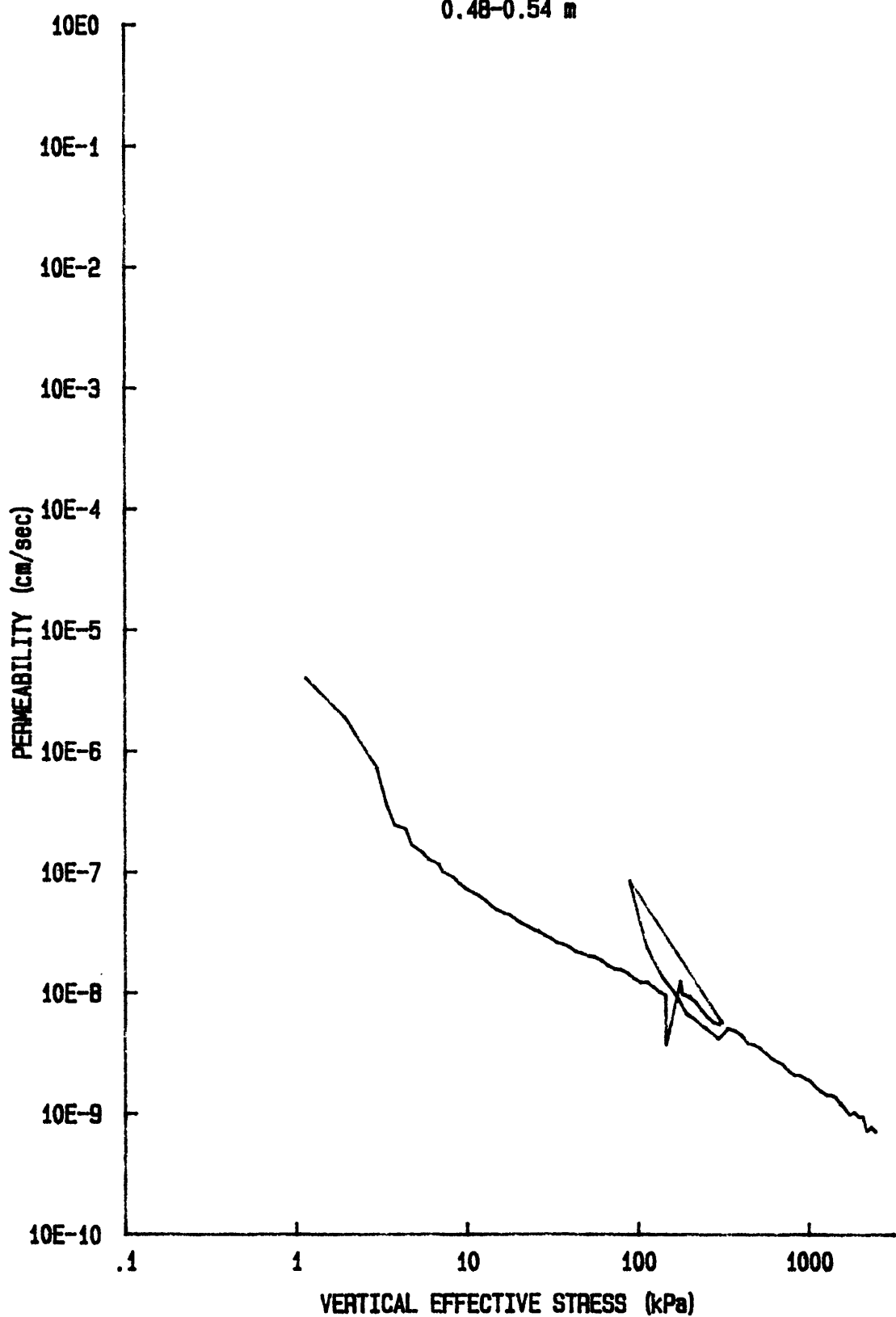
0.48-0.54 m



Cv vs log p' for: CR059S8511
YS-85-08
CORE BC-11
0.48-0.54 m



k vs $\log p'$ for: CR059S8511
YS-85-08
CORE BC-11
0.48-0.54 m



Appendix D

Results of Consolidated-Isotropic-Undrained Triaxial Tests

**tabular data
unedited individual test plots
unedited multiple test plots**

TABULAR DATA

Consolidated-Isotropic-Undrained Triaxial Test Results

Core	Test	Depth [*]	w	w_s^+	σ'_c	A_f	Strain at failure	S_u	S_u / σ'_c	ϕ'	θ'	θ'^{**}	c'^{**}
no.		in core	(m)	(%)	(%)	kPa	(%)	kPa		max oblique (c' = 0) deg.	max q (c' = 0) deg.	max oblique (c' ≠ 0) deg.	kPa
BC-5	1	0.42	105	46	210.3	0.81	11.1	88.1	0.42	36.1	34.6		
	2	"	102	50	138.3	0.89	17.3	56.5	0.41	37.0	36.8		
	3	"	105	56	66.9	0.66	16.3	37.0	0.55	42.8	42.4		
	4	"	100	78	1.7	0.42	19.0	3.4	2.00	—	—	35.4	3.1
BC-6	1	0.36	119	50	208.1	0.92	11.9	76.9	0.37	33.7	32.2		
	2	"	120	54	141.3	1.00	9.0	44.8	0.32	28.6	27.8		
	3	"	116	61	67.3	0.75	10.2	31.6	0.47	40.0	38.5		
	4	"	114	92	1.3	0.29	9.9	3.8	2.92	—	—	—	
BC-7	1	0.39	47	28	259.9	1.00	19.9	97.2	0.37	36.9	36.8		
	2	"	47	29	190.3	1.07	11.4	68.2	0.36	37.8	37.6		
	3	"	46	31	116.1	0.89	13.0	49.0	0.42	38.6	38.4		
	4	"	46	43	2.6	0.10	19.1	8.5	3.27	—	—	35.5	4.2
BC-8	1	0.44	45	29	208.4	0.85	19.9	88.7	0.43	37.9	37.6		
	2	"	48	31	99.8	0.77	17.6	44.1	0.44	37.1	36.5		
	3	"	45	43	3.1	-0.23	18.0	2.5	0.81	—	—	38.5	0.0
	4	"											
BC-11	1	0.41	58	32	209.4	0.95	10.6	80.9	0.39	36.6	36.4		
	2	"	59	36	137.7	0.97	10.0	51.4	0.37	35.5	35.3		
	3	"	58	38	67.8	0.66	15.2	38.6	0.57	44.1	43.8		
	4	"	61	52	2.5	0.06	16.9	5.4	2.10	—	—	34.9	3.8

* Depth in core is sampling midpoint for test series

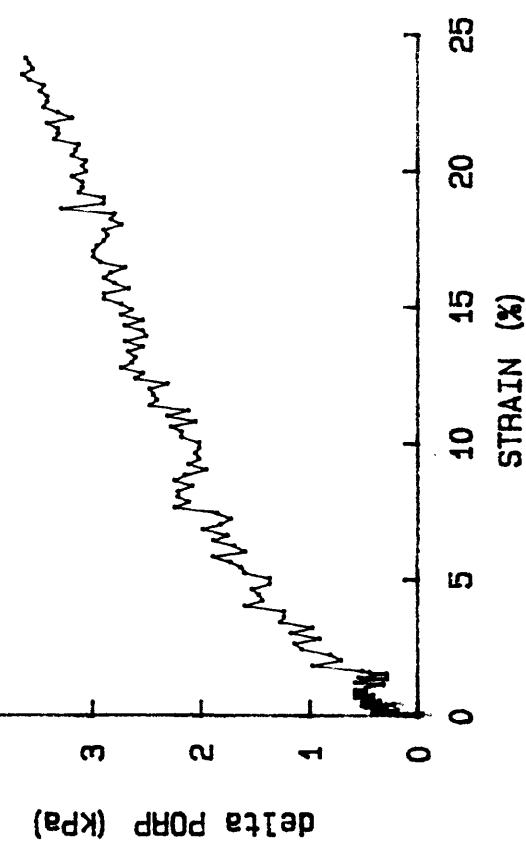
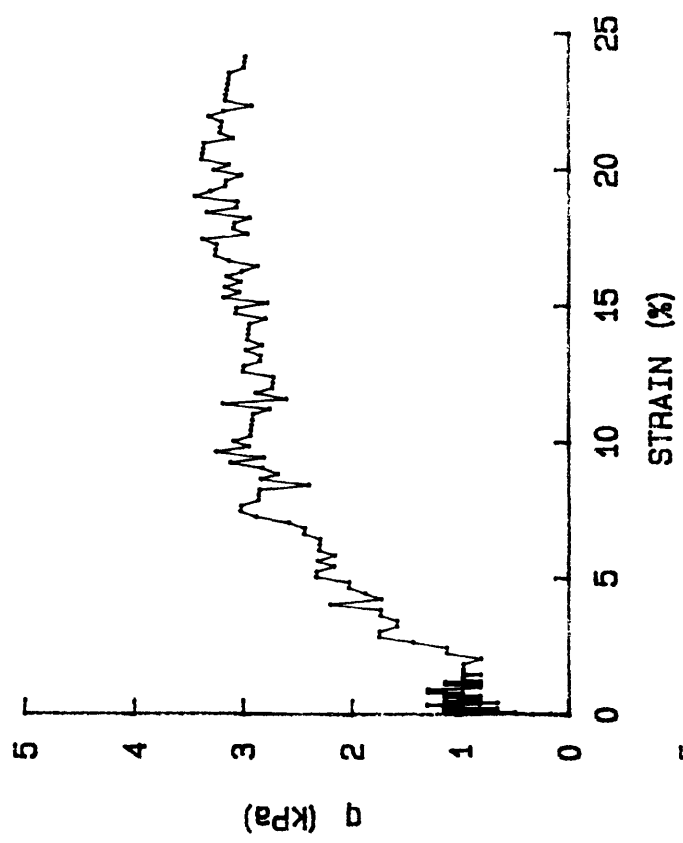
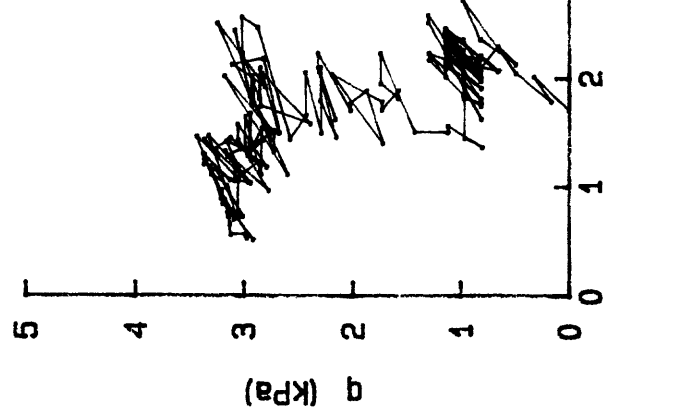
† Water content at end of test

** σ', c' values based on 3-4 tests

†† obliquity = σ'_1 / σ'_3

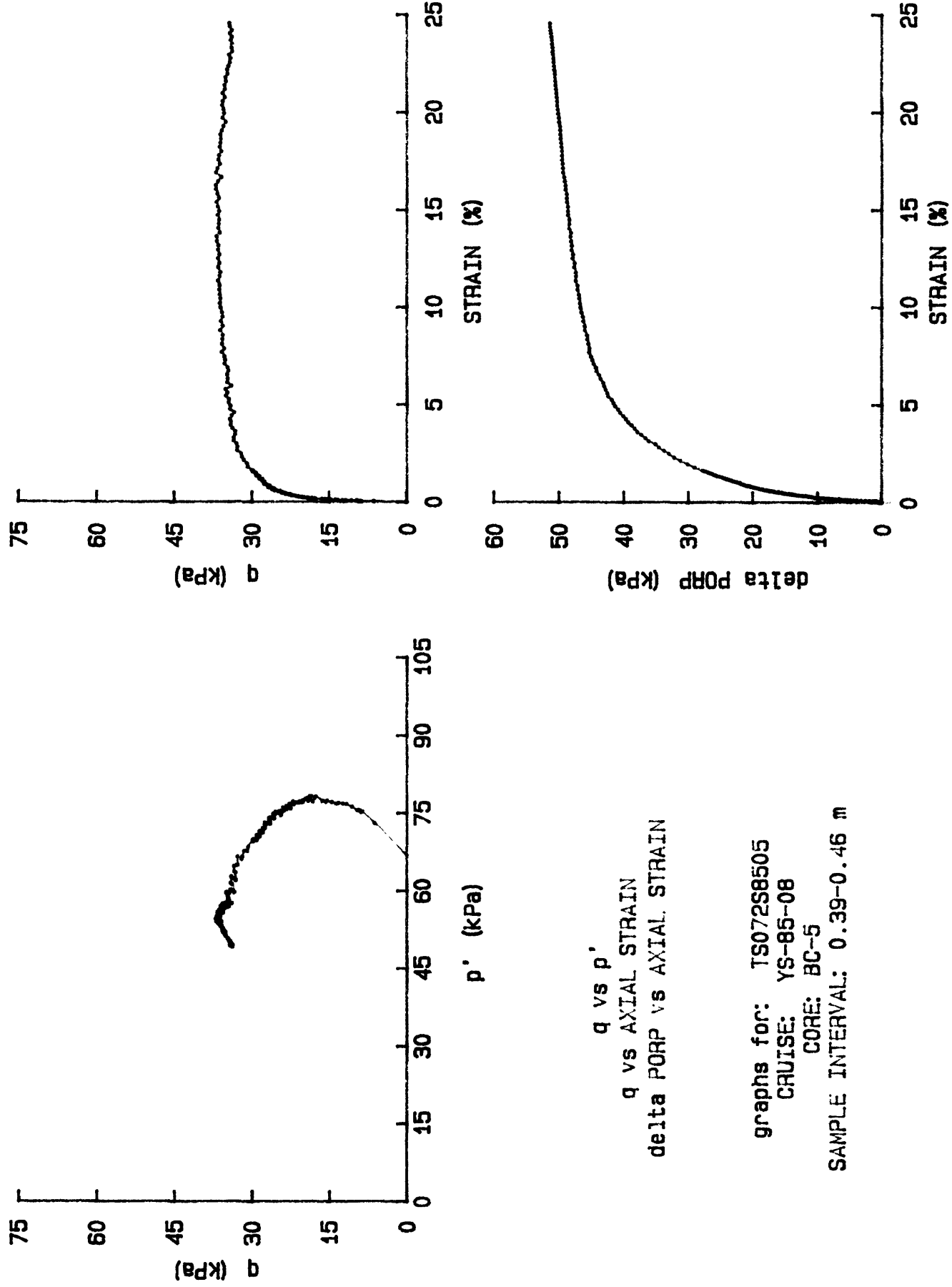
Symbols are explained in Appendix A.

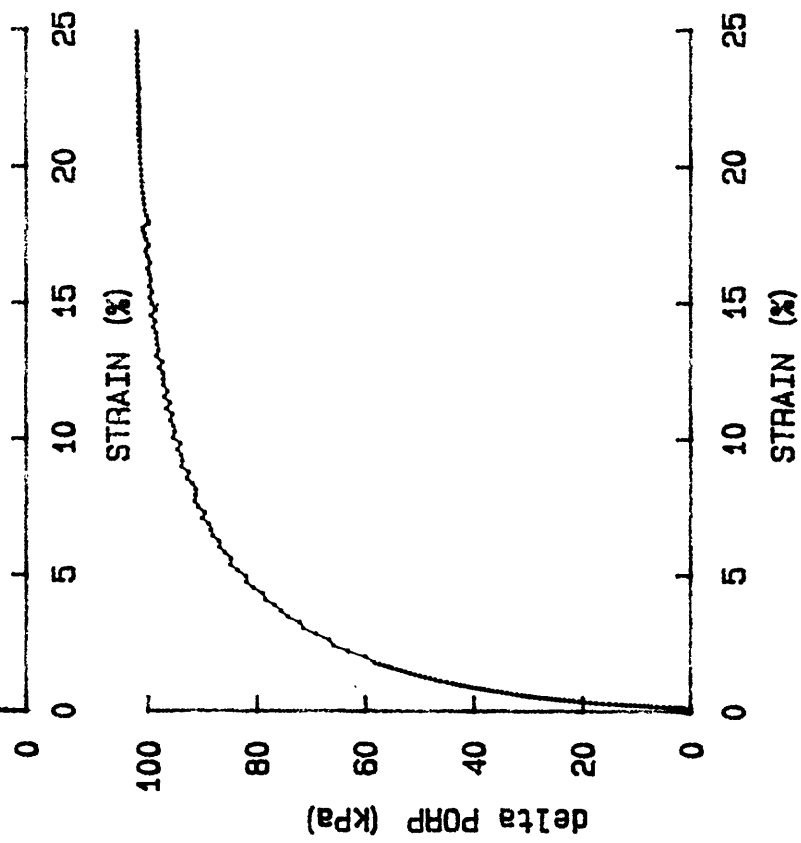
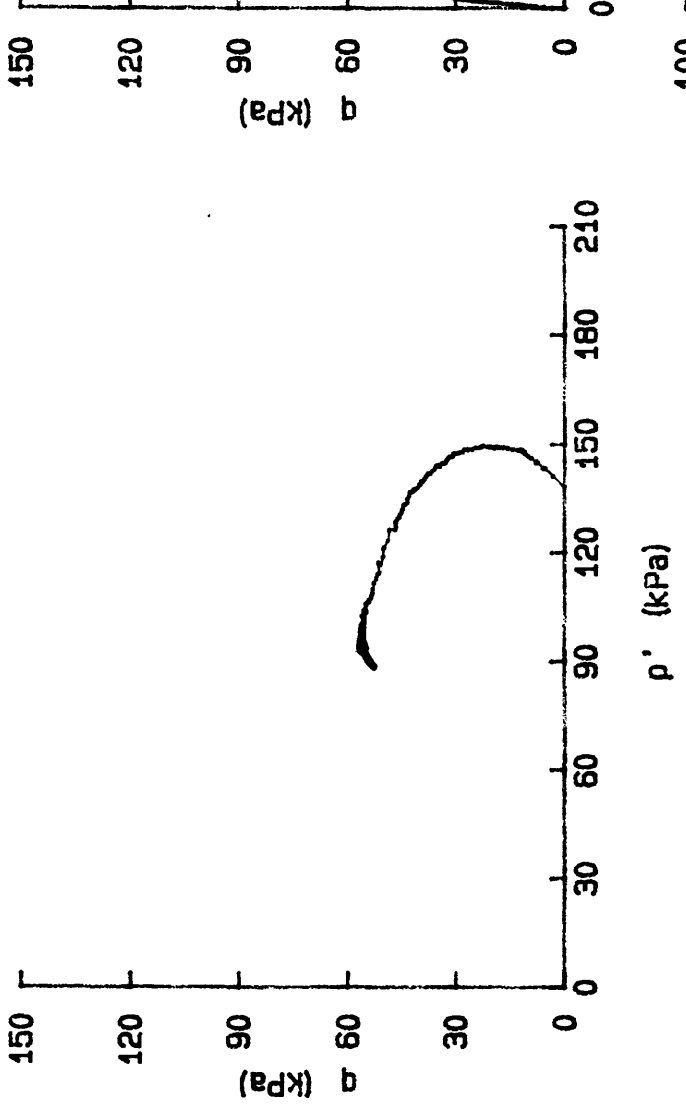
INDIVIDUAL TEST PLOTS



q vs p'
 q vs AXIAL STRAIN
 ΔPORP vs AXIAL STRAIN

graphs for: TS075S8505
 CRUISE: YS-85-08
 CORE: BC-5
 SAMPLE INTERVAL: 0.39-0.46 m



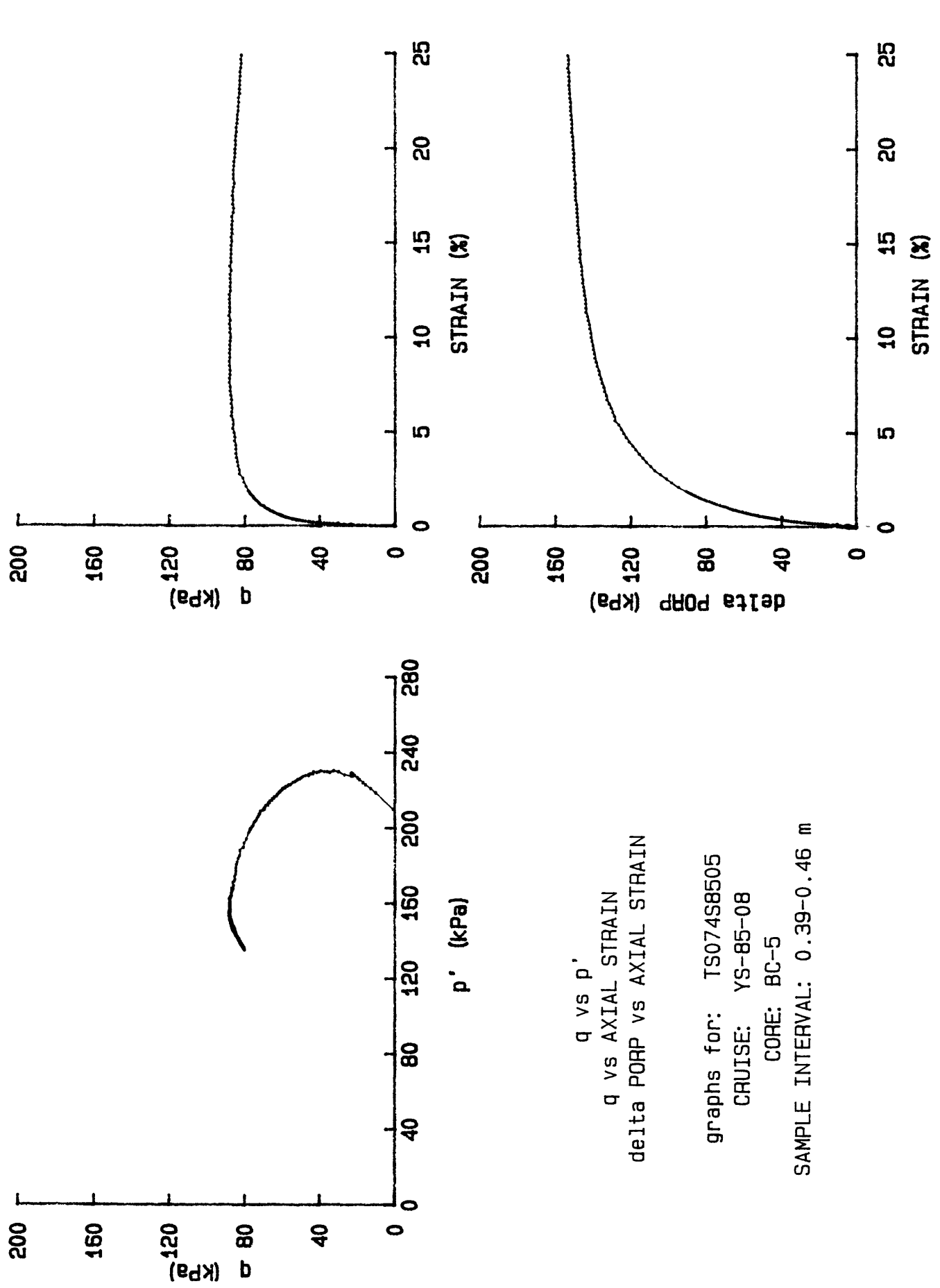


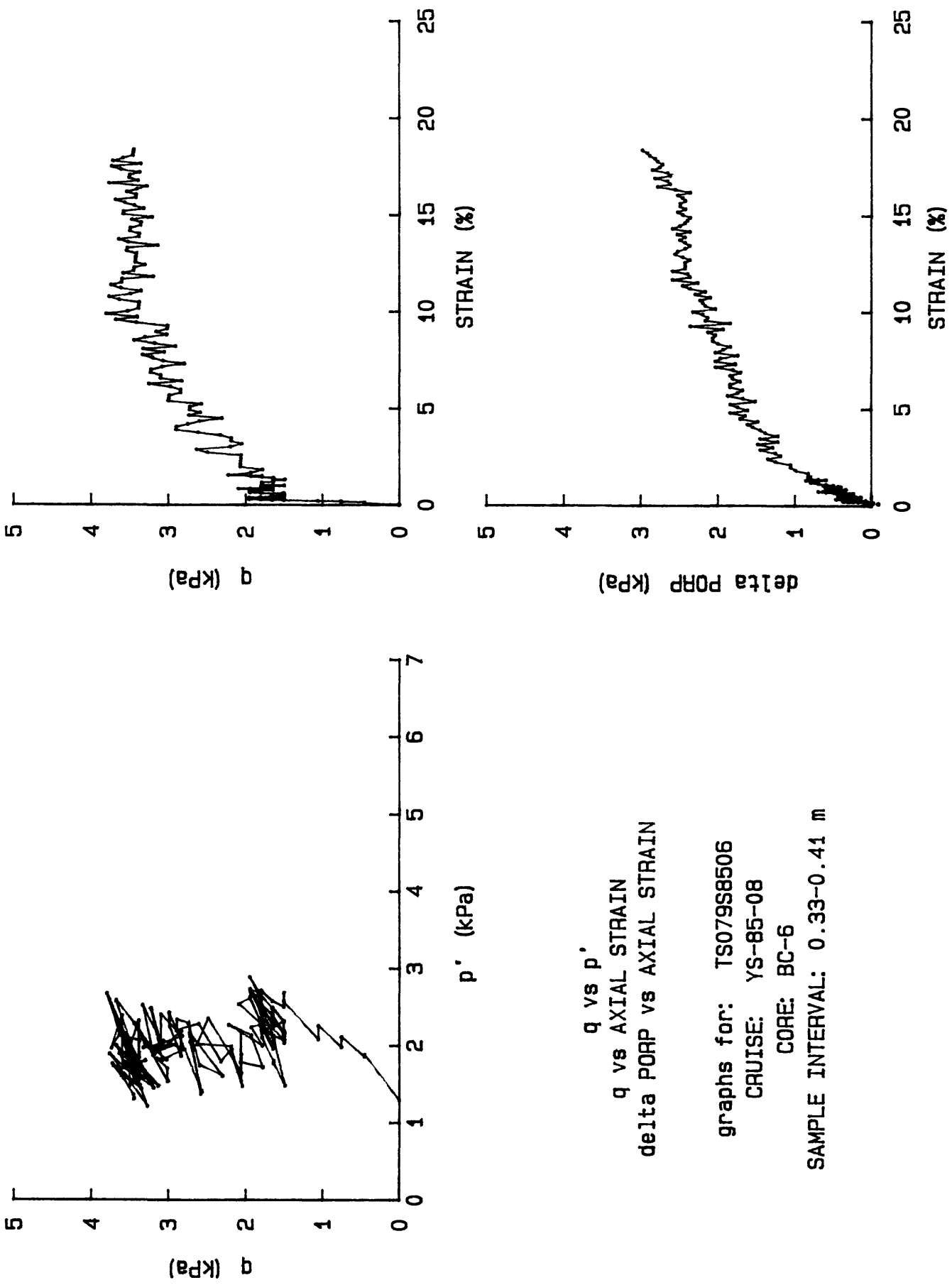
q vs p'
q vs AXIAL STRAIN
delta PORP vs AXIAL STRAIN

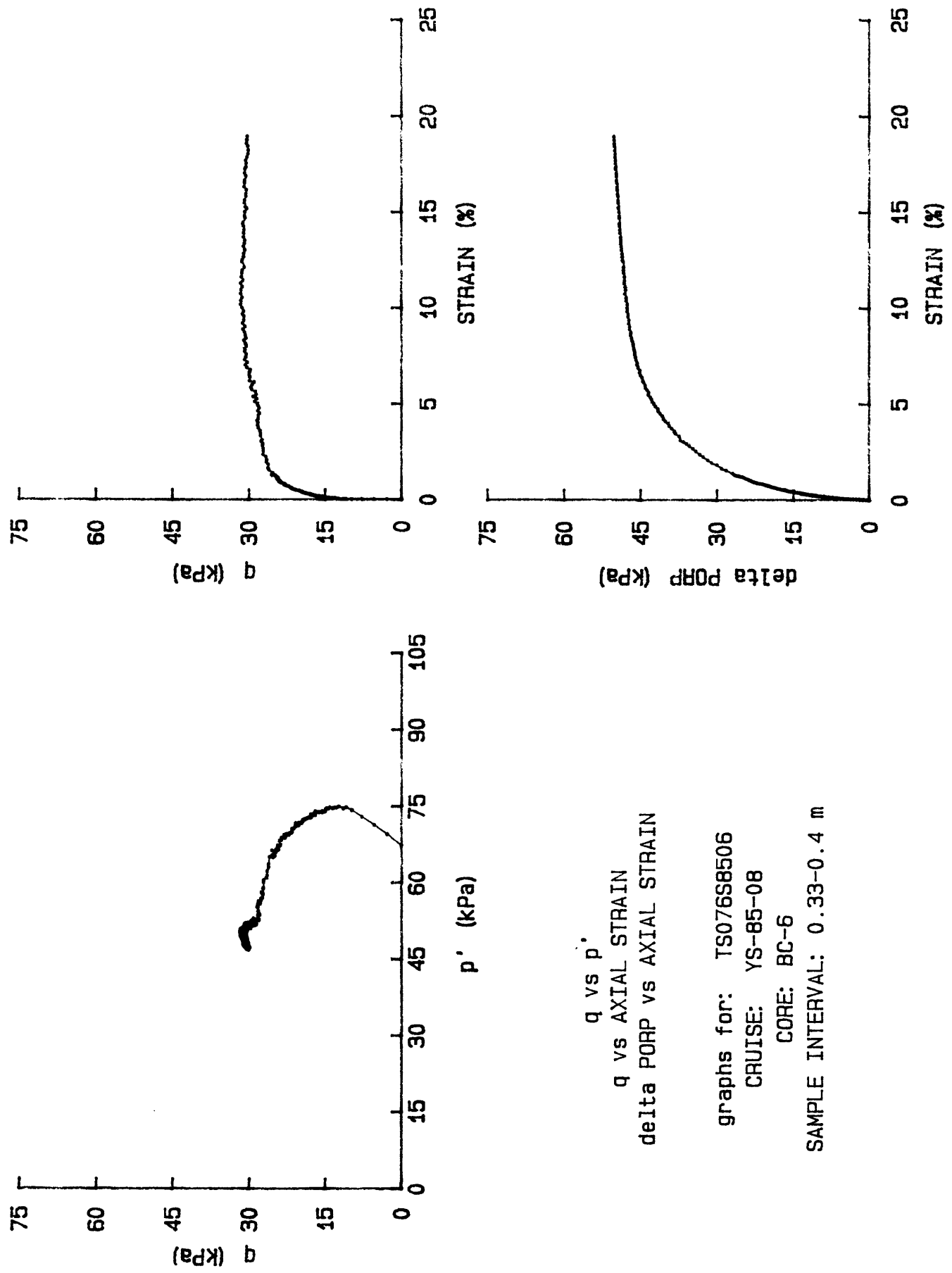
graphs for: CRUISE: TS-85-08
TS073S8505

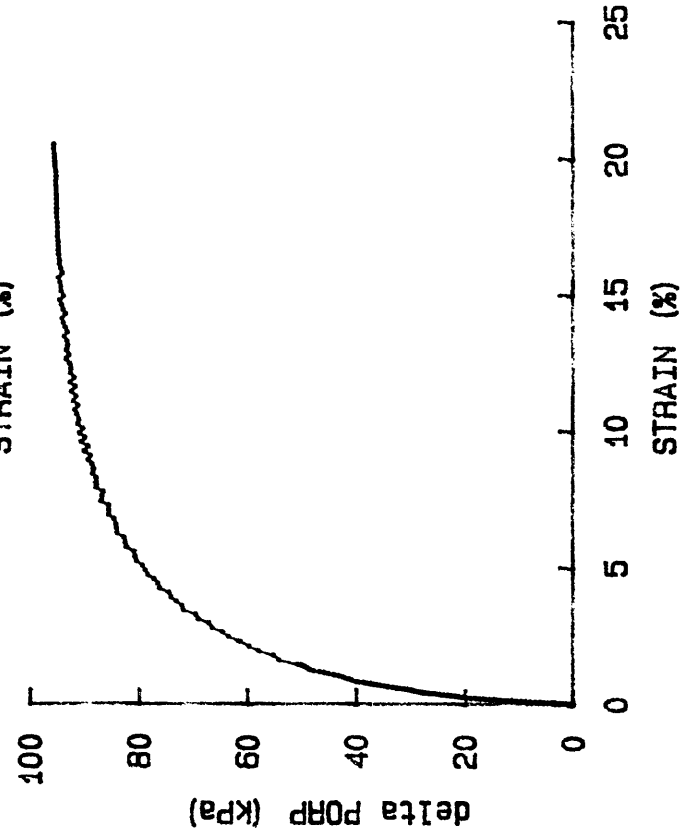
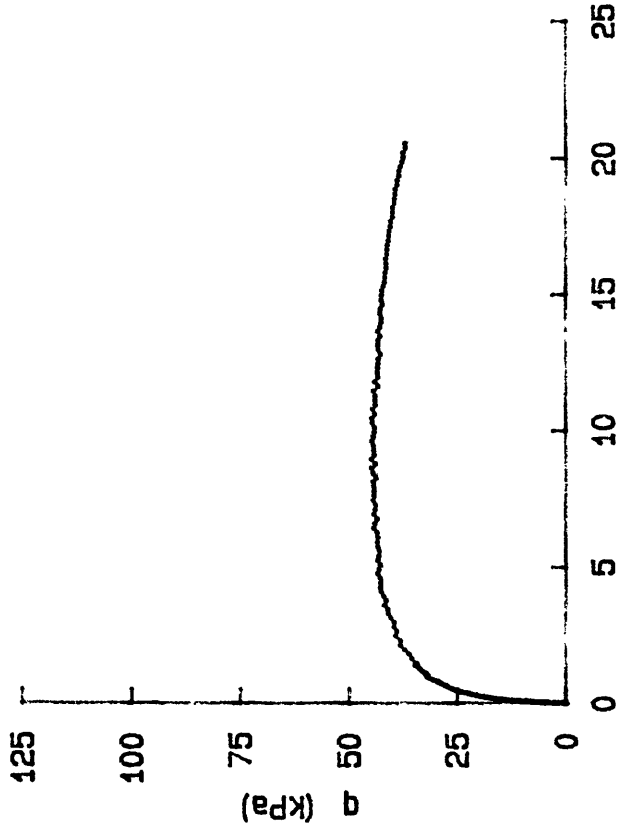
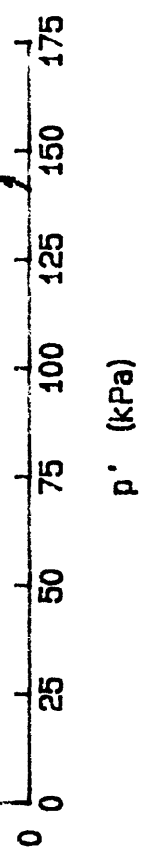
CORE: BC-5

SAMPLE INTERVAL: 0.39-0.46 m



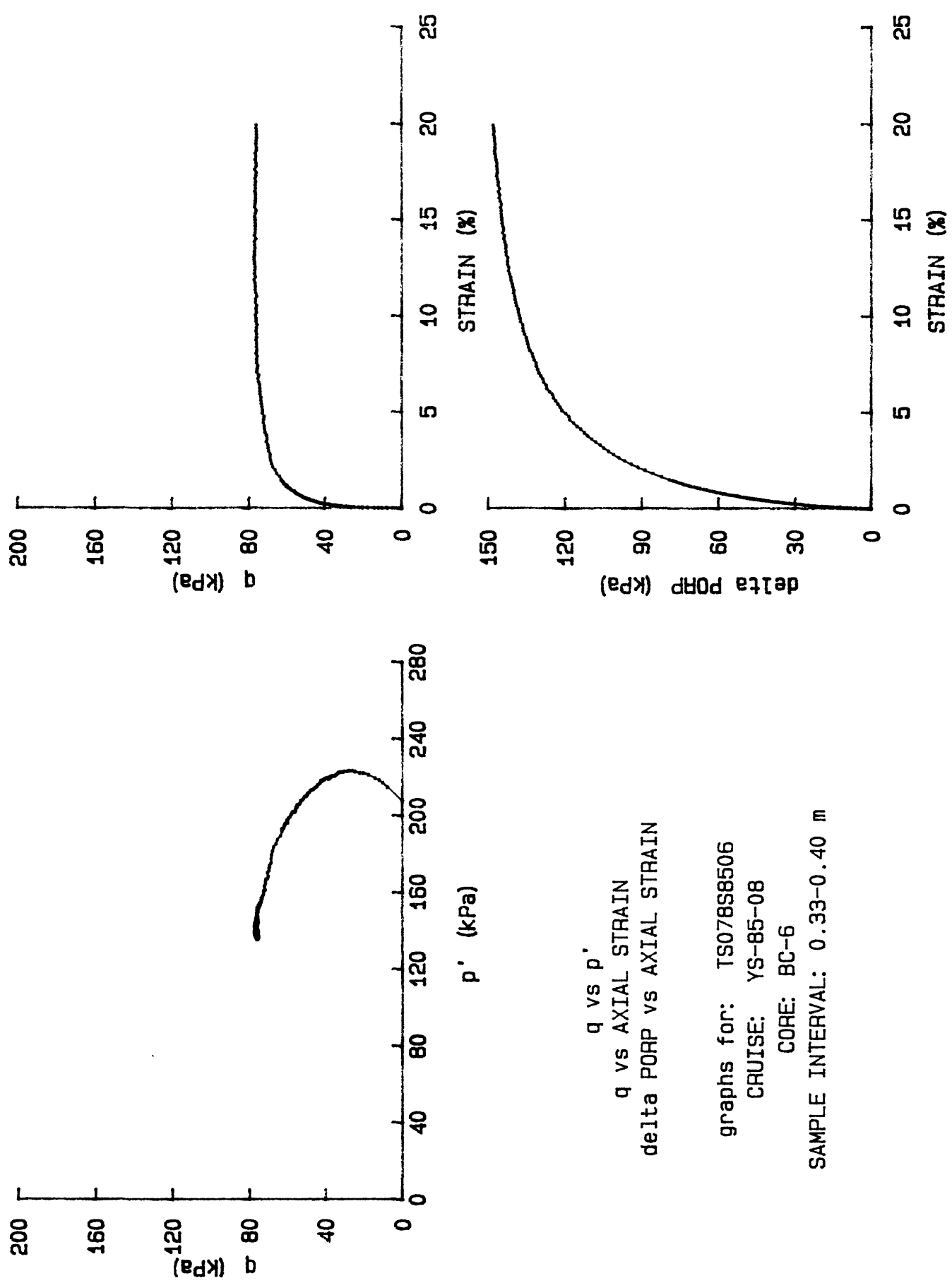


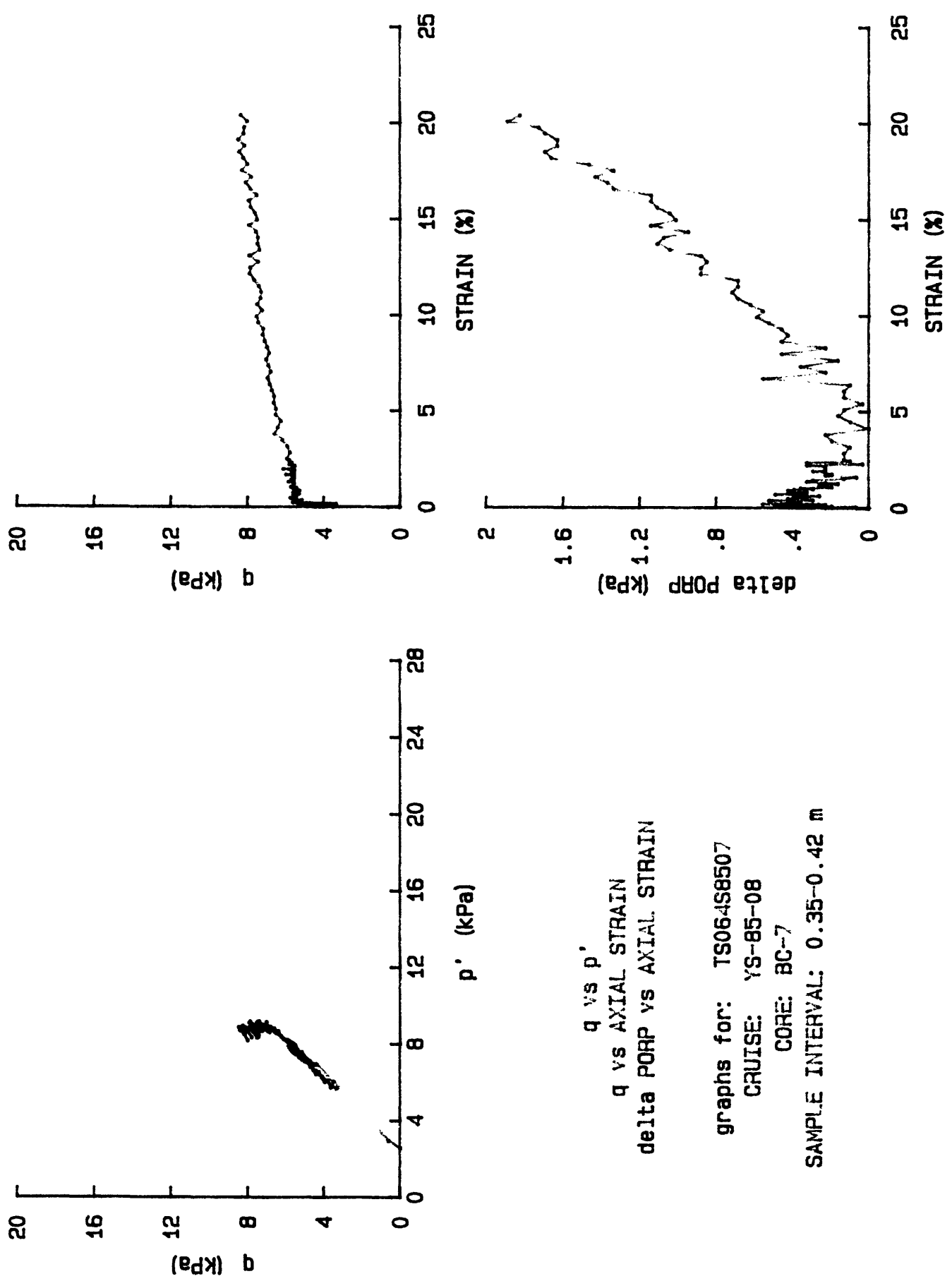


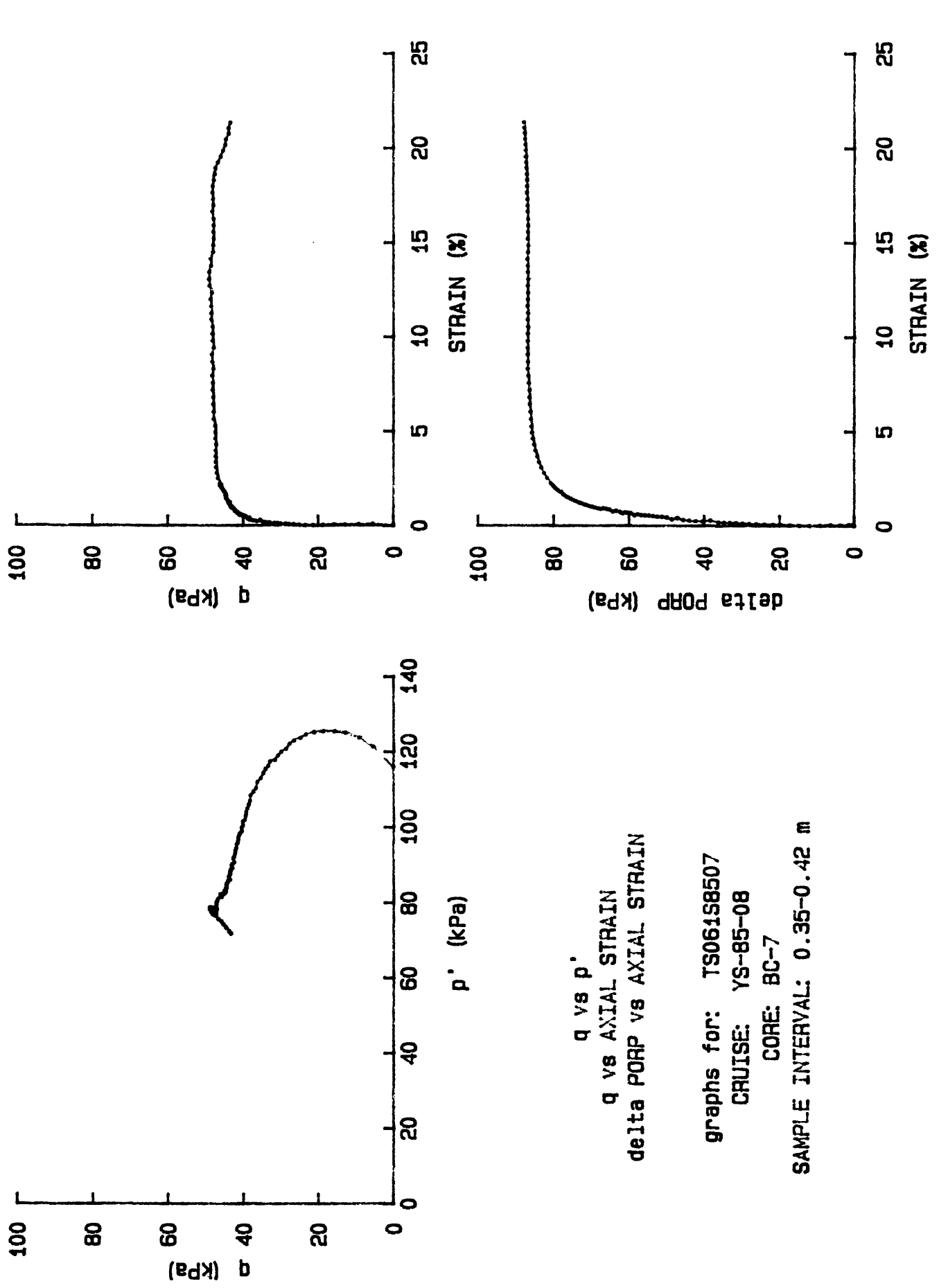


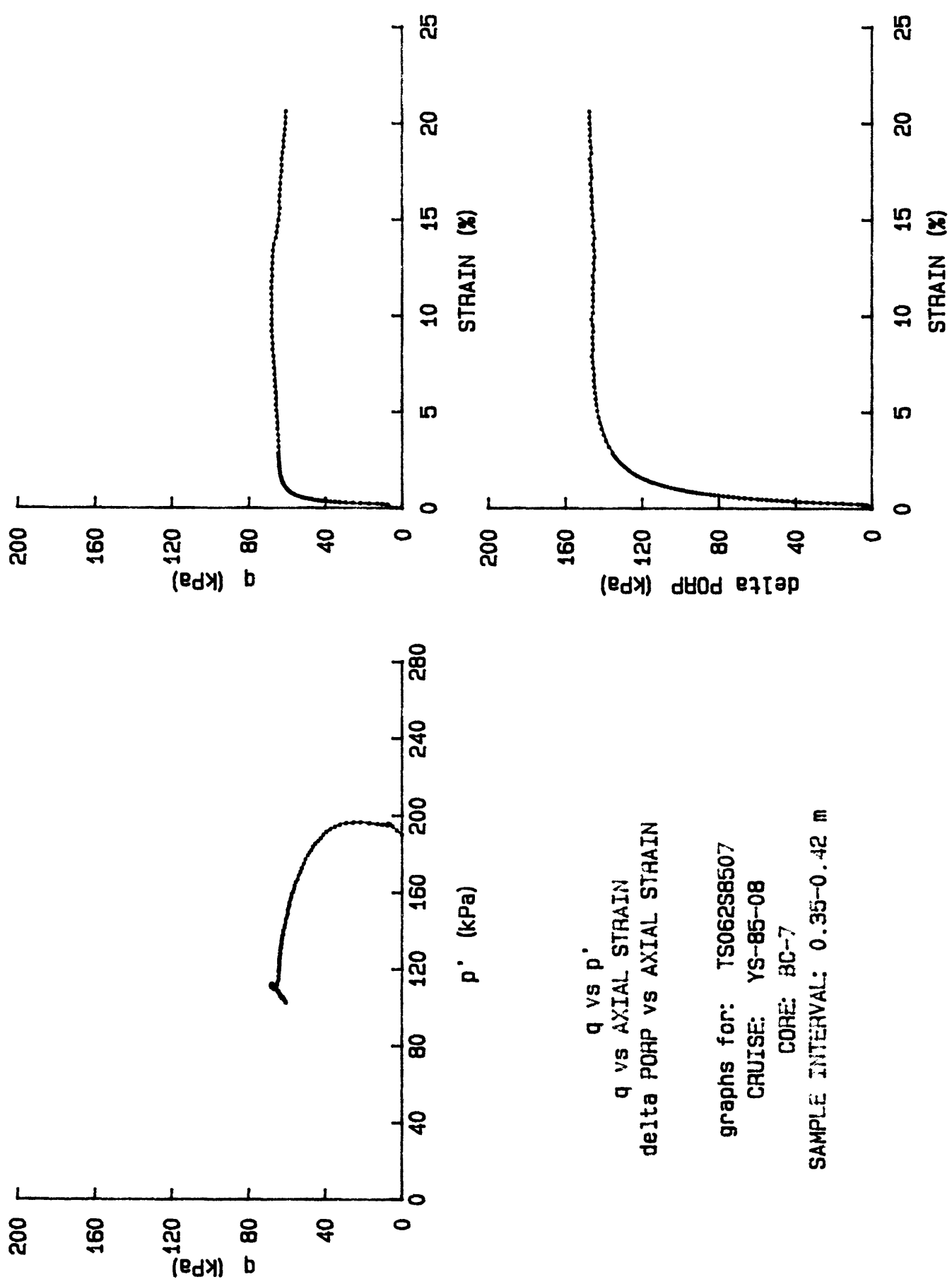
q vs p'
 q vs AXIAL STRAIN
 delta PORE vs AXIAL STRAIN

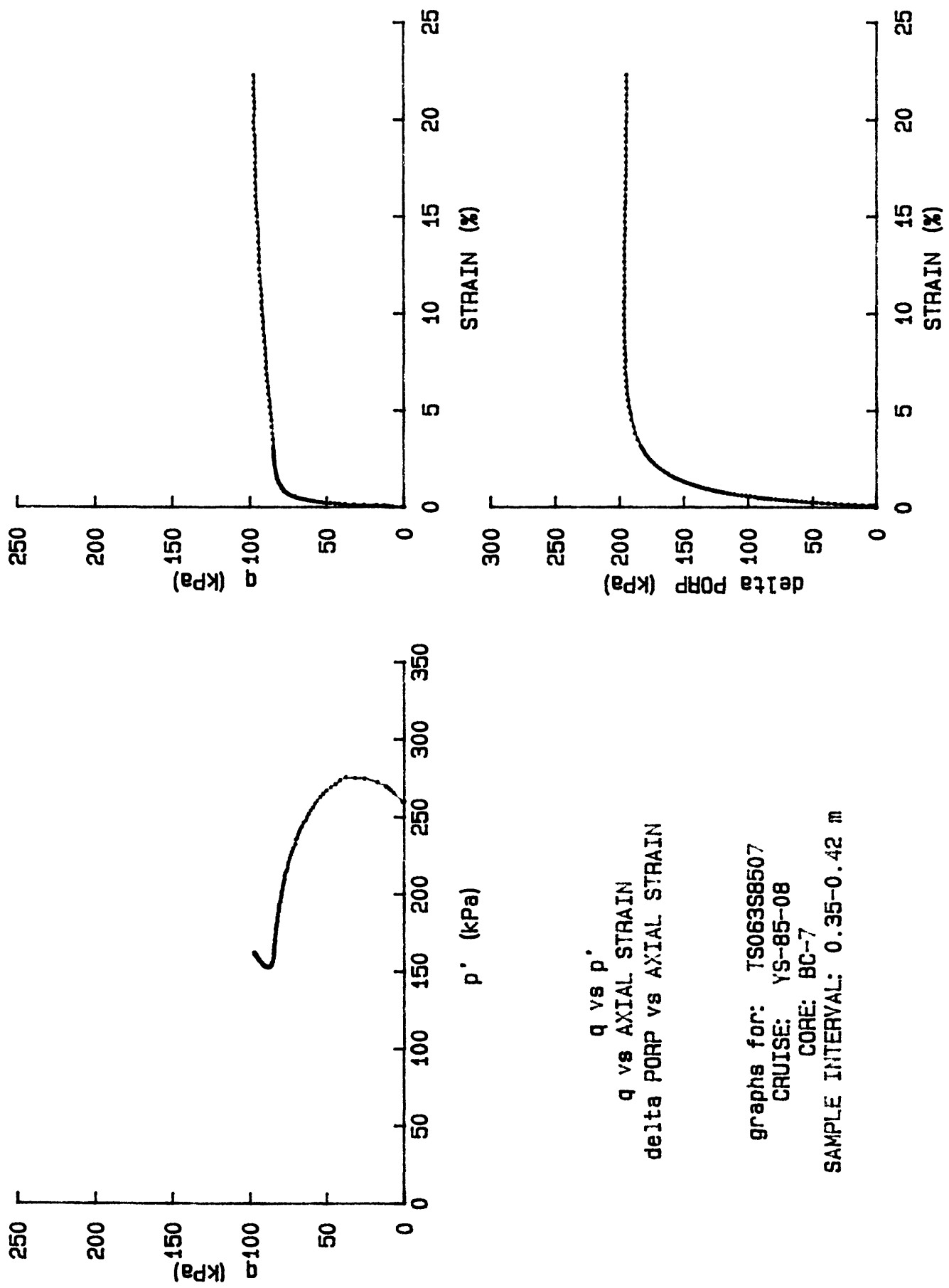
graphs for: TS077S8506
 CRUISE: YS-85-08
 CORE: BG-6
 SAMPLE INTERVAL: 0.33-0.40 m

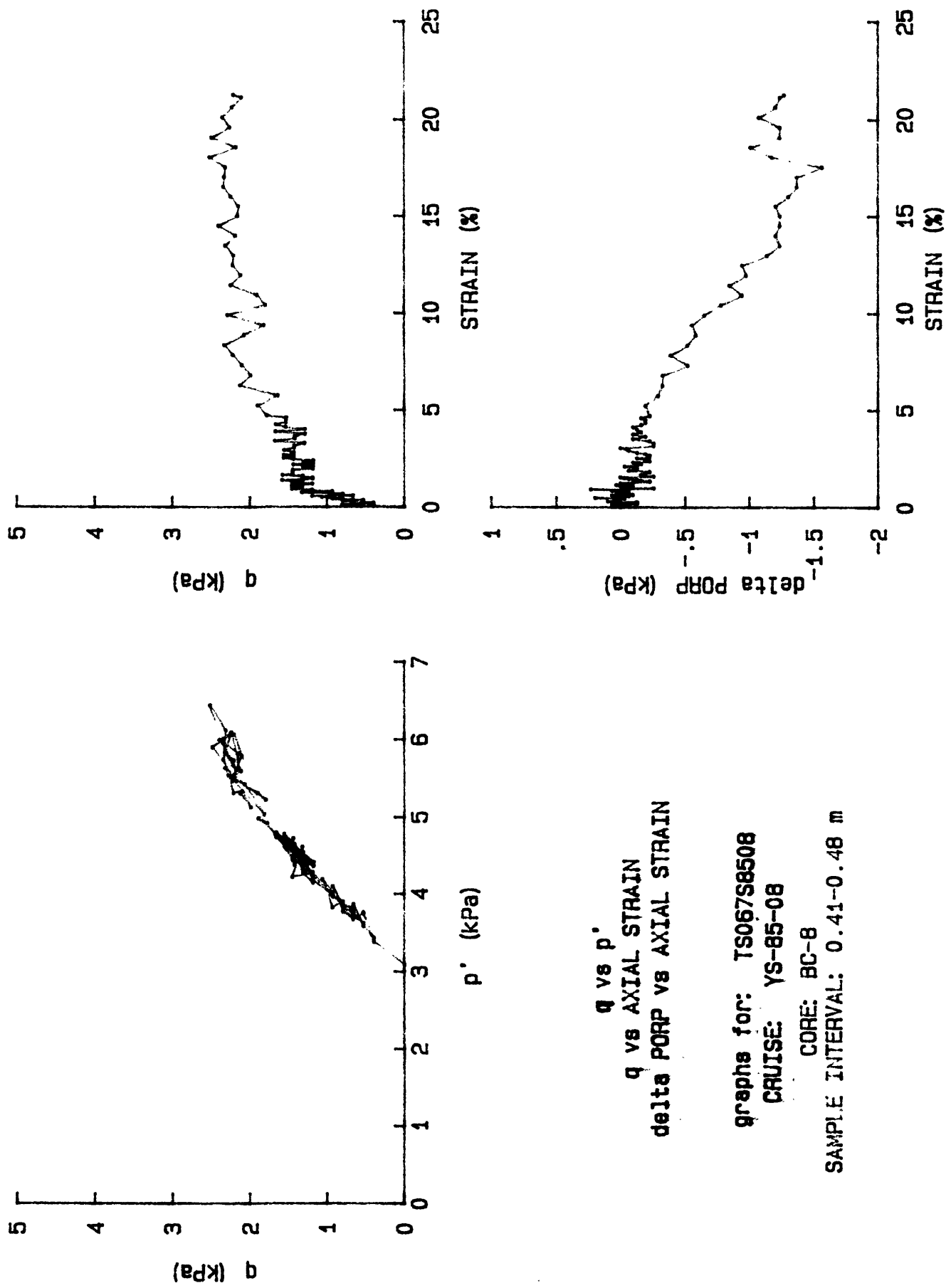


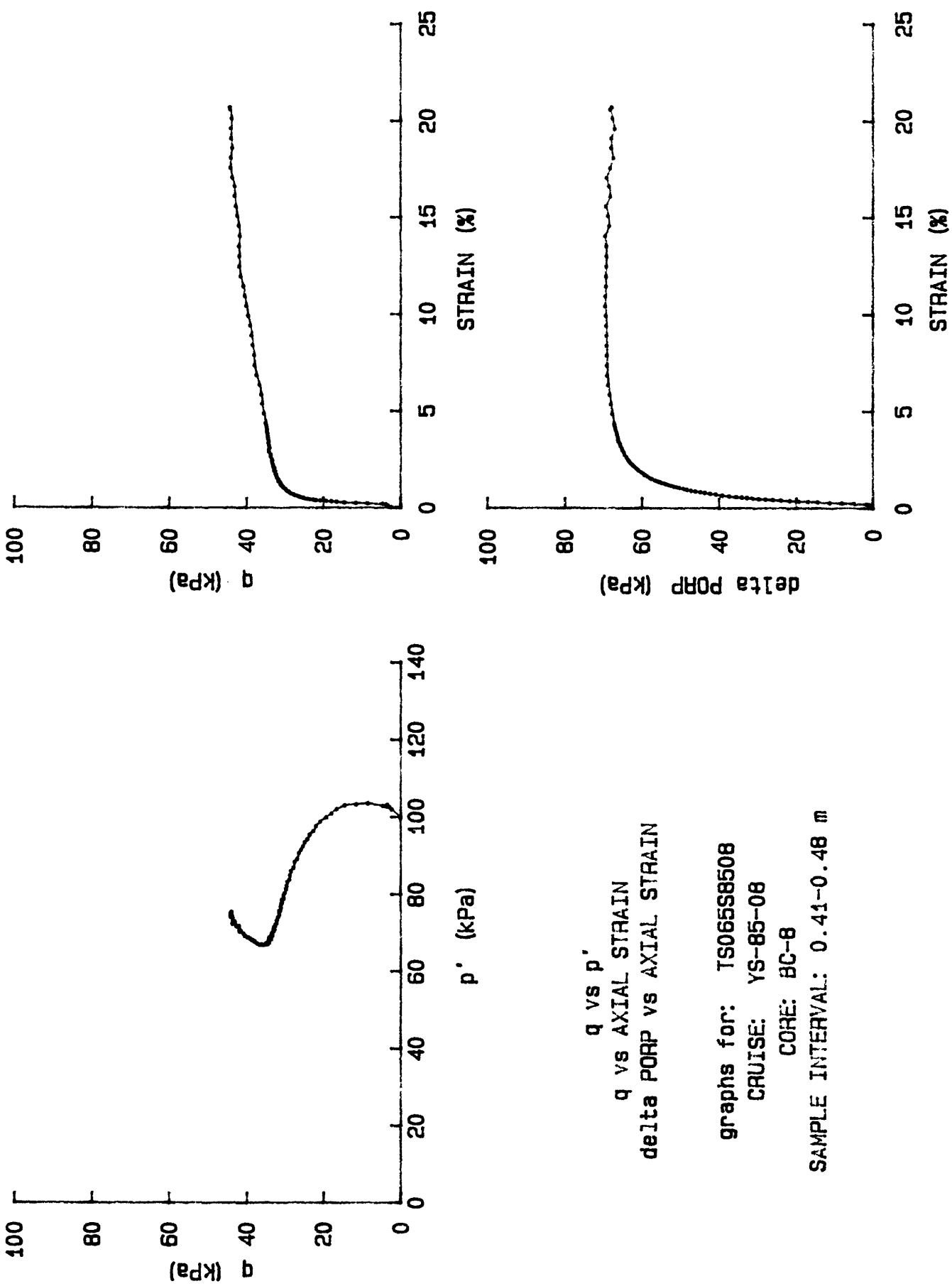


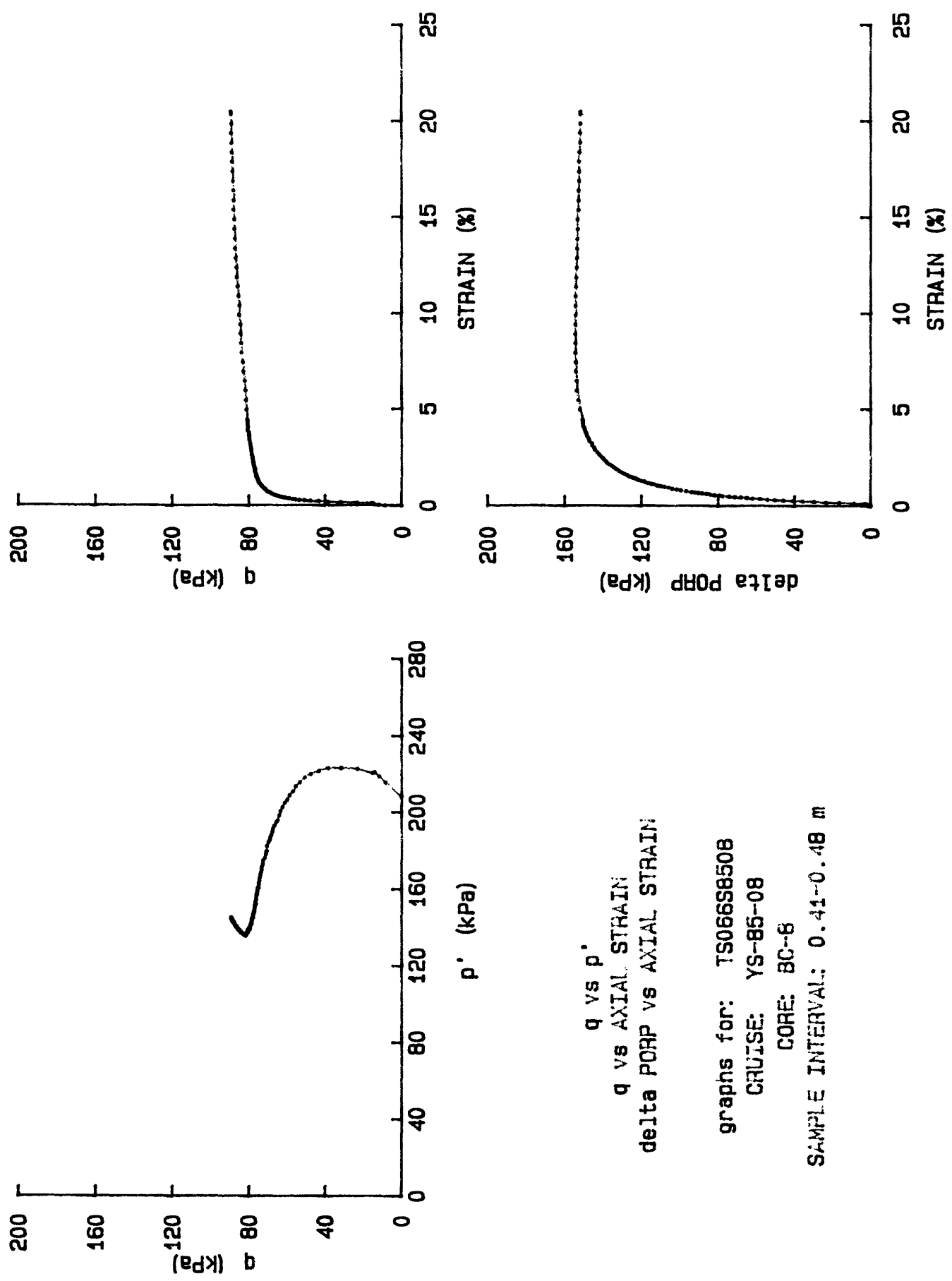


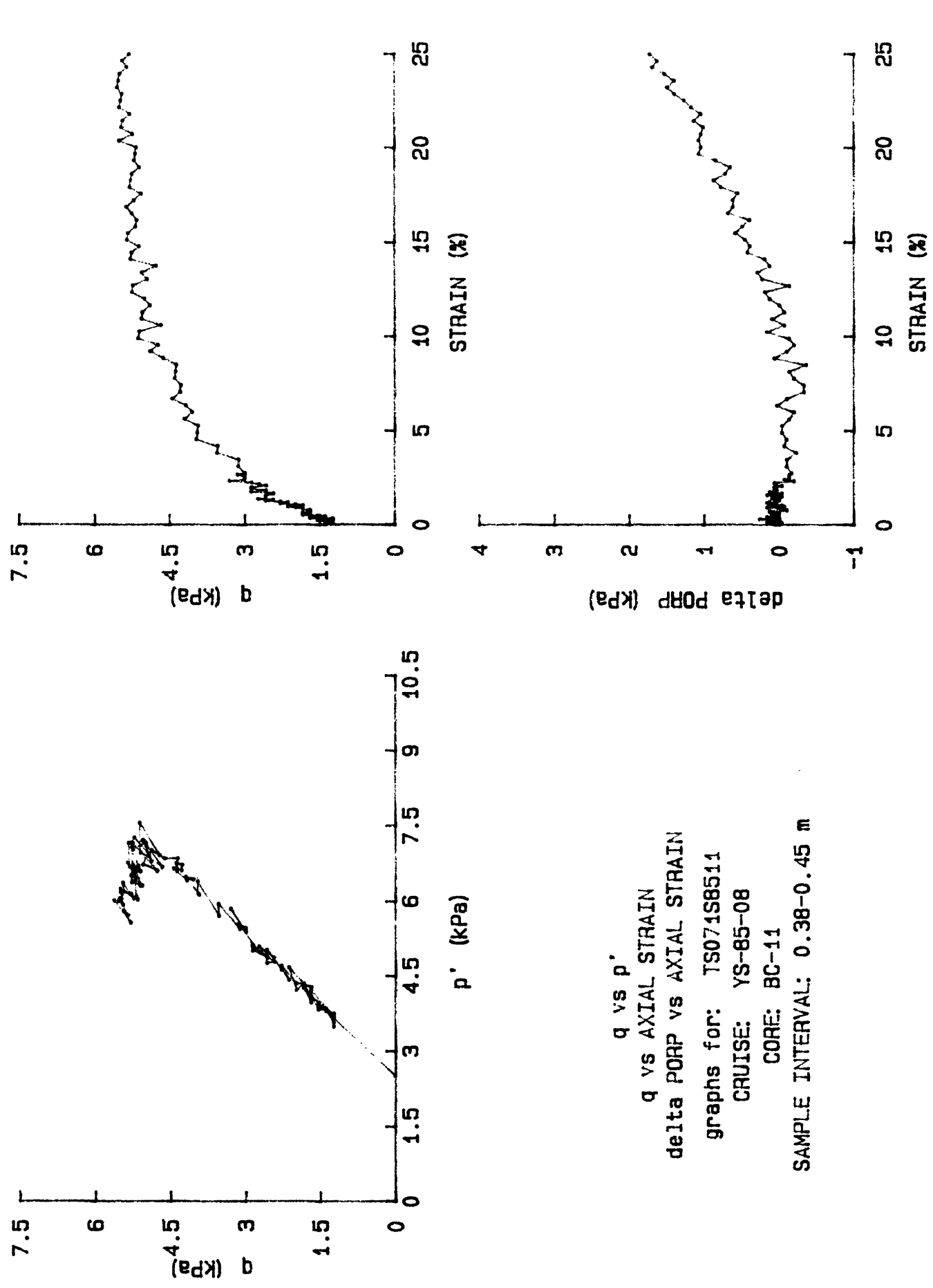


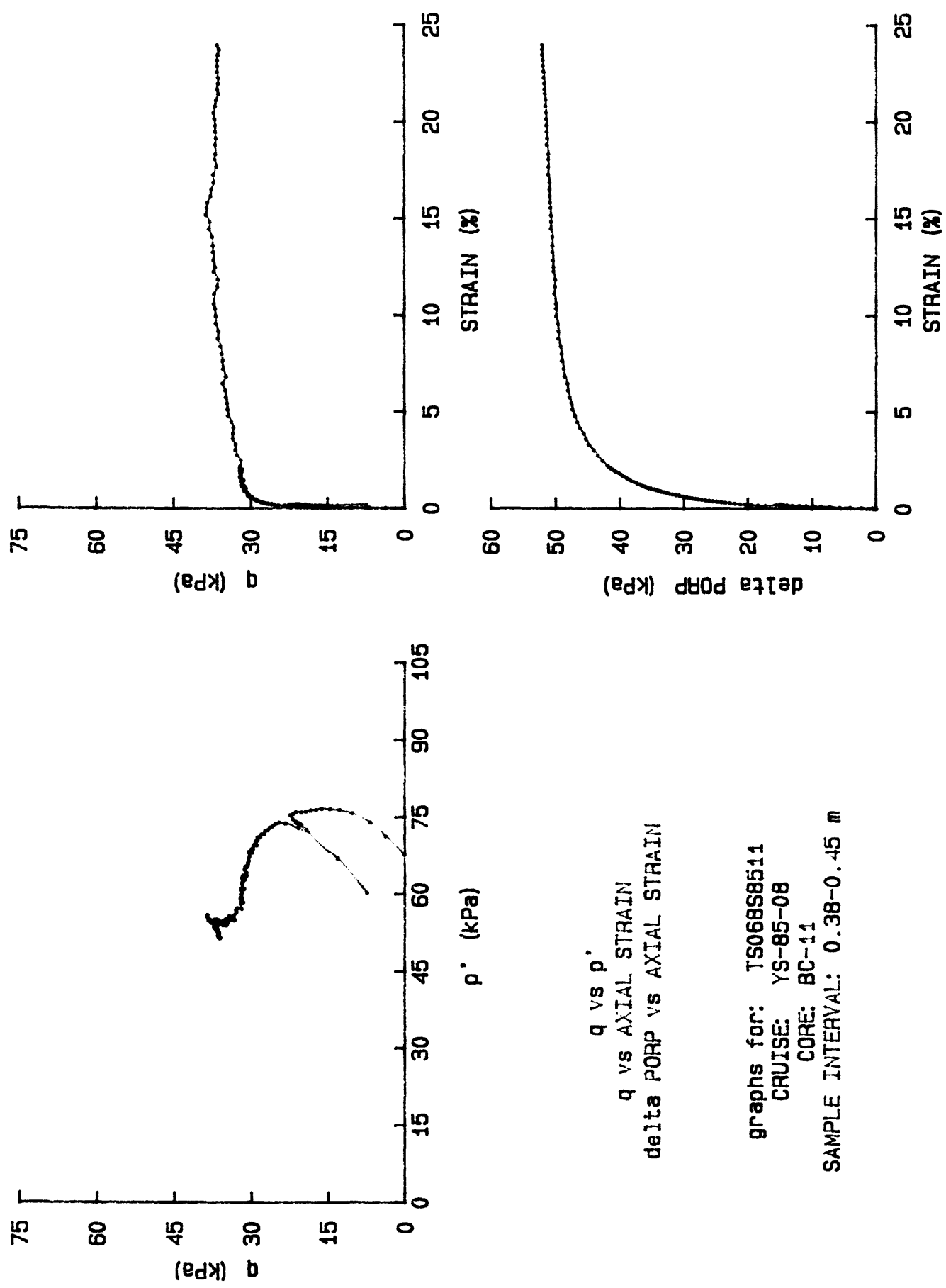


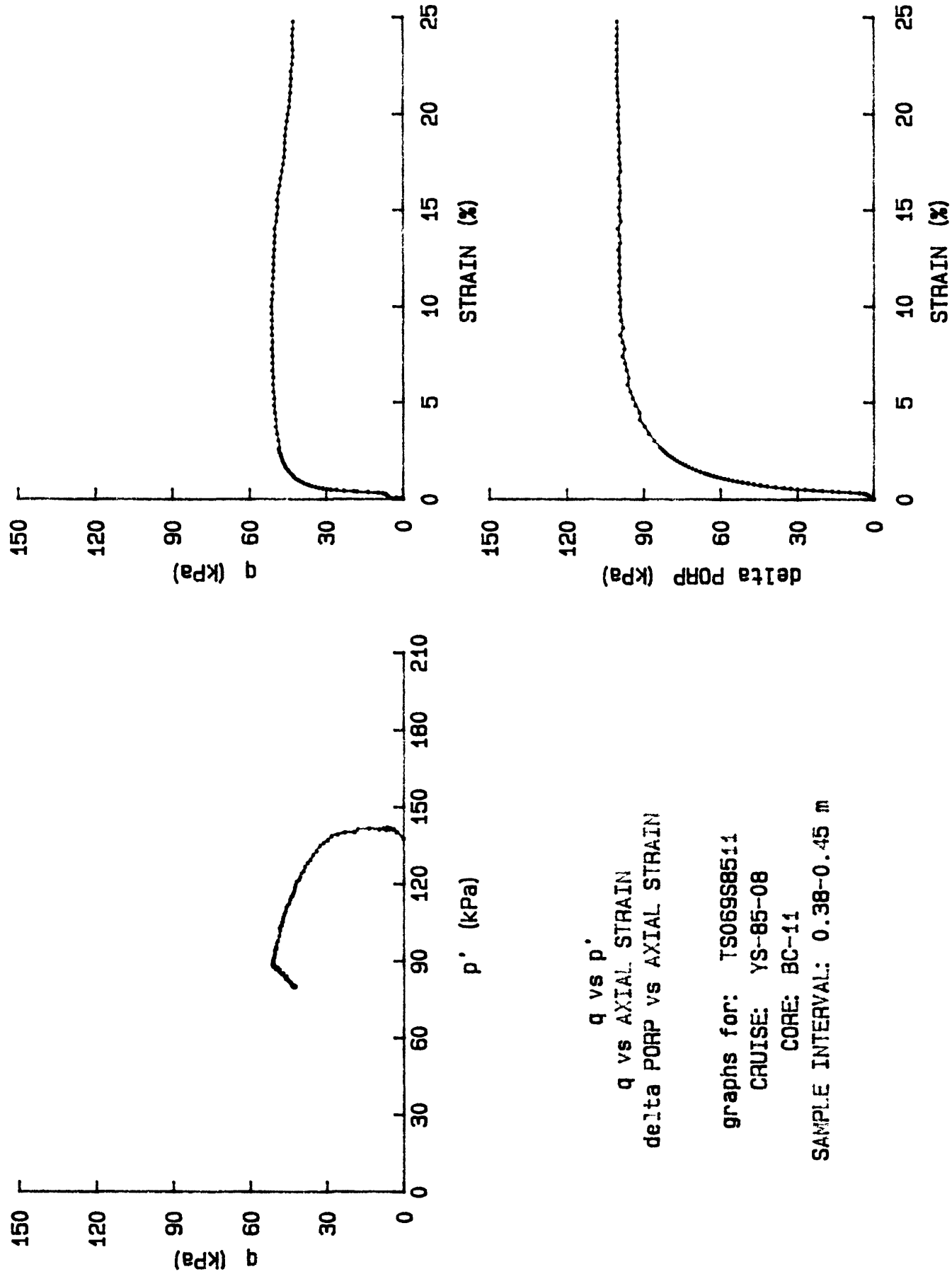


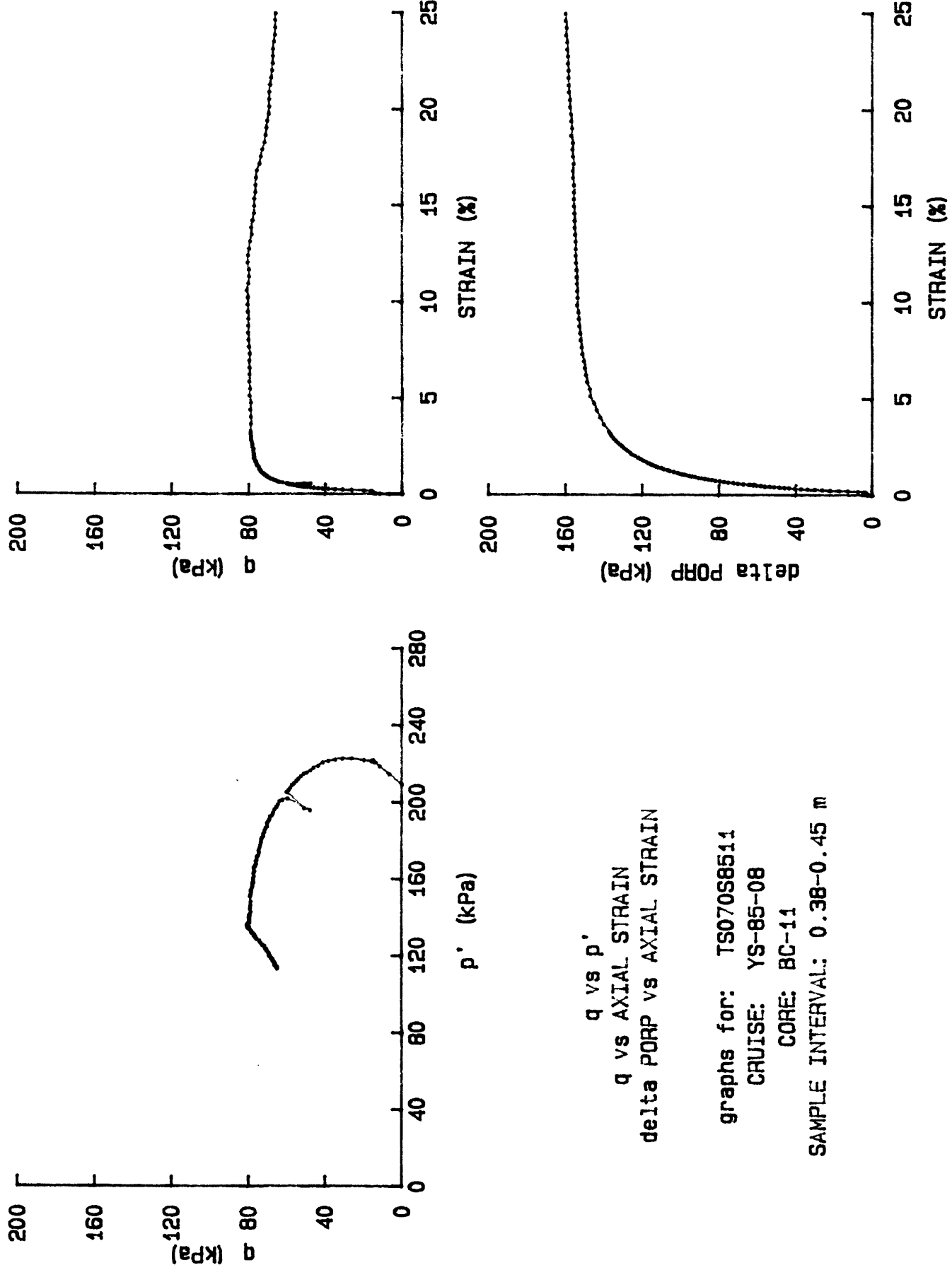




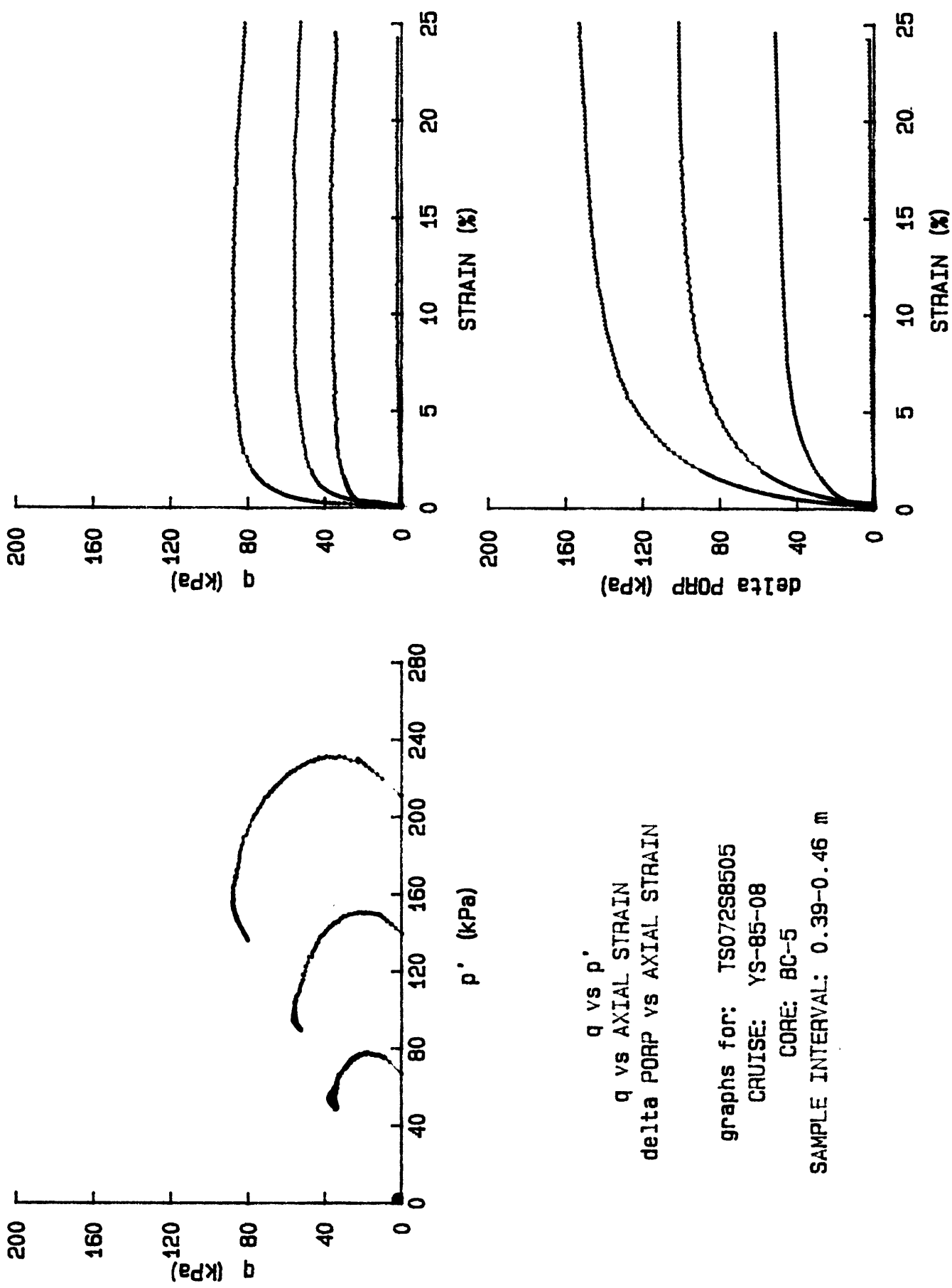


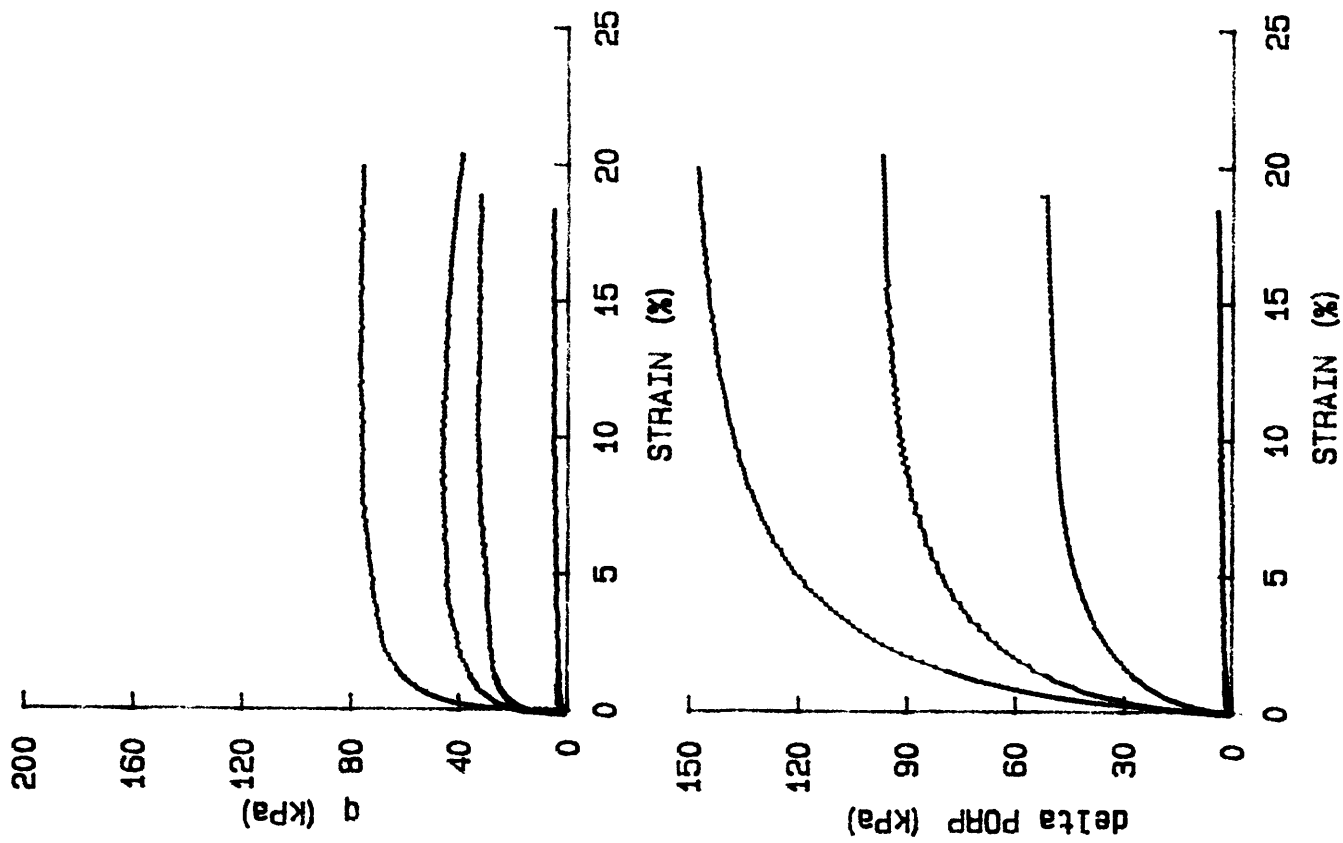
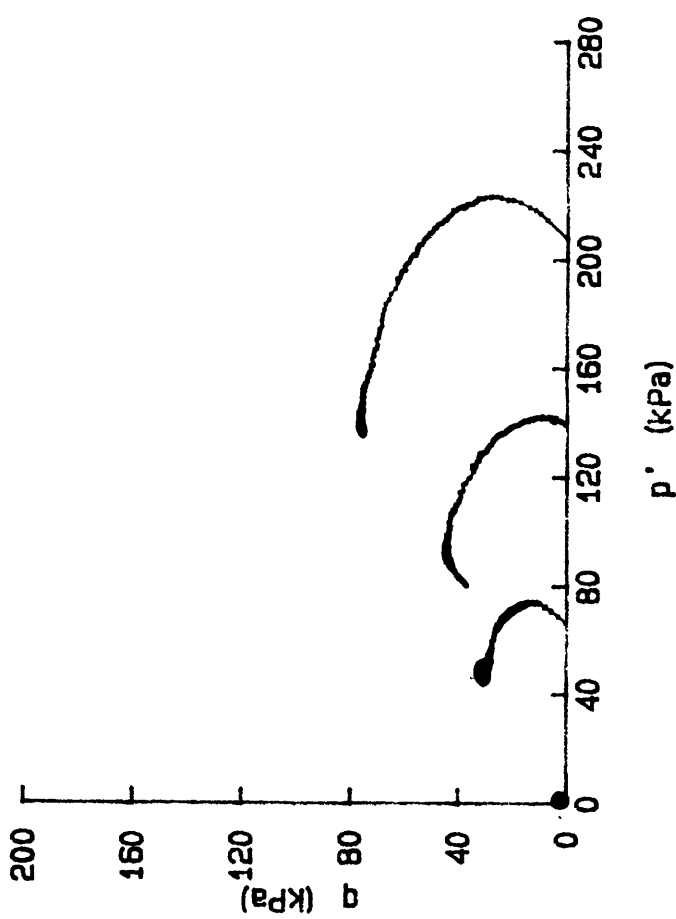






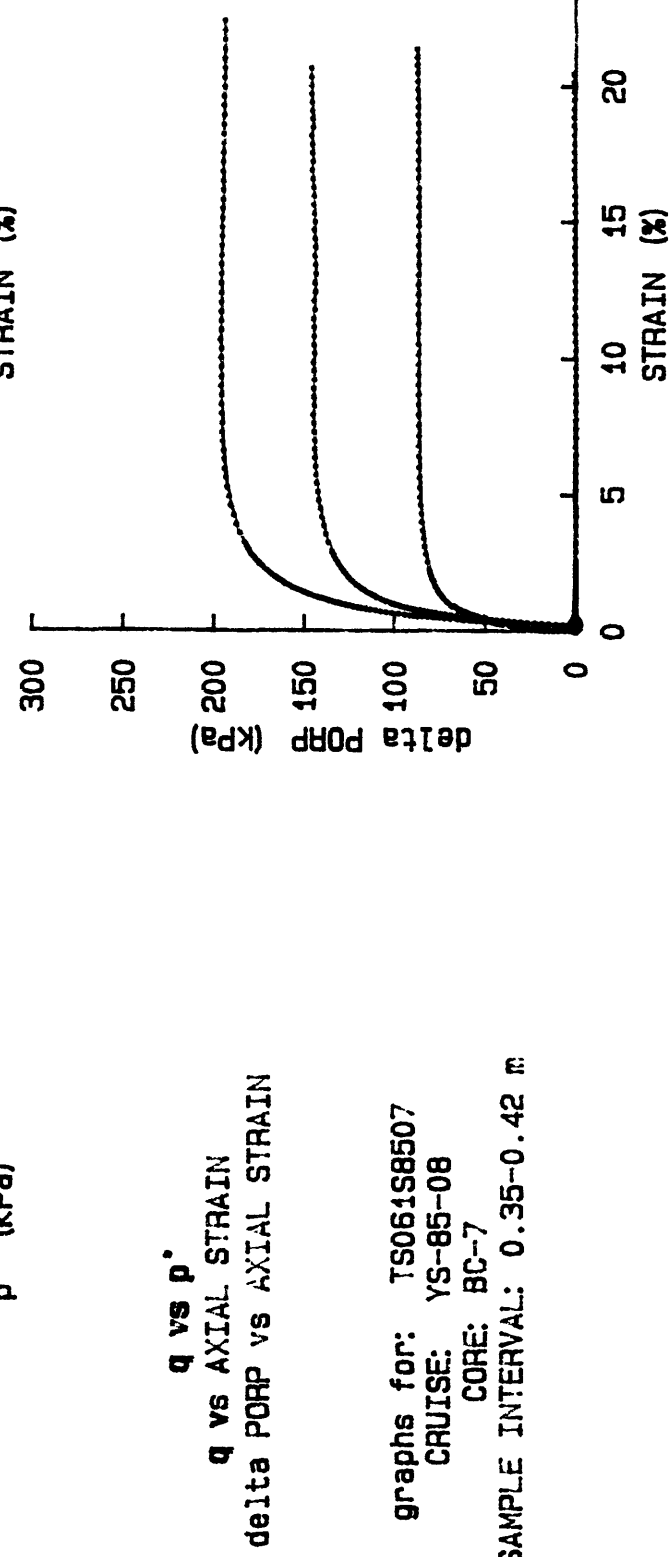
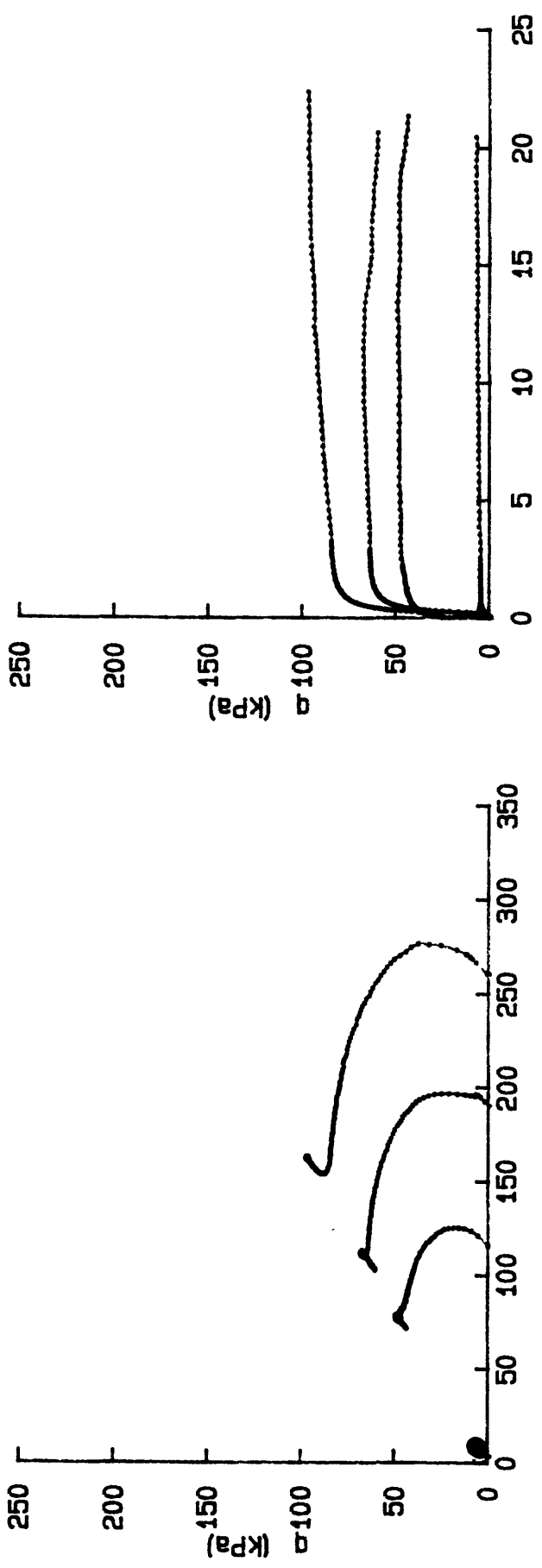
MULTIPLE TEST PLOTS



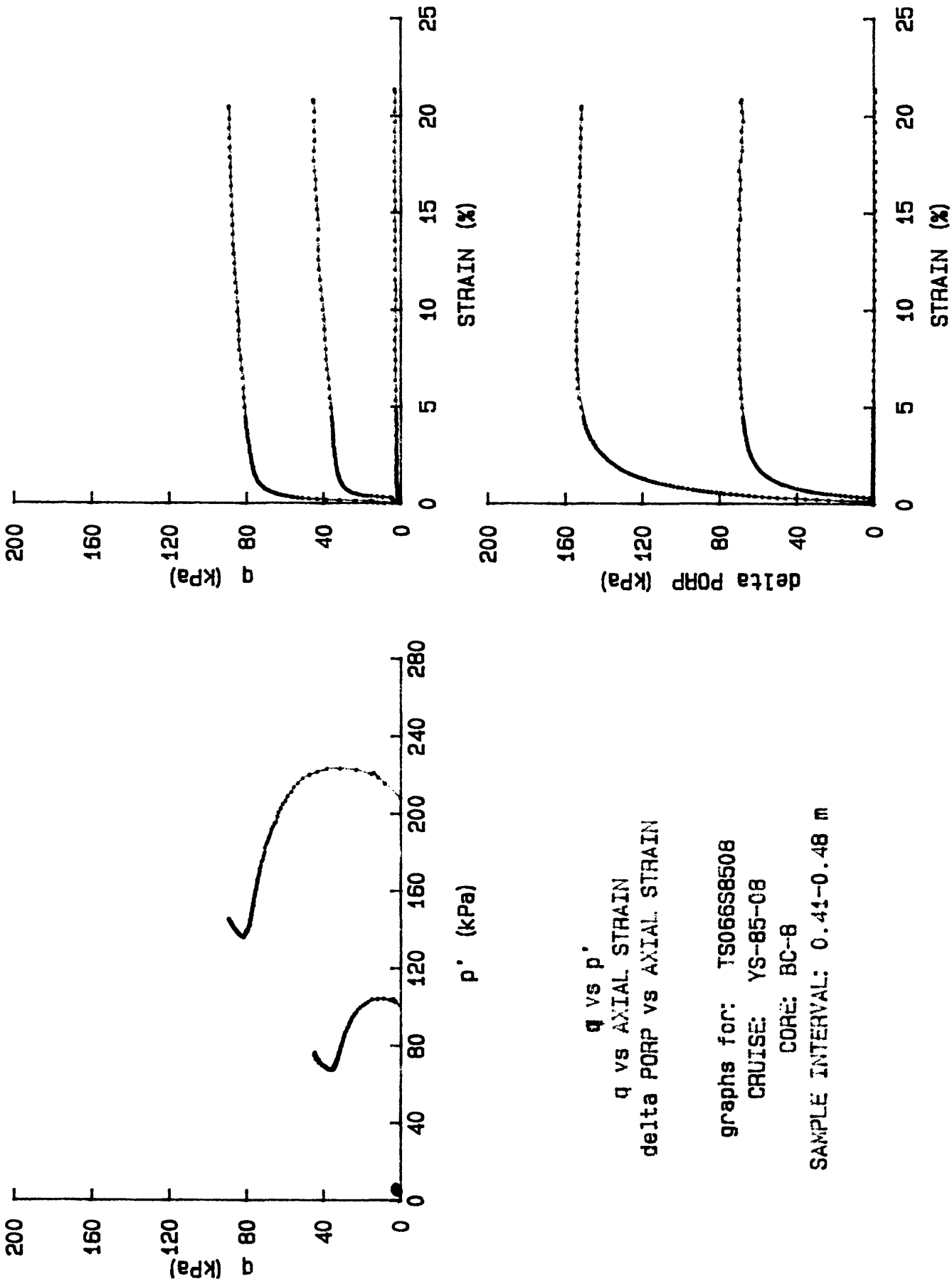


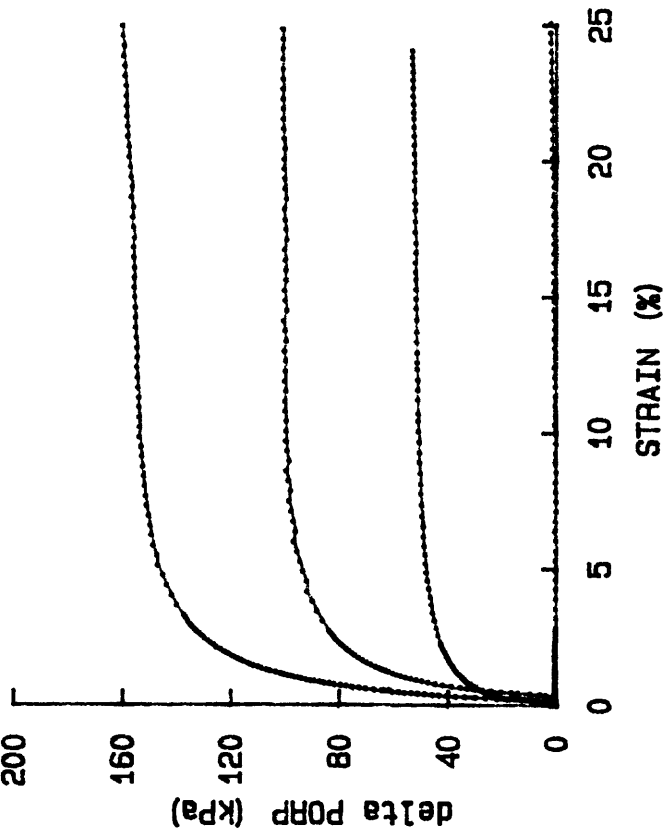
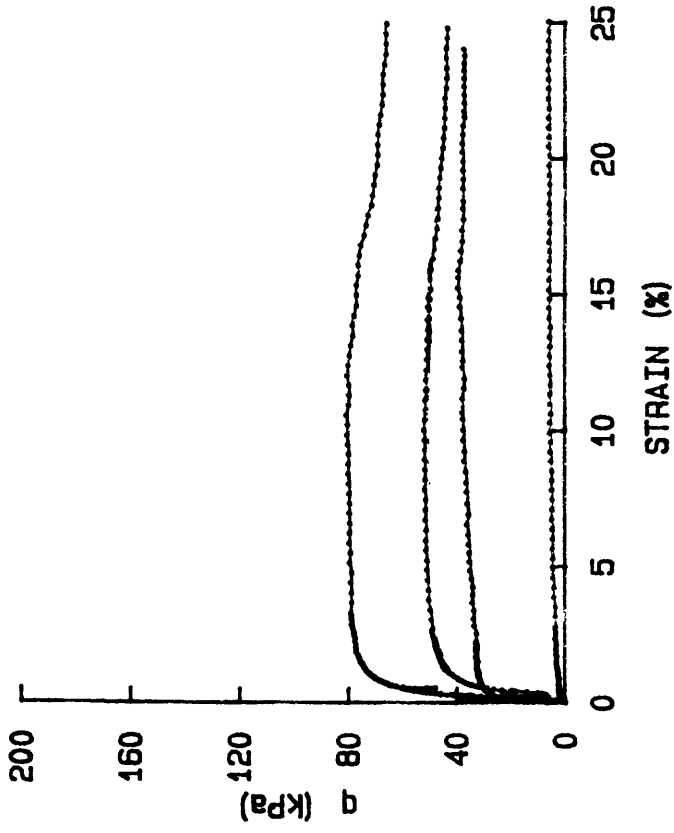
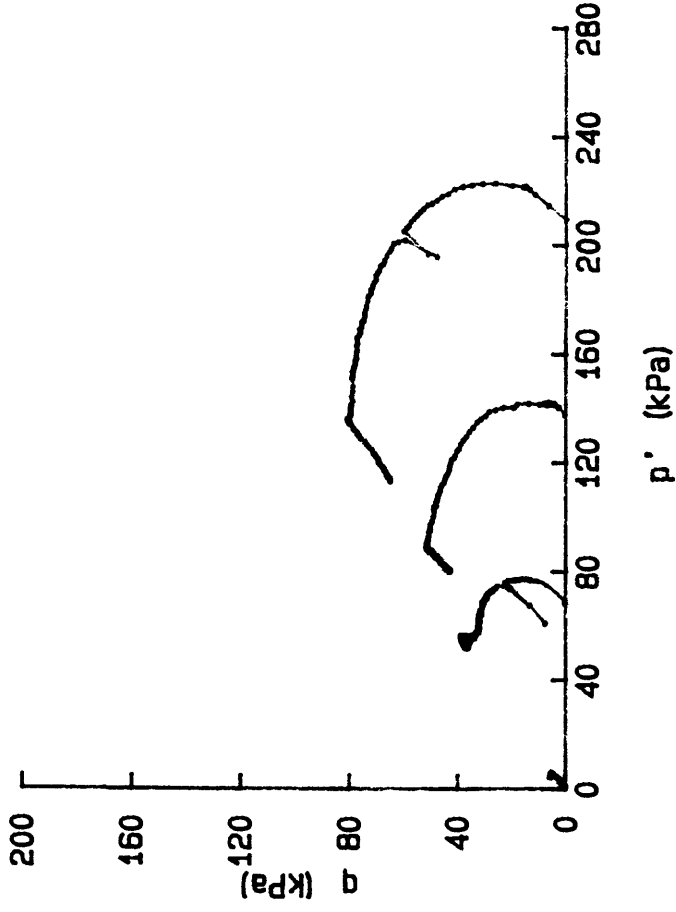
q vs p'
 q vs AXIAL STRAIN
 ΔP_{RP} vs AXIAL STRAIN

graphs for: TS07888506
 CRUISE: YS-85-08
 CORE: BC-6
 SAMPLE INTERVAL: 0.33-0.40 m



graphs for: TS061S8507
CRUISE: YS-85-08
CORE: BC-7
SAMPLE INTERVAL: 0.35-0.42 m





q vs p'
 q vs AXIAL STRAIN
 ΔPoreP vs AXIAL STRAIN

graphs for: TS070S8511
 CRUISE: YS-85-08
 CORE: BC-11
 SAMPLE INTERVAL: 0.38-0.45 m